



**Diogo Ribeiro do Couto**

**A PHYLOGENETIC ANALYSIS OF FASCIOLARIIDAE (GASTROPODA: BUCCINOIDEA)**

**ANÁLISE FILOGENÉTICA DE FASCIOLARIIDAE (GASTROPODA: BUCCINOIDEA)**

Dissertation presented to the post-graduate programme of the Museu de Zoologia da Universidade de São Paulo as a requirement for the acquisition of a Doctorate degree in Systematics, Animal Taxonomy and Biodiversity

Tese apresentada ao Programa de Pós Graduação do Museu de Zoologia da Universidade de São Paulo para obtenção do título de Doutor em Sistemática, Taxonomia Animal e Biodiversidade.

Supervisor/Orientador: Prof. Dr. Luiz Ricardo Lopes de Simone

**São Paulo, 2016**



## **AUTHORIZATION/AUTORIZAÇÃO**

*I authorize the reproduction and dissemination of this work in part or entirely by any electronic or conventional means, for study or research, provide the source is cited.*

*Autorizo a reprodução e divulgação total ou parcial deste trabalho, por qualquer meio convencional ou eletrônico, para fins de estudo e pesquisa, desde que citada a fonte.*

## FICHA CATALOGRÁFICA

Couto, Diogo Ribeiro

A phylogenetic analysis of Fasciolariidae (Gastropoda: Buccinoidea) /  
Análise filogenética de Fasciolariidae (Gastropoda: Buccinoidea) / Diogo  
Ribeiro do Couto; supervisor Luiz Ricardo Lopes de Simone – São Paulo,  
SP, 2016. Dissertation (doctorate) – Programa de Pós Graduação em  
Sistemática, Taxonomia Animal e Biodiversidade, Museu de Zoologia da  
Universidade de São Paulo..

1. Neogastropoda - phylogeny. 2. Morphology - Gastropod. 3. Total-  
evidence - analysis. I. Simone, Luiz Ricardo, orient. II. Título.

### Banca examinadora

Prof. Dr. \_\_\_\_\_ Instituição: \_\_\_\_\_

Julgamento: \_\_\_\_\_ Assinatura: \_\_\_\_\_

Prof. Dr. \_\_\_\_\_ Instituição: \_\_\_\_\_

Julgamento: \_\_\_\_\_ Assinatura: \_\_\_\_\_

Prof. Dr. \_\_\_\_\_ Instituição: \_\_\_\_\_

Julgamento: \_\_\_\_\_ Assinatura: \_\_\_\_\_

Prof. Dr. \_\_\_\_\_ Instituição: \_\_\_\_\_

Julgamento: \_\_\_\_\_ Assinatura: \_\_\_\_\_

Prof. Dr. \_\_\_\_\_ Instituição: \_\_\_\_\_

Julgamento: \_\_\_\_\_ Assinatura: \_\_\_\_\_

## ACKNOWLEDGMENTS

First and foremost, I thank my family for the love and support I received throughout all my life: Martha, Lize, Anna and Edra Lee; Dilton Couto and D.C. Jr. Alexandre Selvatti and Maria Augusta and Terezinha Maria. My advisor, Luiz Simone, for the opportunity and aid in the fine craft of molluscan anatomy. To my friends and colleagues in the malacology lab of MZSP (and to those already departed), in which the daily life together brought much learning and maturing: Ana Paula Dornellas, Vanessa Simão, Daniel and Patrícia Abbate, Jaime Jardim, Sérgio Mendonça, Hilton Galvão, Bárbara Louise, Rodrigo César Marques and Carlo Magenta. To all the technical staff and interns of the lab, that keep the wheels running: Daniel Cavallari, Isac Balbino, Natan Carvalho, Eugenio Melo, Cibele Carvalho, Fernanda Silva. Lara Guimarães for the SEM sessions, to the academic staff Marta Maria, Omair Filho and Sonia de Araújo for their help. To Dione Seripierri, for the immense help in the Reference section of this dissertation. I thank Gary Rosenberg (ANSP), Gustav Paulay (FMNH), Daniel Geiger (SBMNH) and Gregory Herbert (USF) for loan of additional specimens and sending of molecular samples for this work; Philippe Bouchet kindly loaned specimens from the Museum in Paris, and greatly helped in the taxonomy. Virginie Héros, Philippe Maestrati, Pierre Lozouet, Barbara Buge, Laurent Charles (MNHN) and Ellen Strong (NMNH) for their role in specimen processing during the expeditions and curation. Martin Snyder, Paul Callomon (ANSP) and Yuri Kantor (SIEEM) for their help in species identification and other insights. Other friends, in different spheres of life, include, but are not limited to: Babies: Renata Novaes, Gabriel Costa and Andre Costa; Julia Castro, Gabi and Gisa Sobral, Fernanda Oliveira, Luiz Renato, Simeão Moraes, the [bio]family: Flavia Sant'Anna, Raíssa Rosa, Victor Santos, Veronica Slobodian, Eloísa Zanin; to my brothers in UFRJ: Daniel Paiva, Elias Viana and Filipe Alonso; Beta Graboski and Felipe Grazziotin, Jorge Calvimontes, Vanessa Pose, Barbara Vale, Paula Garcia, Felipe Bastos and Dudu Dvogt, Marina Avila; Nathalia Granado, Jesine Falcão and Luiza Gondin; Rafa Lumi and Andre Giroti; Rafaela Jorge Trad and Cristiano Sampaio; finally, Nathalia Machado and Leandro Grance. Gonzalo Giribet (MCZ) made the molecular part of this work possible, opening up his lab and allowing the most fruitful experience of my academic career. To all his team, Rosa Fernández, Sarah Lemer, David Combosch, Erin McIntyre, Tauana Cunha, Ana Tourinho and Beka Buckham, that helped with many aspects of bench work and analysis and Adam Baldinger (MCZ) for help in collection and

management. Lee Ann Galindo (MNHN) and Patricia Álvarez (UAM) provided helpful insights during the early stages of the lab work; Alexander Fedosov and Nicolas Puillandre (MNHN) for sending useful sequence information; John Slapcinsky (FMNH) sent photographic material. Jeffrey Doucette, David Becker, Augustin (A.J.) Rodriguez and Bruna Palsen were essential friends during the making of this dissertation abroad. This work was funded by grant #2012/14821-3, Fundação de Amparo à Pesquisa do Estado de São Paulo (FAPESP), Brazil. Funds abroad came from grant #2014/10951-5 of FAPESP and by internal funds from the MCZ and the Faculty of Arts and Sciences, Harvard University.

## ABSTRACT

The neogastropod family Fascioliariidae comprise of important representatives of tropical and subtropical molluscan assemblages, with over 500 species in the subfamilies Fascioliariinae, Fusininae and Peristerniinae. Fascioliariids – with many well-known species such as tulip shells, horse-conchs, spindles, among others – have a long complicated taxonomical history, with several genus names being used to group heterogeneous contingents of many unrelated species. Recently, however, taxonomical revisions have begun to set straight its taxonomy. The present work aims to resolve the phylogeny of the family Fascioliariidae, through: 1) a morphological phylogenetic parsimony analysis in TnT based on 95 characters and 53 taxa which revealed a monophyletic Fascioliariidae, with the genera *Dolicholatirus* and *Teralatirus* representing the first split in the family, followed by three splits that correspond to a fusinine grade, which also include the genus *Pseudolatirus* (Peristerniinae); a last split groups the peristerniine genera *Peristernia* and *Fusolatirus*, while the last group comprises of fascioliariines and the remaining peristerniines. None of these clades correspond to the present-day accepted circumscription of the three recognized subfamilies. 2) Complementing the work of Couto *et al.* (2016), which used a five-gene molecular dataset to analyze the phylogeny of the family. To this dataset, the previous morphological matrix was added, generating a total evidence dataset that was implemented in POY. This analysis revealed a non-monophyletic family with the genera *Dolicholatirus* and *Teralatirus* as non-fascioliariids; the remaining fascioliariids are well-supported, with the first split a monophyletic Fusininae and *Pseudolatirus*; a second split groups *Peristernia* and *Fusolatirus*; while the last, the remaining peristerniines and fascioliariines. Total evidence was congruent with the morphological data with the exception of the Fusininae that appeared as a crown-group and not as a grade; *Lamellilatirus lamyi* (Peristerniinae) nested within the fascioliariines. Finally, 3) supplement the phylogenetic analysis of Simone (2011), inserting the analyzed taxa from the morphological analysis in the same dataset. This resulted in a monophyletic Buccinoidea superfamily, a monophyletic Fascioliariidae, despite low resolution of relationship for internal taxa; *Dolicholatirus* nested within Fascioliariidae and the fusinines with *Pseudolatirus* appeared as a monophyletic crown-group.

**Key-words:** Neogastropoda, Fascioliariinae, Peristerniinae, Fusininae, *Dolicholatirus*, morphology, total-evidence

## RESUMO

A família de neogastropodes Fascioliidae é composta por representantes significativos da malacofauna em mares tropicais e subtropicais, com mais de 500 espécies descritas nas subfamílias Fascioliinae, Fusininae e Peristerniinae. Os fasciolarídeos possuem um longo e confuso histórico taxonômico, com muitas espécies sendo alocados em gêneros claramente heterogêneos, resultando em agrupamentos que não refletem relação de parentesco. O presente estudo tem como objetivo gerar hipóteses de filogenia da família Fascioliidae; dessa maneira, foi realizada: 1) uma análise filogenética através de parcimônia no programa TnT, baseada em 95 caracteres morfológicos e 53 espécies, na qual demonstrou a monofilia da família. Em relação aos arranjos internos dos fasciolarídeos, as subfamílias que compõem esse clado não são monofiléticas. Segundo a topologia obtida, observou-se que a primeira divergência separa um grupo com os gêneros *Dolicholattirus* e *Terralattirus*; a seguir, três divisões que correspondem a um grupo de fusiníneos, que também inclui o gênero *Pseudolattirus* (Peristerniinae); uma última divisão, na qual se observa uma dicotomia que agrupa os gêneros de peristerníneos *Peristernia* e *Fusolattirus*, e os demais peristerníneos e fasciolaríneos. 2) Complementar o trabalho de Couto *et al.* (2016), que utilizaram dados moleculares de cinco genes para analisar a filogenia da família. A esses dados, foram incluídos também a matriz da análise morfológica, a fim de realizar uma análise de evidência total implementada no programa POY. O resultado dos dados concatenados corrobora com a análise molecular evidenciando a família Fascioliidae como um clado não monofilético, uma vez que os gêneros *Dolicholattirus* e *Terralattirus* não estão incluídos na família; os demais fasciolarídeos formam um clado com uma primeira divisão que separa os fusiníneos e *Pseudolattirus* dos demais; uma segunda divisão compondo os peristerníneos *Peristernia* e *Fusolattirus* e a última agrupa os demais peristerníneos e fasciolaríneos. Dados de evidência total foram congruentes com a análise morfológica, com exceção dos fusiníneos, que apareceram como um grupo monofilético e *Lamellilattirus lamyi* (Peristerniinae) dentro dos fasciolaríneos. Finalmente, 3) inserir as espécies analisadas na análise morfológica, na matriz de dados de Simone (2011). Esta última análise resultou em uma superfamília Buccinoidea monofilética, a família Fascioliidae sendo monofilético apesar de com uma topologia com pouca resolução interna para os táxons internos; *Dolicholattirus* e *Terralattirus* estão incluídos na família e os fusiníneos mais o gênero *Pseudolattirus* como um grupo monofilético.

**Palavras-chave:** Neogastropoda, Fascioliinae, Peristerniinae, Fusininae, *Dolicholattirus*, morfologia, evidência-total

## LIST OF FIGURES

### Chapter I

---

<b>Figure 1A.</b> Phylogenetic tree obtained through parsimonious analysis in TnT using prior, unweighted characters.....	20
<b>Figure 1B.</b> Phylogenetic tree obtained through parsimonious analysis in TnT using prior, unweighted characters.....	21
<b>Figure 2.</b> Phylogenetic tree (part one) indicating the synapomorphies that support them.....	22
<b>Figure 3.</b> Phylogenetic tree (part two) indicating the synapomorphies that support them.....	23
<b>Figure 4.</b> Phylogenetic tree (part three) indicating the synapomorphies that support them.....	24
<b>Figure 5.</b> Phylogenetic tree (part four) indicating the synapomorphies that support them.....	25
<b>Figure 6.</b> Phylogenetic tree obtained through parsimonious analysis in TnT with prior weighing. Numbers in nodes indicate node numbers.....	26
<b>Figure 7.</b> <i>Thais speciosa</i> , shell.....	28
<b>Figure 8.</b> <i>Thais speciosa</i> , radula.....	28
<b>Figure 9.</b> <i>Pugilina tupiniquim</i> , shell.....	29
<b>Figure 10.</b> <i>Pugilina tupiniquim</i> , radula.....	29
<b>Figure 11.</b> <i>Engoniophos uncinatus</i> , shell.....	31
<b>Figure 12.</b> <i>Engoniophos uncinatus</i> , radula.....	31
<b>Figure 13.</b> <i>Nassarius reticulatus</i> , shell.....	32
<b>Figure 14.</b> <i>Nassarius reticulatus</i> , radula.....	32
<b>Figure 15.</b> <i>Bullia laevissima</i> , shell and operculum.....	33
<b>Figure 16.</b> <i>Bullia laevissima</i> , radula.....	33
<b>Figure 17.</b> <i>Buccinum undatum</i> , shell and operculum.....	35
<b>Figure 18.</b> <i>Buccinum undatum</i> , radula.....	35
<b>Figure 19.</b> <i>Pisania pusio</i> , shell.....	37
<b>Figure 20.</b> <i>Pisania pusio</i> , radula.....	37
<b>Figure 21.</b> <i>Dolicholatirus</i> sp. shell.....	38
<b>Figure 22.</b> <i>Dolicholatirus</i> sp. radula.....	38
<b>Figure 23.</b> <i>Teralatirus roboreus</i> , shell.....	39
<b>Figure 24.</b> <i>Teralatirus roboreus</i> , radula.....	39

<b>Figure 25.</b> <i>Dolicholatirus</i> aff. <i>cayohuesonicus</i> , shell.....	40
<b>Figure 26.</b> <i>Dolicholatirus</i> aff. <i>cayohuesonicus</i> , radula.....	40
<b>Figure 27.</b> <i>Pseudolatirus kuroseanus</i> , shell.....	42
<b>Figure 28.</b> <i>Pseudolatirus kuroseanus</i> , radula.....	42
<b>Figure 29.</b> <i>Amiantofusus pacificus</i> , shell.....	43
<b>Figure 30.</b> <i>Amiantofusus pacificus</i> , radula.....	43
<b>Figure 31.</b> <i>Amiantofusus candoris</i> , shell.....	44
<b>Figure 32.</b> <i>Amiantofusus candoris</i> , radula.....	44
<b>Figure 33.</b> <i>Pseudolatirus pallidus</i> , shell. ....	47
<b>Figure 34.</b> <i>Pseudolatirus pallidus</i> , radula.....	47
<b>Figure 35.</b> <i>Chryseofusus archerusicus</i> , shell.....	48
<b>Figure 36.</b> <i>Chryseofusus archerusicus</i> , radula.....	48
<b>Figure 37.</b> <i>Chryseofusus graciliformis</i> , shell.....	50
<b>Figure 38.</b> <i>Chryseofusus graciliformis</i> , radula.....	50
<b>Figure 39.</b> <i>Fusinus brasiliensis</i> , shell and operculum.....	51
<b>Figure 40.</b> <i>Fusinus brasiliensis</i> , radula.....	51
<b>Figure 41.</b> <i>Fusinus marmoratus</i> , shell and operculum.....	52
<b>Figure 42.</b> <i>Fusinus marmoratus</i> , radula.....	53
<b>Figure 43.</b> <i>Fusinus</i> sp., shell.....	54
<b>Figure 44.</b> <i>Fusinus</i> sp., radula.....	54
<b>Figure 45.</b> <i>Fusinus frenguelli</i> , shell.....	56
<b>Figure 46.</b> <i>Fusinus frenguelli</i> , radula.....	56
<b>Figure 47.</b> <i>Fusinus australis</i> , shell.....	57
<b>Figure 48.</b> <i>Fusinus australis</i> , radula.....	57
<b>Figure 49.</b> <i>Cyrtulus serotinus</i> , shell in growth series.....	58
<b>Figure 50.</b> <i>Cyrtulus serotinus</i> , radula.....	58
<b>Figure 51.</b> <i>Granulifusus</i> sp. shell.....	60
<b>Figure 52.</b> <i>Granulifusus</i> sp. radula.....	60
<b>Figure 53.</b> <i>Granulifusus hayashi</i> , shell.....	61
<b>Figure 54.</b> <i>Granulifusus hayashi</i> , radula.....	61
<b>Figure 55.</b> <i>Granulifusus kiranus</i> , shell.....	62



<b>Figure 56.</b> <i>Granulifusus kiranus</i> , radula.....	62
<b>Figure 57.</b> <i>Pseudolatirus discrepans</i> , shell.....	64
<b>Figure 58.</b> <i>Pseudolatirus discrepans</i> , radula.....	64
<b>Figure 59.</b> <i>Fusolatirus bruijnii</i> . shell and operculum.....	66
<b>Figure 60.</b> <i>Fusolatirus bruijnii</i> , radula.....	66
<b>Figure 61.</b> <i>Peristernia nassatula</i> , shell and operculum.....	67
<b>Figure 62.</b> <i>Peristernia nassatula</i> , radula.....	67
<b>Figure 63.</b> <i>Peristernia marquesana</i> , shell.....	68
<b>Figure 64.</b> <i>Peristernia marquesana</i> , radula.....	68
<b>Figure 65.</b> <i>Nodolatirus nodatus</i> , shell.....	70
<b>Figure 66.</b> <i>Nodolatirus nodatus</i> , radula.....	70
<b>Figure 67.</b> <i>Latirus vischii</i> , shell.....	70
<b>Figure 68.</b> <i>Latirus vischii</i> , radula.....	70
<b>Figure 69.</b> <i>Fasciolaria tulipa</i> , shell and operculum.....	72
<b>Figure 70.</b> <i>Fasciolaria tulipa</i> , radula.....	72
<b>Figure 71.</b> <i>Aurantilaria aurantiaca</i> , shell and operculum.....	74
<b>Figure 72.</b> <i>Aurantilaria aurantiaca</i> , radula.....	75
<b>Figure 73.</b> <i>Filifusus filamentosus</i> . shell and operculum.....	76
<b>Figure 74.</b> <i>Filifusus filamentosus</i> , radula.....	76
<b>Figure 75.</b> <i>Australaria australasia</i> , shell.....	77
<b>Figure 76.</b> <i>Australaria australasia</i> , radula.....	77
<b>Figure 77.</b> <i>Pleuroploca trapezium</i> , shell.....	78
<b>Figure 78.</b> <i>Pleuroploca trapezium</i> , radula.....	78
<b>Figure 79.</b> <i>Hemipolygona armata</i> , shell.....	79
<b>Figure 80.</b> <i>Hemipolygona armata</i> , radula.....	79
<b>Figure 81.</b> <i>Pustulatirus mediamericanus</i> , shell.....	80
<b>Figure 82.</b> <i>Pustulatirus ogum</i> , shell and operculum.....	81
<b>Figure 83.</b> <i>Pustulatirus ogum</i> , radula.....	81
<b>Figure 84.</b> <i>Polygona angulata</i> , shell and operculum.....	82
<b>Figure 85.</b> <i>Polygona angulata</i> , radula.....	83
<b>Figure 86.</b> <i>Latirus polygonus</i> , shell.....	84

<b>Figure 87.</b> <i>Polygona infundibulum</i> , shell.....	85
<b>Figure 88.</b> <i>Polygona infundibulum</i> , radula.....	85
<b>Figure 89.</b> <i>Hemipolygona beckyae</i> , shell and operculum.....	86
<b>Figure 90.</b> <i>Hemipolygona beckyae</i> , radula.....	86
<b>Figure 91.</b> <i>Latirus pictus</i> , shell.....	88
<b>Figure 92.</b> <i>Latirus pictus</i> , radula.....	88
<b>Figure 93.</b> <i>Leucozonia ocellata</i> , shell and operculum.....	89
<b>Figure 94.</b> <i>Leucozonia ocellata</i> , radula.....	89
<b>Figure 95.</b> <i>Leucozonia cerata</i> , shell.....	90
<b>Figure 96.</b> <i>Leucozonia cerata</i> , radula.....	90
<b>Figure 97.</b> <i>Opeatostoma pseudodon</i> , shell and operculum.....	92
<b>Figure 98.</b> <i>Opeatostoma pseudodon</i> , radula.....	92
<b>Figure 99.</b> <i>Leucozonia nassa nassa</i> , shell.....	93
<b>Figure 100.</b> <i>Leucozonia nassa cingulifera</i> , shell.....	94
<b>Figure 101.</b> <i>Leucozonia nassa brasiliiana</i> , shell.....	95
<b>Figure 102.</b> <i>Leucozonia nassa brasiliiana</i> , radula.....	95
<b>Figure 103.</b> <i>Leucozonia ponderosa</i> , shell and operculum.....	96
<b>Figure 104.</b> <i>Leucozonia ponderosa</i> , radula.....	96
<b>Figure 105.</b> Strict consensus of the obtained trees from Ponder & Lindberg (1997).....	99
<b>Figure 106.</b> Strict consensus tree of the analysis of Caenogastropoda based on morphological characters of Strong (2003).....	100
<b>Figure 107.</b> Strict consensus tree of the Caenogastropoda analysis of Simone (2011).....	101
<b>Figure A.</b> Shell in apertural and abapertural view. A1-2. <i>Monetaria annulus</i> (modified from Simone, 2004); A3. <i>Opeatostoma pseudodon</i> ; 4A. <i>Fusinus frenguelli</i> .....	142
<b>Figure B.</b> Shell in apertural view. B1. <i>Aurantilaria aurantiaca</i> ; B2. <i>Amiantofusus candoris</i> ; B3. <i>Pseudolatirus</i> sp.....	143
<b>Figure C.</b> Shell in apertural view. C1. <i>Dolicholatirus</i> sp.; C2. <i>Chryseofusus graciliformis</i> ; C3. <i>Aurantilaria aurantiaca</i> .....	143
<b>Figure D.</b> Shell in apertural view and detail of aperture. D1. <i>Pisania pusio</i> ; D2-3. <i>Angulofusus nedae</i> (modified from Fedosov & Kantor, 2012).....	144

<b>Figure E.</b> Shell in apertural and lateral view. E1. <i>Latirus vischii</i> ; E2-3. <i>Leucozonia nassa cingulifera</i> ; E4-5. <i>Opeatostoma pseudodon</i> .....	145
<b>Figure F.</b> Shell, lateral view. F1. <i>Pisania pusio</i> ; F2. <i>Hemipolygona beckyae</i> .....	146
<b>Figure G.</b> Apertural view of shell. G1. <i>Pseudolatirus discrepans</i> ; G2. <i>Pleuroploca trapezium</i> ; G3. <i>Leucozonia nassa</i> .....	146
<b>Figure H.</b> Apertural view of shell. H1. <i>Granulifusus</i> sp.; H2. <i>Filifusus filamentosus</i> .....	147
<b>Figure I.</b> Shell in apertural view. I1. <i>Buccinum undatum</i> ; I2. <i>Leucozonia ocellata</i> ; I3. <i>Fusinus brasiliensis</i> .....	148
<b>Figure J.</b> Shell in apertural view 1J. <i>Pseudolatirus pallidus</i> ; 2J. <i>Fusolatirus bruijnii</i> .....	148
<b>Figure K.</b> Live specimens with body extended. K1. <i>Buccinum undatum</i> , (0); K2. <i>Fusinus brasiliensis</i> ; K3. <i>Aurantiaca aurantiaca</i> ; K4. <i>Leucozonia nassa brasiliensis</i> .....	149
<b>Figure L.</b> Head in ventral view. L1. <i>Buccinum undatum</i> ; L2. <i>Polygona angulata</i> .....	150
<b>Figure M.</b> Head in ventral view. M1. <i>Pseudolatirus pallidus</i> ; M2. <i>Fusinus brasiliensis</i> ; M3. <i>Granulifusus</i> sp.....	150
<b>Figure N.</b> <i>Bullia laevissima</i> (modified from Abbate & Simone, 2016).....	152
<b>Figure O.</b> Shell in apertural view. O1. <i>Granulifusus kiranus</i> ; O2. <i>Latirus polygonus</i> .....	152
<b>Figure P.</b> Operculum in dorsal view. P1. <i>Granulifusus poppei</i> (modified from Preetha <i>et al.</i> , 2014); P2. <i>Fusinus frenguelli</i> .....	153
<b>Figure Q.</b> Operculum in ventral view. Q1. <i>Buccinum undatum</i> ; Q2. <i>Fusinus marmoratus</i> ; Q3. <i>Peristernia nassatula</i> .....	153
<b>Figure R.</b> head-foot and visceral mass. R1. <i>Buccinum undatum</i> (1); R2. <i>Pisania pusio</i> .....	154
<b>Figure S.</b> Ventral view of the roof of the pallial cavity evidencing the osphradium. 1S. <i>Dolicholatirus cayohuesonicus</i> ; 2S. <i>Fusinus frenguelli</i> ; 3S. <i>Amiantofusus candoris</i> .....	155
<b>Figure T.</b> Ventral view of osphradium and transversal section of the roof of the pallial cavity, evidencing the osphradium. T1-2. <i>Aurantilaria aurantiaca</i> ; T3-4. <i>Opeatostoma pseudodon</i> .....	156
<b>Figure U.</b> Transversal section of the roof of the pallial cavity in the osphradium region. U1. <i>Dolicholatirus cayohuesonicus</i> ; U2. <i>Fusinus australis</i> .....	156
<b>Figure V.</b> Transversal section of the roof of the pallial cavity in the osphradium and ctenidium region. V1. <i>Opeatostoma pseudodon</i> ; V2. <i>Granulifusus</i> sp.....	157

<b>Figure W.</b> Roof of the pallial cavity in the osphradium and ctenidium region. W1. <i>Peristernia nassatula</i> ; W2. <i>Dolicholatirus</i> sp.; W3. <i>Buccinum undatum</i> .....	158
<b>Figure X.</b> Siphon X1. <i>Granulifusus</i> sp.; X2. <i>Leucozonia cerata</i> .....	159
<b>Figure Y.</b> Siphon. Y1. <i>Amiantofusus candoris</i> ; Y2. <i>Fusinus marmoratus</i> .....	159
<b>Figure Z.</b> Kidney and pericardium. 1Z. <i>Polygona angulata</i> ; 2Z. <i>Granulifusus</i> sp.....	161
<b>Figure AA.</b> Kidney and pericardium. 1AA. <i>Pustulatirus ogum</i> ; AA2. <i>Aurantilaria aurantiaca</i> .....	162
<b>Figure AB.</b> Head in ventral view. AB1. <i>Granulifusus kiranus</i> ; AB2. <i>Leucozonia cerata</i> ; AB3. <i>Hemipolygona beckyae</i> .....	163
<b>Figure AC.</b> Head in ventral view. 1AC. <i>Granulifusus</i> sp.; 2AC. <i>Dolicholatirus cayohuesonicus</i> .....	163
<b>Figure AD.</b> Proboscis opened laterally. AD1. <i>Polygona angulata</i> ; AD2. <i>Thais speciosa</i> .....	164
<b>Figure AE.</b> Proboscis opened laterally AE1. <i>Thais speciosa</i> ; AE2. <i>Granulifusus</i> sp.; AE3. <i>Fusinus brasiliensis</i> .....	165
<b>Figure AF.</b> Ventral view of odontophore cartilages and associated muscles AF1. <i>Thais speciosa</i> ; AF2. <i>Chryseofusus archeruisius</i> ; AF3. <i>Fusinus brasiliensis</i> .....	166
<b>Figure AG.</b> Odontophore in ventral view. AG1. <i>Pustulatirus ogum</i> ; AG2. <i>Fusinus</i> sp.....	167
<b>Figure AH.</b> Radula. HA1. <i>Monetaria annulus</i> (modified from Simone, 2004); AH2. <i>Fusinus australis</i> .....	168
<b>Figure AI.</b> Radula, detail of rachidian. AI1. <i>Fusinus frenguelli</i> ; AI2. <i>Pseudolatirus kuroseanus</i> .....	169
<b>Figure AJ.</b> Radula. AJ1. <i>Latirus pictus</i> ; AJ2. <i>Fusolatirus bruijnii</i> ; AJ3. <i>Cyrtulus serotinus</i> .....	169
<b>Figure AK.</b> Radula detail of rachidian. AK1. <i>Latirus</i> sp.; AK2. <i>Pugilina tupiniquim</i> , (modified from Abbate & Simone, 2015); AK3. <i>Nodolatirus nodatus</i> ; AK4. <i>Pustulatirus ogum</i> ; AK5. <i>Buccinum undatum</i> .....	170
<b>Figure AL.</b> Radula, detail of rachidian. AL1. <i>Aurantilaria aurantiaca</i> ; AL2. <i>Pustulatirus pallidus</i> .....	171
<b>Figure AM.</b> Radula. AM1. <i>Dolicholatirus cayohuesonicus</i> ; AM2. <i>Pisania pusio</i> ; AM3. <i>Leucozonia nassa</i> ; AM4. <i>Latirus vischii</i> .....	172

<b>Figure AN.</b> Radula. AN1. <i>Dolicholatirus cayohuesonicus</i> ; AN2. <i>Buccinum undatum</i> ; AN3. <i>Amiantofusus candoris</i> ; AN4. <i>Chryseofusus graciliformis</i> ; AN5. <i>Peristernia marquesana</i> .....	173
<b>Figure AO.</b> Radula. AO1. <i>Hemipolygona armata</i> ; AO2. <i>Dolicholatirus cayohuesonicus</i> .....	174
<b>Figure AP.</b> Radula, detail of lateral. AP1. <i>Fusolatirus bruijnii</i> ; AP2. <i>Latirus pictus</i> .....	175
<b>Figure AQ.</b> Radula. AQ1. <i>Dolicholatirus cayohuesonicus</i> ; AQ2. <i>Amiantofusus pacificus</i> ; AQ3. <i>Hemipolygona armata</i> ; AQ4. <i>Pleuroploca trapezium</i> .....	175
<b>Figure AR.</b> Radula. AR1. <i>Amiantofusus candoris</i> ; AR2. <i>Polygona angulata</i> .....	176
<b>Figure AS.</b> Radula, detail of lateral. AS1. <i>Pisania pusio</i> ; AS2. <i>Pseudolatirus discrepans</i> ; AS3. <i>Filifusus filamentosus</i> ; AS4. <i>Leucozonia ocellata</i> .....	177
<b>Figure AT.</b> Radula. AT1. <i>Cyrtulus serotinus</i> ; AT2. <i>Pseudolatirus discrepans</i> .....	178
<b>Figure AU.</b> Radula. AU1. <i>Peristernia nassatula</i> ; AU2. <i>Leucozonia ponderosa</i> .....	179
<b>Figure AV.</b> Proboscis. AV1. <i>Granulifusus</i> sp.; AV2. <i>Fusinus frenguelli</i> .....	180
<b>Figure AW.</b> Proboscis. AW1. <i>Pisania pusio</i> ; AW2. <i>Pustulatirus ogum</i> ; AW3. <i>Fusinus marmoratus</i> .....	182
<b>Figure AX.</b> Proboscis. AX1. <i>Dolicholatirus cayohuesonicus</i> ; AX2. <i>Fusinus frenguelli</i> .....	183
<b>Figure AY.</b> Mid-esophagus. AY1. <i>Fasciolaria tulipa</i> ; AY2. <i>Fusinus</i> sp.....	184
<b>Figure AZ.</b> Section of the anterior esophagus immediately after valve of Leiblein. AZ1. <i>Buccinum undatum</i> ; AZ2. <i>Polygona infundibulum</i> ; AZ3. <i>Fusinus australis</i> .....	184
<b>Figure BA.</b> Anterior and middle esophagus. BA1. <i>Pugilina tupiniquim</i> (modified from Abbate & Simone, 2015); BA2. <i>Aurantilaria aurantiaca</i> ; BA3. <i>Fusinus frenguelli</i> .....	185
<b>Figure BB.</b> Anterior digestive system. BB1. <i>Teralatirus roboreus</i> (modified from Simone <i>et al.</i> , 2013); BB2. <i>Granulifusus</i> sp.; BB3. <i>Pugilina tupiniquim</i> (modified from Abbate & Simone, 2015).....	188
<b>Figure BC.</b> Visceral mass. BC1. <i>Polygona angulata</i> ; BC2. <i>Aurantilaria aurantiaca</i> .....	189
<b>Figure BD.</b> Stomach in dorsal view and lumen. BD1. <i>Monetaria annulus</i> (modified from Simone, 2011); BD2. <i>Pisania pusio</i> ; BD3. <i>Fasciolaria tulipa</i> .....	190
<b>Figure BE.</b> Roof of the pallial cavity in ventral view. BE1. <i>Opeatostoma pseudodon</i> ; BE2. <i>Amiantofusus candoris</i> .....	192
<b>Figure BF.</b> Pallial oviduct. BF1. <i>Leucozonia ocellata</i> ; BF2. <i>Opeatostoma pseudodon</i> .....	193

<b>Figure BG.</b> Terminal portion of pallial oviduct. BG1. <i>Granulifusus hayashi</i> ; BG2. <i>Polygona angulata</i> .....	194
<b>Figure BH.</b> Longitudinal section of foot and columellar muscle, haemocoel removed. BH1. <i>Pseudolatirus discrepans</i> ; BH2. <i>Filifusus filamentosus</i> ; BH3. <i>Dolicholatirus cayohuesonicus</i> .....	194
<b>Figure BI.</b> Right side of roof of pallial cavity, male. BI1. <i>Latirus vischii</i> ; BI2. <i>Buccinum undatum</i> .....	196
<b>Figure BJ.</b> Penis and adjacent head-foot in dorsal view. BJ1. <i>Pustulatirus ogum</i> ; BJ2. <i>Pseudolatirus pallidus</i> ; BJ3. <i>Dolicholatirus cayohuesonicus</i> .....	196
<b>Figure BK.</b> Penis. BK1. <i>Leucozonia ocellata</i> ; BK2. <i>Dolicholatirus cayohuesonicus</i> ; BK3. <i>Pisania pusio</i> .....	198
<b>Figure BL.</b> Penis and section of tegument. BL1. <i>Fusinus frenguelli</i> ; BL2. <i>Opeatostoma pseudodon</i> .....	198
<b>Figure BM.</b> Nerve ring in dorsal view. BM1. <i>Fusinus</i> sp.; BM2. <i>Filifusus filamentosus</i> .....	199
<b>Figure BN.</b> Nerve ring in dorsal view. BN1. <i>Buccinum undatum</i> ; BN2. <i>Hemipolygona beckyae</i> .....	200
<b>Figure BO.</b> Nerve ring in dorsal view. BO1. <i>Leucozonia ponderosa</i> ; BO2. <i>Pustulatirus ogum</i> .....	201
<b>Figure BP.</b> Nerve ring in dorsal view. BP1. <i>Granulifusus</i> sp.; BP2. <i>Filifusus filamentosus</i> .....	201
<b>Figure BQ.</b> Nerve ring. <b>BQ1.</b> <i>Teralatirus roboreus</i> (modified from Simone <i>et al.</i> , 2013); <b>BQ2.</b> <i>Polygona angulata</i> .....	203

---

## Chapter II

---

<b>Figure 1.</b> Phylogenetic relationships based on a parsimonious analysis done in POY under parameter 3221.....	232
<b>Figure 2.</b> Phylogenetic relationships (part one) based on a parsimonious analysis done in POY under parameter 322. Navajo rugs indicate support for the given parameter.....	233
<b>Figure 3.</b> Phylogenetic relationships (part one) based on a parsimonious analysis done in POY under parameter 3221. Navajo rugs indicate support for the given parameter.....	234
<b>Figure 4.</b> Phylogenetic relationships (part two) based on a parsimonious analysis done in POY under parameter 3221. Navajo rugs indicate support for the given parameter.....	235

**Figure 5.** Phylogenetic relationships (part three) based on a parsimonious analysis done in POY under parameter 3221. Navajo rugs indicate support for the given parameter.....236

**Figure 6.** Phylogenetic relationships (part four) based on a parsimonious analysis done in POY under parameter 3221. Navajo rugs indicate support for the given parameter.....237

**Figure 7.** Phylogenetic relationships of Fasciolariidae for the total evidence analysis as implemented in POY under parameter 3221.....238

**Chapter III**

---

**Figure 1.** Phylogenetic tree obtained through parsimonious analysis in TnT using prior, unweighted characters.....251

**Figure 2A.** Phylogenetic tree of the included taxa.....252

**Figure 2B.** Phylogenetic tree of the included taxa.....253

**LIST OF TABLES**

**Chapter I**

---

**Table 1.** Species used for the morphological analysis, with voucher numbers, species count and locality.....11

**Chapter II**

---

**Table 1.** Number of taxa and fragments analyzed for each coding or non-coding loci.....228

**Table 2.** Taxa used for morphological (chapter I) and molecular analyses.....229



## CONTENTS

<b>Chapter I</b>	<b>1</b>
<b>1. Introduction</b>	<b>2</b>
<b>2. Objectives</b>	<b>9</b>
<b>3. Material and Methods</b>	<b>10</b>
<b>3.1 Taxon sampling</b>	<b>10</b>
<b>3.2 Morphological data</b>	<b>14</b>
<b>3.3 Phylogenetic analysis</b>	<b>16</b>
<b>4. Results</b>	<b>18</b>
<b>5. Phylogenetic descriptions</b>	<b>27</b>
<b>6. Phylogenetic discussion</b>	<b>98</b>
<b>7. Character discussion</b>	<b>142</b>
<b>7.1 Character matrix</b>	<b>205</b>
<b>8. References</b>	<b>209</b>
<b>Chapter II</b>	<b>225</b>
<b>1. Introduction</b>	<b>226</b>
<b>2. Objectives</b>	<b>226</b>
<b>3. Material and Methods</b>	<b>227</b>
<b>3.1 Parsimony analyses – molecular data</b>	<b>227</b>
<b>3.2 Parsimony analyses – total evidence data</b>	<b>228</b>
<b>4. Results</b>	<b>230</b>
<b>5. Discussion</b>	<b>239</b>
<b>5.1 Outgroup species</b>	<b>239</b>
<b>5.2 Dolicholatirus and Teralatirus clade</b>	<b>239</b>
<b>5.3 Fusinus colus clade</b>	<b>240</b>
<b>5.4 Peristernia nassatula clade</b>	<b>240</b>
<b>5.5 Fasciolaria tulipa clade</b>	<b>240</b>
<b>6. Conclusions</b>	<b>242</b>
<b>7. References</b>	<b>243</b>

<b>Chapter III</b>	247
<b>1. Introduction</b>	248
<b>2. Objectives</b>	249
<b>3. Material and Methods</b>	249
<b>4. Results</b>	249
<b>5. Discussion</b>	254
<b>5.1 Character matrix</b>	256
<b>6. References</b>	273
<b>Appendix</b>	274

## CHAPTER I

---

# **Phylogenetic analysis of Fasciolaridae based on comparative morphology (Gastropoda: Buccinoidea)**

## 1. Introduction

The phylum Mollusca, is one of the most important invertebrate group, second-most important according to species richness (topped only by the arthropods), with circa 130,000 extant species (WoRMS, 2016). Mollusks are extremely diverse biologically, not just in size and in anatomical structure, but also in behavior and in habitat, with great success in colonizing marine, terrestrial and freshwater environments. Gastropoda, the main class of the phylum and contributing to about 70% of the species, has achieved great success, particularly in marine environment. Gastropods are the main representatives in regards to biomass, ecological diversity and biogeographical patterns. They explore habitats from mangroves to hydrothermal vents to rocky coastal mesolittoral zone, have pelagic to epifaunal to infaunal lifestyles, occupying most ecological niches (Bronwen *et al.*, 1998).

Despite the importance of the group, mollusks are likely sub-represented in areas with little or no collective and taxonomic effort, especially for deep-water species. In Brazil for example, only 1,776 taxa, including species and subspecies, occur according to Rios (2009), surely a portion of the real number. Trawling of economically important areas have only now been endeavored, as done by the REVIZEE program (Absalão *et al.*, 2006) and this will most certainly increase the number of species reported for Brazilian waters.

The order Neogastropoda comprises the most diverse caenogastropod mollusk clade, and is currently divided in the superfamilies: Buccinoidea, Cancellarioidea, Conoidea, Muricoidea, Olivoidea and Pseudolivoidea (Bouchet & Rocroi, 2005).

The monophyly of Neogastropoda is supported by recent morphology-based phylogenetic analyses (*e.g.*, Ponder & Lindberg, 1997; Strong, 2003; Simone, 2011). Ponder & Lindberg (1997) analyzed 117 characters in 40 taxa of mainly prosobranch gastropods, and found that the Neogastropoda, included within the prosobranchs, are monophyletic; Caenogastropoda, a more inclusive group that encompasses neogastropods, mesogastropods and other small lineages, was also recovered monophyletic. Strong (2003) inferred the monophyly of Neogastropoda and Caenogastropoda utilizing 64 characters (mainly midgut) in 18 taxa, as well as establishing character homologies. The extensive Caenogastropoda phylogeny of Simone (2011) once again recovered a monophyletic Neogastropoda; this study sampled 676 characters in 305 species. All

the above cited studies point to a well-supported Neogastropoda with several unambiguous synapomorphies corroborating it.

A Bayesian inference analysis of a combined morphological and molecular data was done by Ponder *et al.* (2008) with data from Colgan *et al.* (2007) and compiled morphological characters from the literature. Neogastropods appeared highly supported within a more inclusive ‘siphonated’ clade.

Several are the neogastropod synapomorphies that have been phylogenetically tested by Ponder & Lindberg (1997) and Strong (2003): the presence of a pair of accessory salivary glands, a valve of Leiblein and an anal or rectal gland (the homology of the latter one was disputed by Kantor & Fedosov, 2009). Based on these generally accepted morphological synapomorphies, Simone (2011) added: the pair of retractor muscles of the buccal mass passing through the nerve ring, the loss of jaws, the ducts of salivary glands free from the nerve ring and a high concentration of the ganglia, although this author retracted the synapomorphy of the valve of Leiblein to Muricoidea only. Ponder *et al.* (2008) stated that Neogastropoda tend to have higher chromosome numbers and larger cellular DNA content than other gastropods.

Most other analyses based solely in molecular data were not able to recover a monophyletic Neogastropoda (Harasewych *et al.*, 1997; Colgan *et al.*, 2000, 2003, 2007). Harasewych *et al.* (1997) based its molecular results in a two gene analysis of 18S rRNA and cytochrome *c* oxidase subunit I (COI), and, although Caenogastropoda (including Neogastropoda and architaenioglossates) and heterobranchs were recovered, they were incapable of resolving relationships among neogastropod families, or between Neogastropoda and other higher Caenogastropoda.

Colgan *et al.* (2000) sampled partial 28S rRNA and Histone H3 and failed to recover a monophyletic Neogastropoda due to the low support of its branches. Colgan *et al.* (2003) used these same gene fragments plus 18S rRNA, COI and small nuclear U2 RNA (*snU2* RNA) to infer the relationships of gastropods; neogastropod taxa appeared as several lineages in caenogastropods (also non-monophyletic), and also not well supported. Finally, Colgan *et al.* (2007) collected data from partial 18S rRNA, 28S rRNA, 12S rRNA, COI, histone H3 and elongation factor 1 $\alpha$ ; despite a monophyletic Caenogastropoda, Neogastropoda was contradicted by their analyses.

In their complete mitochondrial genome, Cunha *et al.* (2009) revisited the Neogastropoda concept with the inclusion of littoriniomorph lineages within the group. In another mitochondrial genome phylogeny, plus three nuclear genes, Osca *et al.* (2015), proposed the inclusion of Tonnoidea, or the exclusion of cancellarioids and possibly volutids from Neogastropoda; in the first case tonnoideans would have secondarily lost the traditional neogastropod synapomorphies, while in the latter these synapomorphies would be considered homoplastic, in this sense agreeing with Kantor and Fedosov (2009). Both of these studies prove the need to further increase gene sampling, as both mitochondrial genomes (circa 15-16k bp) were unable to achieve conclusive results regarding phylogenetic relationships within Neogastropoda, nevertheless, the rapid radiation at the Neogastropoda origin may not allow a fully resolution based only on such data. Another possible solution to these outcomes would be to include morphological data in these analyses.

Not all molecular-based analyses contest the monophyly of neogastropods. Zou *et al.* (2011), using data collected from entire nuclear 18S rRNA, histone H3, and three partial mitochondrial genes (COI, 16S rRNA and 12S rRNA) were able to recover a monophyletic Neogastropoda. In their analyses, all neogastropod families were strongly supported except for the buccinids, turrids and cancellariids.

Despite these mentioned controversies, Neogastropoda has maintained its monophyletic status ('Archaeogastropoda' and 'Mesogastropoda' from Thiele [1925] proved to be artificial groups) until definitive conclusions prove otherwise (Bouchet & Rocroi, 2005; WoRMS, 2016).

Within the Neogastropoda scheme, the superfamily Buccinoidea is considered highly derived due to several losses of typical neogastropod synapomorphies: mainly the accessory salivary glands and the rectal gland. The superfamily typically includes the families Buccinidae, Belomitridae, Busyconidae, Colubrariidae, Columbelloidea, Nassariidae, Melongenidae and Fasciolaridae (Bouchet & Rocroi, 2005; WoRMS, 2016).

There is usually consensus among researchers that the superfamily is monophyletic and a crown group of Neogastropoda (*e.g.*, Oliverio & Modica, 2010; Fedosov *et al.*, 2015). In the work of Simone (2011), the families included in Buccinoidea are present in the more inclusive clade Muricoidea.

Oliverio & Modica (2010) included the first molecular analysis of Neogastropoda based on more than 50% of the recognized families. On their molecular dataset analyzing neogastropod

families (28S rRNA, 16S rRNA, 12S rRNA and COI), Buccinoidea resulted in a monophyletic clade, with cancellariids the first offspring of the Neogastropoda (Rachiglossate) and the toxoglossate conoideans the sister group to it. On their second dataset (16S rRNA) that analyzed a more inclusive buccinoid ingroup, all families sampled except buccinids were recovered as monophyletic.

Fedosov *et al.* (2015) sequenced COI, 16S rRNA, 12S rRNA and Histone H3 for over 90 species in 20 genera and this molecular data set was supplemented by studies of radula morphology. Their results (which focused on mitriform gastropods) confirmed the monophyly of the neogastropod superfamilies Buccinoidea and Conoidea.

Phylogenetic studies are more common among more inclusive groups, especially those that have had a troubled taxonomic history, *e.g.*, Buccinidae. WoRMS (2016) cites the family as accepted taxonomically; however, several works have refuted this hypothesis. Hayashi (2005) based its phylogeny on complete 16S rRNA sequences for buccinid species, and due to the intercalation by nassariid and fascioliid species, the family was evidenced as polyphyletic. Kosyan *et al.* (2009) studied the phylogeny of buccinid species through a 16S rRNA dataset, partially from the sequences of Hayashi (2005), and the family was also reported as non-monophyletic.

Kantor *et al.* (2013) endeavored in a phylogeny of deep-water buccinids based on COI, 12S rRNA and 28S rRNA genes, revealing that these taxa are closely related to taxa from vents. Although this study did not shed any lights into a more inclusive Buccinoidea, it shows a monophyletic Buccinidae family, despite a desired more extensive taxon sampling.

Galindo *et al.* (2016), through a five-gene phylogeny (COI, 16S rRNA, 12S rRNA, 28S rRNA and Histone H3) of 218 putative nassariid species, proved the monophyly of the family if one includes traditional buccinid species (*e.g.*, *Engoniophos* Woodring, 1928, *Nassaria* Link, 1807). Their result confirmed the monophyletic families within Buccinoidea, with the exception of Buccinidae. Abbate (2016) has since confirmed the inclusion of the genus *Engoniophos* in Nassariidae.

The buccinoid family Fascioliidae comprehends species that form a diverse element of the molluscan predatory fauna in shallow to deep coastal waters, especially on soft bottoms. With 540 extant species in 51 genera worldwide (WoRMS, 2016), fascioliids are gonochoristic with internal fertilization and, usually, direct development (Leal, 1991), meaning that their distribution

is more-or-less restricted to isolated geographical areas. They inhabit depths of up to 1900m (Callomon & Snyder, 2009) where they prey on polychaetes, sipunculans, bivalves and other gastropods (Rosenberg, 1992; Taylor & Lewis, 1995).

Couto *et al.* (2016), in a study also related to this one, sampled 116 fascioliid taxa and 17 outgroup species for its five-gene (COI, 18S rRNA, 28S rRNA, 16S rRNA and Histone H3) molecular phylogeny. These authors based their result on a maximum likelihood and a Bayesian inference analyses. All fascioliids except *Dolicholattirus* Bellardi, 1884 and *Teralattirus* Coomans, 1965 were recovered within three subfamilies: Fusiniinae, Peristerniinae and Fascioliinae; although with an extensively revised inclusion of species and genera. The subfamily Fusiniinae, includes the spindles (*e.g.*, *Fusus* Rafinesque, 1815, *Chryseofusus* Hadorn & Fraussen, 2003 and related genera) including the genus *Pseudolattirus* Bellardi, 1884; Peristerniinae includes the genera *Peristernia* Mörch, 1852 and *Fusolattirus* Kuroda & Habe, 1971; finally, Fascioliinae includes the bulk of peristerniines *sensu lato* (*e.g.*, *Lattirus* Montfort, 1810, *Polygona* Schumacher, 1817) and fascioliines, with the conspicuous and well-known tulips and horse-conchs (the only traditional clade that maintained its monophyly). The genera *Teralattirus* and *Dolicholattirus* formed a separate group from the remaining fascioliids, although its position remains uncertain, as the statistic tests made were not able to correctly access its position.

The analysis of Couto *et al.* (2016) is so far the only extensive phylogenetic study of the family, since past works which included some fascioliid taxa did not have the internal resolution to solve most internal clades (Hayashi, 2005; Kosyan *et al.*, 2009; Zou *et al.*, 2011). Other works in which fascioliid taxa were present it was usually not possible to infer any phylogenetic position because of scarce taxon sampling and they lack the resolution and coverage to clarify its relationships or to test its monophyly, as the family was thought to potentially comprise multiple paraphyletic groups (Fedosov & Kantor, 2012), until the work of Couto *et al.* (2016) which clarified the relationships among major fascioliid lineages.

Despite sub-familiar names being conserved in the current taxonomy of the family, Fusiniinae, Peristerniinae and Fascioliinae have had a complicated history. For a long time, the name '*Fusus*' has been used indiscriminately for numerous Cretaceous, Cenozoic and Recent spindle-shaped shells (Snyder, 2003), and likewise *Lattirus*, *Fasciolaria* Lamarck, 1799 and *Pleuroploca* Fischer, 1884 were also used for evidently heterogeneous assemblages. More



recently, however, the group has undergone extensive taxonomical revision (*e.g.*, Vermeij & Snyder, 2002: *Leucozonia* Gray, 1847; Vermeij & Snyder, 2006: *Latirus* and related genera; Snyder *et al.*, 2012: fascioliariines; Lyons & Snyder, 2013: *Pustulatirus* Vermeij & Snyder, 2006), elevating several subgenera to genus rank and establishing new ones. Of noteworthy reference is the genus *Dolicholatirus* that has had a confusing history in which its taxonomic position within Fascioliariidae is ambiguous, although currently generally accepted (*e.g.*, Snyder, 2003; WoRMS, 2016), an issue unresolved by the analyses of Couto *et al.* (2016).

Fascioliariidae, Melongenidae, Cancellariidae and Buccinidae date back to the early Cretaceous (Valanginian, ~140 Mya) (Benton, 1993), whereas other neogastropod families appeared between the late Cretaceous to early Paleogene, suggesting that the former families represent the first offshoots of Neogastropoda (Hayashi, 2005). While Fascioliariinae appeared during the Albian (Bandel, 1993), the fossil record indicates that the family – especially Fascioliariinae and Peristerniinae (Vermeij & Snyder, 2006) – diversified extensively during the early Neogene (Aquitainian, 24 Mya). This rapid speciation endeavored by the group is evidenced by the many short branches of molecular analysis, because if speciation events are closely spaced in time, the amount of phylogenetic signal is often small, leading to short internal tree branches that are difficult to resolve (Philippe *et al.*, 2011) such as those in Couto *et al.* (2016).

Like most gastropods, fascioliariids have a taxonomy based mostly on the shell and radula (*e.g.*, Tryon, 1880; Thiele, 1929-1935; Vermeij & Snyder, 2002; 2006), likewise, taxonomic and phylogenetic approaches based on soft-part anatomy are scarce. Even in the context of the superfamily, the anatomical framework of the buccinoideans is especially scant, for they are considered highly advanced Neogastropoda (Kantor, 1996), lacking accessory salivary glands, anal glands and ingesting gland in the oviduct (Harasewych 1998). Typical for fascioliariids is the orange-red color of the foot and head-foot mass. Fraussen *et al.* (2007) reported that a combination of traits is diagnostic for Fascioliariidae: multicuspidate lateral teeth and narrow rachidian teeth, proboscis retractor muscle as a single or paired tuft of fibers, ducts of the salivary glands immersed in the esophagus wall, and a stomach without a posterior caecum. Furthermore, Kosyan *et al.* (2009) studied the anatomy of fascioliariids based in eight species and seven genera arranged in all subfamilies. These authors distinguished fascioliariids from buccinids studied by them and by Kosyan & Kantor (2009) based on stomach and proboscis retractor muscle characters, as appointed by Fraussen *et al.* (2007).

The work of Simone (2011) is based on thorough anatomical analysis of caenogastropods, which was stemmed on several previous publications that were employed in his phylogeny of the subclass (*e.g.*, Simone, 2004; Bieler & Simone, 2005; Simone *et al.*, 2009). Such detailed morphological studies are scarce. Kosyan *et al.* (2009) studied the anatomy of eight fascioliids: *Turrilatirus turritus* (Gmelin, 1791), *Pustulatirus mediamericus* (Hertlein & Strong, 1951), *Latirus polygonus* (Gmelin, 1791), *Peristernia nassatula* (Lamarck, 1822), *Peristernia ustulata* (Reeve, 1847), *Opeatostoma pseudodon* (Burrow, 1815), *Fusinus tenerifensis* Hadorn & Rolán, 1999 and *Tarantinae lignaria* (Linnaeus, 1758). Marcus & Marcus (1962) made detailed anatomical descriptions of *Leucozonia nassa* (Gmelin, 1791) from Brazil, while Couto & Pimenta (2012) studied the Brazilian *Leucozonia* species: *L. nassa* (Gmelin, 1791), *L. ocellata* (Gmelin, 1791) and *L. ponderosa* Vermeij & Snyder, 1998. Couto *et al.* (2015a) investigated *Pustulatirus ogum* (Petuch, 1979) and *Hemipolygona beckyae* (Snyder, 2000) and Couto *et al.* (2015b) *Fasciolaria tulipa* (Linnaeus, 1758). Finally, Simone *et al.* (2013) described the anatomy of *Teralatirus roboreus* (Reeve, 1845).

Phylogenetic analyses of gastropods based on morphological data have greatly fallen in disuse, as molecular-based multi-gene or even next-generation sequencing (NGS), gains popularity. The work of Ponder & Lindberg (1997), Strong (2003) and Simone (2011) were based solely on anatomical characters. Galindo *et al.* (2016), through an approach based on the reconstruction of the ancestral character, eight characters supposedly informative for taxonomy were coded in the final Nassariidae tree; this approach is relatively common. A phylogenetic approach, though parsimony or otherwise, that takes into consideration the transformation in morphological characters increasingly more infrequent; this is due to homology statements issues, the choice of higher taxa as terminals, and most importantly due to the cheapening of molecular analyses (Shendure & Ji, 2008; McCormack *et al.*, 2013; Giribet, 2015)

The use of morphology has traditionally been employed by phylogeneticists to infer the relationship of major groups since the first evolutionary biologists began to decipher the animal tree of life. The amount of molecular data has increased in a way that is unprecedented when compared to morphological ones (morphological or developmental data [*e.g.*, patterns in egg cleavage, mesoderm formation, segmentation, etc.] are considered morphological characters and are treated as such), and that has enticed researchers into favoring the former over the latter. The

amount of training required for a detailed anatomical study also greatly increases the cost of training morphologists over “molecular zoologists”.

It is essential that morphological characters do not come into disuse for innumerable reasons. Giribet (2015) stressed that a zoologist’s interest is to understand form and function, and how this evolved over its history; hence why morphology should not be left aside. It is pivotal that fossils be incorporated, not just in constraining a node, but as terminals, which proves to me a more realistic way of dating the evolution. Morphological characters prove useful in validating phylogenetic relationships and helps to resolve many internal clades, (*e.g.*, as encountered in other groups such as butterflies by Wahlberg *et al.*, 2005; arthropods by Giribet *et al.*, 2001; Opiliones by Giribet *et al.*, 2002).

Because of the difficulties in delimiting groups in fascioliids especially those distinguished solely on shell features (Vermeij & Snyder, 2006; Lyons & Snyder, 2013), hence prone to issues regarding polymorphisms and convergence, it is essential that a morphology based phylogenetic analysis be implemented. In order to compare the morphological results obtained here with previous studies, the analysis of Couto *et al.* (2016) proves especially useful. The following work is, therefore, a comprehensive extensive phylogenetic study of the family Fascioliidae.

## **2. Objectives**

1. To provide a hypothesis, in hopes to further clarify the phylogeny of the family Fascioliidae, based on a parsimonious analysis of morphological data.

2. To test the monophyly of the Fascioliidae through inclusion of many outgroup.

3. To provide a comprehensive framework in morphological characters for a more inclusive Neogastropoda.

4. In light of the putative phylogeny, propose a tentative taxonomic scheme for the analyzed taxa.

### 3. Material and Methods

#### 3.1 Taxon sampling

Material for this study was obtained from deposited material in the Museum of Zoology, São Paulo University and foreign collections; through loan and/or visit to these institutions. A complete list of examined material is presented in table 1. The foreign institutions, abbreviated throughout the text, with their respective curators: **ANSP** – Academy of Natural Sciences, Drexel University, Philadelphia, PA, USA. Curator: Gary Rosenberg. **CMPHRM** – Federal University of Ceará, Brazil. Curator: Helena Matthews-Cascon. **FMNH** – Florida Museum of Natural History, Gainesville, FL, USA. Curator: Gustav Paulay. **KZN** – KwaZulu-Natal Museum, Pietermaritzburg, South Africa. **MCZ** – Museum of Comparative Zoology, Harvard University, Cambridge, MA, USA. Curator: Gonzalo Giribet. **MNHN** – National Museum of Natural History, University of Sorbonne, Paris, France. Curator: Philippe Bouchet. **MNRJ** – National Museum of Brazil, Federal University of Rio de Janeiro (UFRJ), Rio de Janeiro, RJ, Brazil. Curator: Alexandre Pimenta. **MORG** – Oceanographic Museum "Prof. Eliézer de Carvalho Rios", Federal University of Rio Grande (FURG), Rio Grande do Sul, Brazil. **MZSP** – Museum of Zoology, University of São Paulo (USP), São Paulo, SP, Brazil. Curator: Luiz R. L. Simone. **NHMUK** – National History Museum of London, England, UK. Curator: Andreia Salvador. **SBMNH** – Santa Barbara Museum of Natural History, Santa Barbara, CA, USA. Curator: Daniel Geiger.

In order to obtain a broad taxonomical sample of fasciolariids, 53 specimens in 21 genera were chosen: *Amiantofusus* Fraussen *et al.*, 2007, *Aurantilaria* Snyder *et al.*, 2012, *Australaria* Snyder *et al.*, 2012, *Chryseofusus*, *Cyrtulus* Hinds, 1843, *Dolicholatirus*, *Fasciolaria*, *Filifusus* Snyder *et al.*, 2012, *Fusinus*, *Fusolatirus*, *Granulifusus* Kuroda & Habe, 1954, *Hemipolygona* Rovereto, 1899, *Leucozonia*, *Latirus*, *Nodolatirus* Bouchet & Snyder, 2013, *Peristernia*, *Pleuroploca*, *Polygona*, *Pseudolatirus*, *Pustulatirus* and *Teralatirus*. Data from *Angulofusus neda* Fedosov & Kantor, 2012 and *Teralatirus roboreus* were taken from the literature; table 1 lists the origin of the morphological material, novel or excerpt from the literature.

Outgroup taxa were added in order to confirm the monophyly of Fasciolariidae, in particular, the positioning of *Dolicholatirus* and *Teralatirus*, in which doubt was raised by previous authors (Vermeij & Snyder, 2006; Beu, 2011) and undetermined by Couto *et al.* (2016).

Hence, species comprising of a broad taxonomic spectrum were chosen as outgroups, occurring in the families: Cypraeidae (Cypraeoidea), Rapaninae (Muricoidea), Melongenidae, Nassariidae and Buccinidae (Buccinoidea). In total, eight outgroup species were used.

Couto *et al.* (2016) is the culmination of the work endeavored in the MCZ (Appendix), and although only molecular data as used, it comprehends part of this dissertation. More on molecular data will be discussed on chapter II of the present dissertation. In order to compare the morphological results obtained here, most terminals also occur in Couto *et al.* (2016) providing a useful tool for comparison.

Table 1: Species used for the morphological analysis, with voucher numbers, species count and locality. Morphological data compiled from the literature is indicated after the species name, and highlighted in grey. For full voucher detail refer to Phylogenetic description section, following each species name. **Cy**: Cypraeidae. **Me**: Melongenidae. **Na**: Nassariidae. **Th**: Thaididae. **Bu**: Buccinidae. **Fa**: Fasciolaridae (continues in the next four pages).

	SPECIES	VOUCHER NUMBER	#	LOCALITY
<b>Me</b>	<i>Pugilina tupiniquim</i>	Abbate & Simone (2015)		
<b>Na</b>	<i>Engoniophos unicinctus</i>	Abbate (2016)		
<b>Na</b>	<i>Nassarius reticulatus</i>	Abbate (2016)		
<b>Na</b>	<i>Bullia laevis</i>	Abbate (2016)		
<b>Fa</b>	<i>Dolicholattirus</i> sp.	Couto <i>et al.</i> (2016)		
<b>Fa</b>	<i>Teralattirus roboreus</i>	Simone <i>et al.</i> (2013)		
<b>Fa</b>	<i>Angulofusus nedae</i>	Fedosov & Kantor (2012)		
<b>Th</b>	<i>Thais speciosa</i>	MZSP 67772	2	Ecuador
<b>Th</b>	<i>Thais speciosa</i>	MZSP 95270	1	Ecuador
<b>Bu</b>	<i>Buccinum undatum</i>	MZSP 98217	10	France
<b>Bu</b>	<i>Buccinum undatum</i>	MZSP 58732	1	North Sea
<b>Bu</b>	<i>Pisania pusio</i>	MZSP 105583	18	Brazil, São Paulo state
<b>Bu</b>	<i>Pisania pusio</i>	MZSP 105690	2	Brazil, São Paulo state
<b>Bu</b>	<i>Pisania pusio</i>	MZSP 111471	6	Brazil, Espírito Santo state
<b>Bu</b>	<i>Pisania pusio</i>	MZSP 11290	6	Brazil, Fernando de Noronha Archipelago
<b>Fa</b>	<i>Dolicholattirus</i> aff. <i>Cayohuesonicus</i>	ANSP A8131	2	Cayman Islands
<b>Fa</b>	<i>Dolicholattirus</i> aff. <i>Cayohuesonicus</i>	ANSP 338609/A5642	9	British Virgin Islands
<b>Fa</b>	<i>Dolicholattirus</i> aff. <i>Cayohuesonicus</i>	ANSP A18293	1	Puerto Rico
<b>Fa</b>	<i>Pseudolattirus kuroseanus</i>	MNHN IM-2013-14709	1	Papua New Guinea
<b>Fa</b>	<i>Amiantofusus pacificus</i>	MNHN IM-2013-42508	1	China Sea
<b>Fa</b>	<i>Amiantofusus pacificus</i>	MNHN IM-2013-44179	1	China Sea
<b>Fa</b>	<i>Amiantofusus candoris</i>	MNHN IM-2013-19759	1	Papua New Guinea
<b>Fa</b>	<i>Pseudolattirus pallidus</i>	MNHN IM-2013-19937	1	Papua New Guinea
<b>Fa</b>	<i>Pseudolattirus pallidus</i>	MNHN IM-2007-32537	1	Salomon Islands
<b>Fa</b>	<i>Pseudolattirus pallidus</i>	MNHN IM-2013-19011	1	Papua New Guinea
<b>Fa</b>	<i>Pseudolattirus pallidus</i>	MNHN IM-2007-32913	1	Philippines
<b>Fa</b>	<i>Pseudolattirus pallidus</i>	MNHN IM-2013-44506	1	China Sea
<b>Fa</b>	<i>Pseudolattirus pallidus</i>	MNHN IM-2013-44495	1	China Sea
<b>Fa</b>	<i>Chryseofusus archerius</i>	MNHN IM-2013-44363	1	China Sea

<b>Fa</b>	<i>Chryseofusus archeruisius</i>	MNHN IM-2013-44302	1	China Sea
<b>Fa</b>	<i>Chryseofusus graciliformis</i>	MNHN IM-2007-32797	1	Salomon Islands
<b>Fa</b>	<i>Chryseofusus graciliformis</i>	MNHN IM-2013-19921	1	Salomon Islands
<b>Fa</b>	<i>Chryseofusus graciliformis</i>	MNHN IM-2013-19938	1	Salomon Islands
<b>Fa</b>	<i>Fusinus brasiliensis</i>	MZSP 70512	~80	Brazil, Espírito Santo state
<b>Fa</b>	<i>Fusinus brasiliensis</i>	MNRJ 8660	8	Brazil, Espírito Santo state
<b>Fa</b>	<i>Fusinus brasiliensis</i>	MNRJ 8960	1	Brazil, Rio de Janeiro state
<b>Fa</b>	<i>Fusinus marmoratus</i>	MNRJ 14243	2	Brazil, Rio de Janeiro state
<b>Fa</b>	<i>Fusinus marmoratus</i>	MNRJ 14489	2	Brazil, Rio de Janeiro state
<b>Fa</b>	<i>Fusinus marmoratus</i>	MNRJ 14588	1	Brazil, Rio de Janeiro state
<b>Fa</b>	<i>Fusinus marmoratus</i>	MZSP 77515	3	Brazil, São Paulo state
<b>Fa</b>	<i>Fusinus sp.</i>	MNRJ 6258	1	Brazil, Rio de Janeiro state
<b>Fa</b>	<i>Fusinus sp.</i>	MNRJ 6259	1	Brazil, Rio de Janeiro state
<b>Fa</b>	<i>Fusinus frenguelli</i>	MNRJ 14414	3	Brazil, Rio de Janeiro state
<b>Fa</b>	<i>Fusinus frenguelli</i>	MNRJ 7829	1	Brazil, Rio de Janeiro state
<b>Fa</b>	<i>Fusinus frenguelli</i>	MNRJ 14595	5	Brazil, Rio de Janeiro state
<b>Fa</b>	<i>Fusinus frenguelli</i>	MNRJ 14487	1	Brazil, Rio de Janeiro state
<b>Fa</b>	<i>Fusinus frenguelli</i>	MNRJ 14709	1	Brazil, Santa Catarina state
<b>Fa</b>	<i>Fusinus frenguelli</i>	MZSP 77531	17	Brazil, Trindade Island
<b>Fa</b>	<i>Fusinus australis</i>	MNHN IM-2013-42513	1	Australia
<b>Fa</b>	<i>Fusinus australis</i>	MNHN IM-2013-42517	1	Australia
<b>Fa</b>	<i>Cyrtulus serotinus</i>	MNHN IM-2013-42529	1	Marchesas Archipelago
<b>Fa</b>	<i>Cyrtulus serotinus</i>	MNHN IM-2013-42530	1	Marchesas Archipelago
<b>Fa</b>	<i>Cyrtulus serotinus</i>	MNHN IM-2013-42531	1	Marchesas Archipelago
<b>Fa</b>	<i>Cyrtulus serotinus</i>	MNHN IM-2013-42532	1	Marchesas Archipelago
<b>Fa</b>	<i>Granulifusus sp.</i>	MNHN IM-2013-19724	1	Bismarck Sea, Papua New Guinea
<b>Fa</b>	<i>Granulifusus hayashi</i>	MNHN IM-2013-19210	1	Bismarck Sea, Papua New Guinea
<b>Fa</b>	<i>Granulifusus kiranus</i>	MNHN IM-2013-44502	1	China Sea
<b>Fa</b>	<i>Granulifusus kiranus</i>	MNHN IM-2013-19037	1	Bismarck Sea, Papua New Guinea
<b>Fa</b>	<i>Granulifusus kiranus</i>	MNHN IM-2013-44449	1	China Sea
<b>Fa</b>	<i>Pseudolatirus discrepans</i>	MNHN IM-2013-9777	1	Papua New Guinea
<b>Fa</b>	<i>Pseudolatirus discrepans</i>	MNHN IM-2007-34604	1	Philippines
<b>Fa</b>	<i>Fusolatirus bruijnii</i>	MNHN IM-2013-16671	1	Papua New Guinea
<b>Fa</b>	<i>Fusolatirus bruijnii</i>	MNHN IM-2013-18013	1	Papua New Guinea
<b>Fa</b>	<i>Peristernia nassatula</i>	MNHN IM-2007-32487	1	Vanuatu
<b>Fa</b>	<i>Peristernia nassatula</i>	MNHN IM-2013-18061	1	Papua New Guinea
<b>Fa</b>	<i>Peristernia nassatula</i>	MZSP 71241	2	Fiji
<b>Fa</b>	<i>Peristernia nassatula</i>	MNHN IM-2007-32541	1	Philippines
<b>Fa</b>	<i>Peristernia nassatula</i>	MNHN IM-2013-10796,	1	Papua New Guinea
<b>Fa</b>	<i>Peristernia marquesana</i>	MZSP 68507	2	Japan
<b>Fa</b>	<i>Peristernia marquesana</i>	MZSP 69249	2	Japan
<b>Fa</b>	<i>Nodolatirus nodatus</i>	MNHN IM-2013-42533	1	Austral Islands
<b>Fa</b>	<i>Nodolatirus nodatus</i>	MNHN IM-2013-42533	1	Austral Islands
<b>Fa</b>	<i>Latirus vischii</i>	MNHN IM-2009-15038	1	Madagascar
<b>Fa</b>	<i>Fasciolaria tulipa</i>	MZSP 69277	1	Honduras
<b>Fa</b>	<i>Fasciolaria tulipa</i>	MZSP 35530	2	Venezuela
<b>Fa</b>	<i>Fasciolaria tulipa</i>	MZSP 56870	2	Venezuela

<b>Fa</b>	<i>Aurantilaria aurantiaca</i>	CMPHRM 2765	1	Brazil, Ceará state
<b>Fa</b>	<i>Aurantilaria aurantiaca</i>	MNRJ 8372	1	Brazil, Ceará state
<b>Fa</b>	<i>Aurantilaria aurantiaca</i>	MNRJ 993	2	Brazil, Bahia state
<b>Fa</b>	<i>Aurantilaria aurantiaca</i>	MNRJ 8304	1	Brazil, Bahia state
<b>Fa</b>	<i>Aurantilaria aurantiaca</i>	MNRJ 15161	2	Brazil, Bahia state
<b>Fa</b>	<i>Aurantilaria aurantiaca</i>	MNRJ 14346	2	Brazil, Espírito Santo state
<b>Fa</b>	<i>Aurantilaria aurantiaca</i>	MNRJ 8369	1	Brazil, Espírito Santo state
<b>Fa</b>	<i>Aurantilaria aurantiaca</i>	MNRJ 6678	1	Brazil, Paraíba state
<b>Fa</b>	<i>Aurantilaria aurantiaca</i>	MZSP 33005	1	Brazil, Paraíba state
<b>Fa</b>	<i>Aurantilaria aurantiaca</i>	MZSP 77496	2	Brazil, Alagoas state
<b>Fa</b>	<i>Aurantilaria aurantiaca</i>	MZSP 35976	3	Brazil, Bahia state
<b>Fa</b>	<i>Filifusus filamentosus</i>	MNHN IM-2013-13107	1	Papua New Guinea
<b>Fa</b>	<i>Filifusus filamentosus</i>	MNHN IM-2007-32592	1	Vanuatu
<b>Fa</b>	<i>Australaria australasia</i>	MNHN IM-2013-42514	1	Australia
<b>Fa</b>	<i>Australaria australasia</i>	MNHN IM-2013-42516	1	Australia
<b>Fa</b>	<i>Pleuroploca trapezium</i>	MNHN IM-2009-15358	1	Madagascar
<b>Fa</b>	<i>Pleuroploca trapezium</i>	MNHN IM-2007-32591	1	Vanuatu
<b>Fa</b>	<i>Hemipolygona armata</i>	MNHN IM-2013-42511	1	Senegal
<b>Fa</b>	<i>Hemipolygona armata</i>	MNHN IM-2013-42509	1	Senegal
<b>Fa</b>	<i>Pustulatirus mediamericanus</i>	MZSP 69500	2	Ecuador
<b>Fa</b>	<i>Pustulatirus mediamericanus</i>	MZSP 95273	15	Ecuador
<b>Fa</b>	<i>Pustulatirus mediamericanus</i>	MZSP 67752	1	Ecuador
<b>Fa</b>	<i>Pustulatirus ogum</i>	MZSP 68475	16	Brazil, Espírito Santo state
<b>Fa</b>	<i>Pustulatirus ogum</i>	MZSP 69477	5	Brazil, Bahia state
<b>Fa</b>	<i>Pustulatirus ogum</i>	MZSP 69301	2	Brazil, Rio de Janeiro state
<b>Fa</b>	<i>Polygona angulata</i>	MZSP 31125	4	Brazil, Fernando de Noronha Archipelago
<b>Fa</b>	<i>Polygona angulata</i>	MZSP 112907	1	Brazil, Fernando de Noronha Archipelago
<b>Fa</b>	<i>Polygona angulata</i>	MZSP 90774	2	Brazil, Fernando de Noronha Archipelago
<b>Fa</b>	<i>Polygona angulata</i>	MZSP 112826	6	Brazil, Fernando de Noronha Archipelago
<b>Fa</b>	<i>Polygona angulata</i>	MZSP 90047	2	Brazil, Fernando de Noronha Archipelago
<b>Fa</b>	<i>Latirus polygonus</i>	MZSP 71428	1	Fiji
<b>Fa</b>	<i>Latirus polygonus</i>	MZSP 71869	1	Fiji
<b>Fa</b>	<i>Polygona infundibulum</i>	MNHN IM-2013-19591	1	Guadeloupe
<b>Fa</b>	<i>Hemipolygona beckyae</i>	MNRJ 7696	1	Brazil, Espírito Santo state
<b>Fa</b>	<i>Hemipolygona beckyae</i>	MZSP 69482	3	Brazil, Espírito Santo state
<b>Fa</b>	<i>Hemipolygona beckyae</i>	MZSP 57053	1	Brazil, Espírito Santo state
<b>Fa</b>	<i>Hemipolygona beckyae</i>	MZSP 69764	1	Brazil, Espírito Santo state
<b>Fa</b>	<i>Leucozonia ocellata</i>	MNRJ 11174	1	Brazil, Fernando de Noronha Archipelago
<b>Fa</b>	<i>Leucozonia ocellata</i>	MNRJ 11200	1	Brazil, Fernando de Noronha Archipelago
<b>Fa</b>	<i>Leucozonia ocellata</i>	MNRJ 4276	10	Brazil, Atol das Rocas Archipelago
<b>Fa</b>	<i>Leucozonia ocellata</i>	MNRJ 5357	4	Brazil, Bahia state
<b>Fa</b>	<i>Leucozonia ocellata</i>	MNRJ 12963	35	Brazil, Abrolhos Archipelago

<b>Fa</b>	<i>Leucozonia ocellata</i>	MNRJ 10735	11	Brazil, Abrolhos Archipelago
<b>Fa</b>	<i>Leucozonia ocellata</i>	MNRJ 14223	1	Brazil, Rio de Janeiro state
<b>Fa</b>	<i>Leucozonia ocellata</i>	MNRJ 10736	1	Brazil, Rio de Janeiro state
<b>Fa</b>	<i>Leucozonia cerata</i>	MZSP 64252	2	Panama
<b>Fa</b>	<i>Leucozonia cerata</i>	MZSP 64210	2	Panama
<b>Fa</b>	<i>Leucozonia cerata</i>	MZSP 95287	8	Ecuador
<b>Fa</b>	<i>Opeatostoma pseudodon</i>	MZSP 64204	6	Panama
<b>Fa</b>	<i>Opeatostoma pseudodon</i>	MZSP 67764	3	Ecuador
<b>Fa</b>	<i>Opeatostoma pseudodon</i>	MZSP 68483	3	Ecuador
<b>Fa</b>	<i>Leucozonia nassa nassa</i>	MNRJ 584	2	USA, Florida
<b>Fa</b>	<i>Leucozonia nassa cingulifera</i>	MNRJ 14848	2	Brazil, Bahia state
<b>Fa</b>	<i>Leucozonia nassa cingulifera</i>	MNRJ 10710	7	Brazil, Pernambuco state
<b>Fa</b>	<i>Leucozonia nassa cingulifera</i>	MNRJ 11065	1	Brazil, Fernando de Noronha Archipelago
<b>Fa</b>	<i>Leucozonia nassa cingulifera</i>	MNRJ 14485	1	Brazil, Trindade Island
<b>Fa</b>	<i>Leucozonia nassa brasiliiana</i>	MNRJ 10993	66	Brazil, Rio de Janeiro state
<b>Fa</b>	<i>Leucozonia nassa brasiliiana</i>	MZSP 69496	2	Brazil, Espírito Santo state
<b>Fa</b>	<i>Leucozonia nassa brasiliiana</i>	MZSP 41814	14	Brazil, Espírito Santo state
<b>Fa</b>	<i>Leucozonia ponderosa</i>	MORG 39299	1	Brazil, Trindade Island
<b>Fa</b>	<i>Leucozonia ponderosa</i>	MNRJ 14607	1	Brazil, Fernando de Noronha Archipelago
<b>Fa</b>	<i>Leucozonia ponderosa</i>	MNRJ 5220	2	Brazil, Trindade Island
<b>Fa</b>	<i>Leucozonia ponderosa</i>	MNRJ 5138	6	Brazil, Trindade Island
<b>Fa</b>	<i>Leucozonia ponderosa</i>	MNRJ 5137	3	Brazil, Trindade Island

### 3.2 Morphological data

Novel morphological data was obtained through dissection of preserved animal immersed in ethanol 70% on a camera lucida attached to stereoscope microscope Zeiss SV6, through standard techniques (*e.g.*, Simone, 2005; 2007). Whenever possible, individuals were removed from their shells through drilling of a whole in the spire, in order access the soft-parts and push the animal through the aperture. In this way it is possible to detach the animal when the columellar muscle is cut off. In some cases, whenever necessary, the shell was destroyed by use of a vise, if the number of individuals allowed for the destruction of one or some individuals. Most specimens from MNHN were removed through the use of a microwave oven (Galindo *et al.*, 2014). The electromagnetic radiation very quickly heats both the animal and the water trapped inside the shell, resulting in separation of the muscles that anchor the animal to the shell, when done properly the body can be removed intact from the shell and the shell voucher is preserved undamaged (Galindo *et al.*, 2014). Drilling or destruction of the shell on these individuals was not needed.



Shells were photographed using a Canon PowerShot G1X camera, on a static photographic table, attached to stereoscope microscope, or in Auto-montage (image stacking) camera model Zeiss Axio Scope A1. Scanning electron microscopy (SEM) photography was done in a Leica model LEO 440; gold (Au) was used for the ultra-thin coating of the radulae.

Dissections were done with the use of ophthalmological surgical material, fixed in place by entomological pins. As most gastropods, for the sake of dissections, animals herein have the body divided in the following regions: mantle cavity, visceral mass and head-foot mass. The mantle border was cut laterally in order to gain access to the pallial organs, following the section of the posterior esophagus and anterior aorta in order to separate the visceral mass from the adjacent head-foot mass. For the remainder of the head-foot mass, a longitudinal incision was made in order to separate the haemocoelic content from the foot mass.

Terminology for the anatomical study followed traditional studies (*e.g.*, Simone, 2005, 2007; 2011), and modified by the author (*e.g.*, Couto & Pimenta, 2012; Couto *et al.*, 2015a; 2015b). Imaging material was edited in Corel Photo-Paint X8 and Adobe Illustrator CC 2015.

Description for each analyzed taxa is present in a phylogenetic description model, in which the description of the clade is given (synapomorphy) and the included species (autapomorphy). Routinely, a thorough description of each species is endeavored, with anatomical observations and illustrations of all organs. Published articles containing species descriptions are found in the Appendix section, for the reader's perusal.

Delimiting characters and character states was based on personal observations of variation among species with respect to each other but also between individuals of the same species. With the exception of shell and radula (which have a terminology relatively well established *e.g.*, Vermeij & Snyder, 2002; Snyder *et al.*, 2012 for shell; Bandel, 1984 for radula) anatomical characters were novel endeavors. Previous morphological analysis of related groups (*e.g.*, Ponder & Lindberg, 1997; Strong, 2003; Simone, 2011) were not helpful for most morphological data collected here because these were hierarchically more inclusive (order, suborder, etc.).

Qualitative characters were preferred, and whenever possible were expressed as so, despite no analytical difference between quantitative or qualitative characters. Ratios and measures, although useful for morphological characterizations, were not used for the analysis, even if they were present in non-overlapping intervals.

Characters were analyzed as non-additive (unordered: cc -) except when there was a logical basis for doing so (Fitch, 1971); in this case the logical basis for additive characters (ordered: cc +) this is present in the character description.

The character matrix was compiled in Mesquite v3.10 (build 765) (Maddison & Maddison, 2010). Inapplicable characters scored '-'; unavailable or unknown scored '?' (Platnick *et al.*, 1991).

### 3.3 Phylogenetic analysis

The character matrix from Mesquite v3.10 was analyzed in TNT, that runs via a parsimonious optimality criterion (Tree analysis using new technology: Goloboff *et al.*, 2008), using heuristic algorithms to search off possible local optima into a global optimum. The algorithms of TNT are designed to deal with the problem of composite optima, (mixture of local optima of various heights, one of which is the global optimum, caused by large phylogenies having subtrees) in large datasets (Goloboff, 1999; Goloboff *et al.*, 2008). The polarization of character states was done posteriorly, in which the plesiomorphic state is decided post rooting, *i.e.*, simultaneously on ingroup and outgroup taxa (Nixon & Carpenter, 1993).

All analyses were performed using equally weighted characters (prior weighting), initially through a traditional search engine using Tree bisection and reconnection (TBR). When using the TBR algorithm, a subtree is clipped from one portion of the tree and reattached at another node in the tree in any orientation, not necessarily maintaining sister group relationships within the subtree (Goloboff, 1999). A TBR search was performed on 1000 replicates (number of added sequences) saving 50 trees per TBR replication (10,000 trees retained in memory); in case of overflow (*i.e.*, in at least some replicates, the TBR algorithm retained more trees than the designated number of trees retained in memory) an additional traditional search was done with the trees saved in memory. The trees were collapsed after each search. This method was repeated several times until the same TBR score and topology was conserved.

Another search was performed using an implied weighting method (Goloboff, 1993; Goloboff *et al.*, 2008), using the same TBR search parameters cited above. Implied weighting is a method for attributing different weights during tree search, and is independent of previous analysis and weights (unlike successive weighting: Farris, 1969). This scheme utilizes a

concavity constant ( $k$ ) (higher  $k$  values weight more strongly against characters with homoplasy); in order to determine  $k$  for the dataset, a TNT script (setk.run) (Goloboff *et al.*, 2008) was used.

Bremer support for each node (decay index) was calculated using the Bremer algorithm implemented in the TNT script Bremer.run (this script and setk.run are freely available at <http://phylo.wikidot.com/tntwiki>, last access ix/08/2016).

ACCTRAN (accelerated transformation) or DELTRAN (delayed transformation) character optimization was done in WinClada ver 1.00.08 (Nixon, 1999), which allows visualization of each character transformation along branches. Tree files were exported in .emf format and edited in Adobe Illustrator CC 2015. Fasciolariidae clades were numbered 1 through  $n$  for deeper nodes (-1 through  $-n$  for outgroups) with subsequent inner clades numbered  $na$ ,  $nb$ ,  $nc$ , etc.

#### 4. Results

The morphological analysis was based on 95 characters: ten relative to the shell; eight to the head-foot mass; 14 to the pallial cavity; four to the circulatory and excretory systems; 41 relative to the digestive system (18 of which were radular characters); seven based on female reproductive; six to male reproductive and finally; six based on the nervous system. All morphological character listings were novel acquisitions.

The traditional search through a TBR algorithm using prior weighting (best hit scored 98 times out of 1000, best TBR = 369) generated 20 equally parsimonious trees of 394 steps (L), a consistency index of 33 (Ci) and a retention index of 70 (Ri). The resulting strict consensus generated a tree with L = 407, Ci = 32 and Ri = 68 (Fig. 1A). Implied weighing search using  $k = 12.4$  (determined by setk.run script) provided a tree with L = 394, Ci = 33 and Ri = 70 (Fig. 1B).

Goloboff (1993) argues in favor of the use of implied weighting because the ‘fittest’ tree is the one that explains the data most parsimoniously, *i.e.*, with fewer number of steps. It has been argued that results based on characters properly weighted (*e.g.*, implied, successive) are to be preferred to those with all characters given the same weight (Farris, 1969; Goloboff, 1993; Goloboff *et al.*, 2008). There is some debate regarding down-weighting homoplasies in cladistic analyses, and this has been intensely criticized (*e.g.*, Turner & Zandee, 1995), also contributing to a lower Bremer support scores. The topologies between the strict consensus of the non-weighted analysis (Fig. 1A) and the weighed one (Fig. 1B) differ only slightly (mainly in resolving terminal polytomies); for this reason, because of the lower Bremer scores of the weighted tree, and the criticism of weighting, it seems logical that all optimizations and character discussion relate to the unweighted one.

The topology of the tree (Fig. 1A) revealed a monophyletic Fasciolariidae (Bremer = 3) consisting of roughly seven major groups: 1) the genera *Dolicholatirus* and *Teralatirus*; 2) *Angulofusus neda*, *Pseudolatirus kuroseanus* (Okutani, 1975) and the genus *Amiantofusus*; 3) *Pseudolatirus pallidus* Kuroda & Habe, 1961 with the genera *Chryseofusus*, *Fusinus* and *Cyrtulus*; 4) *Pseudolatirus discrepans* Kuroda & Habe, 1961 and the genus *Granulifusus*; 5) the genera *Peristernia* and *Fusolatirus*; 6) *Nodolatirus nodatus* (Gmelin, 1791) and *Latirus vischii* Bozzetti, 2008 and all previously designated Fasciolariinae; and 7) the bulk of the previously

designated Peristerniinae, including *Leucozonia*, *Opeatostoma* Berry, 1958, *Polygona*, *Hemipolygona*, *Pustulatirus* and *Latirus polygonus*.

A first split, group 1, separates the non-monophyletic *Dolicholatirus* and *Teralatirus* from the remaining fasciolariids (Clade 1a, Bremer = 4). A highly supported clade (clade 2: Bremer = 8) groups all non-*Dolicholatirus* or *Teralatirus* fasciolariids, with clade 2a, 3a and 4a (Bremer = 2, 2 and 2, respectively) represented by the fusinines, that forms a stem paraphyletic group that also includes the genus *Pseudolatirus*. Group 5a (Bremer = 2) is the Peristerniine genera *Fusolatirus* and *Peristernia* (including the type of the subfamily, *Peristernia nassatula*). Groups 6a and 7 (Bremer = 2 and 2, respectively) include the bulk of peristerniine species and all fasciolariines (including the type of the subfamily *Fasciolaria tulipa*). Bremer supports for all clades are indicated in Fig. 1A (unweighted) and Fig. 1B (weighted).

In order to evaluate the current taxonomical scheme, prior to this analysis, color scheme used for all terminals and branches in the trees correspond to each of the assigned subfamilies: black: outgroup species, non-fasciolariids; blue: fusinines; red: peristerniines; green: fasciolariines. This does not correspond to the natural subfamilies but the one previously assigned (pre-analysis).

The evolution of each of the 95 characters used for this analysis is seen in Figs. 3-6. Discussion of each character follows on the Character discussion section.

A

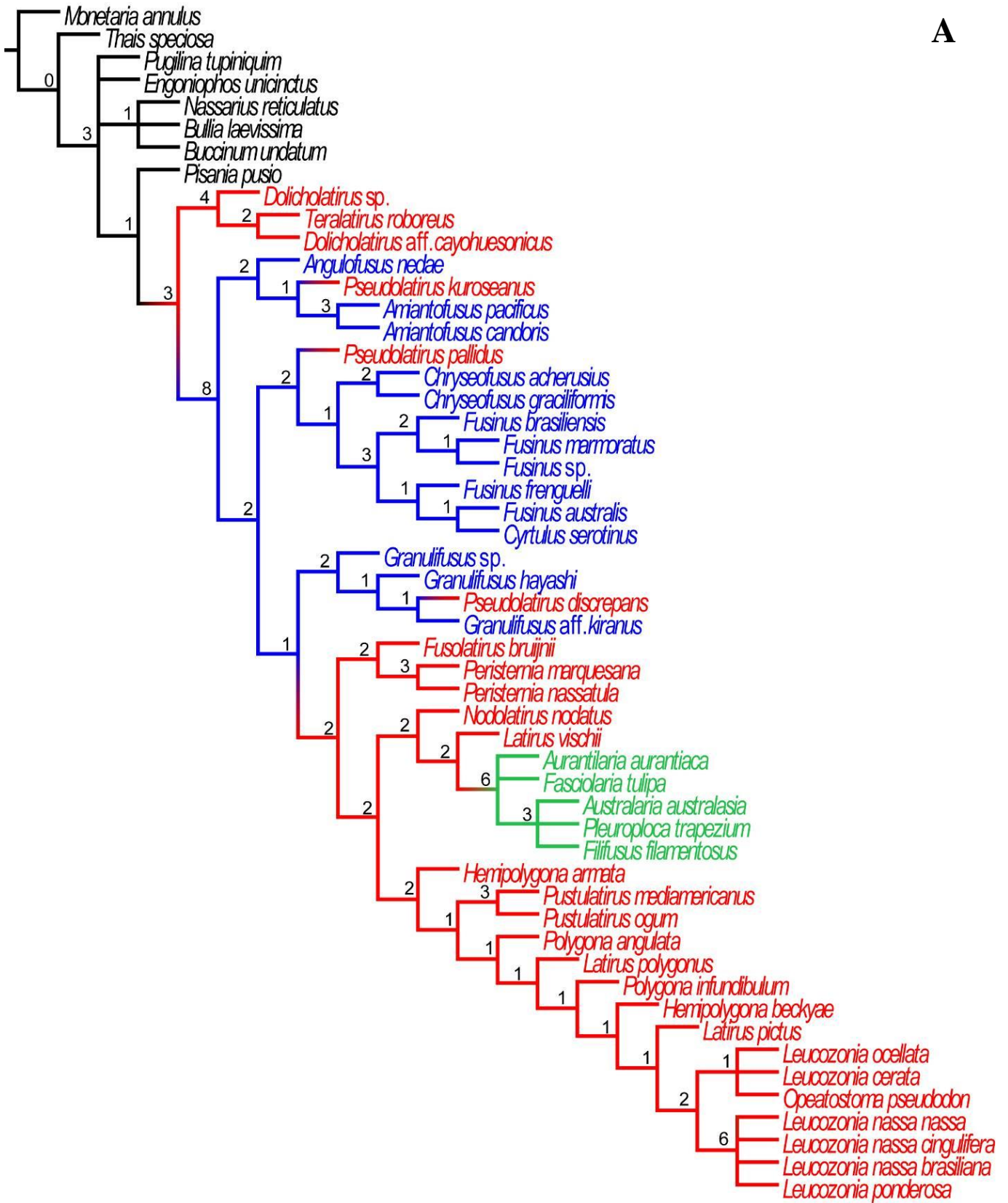


Figure 1. A: Phylogenetic tree obtained through parsimonious analysis in TnT using prior, unweighted characters. Numbers in nodes indicate Bremer support values. Color scheme: Black: non-fascioliariids. Blue: fusinines. Red: peristerniines. Green: fascioliariines.

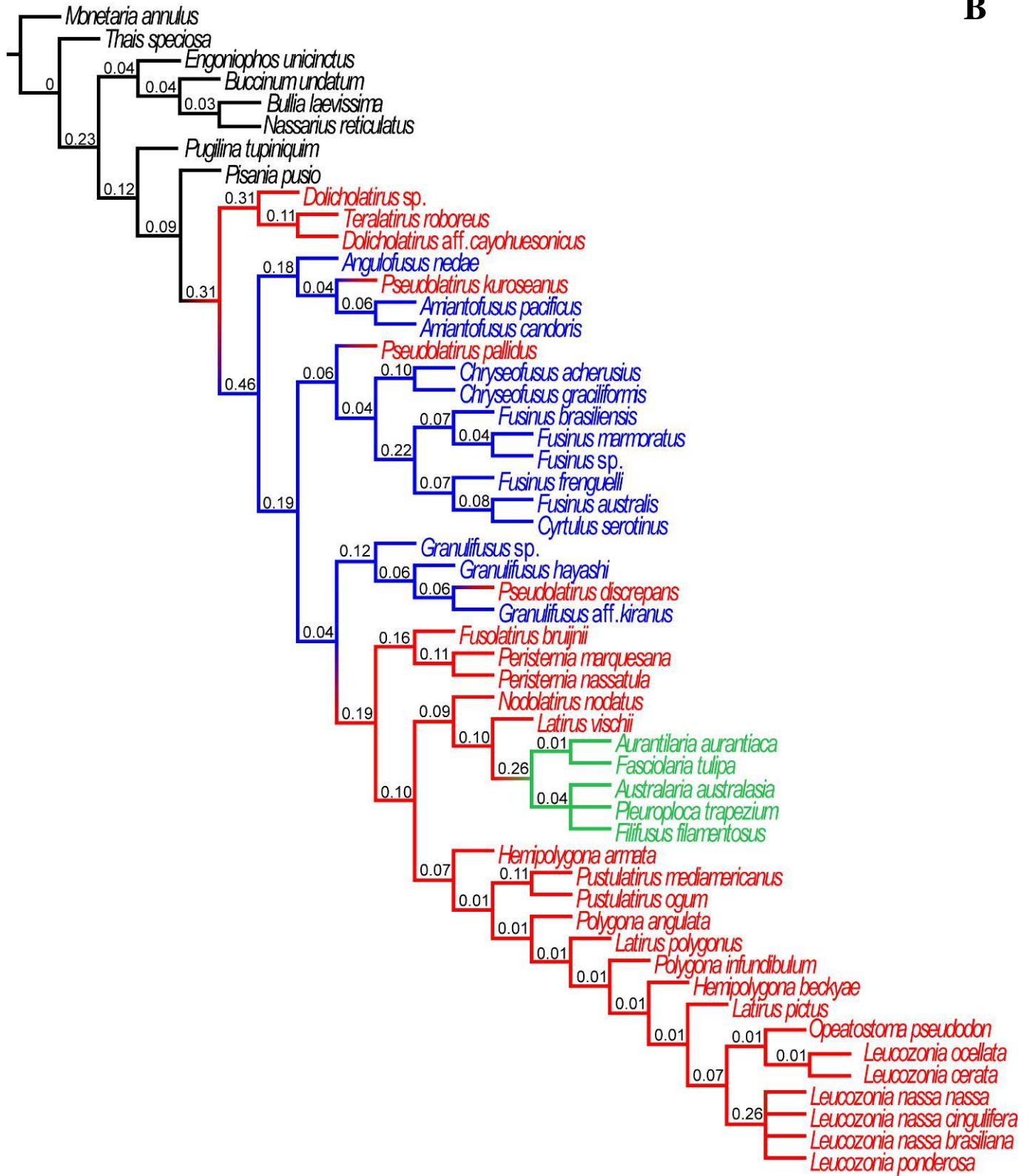
**B**

Figure 1 (cont.). B: Phylogenetic tree obtained through parsimonious analysis in TnT using implied weighing ( $k = 12.4$ ). Numbers in nodes indicate Bremer support values. Color scheme: Black: non-fascioliids. Blue: fusinines. Red: peristerniines. Green: fascioliines.

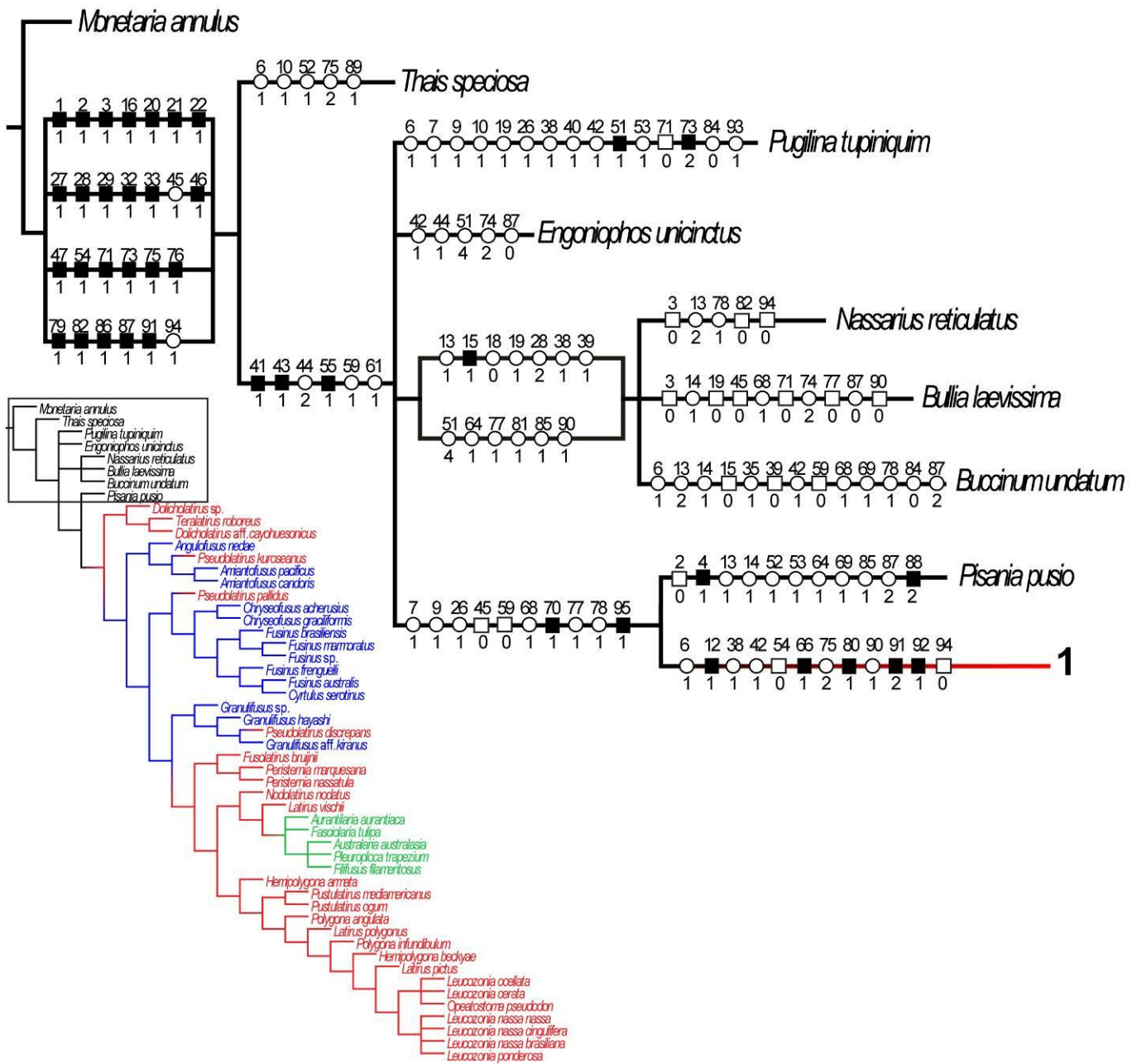


Figure 2. Phylogenetic tree (part one) indicating the synapomorphies that support them. The number above each symbol represents the character, while the number below indicates the character state. Dark squares: non-homoplastic synapomorphy. Empty square: reversion. Circle: convergence. Color scheme: Black: non-fasciolariaids. Blue: fusinines. Red: peristerniines. Green: fasciolariaines.



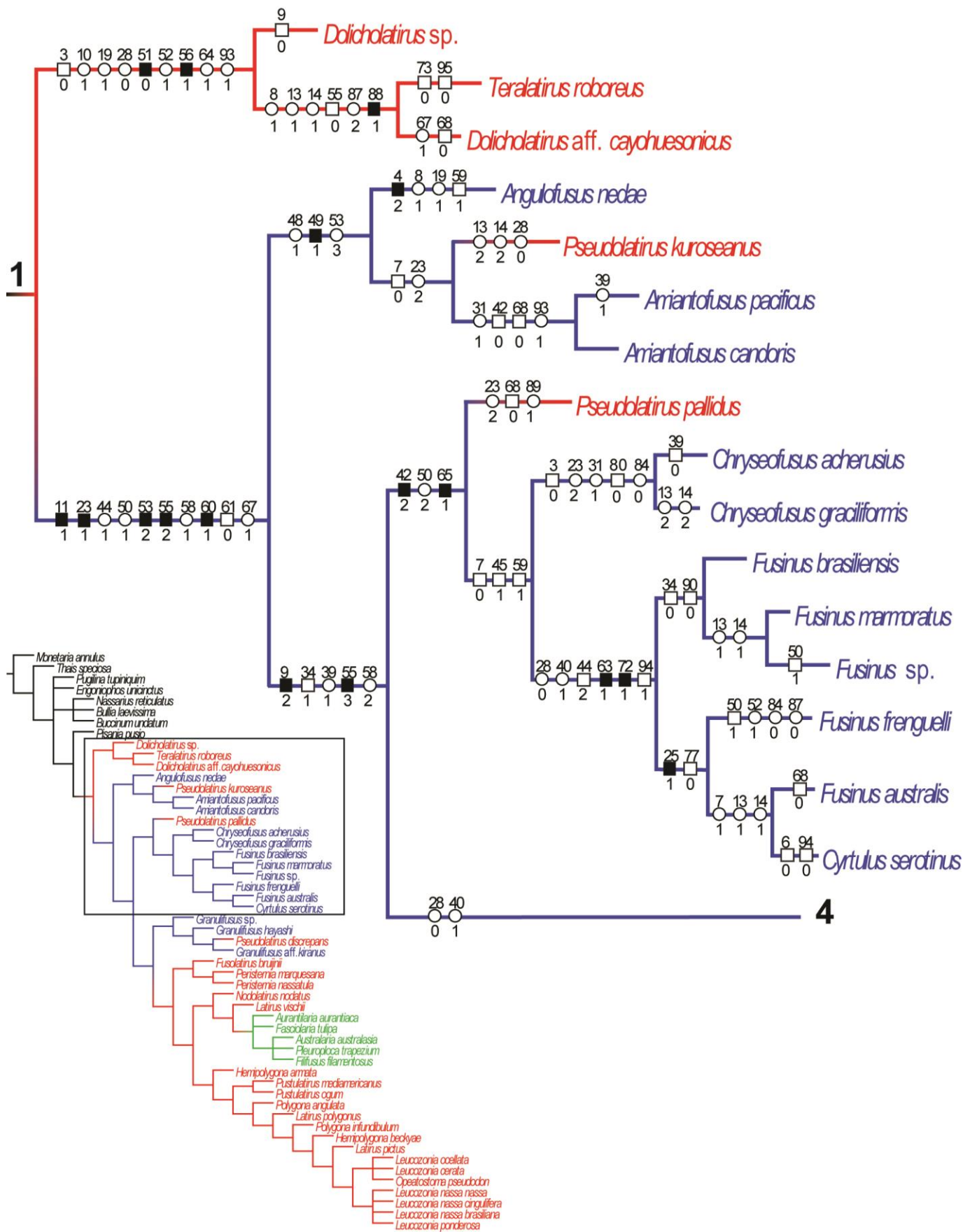


Figure 3. Phylogenetic tree (part two) indicating the synapomorphies that support them. The number above each symbol represents the character, while the number below indicates the character state. Dark squares: non-homoplastic synapomorphy. Empty square: reversion. Circle: convergence. Color scheme: Black: non-fascioliariids. Blue: fusinines. Red: peristerniines. Green: fascioliariines.

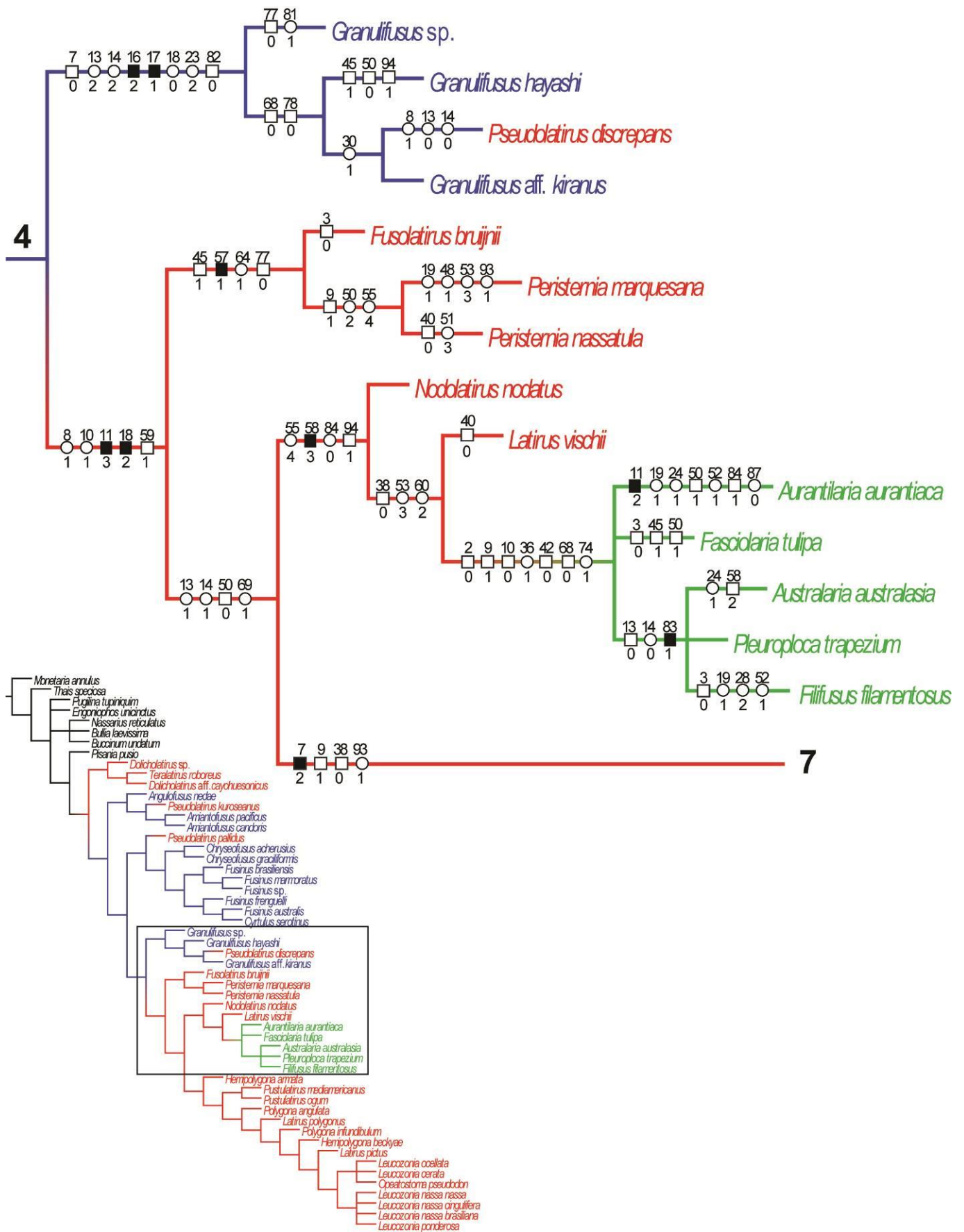


Figure 4. Phylogenetic tree (part three) indicating the synapomorphies that support them. The number above each symbol represents the character, while the number below indicates the character state. Dark squares: non-homoplastic synapomorphy. Empty square: reversion. Circle: convergence. Color scheme: Black: non-fascioliariids. Blue: fusinines. Red: peristerniines. Green: fascioliariines.

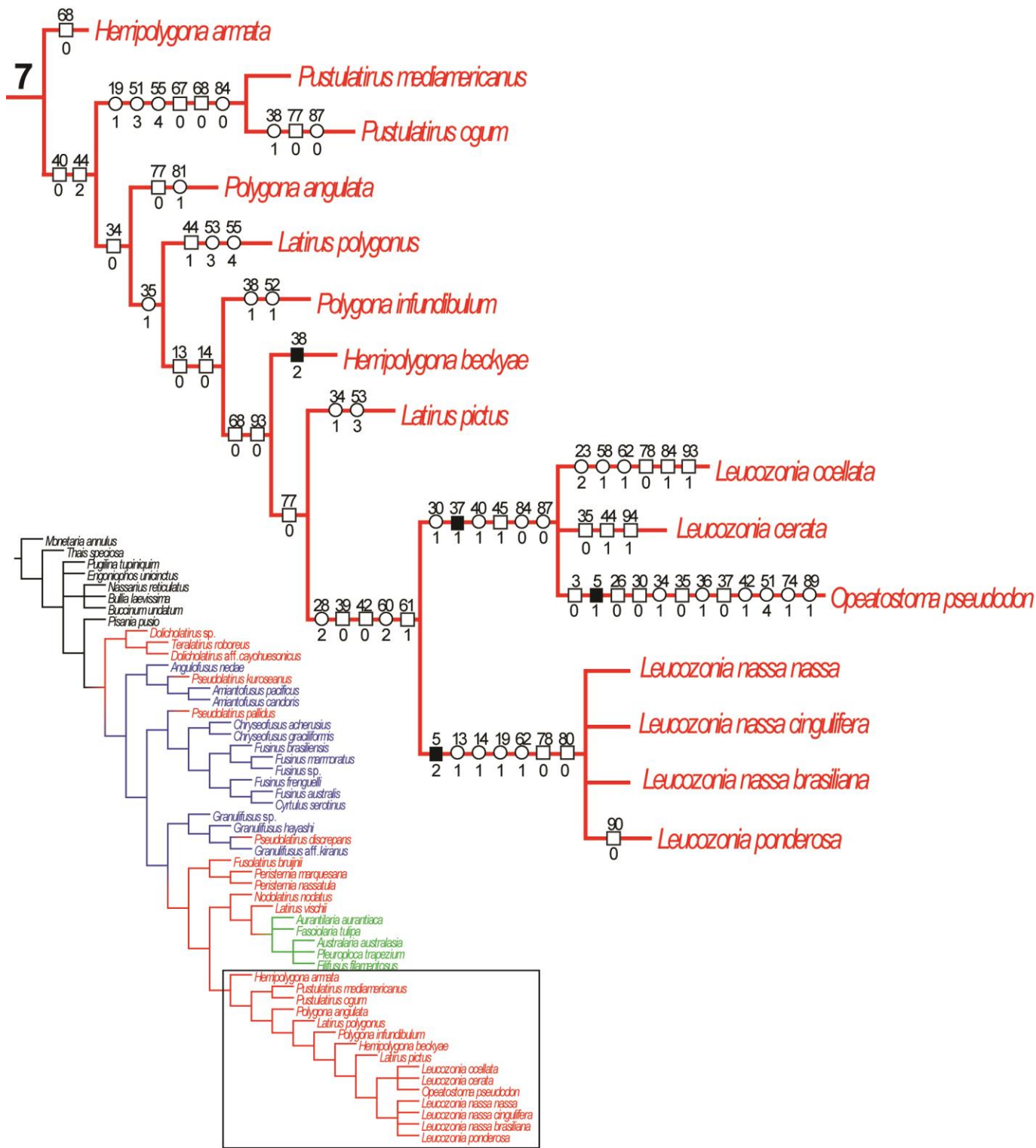


Figure 5. Phylogenetic tree (part four) indicating the synapomorphies that support them. The number above each symbol represents the character, while the number below indicates the character state. Dark squares: non-homoplastic synapomorphy. Empty square: reversion. Circle: convergence. Color scheme: Black: non-fascioliariids. Blue: fusinines. Red: peristerniines. Green: fascioliariines.

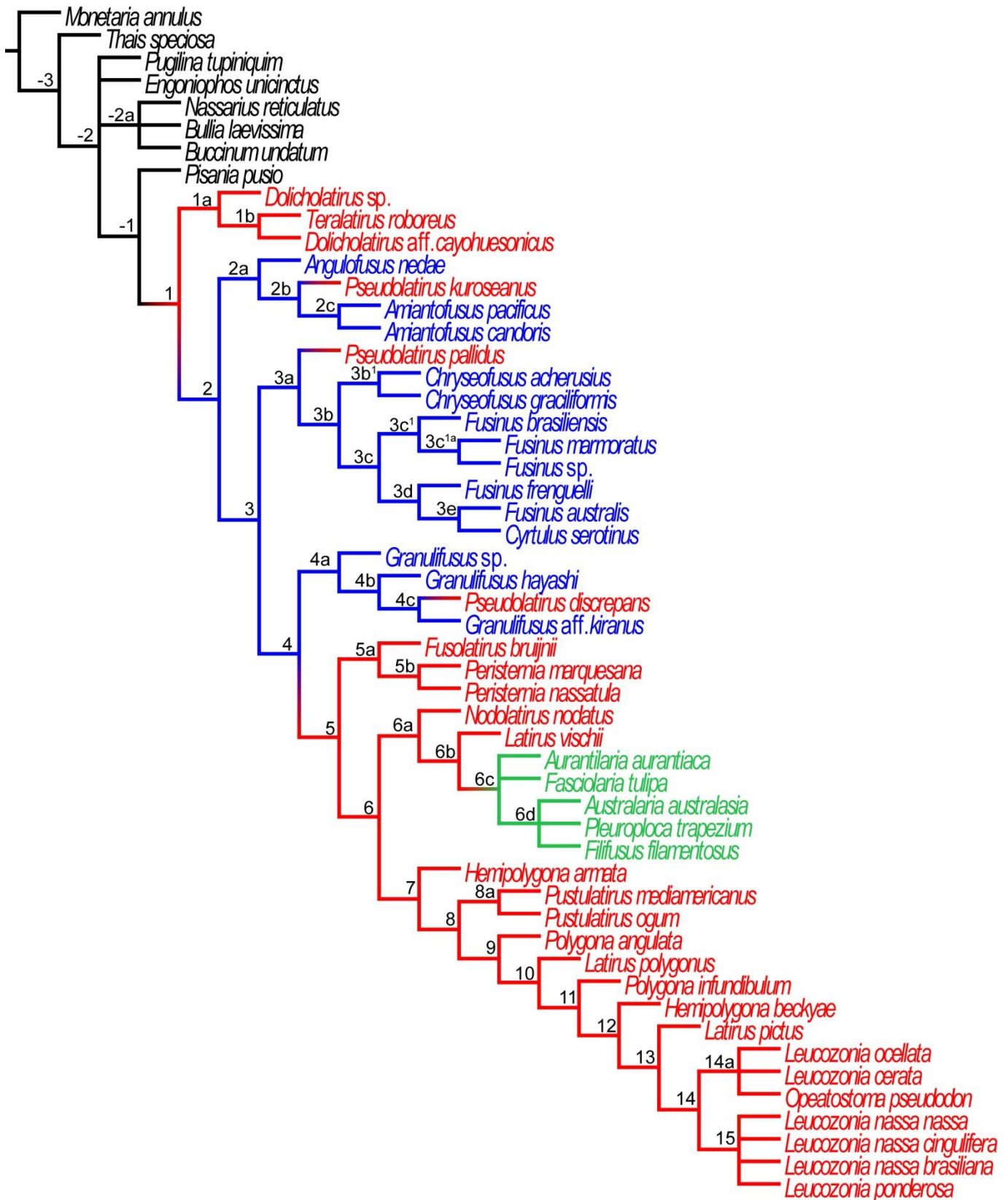


Figure 6. Phylogenetic tree obtained through parsimonious analysis in TnT with prior weighing. Numbers in nodes indicate node numbers (see text for reference and discussion of each number). Color scheme: Black: non-fascioliariids. Blue: fusinines. Red: peristerniines. Green: fascioliariines.



## 5. Phylogenetic descriptions

The following discussion corresponds to the unweighted phylogenetic analysis, as specified in the Material and Methods section. For a reference to the following section see Figures 2-5.

### Outgroup taxa

#### Clade -3 Neogastropoda

Shell spire visible (1: 1), coloration absent or regularly spaced in spiral bands or axial nodes (2: 1); sculpture of spiral bands present (3: 1) throughout teleoconch. Operculum present, filling entire shell aperture (16: 1). Mantle border with single lobe (20: 1) without papilla (21: 1) on its outer surface. Osphradium bearing two branches (anterior-posterior) (22: 1). Ctenidium adjacent to osphradium (27: 1), ctenidium width: osphradium width 1–1.5 (28: 1); its posterior tip directly adjacent to pericardium wall (29: 1). Anal (exhalant) siphon absent (32: 1). Kidney with interdigitating lamellae (pycnonephridial) (33: 1). Odontophore m6 muscle posterior free portion: odontophore length  $\leq 1/6$  (45: 1); origin of m11 muscle posteriorly in odontophore cartilages (46: 1). Radula marginal teeth absent (47: 1); laterals not adjacent to rachidians (54: 1). Valve of Leiblein present (71: 1). Esophageal gland as gland of Leiblein (73: 1). Stomach bearing posterior bulge with sorting area (caecum) (75: 1). Rectum enveloped with pallial gonoduct (76:1) by thin longitudinal membrane. Bursa copulatrix anterior (79: 1), terminally in pallial oviduct. Cement gland present (82: 1). Penis duct (vas deferens) closed (86: 1) throughout, its shape sinuous (87: 1). Buccal ganglia dorsally in nerve ring, connectives visible (91: 1); its commissure length: buccal ganglia length  $\geq 1/2$  (94:1).

#### *Thais speciosa* (Figs. 7-8)

**Examined material:** MZSP 67772, Bajo Copé, off Ayangue, Guayas, Ecuador, Taken under rocks at 10-12m, by dive. Col. Femorale, vi/2006 [2 specimen]. MZSP 95270, Ecuador. Col. J. Coltro, 2009 [1 specimen].

Shell apical growth of outer lip absent (6: 1); pseudo-umbilicus (10: 1) as shallow slit. Radula rachidian bearing minute, secondary cusps (52: 1). Stomach bearing posterior bulge without sorting area (75: 2). Penis ejaculatory duct long convoluted tube immersed in haemocoel (89: 1).

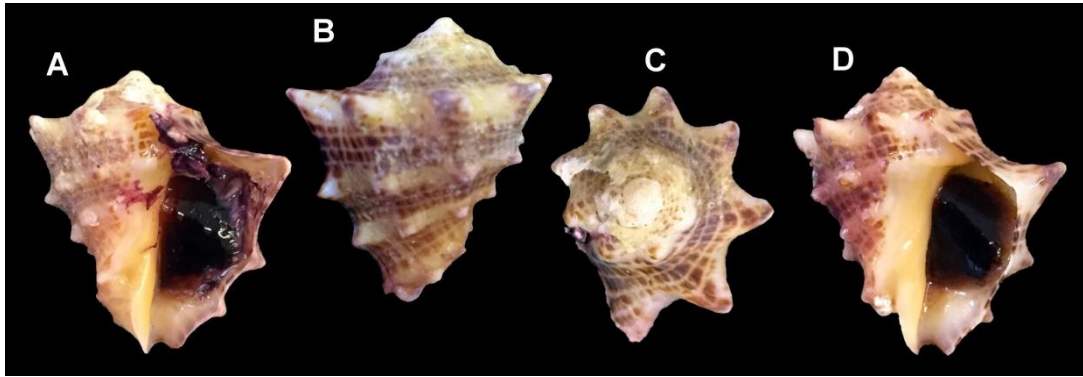


Figure 7. *Thais speciosa*, shell. **A-C**: MZSP 67772 (27.2mm). **D**: MZSP 97270 (23.5mm).

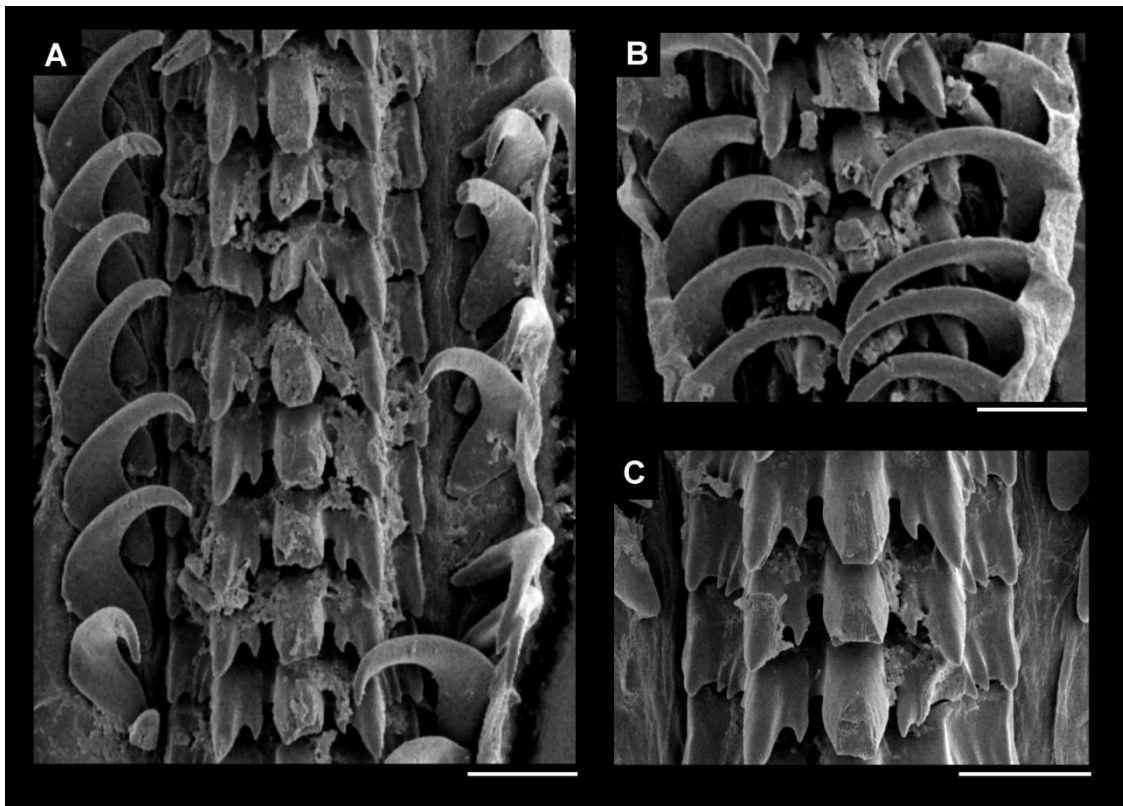


Figure 8. *Thais speciosa*, radula. **A-C**: MZSP 95270. **A**: panoramic view. **B**: detail of lateral tooth of radula. **C**: detail of rachidian tooth of radula. Scale bars = 50 $\mu$ m.

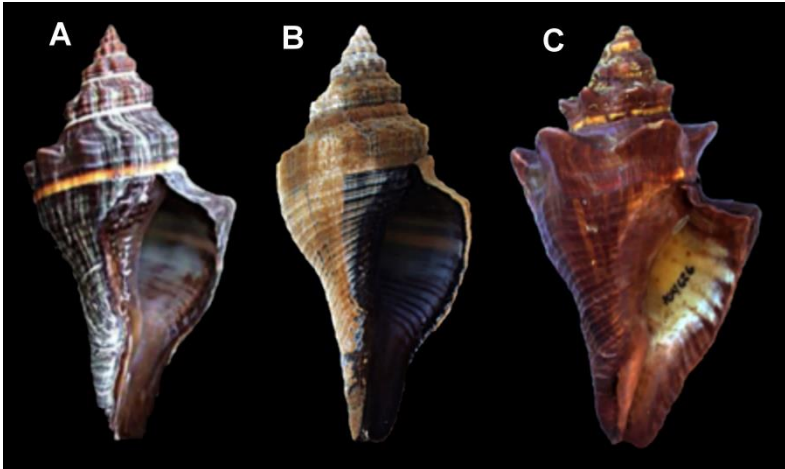


Figure 9. *Pugilina tupiniquim*, shell (modified from Abbate & Simone, 2015). **A:** MZSP 73487 (120mm). **B:** MZSP 116299 (80mm). **C:** MZSP 116299 (110mm).

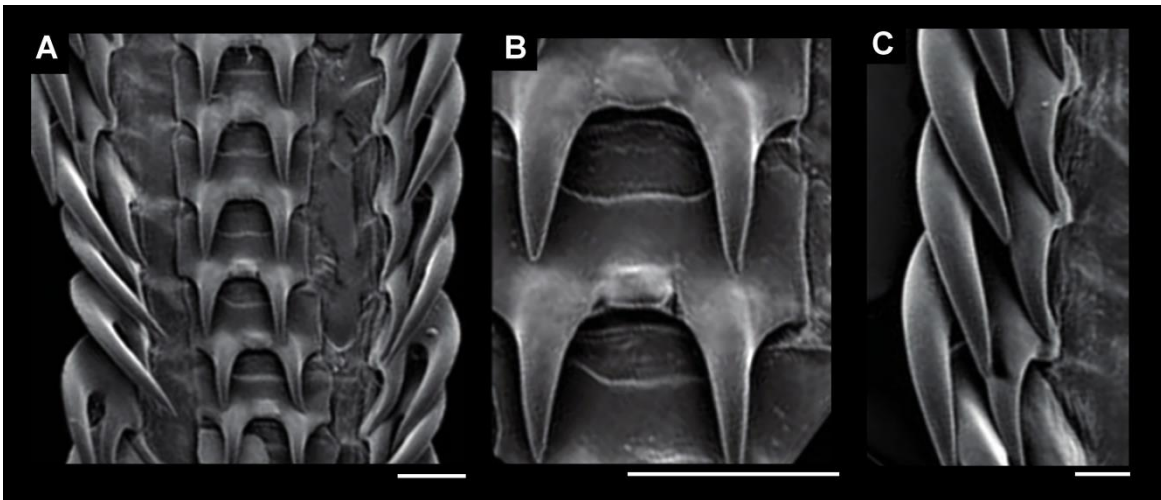


Figure 10. *Pugilina tupiniquim*, radula (modified from Abbate & Simone, 2015). A-C: MZSP 91653. **A:** panoramic view. **B:** detail of rachidian tooth of radula. **C:** detail of lateral tooth of radula. Scale bars = 100 $\mu$ m.

### Clade -2 Buccinoidea

Odontophore radular sac contained within proboscis (41: 1) not extending outwards; cartilages concave (43: 1) slender and elongated; fused anteriorly  $\geq 15\%$  of total odontophore length (44: 2). Lateral tooth of radula as long as wide, its length: width  $\sim 1$  (55: 1), its base curved (59: 1); length of cusp 2 of lateral  $\sim$ twice as other cusps (61: 1).

***Pugilina tupiniquim* (Figs. 9-10)**

**Examined material:** data from Abbate & Simone (2015).

Shell apical growth of outer lip present (6: 1); inner sculpture of outer lip bearing continuous spiral cord (7: 1); siphonal canal moderate-sized, its length: total shell length  $1/6-1/4$  (9: 1); pseudo-umbilicus present (10: 1) as shallow slit. Pallial cavity long, its extension  $\geq 3/4$  whorls (19: 1). Osphradium leaflets high, its height: ctenidium height  $\geq 1/2$  (26: 1). Rhynchostome as longitudinal (38: 1); simple (40: 1), slit. Odontophore medium-sized, its length: proboscis length  $1-1/2$  (42: 1). Rachidian tooth of radula bearing two principal cusps (51: 1), small, its width: lateral tooth width  $1/2 \leq 1$  (53: 1). Loss of valve of Leiblein (71: 0) and esophageal gland (73: 2). Cement gland opening centrally (84: 0) in foot sole. Commissure of buccal ganglia inconspicuous (93: 1).

***Engoniophos uncinctus* (Figs. 11-12)**

**Examined material:** data from Abbate (2016).

Odontophore medium-sized, its length: proboscis length  $1-1/2$  (42: 1), fused anteriorly  $\leq 15\%$  of total odontophore length (44: 1). Rachidian tooth of radula with  $\geq 5$  cusps (51: 4). Posterior esophagus bearing sudden broadening in haemocoel region (74: 2), anterior to diaphragmatic septum. Duct of penis linear (87: 0).

**Clade -2a Clade Buccinidae + Nassariidae**

Head medium-sized, its width: head-foot mass width  $1/4-1/2$  (13: 1). Foot with metapodial 1 or 2 tentacles (15: 1) in posterior dorsal region of foot. Operculum eccentric, its lateral margin rounded (18: 0). Pallial cavity long, its extension  $\geq 3/4$  whorls (19: 1). Ctenidium ample, its width: osphradium width  $\geq 1.5$  (28: 2). Rhynchostome as longitudinal slit (38: 1), bearing longitudinal folds in its margin that extend inwards (39: 1). Rachidian tooth of radula with  $\geq 5$  cusps (51: 4); secondary cusps on lateral tooth present (64: 1). Anus far from mantle border, its distance from mantle border: total pallial cavity length  $\geq 1/3$  (77: 1). Bursa copulatrix bearing anterior muscular bulb (81: 1) close to gonopore. Prostate as simple tube (85: 1). Pedal ganglia elongated, its length: nerve ring length  $\geq 1/2$  (90: 1).



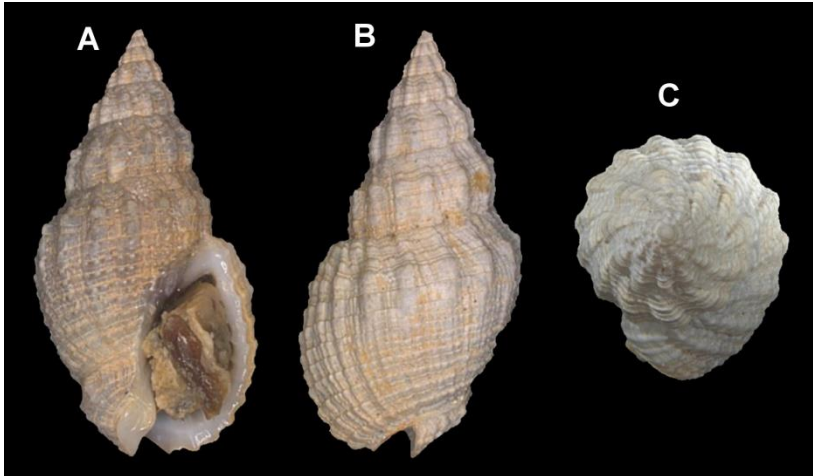


Figure 11. *Engoniophos uncinatus*, shell (modified from Abbate, 2016).  
**A-B:** MZSP 77798 (18.7mm). **C:** MZSP 77798.

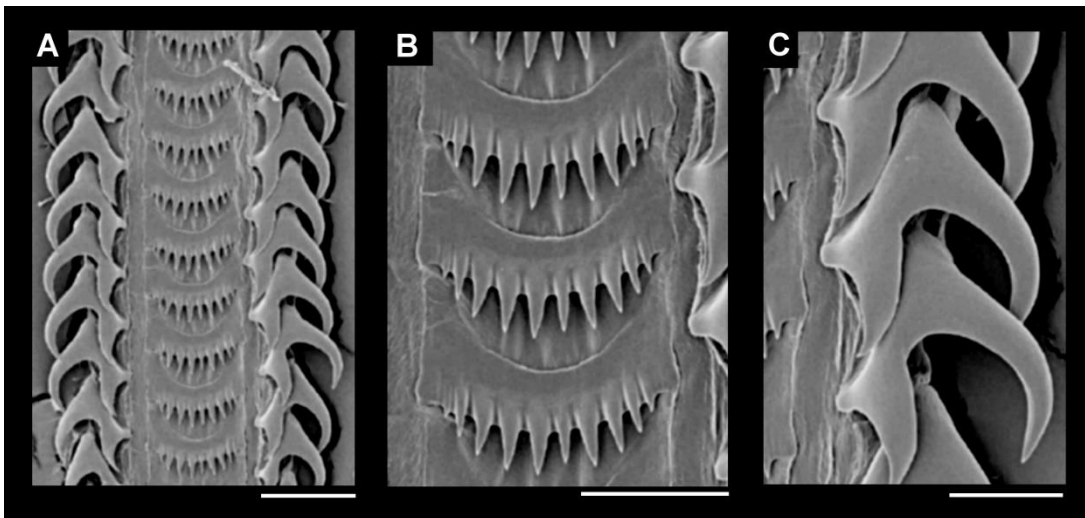


Figure 12. *Engoniophos uncinatus*. radula (modified from Abbate, 2015). **A-C:** MZSP 77798. **A:** panoramic view. **B:** detail of rachidian tooth of radula. **C:** detail of lateral tooth of radula. Scale bars = 50 $\mu$ m.

### *Nassarius reticulatus* (Figs. 13-14)

**Examined material:** data from Abbate (2016).

Loss of spiral sculpture of shell (3: 0). Head large, its width: head-foot mass width  $\geq 1/2$  (13: 2).  
 Seminal receptacle in pallial oviduct absent (78: 1). Loss of cement gland (82: 0). Buccal ganglia  
 commissure diminute, its length: buccal ganglia length  $\leq 1/2$  (94: 0).

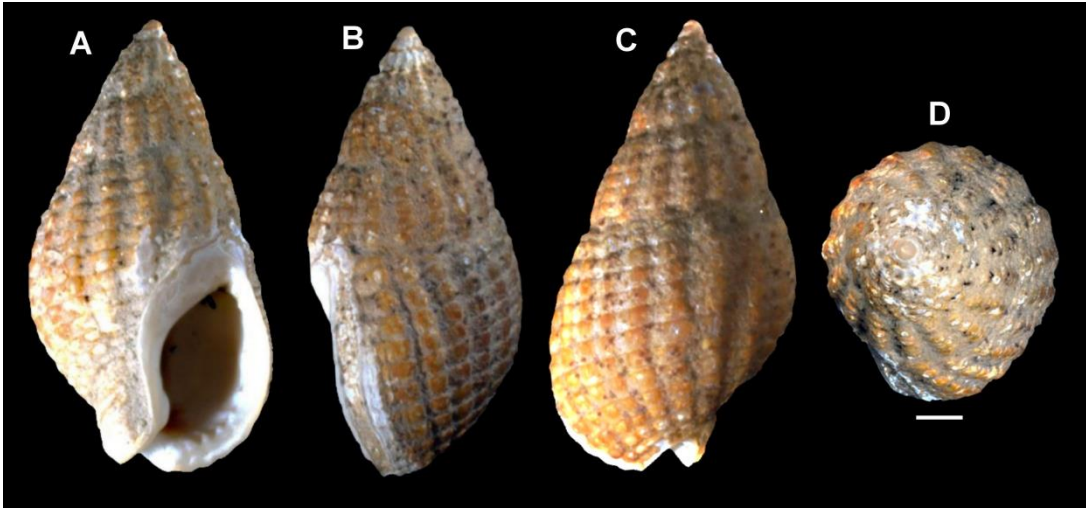


Figure 13. *Nassarius reticulatus*, shell (modified from Abbate, 2016). A-D: MZSP 92087. Scale bars = 2mm.

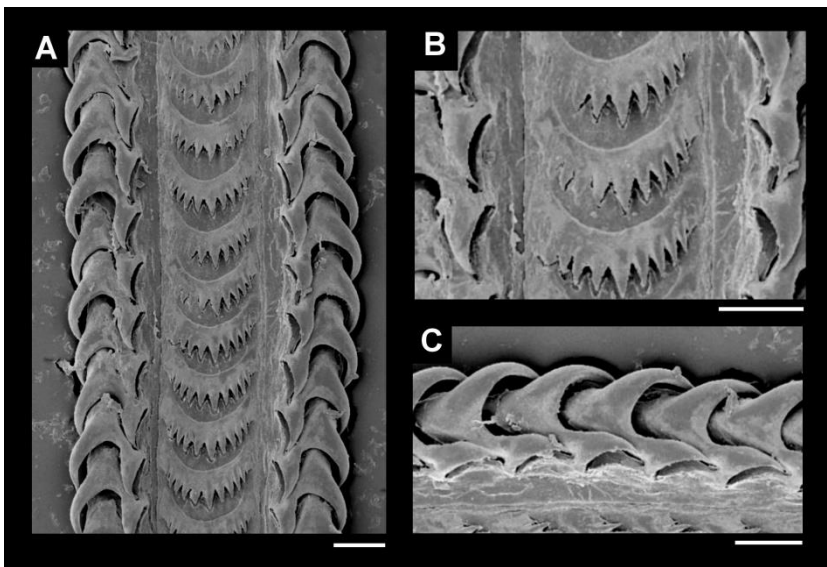


Figure 14. *Nassarius reticulatus*, radula (modified from Abbate, 2016). A-D: MZSP 92087. A: panoramic view. B: detail of rachidian tooth. C: detail of lateral tooth. Scale bars = 30µm.

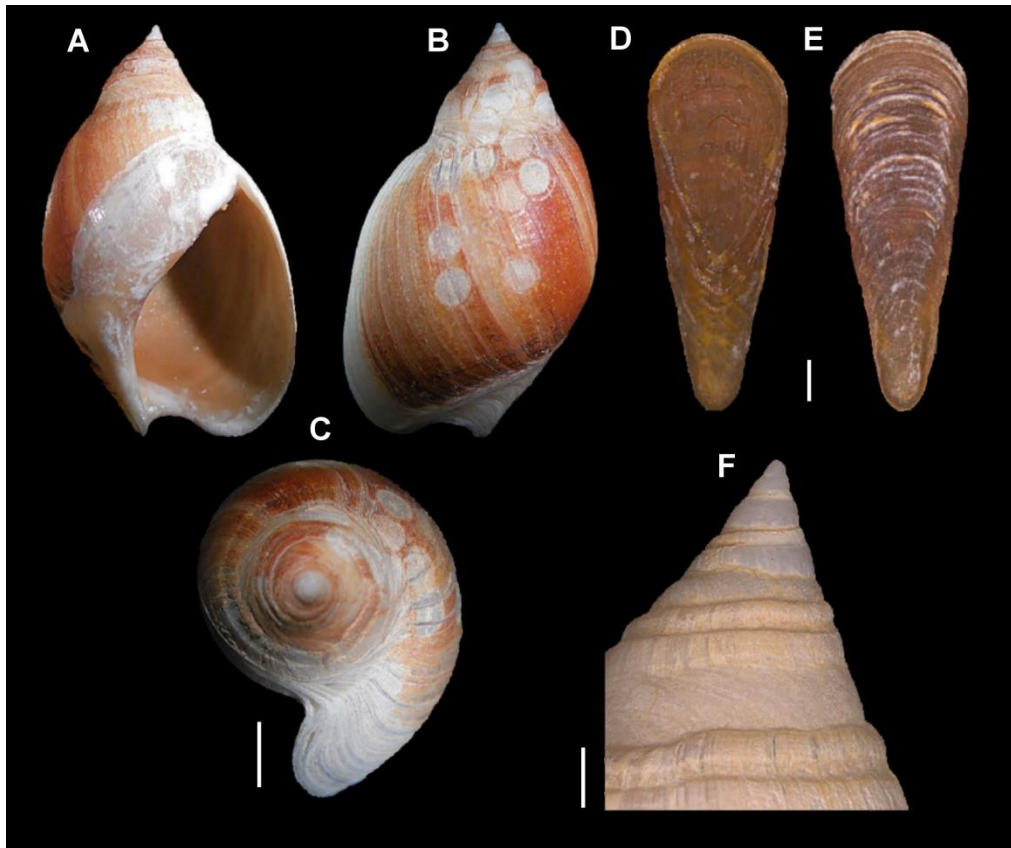


Figure 15. *Bullia laevissima*, shell and operculum (modified from Abbate & Simone, 2016). A-F: KZN S3741. A-C: (41.7mm). D-E: operculum ventral and dorsal view. F: detail of protoconch. Scale bars = 1mm.

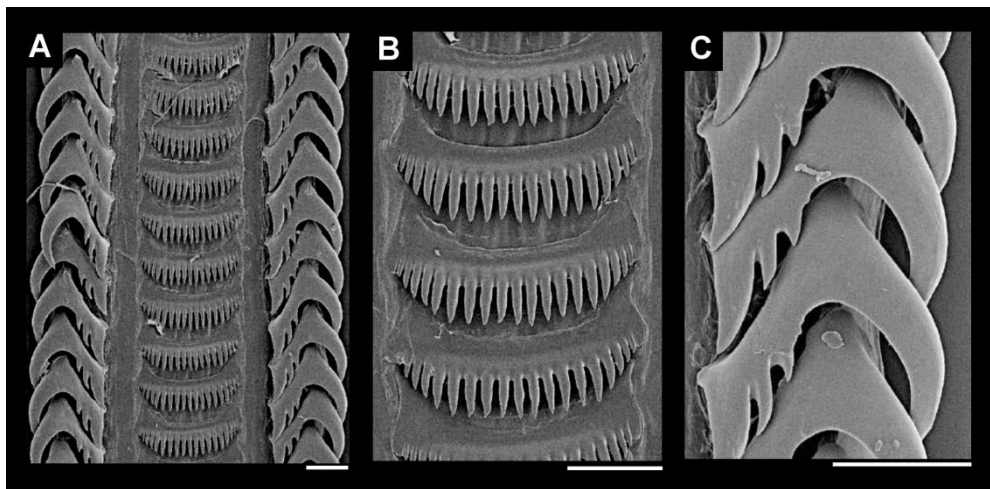


Figure 16. *Bullia laevissima*, radula (modified from Abbate & Simone, 2016). A-C: KZN S3741. A: panoramic view. B: detail of rachidian tooth. C: detail of lateral tooth. Scale bars = 200µm.

***Bullia laevissima* (Figs. 15-16)**

**Examined material:** data from Abbate (2016).

Loss of spiral sculpture of shell (3: 0). Head with short cephalic tentacles, its length: head width  $1/2-2/3$  (14: 1). Pallial cavity short, its extension  $\leq 3/4$  whorls (19: 0). Odontophore m6 muscle posterior free portion: odontophore length  $>1/6$  (45: 0). Proboscis retractor muscles originating mid-proboscis (68: 1). Loss of valve of Leiblein (71: 0). Posterior esophagus constant in diameter (74: 2) throughout its extension. Anus close to mantle border, its distance from mantle border: total pallial cavity length  $<1/3$  (77: 0). Duct of penis linear (87: 0). Pedal ganglia short, its length: nerve ring length  $<1/2$  (90: 0).

***Buccinum undatum* (Figs. 17-18)**

**Examined material:** MZSP 98217, off Calais, North Sea, France, Taken by nets at 15-20 meters, bought at local market in Paris. xii/2010 [10 specimens]. MZSP 58732, Amrun Island, North Sea. L. Forneris col. vi/23/1960 [1 specimen].

Shell apical growth of outer lip absent (6: 1). Head large, its width: head-foot mass width  $\geq 1/2$  (13: 2). Head with short cephalic tentacles, its length: head width  $1/2-2/3$  (14: 1). Loss of metapodial tentacles (15: 0). Nephridial gland present in membrane between renal cavity and pericardium (35: 1). Loss of longitudinal folds in margin of rhynchostome (39: 0). Odontophore medium-sized, its length: proboscis length  $1-1/2$  (42: 1). Base of lateral tooth of radula straight (59: 0). Proboscis retractor muscles originating mid-proboscis (68: 1). Salivary glands as free amorphous masses (69: 1) present in haemocoel. Seminal receptacle of oviduct absent (78: 1); cement gland opening centrally (84: 0) in foot sole. Penis duct highly convoluted (87: 2).



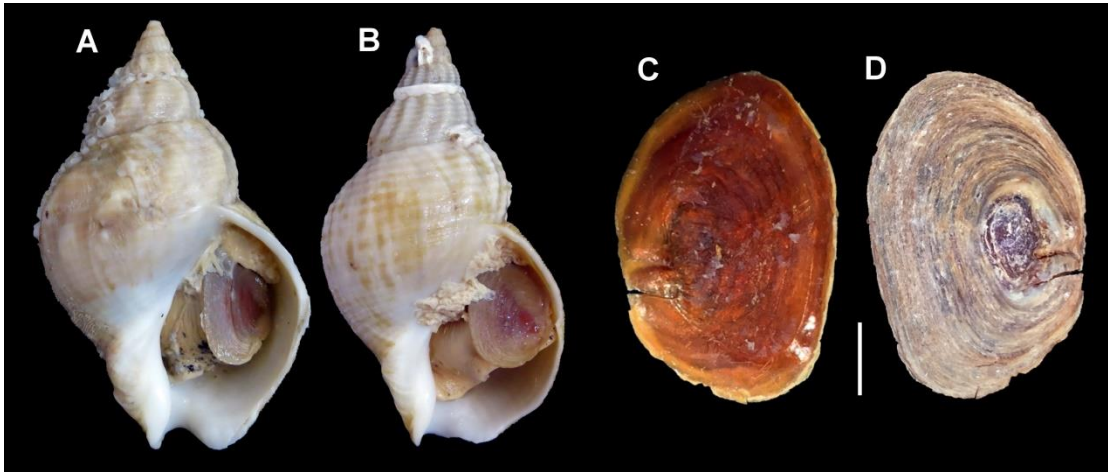


Figure 17. *Buccinum undatum*, shell and operculum. A-D: MZSP 98217. A: 67.7mm. B: 85.4mm. C: operculum, inner view. D: operculum, outer view. Scale bars = 10mm.

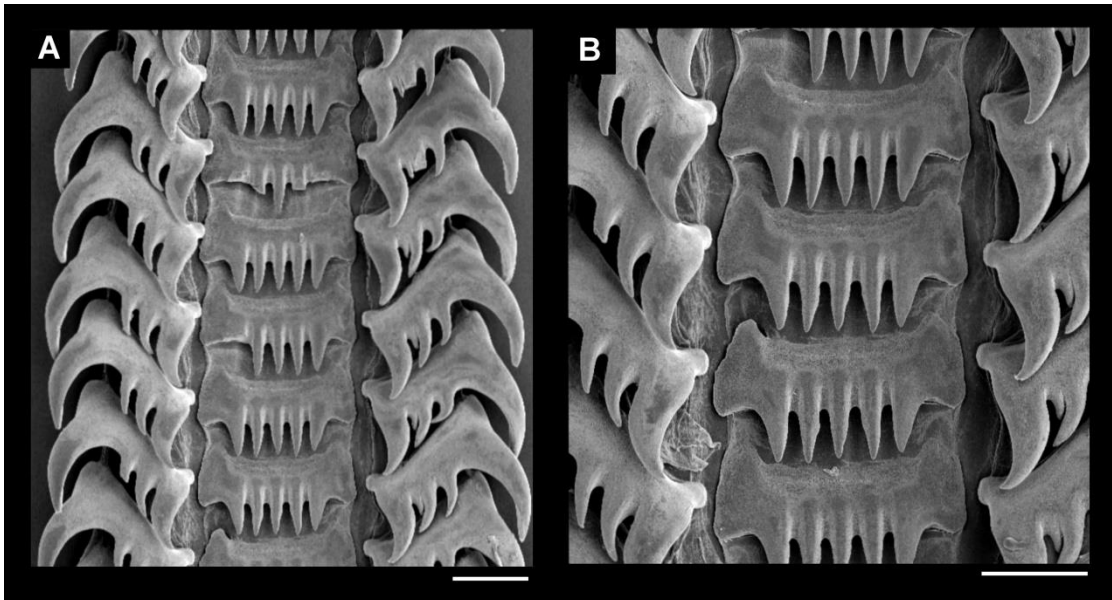


Figure 18. *Buccinum undatum*, radula. A-B: MZSP 98217. A: panoramic view. B: detail of rachidian tooth of radula. Scale bars = 200µm.

### Clade -1 Pisaniinae + Fasciolariidae “salivary ducts immersed in esophagus wall”

Shell outer lip bearing inner sculpture of continuous spiral cord (7: 1); siphonal canal of moderate size, its length: total shell length  $1/6-1/4$  (9: 1). Osphradium leaflets high, its height: ctenidium height  $\geq 1/2$  (26: 1). Odontophore m6 muscle posterior free portion: odontophore length  $>1/6$  (45: 0). Base of lateral tooth of radula straight (59: 0). Proboscis retractor muscles originating mid-proboscis (68: 1). Salivary ducts immersed in its ventral-laterally walls of anterior esophagus (70: 1), anteriorly to valve of Leiblein. Anus distance from mantle border: total pallial cavity length  $\geq 1/3$  (77: 1). Seminal receptacle in pallial oviduct absent (78: 1). Statocysts in nerve ring asymmetrical, right anterior and left posterior (95: 1).

***Pisania pusio* (Figs. 19-20)**

**Examined material:** MZSP 105583, Búzios, Ilhabela, São Paulo state, 23°47.762'S 45°09.282'W, 10m depth. Coltro col. vi/2003 [18 specimens]. MZSP 105690. São Paulo state, Brazil. v/15/2012 [6 specimens]. MZSP 111471 Guarapará, Espírito Santo state, Brazil. ii/17/2013 [7 specimens]. MZSP 112908, Fernando de Noronha, Pernambuco state, Brazil. FAPESP col v/04/2013. [4 specimens].

Shell coloration blotchy spots, irregularly spaced (2: 0); anal notch in outer lip, ventral to aperture (4: 1). Head medium-sized, its width: head-foot mass width  $1/4-1/2$  (13: 1), with short cephalic tentacles, length: head width  $1/2-2/3$  (14: 1). Radula rachidian bearing minute, secondary cusps (52: 1), small, width: lateral tooth width  $1/2 \leq 1$  (53: 1); lateral tooth bearing secondary cusps (64: 1). Salivary glands as free amorphous masses (69: 1). Prostate as simple tube (85: 1). Penis duct highly convoluted (87: 2), pre-copulatory chamber bearing long terminal papilla (88: 2).

**Ingroup taxa**

**Clade 1 Family Fasciolariidae**

Shell apical growth of outer lip absent (6: 1). Head with cephalic tentacles positioned with its bases side by side (12: 1), lacking forehead. Rhynchostome as longitudinal slit (38: 1). Odontophore medium-sized, its length: proboscis length  $1-1/2$  (42: 1). Lateral tooth of radula directly adjacent to rachidian (54: 0). Single or paired proboscis retractor muscles originate in columellar muscle (66: 1). Stomach bearing posterior bulge without sorting area (75: 2). Bursa copulatrix long, its length: oviduct length  $\geq 1/4$  (80: 1). Pedal ganglia elongated, its length: nerve ring length  $\geq 1/2$  (90: 1); buccal ganglia immersed in nerve ring (91: 2), its connectives not visible, positioned dorsal to cerebro-pleural ganglia (92: 1); buccal ganglia commissure diminute, its length: buccal ganglia length  $\leq 1/2$  (94: 0).

**Clade 1a *Dolicholatirus* + *Teralatirus***

Loss of shell spiral sculpture (3: 0); pseudo-umbilicus (10: 1). Pallial with extension  $\geq 3/4$  whorls (19: 1). Ctenidium width: osphradium width  $< 1$  (28: 0). radula rachidian tooth with 1 principal cusp (51: 0), bearing secondary cusps (52: 1); lateral tooth curved outward (56: 1), secondary cusps on lateral tooth absent (64: 1). Commissure of buccal ganglia inconspicuous (93: 1).

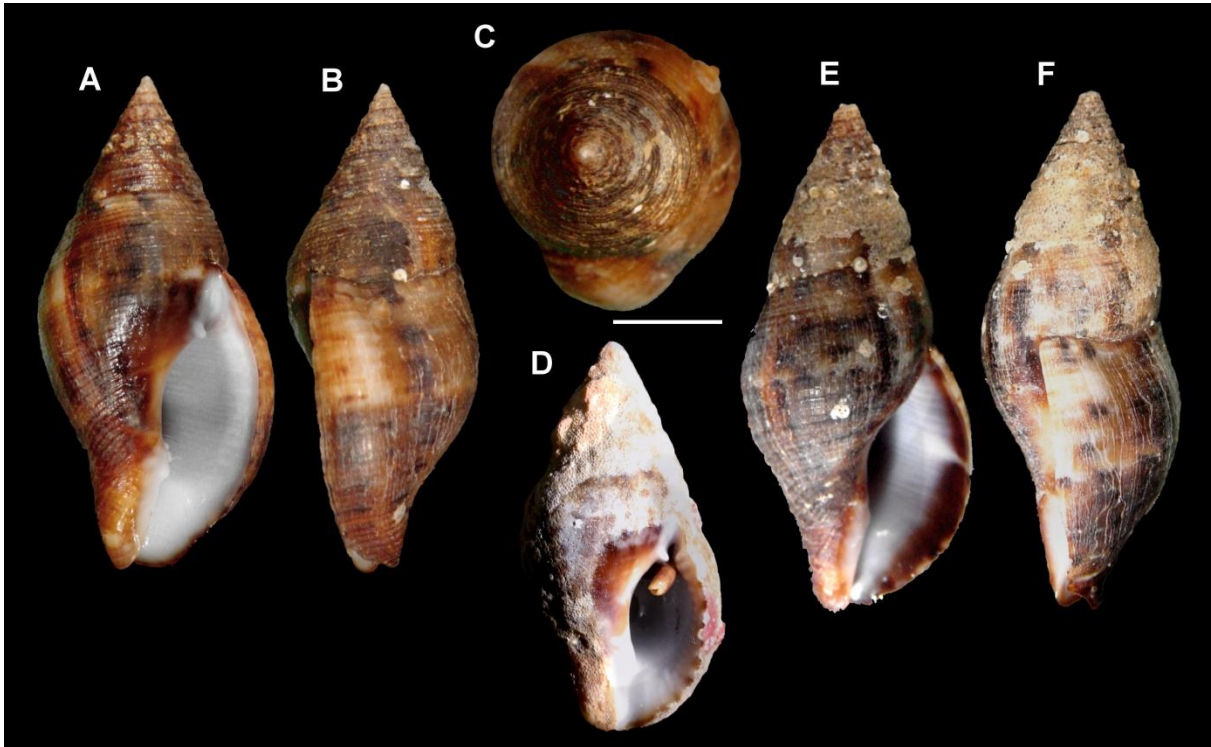


Figure 19. *Pisania pusio*, shell. A-C: MZSP 111471 (26,3mm). D: MZSP 105583 (38,0mm). E-F: MZSP 105690 (35,2mm). Scale bars = 10mm.

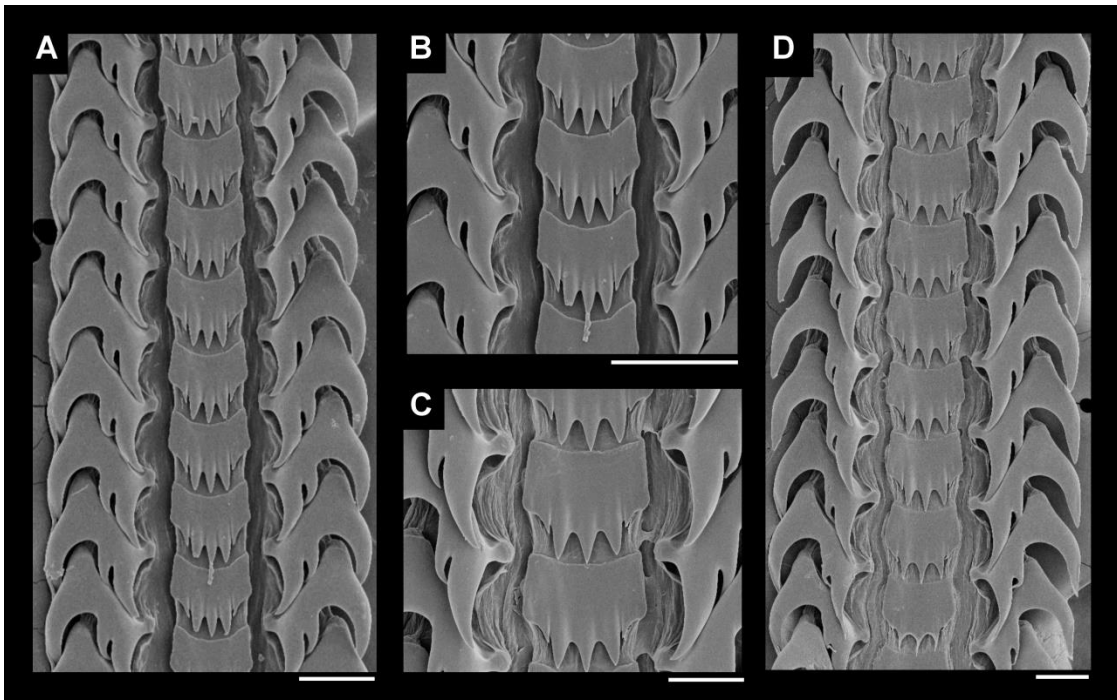


Figure 20. *Pisania pusio*, radula. A-B: MZSP 105690. A: panoramic view. B: detail of rachidian tooth of radula. C-D: MZSP 111471. C: radula. D: detail of rachidian tooth of radula. Scale bars = 50µm.



Figure 21. *Dolicholatirus* sp. shell (modified from Couto *et al.*, 2016), MNHN IM-2009-29739.

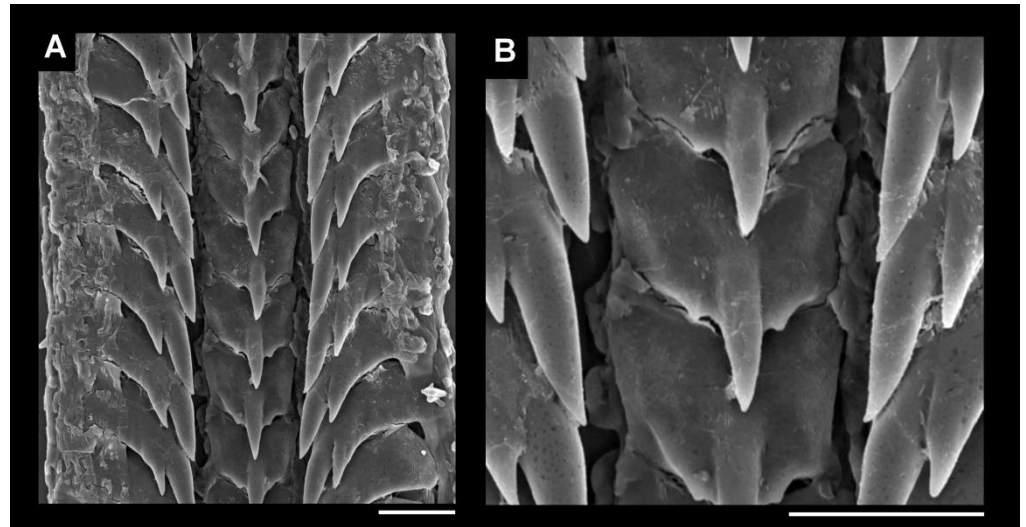


Figure 22. *Dolicholatirus* sp. radula (modified from Couto *et al.*, 2016). **A-B**: MNHN IM-2009-29739. **A**: panoramic view. **B**: detail of rachidian tooth. Scale bars = 10 $\mu$ m.

### ***Dolicholatirus* sp. (Figs. 21-22)**

**Examined material:** data from Couto *et al.* (2016).

Shell with short siphonal canal, its length: total shell length  $\leq 1/6$  (9: 0).

#### **Clade 1b**

Shell with columellar folds (8: 1) present in mid-aperture. Head medium-sized, its width: head-foot mass width  $1/4$ – $1/2$  (13: 1), bearing short cephalic tentacles, its length: head width  $1/2$ – $2/3$  (14: 1). Radula lateral tooth longer than wide, its length: width  $>1$  (55: 0). Penis duct highly convoluted (87: 2), pre-copulatory chamber bearing short terminal papilla (88: 1) contained within.

### ***Teralatirus roboreus* (Figs. 23-24)**

**Examined material:** data from Simone *et al.* (2013).

Esophageal gland as ventral septated sac (73: 0). Statocysts in nerve ring symmetrical (95: 0), anterior in pedal ganglia.



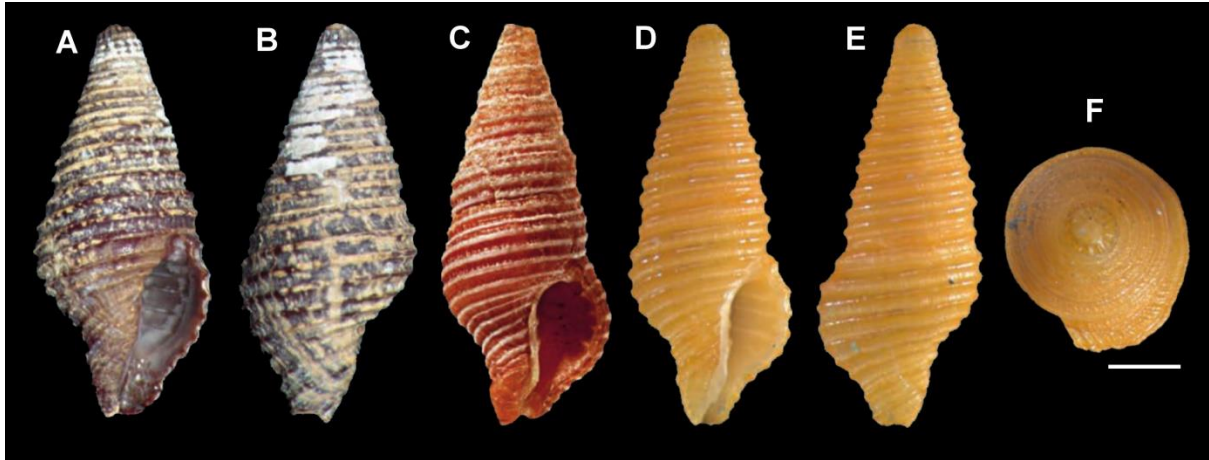


Figure 23. *Teralatirus roboreus*, shell (modified from Simone *et al.*, 2013). **A-B**: MZSP 92195 (9mm). **C**: NHMUK 1854, holotype (9.3mm). **D-F**: MZSP 87285 (10.2mm). Scale bars = 1mm.

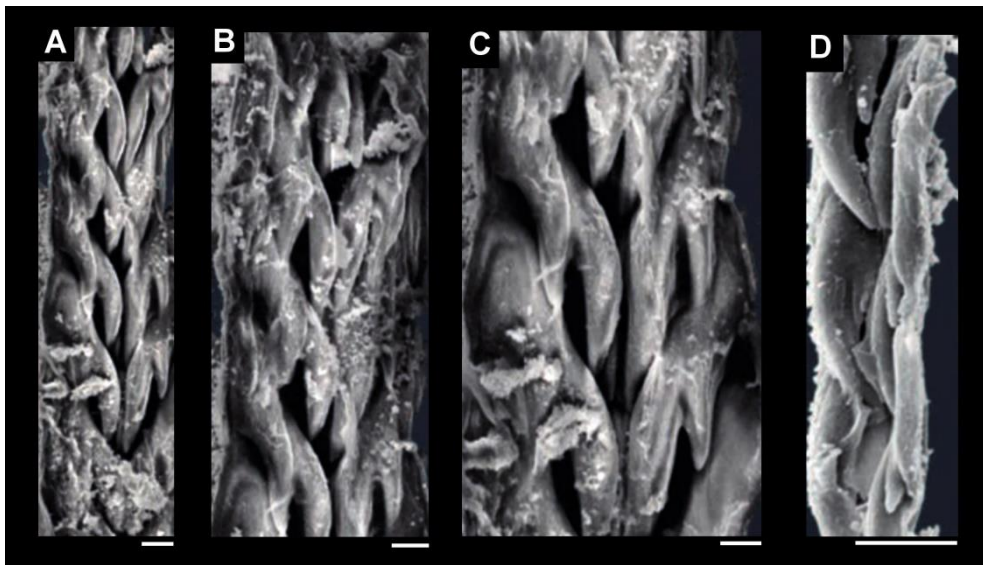


Figure 24. *Teralatirus roboreus*, radula (modified from Simone *et al.*, 2013). **A-D**: MZSP 92195. Scale bars = 2 $\mu$ m.

***Dolicholatirus aff. cayohuesonicus* (Figs. 25-26)**

**Examined material:** ANSP A8131, Cayman Brac, Southwest Point, Cayman Islands. Maes, R. A. & V. O. col. ii/1968 [2 specimens]. ANSP 338609/A5642, White Bay, Guana Island, British Virgin Islands, in drifted sand on rocks, 2-3m depth. Maes, V. O. col. ii/15-28/1975 [9 specimens]. ANSP A18293, Reef, mouth of Puerto Yabucoa, Yabucoa, Puerto Rico. Loos, J. col. vii/22-23/1969. [1 specimen].

Proboscis retractor muscles as single bundle (67: 1), inserting posteriorly (68: 0).

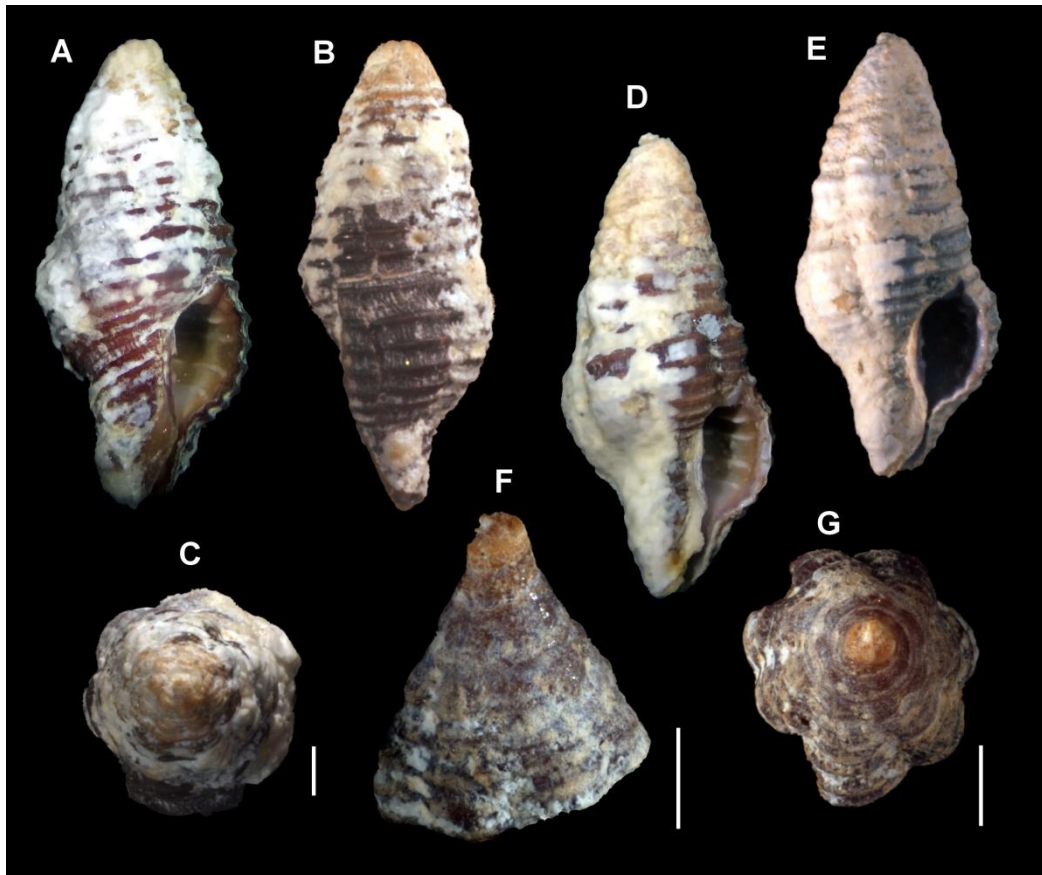


Figure 25. *Dolicholatirus* aff. *cayohuesonicus*, shell. **A-C**: ANSP 338609/A5642 (9.9mm). **D-E**: ANSP A18293. **D**: (13.2mm). **E**: (10.7mm). **F-G**: ANSP A8131. Scale bars = 1mm.

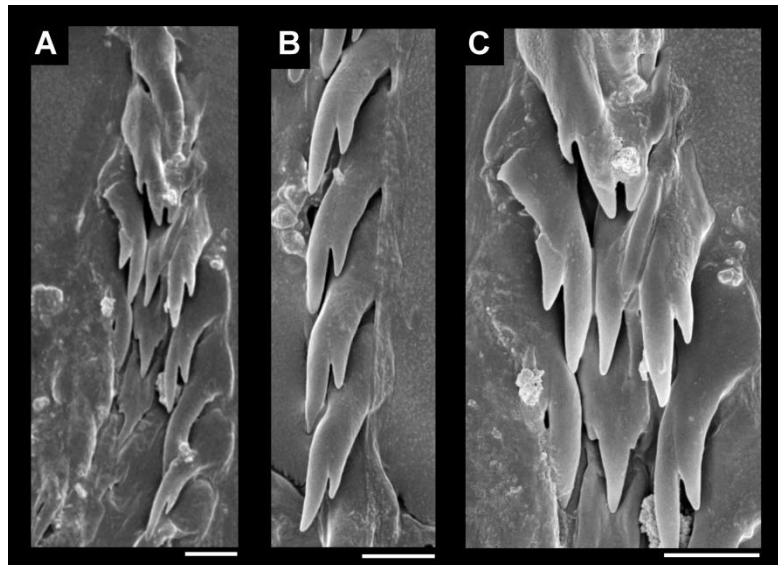


Figure 26. *Dolicholatirus* aff. *cayohuesonicus*, radula. **A-C**: ANSP 338609/A5642. **A**: panoramic view. **B**: detail of rachidian tooth. **C**: detail of lateral teeth. Scale bars = 10 $\mu$ m.

**Clade 2 Fasciolaridae non *Dolicholattirus* and *Teralattirus***

Body pigmentation orange to light-red (11: 1), present in head-foot mass and mantle border. Osphradium slightly asymmetrical (23: 1), its right leaflets longer than left. Odontophore fused anteriorly  $\leq 15\%$  of total odontophore length (44: 1). Rachidian tooth of radula trapezoidal-shaped, its base width: edge width 1/2–1 (50: 1), small, its width: lateral tooth width 1/4–1/2 (53: 2); lateral tooth wider than long, its length: width 1/2–1 (55: 2), bearing 5–6 cusps (58: 1), the innermost one, cusp 1, is present in reduced size (60: 1), cusp 2 has same size or smaller than other cusps (61: 0). Proboscis retractor muscles as single bundle (67: 1).

**Clade 2a *Angulofusus* + *Amiantofusus***

Rachidian tooth of radula triangle-shaped (48: 1), with sub-terminal cusps (49: 1), diminute, its width: lateral tooth width  $< 1/4$  (53: 3).

***Angulofusus nedae***

**Examined material:** data from Fedosov & Kantor (2012).

Anal notch present in outer lip of shell, laterally in aperture (4: 1), inner side of aperture bearing distinct columellar folds (8: 1). Pallial cavity long, its extension  $\geq 3/4$  whorls (19: 1). Base of lateral tooth of radula curved (59: 1).

**Clade 2b *Amiantofusus***

Loss of inner sculpture of outer lip (7: 0). Osphradium heavily asymmetrical (23: 2), its right leaflets longer than left.

***Pseudolattirus kuroseanus* (Figs. 27-28)**

**Examined material:** MNHN IM-2013-14709, Rempi Area, Papua New Guinea, 5°2'56.6592"S; 145°49'5.6748"E. PAPUA NIUGINI expedition, ship Alis col. xi/22/2012 [1 specimen].



Figure 27. *Pseudolatirus kuroseanus*, shell. MNHN IM-2013-14709 (41.3mm).

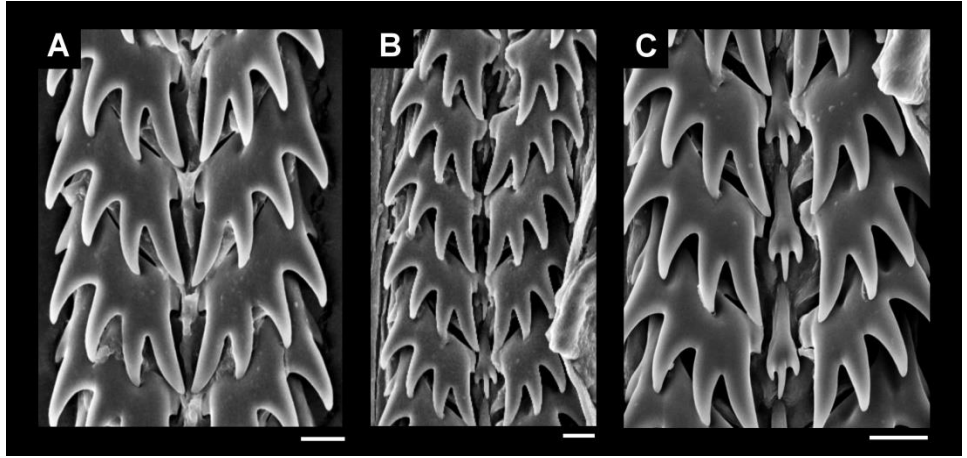


Figure 28. *Pseudolatirus kuroseanus*, radula. A-C: MNHN IM-2013-14709. A-B: panoramic view. C: detail of rachidian tooth. Scale bars = 10 $\mu$ m.

Head large, its width: head-foot mass width  $\geq 1/2$  (13: 2), bearing long cephalic tentacles, its length: head width  $\leq 2/3$  (14: 2). Ctenidium narrow, its width: osphradium width  $< 1$  (28: 0).

#### **Clade 2c *Amiantofusus***

Ventral fold of siphon in pallial cavity with a wide base (31: 1). Odontophore long, its length: proboscis length  $\sim 1$  (42: 0). Proboscis retractor muscles inserting posteriorly (68: 0). Commissure of buccal ganglia inconspicuous (93: 1).

#### ***Amiantofusus pacificus* (Figs. 29-30)**

**Examined material:** MNHN IM-2013-42508, China Sea, off An-Da Chiao, 10°24'52.398"N; 114°46'9.4872"E. NanHai 2014 expedition, Ocean Researcher 5 ship, Chen Wei-jen col. i/07/2014 [1 specimen]. MNHN IM-2013-44179, China Sea, V bis (seamount), 15°5'22.434"N ; 116°29'39.84"E. NanHai 2014 expedition, Ocean Researcher 5 ship, Chen Wei-jen col. i/02/2014. [1 specimen].

Rhynchostome bearing longitudinal folds in its margin that extend inwards (39: 1).



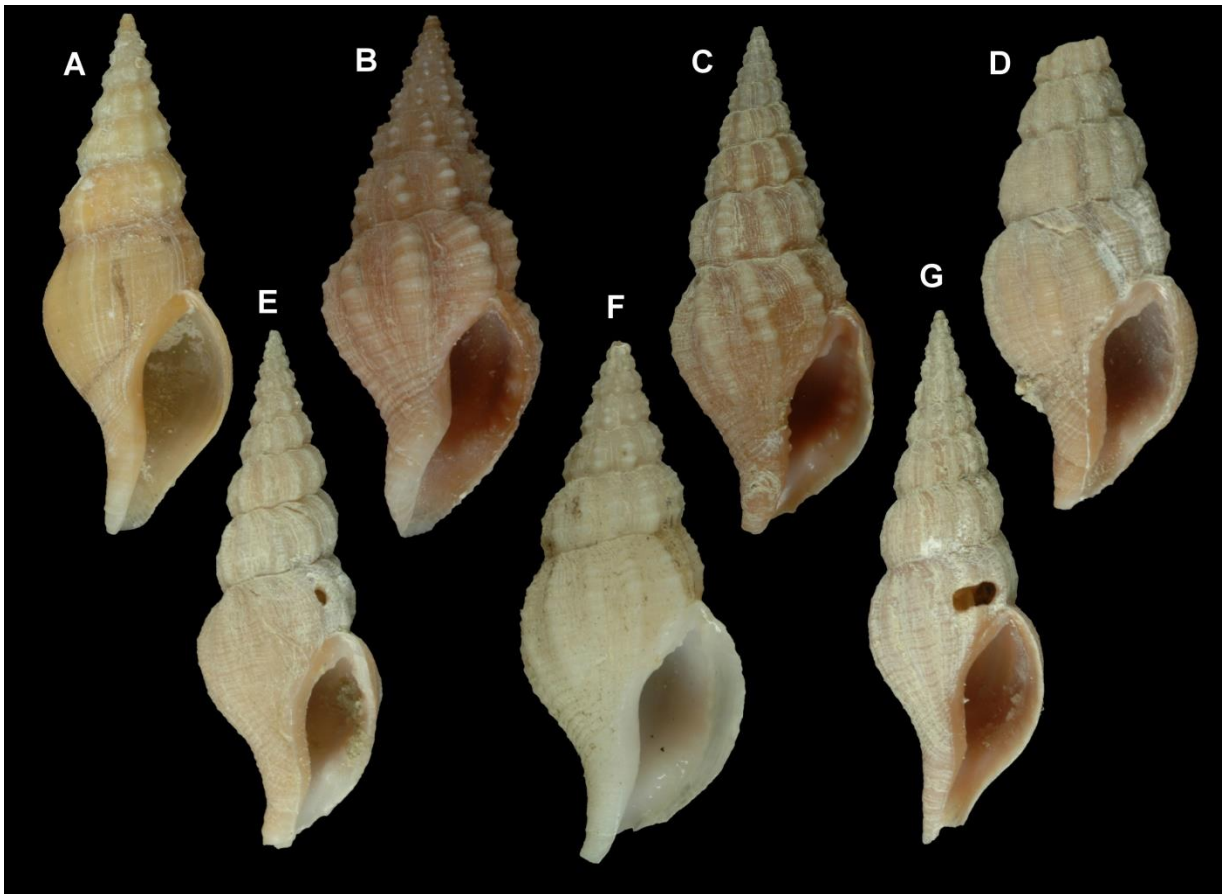


Figure 29. *Amiantofusus pacificus*, shell. **A**: MNHN IM-2009-13533 (28.1mm). **B**: MNHN IM-2013-41243 (23.2mm). **C**: MNHN IM-2013-44400 (29.3mm). **D**: MNHN IM-2013-42506 (30.3mm). **E**: MNHN IM-2013-42508 (36.9mm). **F**: MNHN IM-2013-44179 (28.8mm). **G**: MNHN IM-2013-42464 (37.1mm).

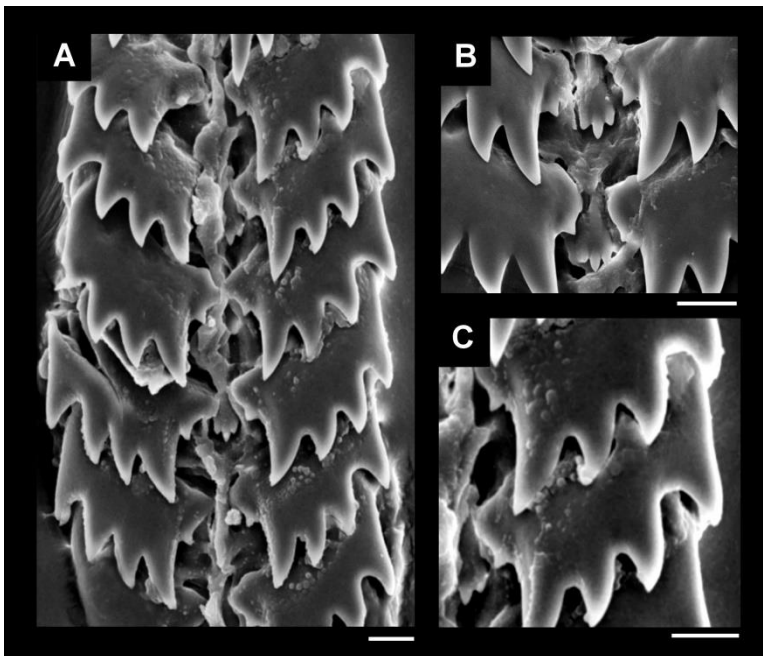


Figure 30. *Amiantofusus pacificus*, radula. **A-C**: MNHN IM-2013-44179. **A**: panoramic view. **B**: detail of rachidian tooth. **C**: detail of lateral tooth. Scale bars = 10 $\mu$ m.

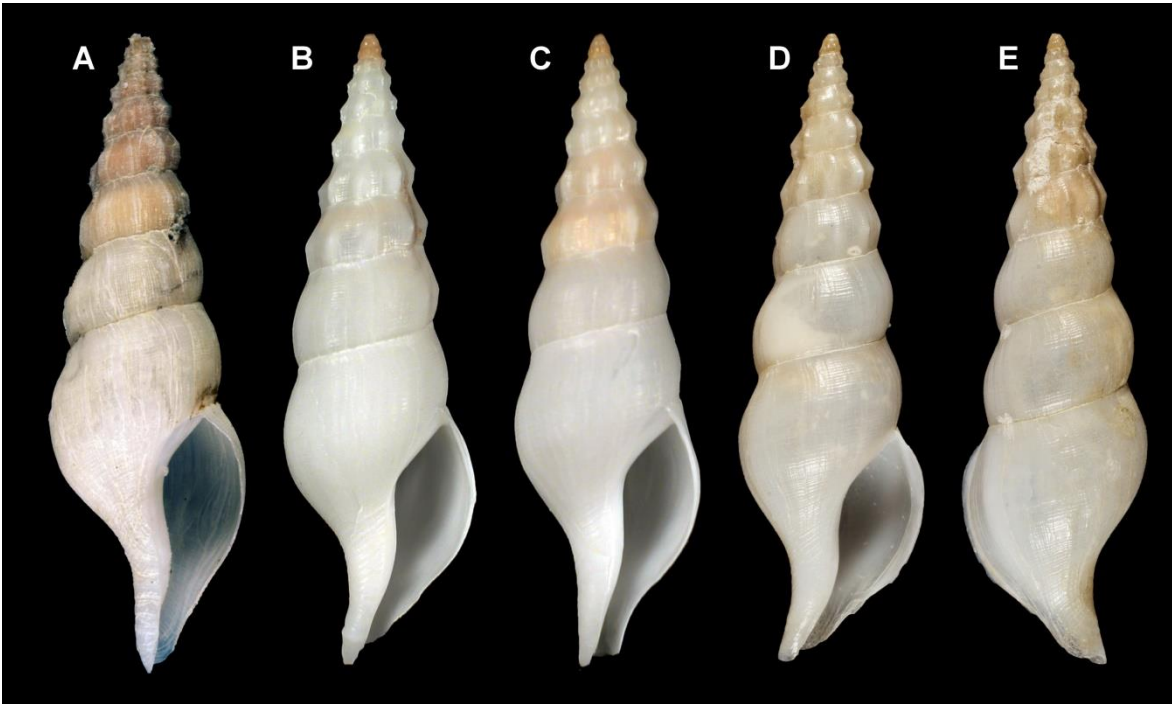


Figure 31. *Amiantofusus candoris*, shell. **A**: MNHN IM-2013-19759 (32.5mm). **B**: MNHN IM-2007-32813 (28mm). **C**: MNHN IM-2007-32814 (26.4mm). **D-E**: holotype MNHN-IM-2007-32814 (26.4mm).

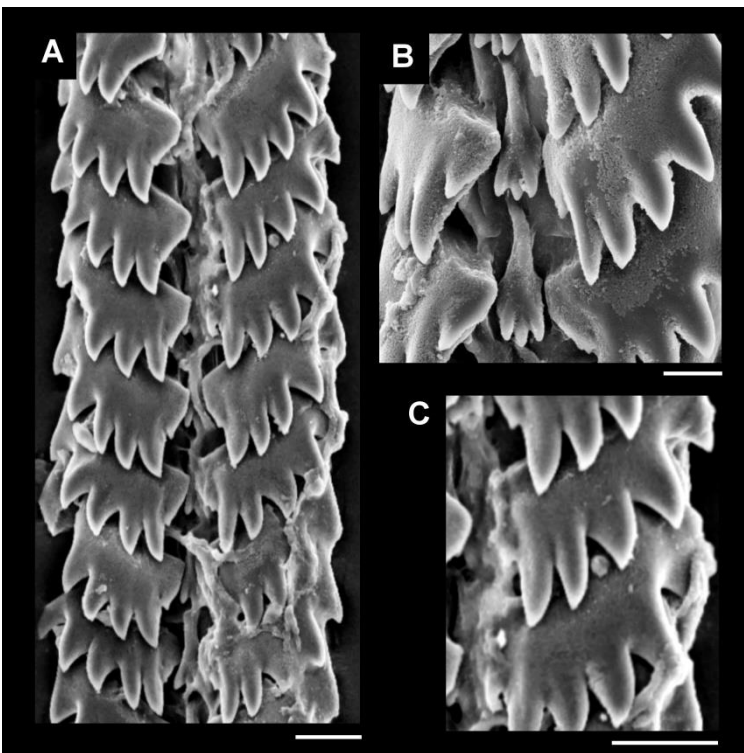


Figure 32. *Amiantofusus candoris*, radula. **A-C**: MNHN 2013-19759. **A**: panoramic view. **B**: detail of rachidian tooth. **C**: detail of lateral tooth. Scale bars = 10 $\mu$ m.

***Amiantofusus candoris* (Figs. 31-32)**

**Examined material:** MNHN IM-2013-19759, N. Long Island, Bismarck Sea, 5°10'27.84"S; 147°2'53.8584"E. PAPUA NIUGINI expedition, ship Alis col. xii/06/2012 [1 specimen].

No known autapomorphies.

**Clade 3**

Siphonal canal of shell long, its length: total shell length  $>1/4$  (9: 2). Margin of renal aperture lipped (34: 1). Rhynchostome bearing longitudinal folds in its margin (39: 1). Lateral tooth of radula much wider than long, its length: width  $1/3-1/2$  (55: 3), bearing 7–15 cusps (58: 2).

**Clade 3a**

Odontophore very short, length: proboscis length  $\leq 1/2$  (42: 2). Rachidian tooth trapezoidal-shaped, its base width: edge width  $\leq 1/2$  (50: 2). Proboscis very long, coiled within sheath (65: 1).

***Pseudolatirus pallidus* (Figs. 33-34)**

**Examined material:** MNHN IM-2013-19937, Dampier Strait, E Umboi Island, Salomon Sea, 5°36'18.2988"S; 148°12'38.4408"E. PAPUA NIUGINI expedition, ship Alis col. xii/12/2012 [1 specimen]. MNHN IM-2007-32537, Tetepare, Salomon Islands, 384-418m depth 8°39'58.1976"S; 157°31'40.1952"E. SALOMON 2 expedition, Alis ship col. xi/07/2004. [1 specimen]. MNHN IM-2013-19011, Bismarck Sea, NE Sissano, 2°55'19.6212"S; 142°10'41.8764"E. PAPUA NIUGINI expedition, ship Alis col. xii/20/2012 [1 specimen]. MNHN IM-2007-32913, Bohol Sea, Maribojoc Bay, Philippines, 382-434m depth, 9°36'11.9988"N; 123°43'48.0108"E. PANGLAO 2005 expedition, DA-BFAR ship col. v/31/2005 [1 specimen]. MNHN IM-2013-44506, China Sea, Continental slop, 333-421m depth, 20°1'52.3704"N; 114°9'21.3192"E. NanHai 2014 expedition, Ocean Researcher 5 ship, Chen Wei-jen col. i/11/2014 [1 specimen]. MNHN IM-2013-44495, China Sea, continental slop, 333-421m depth, 20°1'52.3704"N; 114°9'21.3192"E. NanHai 2014 expedition, Ocean Researcher 5 ship, Chen Wei-jen col. i/11/2014 [1 specimen].

Osphradium heavily asymmetrical (23: 2), its right leaflets longer than left. Proboscis retractor muscles inserting posteriorly (68: 0). Penis ejaculatory duct as long convoluted tube immersed in haemocoel (89: 1).

**Clade 3b *Chryseofusus* + *Fusinus***

Loss of inner sculpture of outer lip (7: 0). Odontophore m6 muscle posterior free portion: odontophore length  $\leq 1/6$  (45: 1). Base of lateral tooth of radula curved (59: 1).

**Clade 3b<sup>1</sup> *Chryseofusus***

Loss of spiral sculpture of shell (3: 0). Osphradium heavily asymmetrical (23: 2), its right leaflets longer than left. Ventral fold of siphon in pallial cavity with a wide base (31: 1). Bursa copulatrix short, its length: oviduct length  $< 1/4$  (80: 0). Female cement gland opening centrally (84: 0) in foot sole.

***Chryseofusus acherusius* (Figs. 35-36)**

**Examined material:** MNHN IM-2013-44302, China Sea, off Taiping Island, 1707-1799m depth, 10°25'37.056"N; 114°14'20.5044"E. NanHai 2014 expedition, Ocean Researcher 5 ship, Chen Wei-jen col. i/06/2014 [1 specimen]. MNHN IM-2013-44363, China Sea, off An-Da Chiao, 464-1076m depth, 10°24'52.398"N; 114°46'9.4872"E. NanHai 2014 expedition, Ocean Researcher 5 ship, Chen Wei-jen col. i/07/2014 [1 specimen].

Loss of longitudinal folds in margin of rhynchostome (39: 0).



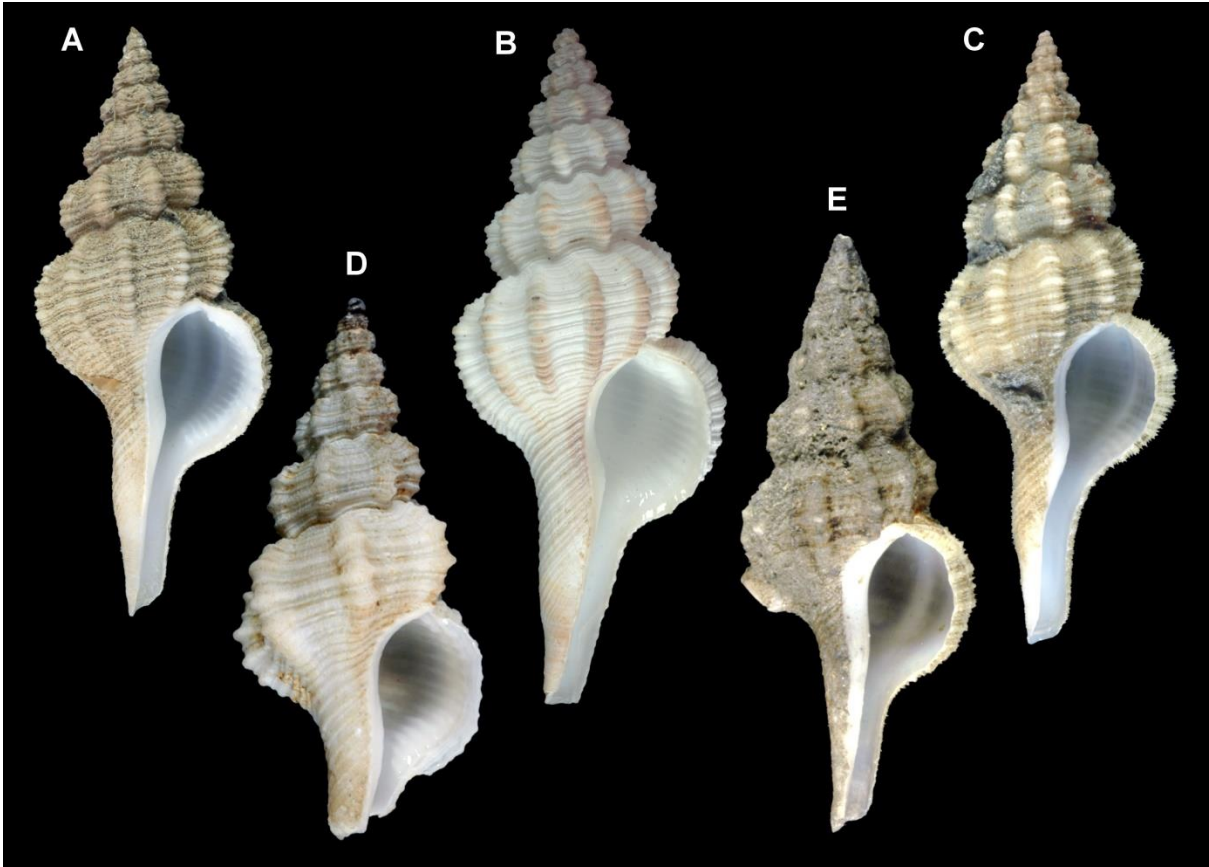


Figure 33. *Pseudolatirus pallidus*, shell. **A**: MNHN IM-2013-19937 (49.3mm). **B-E**: modified from Muséum national d'Histoire naturelle, Paris (France) Collection: Molluscs (IM). **B**: MNHN IM-2007-32537 (63.5mm). **C**: MNHN IM-2013-19011 (56.7mm). **D**: MNHN IM-2007-32913 (24.3mm). **E**: MNHN IM-2013-44506 (39.8mm).

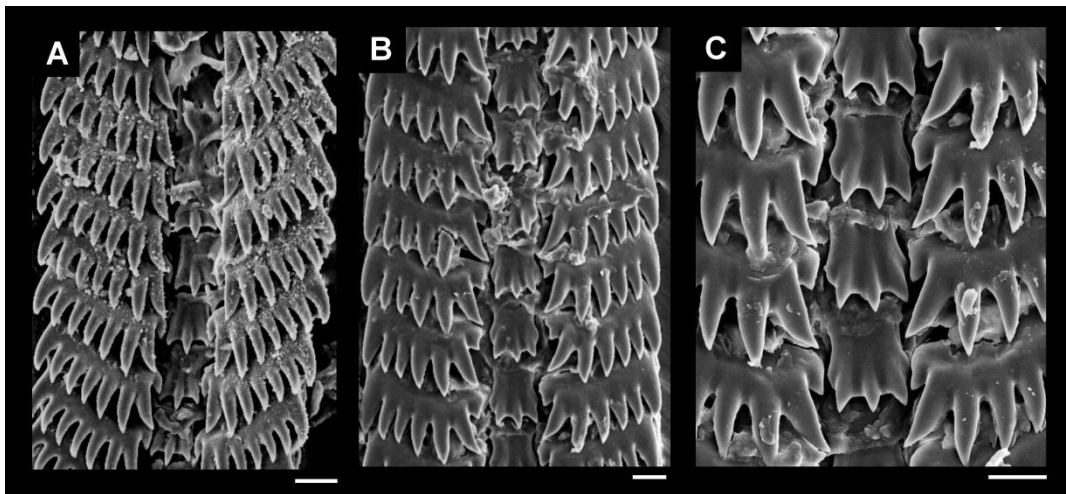


Figure 34. *Pseudolatirus pallidus*, radula. **A**: MNHN IM-2013-19937, panoramic view. **B-C**: MNHN IM-2013-44506. **B**: panoramic view. **C**: detail of rachidian tooth. Scale bars = 20µm.



Figure 35. *Chryseofusus archerius*, shell. MNHN IM-2013-44302 (56.2mm).

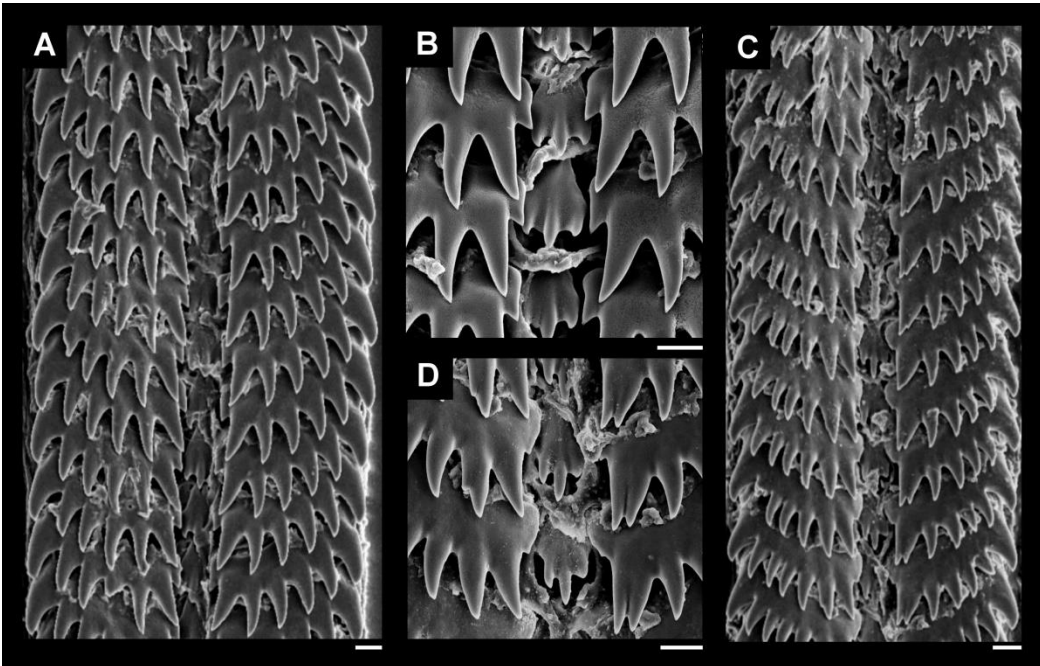


Figure 36. *Chryseofusus archerius*, radula. **A-B**: MNHN IM-2013-44302. **A**: panoramic view. **B**: detail of rachidian tooth. **C-D**: MNHN IM-2013-44363. **C**: panoramic view. **D**: detail of rachidian tooth. Scale bars = 20 $\mu$ m.

***Chryseofusus graciliformis* (Figs. 37-38)**

**Examined material:** MNHN IM-2007-32797, Salomon Islands, 650-673m depth, 7° 42'30.5388"S; 156°24'50.076"E. SALOMON 2 expedition, Alis ship col. xi/01/2004. [1 specimen]. MNHN IM-2013-19921, SE Tuam Island, Salomon Sea, 500-555m depth, 6°4'15.1788"S; 148°10'25.3416"E. PAPUA NIUGINI expedition, ship Alis col. xii/11/2012 [1 specimen]. MNHN IM-2013-19938, Dampier Strait, E Umboi Island, Salomon Sea, 500-640m depth, 5°36'18.2988"S; 148°12'38.4408"E. PAPUA NIUGINI expedition, ship Alis col. xii/12/2012 [1 specimen].

Head large, its width: head-foot mass width  $\geq 1/2$  (13: 2), bearing long cephalic tentacles, its length: head width  $\leq 2/3$  (14: 2).

**Clade 3c *Fusinus* + *Cyrtulus***

Ctenidium narrow, its width: osphradium width  $< 1$  (28: 0). Rhynchostome as simple, not lipped, slit (40: 1). Odontophore cartilages fused anteriorly  $\geq 15\%$  of total odontophore length (44: 2). Radula bearing lateral tooth with progressive increase in innermost cusps 1–3 length (63: 1). Medium esophagus with posterior ventral glandular region (72: 1) posterior to valve of Leiblein and anterior to nerve ring. Buccal ganglia commissure length: buccal ganglia length  $\geq 1/2$  (94:1).

**Clade 3c<sup>1</sup>**

Loss of lipped margin of renal aperture (34: 0). Pedal ganglia short, its length: nerve ring length  $< 1/2$  (90: 0).

***Fusinus brasiliensis* (Figs. 39-40)**

**Examined material:** MZSP 70512, off Vitoria, Espírito Santo State, Brazil, trawled by shrimp boats, 30-40m depth. xii/2003 [~80 specimens]. MNRJ 8660, off Vitoria, Espírito Santo State, Brazil. 2001 [8 specimens]. MNRJ 8960, northern Rio de Janeiro state, Brazil. x/15/1963 [1 specimen].

No known autapomorphies.



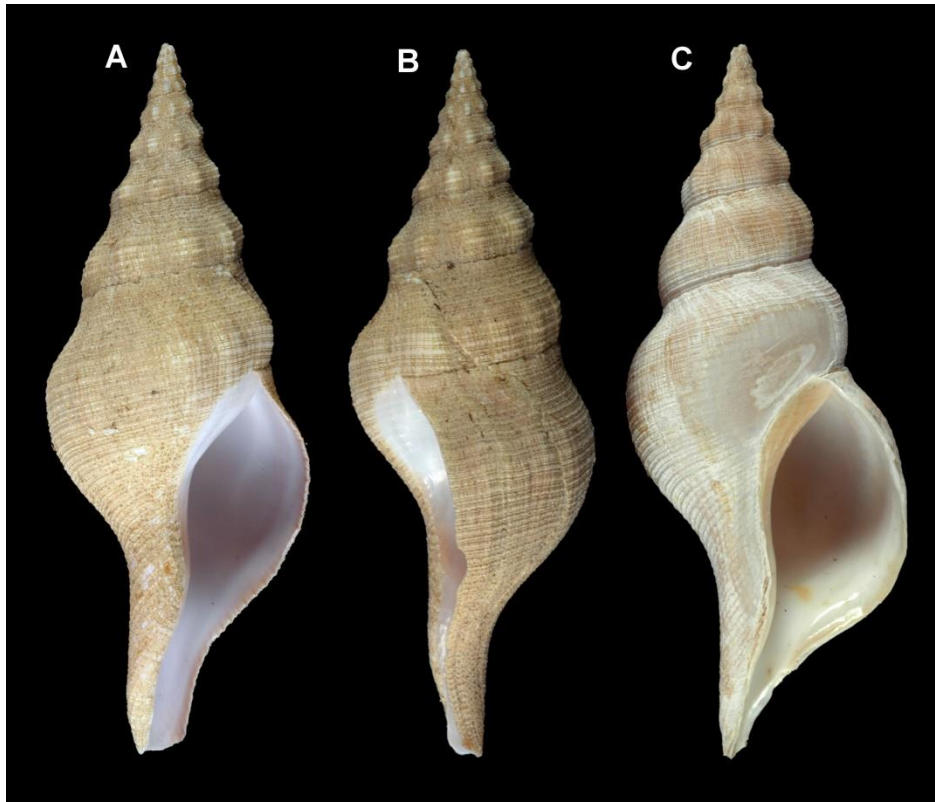


Figure 37. *Chryseofusus graciliformis*, shell. **A-B**: MNHN IM-2013-19921 (88.4mm). **C**: MNHN IM-2007-32797 (84mm).

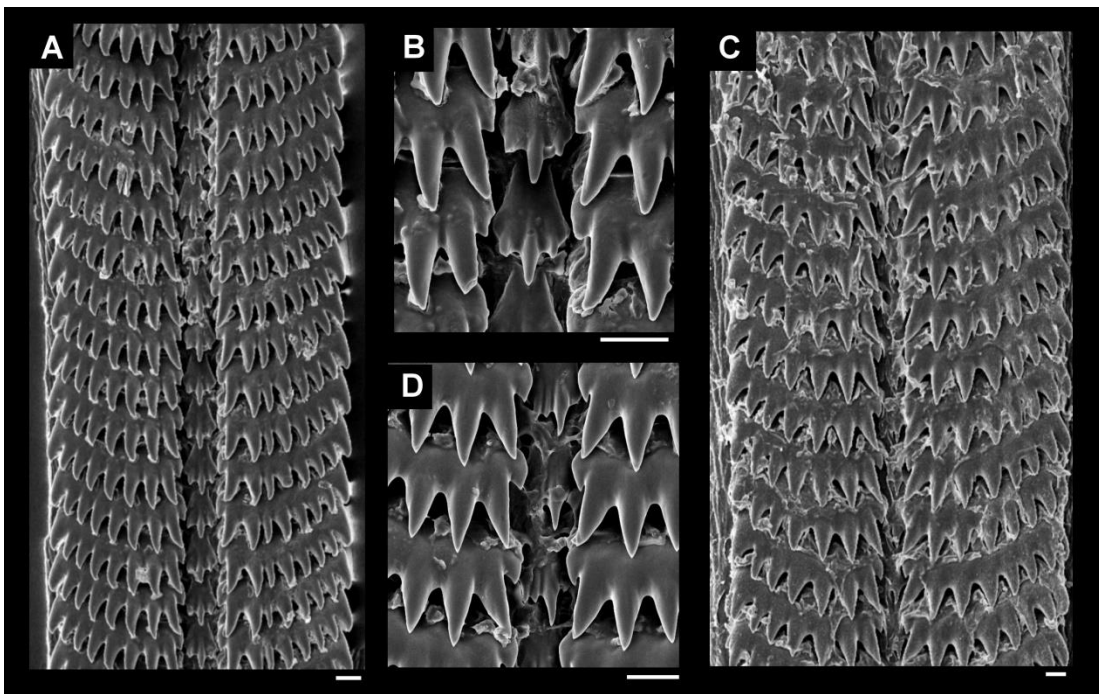


Figure 38. *Chryseofusus graciliformis*, radula. **A-B**: MNHN IM-2013-19938. **A**: panoramic view. **B**: detail of rachidian tooth. **C-D**: MNHN IM-2013-19921. **D**: panoramic view. **D**: detail of

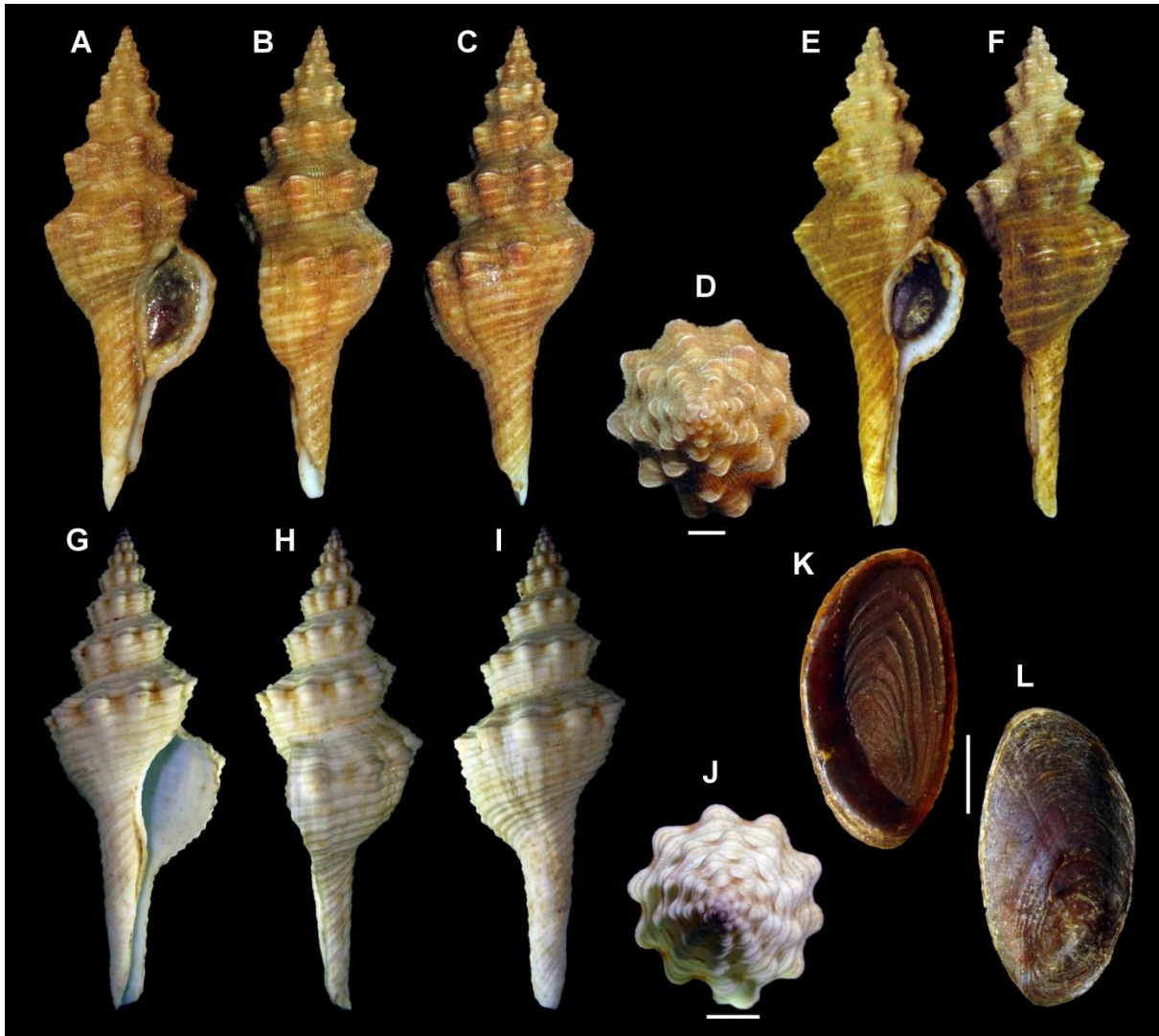


Figure 39. *Fusinus brasiliensis*, shell and operculum. **A-D**: MZSP 70512 (97.4mm). **E-F**: MNRJ 8660 (96.4mm). **G-I**: MNRJ 8960 (97.4mm). **K**: operculum, inner view. **L**: operculum, outer view. Scale bars = 5mm.

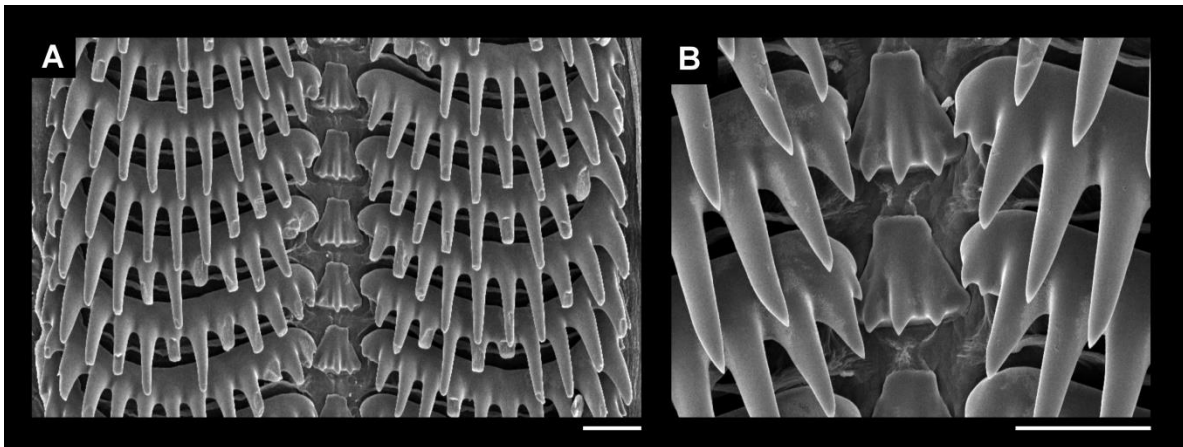


Figure 40. *Fusinus brasiliensis*, radula. **A-B**: MNRJ 8660. **A**: panoramic view. **B**: detail of rachidian tooth. Scale bars = 50µm.

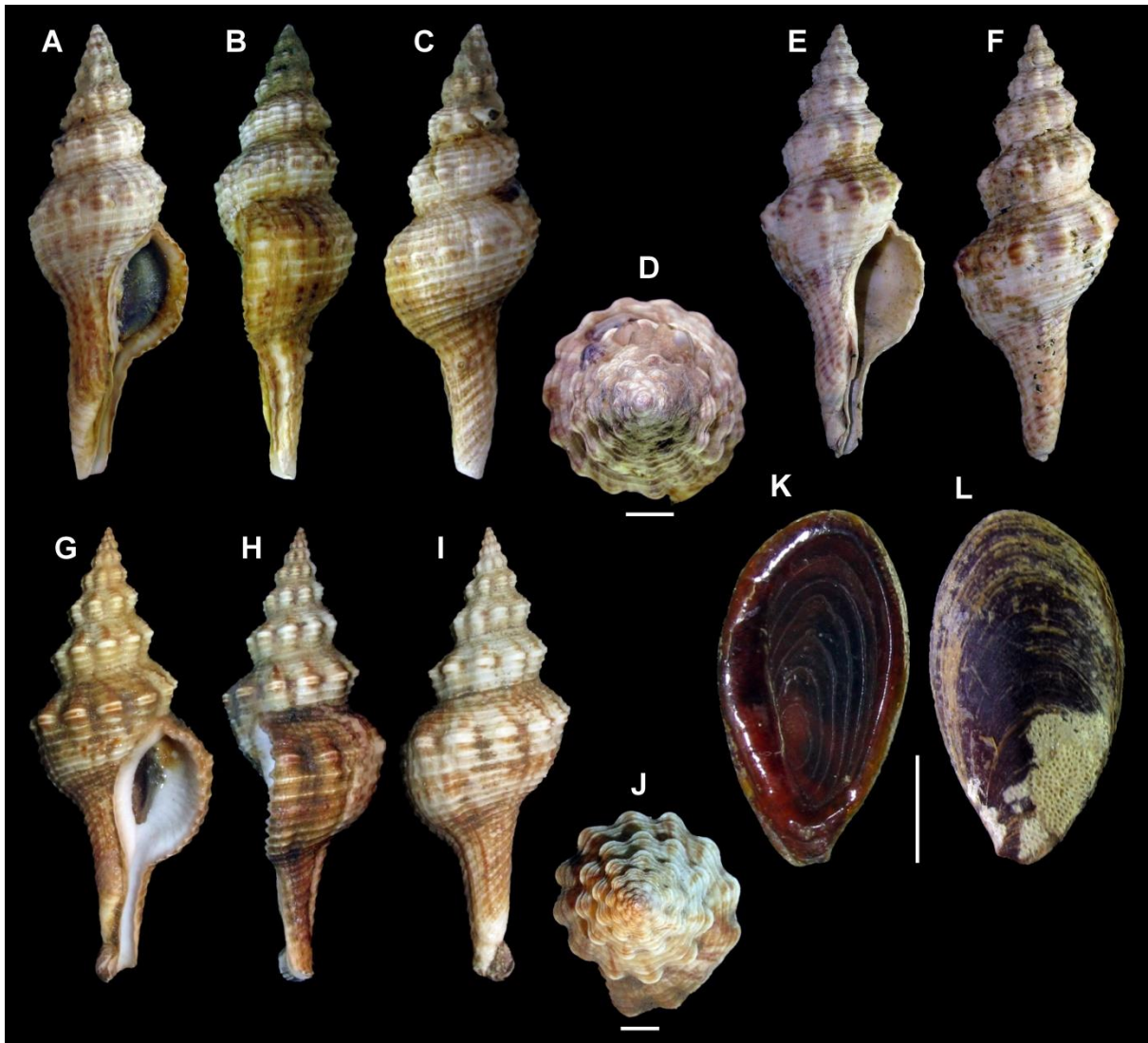


Figure 41. *Fusinus marmoratus*, shell and operculum. A-D: MNRJ 14489 (97.8mm). E-F: MNRJ 14588 (89.1mm). G-J: MZSP 77515 (87.8mm). K: operculum, inner view. L: operculum, outer view. Scale bars = 5mm.



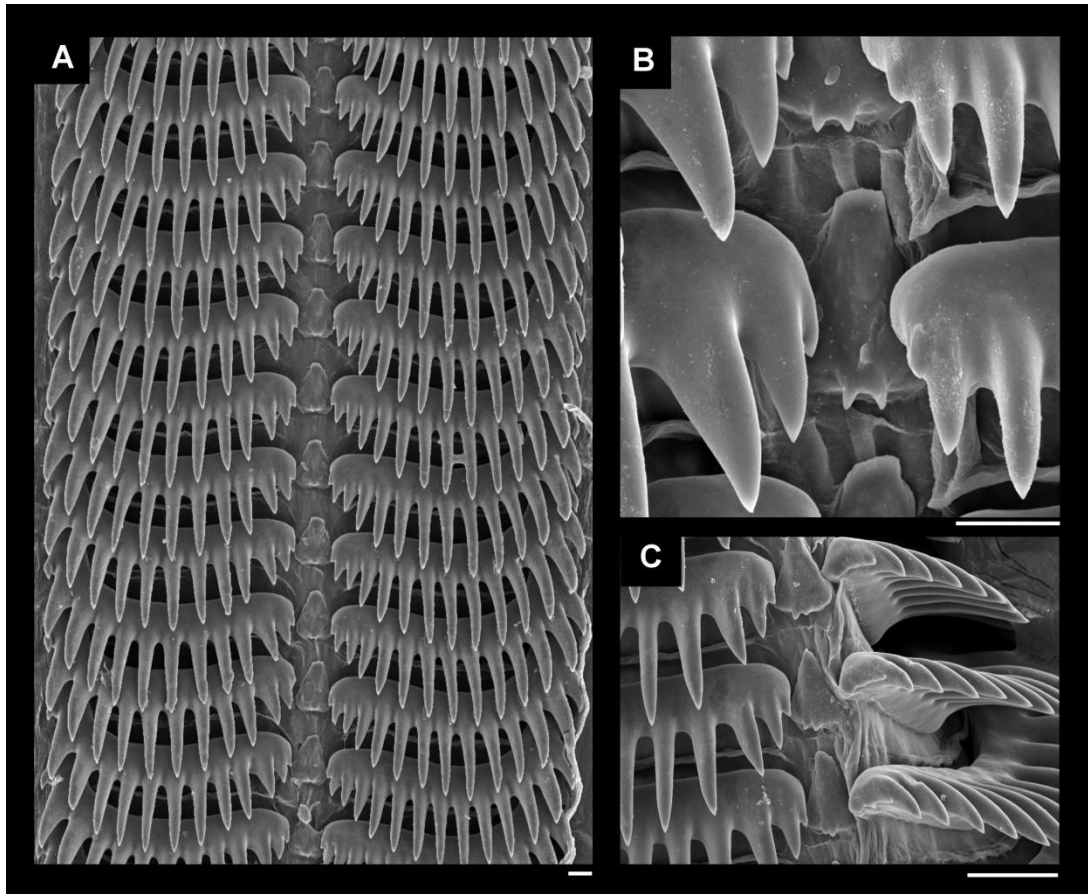


Figure 42. *Fusinus marmoratus*, radula. A-D: MNRJ 10715. A: panoramic view. B-C: detail of rachidian tooth. Scale bars = 20 $\mu$ m.

**Clade 3c<sup>1a</sup> *Fusinus marmoratus* + *Fusinus* sp.**

Head medium-sized, its width: head-foot mass width 1/4–1/2 (13: 1), bearing short cephalic tentacles, its length: head width 1/2–2/3 (14: 1).

***Fusinus marmoratus* (Figs. 41-42)**

**Examined material:** MNRJ 14243, Mangunho, Búzios, Rio de Janeiro state, Brazil. R. Arlé, B. M. Tursh, A. Coelho, S. Buitone & A. Rosas cols. iii/31/1962 [2 specimens]. MNRJ 14489, João Fernandes Beach, Búzios, Rio de Janeiro state, Brazil. R. Novelli & O. S. I. Neto cols. vii/20/1982 [2 specimens]. MNRJ 14588, Santana Island, Cabo Frio, Rio de Janeiro state, Brazil, 23°36'S; 41°26'W. Santo Antônio ship col. x/09-23/1964 [1 specimen]. MZSP 77515, Ubatuba, São Paulo state, 4m depth. L.R.L. Simone col. ix/29/1991 [3 specimens].

No known autapomorphies.

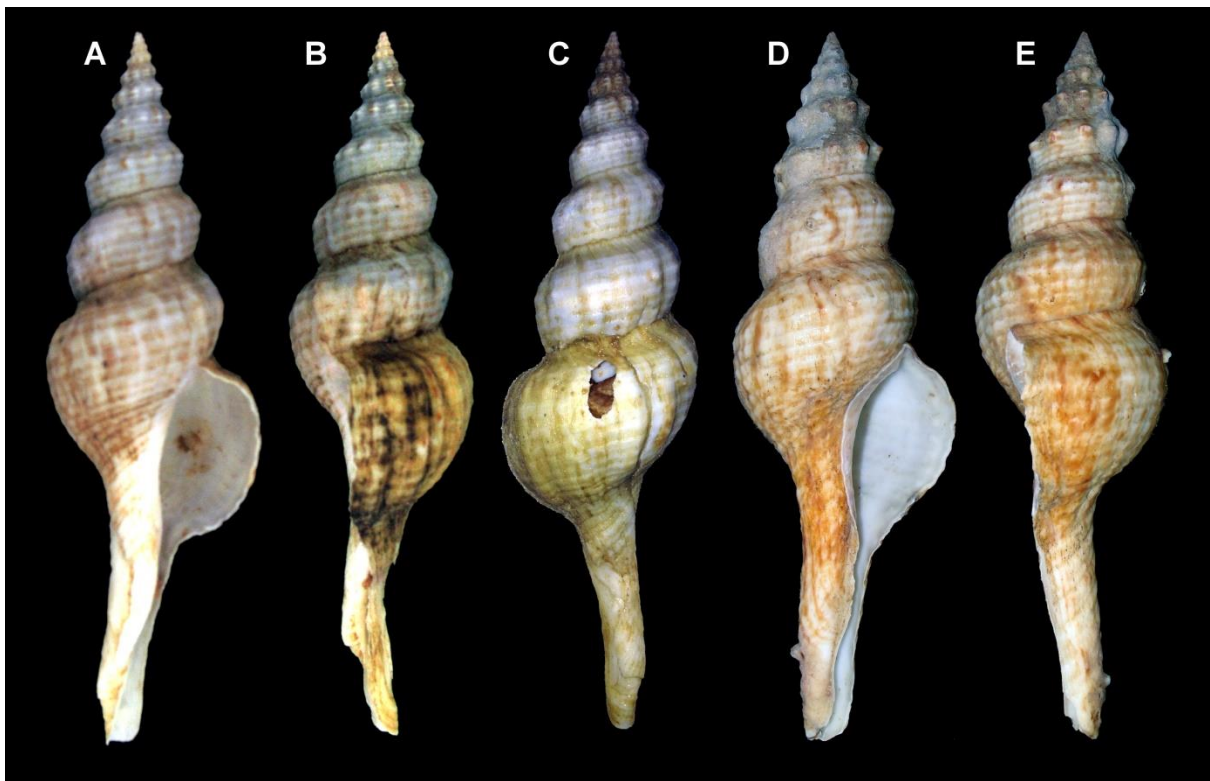


Figure 43. *Fusinus* sp., shell. A-C: MNRJ 6258 (183.5mm). D-E: MNRJ 6259 (203mm).

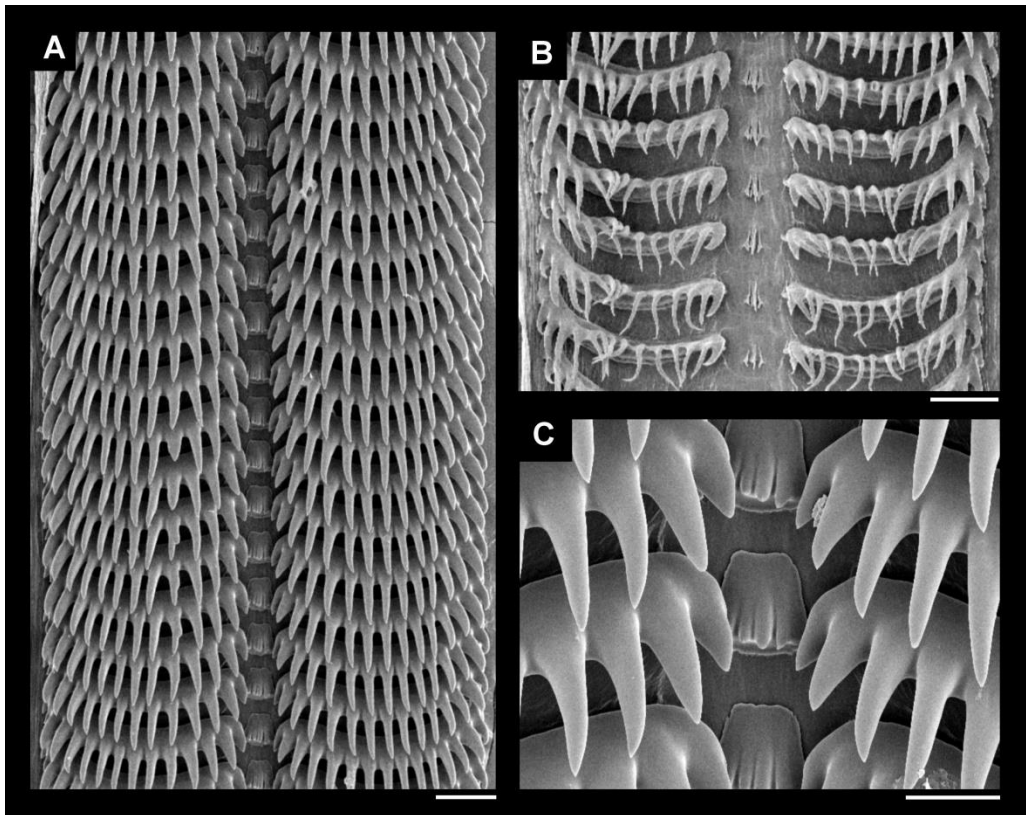


Figure 44. *Fusinus* sp., radula. A-C: MNRJ 6259. A: posterior region panoramic view. B: anterior region panoramic view. C: detail of rachidian tooth. Scale bars = 100 $\mu$ m.



***Fusinus* sp. (Figs. 43-44)**

**Examined material:** MNRJ 6258, Paulista beach, Macaé, Rio de Janeiro state, Brazil, 70m depth, 22°59'S; 41°13'W. v/10/1974 [1 specimen]. MNRJ 6259, Paulista beach, Macaé, Rio de Janeiro state, Brazil, 78m depth, 23°02'S; 41°17'W. v/10/1974 [1 specimen]

Rachidian tooth of radula trapezoidal-shaped, its base width: edge width 1/2–1 (50: 1).

**Clade 3d *Fusinus* “osphradium digitated”**

Osphradium bearing leaflets with digitated terminal shape (25: 1). Anus close to mantle border, its distance from mantle border: total pallial cavity length <1/3 (77: 0).

***Fusinus frenguelli* (Figs. 45-46)**

**Examined material:** MNRJ 14414 (paratype), Rio de Janeiro state, Brazil. Santo M.S. Neves Antônio ship col. 1966 [3 specimens]. MNRJ 7829, Rio de Janeiro state, Brazil. xi/17/1995 [1 specimen]. MNRJ 14595, 35 miles off the coast of Guaratiba, Rio de Janeiro state, Brazil, 35-40m depth. M.S. Neves col. iv/1963 [5 specimens]. MNRJ 14487, Rio de Janeiro state, Brazil 23°6'S; 43°17'W. 1976 [1 specimen]. MNRJ 14488, Laje dos Santos, Queimada Grande Island, São Paulo state, Brazil. M.S. Neves col. iv/1964 [2 specimens]. MNRJ 14709, Cape of Santa Marta, Santa Catarina state, Brazil, 85m depth, 29°18'80"S; 49°01'W. Almirante Saldanha oceanographic ship col. ix/25/1967 [1 specimen]. MZSP 77531, Alcatrazes Island, São Paulo state, Brazil, 32m depth. viii/1998 [17 specimens].

Rachidian tooth of radula trapezoidal-shaped, its base width: edge width 1/2–1 (50: 1), bearing minute, secondary cusps (52: 1). Cement gland opening centrally in foot sole (84: 0). Duct of penis linear (87: 0).

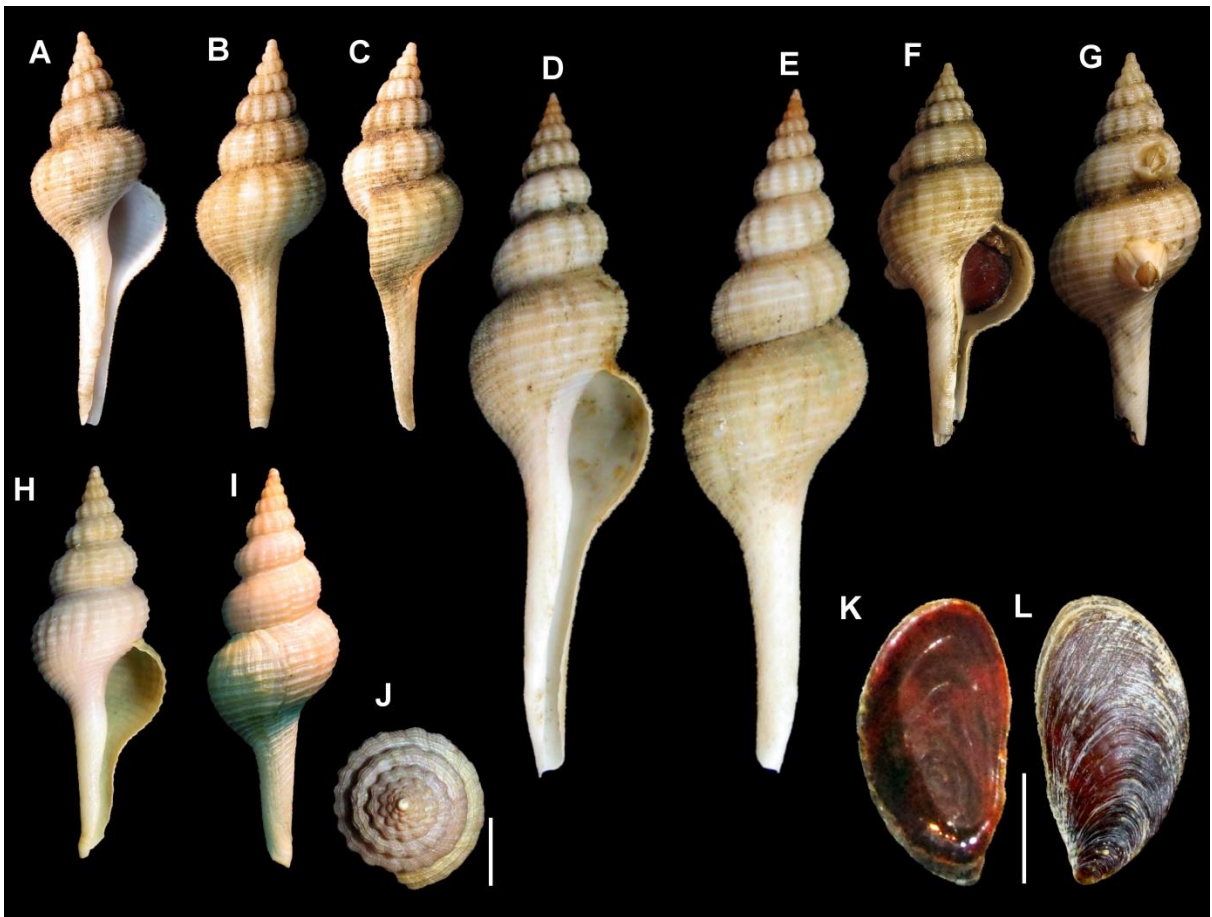


Figure 45. *Fusinus frenguelli*, shell. **A-C**: MNRJ 7829 (51.6mm). **D-E**: MZSP 77531 (89.2mm). **F-G**: MNRJ 14488 (56mm). **H-I**: MNRJ 14487 (50.4mm). **K**: operculum, inner view. **L**: operculum, outer view. Scale bars = 5mm.

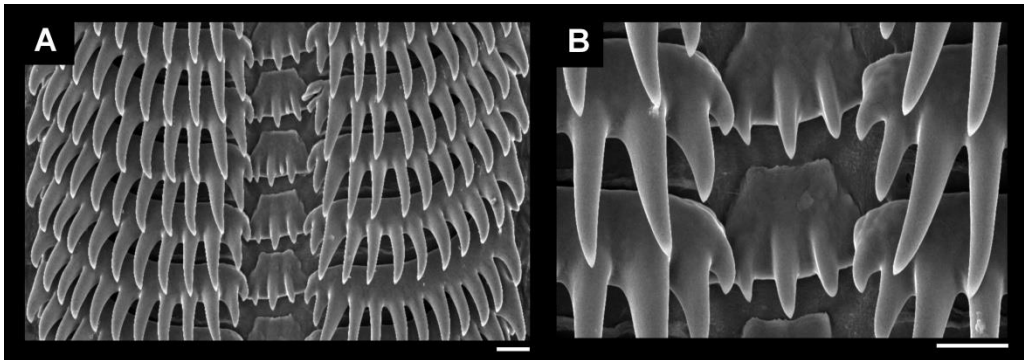


Figure 46. *Fusinus frenguelli*, radula. **A-B**: MZSP 47147. **A**: panoramic view. **B**: detail of rachidian tooth. Scale bars = 20µm.



Figure 47. *Fusinus australis*. shell. MNHN IM-2013-42513 (57.1mm).

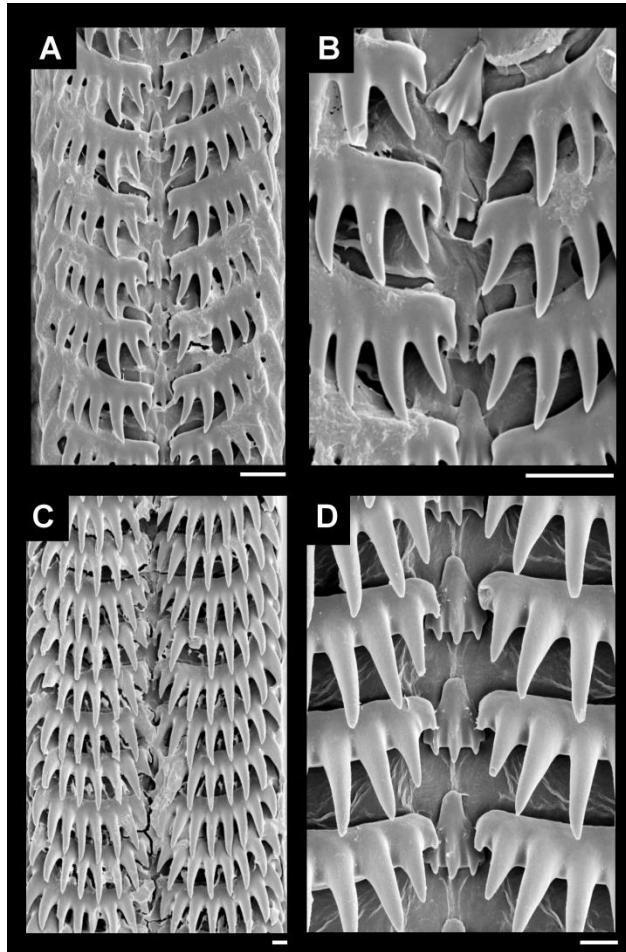


Figure 48. *Fusinus australis*. radula. **A-D**: MNHN IM-2013-42513. **A**: panoramic view. **B**: detail of rachidian tooth. **C**: panoramic view. **D**: detail of rachidian tooth. Scale bars = 20 $\mu$ m.

### Clade 3e *Fusinus australis* + *Cyrtulus serotinus*

Outer lip of shell with continuous spiral cord sculpture (7: 1). Head medium-sized, its width: head-foot mass width 1/4–1/2 (13: 1), bearing short cephalic tentacles, its length: head width 1/2–2/3 (14: 1).

#### *Fusinus australis* (Figs. 47-48)

**Examined material:** MNHN IM-2013-42513, Albany, Mistaken Island, King George Sound, Australis. 5-12m depth, 35°3'43.344"S; 117°56'54.06"E. WESTERN AUSTRALIA 2011 expedition. xi/30/2011 [1 specimen]. MNHN IM-2013-42517. Albany, Cheyne Ledge, King George Sound, 35°0'30.672"S; 117°57'6.84"E. WESTERN AUSTRALIA 2011 expedition. xi/27/2011 [1 specimen].

Proboscis retractor muscles inserting posteriorly (68: 0).

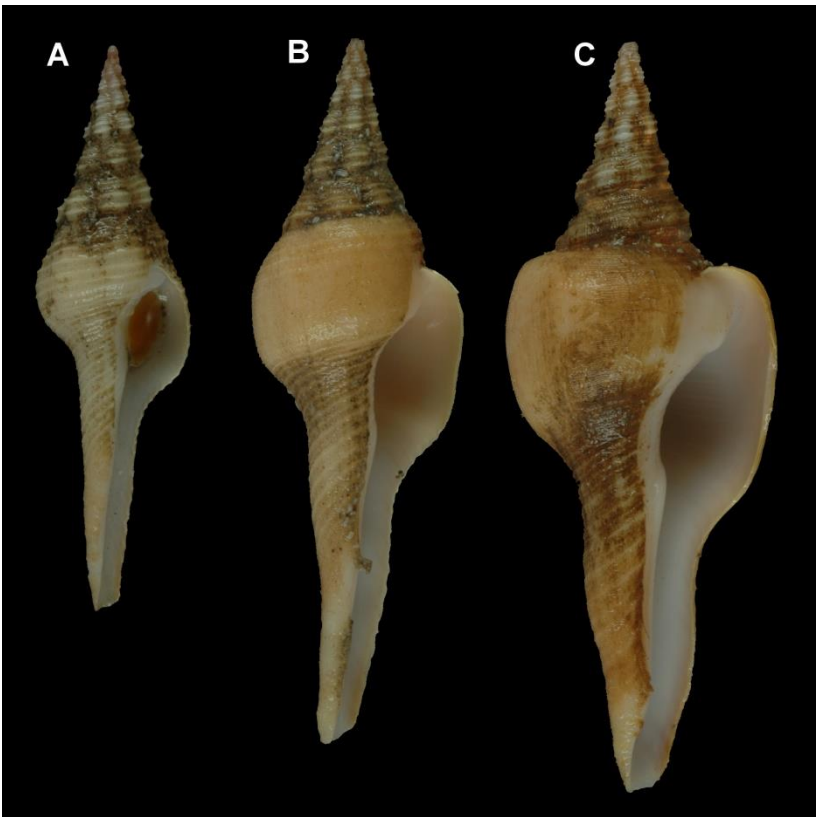


Figure 49. *Cyrtulus serotinus*, shell in growth series. **A**: MNHN IM-2013-42530 (36.7mm). **B**: MNHN IM-2013-42531 (54.5mm). **C**: MNHN IM-2013-42532 (57.3mm).

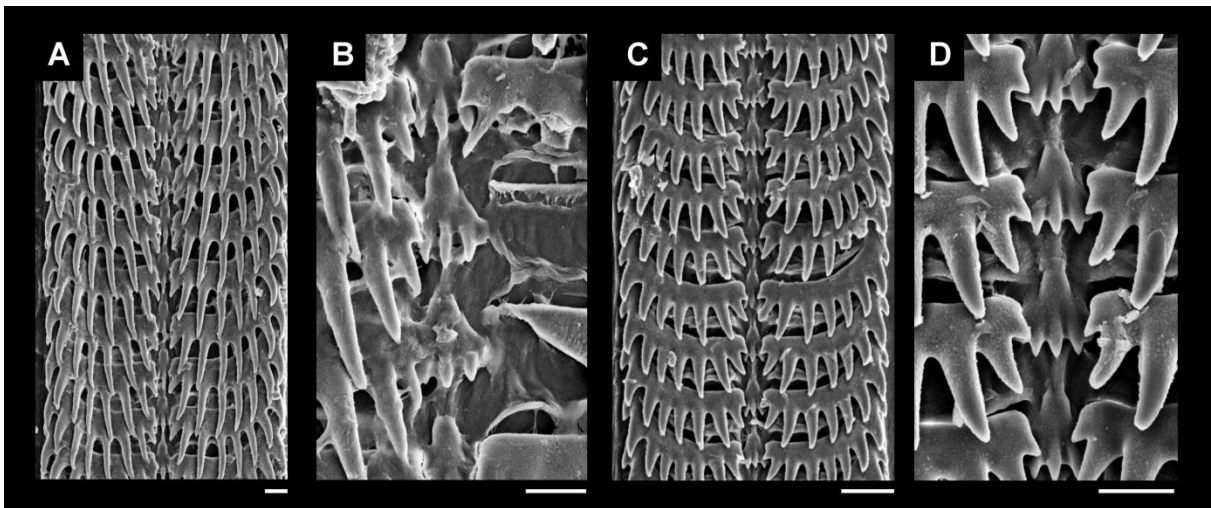


Figure 50. *Cyrtulus serotinus*, radula. **A-B**: MNHN IM-2013-42531. **A**: panoramic view. **B**: detail of rachidian tooth. **C-D**: MNHN IM-2013-42529. **C**: panoramic view. **D**: detail of rachidian tooth. Scale bars = 20 $\mu$ m.

***Cyrtulus serotinus* (Figs. 49-50)**

**Examined material:** MNHN IM-2013-42529, Marquesas Archipelago, N bay of Vaituha, 7°58'46.4412"S; 140°42'42.3"W. PAKAIHI I TE MOANA expedition. xi/24/2011 [1 specimen]. MNHN IM-2013-42530, Marquesas Archipelago, Tahuata, 9°58'49.9188"S; 139°7'47.1"W. PAKAIHI I TE MOANA expedition. xii/05/2011 [1 specimen]. MNHN IM-2013-42531, Marquesas Archipelago, Tahuata, 9°58'49.9188"S; 139°7'47.1"W. PAKAIHI I TE MOANA expedition. xii/05/2011 [1 specimen]. MNHN IM-2013-42532, Marquesas Archipelago, N bay of Vaituha, 7°58'46.4412"S; 140°42'42.3"W. PAKAIHI I TE MOANA expedition. xi/24/2011 [1 specimen].

Outer lip of shell with apical growth (6: 0). Buccal ganglia commissure diminute, its length: buccal ganglia length  $\leq 1/2$  (94: 0).

**Clade 4 *Granulifusus* + Peristerniinae + Fasciolarinae**

Ctenidium narrow, its width: osphradium width  $< 1$  (28: 0). Rhynchostome bearing lipped rim (40: 1).

**Clade 4a *Granulifusus* “round opercula, not filling entire aperture”**

Loss of inner sculpture of outer lip (7: 0). Head large, its width: head-foot mass width  $\geq 1/2$  (13: 2), bearing long cephalic tentacles, its length: head width  $\leq 2/3$  (14: 2). Operculum small, not filling entire shell aperture (16: 2), its nucleus eccentric (17: 1) and lateral margin rounded (18: 0). Osphradium with right leaflets longer than left, heavily asymmetrical (23: 2). Loss of female cement gland (82: 0).





Figure 51. *Granulifusus* sp. shell. MNHN IM-2013-19724 (56.2mm).

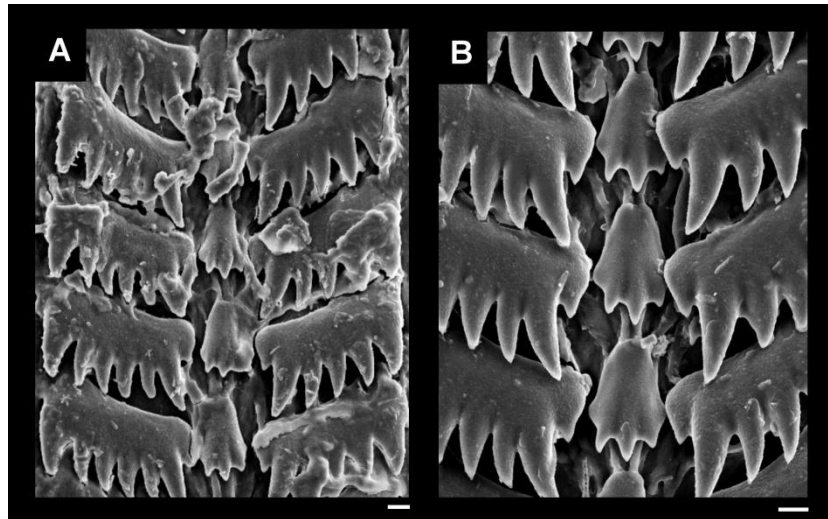


Figure 52. *Granulifusus* sp. radula. **A-B**: MNHN IM-2013-19724. **A**: panoramic view. **B**: detail of rachidian tooth. Scale bars = 10µm.

***Granulifusus* sp. (Figs. 51-52)**

**Examined material:** MNHN IM-2013-19724. N Long I. Bismarck Sea, 5°10'51.4812"S; 147°3'3.4164"E. PAPUA NIUGINI expedition, ship Alis col. xii/06/2012 [1 specimen].

Anus close to mantle border, its distance from mantle border: total pallial cavity length <math>< 1/3</math> (77: 0). Bursa copulatrix bearing anterior muscular bulb (81: 1) close to gonopore.

**Clade 4b**

Proboscis retractor muscles inserting posteriorly (68: 0). Seminal receptacle in pallial oviduct present (78: 0).



Figure 53. *Granulifusus hayashi*, shell. MNHN IM-2013-19210 (48.7mm).

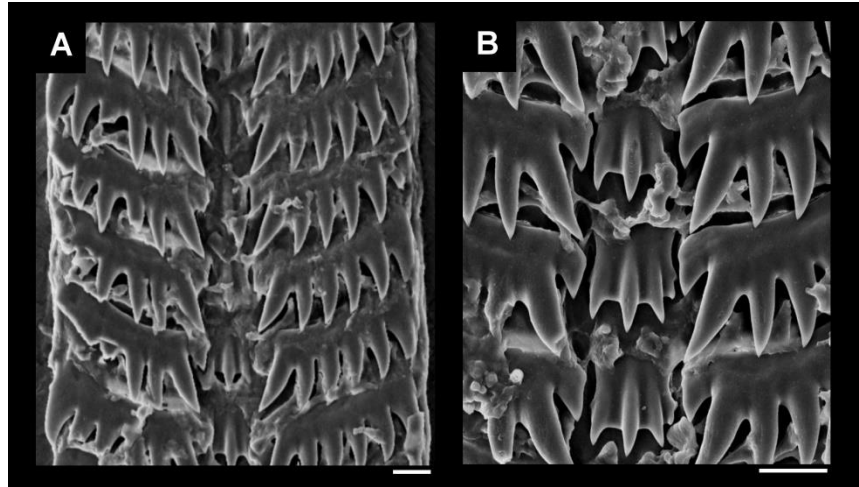


Figure 54. *Granulifusus hayashi*, radula. **A-B**: MNHN IM-2013-19210. **A**: panoramic view. **B**: detail of rachidian tooth. Scale bars = 20 $\mu$ m.

***Granulifusus hayashi* (Figs. 53-54)**

**Examined material:** MNHN IM-2013-19210, Dogreto Bay, Bismarck Sea, 3°17'41.7012"S; 143°2'22.3296"E. PAPUA NIUGINI expedition, ship Alis col. xii/22/2012 [1 specimen].

Odontophore m6 muscle posterior free portion: odontophore length  $\leq 1/6$  (45: 1). Rachidian tooth of radula square-shaped, its base width: edge width 1/2–1 (50: 0). Buccal ganglia commissure length: buccal ganglia length  $\geq 1/2$  (94:1).

**Clade 4c *Granulifusus kiranus* + *Pseudolatirus discrepans***

Margin of siphon bearing many longitudinal folds (30: 1).

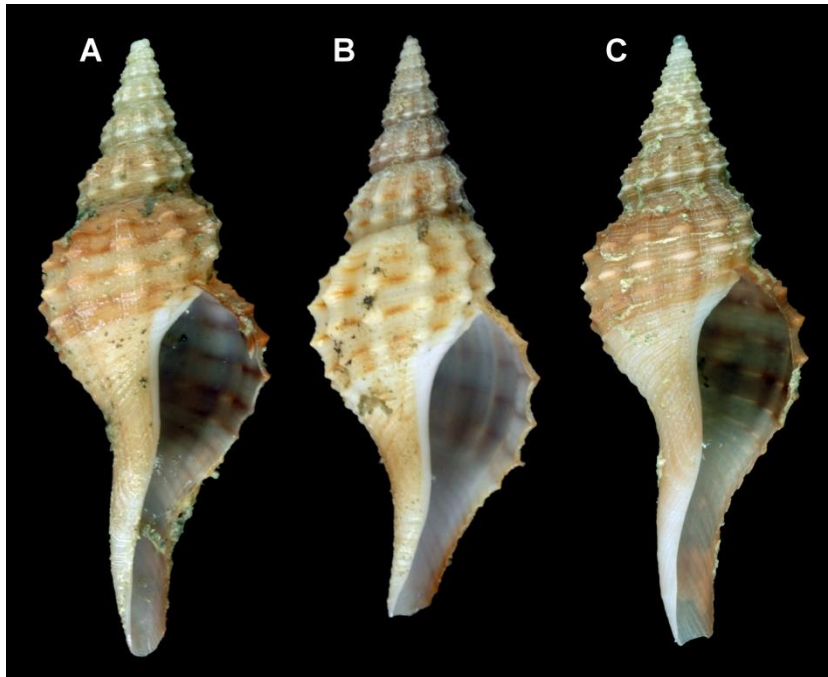


Figure 55. *Granulifusus kiranus*, shell. **A**: MNHN IM-2013-44502 (37.6mm). **B**: MNHN IM-2013-19037 (45.2mm). **C**: MNHN IM-2013-44449 (33.9mm).

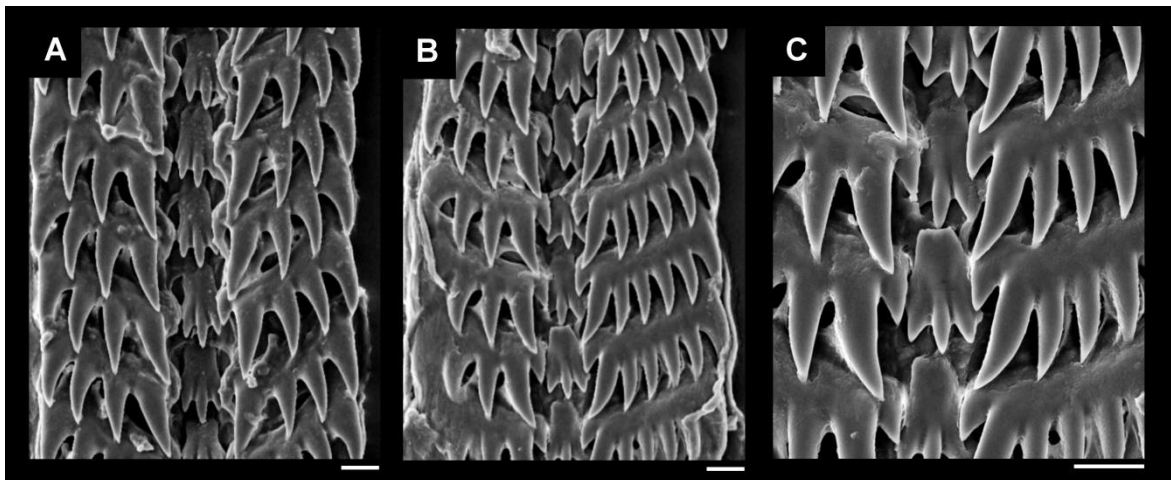


Figure 56. *Granulifusus kiranus*, radula. **A**: MNHN IM-2013-44502, panoramic view. **B-C**: MNHN IM-2013-44449. **B**: panoramic view. **C**: detail of rachidian tooth. Scale bars = 20 $\mu$ m.



***Granulifusus kiranus* (Figs. 55-56)**

**Examined material:**

MNHN IM-2013-44502, continental slope, China Sea, 333-421m depth, 20°1'52.3704"N; 114°9'21.3192"E. NanHai 2014 expedition, Ocean Researcher 5 ship, Chen Wei-jen col. i/11/2014. [1 specimen]. MNHN IM-2013-19037, NE of Sissano, Bismarck Sea, 535-540m depth. 2°54'40.14"S; 142°10'46.326"E. PAPUA NIUGINI expedition, ship Alis col. xii/20/2012 [1 specimen]. MNHN IM-2013-44449, Continental slop, China Sea, 262-298m depth, 20°2'55.4532"N; 114°11'17.4984"E. NanHai 2014 expedition, Ocean Researcher 5 ship, Chen Wei-jen col. i/03/2014 [1 specimen].

No known autapomorphies.

***Pseudolatirus discrepans* (Figs. 57-58)**

**Examined material:** MNHN IM-2013-9777, Astrolabe Bay, Papua New Guinea, 340-385m depth, 5°21'54.36"S; 145°47'48.9696"E. PAPUA NIUGINI expedition, ship Alis col. xii/14/2014 [1 specimen]. MNHN IM-2007-34604, Philippines, 342-358m depth, 16°0'52.2"N; 121°51'11.9988"E. AURORA 2007 expedition, DA-BFAR ship col. v/20/2007 [1 specimen].

Shell with columellar folds presently in mid-aperture (8: 1). Head very small, its width: head-foot mass width <1/4 (13: 0), bearing very short cephalic tentacles, its length: head width <1/2 (14: 0).

**Clade 5 Peristerniinae + Fasciolarinae**

Shell with columella bearing folds (8: 1) medially, pseudo-umbilicus (10: 1) as shallow slit. Head-foot mass pigmentation dark-red (11: 3). Lateral margin of operculum hook-like (18: 2). Base of lateral tooth of radula slightly curved (59: 1).

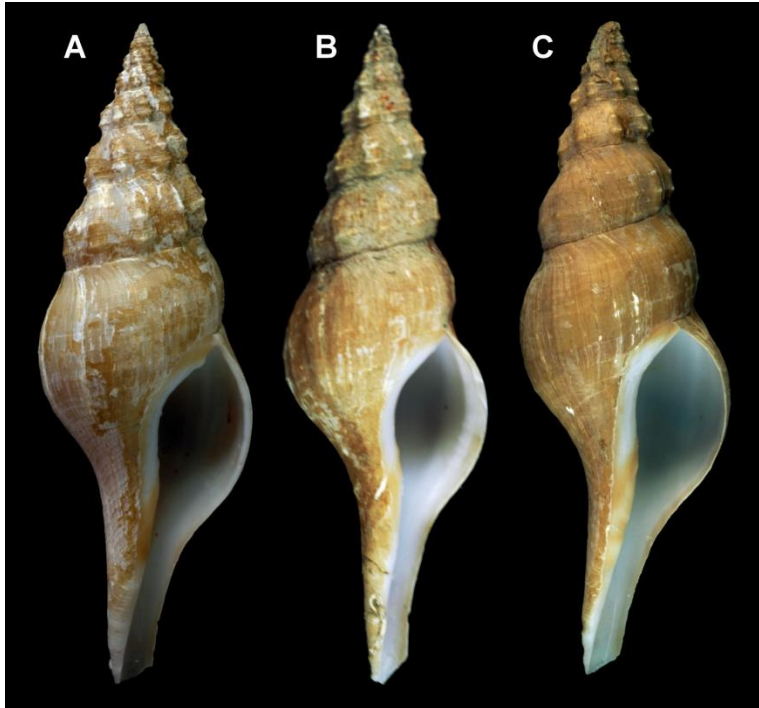


Figure 57. *Pseudolatirus discrepans*, shell. **A**: MNHN IM-2007-34604 (58.3mm). **B**: MNHN IM-2013-9777 (66mm). **C**: MNHN IM-2007-32791 (68.7mm).

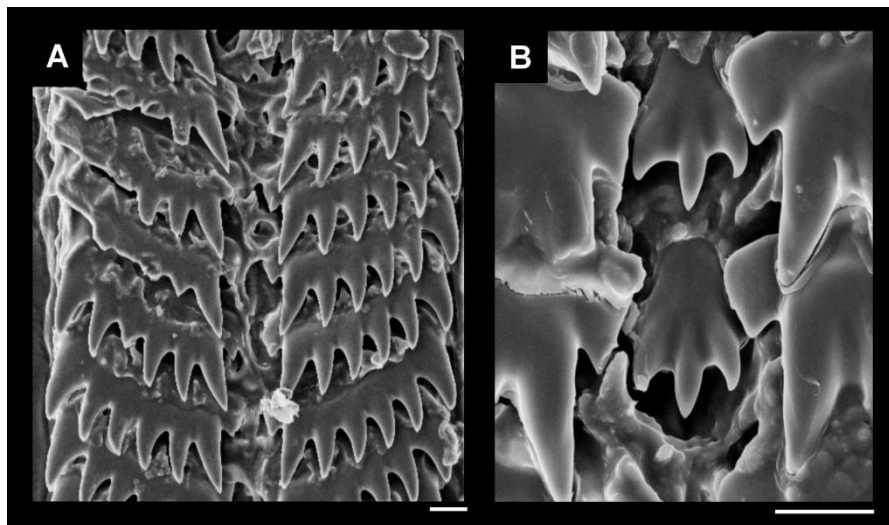


Figure 58. *Pseudolatirus discrepans*, radula. **A-B**: MNHN IM-2013-9777. **A**: panoramic view. **B**: detail of rachidian tooth. Scale bars = 20um.

### **Clade 5a Peristerniinae**

Odontophore m6 muscle posterior free portion: odontophore length  $\leq 1/6$  (45: 1). Cusps of lateral tooth of radula non-uniform in length and distribution (57: 1), and bearing many secondary cusps (64: 1). Anus close to mantle border, its distance from mantle border: total pallial cavity length  $< 1/3$  (77: 0).

#### ***Fusolatirus bruijnii* (Figs. 59-60)**

**Examined material:** MNHN IM-2013-16671, inner slope, Papua New Guinea, 7-22m depth, 5°10'6.0024"S; 145°50'14.9784"E. PAPUA NIUGINI expedition. xii/03/2012 [1 specimen]. MNHN IM-2013-18013, Papua New Guinea, 1-19m depth, 5°10'18.0012"S; 145°48'30.0024"E. PAPUA NIUGINI expedition. xii/07/2012 [1 specimen].

Loss of spiral sculpture of shell (3: 0).

### **Clade 5b Peristernia**

Siphonal canal of shell moderate-sized, its length: total shell length  $1/6-1/4$  (9: 1). Rachidian tooth of radula trapezoidal-shaped, its base width: edge width  $\leq 1/2$  (50: 2); lateral tooth much wider than long, its length: width  $< 1/3$  (55: 4).

#### ***Peristernia nassatula* (Figs. 61-62)**

**Examined material:** MNHN IM-2007-32487, N of Malu Island, Vanuatu, 15°37'41.502"S; 167°11'2.004"E. SANTO 2006 expedition, Aldric ship col. ix/16/2006. [1 specimen]. MNHN IM-2013-18061, Papua New Guinea, 1-8m depth. PAPUA NIUGINI expedition. xii/08/2012 [1 specimen]. MZSP 71241. Sovi Bay, Baravi, Southern Viti-Levu, Fiji. J coltro Femorale col. ix/10/2006 [2 specimens]. MNHN IM-2007-32541, Panglao Island, Napaling, Philippines, 9°37'12"N; 123°46'23.9916"E. PANGLAO 2004 expedition. vi/15/2004 [1 specimen]. MNHN IM-2013-10796, Papua New Guinea, 5°10'7.7412"S; 145°50'32.4996"E. PAPUA NIUGINI expedition. xi/07/2012. [1 specimen].

Loss of lipped margin of rhynchostome (40: 0). Rachidian tooth of radula with 4 cusps (51: 3).

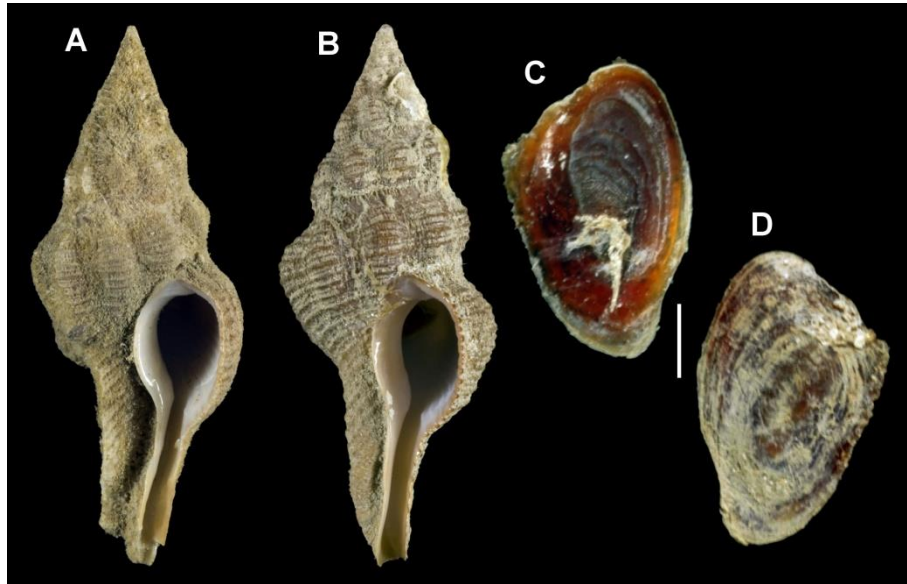


Figure 59. *Fusolatirus bruijnii*. shell and operculum. **A**: MNHN IM-2013-18013 (45.5mm). **B**: MNHN IM-2013-16671 (40mm). **C**: operculum, inner view. **D**: operculum, outer view. Scale bars = 1mm.

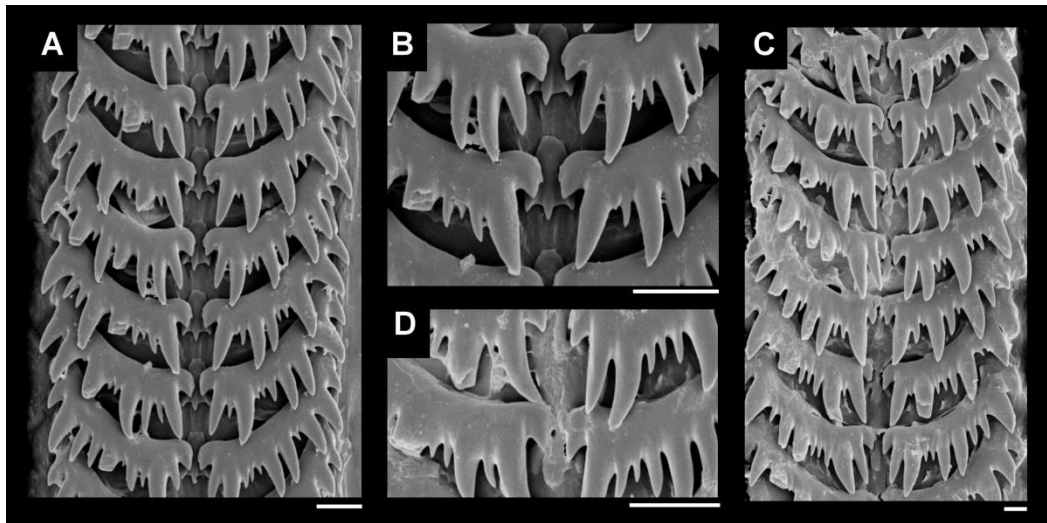


Figure 60. *Fusolatirus bruijnii*, radula. **A-B**: MNHN IM-2013-18013. **A**: panoramic view. **B**: detail of rachidian tooth. **C-D**: MNHN IM-2013-16671. **C**: panoramic view. **D**: detail of rachidian tooth. Scale bars = 20 $\mu$ m.

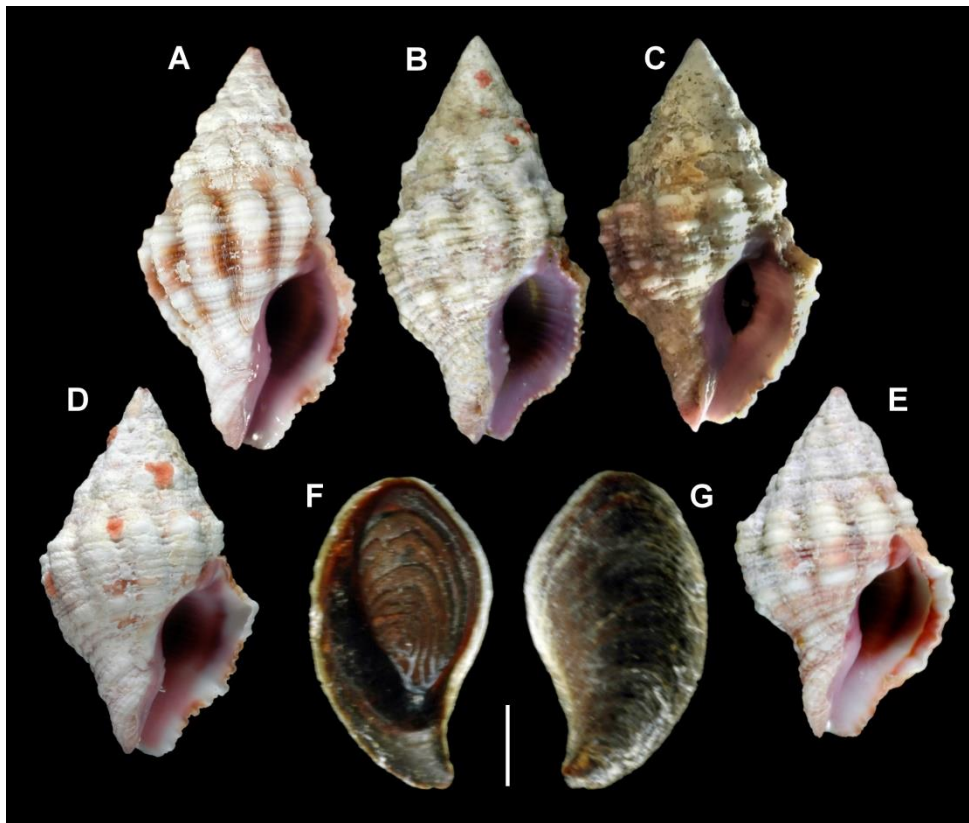


Figure 61. *Peristernia nassatula*, shell and operculum. **A**: MNHN IM-2007-32487 (28.6mm). **B**: MNHN IM-2013-18061 (35.5mm). **C**: MZSP 71241 (25mm). **D**: MNHN IM-2007-32541 (30.1mm). **E**: MNHN IM-2013-10796 (16.5mm). **F**: operculum, inner view. **G**: operculum, outer view. Scale bars = 2mm.

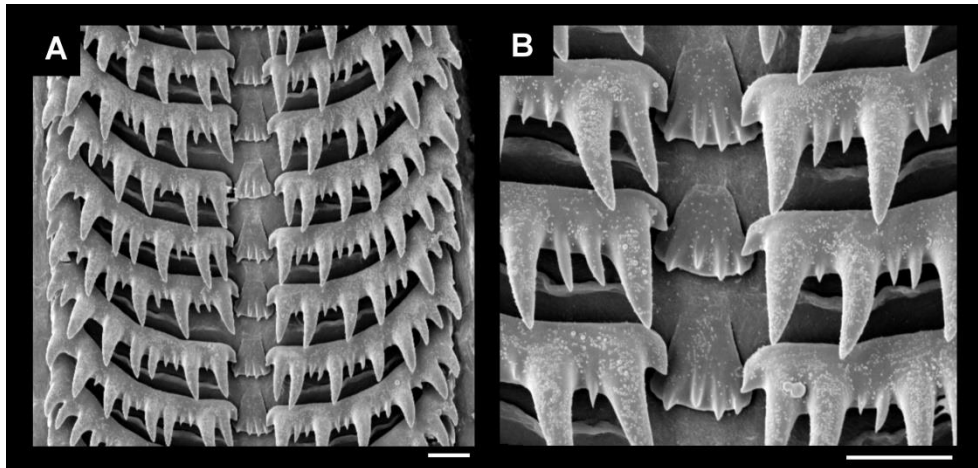


Figure 62. *Peristernia nassatula*, radula. **A-B**: MNHN IM-2013-18061. **A**: panoramic view. **B**: detail of rachidian tooth. Scale bars = 20µm.



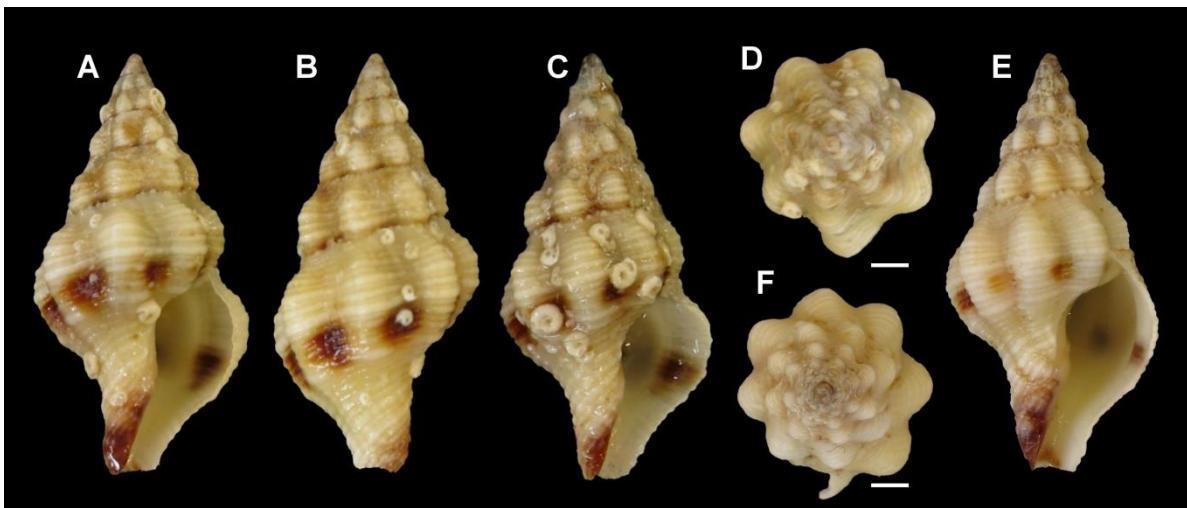


Figure 63. *Peristernia marquesana*, shell. A-D: MZSP 68507. A-B: (17.2mm). C: (18.3mm). E-F: MZSP 69249 (21.2mm). Scale bars = 2mm.

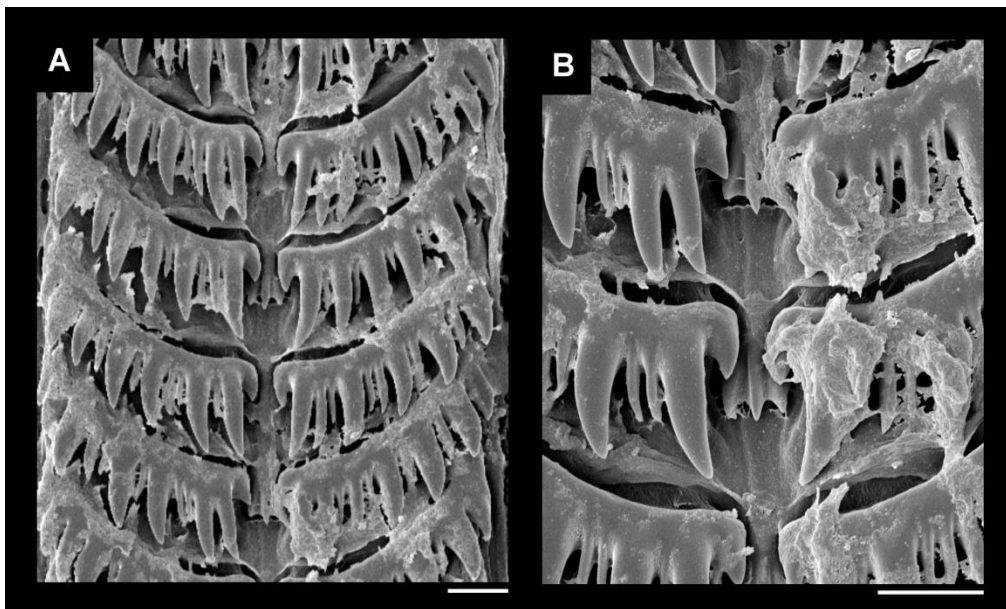


Figure 64. *Peristernia marquesana*, radula. A-B: MZSP 69249. A: panoramic view. B: detail of rachidian tooth. Scale bars = 20 $\mu$ m.

***Peristernia marquesana* (Figs. 63-64)**

**Examined material:** MZSP 68507, Okinawa city, Okinawa, Japan. J. Coltro Femorale col. v/2006 [2 specimens]. MZSP 69249, Malibu Beach, West Okinawa, Japan. . Coltro Femorale col. v/2006 [2 specimens].

Pallial cavity long, its extension  $\geq 3/4$  whorls (19: 1). Rachidian tooth of radula triangle-shaped (48: 1), diminute, its width: lateral tooth width  $< 1/4$  (53: 3). Commissure of buccal ganglia inconspicuous (93: 1).

### **Clade 6 Fasciolarinae**

Head medium-sized, its width: head-foot mass width  $1/4-1/2$  (13: 1), with short cephalic tentacles, its length: head width  $1/2-2/3$  (14: 1). Rachidian tooth of radula square-shaped, its base width: edge width  $1/2-1$  (50: 0). Salivary glands as free amorphous masses (69: 1).

### **Clade 6a**

Lateral tooth of radula much wider than long, its length: width  $<1/3$  (55: 4), bearing  $\geq 16$  cusps (58: 3). Cement gland opening in foot sole centrally (84: 0). Commissure of buccal ganglia long, its length: buccal ganglia length  $\geq 1/2$  (94:1).

#### ***Nodolatirus nodatus* (Figs. 65-66)**

**Examined material:** MNHN IM-2013-42533, Tubuai, French Polynesia, Austral Archipelago,  $23^{\circ}19'41.4012''S$ ;  $149^{\circ}29'17.9772''W$ . Tuhaa Pae 2013 expedition, Alis ship col. iii/24/2013 [1 specimen]. NHN IM-2013-42533, Tubuai, French Polynesia, Austral Archipelago,  $23^{\circ}25'7.7988''S$ ;  $149^{\circ}27'0.3744''W$ . Tuhaa Pae 2013 expedition, Alis ship col. iii/23/2013 [1 specimen].

No known autapomorphies.

### **Clade 6b**

Rhynchostome transverse (38: 0). Rachidian tooth of radula diminute, its width: lateral tooth width  $<1/4$  (53: 3); cusp 1 of lateral tooth absent (60: 2).

#### ***Latirus vischii* (Figs. 67-68)**

**Examined material:** MNHN IM-2009-15038, Choumare Islet, S Madagascar,  $24^{\circ}50'28.7376''S$ ;  $47^{\circ}10'26.4''E$ . ATIMO VATAE expedition vi/07/201 [1 specimen].

Loss of lipped margin of rhynchostome (40: 0).



Figure 65. *Nodolattirus nodatus*, shell. MNHN IM-2013-42534 (76.5mm).

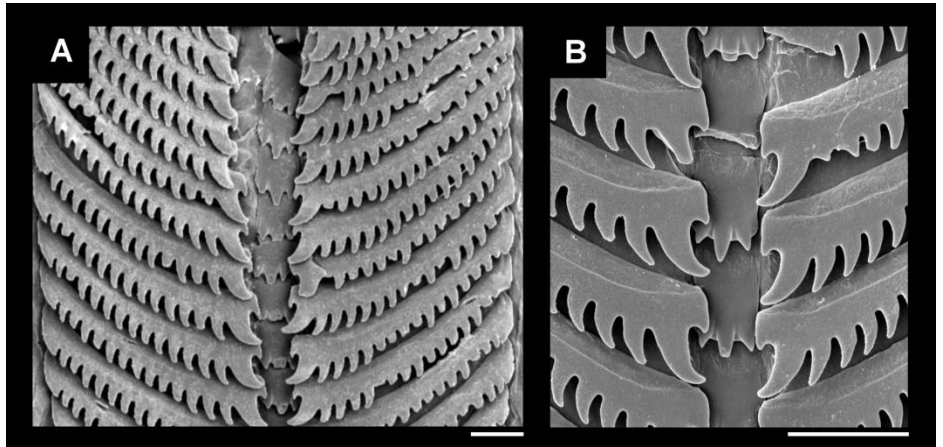


Figure 66. *Nodolattirus nodatus*, radula. A-B: MNHN IM-2013-42534. A: panoramic view. B: detail of rachidian tooth. Scale bars = 40µm.

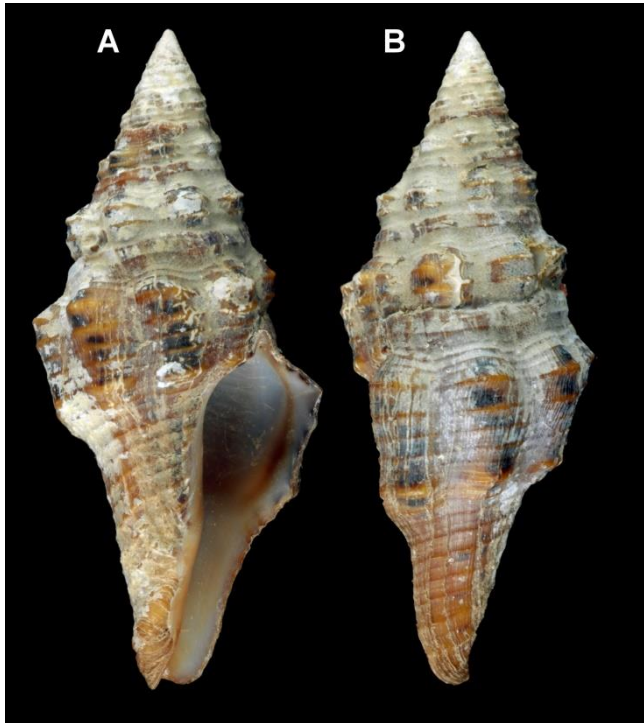


Figure 67. *Latirus vischii*, shell. A-B: MNHN IM-2009-15038 (66.6mm).

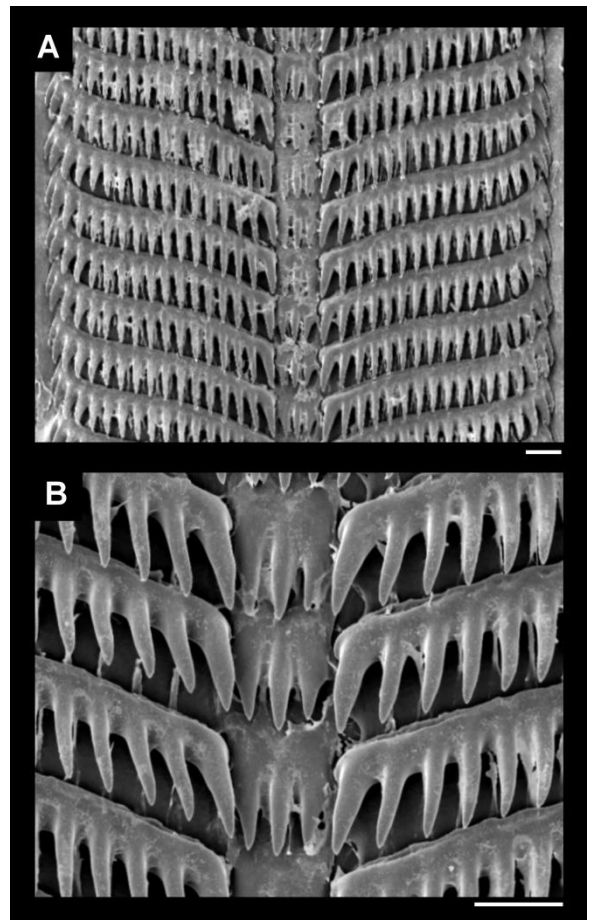


Figure 68. *Latirus vischii*, radula. A-B: MNHN IM-2009-15038. A: panoramic view. B: detail of rachidian tooth. Scale bars = 50µm.



**Clade 6c Fasciolarinae *sensu stricto***

Shell coloration as blotchy spots, irregularly spaced (2: 0); siphonal canal moderate-sized, its length: total shell length  $1/6$ – $1/4$  (9: 1); loss of pseudo-umbilicus (10: 0). Renal aperture situated close to pericardium (36: 1). Odontophore long, its length: proboscis length  $\sim 1$  (42: 0). Retractor muscle of proboscis inserting posteriorly (68: 0). Posterior esophagus bearing sudden broadening in visceral region (74: 1), anterior to stomach.

***Fasciolaria tulipa* (Figs. 69-70)**

**Examined material:** MZSP 69277, Roatan Island, Honduras, 80-100m depth. Femorale col. iii/2006 [1 specimen]. MZSP 35530, Marguerita Island, Venezuela, 3m depth. L.R. Simone col. [2 specimens]. MZSP 56870, Marguerita Island, El Yaque, Venezuela, 2m depth. L.R. Simone col. i/28/1998 [2 specimens].

Loss of spiral shell sculpture (3: 0). Odontophore m6 muscle posterior free portion: odontophore length  $\leq 1/6$  (45: 1). Rachidian tooth of radula trapezoidal-shaped, its base width: edge width  $1/2$ –1 (50: 1).

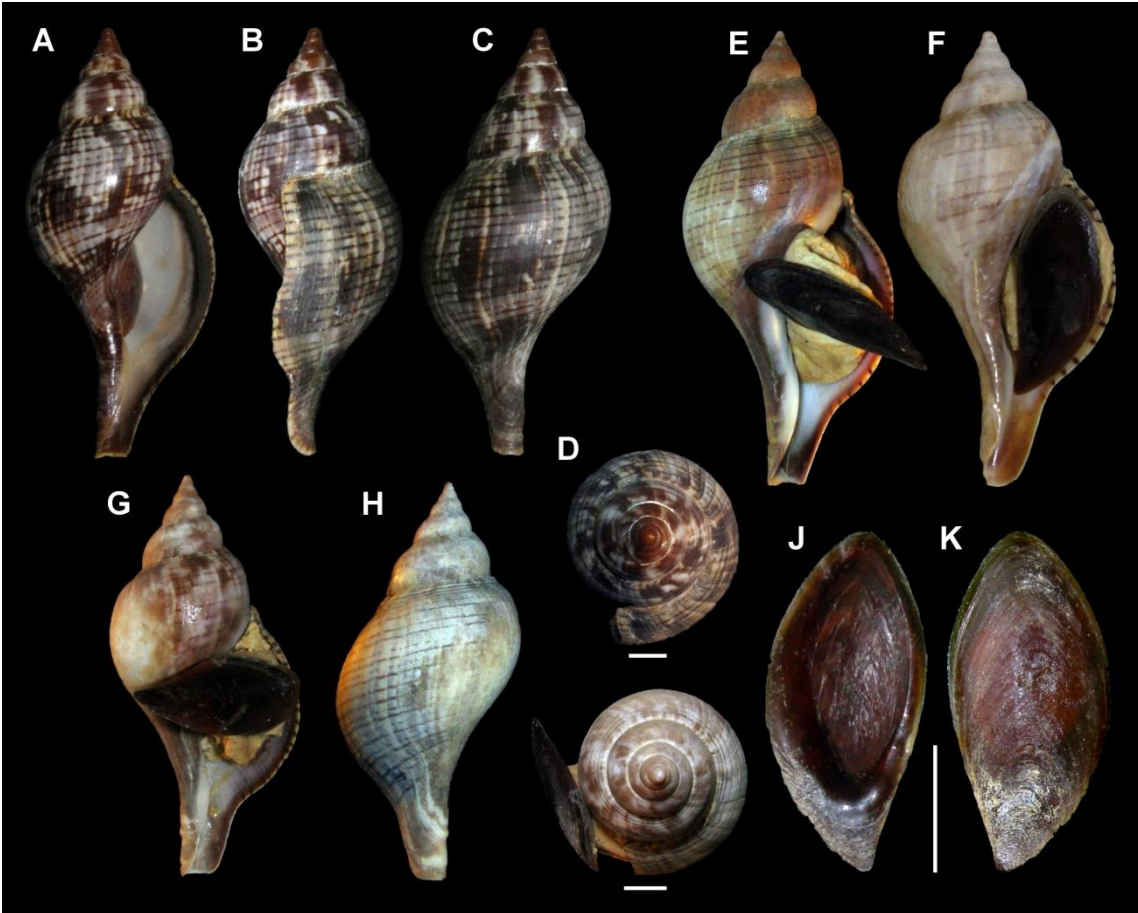


Figure 69. *Fasciolaria tulipa*, shell and operculum. **A-D**: MZSP 69277 (69,5mm). **E-F**: MZSP 35530. **E**: (77,5mm). **F**: (107,9mm). **G-I**: MZSP 56870 (92,3mm). **J**: operculum, inner view. **K**: operculum, outer view. Scale bars = 10mm.

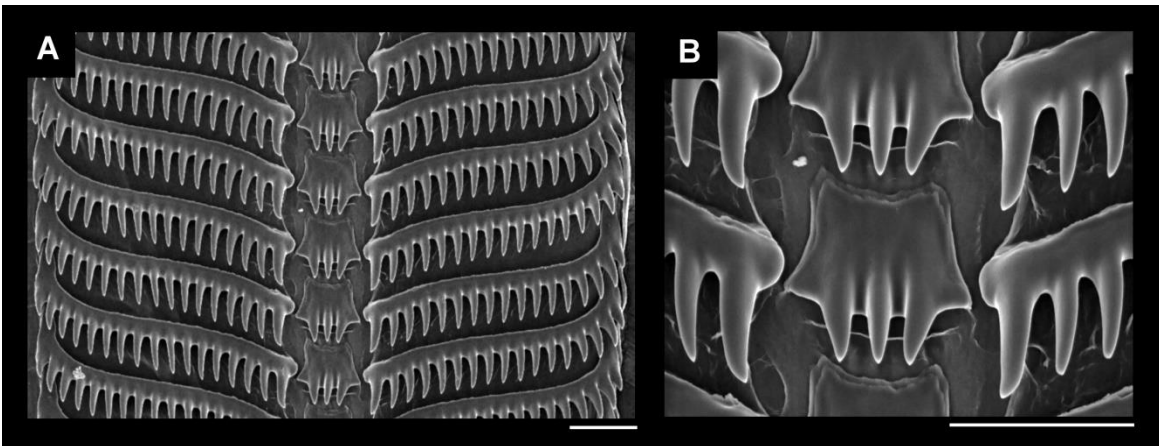


Figure 70. *Fasciolaria tulipa*, radula. **A-B**: MZSP 35530. **A**: panoramic view. **B**: detail of rachidian tooth. Scale bars = 100µm.

***Aurantilaria aurantiaca* (Figs. 71-72)**

**Examined material:** CMPHRM 2765, Redonda Beach, Icapuí, Ceará state, Brazil. H. Matthews-Cascon col. ix-18-2009 [2 specimens]. MNRJ 8372, Retiro grande Beach, Aracati, Ceará state, Brazil. A.L. Castro col. i/1964 [1 specimen]. MNRJ 993, Itapagipe, Salvador, Bahia state, Brazil. , H. Souza Lopes col. [2 specimens]. MNRJ 8304, Nova Viçosa Reef, Nova Viçosa Bay, Bahia state, Brazil. P.S. Young & C.B. Castro col. vii/18/1993 [1 specimen]. MNRJ 15161, Conceição, Itaparica Island, Bahia state, Brazil. D.R. Couto col. i/4/2010 [2 specimens]. MNRJ 14346, Santa Cruz, Espírito Santo state, Brazil. P. Jurberg col. i/18/1973 [2 specimens]. MNRJ 8369, Piloto Beach, Santa Cruz, Espírito Santo state, Brazil. D. Campos & D. Campos col. viii/1973 [1 specimen]. MNRJ 6678, Rio de Janeiro state, Brazil. H.S. Lopes col. [1 specimen]. MZSP 33005, Cabo Branco Beach, João Pessoa, Paraíba state, Brazil. R. Leonel col. v/25/1998 [1 specimen]. MZSP 77496, Francês Beach, Marechal Deodoro, Alagoas state, Brazil, 5m depth. L.R.S. Simone col. vii/17/1989 [2 specimens]. MZSP 35976, Alcaçoba, Bahia state, Brazil. Coltro col. ix/2002 [3 specimens].

Body pigmentation orange to light red with reticulated lighter pattern (11: 2). Pallial cavity long, its extension  $\geq 3/4$  whorls (19: 1). Osphradium leaflets non uniform (24: 1). Rachidian tooth of radula trapezoidal-shaped, its base width: edge width  $1/2-1$  (50: 1), bearing minute, secondary cusps (52: 1). Female cement gland opening anteriorly (84: 1) in foot sole. penis duct linear (87: 0).

**Clade 6d**

Head very small, its width: head-foot mass width  $< 1/4$  (13: 0), bearing very short cephalic tentacles, its length: head width  $< 1/2$  (14: 0). Cement gland immersed in foot as several saccular vesicles, branching from single opening (83: 1).

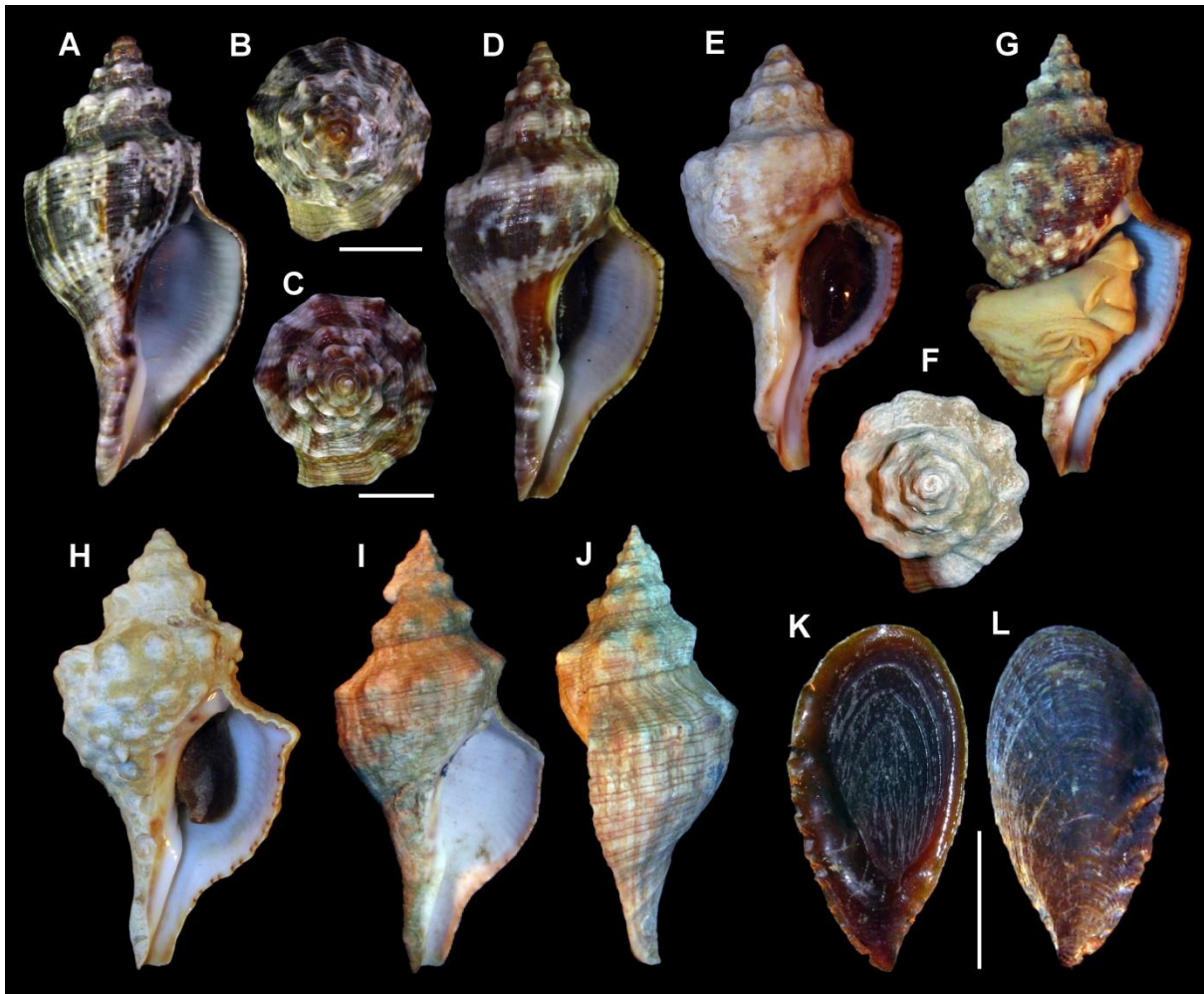


Figure 71. *Aurantilaria aurantiaca*, shell and operculum. **A-D**: CMPHRM 2765. **A-B**: (48.3mm). **C-D**: (48.7mm). **E-F**: MZSP 77496 (75.8mm). **G**: MZSP 33005 (75.6mm). **H**: MNRJ 8304 (100.4mm). **I-J**: MNRJ 993 (75.9mm). **K**: operculum, inner view. **L**: operculum, outer view. Scale bars = 10mm.

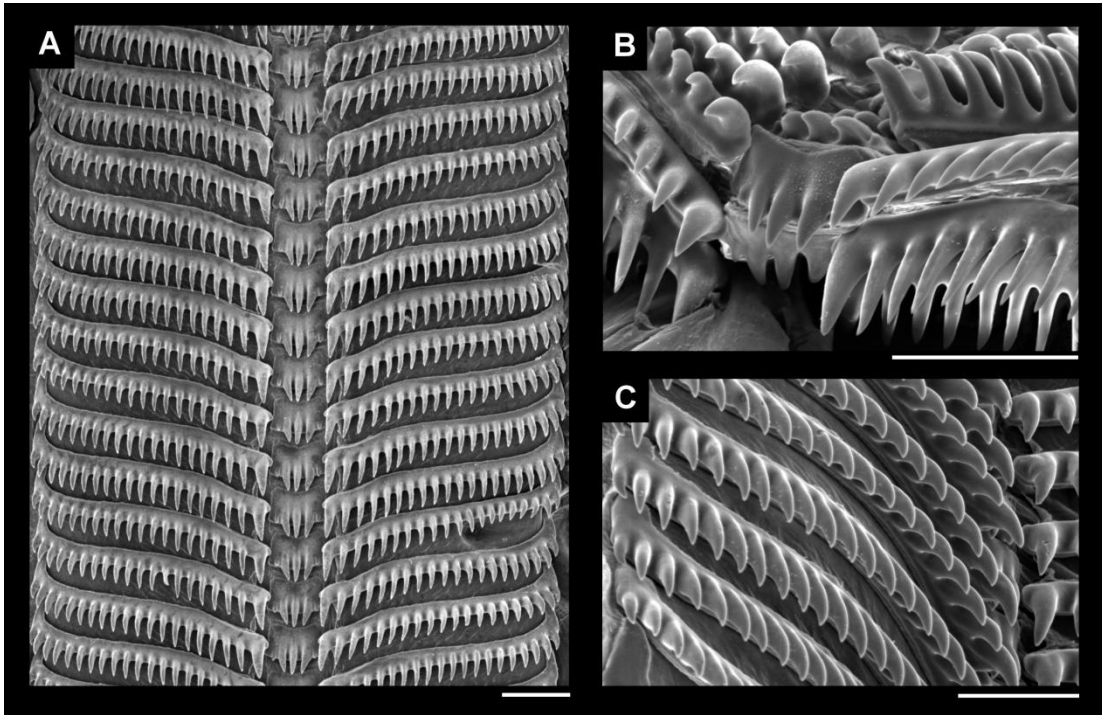


Figure 72. *Aurantilaria aurantiaca*, radula. **A-B**: MNRJ 15161. **A**: panoramic view. **B**: detail of rachidian tooth. **C**: MNRJ 14346 detail of lateral tooth. Scale bars = 100 $\mu$ m.

***Filifusus filamentosus* (Figs. 73-74)**

**Examined material:** MNHN IM-2013-13107, Papua New Guinea, 5°4'43.968"S; 145°48'53.1108"E. PAPUA NIUGINI expedition. xi/14/2012 [1 specimen]. MNHN IM-2007-32592, Palikulo Bay, N Cape Undine, Vanuatu, 9-30m depth, 15°25'50.9412"S; 167°12'59.688"E. SANTO 2006 expedition, Aldric ship col. ix/26/2006 [1 specimen].

Loss of spiral sculpture of shell (3: 0). Pallial cavity long, its extension  $\geq 3/4$  whorls (19: 1). Ctenidium ample, its width: osphradium width  $\geq 1.5$  (28: 2). Radula rachidian bearing minute, secondary cusps (52: 1).



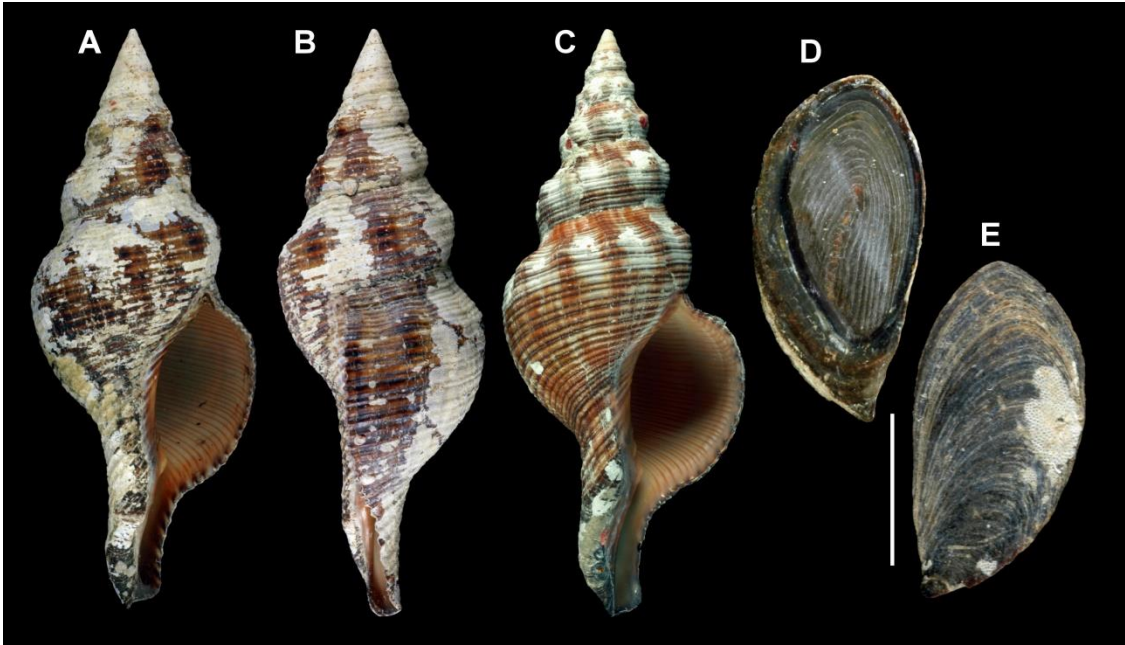


Figure 73. *Filifusus filamentosus*. shell and operculum. **A-B**: MNHN IM-2013-13107 (102.5mm). **C**: MNHN IM-2007-32592 (130mm). **D**: operculum, inner view. **E**: operculum, outer view. Scale bars = 10mm.

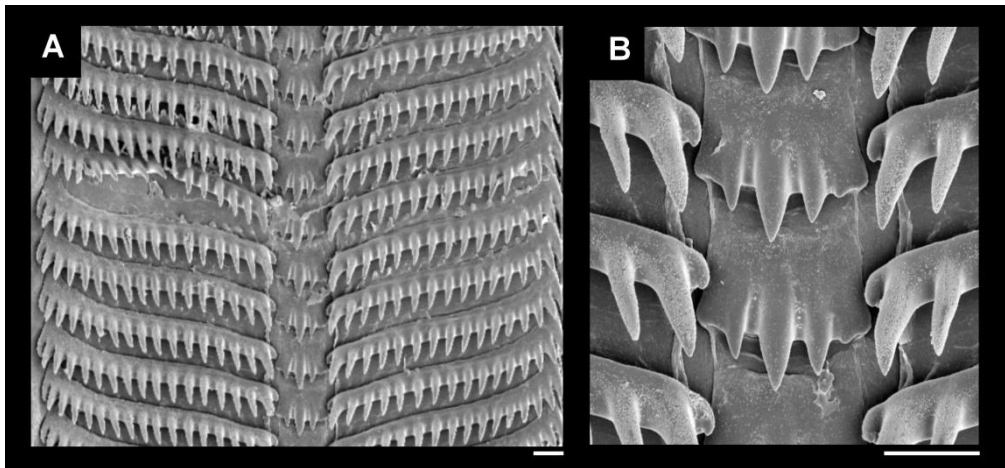


Figure 74. *Filifusus filamentosus*, radula. **A-B**: MNHN IM-2013-13107. **A**: panoramic view. **B**: detail of rachidian tooth. Scale bars = 50 $\mu$ m.



Figure 75. *Australaria australasia*, shell. MNHN IM-2013-42514 (61.2mm).

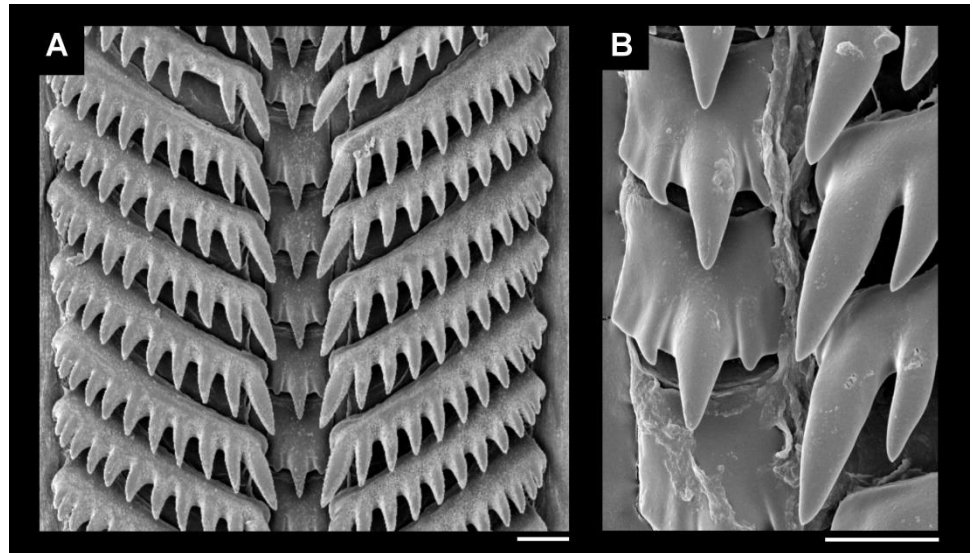


Figure 76. *Australaria australasia*, radula. **A-B**: MNHN IM-2013-42514. **A**: panoramic view. **B**: detail of rachidian tooth. Scale bars = 40µm.

***Australaria australasia* (Figs. 75-76)**

**Examined material:** MNHN IM-2013-42514, Island off Cape Le Grande, Esperance, Australia, 34°1'15.672"S; 122°8'29.328"E. WESTERN AUSTRALIA 2011 expedition. xi/20/2011 [1 specimen]. MNHN IM-2013-42516, Island off Cape Le Grande, south side, Esperance, Australia, 34°1'15.672"S; 122°8'29.328"E. WESTERN AUSTRALIA 2011 expedition. xi/20/2011. [1 specimen].

Osphradium leaflets non uniform in profile (24: 1). Lateral tooth of radula bearing 7–15 cusps (58: 2).

***Pleuroploca trapezium* (Figs. 77-78)**

**Examined material:** MNHN IM-2009-15358, Ambatobe, Madagascar, 0-1m depth, 25°27'23.6988"S; 44°57'23.4036"E. ATIMO VATAE expedition v/24/2010 [1 specimen]. MNHN IM-2007-32591, Vanuatu. SANTO 2006 expedition, Alis ship col. [1 specimen].

No known autapomorphies.

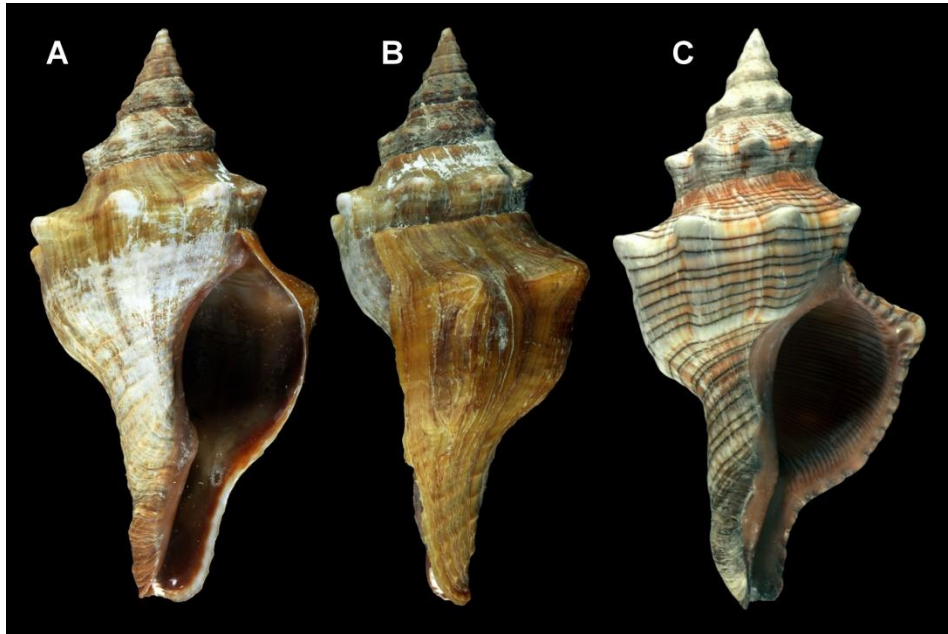


Figure 77. *Pleuroploca trapezium*, shell. **A-B**: MNHN IM-2009-15358 (66.5mm). **C**: MNHN IM-2007-32591 (185.5mm).

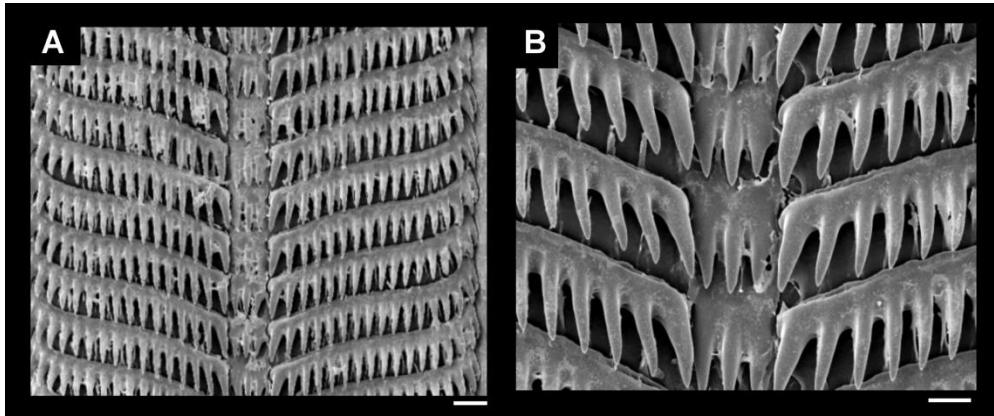


Figure 78. *Pleuroploca trapezium*, radula. **A-B**: MNHN IM-2009-15358. **A**: panoramic view. **B**: detail of rachidian tooth. Scale bars = 50 $\mu$ m.





Figure 79. *Hemipolygona armata*, shell. MNHN IM-2013-42509 (46.7mm).

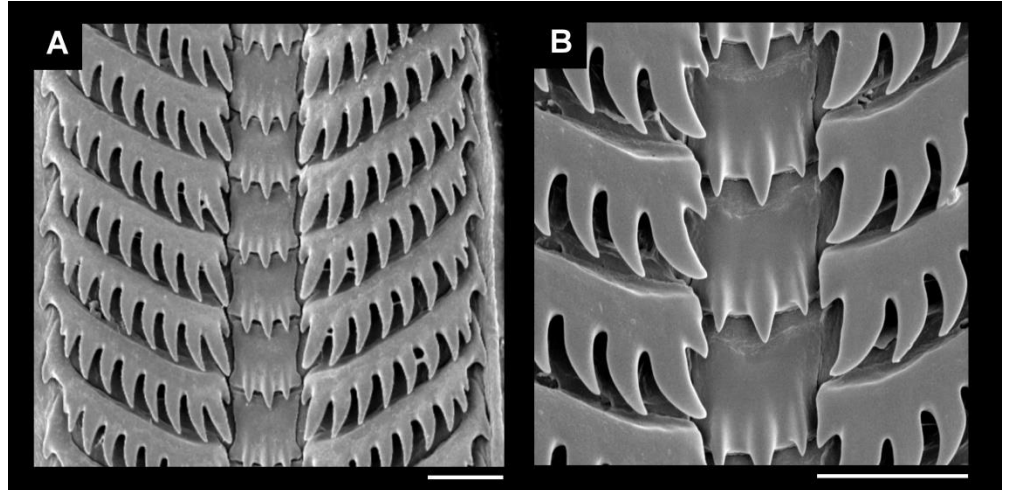


Figure 80. *Hemipolygona armata*, radula. **A-B**: MNHN IM-2013-42509. **A**: panoramic view. **B**: detail of rachidian tooth. Scale bars = 40 $\mu$ m.

### Clade 7

Inner sculpture of outer lip of shell bearing discontinuous spiral cords (7: 2) or lirae; siphonal canal moderate-sized, its length: total shell length 1/6–1/4 (9: 1). Rhynchostome transverse slit (38: 0). Commissure of buccal ganglia inconspicuous (93: 1).

#### *Hemipolygona armata* (Figs 79-80)

**Examined material:** MNHN IM-2013-42511, Gorée Island, Senegal, 14°40'12"N; 17°23'48.0012"W. Dakar'09 expedition [1 specimen]. MNHN IM-2013-42509, Gorée Island, Senegal, 14°40'12"N; 17°23'48.0012"W. Dakar'09 expedition [1 specimen].

Proboscis retractor muscle inserting posteriorly (68: 0).

### Clade 8

Rhynchostome lipped margin lost (40: 0). Odontophore cartilages fused anteriorly  $\geq 15\%$  of total odontophore length (44: 2).

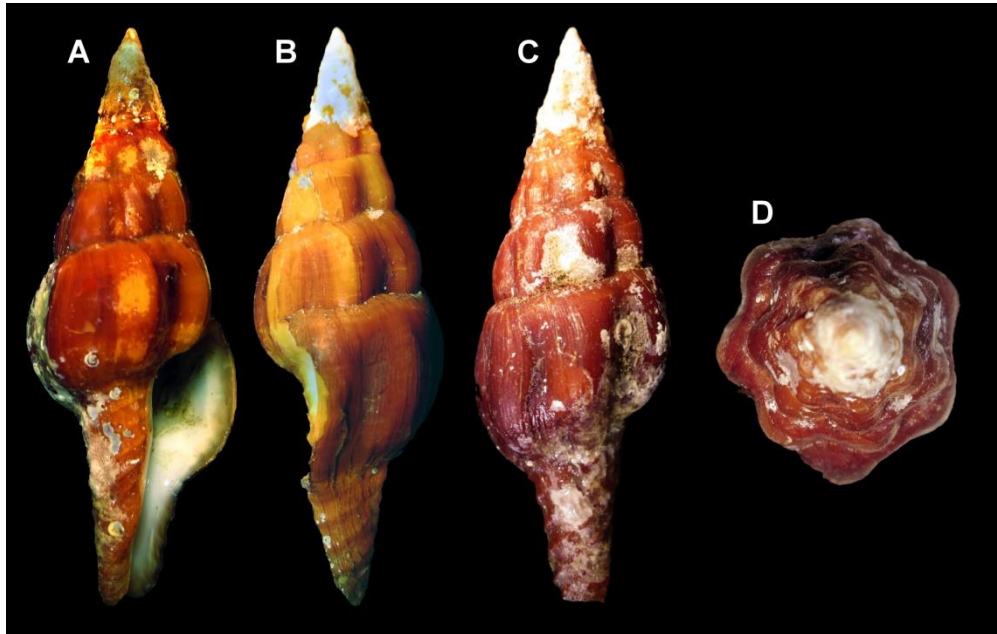


Figure 81. *Pustulatirus mediamericus*, shell. A-D: MZSP 69500 (57.5mm).

### Clade 8a *Pustulatirus*

Pallial cavity long, its extension  $\geq 3/4$  whorls (19: 1). Rachidian tooth of radula bearing 4 cusps (51: 3); lateral tooth much wider than long, its length: width  $< 1/3$  (55: 4). Paired proboscis retractor muscles (67: 0), inserting posteriorly in proboscis (68: 0). Female cement gland opening centrally in foot (84: 0).

### *Pustulatirus mediamericus* (Fig. 81)

**Examined material:** MZSP 69500, La Plata Island, Manabi, Ecuador. J. Coltro col. x/2002 [2 specimens]. MZSP 95273, Ecuador. Simone col. 2009 [15 specimens]. MZSP 67752, La Plata Island, Manabi, Ecuador. J. Coltro col. vi/2006 [1 specimen].

No known autapomorphies.

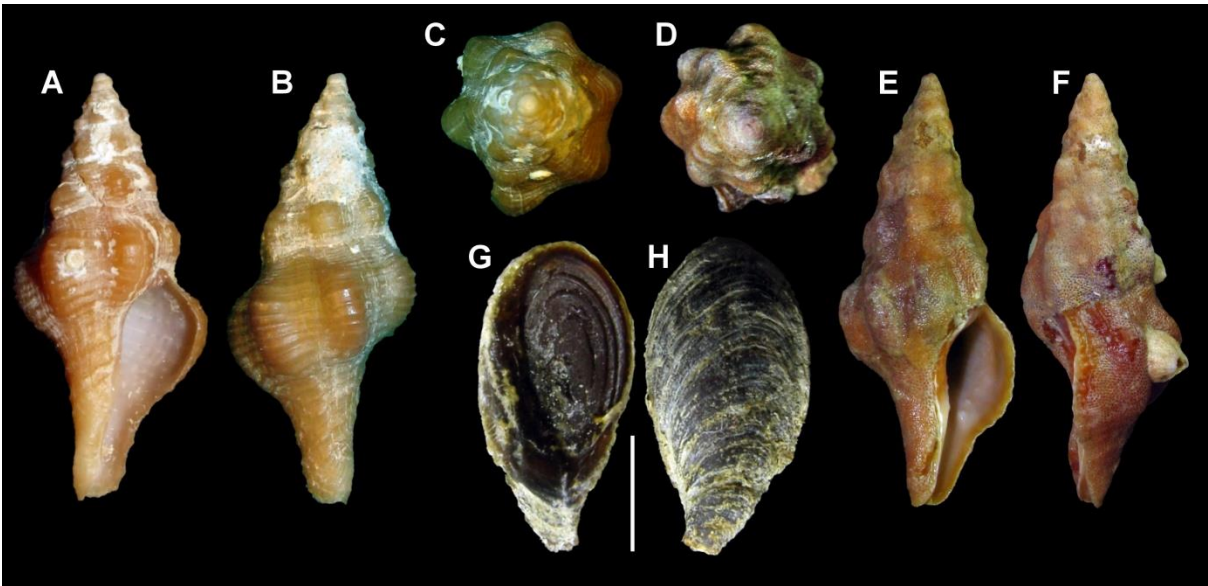


Figure 82. *Pustulaturus ogum*, shell and operculum. **A-C**: MZSP 68475 (22.2mm). **D-F**: MZSP 69301 (39.2mm). **G**: operculum, inner view. **H**: operculum, outer view. Scale bars = 3mm.

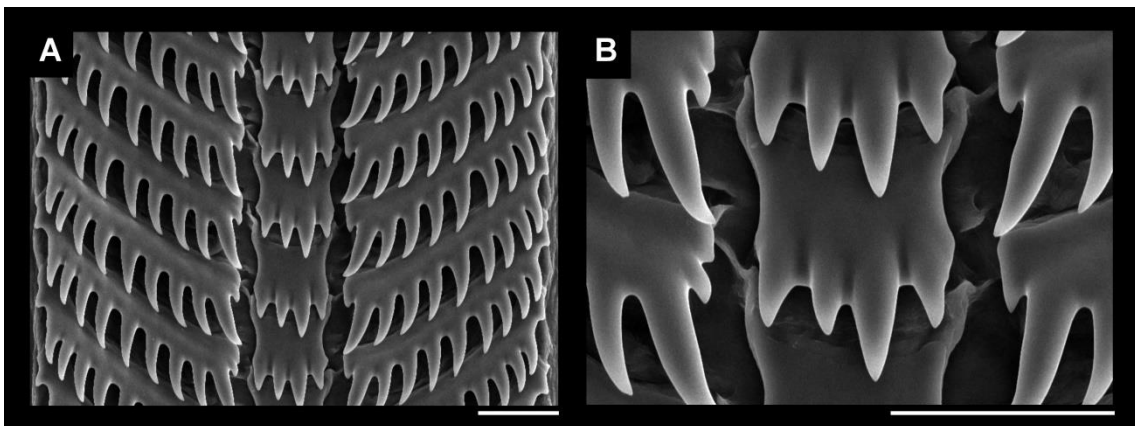


Figure 83. *Pustulaturus ogum*, radula. **A-B**: MZSP 69301. **A**: panoramic view. **B**: detail of rachidian tooth. Scale bars = 30µm.

***Pustulaturus ogum* (Figs. 82-83)**

**Examined material:** MZSP 68475, Alcaçoba, Bahia state, Brazil, 20-30m depth Femorale col. vi/2006 [16 specimens]. MZSP 69477, Guarapari, Espírito Santo state, Brazil, 20-30m depth. A. Bodart Femorale col. i/2006 [6 specimens]. MZSP 69301, Arraial do Cabo, Rio de Janeiro State, 30-35m depth. P. Gonçalves Femorale col. i/2005 [2 specimens].

Rhynchostome longitudinal slit (38: 1). Anus situated close to mantle border, its distance from mantle border: total pallial cavity length <math><1/3</math> (77: 0). Duct of penis linear shape (87: 0).

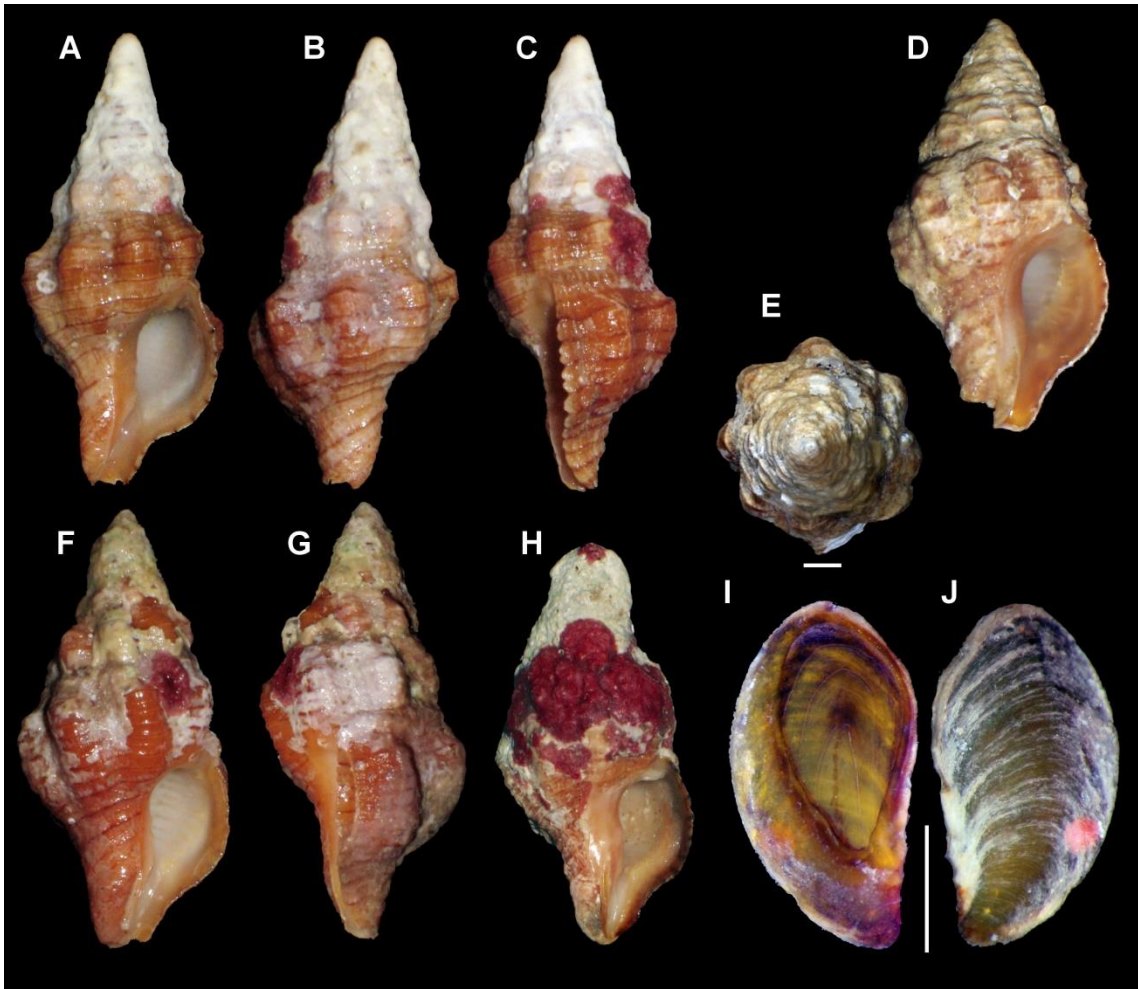


Figure 84. *Polygona angulata*, shell and operculum. A-C: MZSP 90047 (23.3mm). D-E: MZSP 31125 (18.7mm). F-G: MZSP 90774 (24.5mm). H: MZSP 112907 (29mm). I: operculum, inner view. J: operculum, outer view. Scale bars = 2mm.



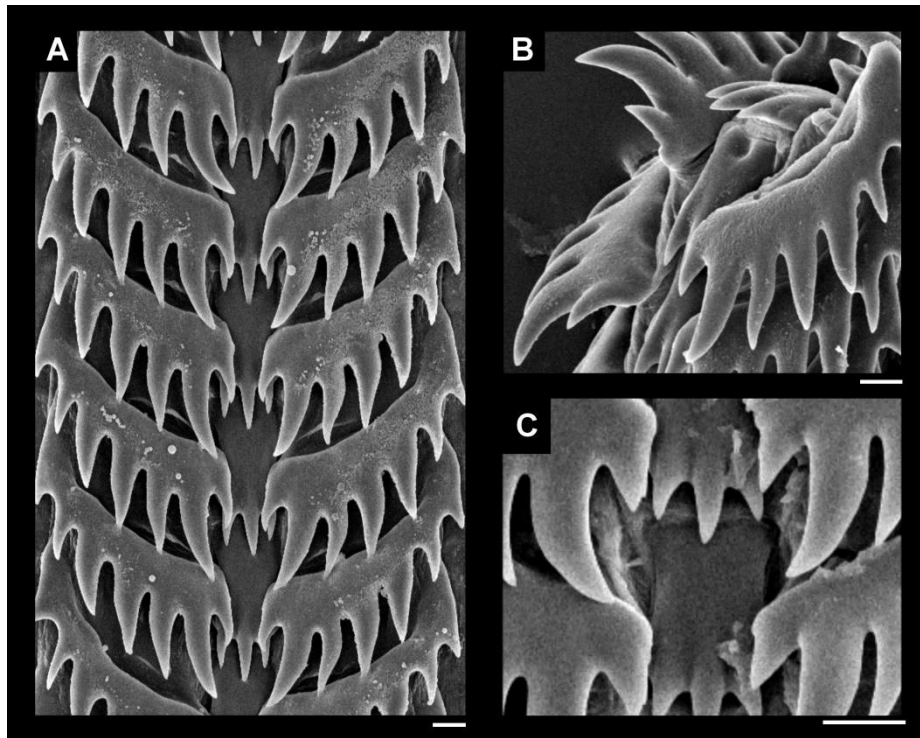


Figure 85. *Polygonia angulata*, radula. **A-B**: MZSP 112907. **A**: panoramic view. **B**: detail of lateral tooth. **C**: MZSP 90774, detail of rachidian tooth. Scale bars = 10µm.

## Clade 9

Loss of lipped margin of renal aperture (34: 0).

### *Polygonia angulata* (Figs 84-85)

**Examined material:** MZSP 31125, Fernando de Noronha Archipelago, Pernambuco state, Brazil. L.R.L. Simone & Souza col. vii/19/1999 [4 specimens]. MZSP 112907, Fernando de Noronha Archipelago, Pernambuco state, Brazil, 03°49'44"S; 32°23'52"W. L.R.L. Simone cols. v/04/2013 [1 specimen]. MZSP 90774, Fernando de Noronha Archipelago, Pernambuco state, Brazil, 0349'48"S; 3223'57,3"W. L.R.L. Simone & Cunha col. iii/11/2009 [2 specimens]; MZSP 112826, Fernando de Noronha Archipelago, Pernambuco state, Brazil, 5-10m depth, 03°48'42"S; 32°23'45,18"W. L.R.L. Simone col. v/03/2013 [6 specimens]. MZSP 90047, Fernando de Noronha Archipelago, Pernambuco state, Brazil. L.R.L. Simone col. iii/10/2009 [2 specimens].

Anus located close to mantle border, its distance from mantle border: total pallial cavity length <1/3 (77: 0). Bursa copulatrix bearing anterior muscular bulb, close to gonopore (81: 1).

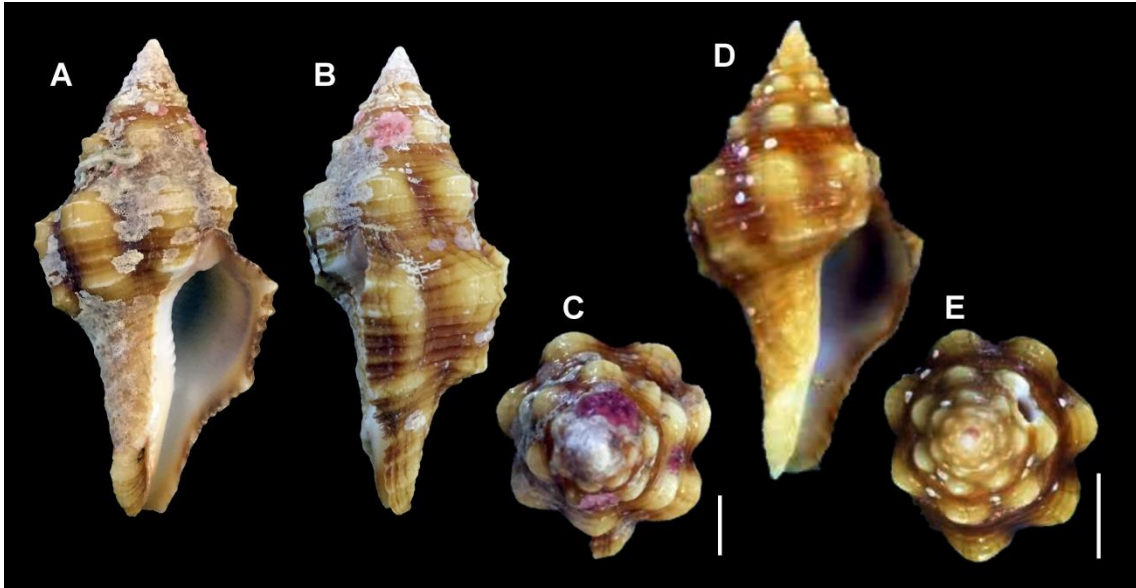


Figure 86. *Latirus polygonus*, shell. **A-C**: MZSP 71428 (65mm). **D-E**: MZSP 71869 (37.9mm). Scale bars = 1mm.

### Clade 10

Kidney nephridial gland present in membrane between renal cavity and pericardium (35: 1).

#### *Latirus polygonus* (Fig. 86)

**Examined material:** MZSP 71428, Natandola Bay, west Sigatoka, Viti-Levu, Fiji. Coltro col. ix/06/2006 [1 specimen]. MZSP 71869, Viti-Levu, Fiji. C Henckes col. ix/10/2006 [1 specimen].

Odontophore fused anteriorly  $\leq 15\%$  of total odontophore length (44: 1). Rachidian tooth of radula diminute, its width: lateral tooth width  $< 1/4$  (53: 3); lateral tooth much wider than long, its length: width  $< 1/3$  (55: 4).

### Clade 11

Head diminute, its width: head-foot mass width  $< 1/4$  (13: 0), bearing very short cephalic tentacles, its length: head width  $< 1/2$  (14: 0).





Figure 87. *Polygona infundibulum*, shell. **A-B:** MNHN IM-2013-19591 (66.5mm).

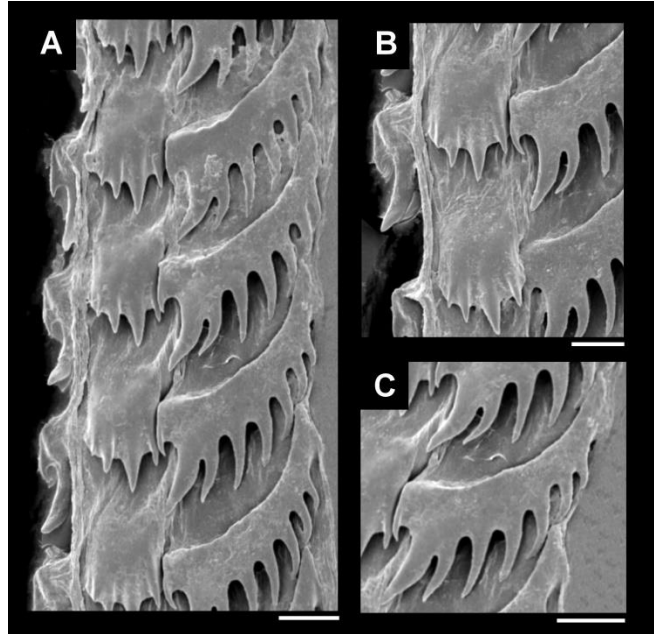


Figure 88. *Polygona infundibulum*, radula. **A-C:** MNHN IM-2013-19591. **A:** panoramic view. **B:** detail of rachidian tooth. **C:** detail of lateral tooth. Scale bars = 20 $\mu$ m.

***Polygona infundibulum* (Figs. 87-88)**

**Examined material:** MNHN IM-2013-19591, Guadeloupe, 16°22'47.8812"N; 61°33'26.5212"W. KURUBENTHOS expedition. v/18/2012 [1 specimen].

Rhynchostome located longitudinally (38: 1). Rachidian teeth of radula bearing minute, secondary cusps (52: 1).

**Clade 12**

Proboscis retractor muscle inserting posteriorly (68: 0). Commissure of buccal ganglia conspicuous (93: 0).

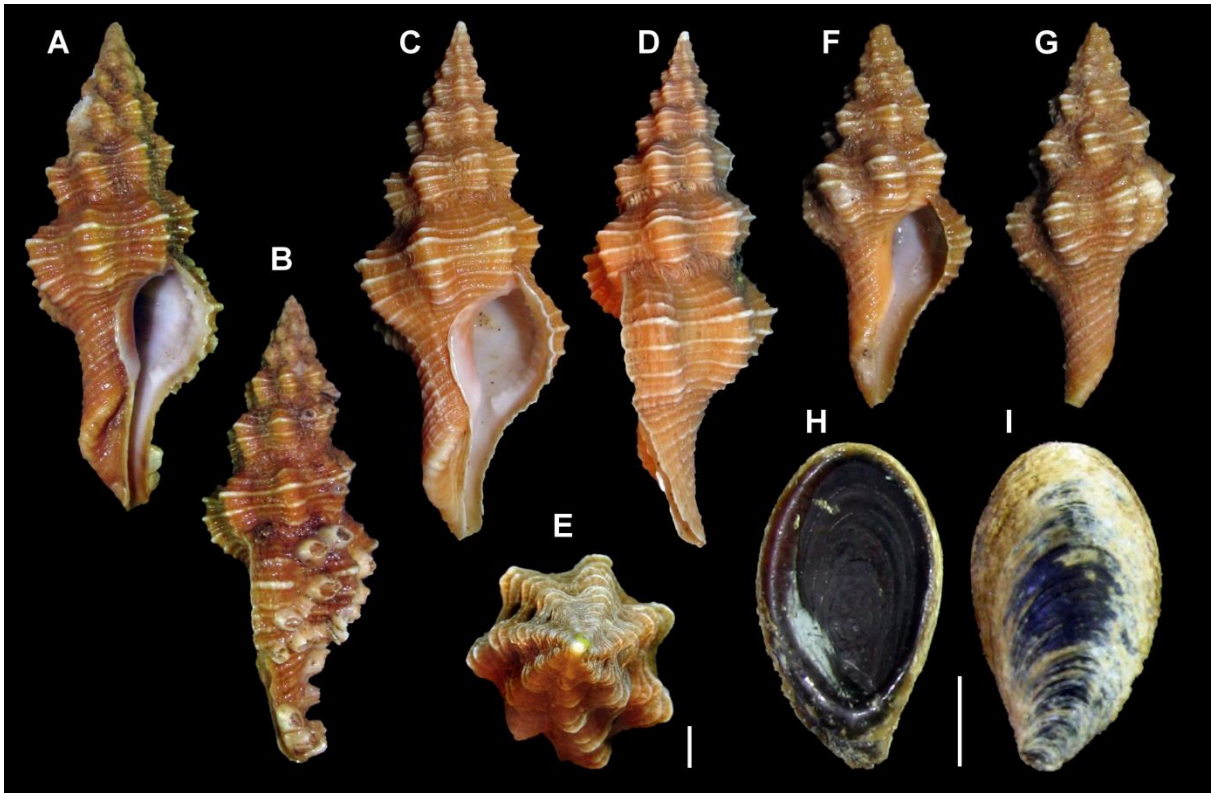


Figure 89. *Hemipolygona beckyae*, shell and operculum. **A-B**: MZSP 69764 (55.4mm). **C-E**: MZSP 57053 (52.4mm). **F-G**: MZSP 69482 (32.8mm). **H**: operculum, inner view. **I**: operculum, outer view. Scale bars = 3mm.

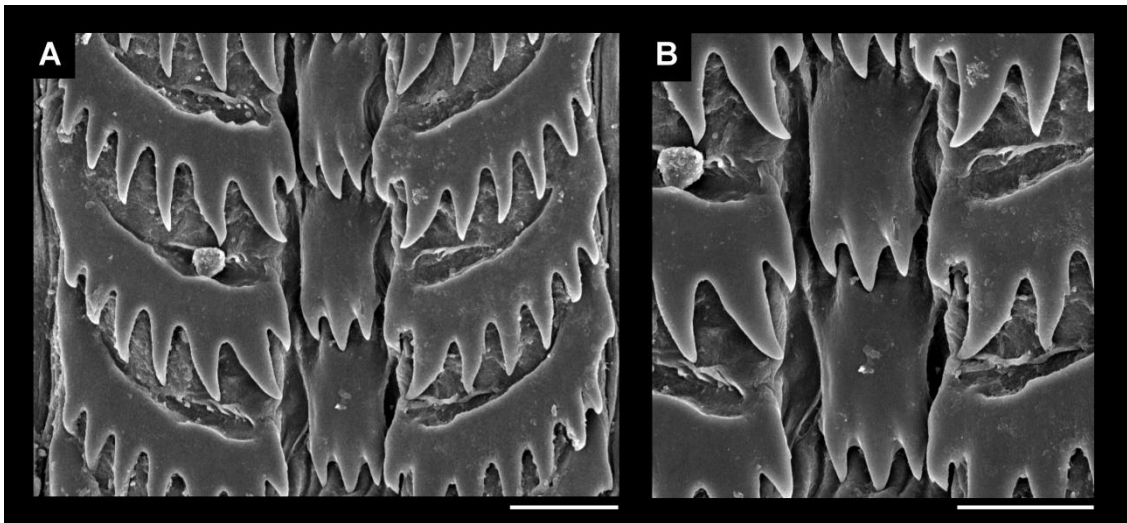


Figure 90. *Hemipolygona beckyae*, radula. **A-B**: MZSP 57053. **A**: panoramic view. **B**: detail of rachidian tooth. Scale bars = 30µm.

***Hemipolygona beckyae* (figs. 89-90)**

**Examined material:** MNRJ 7696, Vitória, Espírito Santo state, Brazil, 30-50m depth. v/1994 [1 specimen, holotype]. MZSP 69482, Vitória, Espírito Santo state, Brazil, 30-35m depth. Femorale col. viii/2003 [3 specimens]. MZSP 57053, Guarapari, Espírito Santo state, Brazil. Coltro col. 2005 [1 specimen]. MZSP 69764, Espírito Santo state, Brazil, 30-35m depth. Femorale col. viii/2000 [1 specimen].

Rhynchostome positioned obliquely between cephalic tentacles (38: 2).

**Clade 13**

Anus sited close to mantle, distance to mantle border: total pallial cavity length  $<1/3$  (77: 0).

***Latirus pictus* (Figs. 91-92)**

**Examined material:** MNHN IM-2013-10540, Kranket Island, Papua New Guinea, 15-17m depth, 5°12'9"S; 145°49'18.6168"E. PAPUA NIUGINI expedition. xi/06/2012 [1 specimen].

Margin of renal aperture emarginated by lipped rim (34: 1). Rachidian tooth of radula diminute, its width: lateral tooth width  $<1/4$  (53: 3).

**Clade 14 *Leucozonia* and *Opeatostoma***

Ctenidium ample, its width: osphradium width  $\geq 1.5$  (28: 2). Loss of longitudinal folds in margin of rhynchostome (39: 0). Odontophore long, its length: proboscis length  $\sim 1$  (42: 0). Cusp 1 of lateral tooth of radula absent (60: 2), cusp 2  $\sim$ twice as other cusps (61: 1).

**Clade 14a *Leucozonia ocellata*, *L. cerata* and *Opeatostoma pseudodon***

Margin of siphon bearing many longitudinal folds (30: 1). Rhynchostome distanced longitudinally from cephalic tentacles, not adjacent to them (37: 1), non-lipped (40: 1). Odontophore m6 muscle posterior free portion: odontophore length  $\leq 1/6$  (45: 1). Female cement gland opening centrally in foot sole (84: 0). Duct of penis linear (87: 0).



Figure 91. *Latirus pictus*, shell.  
MNHN IM-2013-10540  
(66mm).

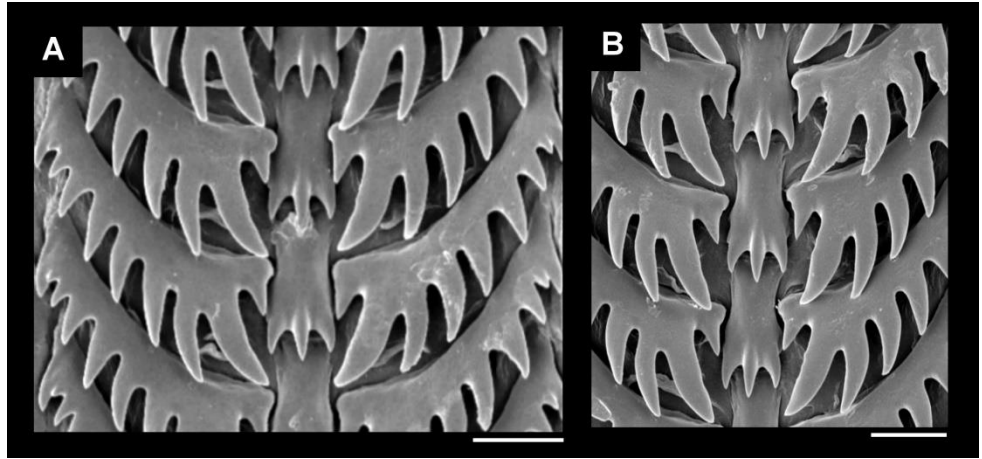


Figure 92. *Latirus pictus*, radula. **A-B**: MNHN IM-2013-10540. **A**: panoramic view. **B**: detail of rachidian tooth. Scale bars = 20 $\mu$ m.

#### *Leucozonia ocellata* (Figs. 93-94)

**Examined material:** MNRJ 11174, Rasa Island, Fernando de Noronha Archipelago, Pernambuco state, Brazil. P.M.S. Costa col. vii/10/1999 [1 specimen]. MNRJ 11200, Fernando de Noronha Archipelago, Pernambuco state, Brazil. P.M.S. Costa col. vii/09/1999 [1 specimen]. MNRJ 4276, Atol das Rocas, Pernambuco state, Brazil. J.H.Leal, G.W.Nunam, C.B. Castro, D.F. Moraes. col. ii-iii/1982 [10 specimens]. MNRJ 5357, Itapoã Beach, Salvador state, Brazil. P. Jurberg col. vii/11/1980 [4 specimens]. MNRJ 12963, Santa Bárbara Island, Abrolhos Archipelago, Bahia state, Brazil. A.L. Castro, J. Becker, P. Jurberg & A. Coelho col. ix/1968 [35 specimens]. MNRJ 10735, Santa Bárbara Island, Abrolhos Archipelago, Bahia state, Brazil. A.L. Castro, J. Becker, P. Jurberg & A. Coelho col. ix/1969 [11 specimens]. MNRJ 14223, Rio de Janeiro state, Brazil. L.R. Tostes col. iii/1975 [1 specimen]. MNRJ 10736, Prainha Beach, Arraial do Cabo, Rio de Janeiro state, Brazil. A.L. Castro, J. Becker, P. Jurberg & E.A. Coelho col. ix/1969 [1 specimen].

Osphradium heavily asymmetrical (23: 2). Rachidian tooth of radula bearing 5–6 cusps (58: 1); cusp 2 bearing secondary inner cusp (62: 1). Loss of seminal receptacle in pallial oviduct (78: 0). (84: 1). Female cement gland opening anteriorly in foot (84: 1). Commissure of buccal ganglia inconspicuous (93: 1).



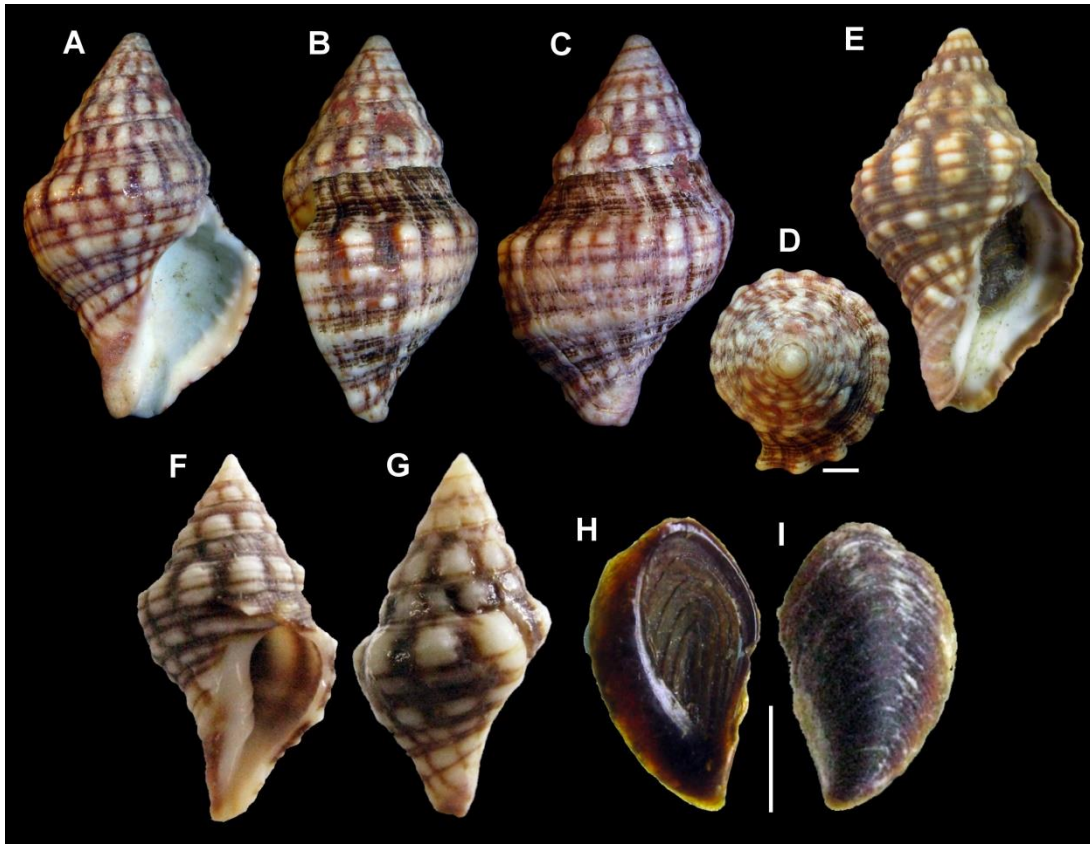


Figure 93. *Leucozonia ocellata*, shell and operculum. **A-D**: MNRJ 5357 (35.9mm). **E**: MNRJ 14223 (22.1mm). **F-G**: MNRJ 10735 (17mm). **H**: operculum, inner view. **I**: operculum, outer view. Scale bars = 3mm.

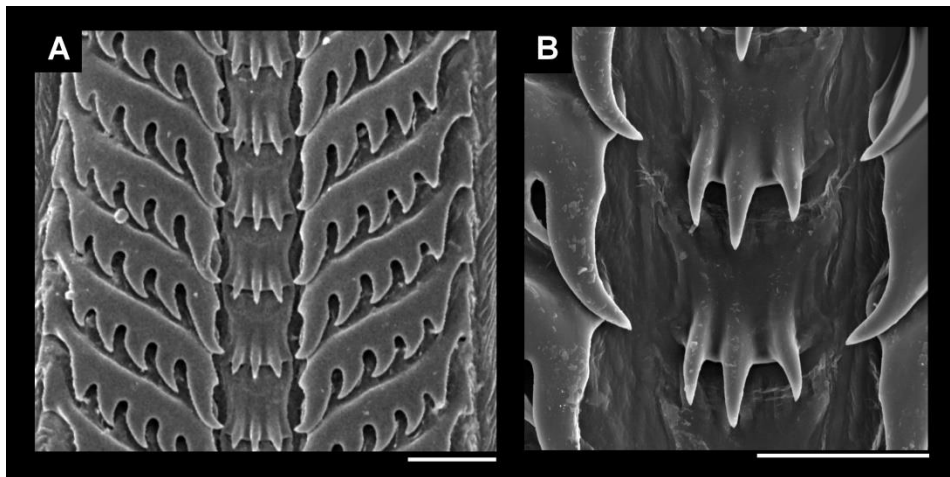


Figure 94. *Leucozonia ocellata*, radula. **A-B**: MNRJ 10735. **A**: panoramic view. **B**: detail of rachidian tooth. Scale bars = 50 $\mu$ m.

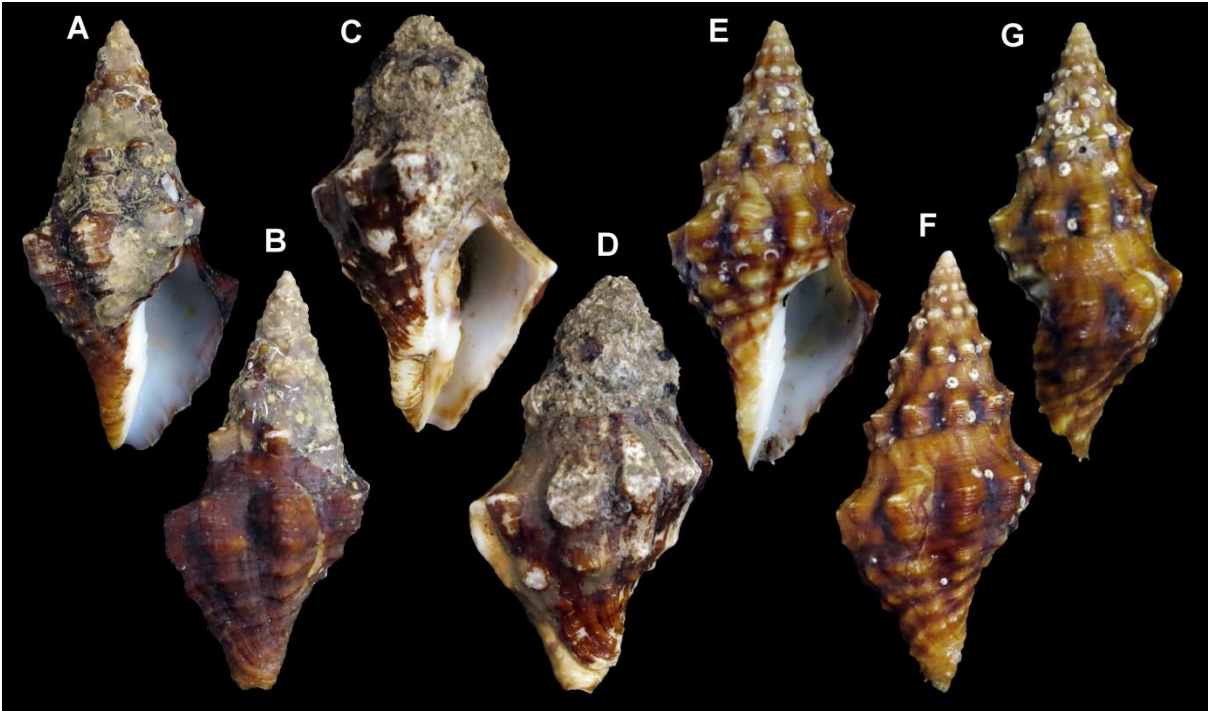


Figure 95. *Leucozonia cerata*, shell. **A-B**: MZSP 64252 (57.5mm). **C-D**: MZSP 64210 (62.1mm). **E-G**: MZSP 95287 (49mm).

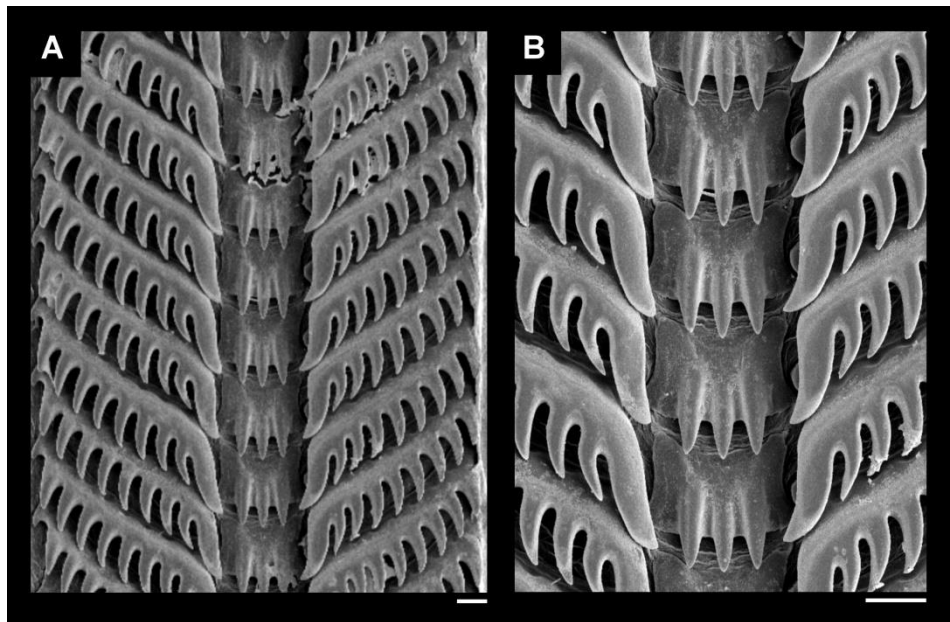


Figure 96. *Leucozonia cerata*, radula. **A-B**: MZSP 64252. **A**: panoramic view. **B**: detail of rachidian tooth. Scale bars = 30 $\mu$ m.



***Leucozonia cerata* (Figs. 95-96)**

**Examined material:** MZSP 64252, Venedo Island, Panama. L.R.L. Simone col. i/30/2006 [2 specimens]. MZSP 64210, Venedo Island, Panama. L.R.L. Simone col. i/30/2006 [2 specimens]. MZSP 95287, Ecuador. J. Coltro col. 2009 [8 specimens].

Nephridial gland present in membrane between renal cavity and pericardium (35: 1). Odontophore fused anteriorly  $\leq 15\%$  of total odontophore length (44: 1). Buccal ganglia commissure long, its length: buccal ganglia length  $\geq 1/2$  (94: 1).

***Opeatostoma pseudodon* (Figs. 97-98)**

**Examined material:** MZSP 64204, Venedo Island, Panama. L.R.L. Simone col. i/30/2006 [6 specimens]. MZSP 67764, la de la Plata, Manabi, Ecuador. J. Coltro col. vi/2006 [3 specimens]. MZSP 68483, Isla Salango, Manabi, Ecuador. J. Coltro col. vii/2006 [3 specimens].

Loss of spiral sculpture of shell (3: 0). Labral tooth present in outer lip covered by mantle (5: 1) as a sharp ventrally pointed tooth. Osphradium leaflets low, its height: height of ctenidium  $< 1/2$  (26: 0). Loss of longitudinal folds in margin of siphon (30: 0). Margin of renal aperture emarginated by lipped rim (34: 1). Loss of nephridial gland in membrane between renal cavity and pericardium (35: 0). Renal aperture situated close to pericardium (36: 1). Rhynchostome longitudinally adjacent to cephalic tentacles (37: 0). Odontophore medium-sized, its length: proboscis length  $1-1/2$  (42: 1). Rachidian tooth of radula may bear  $\geq 5$  cusps (51: 4). Posterior esophagus bearing sudden broadening in visceral region (74: 1), anterior to stomach. Penis ejaculatory duct as long convoluted tube immersed in haemocoel (89: 1).

**Clade 14b “*Leucozonia nassa* complex”**

Labral tooth may be present in outer lip, not covered by mantle as a blunt, short, ventral tooth. (5: 2). Head medium-sized, its width: head-foot mass width  $1/4-1/2$  (13: 1), bearing short cephalic tentacles, its length: head width  $1/2-2/3$  (14: 1). Pallial cavity long, its extension  $\geq 3/4$  whorls (19: 1). Cusp of 2 lateral tooth of radula bearing secondary inner cusp (62: 1). Seminal receptacle in pallial oviduct present (78: 0). Bursa copulatrix short, its length: oviduct length  $< 1/4$  (80: 0).

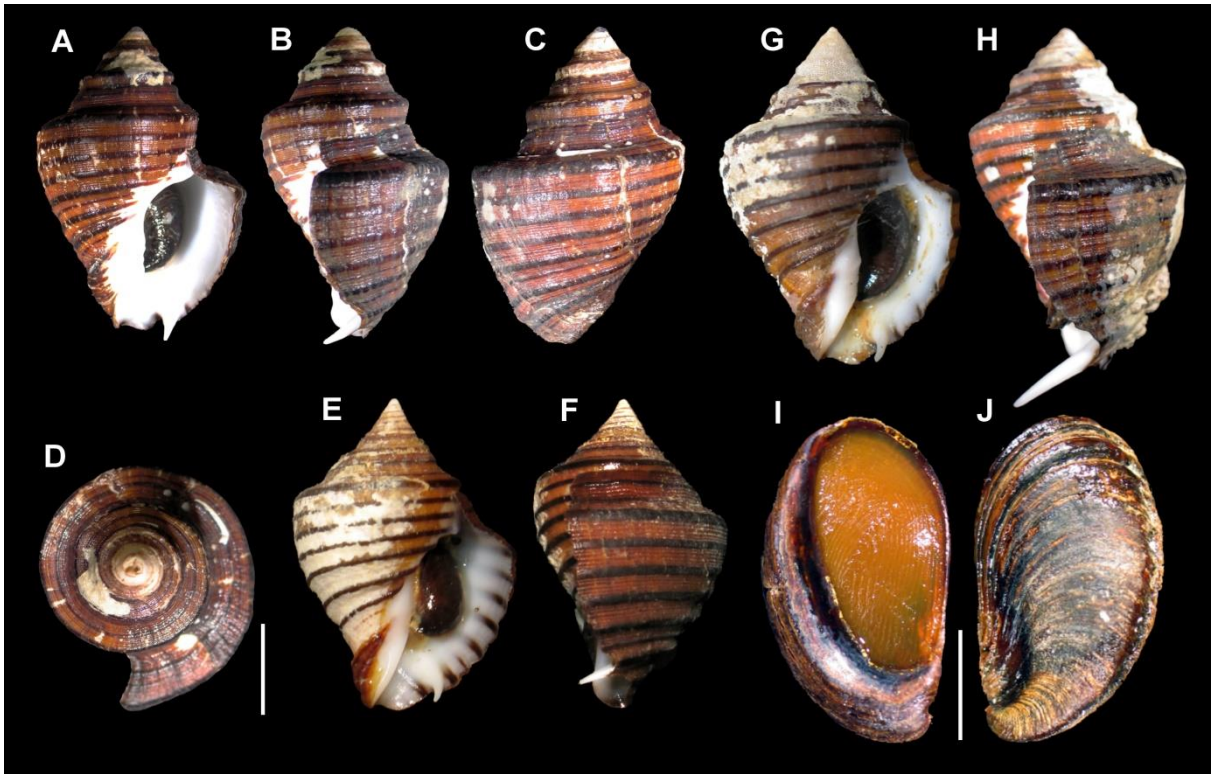


Figure 97. *Opeatostoma pseudodon*, shell and operculum. A-D: MZSP 64204 (54.3mm). E-F: MZSP 67764 (28.3mm). G-H: MZSP 68483 (65.7mm). I: operculum, inner view. J: operculum, outer view. Scale bars = 10mm.

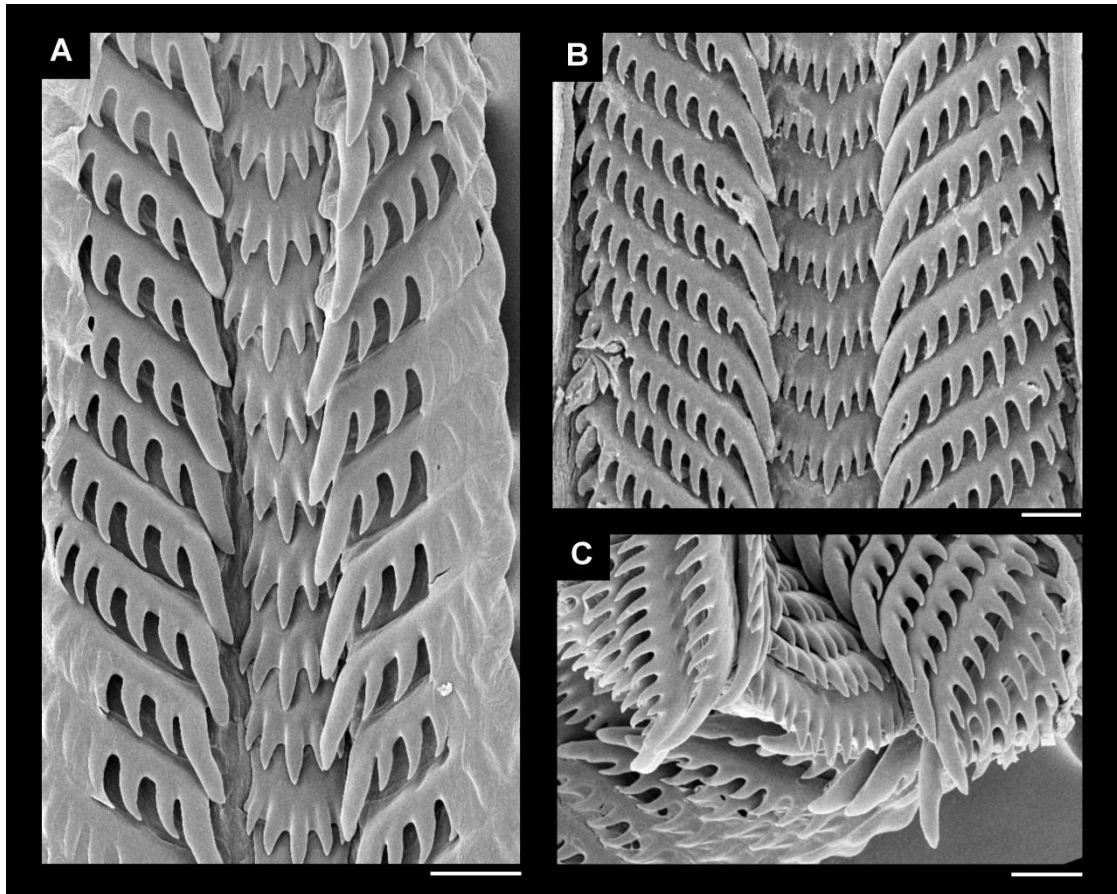


Figure 98. *Opeatostoma pseudodon*, radula. A-C: MZSP 68483. A: panoramic view, male. B: panoramic view, female. C: detail of rachidian tooth, female. Scale bars = 50 $\mu$ m.

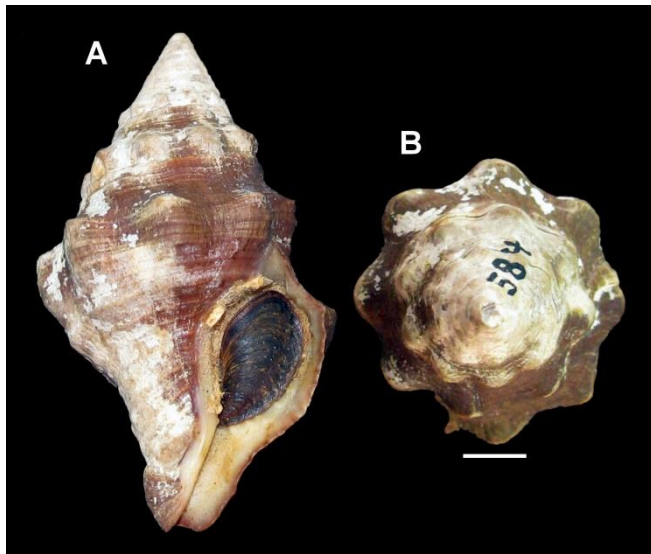


Figure 99. *Leucozonia nassa nassa*, shell. A-B: MNRJ 584 (36mm). Scale bars = 5mm.

***Leucozonia nassa nassa* (Figs. 99)**

**Examined material:** MNRJ 584, Marathon Key, Florida, USA. Mata col. iii/1951 [2 specimens]

No known autapomorphies.

***Leucozonia nassa cingulifera* (Fig. 100)**

**Examined material:** MNRJ 14848, Itapuã, Salvador, Bahia state, Brazil. D. Mendonça col. xi/1964 [2 specimens]. MNRJ 10710, Tamandaré Bay, Pernambuco state, Brazil. S. Ypiranga col. xii/1962 [7 specimens]. MNRJ 11065, Fernando de Noronha Archipelago, Pernambuco state, Brazil. P.M.S. Costa col. vi/17/2000 [1 specimen]. MNRJ 14485, Trindade Island, Espírito Santo state, Brazil. F. Moraes col. xi/18/2003 [1 specimen].

No known autapomorphies.

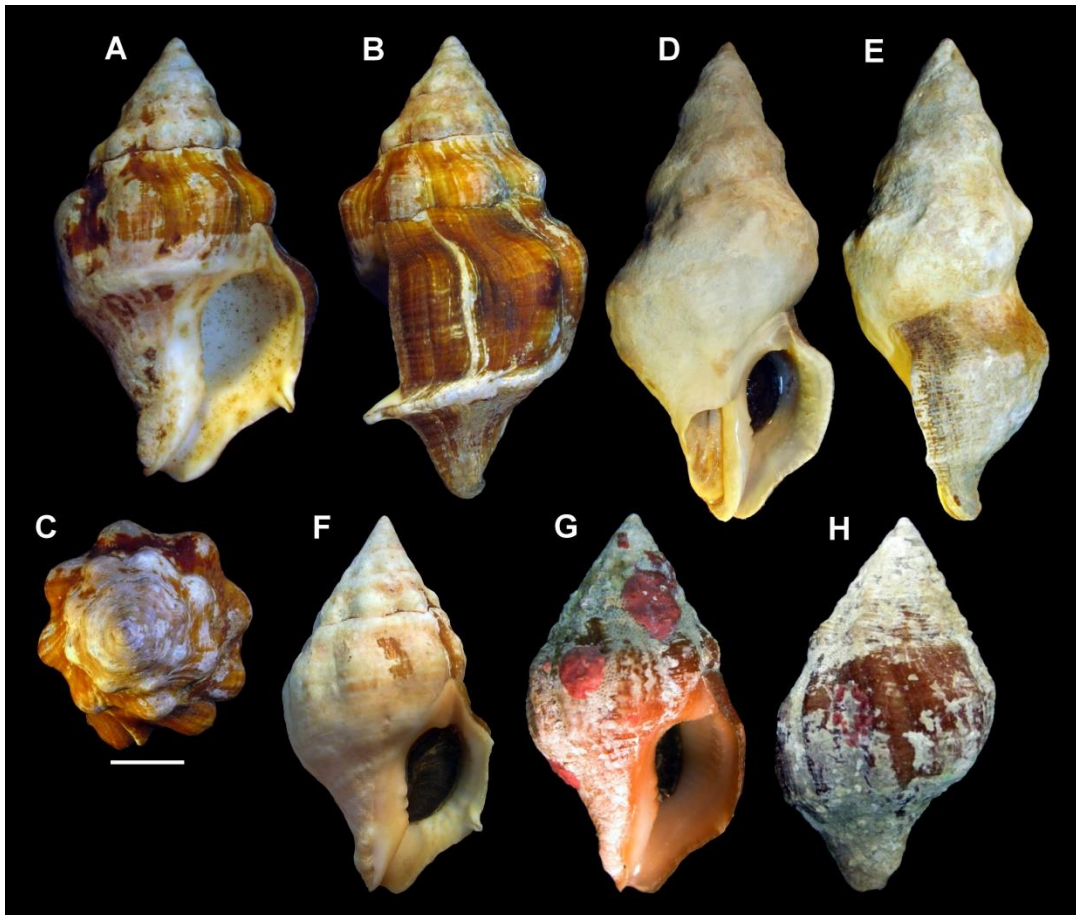


Figure 100. *Leucozonia nassa cingulifera*, shell. **A-C**: MNRJ 14848 (57.9mm). **D-E**: MNRJ 10710 (69.9mm). **F**: MNRJ 11065 (48.8mm). **G-H**: MNRJ 14485 (27.4mm). Scale bars = 10mm.

***Leucozonia nassa brasiliiana* (Figs. 101-102)**

**Examined material:** MNRJ 10993, Japonês Beach, Cabo Frio, Rio de Janeiro state, Brazil. A.D. Pimenta, M.S. Costa, J.B. Alvim & D.R. Couto col. i/18/2007 [66 specimens]. MZSP 69496, Scalvada Island, Guarapari, Espírito Santo state, Brazil, 12-20m depth. A. Bodart Femorale col. i/2005 [2 specimens]. MZSP 41814, Guarapari, Espírito Santo state, Brazil. Coltro col. 2003 [14 specimens].

No known autapomorphies.



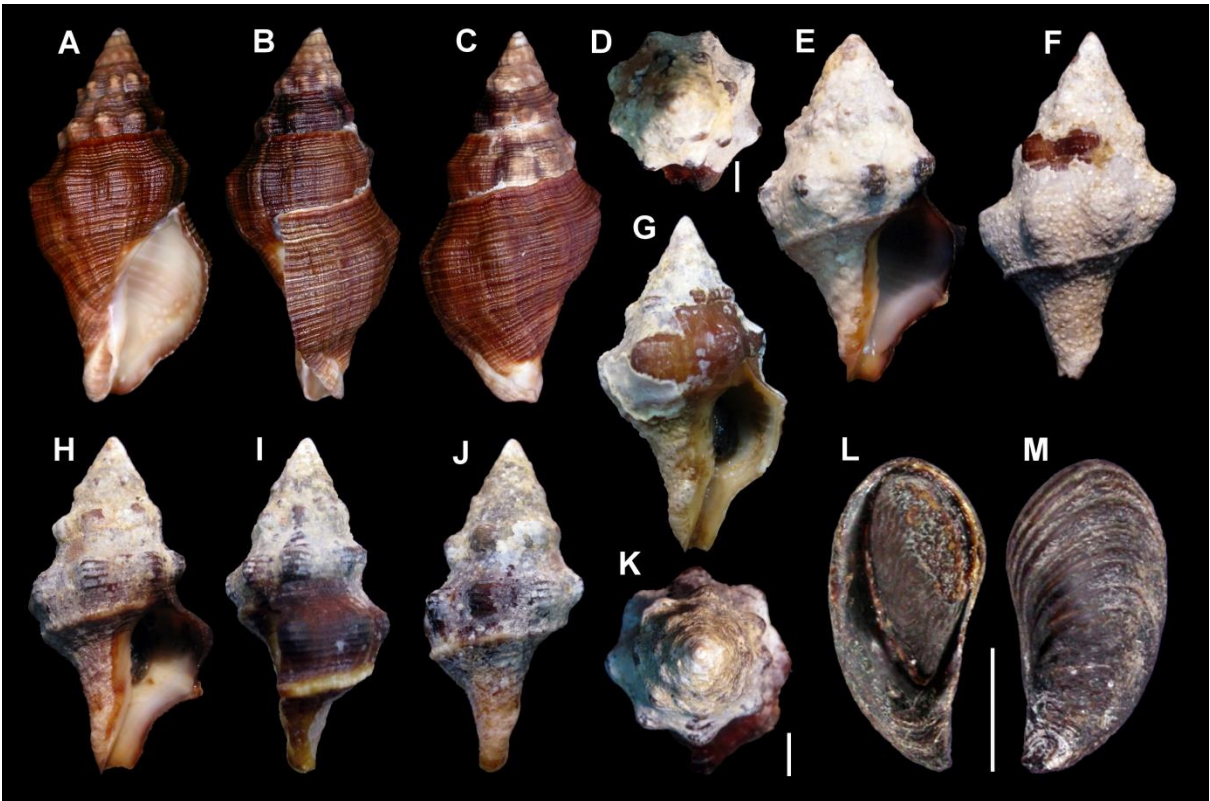


Figure 101. *Leucozonia nassa brasiliiana*, shell. **A-C**: MNRJ 10993 (55.5mm). **D-F**: MZSP 69496 (28.1mm). **G**: MZSP 41814 (29.3mm). **H-K**: MZSP 69496 (34.5mm). **L**: operculum, inner view. **M**: operculum, outer view. Scale bars = 3mm.

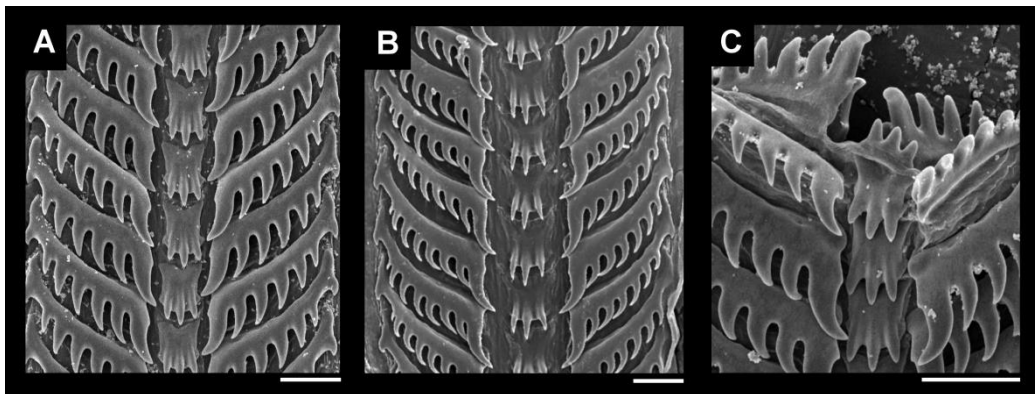


Figure 102. *Leucozonia nassa brasiliiana*, radula. **A-C**: MNRJ 10993. **A-B**: panoramic view. **C**: detail of rachidian tooth. Scale bars = 50µm.

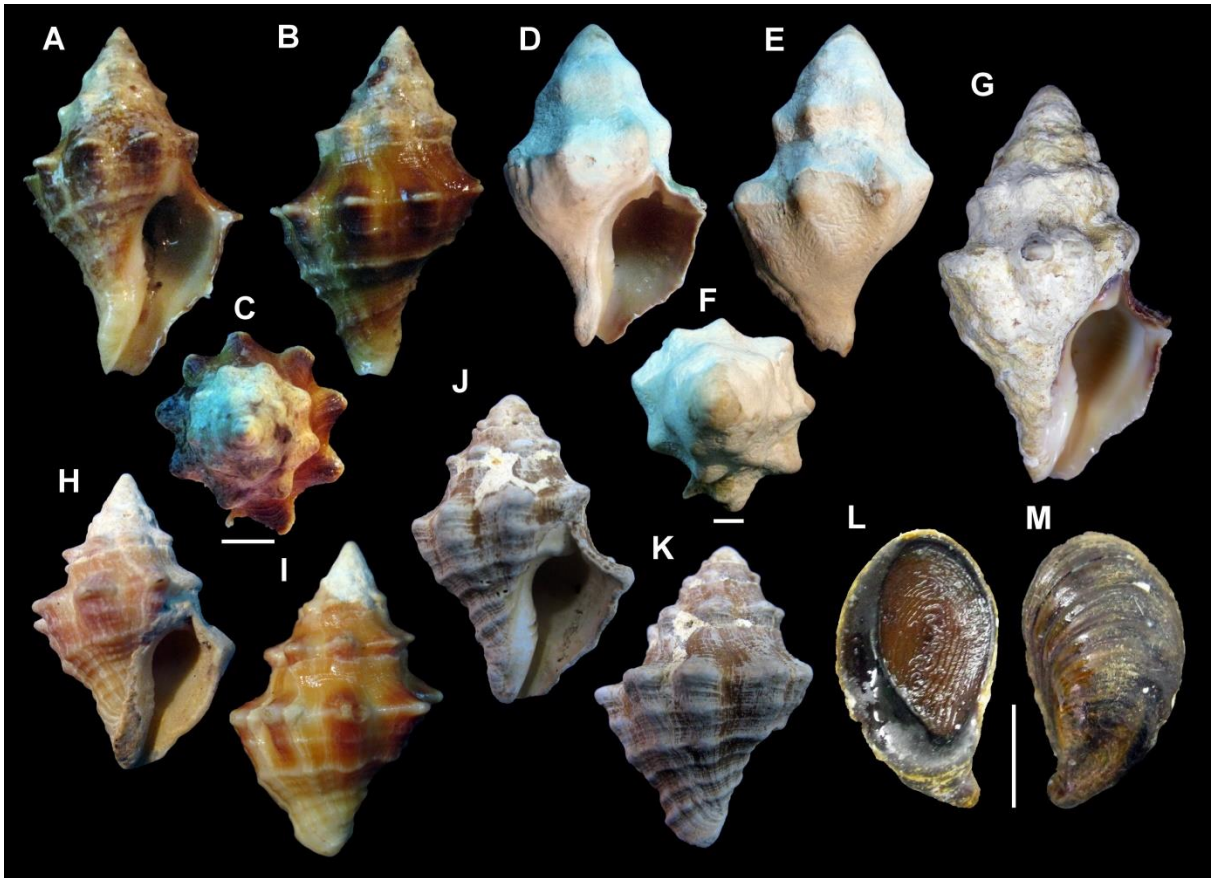


Figure 103. *Leucozonia ponderosa*, shell and operculum. **A-C**: MNRJ 14607 (28.6mm). **D-F**: MNRJ 5220 (44.2mm). **G**: holotype, MORG 39599 (47.3mm). **H-I**: MNRJ 5138 (31.4mm). **J-K**: MNRJ 5137 (37.3mm). **L**: operculum, inner view. **M**: operculum, outer view. Scale bars = 5mm.

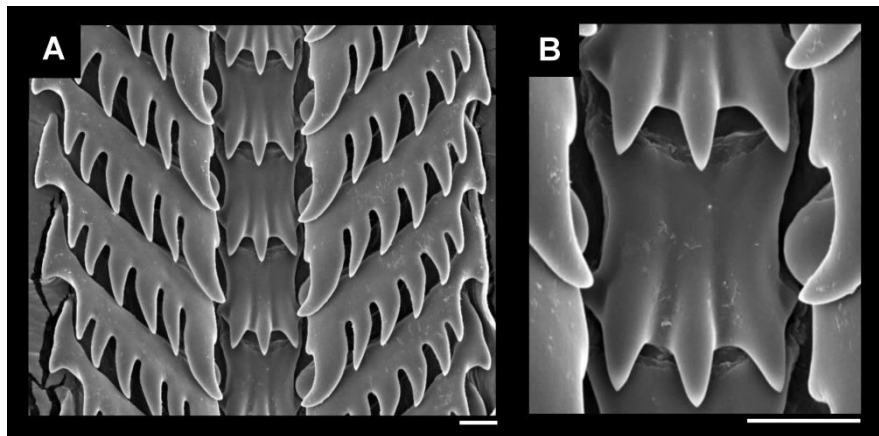


Figure 104. *Leucozonia ponderosa*, radula. **A-B**: MNRJ 5220. **A**: panoramic view. **B**: detail of rachidian tooth. Scale bars = 20 $\mu$ m.



***Leucozonia ponderosa* (Figs. 103-104)**

**Examined material:** MORG 39299, Portuguese cove, Trindade Island, Espírito Santo state, Brazil, 10m depth on rocky bottom, 20°30'S; 29°20'W. J.H. Leal & P. Bouchet col. v/22/1987 [1 specimen, holotype]. MNRJ 14607, Fernando de Noronha Archipelago, Pernambuco state, Brazil, 12-18m depth. P.M.S. Costa col. viii/2009 [1 specimen]. MNRJ 5220, Cachoeira Beach, Trindade Island, Espírito Santo state, Brazil. J. Becker col. i/1959 [2 specimens]. MNRJ 5138, Galheta Beach, Trindade Island, Espírito Santo state, Brazil. B Prazeres col. xii/1975 [6 specimens]. MNRJ 5137, Cabritos Beach, Trindade Island, Espírito Santo state, Brazil. B Prazeres col. xii/1975 [3 specimens].

Pedal ganglia short, its length: nerve ring length  $<1/2$  (90: 0).

## **6. Phylogenetic discussion**

The following discussion corresponds to the unweighted phylogenetic analysis, as specified in the Material and Methods section. Clades are numbered 1 through 15 in the main branch (for Fasciolariidae, outgroup taxa are numbered in decreasing order), while subsequent inner branches are labelled 1a, 1b, etc. as seen in Figure 6.

Important morphology morphology-based phylogenetic analyses were endeavored by Ponder & Lindberg (1997), Strong (2003) and Simone (2011). Despite being more inclusive (Gastropoda and Neogastropoda), these important works are of great value to this discussion, and most taxonomical, phylogenetical and morphological considerations will be discussed subsequently in the next section. Figures 105-107 illustrates these phylogenetic hypotheses.

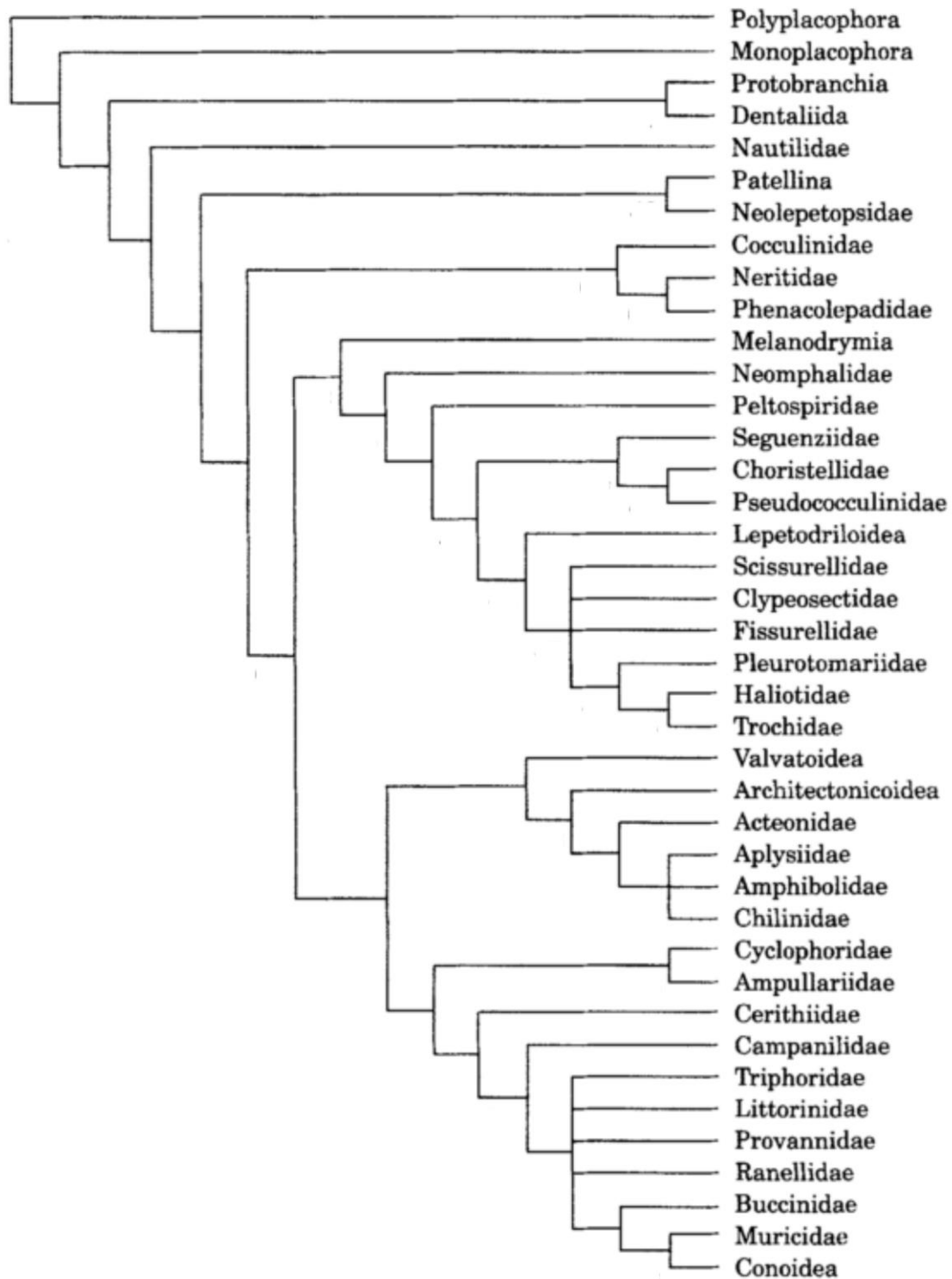


Figure 105. Strict consensus of the obtained trees from Ponder & Lindberg (1997), based on morphological data (modified from Ponder & Lindberg, 1997: Fig. 2)

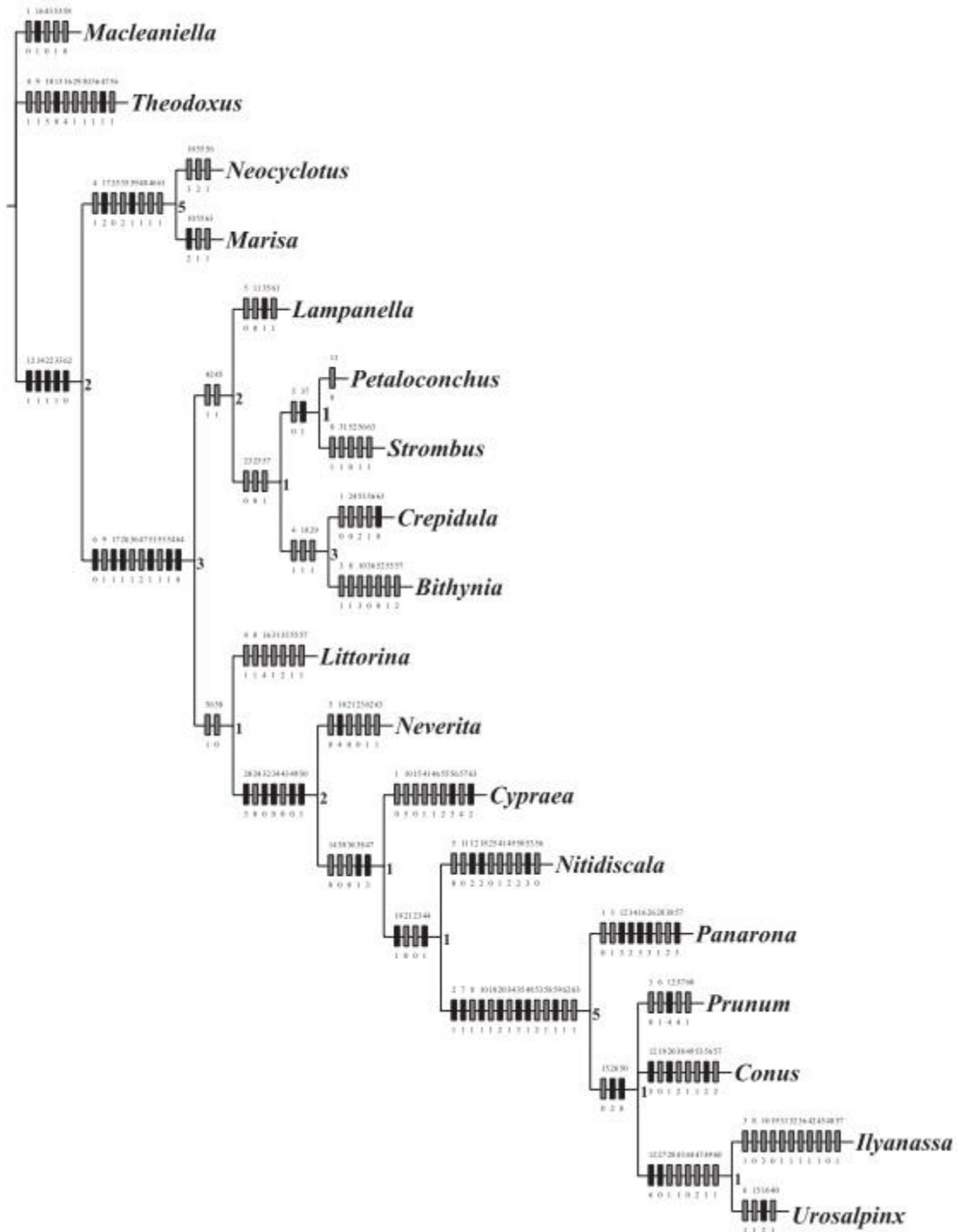


Figure 106. Strict consensus tree of the analysis of Caenogastropoda based on morphological characters of Strong (2003). Tree shows character optimizations, numbers at the nodes indicate Bremer support (modified from Strong, 2003: Fig. 26).

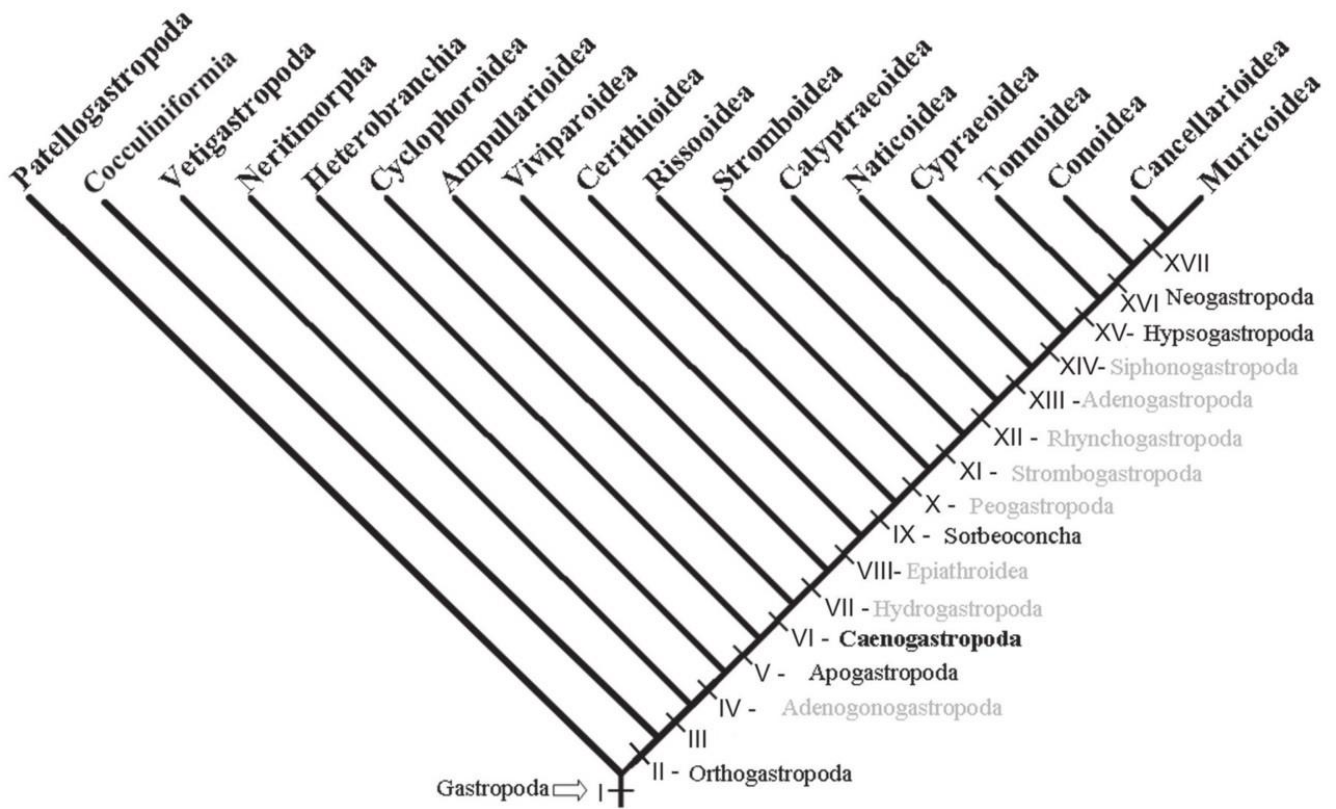


Figure 107. Strict consensus tree of the Caenogastropoda analysis of Simone (2011), based on morphological characters (modified from Simone, 2011: Fig. 21).

### Clade -3 Neogastropoda

Neogastropoda is the most diverse caenogastropod mollusk clade and are traditionally well defined morphologically, and several are its synapomorphies, including: presence of a pair of accessory salivary glands, a valve of Leiblein, and an anal or rectal gland (Kantor & Fedosov, 2009); the work of Simone (2011) added: the loss of the jaws, the pair of retractor muscles of buccal mass passing through the nerve ring, the ducts of the salivary glands free from the nerve ring, the ventral esophageal gland individualized by a duct (known as the gland of Leiblein and the venom gland), and a highly concentration of the nerve ring. A brief discussion of the synapomorphies relevant to this work is ensued; however, a more thorough discussion of each character utilized for this analysis is found in the character discussion section.

Strong (2003) agreed that the pycnonephridial kidney is a synapomorphy of the neogastropods, and this is confirmed here. Although this traditional classification of kidney lamellae has been contested by several authors (*e.g.*, Ponder, 1973), it is undoubted that on the current context, neogastropods have them differentiated: the kidney's interdigitating lamellae that occur in all neogastropod taxa are supplied by a two main branches: the dorsal and the ventral afferent renal vessel; the dorsal branch supplies the lobes while the ventral remains in the kidney floor (Strong, 2003). This is the type of pycnonephridians; in contrast, meronephridians have lamellae that are not interdigitated. Such renal vessel detail was not visualized in the present study. This was interpreted as a secondary reversion to the plesiomorphic state within non-cancellariids neogastropods by Simone (2011).

The neogastropod odontophore cartilages are highly differentiated from other Caenogastropoda. Simone (2011) pointed to the loss of accessory pair of protractor muscles of odontophore (m14) in Neogastropoda; in the present analysis it was observed that the origin of the m11 muscles occur posteriorly in the odontophore cartilages, as opposed to inserted in the haemocoelic wall. This odontophore type occurs in all neogastropods present in the literature (*e.g.*, Simone, 1996; Simone *et al.*, 2009; Simone & Pastorino, 2014; Couto *et al.*, 2015a; 2015b). The m11 muscles are a pair of ventral tensor muscles of the radula, which enables the sliding movement of the radular ribbon (Ponder *et al.*, 2008). In taxa which these muscles are diminute (as in the case of Caenogastropoda *sensu* Simone, 2011) this function is somewhat hampered and there is no sliding movement between the cartilages and the radula (Simone, 2011). Regardless of their true function, which is hard to access by itself, the muscles in the cypraeid *Monetaria*



*annulus* (Linnaeus, 1758) are inserted in the haemocoelic wall, differing from Neogastropods which insert posteriorly in the odontophore.

Radula in Neogastropoda is characterized as being of the rachiglossate type, *i.e.*, one rachidian flanked by one lateral in each side and lacking marginal teeth, adding to three teeth per row. The rachiglossate and toxoglossate (*a posteriori* modification of the rachiglossate type) radulae characterizing neogastropods are assumed to have arisen from a taenioglossate ancestral type (Ponder & Lindberg, 1997). In contrast, non-neogastropod caenogastropods have a taenioglossate type, with a rachidian flanked by a pair of laterals and two pairs of marginals, completing seven teeth per row. Simone (2011) argued that the radula in Conoidea evolved from a taenioglossate type, at least twice in the group, and that the evolution of this character did not pass through a rachiglossate radula.

Another radular modification suffered by the Neogastropods in this analysis is the position of the lateral teeth in relation to the rachidian: in *Monetaria annulus* the teeth are directly adjacent to one another while in non-fascioliid (“basal”) neogastropods the teeth are somewhat apart. All Caenogastropoda radulae figured in the work by Bandel (1984) have this same configuration (*e.g.*, *Cypraea* Linnaeus, 1758: Fig 126; *Murex* Linnaeus, 1758: Fig. 168; *Engina* Gray, 1839: Fig. 201).

One of the more traditional of neogastropod characteristics is the presence of a gland of Leiblein; being utilized as a synapomorphy in several morphological phylogenetic analysis (*e.g.*, Ponder & Lindberg, 1997; Strong, 2003; Simone, 2011). This structure is derived from the esophageal gland of other caenogastropods, and is thought to be homologous to the septated sac in Cypraeidae (Simone, 2011), despite some groups within Neogastropoda lacking this structure and others modified it to a venom gland (for a thorough review of the anatomy and function of the gland of Leiblein see Andrews & Thorogood, 2005). The absence of this structure, along with other factors, has led to the supposition that the neogastropods are not monophyletic (more on this is discussed under Clade -2 Buccinoidea) by Kantor & Fedosov (2009).

*Thais speciosa* (Valenciennes, 1832) (Fig. 7) is regarded as a non-neogastropod because of the absence of typical neogastropod synapomorphies and the radula typical for the genus (Fig. 8) (Bandel, 1984). Despite this species possessing some characteristics of buccinoideans such a pseudoumbilicus, a stomach bearing a posterior bulge and the presence of a penis ejaculatory duct as long convoluted tube, these are considered convergences.

## **Clade -2 Buccinoidea**

The superfamily Buccinoidea includes the families Buccinidae, Belomitridae, Busyconidae, Colubrariidae, Columbellidae, Nassariidae, Melongenidae and Fasciolariidae (Bouchet & Rocroi, 2005; WoRMS, 2016). They are considered highly derived in the Neogastropoda scheme due to the probable loss of the accessory salivary glands and the anal or rectal glands (Fedosov & Kantor, 2012).

Kantor & Fedosov (2009) argued that the valve of Leiblein, an important Neogastropoda synapomorphy, is indeed homoplastic, and emerged at least twice in the evolution of this group. If this proves true, Neogastropoda becomes non-monophyletic because Buccinoidea will lack all of its synapomorphies (until now regarded as secondary losses, *e.g.*, Melongenidae here represented by *Pugilina tupiniquim* Abbate & Simone, 2015, Figs. 9-10).

In their complete mitochondrial genome and three nuclear-gene phylogeny, Osca *et al.* (2015) failed to recover Neogastropoda, and proposed the inclusion of Tonnoidea, or the exclusion of Cancellarioidea and possibly Volutidae from Neogastropoda. In the first case, tonnoideans would have secondarily lost the traditional neogastropod synapomorphies, while in the latter these synapomorphies would be considered homoplastic, in this sense agreeing with Kantor & Fedosov (2009).

## **Clade -2a Clade Buccinidae + Nassariidae**

This clade excludes the genus *Engoniophos* Woodring, 1928 (here represented by *E. uncinatus* [Say, 1826], Figs. 11-12), which has traditionally been recognized as a buccinid, although more recently has been revisited and is thought to belong to Nassariidae in both morphology (Abbate, 2016) and molecular-based (Galindo *et al.*, 2016) analyses. It includes the nassariid species *Nassarius reticulatus* (Linnaeus, 1758) (Figs. 13-14) and *Bullia laevissima* (Gmelin, 1791) (Figs.15-16). In the present work, the probable cause for the exclusion of this taxon is the absence of a dorsal metapodial tentacle in this genus. A more thoroughly sampling will likely obtain similar results to those of Abbate (2016) and Galindo *et al.* (2016), since making any taxonomical decisions for the outgroup species in the present study (due to the lack of sampling) is tentative at best.

The rachidian tooth of species contained in this clade possess five or more sharp principal cusps (Figs. 14.16), which is unique for the Buccinoidea radula; *Nassarius albus* (Say, 1826) may

have up to 18 cusps (Bandel, 1984), *Engoniophos* has a large increase in cusp number of the rachidian, and Bandel (1984) already indicated that they belong in the same family; although, presently, it was interpreted as a convergence. Morphology of the lateral teeth the Nassariidae is similar to most Buccinidae, only the characteristic central tooth of the nassariids differentiates their radula from that of other buccinids (*e.g.*, Bandel, 1984). *Buccinum undatum* Linnaeus, 1758 (Fig. 18) has five cusps on the rachidian, but that is considered few in number for a nassariid, despite currently classified in Buccinidae.

### **Clade -1 Clade Pisaniinae + Fasciolaridae**

The main feature that distinguishes species in this clade is the salivary ducts which merge in the anterior esophagus wall. This was observed for Fasciolaridae and was already reported as a diagnostic feature for the family by Fraussen *et al.* (2007). In Buccinidae, the ducts, after leaving the glands, follow freely along the anterior esophagus towards the anterior part of the proboscis where they enter the walls of the esophagus close to their entrance into the buccal cavity. In Fasciolaridae, on the other hand, the ducts, after leaving the glands, merge with the anterior esophagus walls close to the valve of Leiblein. They then follow to their openings into the buccal cavity under the lateral folds of the esophagus.

Although *Pisania pusio* (Linnaeus, 1758) (Fig. 19-20) is classified under Buccinidae, this group is surely a heterogeneous assemblage that deserves a scope of its own and likely forms several, independent, polyphyletic lineages.

The statocysts present in the nerve ring of all species of *Pisania pusio* occurs asymmetrically, *i.e.*, one anterior, associated to the pedal ganglia, and another more posteriorly, associated to the cerebral ganglia; this situation is reversed in *Teralatirus roboreus*. Although there is some variation in the position of both statocysts (more anterior or posteriorly, *e.g.*, Strong, 2003; Simone, 2011), an asymmetry has never been reported.

### **Clade 1 Family Fasciolaridae**

With 541 extant species in 51 genera worldwide (WoRMS, 2016), fasciolarids comprise of three subfamilies: Peristerniinae Tryon, 1880: which includes, among other genera, *Peristernia* and *Latirus*; Fusiniinae: the spindle shells; and Fasciolarinae: with the conspicuous and well-known tulips and horse-conchs. More recently, however, the group has undergone extensive

taxonomical revision (*e.g.*, Vermeij & Snyder, 2002; 2006; Snyder *et al.*, 2012; Lyons & Snyder, 2013), that elevated several subgenera to genus rank as well as establishing new genera.

The sub-familiar categories for Fasciolariidae have been retained more-or-less stable; Couto *et al.* (2016) on its five-gene molecular phylogeny recovered all three of these subfamilies; although with an extensively revised inclusion of species and genera. This is so far the only extensive phylogenetic study of the family, since past works which included some fascioliid taxa did not have the internal resolution to solve most internal clades. These authors were able to recognize the fusinines, with the inclusion of the genus *Pseudolatirus*; the peristerniines, which include the genera *Peristernia* and *Fusolatirus*; and the fascioliines that include the bulk of Peristerniinae *sensu lato* and the Fascioliinae (the only traditional clade that maintained its monophyly). The traditional peristerniines have representatives in all three clades, while the genera *Teralatirus* and *Dolicholatirus* were a separate group from the remaining fascioliids, although its position remains uncertain, as the statistic tests made were not able to correctly access its position.

Knowledge of the anatomy of the Fasciolariidae is somewhat sparse. Marcus & Marcus (1962) presented a fine anatomical study of *Leucozonia nassa* from Brazil. Although these authors provided a thorough characterization of the species from the state of São Paulo coast in southeastern Brazil, including histological sections, they did not illustrate several features such as the head-foot mass, pallial cavity, and male reproductive and digestive systems. More recently, several anatomical studies of Brazilian species of Fasciolariidae have been undertaken following a thorough anatomical endeavor (*e.g.*, Couto & Pimenta, 2012: on *Leucozonia* Gray, 1847 from Brazil; Couto *et al.*, 2015a: on *Pustulatirus* and *Hemipolygona* species; Couto *et al.*, 2015b: on *Fasciolaria tulipa*).

The current morphological analysis confirms several synapomorphies for Fasciolariidae, five of which are non-homoplastic. Those worth mentioning are: 1) the head with cephalic tentacles positioned with its bases side by side (non-homoplastic) (character 12, Fig. L); 2) the rhynchostome as longitudinal slit (character 38, Fig. AB); 3) the lateral tooth of the radula directly adjacent to rachidian (character 54, Fig. AN); 4) single or paired proboscis retractor muscles originating in the columellar muscle (non-homoplastic) (character 67, Fig. AW); 5) a stomach bearing a posterior bulge without a sorting area (character 75, Fig. BD); 6) a long bursa copulatrix (non-homoplastic) (character 80, Fig. BF); 7) buccal ganglia immersed in the nerve

ring with its connectives not visible (non-homoplastic) (character 91, Fig. BN); and 8) buccal ganglia which is positioned dorsal to cerebro-pleural ganglia (non-homoplastic) (character 92, Fig. BN). For a description of all synapomorphies, in Fasciolariidae as well as all other clades, see section ‘Phylogenetic Description’ and refer to Fig. 6.

Kosyan *et al.* (2009) studied the comparative anatomy of seven fasciolariid species: *Pustulatirus mediamericus*, *Peristernia nassatula*, *P. ustulata*, *Opeatostoma pseudodon*, *Tarantinae lignaria*, *Latirus polygonus*, and *Turrilatirus turritus*. Typically, according to Kosyan *et al.* (2009), fasciolariiids lack a caecum (posterior sorting area) in the stomach and an ingesting gland in the pallial oviduct; additionally, as in buccinids, melongenids, and nassariids, they lack accessory salivary glands and an anal gland (Harasewych, 1998). Species of the family generally have light orange to red head-foot mass; however this characteristic does not take into consideration the clade consisting of the genus *Dolicholatirus* and *Teralatirus* that lack this coloration and is sister group of the remaining fasciolariiids; more on this distinct clade will be discussed later.

A novel characteristic for the clade Fasciolariidae is the position of the cephalic tentacles in relation to each other. In the buccinoidean species, the bases are somewhat apart, while in fasciolariiids they are adjacent to each other. This characteristic has never been reported as diagnostic at this level; all fasciolariid species illustrated in the literature have this conformation as well (*e.g.*, Marcus & Marcus, 1962; Kosyan *et al.*, 2009; Fedosov & Kantor, 2012).

Troschel & Thiele (1865-1893) were the first to characterize the radula of Fasciolariidae, and according to these authors, the radula is characterized as having very wide laterals with many cusps; the rachidians are quadrangular and less wide than the laterals. Although not all fasciolariiids have this conformation (clade of *Dolicholatirus*, discussed later), a single characteristic that can distinguish the fasciolariiids at this level is the position of the rachidian that is adjacent to the lateral; in the buccinoideans the lateral is distanced in a way that you can see the radular ribbon between the teeth. Bandel (1984) illustrated and characterized the radulae of five Caribbean fasciolariiids: *Leucozonia nassa*, *L. ocellata*, *Polygona infundibulum* (Gmelin, 1791), *P. angulata* (Röding, 1798) and *Fasciolaria tulipa*, and this feature conforms to all illustrations.

Fraussen *et al.* (2007) reported that a combination of anatomical characters is diagnostic for the Fasciolariidae, including the multicuspidate lateral teeth and a small rachidian, salivary ducts embedded in the esophagus wall (a feature shared with *Pisania pusio*), but also: a single or paired

proboscis retractor muscle, and the characteristic stomach morphology. Kosyan *et al.* (2009) confirmed the proboscis retractor muscles as characteristic for the fasciolaridiids. The proboscis retractor muscles of fasciolaridiids consists of aggregated fibers that have its origin in the back of the diaphragmatic septum, attached to the columellar muscle. It is hypothesized that this corresponds to the same configuration as that pointed by Fraussen *et al.* (2007) and Kosyan *et al.* (2009). This differs from other Neogastropoda studied because they have the origin of the muscles in the floor of the haemocoel, as well as constituting several tuft of fibers. *Troschelia berniciensis* (King, 1846), a buccinid analyzed by Kosyan *et al.* (2009) has the proboscis attached to the bottom of the body haemocoel by several proboscis retractors emerging from its base, consisting of approximately six muscle tufts.

Kantor (2003) distinguished the Fasciolaridiidae by their distinct stomach morphology with low folds on the inner wall, transverse striations on the longitudinal fold and absence of a posterior mixing area, and stated that the superfamily Buccinoidea can be differentiated based on stomach characters. In the context of the superfamily, the typical fasciolariid stomach is one that lacks a posterior mixing area, (sometimes called as caecum), low relief of the folds on the inner stomach wall, presence of transverse striations on the low longitudinal fold, and the absence of clear differentiation of the gastric chamber into dorsal and ventral parts. Buccinoidean species, non-fasciolaridiids, on the other hand, have a posterior elongation of the stomach wall, and a division into ventral and dorsal chambers connected by a lateral sulcus (Kantor, 2003).

It is worth noting that only the combination of several of these above-mentioned characteristics has been reported as diagnostic for the family. However, other species belonging to other families may possess these characteristics individually. For example, *Troschelia berniciensis* has fasciolariid-like lateral radular teeth with five to ten cusps, but typical buccinid-like proboscis retractor muscles and stomach (Bouchet & Warén, 1985; Kosyan *et al.*, 2009); this species is currently attributed to Buccinidae (WoRMS, 2016). *Thalassoplanes circumreta* Lus, 1973 possesses a clearly fasciolariid-like radula, but the stomach has a very long posterior mixing area and salivary ducts which pass freely along the anterior oesophagus (Fraussen *et al.*, 2007); it is currently a Buccinidae although originally in Fasciolaridiidae. The use of a rigorous phylogenetic analysis allows for the distinction between true synapomorphies and mere diagnostic characteristics, *e.g.*, homoplasies, plesiomorphies or convergences.



There is a general tendency in Caenogastropoda for the buccal mass to be located far from the nerve ring. However, muricoideans (*sensu* Simone, 2011: which includes Buccinoidea) have reverted to the plesiomorphic condition, possessing buccal ganglia closer to, or even incorporated into the nerve ring (Simone, 2011). In the context of the superfamily Buccinoidea, it is observed that fascioliariids have the ganglia incorporated into the nerve ring in a way that the connectives are not visible; being even closer to it, located dorsal to the cerebral ganglia. In non-fascioliariid buccinoideans the buccal commissures are visible and the ganglia are more anterior, less associated to the nerve-ring.

### **Clade 1a *Dolicholaturus* + *Teralaturus***

*Dolicholaturus* and *Teralaturus* (Figs. 21-26) are small buccinoid genera with distinctive shell characters whose taxonomic position in Fascioliariidae is ambiguous, although currently generally accepted (*e.g.*, Snyder, 2003; WoRMS, 2016). Originally established (Bellardi, 1884) as a section of *Latirus* for two fossil species, the genus *Dolicholaturus* was attributed to Fascioliariidae without any arguments or analyses, on the basis of its fusiform shell superficially resembling many fascioliariids, although the presence of paired weak columellar plaits (uncommon in Fascioliariidae) was mentioned. Cossmann (1901) raised *Dolicholaturus* to full genus, designated the type species (*Turbinella bronni* Michelotti, 1847) and classified it in the family Fusidae (which Cossmann used in place of Fascioliariidae), subfamily Fusinae, also without providing supporting arguments. Subsequently, almost half of the genera included in Cossmann's Fusinae have since been transferred to other families of Neogastropoda (*Columbarium* Martens, 1881, now Columbariinae, Turbinellidae; *Exilia* Conrad, 1860, now Ptychatractidae; *Thersitea* Savorin, 1915, now Thersiteidae; *Euthriofusus* Defrance, 1820, now Buccinidae). Thiele (1929) reverted to *Dolicholaturus* as a section of *Latirus*, still included in the family Fascioliariidae, a position followed by Wenz (1943) and finally by Snyder (2003; but see Vermeij & Snyder, 2006). Thus the current inclusion of *Dolicholaturus* in the Fascioliariidae goes back to Bellardi (1884) and is uncritically based on shell characters, which generally proves to be an unreliable diagnosis at best.

Couto *et al.* (2016) demonstrated the monophyly of the clade containing *Dolicholaturus* and *Teralaturus* through maximum likelihood (ML) and Bayesian inference (BI) analyses, and *Dolicholaturus lancea* (Gmelin, 1791), *D. cayohuesonicus* (Sowerby, 1878), *D. spiceri* (Tenison-

Woods, 1876), *Teralatirus noumeensis* (Crosse, 1870) and *T. roboreus* were sampled. Its position as the sister group of the remaining fasciolaridiids remained uncertain, as the tests performed to calculate the probabilities according to the approximately unbiased test (Shimodaira, 2002), the Kishino-Hasegawa test (Kishino & Hasegawa, 1989), and the Shimodaira-Hasegawa test (Shimodaira & Hasegawa, 1999) could not statistically discriminate between the constrained (all fasciolaridiids and *Dolicholatirus/Teralatirus*) and unconstrained topologies. Regardless of their position within or out of Fasciolaridiidae, the deeper nodes between the ML and BI analyses of Couto *et al.* (2016) differed; in this way the clade of *Dolicholatirus* was a sister group of the Conoidea and *Thais* Röding, 1798 clade, but other sister-group inferences diverged between both.

Simone *et al.* (2013) pointed out the similarities between *Dolicholatirus* and *Teralatirus*, and suggested that most likely these should be better placed together, a hypothesis confirmed here and by Couto *et al.* (2016) as *Teralatirus* nested within *Dolicholatirus* in both the morphological and molecular analyses, respectively. Simone *et al.* (2013), nevertheless, followed a conservative approach with regard to their classification and no changes were made. Based on this analysis and in Couto *et al.* (2016), *Teralatirus* should be relocated to the genus *Dolicholatirus*.

The main difference that distinguishes this clade from all other fasciolaridiids is present in the radulae. Based on the differences in radula (also on shell morphology and on the shape of the egg capsules), Vermeij & Snyder (2006) argued that *Dolicholatirus* likely belongs to Turbinellidae, a view followed by Beu (2011). Turbinellid radulae possess lateral teeth which are small, with a single cusp and a rachidian that is thin, with a single central cusp and curved outward (*e.g.*, *Turbinella angulata* (Lightfoot, 1786) in Bandel, 1984: pl. 17, Fig. 4). This radula type is very similar to the *Dolicholatirus* (Fig. 22, 26) and *Teralatirus* presently studied (Fig. 24). This notable radular morphology difference is the sole reason that made previous authors disagree on the position of these taxa within Fasciolaridiidae, attributing the similarities to Turbinellidae as synapomorphic. *Dolicholatirus* and *Teralatirus* have a very minute body size (the largest, *Dolicholatirus lancea*, reaches length of up to 60mm, despite being very slender), it may be the case that this clade has suffered a miniaturization process, and that is evidenced also in shell features. Miniaturization events in nature are common, widespread phenomena in animals that result in extremely small adult body size whose phenotype is a complex combination of ancestral and derived traits, including reduction and structural simplification and increased variability

(Hanken & Wake, 1993). This hypothesis may explain why some typical fasciolariid features are not present in this clade, such as the body pigmentation coloration and the ‘typical fasciolariid-like’ radula.

This clade is characterized by the loss (reversion of Neogastropoda) of the spiral sculpture forming nodes in the shell; that is maintained in all species of this clade, despite some possessing the axial sculpture.

### **Clade 1b**

This clade groups *Teralatirus roboreus* (Fig. 23) and *Dolicholatirus* aff. *cayohuesonicus* (Fig. 25); the most notable characteristics that unite both of these taxa are in the radula and the penis. In the radula, what distinguishes this clade from the remaining *Dolicholatirus* sp. is a much smaller rachidian in relation to the lateral (character: 50, Fig. AJ); in the penis, the clade has a pre-copulatory chamber bearing short terminal papilla contained within (character 88, Fig. BK), absent in *Dolicholatirus* sp.

The genus *Dolicholatirus* is distinguished from *Teralatirus* by the presence of strong spiral ribs and a long siphonal canal (*e.g.*, Bullock, 1974), although it has been previously stated that *Dolicholatirus* contains the genus *Teralatirus*, as proved by the present work and by Couto *et al.* (2016). *Dolicholatirus cayohuesonicus* resembles the Indo-Pacific *D. lancea*, type of the genus, by the presence of strong axial ribs; however, it has a broader profile and shorter siphonal canal. Among the Caribbean species, *D. cayohuesonicus* resembles *Teralatirus roboreus* by the short siphonal canal. All the above cited species have strong spiral ridges along the spire and the base of the shell, and strong lirae on the inner side of the outer lip. Simone *et al.* (2013) argued that a feature that distinguishes *Teralatirus roboreus* from other *Dolicholatirus* species is the absence of strong axial ribs. Although specimens of *T. festivus* (Haas, 1941) may bear strong axial ribs (Simone *et al.*, 2013: Figs. 19-27), the sculpture pattern is much more delicate.

The shell of *Dolicholatirus cayohuesonicus* was figured by Faber (2010: Figs. 4-5 [the type *Latirus cayohuesonicus* after Sowerby, 1878, is illustrated in Fig. 5]). While the figured individuals possess a rather long siphonal canal (approximately half of the total aperture length) and broad axial ribs, the specimens studied here lack such long siphonal canal. *Teralatirus roboreus* figured by Simone *et al.* (2013: Figs. 1-16) resembles somewhat the shell of *D. cayohuesonicus*, especially if one takes into consideration a degree of variation of *Teralatirus*;

e.g., *T. festivus* (Simone *et al.*, 2013: Figs. 17-27). This species is only conchologically recognizable through its spiral bands, which in all figured specimens have the same color pattern; however, there is considerable variation in the position, number and spacing of the axial ribs – some even lacking the axial ribs altogether. The length of the siphonal canal, as well as its proportion to the aperture, and its shape also varies considerably.

The short siphonal canal of *Dolicholatirus cayohuesonicus* favor its inclusion in *Teralatirus*; while the presence of axial ribs favors more adequately its inclusion in *Dolicholatirus*. Because of this variation in form, the species is more adequately designated as *Dolicholatirus* aff. *cayohuesonicus*, in the hopes that future taxonomical works, including a much broader sampling, and molecular analyses will resolve this issue.

If this degree of variability occurred for *D. cayohuesonicus*, perhaps it is the case of a species complex of with *T. roboreus* and *D. cayohuesonicus*, with overlapping geographic variation. Both specimens of *D. cayohuesonicus* in Faber (2010: Figs. 4-5) are from localities in the western Caribbean (Belize and Key West, Florida, USA, respectively), while in this study there are only representatives of eastern Caribbean Puerto Rico. A taxonomical revision with sampling of multiple localities is desirable but beyond the means and scope of this work.

Anatomically, *Dolicholatirus* aff. *cayohuesonicus* is strikingly similar to *Teralatirus roboreus* (Simone *et al.*, 2013). All of them lack a posterior sorting area in the stomach and the proboscis retractor muscles with a columellar muscle origin; however, the huge esophageal gland present in *T. roboreus* differs from *D. cayohuesonicus*, because in the latter a gland of Leiblein occurs. It was not possible to evaluate the ducts of the salivary glands of both species. All the above characteristics, with the exception of the esophageal gland in *T. roboreus*, favor the inclusion in Fascioliariidae.

A notable difference present in *Dolicholatirus* and *Teralatirus* is the radula, extremely slender, with narrow rachidian and bicuspidate laterals, with the internal cusp hook-like. Abbott (1958) was the first to examine the radula of *D. cayohuesonicus* and found it to be “the most highly modified of the Fascioliariidae radulae, and somewhat resembling those of Vasidae [currently Turbinellidae].”

The radulae of *Dolicholatirus spiceri* and another undescribed related species in Couto *et al.* (2015) (the *Dolicholatirus* sp. in this analysis: Fig. 22) are virtually identical to that of *D. cayohuesonicus* (Fig. 26) and *T. roboreus* (Fig. 24. see also Simone *et al.*, 2013: Figs. 31-34).

According to Couto *et al.* (2016) this is the characteristic radula type that likely occurs within all species in the group (a radula of *Dolicholatirus* was supposedly figured by Bandel (1984), however Couto *et al.*, [2016] suspected this to be a misidentification, as this radula does not match their observations, and likely Bandel's specimen is instead a buccinid). The similarity of the radula of *Crassicantharus norfolkensis* Ponder, 1972 illustrated by Ponder (1972) suggests that *Crassicantharus* Ponder, 1972 may belong in the same clade, but Couto *et al.* (2016) did not include any species of this genus in their analysis.

In conclusion, although the molecular results obtained by Couto *et al.* (2016) do not reliably establish the position of *Dolicholatirus* and *Teralatirus* as belonging to, or outside of, fasciolariiids, *Dolicholatirus* and *Teralatirus* formed a monophyletic group. In the morphological results obtained herein, this group also obtained its monophyletic status, but resulted as a sister clade to the remaining fasciolariiids. Despite the radula being a strong morphological evidence that suggests a non-fasciolariid position (implying a possible miniaturization phenomenon), the 'fasciolariid-like' radula does not only include the previously typical morphotype, but rather, this morphotype appeared later in Fasciolariiidae history. Perhaps future studies will be able to recover this part of the Neogastropoda tree with high support.

## **Clade 2 Fasciolariiidae non *Dolicholatirus* and *Teralatirus***

This clade comprises the traditional Fasciolariiidae, *i.e.*, non-*Dolicholatirus* and *Teralatirus* fasciolariiids. This clade has several non-autapomorphic synapomorphies, five in total: 1) body pigmentation orange to light-red (character 11, Fig. K), 2) osphradium slightly asymmetrical character 23, Fig. S), 3) radula rachidian tooth thin (character 50, Fig. AJ), 4) lateral tooth wide and (character 55, Fig. AN) 5) cusp one of the lateral with a reduced size (character 60, Fig. AS). The latter three synapomorphies correspond to radular characters, and all of these will be discussed subsequently.

Body pigmentation has been traditionally used to diagnose species of Fasciolariiidae (Harasewych, 1998; Poppe, 2008). Traditionally, members of the fasciolariid subfamilies Fasciolarinae and Peristerniinae are notable due to the intensive red coloration of their head-foot that makes them easily recognizable at a glance; on the contrary, members of the subfamily Fusininae have bodies of a less intense, light-orange to cream pigmentation. Fedosov & Kantor (2012), upon describing the new monospecific genus *Angulofusus* Fedosov & Kantor, 2012,

utilized the pigmentation of the live specimen to place it in the fasciolariid subfamily Fusininae. Despite difficulties of obtaining fresh material, necessary to analyze the body pigmentation (thus it was impossible to know if the clade of *Dolicholatirus* and *Teralatirus* possessed any), an intense red pigmentation of ‘Peristerniinae’ is a derived state of the ‘Fusininae’ light-orange one.

The asymmetry between the left and right filaments of the sensory organ in the pallial cavity is a synapomorphy of this clade, shared by all species; although this asymmetry is accentuated in certain groups. This has been described for species of the genus *Amiantofusus* and also observed for the eight fasciolariid species studied by Kosyan *et al.* (2009). The osphradium in other buccinoids is usually symmetrical (*e.g.*, *Germonaea rachelae* Harasewych & Kantor 2004: Buccinidae; *Pararetifusus tenuis* [Okutani, 1966], Kosyan, 2006: Buccinidae; *Dorsanum miran* [Bruguère, 1789], Simone & Pastorino, 2014: Nassariidae). However, an asymmetrical osphradium is not exclusive to fasciolariaids, as there are reports of other non-fasciolariid buccinoids that possess it (*e.g.*, *Pararetifusus kantori* Kosyan, 2006: Buccinidae). The asymmetry of the osphradium filaments has been connected to the miniaturization (Simone, 2011), as most of the species that have asymmetrical, or even monopectinated osphradia, are of small size. However, this is not the case of the present branch, which mostly includes large-sized animals.

The most remarkable characteristic of this fasciolariid clade is the highly modified radula, being what most previous authors have referred to as the ‘typical fasciolariid radula’. Troschel & Thiele (1865-1893) characterized the radula of the Fasciolariaidae: the lateral teeth very wide, with many cusps; the central teeth are quadrangular and less wide than the lateral teeth. Bandel (1984), on his Caribbean caenogastropod radula survey (studying five fasciolariid species), observed the same pattern, however corrected that not all rachidian tooth can be called narrow, since in some species the central teeth are wider than long; all radular characterizations of the family have followed a more-or-less similar trend (wide laterals, thin rachidians, *e.g.*, Taylor & Lewis, 1995; Hadorn, 1999); Fraussen *et al.* (2007) included in their diagnosis this radula morphology to identify Fasciolariaidae. All of the above cited authors did not take into consideration *Dolicholatirus* or *Teralatirus* in their diagnosis, and therefore this radula cannot be used to distinguish fasciolariaids, but a more inclusive clade.

In this work, the synapomorphies related to the radula are: the increase in width of the lateral in relation to its length, a decrease of the width of the rachidian in relation to the width of the lateral and the reduction of cusp one of the lateral (characters 53, 55, 58; Figs AM, AN, AQ,



respectively). The former two correspond to the ‘fasciolariid-like’ radula aforementioned, while the latter is a novel observation. The lateral innermost cusp is always reduced in length, when present (a few clades have lost cusp one, in that way the innermost cusp is the same length as the others; this will be discussed subsequently when relevant). All Fasciolariidae radulae figured in the literature possess this reduction in size of cusp one, except when it is absent (clades 6b and 14).

The proboscis retractor muscles suffered a reduction in number, from a pair to one. In all non-fasciolariid neogastropods, a pair was observed; in this fasciolariid clade, only one occurs, likely due to the loss of the left one. A clade of *Pustulatirus* possess a pair, and Kosyan *et al.* (2009) also accounts to the existence of a pair in some Fasciolariidae species (*e.g.*, *Latirus polygonus* and *Fusinus tenerifensis*). It may be the case that these latter cases are incorrectly assigned: a fasciolariid proboscis retractor has its origin in the columellar muscle, not the haemocoelic wall; some secondary muscles that attach to the haemocoel may be more conspicuous than the rest, in this way resembling the main retractors and so a pair may be perceived. This was not true for species of *Pustulatirus*, which will be discussed later.

#### **Clade 2a *Angulofusus* + *Amiantofusus* + *Pseudolatirus kuroseanus***

Clades 2a, 3a and 4a correspond to representatives of the traditionally characterized subfamily Fusininae, plus the genus *Pseudolatirus*. This paraphyletic subfamily corresponds to the monophyletic clade of fusinines in Couto *et al.* (2016), which includes the genus *Pseudolatirus* as well. In their analysis, there were some topological differences between the ML and the BI results for this clade, which will be conveyed at the appropriate time in this discussion.

WoRMS (2016) reports ten extant genera for the subfamily Fusininae: *Fusinus*, *Amiantofusus*, *Angulofusus*, *Chryseofusus*, *Granulifusus*, *Cyrtulus*, *Harasewychia* Petuch, 1987, *Marmarofusus* Snyder & Lyons, 2014, *Trophonofusus* Kuroda & Habe, 1971, and *Viridifusus* Snyder *et al.*, 2012. In this work are present representatives of the six former genera.

Fedosov & Kantor (2012), upon describing the monotypic genus *Angulofusus*, noted a striking anatomical resemblance of *A. nedae* to *Amiantofusus*, both in digestive system anatomy (mainly radula and stomach) and mantle complex. However, upon examination of its Cytochrome *c* oxidase subunit I (COI) sequence through BLAST scores in the NCBI database (<http://www.ncbi.nlm.nih.gov/>), a closer relationship to *Granulifusus* was proposed. A superficial

conchological resemblance to some Conoidea was noted by its authors (Fedosov & Kantor, 2012), notably the distinctive anal sinus (Fedosov & Kantor, 2012: Fig 1H), evidencing once more the problems arising on conchologically based taxonomy.

The clade that contained *Angulofusus nedae* in Couto *et al.* (2016) nested within *Amiantofusus*, *Granulifusus* and *Pseudolatirus kuroseanus* in the ML, and as a sister group of all the remaining fusinines in the BI analysis. The former is a sister taxon to *Granulifusus* and *Pseudolatirus kuroseanus*, while *Amiantofusus* is sister to these. A topology similar to the one presented here, in which *A. nedae* is sister of *Amiantofusus* and *Pseudolatirus kuroseanus* is not observed, although a closer relation to *Amiantofusus* occurs in the ML analysis of Couto *et al.* (2016).

All species present in this clade have a characteristic rachidian tooth of the radula, *i.e.*, very minute, nearly needle shaped and tri-cuspidate. The cusps are sub-terminal; hence they do not originate in the terminal edge of the tooth and project forward, rather the cusps originate somewhat in the lateral edge of the tooth in a way that the edge is not visible (characters 48, 49; Fig. AD). This is typical for this clade, occurring solely on species within (Figs. 28-34).

### **Clade 2b *Amiantofusus* + *Pseudolatirus kuroseanus***

The genus *Amiantofusus* was described to accommodate deep-water species that possess shells that are strikingly similar to Buccinidae, short siphonal canal, but with unique protoconch morphology (multispiral protoconch) and fascioliid-like radula and soft-part morphology (Fraussen *et al.*, 2007). Conchologically, *Pseudolatirus kuroseanus* (Fig. 27) differs from *Amiantofusus* due to its long siphonal canal. In this context, *P. kuroseanus* most closely resembles *Amiantofusus pacificus* Fraussen *et al.*, 2007, a species with much geographical variation, resembling “form B” *sensu* Fraussen *et al.* (2007: Figs. 36-37).

In Couto *et al.* (2016) *Pseudolatirus kuroseanus* maintained its sister group position to *Granulifusus* in both ML and BI analysis; this was not the case in this work, as the species is the sister taxon to *Amiantofusus*. Truly, *P. kuroseanus* shell is more *Granulifusus*-like than *Amiantofusus*-like; however, this only accentuates the troublesome conchologically-based taxonomical issues. Regardless, due to the position of this species, and the non-monophyletic state of the genus *Pseudolatirus*, *P. kuroseanus* is better placed in *Amiantofusus*, despite molecular evidence proving a *Granulifusus* relation.

Morphologically, two synapomorphies support this group: a loss of inner sculpture of outer lip (character 7, Fig. G), and a heavily asymmetrical osphradium (character 23, Fig. S). Both characters are convergent; the latter one occurred also in fusinine genera *Granulifusus* and *Chryseofusus*.

### **Clade 2c *Amiantofusus***

Both *Amiantofusus* species comprise this clade, with one of its synapomorphies, among others, is the insertion of the proboscis retractor muscle posteriorly in the proboscis, as opposed to medially (character 68, Fig. AX). This is a reversion of to the previous state.

The genus *Amiantofusus* was strongly supported in both analyses of Couto *et al.* (2016), but the relationship with other fusinines proved controversial. In the BI analysis, *Amiantofusus* is sister group of *Fusinus* and this clade in turn is the sister group of *Chryseofusus* and *Pseudolatirus*; the clade of *Amiantofusus*, *Fusinus*, *Chryseofusus* and *Pseudolatirus* is the sister group of *Granulifusus* and *Pseudolatirus*; and *Angulofusus* is a basal group of all the remaining fusinines. In the ML analysis, *Amiantofusus* is the sister genus to *Granulifusus*, *Pseudolatirus* and *Angulofusus*, while this group is sister to the remaining fusinines.

*Amiantofusus pacificus* (Figs. 29-30) was characterized by Fraussen *et al.* (2007) as having a strong degree of, mostly, geographic variability; its multispiral protoconch indicates a planktotrophic development and wide distribution, despite its bathymetric range being rather narrow (420-795m). Fraussen *et al.* (2007) pointed that the populations are separated by deeper water, causing a certain geographic isolation which is well reflected by the differences in shell morphology, however several intermediate forms are found between most of the forms, hence these authors considered these populations as not fully separated entities, nor subspecies, but merely variations.

Only one specimen of *A. pacificus* was available for anatomical dissections. The smooth form, from New Caledonia, corresponds to the form figured by Fraussen *et al.* (2007: Figs. 42-43) which occurs in the same locality from circa (650-700m deep). The other, more robust form of *A. pacificus* was studied in the molecular analysis of Couto *et al.* (2016); and both species appeared as sister taxa, which in turn are sister of *A. sebalis* Fraussen *et al.*, 2007 and *A. candoris* Fraussen *et al.*, 2007), the latter (Figs. 31-32) was also available for the morphological analysis herein.

### Clade 3

The presence of a long siphonal canal, which is generally characteristic of fusinines (but also occurring in some *Pseudolatirus* and *Nodolatirus*); and will be reverted in a peristerniine clade (e.g., Clade 8a).

Shells of the fusinine generalized morphology extend back to the early Cretaceous and, based on the fossil record, according to (Harasewych, 1990; Riedel, 2000), it is hypothesized that it is the plesiomorphic shell type of Neogastropoda. In the context of Fasciolaridae, the acquisition of a longer siphonal canal, which most notoriously represents the fusinine-like shell, is plesiomorphic to the peristerniine-like shell (shorter siphonal canal), only because *Amiantofusus* lacks a fossil record.

The continuing trend in the family of increasing the width of the lateral tooth of the radula, with a subsequent increase in the number of cusps, is once again observed in this node. The taxa included have at least five cusps in the lateral; this is not observed in any other buccinoid.

### Clade 3a

The fusinine genera *Fusinus*, *Cyrtulus*, *Chryseofusus* and the previously peristerniine *Pseudolatirus pallidus* encompass this clade. This group is the second split from the paraphyletic Fusininae.

In the ML analysis of Couto *et al.* (2016) this group appeared (although unsupported) with almost the exact topology: *Fusinus* as the crown genus, sister to group of *Chryseofusus* and *Pseudolatirus pallidus*. The difference with the current morphological topology is that *Fusinus* and *Chryseofusus* form a group that is sister of *Pseudolatirus pallidus*. In the BI analysis, *Fusinus* was supported, being the sister genus of *Amiantofusus*, and that grouping with *Chryseofusus* and *Pseudolatirus pallidus*, much like in the ML analysis. In the present study, *Pseudolatirus pallidus* is the first split, followed by the genus *Chryseofusus* and *Fusinus* (including *Cyrtulus*).

The main synapomorphies of the group are the presence of a very long proboscis, in which the buccal mass is located anteriorly occupying only circa a quarter of the total proboscis length (character 42, Fig. AE). This proboscis is also coiled within its sheath (character 65, Fig. AV).

The same proboscis has been reported for other buccinoids in the literature (e.g., *Troschelia berniciensis*: Kosyan *et al.*, 2009; *Aulacofusus* Dall, 1918: Kosyan & Kantor, 2013), all in the family Buccinidae. None of the outgroup species of buccinid studied here (*Pisania pusio* or

*Buccinum undatum*) have such proboscis type, albeit none belong to the same subfamily (as currently accepted: WoRMS, 2016).

Kosyan *et al.* (2009) analyzed the anatomy of *Fusinus tenerifensis* and noted that the proboscis is neither coiled nor long, but straight, and the buccal mass has the same length of the proboscis. These same authors stated that the fascioliid proboscis is straight and never coiled within the rhynchodeum (proboscis sheath); but the only fusinine analyzed by them was *Fusinus tenerifensis*. These results contradict this clade's results, although no illustration of shell or radula was provided by Kosyan *et al.* (2009) in order to confirm the taxonomy of *Fusinus tenerifensis*.

*Pseudolatirus pallidus* (Fig. 33-34) is a Japanese species that appeared as sister species to *Chryseofusus* both here and in Couto *et al.* (2016). According to Callomon & Snyder (2009), this species “may well prove too closely related to *Fusinus* to exclude from that genus”, indicating that the placement in the peristerniine genus *Pseudolatirus* was merely provisional.

Several specimens of *Pseudolatirus pallidus* were analyzed, three of which were sampled in the analysis of Couto *et al.* (2016). Callomon & Snyder (2009) pointed that many shells of this species differ somewhat among them (*e.g.*, having finer and more broadly spaced axial sculpture and a slimmer profile), suggesting that this species, as well as others in the genus, require additional attention. Shell sculpture of *Pseudolatirus pallidus* varies enormously, usually with different placement of the axial sculpture, as noted by Callomon & Snyder (2009) and by Couto *et al.* (2016). According to these last authors, who sampled three specimens, the lineage of *Pseudolatirus* sister of *Chryseofusus* comprises a species complex of *Pseudolatirus pallidus* (*Pseudolatirus pallidus*, *P. aff. pallidus* and *Pseudolatirus* sp. [*sensu* Couto *et al.*, 2016]).

Since grouping with *Chryseofusus* seems an unlikely choice based on conchological characters alone, one must assume that the *Pseudolatirus* shell morphology is plesiomorphic, which is corroborated by the fact that this form is present in three independent clades: 1) sister of the group of *Amiantofusus*, 2) in *Chryseofusus* and 3) nested in *Granulifusus*. In Couto *et al.* (2016), the genus *Pseudolatirus* appeared in two distinct lineages.

### **Clade 3b *Chryseofusus* + *Fusinus***

This clade groups traditionally associated genera: *Chryseofusus* and *Fusinus*. The first was first described as a subgenus of the latter by Hadorn & Fraussen (2003) and later elevated to genus category by Callomon & Snyder (2009).

Species herein are distinguished from others of this clade of fusinines (clade 3a) by the absence of the inner sculpture of the outer lip (character 7, Fig. G). The subfamily Fusininae is known to lack these sculptures, being ordinarily present in peristerniines and fasciolariniines; with the discovery of new species and the re-examination of old taxonomy, this diagnosis can no longer be used precisely.

In Couto *et al.* (2016), who sampled four *Chryseofusus* species, the genera was recovered in both the ML and the BI analyses. The strict relationship with *Fusinus*, as implied in the literature (*e.g.*, Hadorn & Fraussen, 2003; Hadorn *et al.*, 2008; Callomon & Snyder, 2009) was only confirmed, however, in the ML analysis, in which the clade *Chryseofusus* and *Pseudolatirus pallidus* formed a sister group with *Fusinus* (albeit weakly supported). The present analysis corroborates this hypothesis, and *Fusinus* and *Chryseofusus* are grouped together

### **Clade 3b<sup>1</sup> *Chryseofusus***

The deep-sea genus *Chryseofusus*, groups a number of Indo-Pacific deep-water species occurring between 100 and 1900m that share conchological features different from typical *Fusinus*, mainly the reduced spiral and axial sculpture on the body whorl and a shorter spire and siphonal canal (Hadorn & Fraussen, 2003). Upon their original description of the subgenera, Hadorn & Fraussen (2003) distinguished *Chryseofusus* from other subgenera by its slightly convex whorls, axial ribs present only on the upper whorls, weak and close set spiral sculpture and an outer lip that is simple, lacking internal structures; the latter is also shared with *Fusinus* which difficult its diagnosis.

In the current analysis, the genus is characterized by many synapomorphies, including the loss of spiral sculpture of the shell (as originally described) (character 3, Fig. C); a heavily asymmetrical osphradium (character 23, Fig. S) and the female cement gland opening centrally in the sole of the foot (character 84, Fig. BH). *Chryseofusus archeruisius* (Hadorn & Fraussen, 2003) (Figs. 35-36) is distinguished from *C. graciliformis* (Sowerby, 1880) (Figs. 37-38) mainly by the more prominent axial nodes on the shoulder angulation and by a shorter, broader siphonal canal.

### **Clade 3c *Fusinus* + *Cyrtulus***

The name '*Fusus*' has been used arbitrarily for numerous fossil and recent spindle-shaped shells (Snyder, 2003), and species in several distinct families received this designation.



Historically, the genus *Fusinus* grouped species with an overall fusinine-like generalized morphology: a large size, tall elongated spire, long siphonal canal, usually with broad axial ribs and spiral cords, absence of columellar folds and operculum that corresponds to the size of the aperture (Hadorn & Fraussen, 2003). Harasewych (1990) discussed that it likely represents the plesiomorphic shell type of Neogastropoda; Vermeij & Snyder (2002), on the other hand, suggested that fusinines are a stem-group of fasciolaridiids distinguished from the other subfamilies by the absence of columellar folds. Some species of *Fusinus* bear resemblance to the genus *Pseudolatirus* (e.g., *F. annae* Snyder, 1986); however, the former genus lacks the one or two plicae that are characteristic of the latter (despite the fact that the genus *Pseudolatirus* is not monophyletic). More recently, *Fusinus* has undergone intensive taxonomical revisions, including descriptions of new species (Callomon & Snyder, 2004; 2006; 2007; 2009), however, these focus mainly in the Pacific, mainly Japan and China Seas.

Of the nine extant genera of Fusininae (WoRMS, 2016), five have species previously attributed to the genus *Fusus* as the type species: 1) *Amiantofusus* (type: *Fusus amiantus* Dall, 1889); 2) *Chryseofusus* (type: *Fusus chrysodomoides* Schepman, 1911); 3) *Granulifusus* (type: *Fusus niponicus* Smith, 1879); 4) *Viridifusus* (type: *Fusus buxeus* Reeve, 1847); and finally, 5) the genus *Fusinus* (type: *Murex colus* Linnaeus, 1758)

Hadorn & Rogers (2000) reviewed the taxonomy of extant *Fusinus* from the tropical western Atlantic; but out of the 37 species analyzed by these authors, only *F. ansatus* (Gmelin, 1791) has its occurrence assuredly reported for Brazil. Rosenberg (2009), on the other hand, reports seven species in the Brazilian coast, occurring in relatively shallow water (e.g., *F. agatha* [Simone & Abbate, 2005] in 60m depth), this number is likely a sub-representation because of a lack of reported deep-water species.

Here, the genera *Fusinus* and *Cyrtulus* (Figs. 39-50) are grouped together, being corroborated by six synapomorphies, two of which are non-homoplastic and will be discussed here. The typical *Fusinus* radula, including that of *Cyrtulus serotinus* Hinds, 1843, has the lateral tooth with a progressive increase in the innermost cusps length (cusps one to three closest to rachidian) (character 63, Fig. AT); hence cusp one is smallest, followed by cusp two and sometimes cusp three (Figs. 40, 42, 44, 46, 48, 50). All radula figured in the literature (e.g., Hadorn & Fraussen, 2006; Couto *et al.*, [in prep]) have this conformation.

The mid-esophagus of *Fusinus* and *Cyrtulus* has in its posterior side a ventral glandular region, posterior to the valve of Leiblein and anterior to the nerve ring. This structure was not observed for any other fasciolariid. It is worth mentioning that this is not the framboise gland, which will be discussed later.

In the molecular analysis of Couto *et al.* (2016), the authors presented conflicting topological results with the present morphological analysis. In both their analyses (ML and BI), a first split within *Fusinus* separates *F. australis* (Quoy & Gaimard, 1833), which is sister to the remaining *Fusinus*; a second split separates *F. brasiliensis* (Grabau, 1904) and *Cyrtulus serotinus*. On the other hand, in the present topology, two groups of *Fusinus* occur: a coastal Brazilian clade with *F. marmoratus* (Philippi, 1846), *F. brasiliensis* and *Fusinus* sp. and another clade with *F. frenguelli* (Carcelles, 1953), *F. australis*, and *Cyrtulus serotinus*. The biogeographical implications to these conflicting results are unclear, however.

### **Clade 3c<sup>1</sup> “*Fusinus marmoratus* complex”**

The southwestern Atlantic "*Fusinus marmoratus* complex" (*sensu* Hadorn & Rogers, 2000) comprising of *F. brasiliensis* and *F. marmoratus*, are not related to other species in the northwestern Atlantic (Hadorn & Rogers, 2000). This "complex" is extremely confusing and requires extensive taxonomical study (Hadorn & Rogers, 2000) as it encompasses some similar-shelled shallow water forms, with doubtful species-status and overlapping shell distinctions that superficially resemble *F. marmoratus*.

In this analysis, the clade 3c<sup>1</sup> corresponds to the *Fusinus marmoratus* complex (*F. marmoratus*, *F. brasiliensis* and a *Fusinus* sp.); there are two reversions supporting it. First, the loss of the lipped margin of the renal aperture and second, the shorter pedal ganglia (characters 34, 90, Figs. Z, BM, respectively).

Currently in the database WoRMS (2016), *Fusinus marmoratus* is synonymized with *F. verrucosus* (Gmelin, 1791). There was no type locality of *Fusinus marmoratus* given by Philippi (1846), hence historically a lot of confusion over this species occur. Zenetos *et al.* (2005) reported *F. verrucosus* as an invasive Red Sea species in the eastern Mediterranean Sea via the Suez Canal; these authors synonymized *F. verrucosus* with *F. marmoratus*, but gave no basis for this action. WoRMS (2016), citing the Check List of European Marine Mollusca (CLEMAM), concurred with this taxonomic action, as have other authors (*e.g.*, Buzzurro & Russo, 2007);

while many others maintain *F. marmoratus* as valid (e.g., Watson, 1886; Hadorn & Rogers, 2000; Rios, 2009). Because no new designation for the Brazilian *F. marmoratus* was given by Zenetos *et al.* (2005), and because there are sufficient morphological differences that separate it from *F. brasiliensis* (Couto *et al.*, in prep), *Fusinus marmoratus* is considered a valid species in the Brazilian coast.

*Fusinus brasiliensis* (Figs. 39-40) and *F. marmoratus* (Figs. 41-42) have very similar shells, mainly due to its size, the brownish coloration and the convex outline of its whorls. Both species are sympatric in the Southeastern coastal region in Brazil; however, *F. marmoratus* occurs more southward into the state of São Paulo (Rosenberg, 2009). They are distinguished from one another by the number of axial ribs: eight to ten in *F. brasiliensis* and 12 to 15 in *F. marmoratus*; and the sub-sutural ramp: slightly convex in *F. brasiliensis* and straight in *F. marmoratus*; the overall profile of the shell of *F. marmoratus* is somewhat broader and smoother than *F. brasiliensis* (Couto *et al.*, in prep). *Fusinus* sp. (Figs. 43-44) is more closely related to *Fusinus marmoratus* based on head and cephalic tentacle characters.

### **Clade 3d *Fusinus***

The offshore Brazilian species *Fusinus frenguelli* and two pacific species, *F. australis* and *Cyrtulus serotinus* are grouped into this clade. The former species correspond to the first split of this clade, and the latter two are sister taxa. A notable, non-homoplastic synapomorphy of this clade is the presence of a unique osphradium: the leaflets of the right side, and sometimes both sides, possess a terminally digitated shape (character 25, Fig. U).

*Fusinus frenguelli* (Figs. 45-46) is distinguished from the other Brazilian *Fusinus* (*F. marmoratus* and *F. brasiliensis*, which are very similar to each other) based on the osphradium and female system traits (Couto *et al.*, in prep). *Fusinus frenguelli* resembles somewhat *F. lightbourni* Snyder, 1984 from Bermuda however the latter is smaller and bears brownish spiral bands (see Hadorn & Rogers, 2000). This species is the sister species of *F. australis* (Figs. 47-48) and *Cyrtulus serotinus* (Figs. 49-50), which have in common the spiral cords in the outer lip and similar head width and cephalic tentacle length.

The central Pacific species *Cyrtulus serotinus* is endemic to the Marquesas Archipelago in French Polynesia, and is the only species of the genus. The shape of its shell is unique within fusinines, with a last whorl embracing the earlier whorls, accompanied by a loss of ornamentation

(see also Couto *et al.*, 2016). Grabau (1907), in his essay on ontogenetic variation, stated that “no one can distinguish the young of *Cyrtulus serotinus* from that of any member of the *Fusus* series (...). Nevertheless, it remains true that *Cyrtulus serotinus* is a derivation of modern *Fusus*.”

It is clear that this species is a *Fusinus* (*Fusus*, *sensu* Grabau [1907]) if one takes a look at a growth series (Couto *et al.*, 2016: Figs. 6A-C). In light of the analysis of Couto *et al.* (2016), in which the species appeared nested within *Fusinus* and sister to the Philippine *Fusinus longissimus* (Gmelin, 1791) (on both ML and BI), the species is now considered as belonging to *Fusinus* (WoRMS, 2016). Presently, based on the topology presented here (agreeing with Couto *et al.*, 2016 and WoRMS, 2016), this species is confirmed as a *Fusinus*, albeit highly derived.

#### **Clade 4 *Granulifusus* + Peristerniinae + Fasciolarinae**

This clade encompasses the fusinine genera *Granulifusus*, a bulk of the peristerniines and all fasciolarinae. There is no non-homoplastic synapomorphy for the clade, but two homoplasies occur: a narrow osphradium (character 28, Fig. W) and a rhynchostome emarginated by a lipped rim (character 40, Fig. AC). Despite being grouped with Peristerniinae, *Granulifusus* was never suggested to belong with this subfamily; in Couto *et al.* (2016) the genus nested within other fusinines, differing from the topology herein.

#### **Clade 4a *Granulifusus***

The genus *Granulifusus*, along with a species of the polyphyletic genus *Pseudolatirus*, comprehend this clade, being supported by numerous synapomorphies, including the loss of the inner sculpture of the outer lip (character 7, Fig. G), loss of the female cement gland (character 82, Fig. BH), a heavily asymmetrical osphradium (character 23, Fig. S) and features in the operculum (characters 16, 17, Figs. O, P, respectively). Operculum characters represent important non-homoplastic characters supporting this clade.

*Granulifusus* (type: *Fusus niponicus* Smith, 1879) was first described and characterized by Kuroda & Habe (1952), based on *Fusinus*-like individuals with a granulated shell surface, radula with a small number of cusps on the lateral tooth and a small round operculum that does not fit entirely the aperture. The operculum also has a central nucleus, differing from other fasciolariaids which have a terminal nucleus. All species of *Granulifusus* (including *Pseudolatirus discrepans*)

figured in the literature have this operculum type (e.g., Hadorn & Fraussen, 2005; Preetha *et al.*, 2014). The genus currently accommodates 28 valid species worldwide (WoRMS, 2016).

*Granulifusus* is an Indo-Pacific genus and one of the Indo-Pacific elements occurring in Japanese warm waters (Shuto, 1958), being relatively common there. The genus was revised by Hadorn & Fraussen (2005), who described several new species (e.g., *G. bacciballus* Hadorn & Fraussen, 2005; *G. benjamini* Hadorn & Fraussen, 2005) and transferred several others to it. The genus is monophyletic if *Pseudolatirus discrepans* is included (more on this species will be discussed later). In Couto *et al.* (2016) the genus is also monophyletic in both ML and BI analyses, with *P. discrepans* representing a first split in the clade.

An undescribed *Granulifusus* species (Fig. 51-52) with a deeply canaliculated suture and reduced granulated surface is the first split in the clade, while the group formed by *G. Hayashi* Habe, 1961, *G. kiranus* Shuto, 1958 and *Pseudolatirus discrepans* are sister to it. This *Granulifusus* sp. is the same specimen sequenced in Couto *et al.* (2016: Fig. 6L) and on their analysis this species is sister to *G. kiranus*, and this fact differs from the present work.

#### **Clade 4b**

In Couto *et al.* (2016), the whole of *Granulifusus*, *Pseudolatirus discrepans*, *P. kuroseanus* and *P. kurodai* Okutani & Sakurai, 1964 form a monophyletic clade. In their topology, a first split separates *P. kuroseanus* and *P. kurodai* from the remaining; and while these species share some similarities, there are very few resemblances between these shells and the typical *Granulifusus*-like shell (Couto *et al.*, 2016: Fig. 6J). Because of this, a more conservative approach was taken and no taxonomical changes were made. *Pseudolatirus discrepans* corresponds to the sister taxa to all *Granulifusus* species in Couto *et al.* (2016), while here it is nested within the genus.

*Pseudolatirus discrepans* has been considered as a *Granulifusus* by several authors (e.g., Poppe, 2008), and based on the tree topology and on the sculpture of the initial whorls (which closely resembles that of many *Granulifusus*), the placement of *Pseudolatirus discrepans* in *Granulifusus* is likely correct. This is also corroborated by the results in Couto *et al.* (2016).

Clade 4b is supported by two reversions: the proboscis retractor muscles inserting posteriorly and the presence of a seminal receptacle in the pallial oviduct. The Japanese species *Granulifusus hayashi* (Figs. 53-54) is the sister taxon to a group formed by *G. kiranus* (Figs. 55-

56) and *P. discrepans* (Figs. 57-58). The latter two are sister species with a unique lamellated siphon. The speciation events, roughly visualized by the short branch lengths in Couto *et al.* (2016: Figs. 1-2) likely point to a rapid speciation, which may hinder taxonomical differentiation, especially conchological.

### **Clade 5 Peristerniinae + Fascioliariinae**

This is an important clade of mostly peristerniines but also includes the monophyletic Fascioliariinae. Most synapomorphies supporting this clade are traditional diagnostic characteristics for the subfamily Peristerniinae: a shell with columellar folds medially in the aperture (character 8, Fig. H), a pseudoumbilicus (character 10, Fig. J) as a shallow slit, a head-foot mass pigmentation as dark-red (character 11, Fig. K) and a lateral margin of the operculum possessing a hook-like extension (character 18, Fig. Q).

The head-foot mass pigmentation is a non-homoplastic synapomorphy and mentioned by several authors when referring to species within this clade (*e.g.*, Marcus & Marcus, 1962: *Leucozonia nassa*; Poppe, 2008: *Peristernia nassatula*; Okutani, 2000: *Fusolatirus pachyus* Snyder & Bouchet, 2006; Bouchet & Snyder, 2013: *Nodolatirus rapanus* Bouchet & Snyder, 2013). Harasewych (1998) reported as a distinguishing feature for Peristerniinae, and Fedosov & Kantor (2012) used the coloration of the head-foot mass in live *Angulofusus nedae* to place it in the subfamily Fusiniinae.

Another head-foot mass character that is a non-homoplastic synapomorphy for this clade is a hook-like extension in the lateral margin of the operculum. Unlike previous opercula with a terminal nucleus, the nucleus of this type of operculum is located in lateral, hook-like extension (but see character discussion for more on this). Snyder & Callomon (2005) stated the presence of a slightly hooked terminal nucleus for three *Fusolatirus* species, Couto & Pimenta (2012) and Couto *et al.* (2015a; 2015b) for several peristerniine and fascioliariine species from Brazil.

This clade is corroborated by both ML and BI molecular analyses of Couto *et al.* (2016) which obtained a highly supported Peristerniinae and Fascioliariinae clade. In spite of the fact that the scope was not Fascioliariidae, Kosyan *et al.* (2009) obtained the peristerniine species (*Turrilatirus turritus* and *Tarantinea lignaria*) as the sister group of the fusinine species (*Granulifusus niponicus* and *Fusinus akitai* Kuroda & Habe, 1961) based on their 16S rRNA analysis. Other works lack the species sampling to make any inference.



### Clade 5a Peristerniinae

The genus *Fusolaturus* was originally established by Kuroda *et al.* (1971), with the Japanese description a more detailed one than the English translation. Kuroda & Habe (1971) noted that “the radula is the same as that of *Peristernia*, but [the new genus] is taller and more slender and differs particularly in its long siphonal process. [Members of] *Pseudolaturus* Bellardi, 1884 also have tall, slender shells, but they are larger and their siphonal processes” (Snyder & Callomon, 2005). Snyder & Callomon (2005) adds that a further *Fusolaturus* character not mentioned in the original description is a subsutural band found on all teleoconch whorls, which varies in prominence; additionally, there is a constriction of the aperture at the top of the siphonal canal that is caused by a deflection of the parietal wall. *F. bruijnii* (Tapparone-Canefri, 1876) fits this description, being very similar to *Peristernia* except for the long siphonal canal.

The type species of the subfamily Peristerniinae is *Peristernia nassatula*, a species sampled by Couto *et al.* (2016); because of this, on their analyses, the clade that contained this species corresponds to the subfamily Peristerniinae (a highly supported clade both in ML and BI analyses). This clade contained the genera *Peristernia* and *Fusolaturus* in Couto *et al.* (2016) and also in the morphology-based produced here, confirming the subfamily placement, and the relation between both genera, in this sense agreeing with Snyder & Callomon (2005) and Snyder & Bouchet (2006).

This clade is represented by *Fusolaturus bruijnii* (Figs. 59-60), *Peristernia nassatula* (Figs. 61-62) and *P. marquesana* (Adams, 1855) (Figs. 63-64). The radula (character 57, Fig. AP) is the main distinguishing feature for this clade, with the lateral teeth alternating smaller and larger cusps (Figs. 54, 56, 58); in other fasciolaridiids, however, the lateral teeth have regular cusp sizes. In fact all radulae of *Peristernia* and *Fusolaturus* figured in the literature (*e.g.*, Bandel, 1984; Taylor & Lewis, 1995; Kosyan *et al.*, 2009 [*Peristernia*]; Snyder & Bouchet, 2006 [*Fusolaturus*]) have ‘*Peristernia*-like’ radula. This dentition is variable to such a degree, that within one radula almost no lateral tooth is exactly like the other (Bandel, 1984). Other synapomorphies for this clade include reversions in the odontophore and anus (characters 45, 77, Figs. AG, BE, respectively).

Snyder & Bouchet (2006) considered *Fusolaturus* a valid genus of peristerniine fasciolaridiids with long siphonal canal, imbricated subsutural spiral ridge and *Peristernia*-like radula. Despite these distinctions, the genus appeared diphyletic in the analyses of Couto *et al.* (2016) because

*Fusolatirus rikae* (Fraussen, 2003) is the sister taxon of *Peristernia* and all other *Fusolatirus* species, and a clade nested within *Peristernia* comprises *Fusolatirus pearsoni* (Snyder, 2002), *F. pachyus* and *F. bruijnii*.

### **Clade 5b *Peristernia***

This clade groups *Peristernia* has been demonstrated to be non-monophyletic in the analysis of Couto *et al.* (2016), but because few taxa were used for the morphological analysis, this inference is not presently possible. This clade is supported by a reduction of the length of the siphonal canal (character 9, Fig. I), a radula with a more trapezoidal-shaped rachidian tooth and a wider lateral tooth (character 50, 55, Figs. AJ, AN).

The topology of the molecular analysis of Couto *et al.* (2016) shows a non-monophyletic genus: the clade including *Peristernia marquesana* and its closest relatives is supported in ML and BI analyses and it likely includes species related to *P. ustulata* and *P. lyrata* (Reeve, 1847) (see Poppe [2008: 108-109] for the illustration of several forms); the clade containing several species of *Peristernia*, including *P. nassatula* is the sister clade to several *Fusolatirus* and *P. marquesana*. These results contradict the present work, as *Fusolatirus bruijnii* is the sister taxon to the monophyletic *Peristernia* clade of *P. nassatula* and *P. marquesana*.

As these authors pointed out, the genus *Peristernia* and its allies have not been the subject of taxonomical revisions, and several species (Couto *et al.*, 2016: Figs. 5E-F) are most likely new to science.

### **Clade 6 Fasciolarinae**

Vermeij & Snyder (2006) considered Fasciolarinae as derived from early peristerniines and the two groups are part of a single clade Fasciolarinae; Snyder *et al.* (2012) noted that both subfamilies are morphologically similar. Most taxa traditionally classified in Peristerniinae must in fact be relocated to Fasciolarinae, according to this analysis and those of Couto *et al.* (2016). This is due to the topology of their results, as traditional fasciolarines formed a clade derived from a group of Peristerniinae with high support, and in which the type species of Fasciolarinae, *Fasciolaria tulipa*, occurs in this clade containing the bulk of peristerniines non-*Peristernia* (this genus is included in Peristerniinae, as previously discussed).

Morphologically, synapomorphies of this clade, none of which are non-homoplastic, include: head width and cephalic tentacle length (characters 13, 14, Fig. M), a reversion to a square-shaped rachidian tooth of radula (character 50, Fig. AJ) and salivary glands as two amorphous masses that are free from the nerve-ring (character 69, Fig. AY). This last character was only reported, among the seven species studied by Kosyan *et al.* (2009), for *Fusinus tenerifensis* and *Tarantinae lignaria*; however, these glands are usually made of a coarse and saccular structure that may be modified during preservation, interfering with the correct visualization.

Clade 6 comprises two distinct groups: clade 6a, with the previously assigned fasciolariines, *Nodolatirus nodatus* and *Latirus vischii*; and clade 7, with *Hemipolygona*, *Pustulatirus*, *Polygona*, *Leucozonia*, *Opeatostoma*, *Latirus polygonus* and *L. pictus* (Reeve, 1847). Couto *et al.* (2016) obtained three distinct groups for their corresponding clade, in which the topologies are more-or-less congruent between the ML and BI analyses; however, the relationship amongst them could not be discerned due to the low support for the deeper nodes (possibly indicating a fast speciation event). The differences between the morphological analysis undertaken here and the molecular analyses of Couto *et al.* (2016) are discussed in the following pages.

### **Clade 6a**

The overall tendency for fasciolariids to increase the number of cusps in the lateral tooth of the radula attains its utmost extreme in this clade (with laterals bearing more than 16 cusps). Bandel (1984) illustrated many fasciolariid radulae, with three species of *Fasciolaria*, including *F. tulipa*; all radulae described agree with this pattern, despite some evidence that some fasciolariids increase the number of cusps in the lateral as the snail mature (*e.g.*, Abbot, 1958 for *Leucozonia nassa*). All the cusps of the laterals of this clade possess more-or-less equal length, and the number of these is generally larger than in other fasciolariids (see Bandel, 1984: Figs. 257-268, for other examples of other fasciolariid radulae). The lateral teeth of the radula of *Fasciolaria (Tarantinae) lignaria* (Küster & Kobelt, 1876; Kosyan *et al.*, 2009) resemble that of many *Latirus*-like species, in having fewer, shorter and more strongly curved cusps. Snyder *et al.* (2012) placed this species in the genus *Tarantinae* Monterosato (1917) (see also WoRMS, 2016), previously a subgenus of *Fasciolaria*, due to the presence of an adapical sinus on the outer lip.

Moreover, this species was considered a member of Peristerniinae “pending molecular confirmation” by these same authors.

Bouchet & Snyder (2013) distinguished the newly-appointed genus *Nodolatirus* from other peristerniines by the presence of nodes and the heavy cords on the shell and by the “massive lateral tooth”. The radula differs from *Benimakia* Habe, 1958 because this genus bears much thinner laterals, carrying five to six cusps (Bouchet & Snyder, 2013: Figs 3A-F); it is this difference that prompted the consideration of a new genus.

*Nodolatirus nodatus* (Figs. 65-66) appeared on a clade with species of *Latirus*, *Hemipolygona*, *Benimakia* and *Latirolagena* Harris, 1897 in Couto *et al.* (2016), although with conflicting topologies between the ML and BI analyses and low support for some deeper nodes. The placement with *Benimakia* agrees with Bouchet & Snyder (2013), but the radula, which is the main distinguishing feature between them, renders this species more related to clade 6a, and that is confirmed here.

### **Clade 6b**

This clade is characterized, among other features, by the absence of the innermost cusp of the radula’s lateral tooth (cusp one) (character 60, Fig. AS). This is seen in the radula of most fasciolariines and in *Latirus vischii*. This species (Fig. 67) has a radula (Fig. 68) with a ‘rounded’ base of the tooth, (*i.e.*, lacking the first cusp) as described by Couto *et al.* (2015b) for *Fasciolaria tulipa*. This feature according to Bullock (1974) distinguishes *Latirus* and related species (*sic*) from *Leucozonia*; he utilized the term denticle, which corresponds to cusp number one in this analysis. This ‘denticle’ was observed by Couto & Pimenta (2012) and Couto *et al.* (2015a) for some *Leucozonia* species. The present work hypothesizes the loss of cusp one for two independent clades: clade 6b and 14, although in the latter, cusp two has a greatly increased length; all of these features are discussed more thoroughly in the character discussion section.

In Couto *et al.* (2016), *Latirus vischii* appeared as the sister taxon to *Latirus polygonus* and that is corroborated by shell morphology. Both species have very strong nodes on the shoulder angulation which are crossed by two whitish spiral cords, but the radula distinguishes both species: while in *L. vischii* it is a characteristic for this clade, in *L. polygonus* (Kosyan *et al.*, 2009: Fig. 31), it is as most ‘*Latirus*-like’, with cusp one present and in reduced length.

## Clade 6c

Historically, most members of this clade have been assigned to the genera *Fasciolaria* or *Pleuroploca*. However, Snyder *et al.* (2012), after a thorough re-examination of their taxonomy, proposed several additional genera, *e.g.*, *Australaria*, *Aurantilaria*, *Viridifusus*, etc. This clade contains species with broad axial ribs and nodose spiral sculpture (*Aurantilaria aurantiaca* [Lamarck, 1816], *Filifusus filamentosus* [Röding, 1798], *Australaria australasia* [Perry, 1811], *Triplofusus giganteus* [Kiener, 1840] and *Pleuroploca trapezium* [Linnaeus, 1758] – all traditionally in the genus *Pleuroploca*); while *Fasciolaria* and *Cinctura* Hollister, 1957 represent a Caribbean lineage with obsolete axial sculpture and weakly convex spiral whorls. Most other species of this group have some degree of nodose shells, but Snyder *et al.* (2012) noted that some species have both nodose and non-nodose forms, which may represent ecophenotypic, local or regional geographic variation.

In the analyses of Couto *et al.* (2016) the Caribbean species *Fasciolaria tulipa*, *F. bullisi* Lyons, 1972 and the related species *Cinctura hunteria* (Perry, 1811) appeared as a crown group, sister to the Indo-Pacific *Pleuroploca trapezium*. This group is sister to the remaining *Aurantilaria*, *Filifusus*, *Triplofusus* Olsson & Harbison, 1953 and *Australaria* species, without support for their internal relationship and with conflicting ML and BI topologies. In this scenario, Caribbean lineages are present in the two main clades, representing at least two dispersal or vicariance scenarios. On the other hand, in the morphology-based topology presented here, the Caribbean species *Aurantilaria aurantiaca* and *Fasciolaria tulipa* form a polytomy with the remaining Indo-Pacific species *Australaria australasia*, *Pleuroploca trapezium* and *Filifusus filamentosus*. In the latter case only one biogeographic event occurs, a more parsimonious scenario than the one from Couto *et al.* (2016).

This clade seems highly derived, being characterized by several synapomorphies, none of which are non-homoplastic. Among them, noteworthy are the coloration of the shell that form blotchy spots (character 2, Fig. B), as opposed to regularly spaced; the loss of the pseudoumbilicus (character 10, Fig. J); the renal aperture situated close to pericardium (character 36, Fig. AA), as opposed to centrally in the membrane; the retractor muscle of the proboscis inserting posteriorly (character 68, Fig. AX); and an abrupt broadening of the posterior esophagus in the visceral region anterior to the stomach (character 74, Fig. BC). The anatomy of *Fasciolaria*

*tulipa* was studied by Couto *et al.* (2015b) and these authors confirmed all of these characteristics. No other reports in the literature occur for these features, however.

Snyder *et al.* (2012) noted that the two species of Fasciolariinae that occur in Brazilian waters, *Fasciolaria tulipa* (Fig. 69-70) and *Aurantilaria aurantiaca* (Fig. 71-72), overlap in northern Brazil, and some geographic differentiation may occur. The former species has smooth axial sculpture while the latter has broad nodes on its shoulder angulation; a body pigmentation that is orange to light red with reticulated lighter pattern and the opening of the female cement gland is anterior.

Distinction of the *Fasciolaria* species from the West Atlantic is problematic (Lyons, 1972): while Rosenberg (2009) argued to the occurrence of at least seven distinct species occurring in sympatry in the Caribbean Sea: *Fasciolaria tulipa*; *F. bullisi*; *F. hollisteri* Weisbord, 1962; *F. tephрина* de Souza, 2002; *F. branhamae* Rehder & Abbott, 1951; *F. hunteria* and *F. lilium* Fischer, 1807; Snyder *et al.* (2012) only recognized the first four as belonging to the genus. A more extensive sampling than one undergone here and in Couto *et al.* (2016) is necessary to resolve these taxonomic issues, likely due to recent dispersal events.

## **Clade 6d**

This exclusively Indo-Pacific clade differs from the previous fasciolariines by its small head and cephalic tentacles (characters 13, 14, Fig. M) and by the cement gland (character 83, Fig. BH). This latter structure occurs immersed in the foot as several saccular vesicles branching from a single opening, and not as a single sac. Species here possess very broad and ample shells, with nodose sculpture present in the shoulder angulation, except for *Filifusus filamentosus* (Figs. 73-74), which has a more rounded profile. *Australaria australasia* (Figs. 75-76) and *Pleuroploca trapezium* (Figs. 77-78) have very similar shells, and the radula of the first has a reduction in the number of cusps of the lateral (Fig. 76), resembling somewhat other peristerniines in clade 7.

## **Clade 7**

Clade 7 is the other main clade of Fasciolariinae, that includes the bulk of peristerniine-like species, such as *Hemipolygona*, *Pustulatirus*, *Polygona*, *Leucozonia* and certain *Latirus*. The most important synapomorphy of this group is the presence of discontinuous spiral cords, also called lirae, on the inner side of the outer lip (character 7, Fig. G). This feature was used by

Vermeij & Snyder (2006) to characterize the subfamily Peristerniinae; however, Vermeij & Snyder (2002) pointed out that the beaded lirae likely evolved more than once in the Fasciolariidae. In the present analysis, this character is non-homoplastic, not supporting the hypothesis of Vermeij & Snyder (2002).

The first split of this group is *Hemipolygona armata* (Adams, 1855) (Fig. 79-80) that is characterized by a reversion to a proboscis retractor muscle inserting posteriorly (character 68, Fig. AX).

### **Clade 8**

This clade is characterized by two reversions: the loss of the rhynchostome lipped margin (character 40, Fig. AC), and the reduction of the anterior fusion of the odontophore cartilages (character 44, Fig. AF). This clade groups species of peristerniine-like fasciolariines with the exception of *Hemipolygona armata*. The genus *Hemipolygona* is present in this analysis with two species: *H. armata* and *H. beckyae*. As with the analysis of Couto *et al.* (2016), the genus appeared non-monophyletic, with *H. mcgintyi* (Pilsbry, 1939) representing the first split of the Fasciolariinae clade, and *H. armata* sister to the genus *Pustulatirus*. Here, *H. armata* is the sister taxon to clade 8, and *Pustulatirus* the next split in the topology.

The genus *Hemipolygona* appeared as a non-monophyletic assemblage in Couto *et al.* (2016), although with a different taxon sampling than presently. In their ML analysis, *H. mcgintyi* is the basal most species of the clade (although unsupported), and *H. armata* is the sister to *Pustulatirus* species; in the BI analysis, *H. mcgintyi* attained the same position while *H. armata* is sister to *Nodolatirus nodatus*.

### **Clade 8a *Pustulatirus***

Species of *Pustulatirus* were previously classified in the genus *Latirus* (that was known until recently to be a polyphyletic taxon). The genus *Latirus* was restricted to the Indo-Pacific after the taxonomical review by Vermeij & Snyder (2006); several other important taxonomical works on *Latirus*-like fasciolariids split the genus even more (*e.g.*, Vermeij & Snyder 2002; 2006) and the analyses of Couto *et al.* (2016) confirmed the placement of the *Latirus* complex as polyphyletic. *Pustulatirus* is an extant genus confined within the new world Atlantic and Pacific coasts, with a few fossil Neogene species (Lyons & Snyder, 2013). The genus is recognized by



six species in tropical western Atlantic and four in the Indo-Pacific (Lyons & Snyder, 2013; WoRMS, 2016), being one of the few fascioliid shallow-water genus with more representation in the new world.

Vermeij & Snyder (2003) transferred numerous species to *Benimakia*, including *B. ogum*, originally described in the genus *Latirus*. These same authors characterized *Benimakia* as high-spired fascioliids with prominent axial ribs and a labral tooth at the end of the central cord of the outer lip. Couto *et al.* (2015a) noted that *B. ogum* (as *Pustulatirus ogum*) differs from other species of *Benimakia* in having a discontinuous beaded lirae on the inner side of the outer lip, in this respect resembling many *Latirus* (Vermeij & Snyder 2003) and *Pustulatirus* (Vermeij & Snyder, 2006). Species included in *Benimakia* by Habe (1958) and Vermeij & Snyder (2003) occur in the west Indo-Pacific, with the exception of *B. ogum*, which putatively differs from other members of Peristerniinae related to *Latirus* in having a small labral tooth at the end of the basal cord (*sic* Vermeij & Snyder, 2003). The presence of this tooth is questionable at best, as a labral tooth is not mentioned in the original description by Petuch (1979), nor was it found in Couto *et al.* (2015a). A pseudoumbilicus is also present, differentiating it from *Benimakia*, although it does occur in *Pustulatirus*. Based on these arguments, *B. ogum* clearly belongs to the genus *Pustulatirus*; this was evidenced by the topology in this study, sister species to *P. mediamericus* and in the molecular analyses of Couto *et al.* (2016), sister to *P. praestantior* (Melvill, 1891) (in this sense also agreeing with Landau & Vermeij, 2012; Lyons & Snyder, 2013 and Couto *et al.*, 2015a).

This study demonstrates the monophyly of the genus *Pustulatirus*, being supported by many reversions and non-homoplastic synapomorphies, most notable of which are the rachidian tooth bearing four principal cusps (character 55, Fig. AK) (also reported by Kosyan *et al.*, 2009: Fig. 35), the paired proboscis retractor muscles inserting posteriorly (characters 67, 68, Figs. AW, AX, respectively) and the female cement gland opening centrally in the foot (character 84, Fig. BH). It is the first split of the clade 8; in the ML analysis of Couto *et al.* (2016) the genus also appeared monophyletic and is sister *Hemipolygona armata* in the clade that includes *Latirus polygonus*, *L. vischii* and *Latirolagena smaragdulus* (Linnaeus, 1758), among others peristerniine-like, all previously assigned to the genus *Latirus*.

*Pustulatirus mediamericus* (Fig. 81), the type species of the genus was not present in the analysis of Couto *et al.* (2016), although based on the topology presented here one may assume to

belong in the same clade as *P. ogum* and *P. praestantior*. *Pustulatirus mediamericanus* resembles *P. ogum* (Figs. 82-83), and these are the largest congeners in the Pacific and Atlantic America, respectively. As with the shells of *P. mediamericanus*, the broad axial ribs of *P. ogum* assume a relatively lower profile as specimens approach maturity (Lyons & Snyder, 2013); the smooth surfaces of intermediate spire whorls and the initial portion of the body whorl are supplanted by spiral cords that become prominent near the terminal edge of the shell in each species. Anatomically, *P. ogum* has a longitudinal rhynchostome and the duct of the penis is linear, differing from *P. mediamericanus*; both species share the four cusped rachidian tooth (Fig. 83).

### Clades 9 to 13

The following clades form a grade (Figs. 84-92) that encompasses species of previously assigned *Latirus*; a genus in which the taxonomy has been confusing because it was used indiscriminately to include several species, some of them doubtfully related. *Latirus* was initially conceived as distributed worldwide; however, Vermeij & Snyder (2006) constrained the known geographic range of the genus to be restricted to the western Indo-Pacific, and consequently raised several taxa previously considered as subgenera to genus rank (e.g., *Polygona*, *Hemipolygona*) and proposed new genera (e.g., *Pustulatirus*, *Turrilatirus* Vermeij & Snyder, 2006).

The genus *Polygona* is the first split in the clade 9 and 11, evidencing its polyphyletic state. The genus is monophyletic in the analysis by Couto *et al.* (2016), highly supported and always grouped together with genus *Turrilatirus*. Vermeij & Snyder (2006) considered *Polygona* and *Turrilatirus* similar in having broad axial ribs lacking nodes, and abapical denticles on the outer lip; however, *Turrilatirus* differs from *Polygona* in having a high spire, a short siphonal protuberance, and usually lacking a pseudoumbilicus.

Several authors have recognized informal groups within *Polygona* (Lyons, 1991; Vermeij & Snyder, 2006); Vermeij & Snyder (2006) also grouped species of *Polygona* into two groups but opted against giving them formal status in view of the “absence of more definitive molecular evidence”. The first group contains *P. angulata* (Figs. 84-85), and possesses shells that are more stepped and nodose; the second group contains *P. infundibulum* (Figs. 87-88) with shells bearing a low shoulder angulation and axial ribs extending onto the long siphonal canal. In Couto *et al.* (2016), *Polygona infundibulum* grouped with *P. bernadensis* (Bullock, 1974), while this clade is

the sister group of *P. angulata*; although a more thorough sampling of *Polygona* species is desirable, these groups concur with those recognized by Vermeij & Snyder (2006) and may indeed justify formal separation, possibly as subgenera. These results do not agree with the present morphological analysis, since *Polygona* does not form a monophyletic group. The rachidian tooth of the radula of *P. infundibulum* bears secondary cusps in this sense differing from *P. angulata* (Figs. 85, 88).

*Latirus polygonus* (Fig. 86) and *L. pictus* (Figs. 91-92) are another case of the non-monophyletic state of the genus. Both species were used in the analysis of Couto *et al.* (2016) and their results placed them in different positions: the first as the sister taxon to *L. vischii* and the second as sister to the clade of *Turrilatirus* and *Polygona*. *Latirus vischii* has the lateral tooth of the radula (Fig. 68) with the first innermost cusp lacking, and that is a synapomorphy of clade 6a; *L. polygonus* and *L. pictus*, on the other hand, have a typical “*Latirus*-like” (Fig. 92, but see Kosyan *et al.*, 2009: Fig. 31) radula in having the first innermost cusp present, albeit reduced.

*Hemipolygona beckyae* (Figs. 89-90) is a Brazilian species with a prominent shoulder angulation as is characteristic for the genus lacking and a small number (four or five) of high, sharp spiral cords on the central sector of the last whorl and a more-or-less planar outer lip. Typical *Hemipolygona* have a more nodose shell, much like *H. armata* (Fig. 80). Morphologically, *H. beckyae* possess the rhynchostome positioned obliquely between the cephalic tentacles as an autapomorphy.

Fascioliariinae and Peristerniinae have a long history of divergence from the Cretaceous (approximately 140 Mya) but diversifying extensively during the Neogene (circa 24 Mya to the present) (Vermeij & Snyder, 2006; Couto *et al.*, 2016). In the analyses of Couto *et al.* (2016) many deep relationships within this clade received little or no support and are incongruent between the ML and BI analyses. However, all genera, with the exception of *Hemipolygona*, are monophyletic and show high support in both their analyses.

The fact of the short branch lengths and incongruent results of Couto *et al.* (2016) is likely the result of a very rapid speciation, which did not leave an imprint in genetic difference, at least in the analyzed genes. If speciation events are closely spaced in time, the amount of phylogenetic signal is often small, leading to short internal tree branches that are difficult to resolve (Philippe *et al.*, 2011) This hypothesis agrees with the morphological one presented here, as each of the

nodes in clades 9 to 13 is supported by very few synapomorphies (no more than two), none of which are non-homoplastic. This also indicates a rapid speciation event.

#### **Clade 14 *Leucozonia* and *Opeatostoma***

The genus *Leucozonia* comprises shallow water coastal species that are usually very common in low rocky intertidal and sublittoral communities. The genus is exclusive to the new world coast, with nine extant species (WoRMS, 2016); however, it is poorly represented in the fossil record in Neogene fossils from the same locality (Vermeij, 1997).

Morphologically, clade 14 is well supported by many synapomorphies, including the loss of the longitudinal folds in the margin of the rhynchostome (character 39, Fig. AC), a long odontophore (character 42, Fig. AE) and the typical radula: the lateral tooth lacks cusp one, much like the fasciolarine clade 6b, however, unlike species in that clade, cusp two is longer, approximately twice in length as the other cusps (characters 60, 61, Fig. AS). In this sense, the functional innermost cusp is longer, and that is diagnostic for all species of this clade. This characterization of the radula as diagnostic for *Leucozonia* and *Opeatostoma* species seems to be true for all radulae figured in the literature (e.g., *Leucozonia ocellata* and *L. nassa* by Bandel, 1984: Figs. 261, 263; *Leucozonia nassa* by Matthews-Cascon *et al.*, 1989: Fig. 3; *Opeatostoma pseudodon* by Kosyan *et al.*, 2009: Fig. 37; *L. nassa*, *L. ocellata* and *L. ponderosa* by Couto & Pimenta, 2012: Figs. 1P, 5F, 9N)

The radula of *Latirus (sic) smaragdulus (Latirolagena smaragdula)* figured by Bandel (1984: Fig. 264) seems to fit this pattern, with a longer innermost cusp (due to the loss of cusp one). This author considered this to be a transitional form between the radulae of *Latirus* and *Leucozonia* species from the Caribbean and those of *Fasciolaria* species, with the many narrow cusps. The radula of this species is confirmed in Taylor & Lewis (1995: Fig. 8), and indeed this radula type seems to belong to this clade. In the analyses of Couto *et al.* (2016) the position of *L. smaragdula* disagrees with this assumption because this species did not appear closely related to *Leucozonia*; the meaning of this is beyond the means of the present study.

In Couto *et al.* (2016), the genus *Leucozonia* was evidenced as non-monophyletic, with *L. ocellata* and *L. cerata* (Wood, 1828) as a natural group, and the remaining species of the genus and *Opeatostoma pseudodon* in a different clade. There were conflicting topologies between the ML and the BI analyses.

#### **Clade 14a *Leucozonia ocellata*, *L. cerata* and *Opeatostoma pseudodon***

Two Pacific species, *Opeatostoma pseudodon* and *Leucozonia cerata*, and the Atlantic *L. ocellata*, form this clade. The internal relations between these taxa are still dubious, due to the polytomy in the final strict consensus tree.

The present morphology-based topology shows a strong support with many synapomorphies for clade 14a, among the most important ones: the position and margin of the rhynchostome (character 37, Fig. AB), the female cement gland opening (character 84, Fig. BH) and the linear duct of the penis (character 87, Fig. BJ). When analyzed through molecular means, Couto *et al.* (2016) obtained a different result: in both ML and BI analyses, *Leucozonia nassa*, *L. ponderosa* and *Opeatostoma pseudodon* formed a highly supported clade, while *L. ocellata* and *L. cerata* appear as the sister clade to the clade of *Turrilatirus* and *Polygona*.

Couto & Pimenta (2012) analyzed shell morphology and internal anatomy of the *Leucozonia* species from Brazil (*L. nassa*, *L. ponderosa* and *L. ocellata*). Despite *L. nassa* and *L. ponderosa* possessing a very similar internal anatomy, *L. ocellata* was shown to possess more differences; that corroborates with the present results (*L. nassa* more closely related to *L. ponderosa* than to *L. ocellata*). *Leucozonia ocellata* (Figs. 93-94) is usually a smaller *Leucozonia* species characterized by the distinct shoulder axial sculpture bearing a white blotchy coloration and the absence of a labral tooth. Although *L. ocellata* shows considerable variation in shell form and sculpture, it is hard to identify geographical patterns in this species (Vermeij & Snyder, 2002). The heavily asymmetrical osphradium and the rachidian tooth of the radula with fewer cusps (Fig. 98) are autapomorphies of this species.

The closest relative to *L. ocellata*, *L. cerata* (Figs. 95-96) is the sister species in the analysis of Couto *et al.* (2016), and both have many similarities in shell structure, including the absence of a labral tooth. *Leucozonia cerata* differs from the western Atlantic *L. ocellata* by attaining a much larger adult size, and usually having a higher spire, much weaker lirae, and stronger principal spiral cords. The autapomorphies of *L. cerata*, which distinguish it from its closely related *L. ocellata*, occur in the renal cavity, odontophore and nerve ring.

*Opeatostoma pseudodon* (Figs. 97-98) is a unique species characterized by a long and curved labral tooth that is completely enveloped by the mantle when the animal is active, which is evidenced by its very sharp edge (Vermeij, 2001). It is formed differently than that of *Leucozonia* because, in the former, it is formed as an extension of the spiral groove; while in the

latter it is formed as an extension of a cord between the base and the central sector of the outer lip (Vermeij & Snyder, 2002). In the phylogeny of Couto *et al.* (2016), *O. pseudodon* is the sister species to the western Atlantic *Leucozonia nassa* complex clade (clade 15), with high support; in the current morphology-based scenario, this species is grouped with *Leucozonia ocellata* and *L. cerata*, within a polytomy.

*Opeatostoma pseudodon* is highly modified, with many autapomorphies, most notable of which are: a lacking the spiral sculpture; a distinct labral tooth is present in the outer lip; the loss of the longitudinal folds in the margin of the siphon; the renal aperture is emarginated by a lipped rim; the rachidian tooth of the radula that may bear more than five cusps (Figs. 98B-C); the posterior esophagus has a broadening in the visceral region; and the presence of a penis ejaculatory duct as a long convoluted tube (characters 3, 5, 30, 34, 51, 74, 89, Figs. C, E, X, Z, AK, BC, BL, respectively).

This species was analyzed by Kosyan *et al.* (2009) and these authors confirmed its position within the fascioliids based on anatomical features, notably the absence of a posterior sorting area (caecum) in the stomach and the typical radula. The rachidian tooth of the radula was reported possessing five cusps by Kosyan *et al.* (2009); here, up to 12 cusps occur and sexual dimorphism was discarded as all specimens analyzed were female. Bandel (1984) reported that the number of cusps in the lateral tooth grows as the snail matures, and that may be the case here, although a larger number of specimens must be studied in order to confirm this hypothesis.

### **Clade 15 “*Leucozonia nassa* complex”**

The *Leucozonia nassa* complex is here represented as two closely related binomial species, *L. nassa* and *L. ponderosa*, and three subspecies of *L. nassa*. This clade contains a polytomy and it is not possible to more closely infer the relationships between these species.

Unlike the previously discussed *Opeatostoma pseudodon*, a ventral labral tooth may be present in the outer lip in some of these taxa; however, it is not covered by the mantle, being blunt and short (character 5, Fig. E). Other synapomorphies include the medium-sized head and cephalic tentacles (characters 13, 14, Fig. M), a secondary inner cusp present in cusp two of the lateral tooth of the radula (character 62, Fig. AS), a seminal vesicle present in the oviduct and a short bursa copulatrix (characters 78, 80, Fig. BF).

*Leucozonia ponderosa* is endemic of Trindade Island; an oceanic island off the coast of the state of Espírito Santo in southeastern Brazil. *Leucozonia nassa sensu stricto* has a wider geographical range on the continental shelf from the northeastern to the southern coast of Brazil, as well as the oceanic islands of Trindade and Fernando de Noronha (Leal, 1991; Rios, 2009). Both species undergo intracapsular or lecithotrophic development (Leal, 1991), as do other fascioliariids. The most common of these, *Leucozonia nassa*, has a marked geographical differentiation, leading to the occurrence of several synonyms, and at least three distinct morphs based solely on shell characters, which were considered by Vermeij (1997) as three different species, *L. nassa*, *L. cingulifera* (Lamarck, 1816), and *L. brasiliana* (d'Orbigny, 1841). In contrast, Vermeij & Snyder (2002) argued that these characters alone may be insufficient to allow separation of species. Due to overlapping geographic ranges and the presence of intermediate forms, *L. nassa* is recognized as a single species (Rosenberg, 2009; WoRMS, 2015). The endemic species from Trindade Island, *L. ponderosa* was considered by Rios (2009) as a synonym of *L. nassa*.

Couto *et al.* (2016) sampled representatives of all three geographical subspecies of *Leucozonia nassa*, and they grouped as a single well supported clade. Based on their tree topology and the fact that *Leucozonia nassa* has a non-planktotrophic development (Leal, 1991), the forms that are geographical isolates may indeed constitute different species. *Leucozonia ponderosa* appeared as sister to *L. nassa cingulifera* from the Fernando de Noronha Archipelago, northeastern Brazil. These insular subspecies grouped with the coastal southeastern Brazilian *L. nassa brasiliana*, a clade that is sister group of the three Caribbean specimens corresponding to *L. nassa nassa*. The Caribbean clade was highly supported in both ML and BI analysis, albeit the other nodes within this group received weak support and conflicting topologies among analyses. The specimens utilized by Couto *et al.* (2016) correspond to the forms used in the present morphological analysis; hence the subspecies category was used in conformance with these authors.

The typical *Leucozonia nassa nassa* (Fig. 99) has a moderately broad shell and defined spiral and axial sculpture. The basal cord, in which the labral tooth emerges, is enlarged; in addition, spiral threads cover the entire shell surface. The siphonal canal is relatively long in relation to the other forms. *Leucozonia nassa cingulifera* (Fig. 100), is a large, extremely thick-shelled form with a peach-colored aperture. Spiral sculpture in this form is usually in the



presence of very weak cords or may be obsolete. Axial sculpture is also weakly developed, which may be accentuated by the presence of calcareous algae incrusting in the shell. Labral tooth is present and also very thick. *Leucozonia nassa brasiliana* (d'Orbigny, 1841) (Fig. 101-102), has a less nodose shell, with fewer and lower shoulder axial nodes on the shoulder angulations, also the spiral cords are weak and not enlarged as they are in the typical form of *L. nassa nassa*. The aperture is typically peach-colored, and the siphonal canal is short.

Couto & Pimenta (2012) found no anatomical differentiation between these three forms, and they concluded that these forms are merely geographical variants, despite the fact that they do not possess planktotrophic dispersal. In fact, in the level of anatomical dissections presented here, no differences may be observed between these forms, and that is evidenced by the lack of autapomorphies and by the polytomy they occur in. Through molecular means, however, these forms seem to be in speciation, as proven by the topology in Couto *et al.* (2016).

*Leucozonia ponderosa* (Figs. 102-103) has a single autapomorphy (pedal ganglia length) and has been distinguished in shell characters by Couto & Pimenta (2012). These authors distinguished this species as distinct from *L. nassa* on the basis of a more prominent spiral sculpture and a somewhat heavier nodulose shell. According to Vermeij & Snyder (1998) and Couto & Pimenta (2012), in the typical form of *L. nassa*, the two upper main cords lie very close together, whereas in *L. ponderosa* the second cord lies approximately midway between the shoulder cord and the central cord. Anatomically, the only minor difference is in the radula, which has a well-marked denticle on the inner margin of the lateral teeth, according to Couto & Pimenta (2012); this denticle occurs much more pronouncedly in *L. ponderosa* than in other *Leucozonia* species (Fig. 104).

## 7. Character discussion

The following pages list each of the 96 characters used in this analysis, and they are thoroughly discussed in a morphological point of view, as opposed to a phylogenetic point of view as seen in the Phylogenetic Discussion section. As before, discussion is based on the phylogenetic analysis using prior weighting only.

Each character is illustrated by a figure (numbered A, B, AA, AB, etc.) When a figure illustrates more than one character, following each figure caption is the character number (e.g., char. 31), followed by the state in which it is found (e.g., char. 31: 1). Readers are referred to the cladogram (Fig. 6) for the numbering of the clades present in this discussion.

### 1. Shell, spire (fig. A)

(L = 1; Ci = 100; Ri = 100)

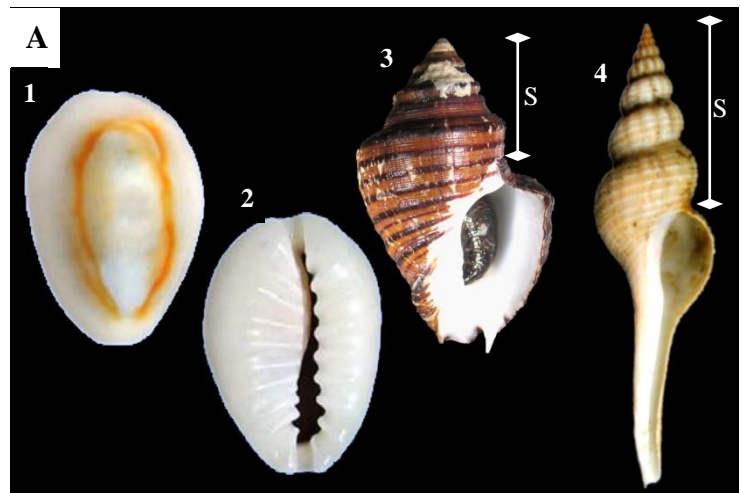
0. Involute

1. Visible

An involute spire occurs in the families included in Cypraeoidea (families Cypraeidae, Eratoidae, Lamellariidae, Ovulidae, Pediculariidae, Triviidae, and Velutinidae) *sensu* Simone (2011).

While there are several degrees of involute shells caused by the apical growth of the outer lip, in most of

these the apex is completely covered as is the case herein for the outgroup species *Monetaria annulus* (0). A visible spire (1) on the other hand is present in most Neogastropoda (Simone, 2011), and all the remaining species. Because of the outgroup choice, this character is plesiomorphic in this analysis, however in the context of Caenogastropoda, it is actually apomorphic, as pointed out by Simone (2011).



A. Shell in apertural and abapertural view. A1-2. *Monetaria annulus* (modified from Simone, 2004) involute spire (0); A3. *Opeatostoma pseudodon* and A4. *Fusinus frenguelli*, visible spire (1). S: spire.

## 2. Shell, pigmentation (fig. B)

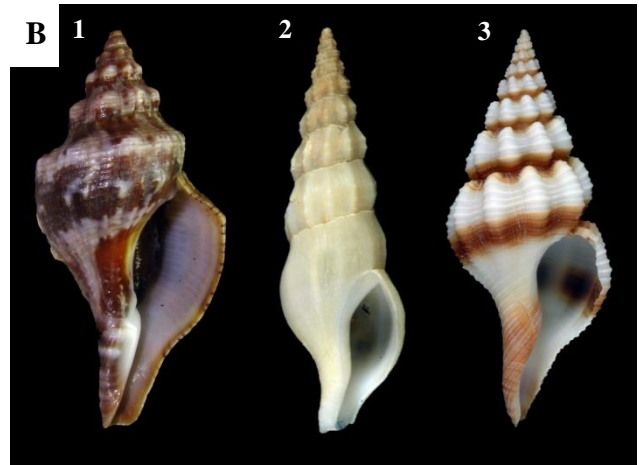
(L = 3; Ci = 33; Ri = 66)

0. Blotchy

1. Absent or regular

Fascioliids, when possessing coloration in the shell, usually have a regular color pattern, with nodes or spiral bands evenly spaced throughout the entire shell (1). A blotchy color pattern (0) occurs when the coloration is not evenly arranged spirally or axially.

Fascioliids have a coloration pattern that is either regular or absent, except for clade 6c of fascioliines.



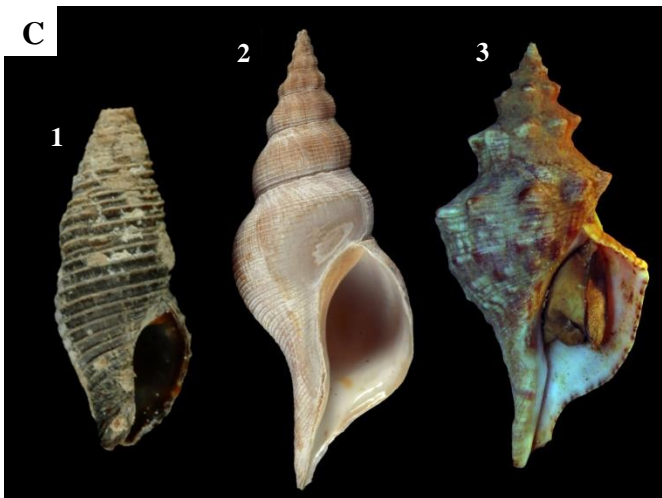
**B.** Shell in apertural view. **B1.** *Aurantilaria aurantiaca*, coloration of shell in blotchy pattern (0); **B2.** *Amiantofusus candoris*, coloration of shell absent (1); **B3.** *Pseudolatirus* sp. regular coloration pattern (1).

## 3. Shell, spiral sculpture forming elevated nodes (fig. C)

(L = 9; Ci = 11; Ri = 27)

0. Absent

1. Present



**C.** Shell in apertural view. **C1.** *Dolicholatirus* sp. and **C2.** *Chryseofusus graciliformis* spiral nodes absent (1); **C3.** *Aurantilaria aurantiaca*, spiral nodes present (0).

The presence of spiral sculpture forming elevated nodes is usually the case for most neogastropods, and it is evidenced here (1). In several cases within Fascioliidae there has been a reversion of the spirally nodulose shell (0), as is the case for the *Dolicholatirus* and *Teralatirus* clade, for *Chryseofusus*, as well as four more times independently as autapomorphies. A DELTRAN optimization was chosen as to force independent reversions in the outgroup species *Nassarius reticulatus* and

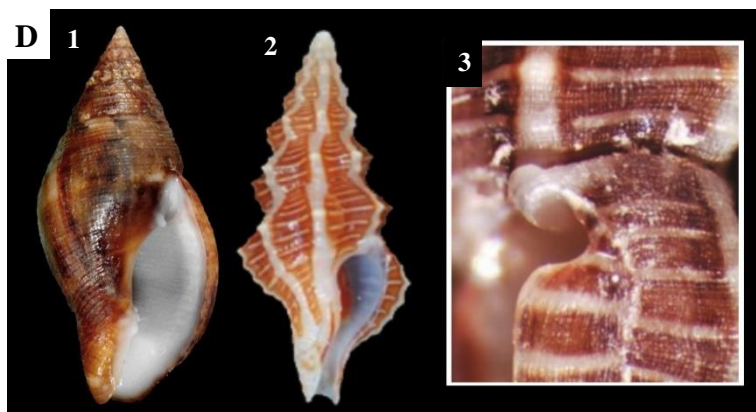
*Bullia laevis*. The presence of strong spiral cords must not be mistaken for the presence of nodes, as most fascioliids possess some spiral sculpture.

Some species (e.g., *Leucozonia nassa*, *Aurantilaria aurantiaca*, *Pugilina tupiniquim*), that normally have elevated nodes, may occur in individuals that lack any sculpture, although the ability to produce such nodes was indicated by the state (1), despite occurring in the (0) state. It is notable ability of shells to be molded by the environment; experimental and accidental transplantations of individuals from one environment to another are typically accompanied by dramatic changes in shell shape, sculpture, and color (Vermeij, 2002). This fact relates to most, if not all, shell characters herein. Fascioliidae have a spiral sculpture forming nodes as a basal state, however clades 1a, 3b<sup>1</sup>, *Fusolatirus bruijnii*, *Fasciolaria tulipa*, *Filifusus filamentosus* and *Opeatostoma pseudodon* have lost this characteristic.

#### 4. Shell, outer lip, anal notch (fig. D)

(L = 3; Ci = 66; Ri = 0)

- 0. Absent
- 1. Present ventral in aperture
- 2. Present lateral in aperture



**D.** Shell in apertural view and detail of aperture. **D1.** *Pisania pusio*, anal notch present ventral to aperture (1); **D2-3.** *Angulofusus nedae* (modified from Fedosov & Kantor, 2012), anal notch present lateral to aperture (2).

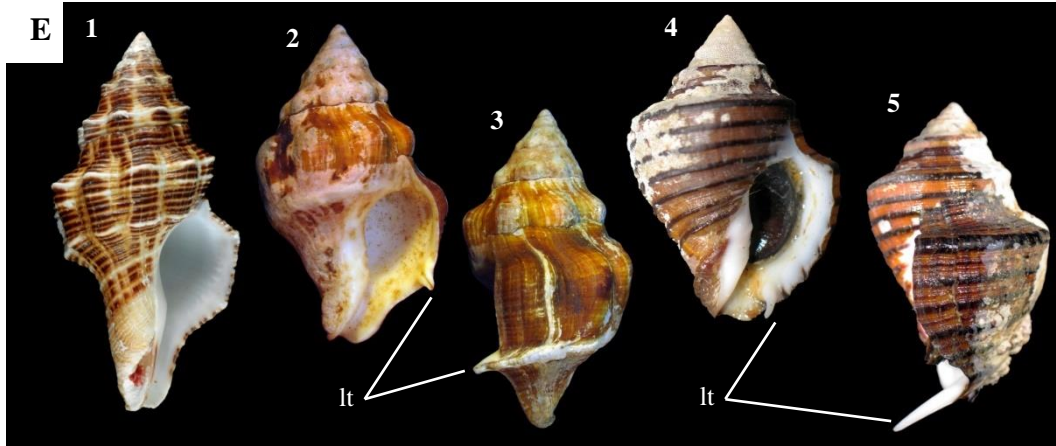
In the original description of *Angulofusus nedae* Fedosov & Kantor, 2012, the only representative of the genus, a superficial conchological resemblance to some Conoidea was noted by its authors notably the distinctive anal notch. Upon closer examination, it was noted the similarity of a sinus in the apical

apertural region of *Pisania pusio* (1), however the sinus in *A. nedae* is more lateral (2), suggesting a dorsal migration of the sinus and forming a notch in the mantle.

## 5. Shell, outer lip, labral tooth (fig. E)

(L = 3; Ci = 66; Ri = 85)

- 0. Absent
- 1. Present, covered by mantle
- 2. Present, not covered by mantle



**E.** Shell in apertural and lateral view. **E1.** *Latirus vischii*, no labral tooth (1); **E2-3.** *Leucozonia nassa cingulifera*, labral tooth not covered by mantle (2); **E4-5.** *Opeatostoma pseudodon*, labral tooth covered by mantle (1). **lt:** labral tooth.

A labral tooth is a downwardly projecting tooth or spine formed at the edge of the outer lip of the shell. The labral tooth plays a more or less active part in predation on relatively large prey animals, such as helping to part bivalve mollusks or even anchorage in the substrate while predation takes place (Vermeij, 2002).

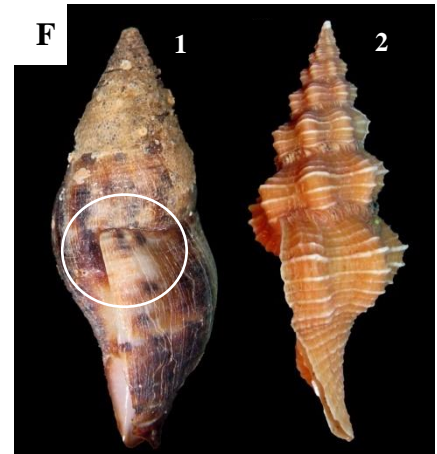
The highly unusual eastern Pacific species *Opeatostoma pseudodon* has the longest known labral tooth of any gastropod, being unusual for at least three reasons other than its length, as pointed out by Vermeij (2001): First, the tip of tooth is always sharp and never worn; second, it is entirely smooth, indicating that it is covered by an extension of the mantle in life; and third, it is separated from the adapical sector of the outer lip by a deep sinus, which exaggerates the tooth's length. This (1) is an autapomorphic state for *Opeatostoma pseudodon*. *Leucozonia nassa nassa* and *L. ponderosa* (clade 15) on the other hand, possesses a labral tooth that is ventrally directed and developed on outer lip at end of central spiral cord (2) and is not enveloped by mantle, as it is blunt and coarse. As pointed out by Simone & Ramos (1986) for the Brazilian *Leucozonia nassa*

complex, some populations lack the labral tooth altogether, not occurring in *Leucozonia nassa brasiliana*.

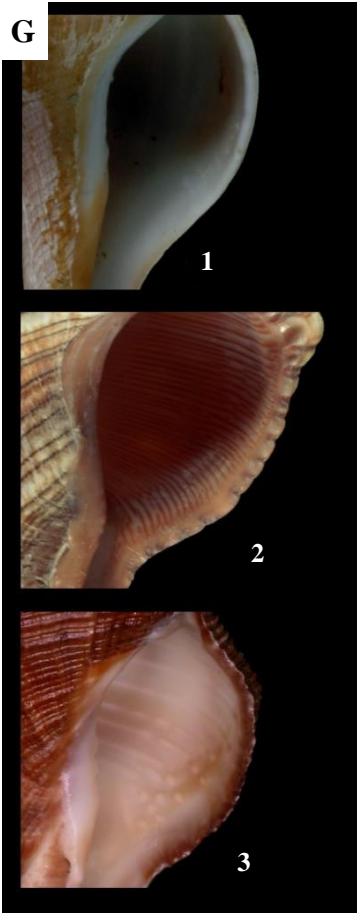
### 6. Shell, outer lip, apical growth of last whorl (fig. F)

(L = 5; Ci = 20; Ri = 20)

- 0. Present
- 1. Absent



F. Shell, lateral view. **F1.** *Pisania pusio*, lateral view evidencing the apical growth of the last whorl (1); **F2.** *Hemipolygona beckyae*, no apical growth (1).



G. Apertural view of shell. **G1.** *Pseudolatirus discrepans*, no inner sculpture on the outer lip (0); **G2.** *Pleuroploca trapezium*, inner sculpture of continuous spiral cords (1); **G3.** *Leucozonia nassa*, inner sculpture of discontinuous spiral cords (2).

During the last stages of growth, the last whorl may grow towards the apex of the shell, or even

encircle earlier whorls, such as in the case of *Monetaria annulus*.

Usually, this apical growth (1) occurs to a certain degree in the outgroup species but never in Fascioliidae, with the exception of *Cyrtulus serotinus*, which has a very aberrant shell in general.

### 7. Shell, outer lip, inner sculpture (fig. G)

(L = 7; Ci = 28; Ri = 84)

- 0. Absent
- 1. Continuous spiral cords
- 2. Discontinuous spiral cords

The sculpture present on the inner side of the outer lip in the form of spiral ridges are lirae. In most gastropods with lirae they are continuous spiral cords (1) extending from near the edge of the outer lip to a variable distance within the aperture. Smooth lirae of this kind characterize the vast majority of fascioliids; on the other

hand, discontinuous lirae which appear granular or beaded (2), are rare among gastropods (Vermeij & Snyder, 2002). The latter occur among neogastropods only in some species in the families Fascioliidae, Costellariidae, and Buccinidae (Vermeij & Rosenberg, 2003).



Beaded lirae have been used to diagnose several fasciolariid groups (*e.g.*, *Latirus* [Vermeij & Snyder, 2006], *Leucozonia* [Vermeij & Snyder, 2002], *Pustulaturus* [Lyons & Snyder, 2013]), which appear distinct from the smooth continuous spiral cords. The presence of such sculpture has not been explicitly discussed in the literature, and nothing is known of their function. Vermeij & Snyder (2002) hypothesized that it likely evolved more than once in the Fasciolaridae, a hypothesis not confirmed here, since it appeared only once: in the group composed of the genera *Leucozonia*, *Hemipolygona*, *Polygona*, *Pustulaturus* and *Latirus polygonus* and *L. pictus* (clade 7).

Continuous cords (1) are present basally in the family, and the absence of any sculpture (0) reversed in several groups within fasciolarids, including clades 2b (*Pseudolaturus kuroseanus* and *Amiantofusus*), 3c (having reappeared in 3e) and 4a (*Granulifusus* and *Pseudolaturus discrepans*) Although such sculpture is present in mature shells, however, it may be poorly developed or absent on immature specimens (Lyons & Snyder, 2013). Because discontinuous spiral lirae are likely derived from the continuous ones, an additive parsimony model was chosen (0–1–2).

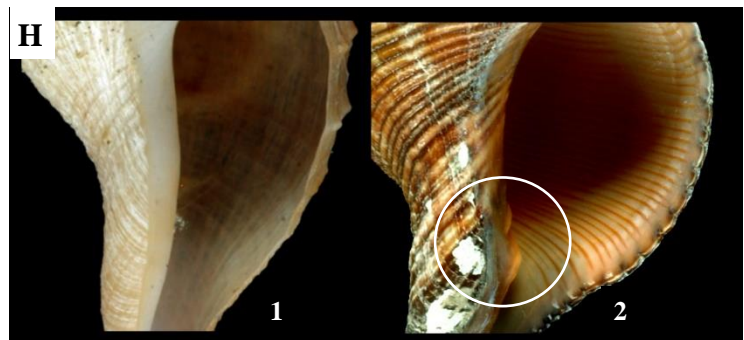
## 8. Shell, columellar folds (fig. H)

(L = 4; Ci = 25; Ri = 86)

- 0. Absent
- 1. Present

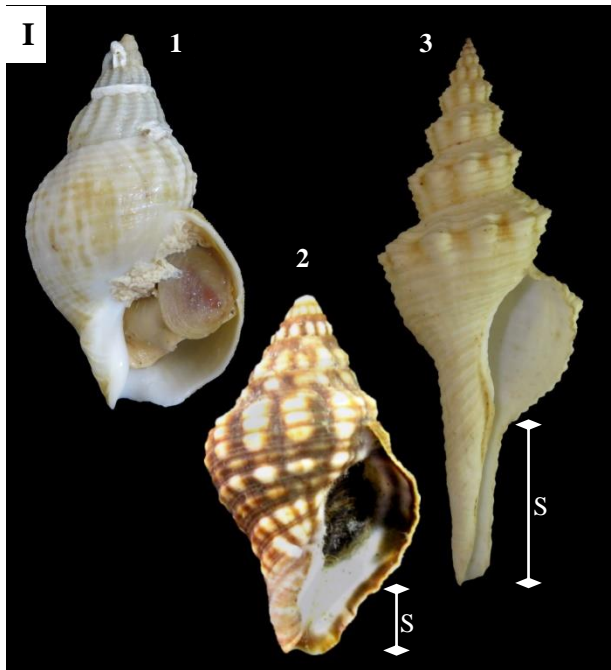
A Columella fold is any ridge on the inner lip of the aperture that extends along the columella for a number of

whorls, but usually all the way to the apex (1). Folds in fasciolarids are the folds located at the bottom of the inner lip of the aperture, near the entrance to the siphonal canal (1), and in some it may be absent (0). Not unlike the beaded lirae discussed earlier, internal ornamentation such as folds are gradually deposited in the wrinkles that would form when the large mantle retracted into the shell (Dall, 1894). Researchers (*e.g.*, Kier & Smith, 1985) often assumed that columellar folds are a type of internal ornamentation that enhances the performance of the columellar muscle, however, Price (2003), through several measurement parameters and biomechanical observations,



**H.** Apertural view of shell. **H1.** *Granulifusus* sp. columella lacking columellar folds (0); **H2.** *Filifusus filamentosus*, evidencing the columellar folds (1).





**I.** Shell in apertural view. **1I.** *Buccinum undatum*, siphonal canal, length: total shell length ratio of 1/6 or less (0); **2I.** *Leucozonia ocellata*, ratio is between 1/6 and 1/4 (1); **3I.** *Fusinus brasiliensis*, ratio is more than 1/4 (2). **S:** siphonal canal.

### 9. Shell, siphonal canal, length: total shell length (fig. I)

(L = 7; Ci = 28; Ri = 76)

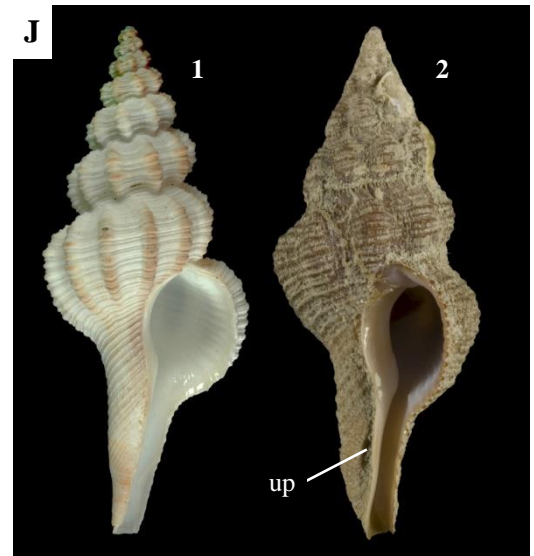
0. 1/6 or less
1. Between 1/6 and 1/4
2. More than 1/4

Simone (2011) described Siphonogastropoda, in which the main characteristic is the development of a pallial siphon; caenogastropod taxa included are Cypraeoidea, Tonnoidea and Neogastropoda (a siphon in the shell is also convergent in Cerithioidea and Stromboidea, but in those cases it is not followed by a pallial siphon).

Fascioliidae (clade 1) has the basal state of a ratio between 1/6 and 1/4 (1), and that is maintained for clade 1a (with a reversion in *Dolicholattirus* sp.) and clade 2a (*Amiantofusus* and *Pseudolattirus discrepans*). Clade 3, the remaining fascioliids, have elongated the siphonal

concluded that the folds neither increase nor decrease the animal's ability to maneuver its shell nor facilitate deeper withdrawal.

For fascioliids, columellar folds are traditionally characteristic for the subfamilies Peristerniinae and Fascioliinae, while Fusiniinae are known for their absence (Harasewych, 1998). Although it is true that most peristerniines *sensu lato* have such folds, it appeared in several clades independently, in clades 1b, 5, *Angulofusus nedae* and *Pseudolattirus discrepans*. Price (2003) augmented that the folds are an easily evolvable solution to many functional problems (none of which are fully understood), and that observable in this analysis.



**J.** Shell in apertural view **1J.** *Pseudolattirus pallidus*, no pseudo-umbilicus (0); **2J.** *Fusolattirus bruijnii*, pseudo-umbilicus is present (1). **up:** pseudo-umbilicus.

canal in relation to the total shell length, to a ratio of more than 1/4 (2), as seen for most of the traditional fusiines. However, most peristerniines and fascioliariines have reversed to a shorter siphonal canal in relation to the aperture (1), as seen for clades 5b, 6c and 7. Due to the quantitative nature of this character, an additive parsimony model was chosen (0–1–2).

#### 10. Shell, pseudo-umbilicus (fig. J)

(L = 5; Ci = 20; Ri = 83)

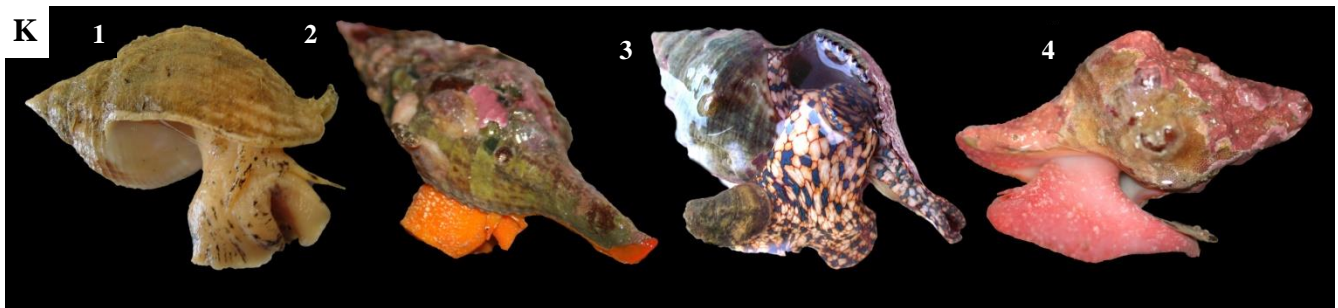
- 0. Absent
- 1. Present

A pseudo-umbilicus is a cavity formed close to the siphonal canal, at base of the shell. It is not a true umbilicus because it is not formed by the complete coiling of the shell. A pseudo-umbilicus can be shallow or deeply-recessed, but in most fascioliariids it is merely a shallow longitudinal slit. In fascioliariids, this structure (1) is found in *Dolicholatirus* and *Teralatirus* (clade 1a) and in the major group of peristerniines (clade 5), however it is lost (0) in the fascioliariines (clade 6c).

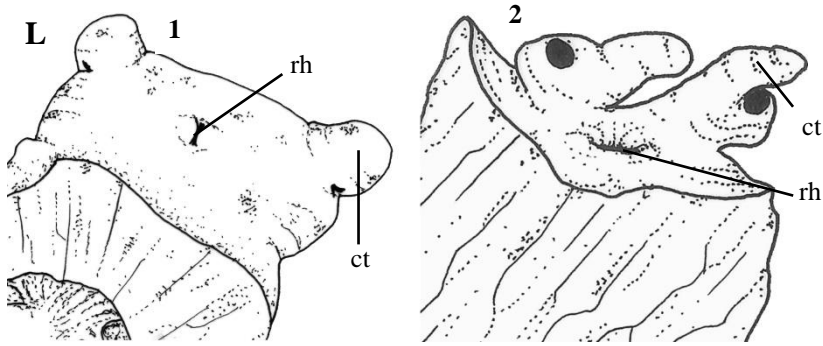
#### 11. head-foot, body pigmentation (fig. K)

(L = 4; Ci = 75; Ri = 95)

- 0. Absent
- 1. Orange to light red
- 2. Orange to light red with a reticulated pattern
- 3. Dark red



**K.** Live specimens with body extended. **K1.** *Buccinum undatum*, ([https://en.wikipedia.org/wiki/Buccinum\\_undatum](https://en.wikipedia.org/wiki/Buccinum_undatum)) no body pigmentation (0); **K2.** *Fusinus brasiliensis*, coloration orange to light red (1); **K3.** *Aurantiaca aurantiaca*, coloration orange to light red with a reticulated pattern (2); **K4.** *Leucozonia nassa brasiliiana*, coloration dark red (3).



L. Head in ventral view. **L1.** *Buccinum undatum*, cephalic tentacles with bases apart (0); **L2.** *Polygona angulata*, bases side by side (1). **ct:** cephalic tentacle; **rh:** rhynchostome.

Kantor (2012) diagnosed the new species *Angulofusus neda* as a Fusiniinae partly due to the soft-orange coloration of the head-foot, as most fusinines are known for. Because color fades over time when in contact with a fixative, this character is not accessible to researchers most of the time. All fascioliids have some color in the head-foot, although in *Dolicholatirus* and *Teralatirus roboreus* it is not possible to infer, traditional fusinines have an orange to light red coloration (1), beginning on clade 2, the traditional peristerniines a darker red (3), clade 5, while *Aurantilaria aurantiaca* a lighter orange with a reticulated pattern (2).

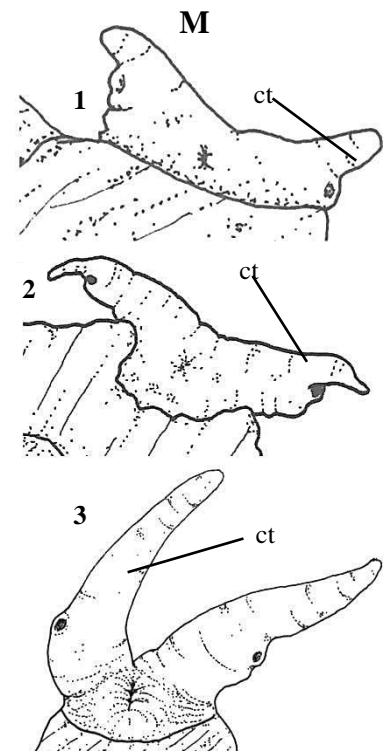
## 12. Head, cephalic tentacles, position (fig. L)

(L = 1; Ci = 100; Ri = 100)

- 0. Bases apart
- 1. Bases side by side

The presence of a pair of cephalic tentacles is a synapomorphy of the Gastropoda (Simone, 2011). The position of the tentacles in relation to each other is an important character; the ancestral state corresponds to a pair not adjacent to each other (0), in all Fascioliariidae, however, their bases are next to each other (1).

Members of Fascioliariidae are known to possess a red-orange color in the head-foot, terminally in the proboscis and edges of the mantle border and siphon. The coloration is a very notable character being used to diagnose members of the family (Harasewych, 1998). Fedosov &



M. Head in ventral view. **M1.** *Pseudolatirus pallidus*, width of head in relation to adjacent head-foot (char. 13: 0) and length of cephalic tentacles in relation to width of head (char. 14: 0); **M2.** *Fusinus brasiliensis* (char. 13 & 14: 1); **M3.** *Granulifusus* sp. (char. 13 & 14: 2). **ct:** cephalic tentacles.

**13. Head, width: head-foot width** (fig. M)

(L = 19; Ci = 10; Ri = 41)

- 0. 1/4 or less
- 1. More than 1/4 and less than 1/2
- 2. 1/2 or more

The width of the head is the transversal distance between both cephalic tentacles, and here it is correlated to the width of the adjacent head-foot. The ancestral state for fasciolariids is a small head relative to the head-foot (0), with groups having a ampler head (1) and culminating in a very broad head (2) in groups such as *Granulifusus*, *Chryseofusus graciliformis* and *Pseudolatirus discrepans*. This is a very homoplastic character, dotted by many reversions, and a DELTRAN optimization was chosen.

Members of fasciolariids have the basal state of 1/4 or less of the ratio between head width by head-foot width (0), although several changes occurred: an increase in the ratio to more than 1/4 to less than 1/2 (1) in clades 1b, 3e, 3c<sup>1a</sup> and 6. For this latter clade, clades 6d and 11 reverted to the previous state 0 (clade 15 reverted yet again to state 1). *Pseudolatirus kuroseanus*, *Chryseofusus graciliformis* and clade 4a (with a posterior reversion in *Pseudolatirus discrepans*) have increased this ratio to 1/2 or more (2).

**14. Head, cephalic tentacles, length: head width** (fig M)

(L = 18; Ci = 11; Ri = 42)

- 0. 2/3 to 2
- 1. Less than 2/3
- 2. More than 2/3

This character is directly correlated to the previous one, as the size of the cephalic tentacles increases as the width of the head, hence longer cephalic tentacles rest on broader heads (the exceptions to this case are *Buccinum undatum* and *Nassarius reticulatus*). As previously, DELTRAN was chosen, and optimization the of character states mimics the previous character.

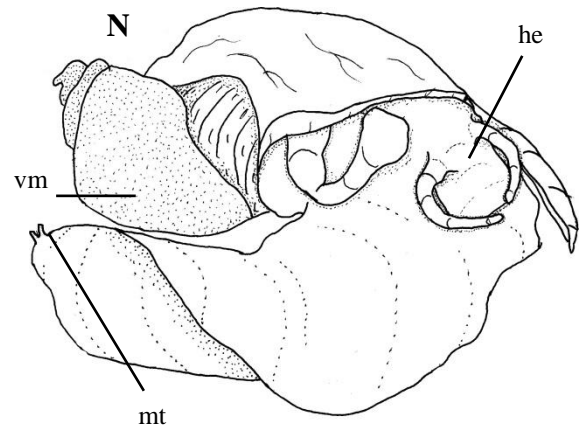
### 15. Foot, metapodial tentacles (fig. N)

(L = 2; Ci = 50; Ri = 0)

0. Absent

1. Present

Metapodial tentacles are (1) dorsal projections of the foot, and are a synapomorphy of Nassariidae. Galindo *et al.* (2016) showed that the ancestor of the Nassariidae probably had a single tentacle and the apparition of the second happened after the divergence of Dorsaninae, while the loss of one or two tentacles happened independently during evolution. *Engoniophos uncinatus*, which closely resembles a nassariid, lack any metapodial tentacles (0), as do all other fasciolariids and outgroups studied (Abbate & Simone, 2016).



N. *Bullia laevisissima* (modified from Abbate & Simone, 2016), head-foot and visceral mass in dorsal view. **he**: head; **mt**: metapodial tentacle; **vm**: visceral mass.

### 16. Operculum (fig. O)

(L = 2; Ci = 100; Ri = 100)

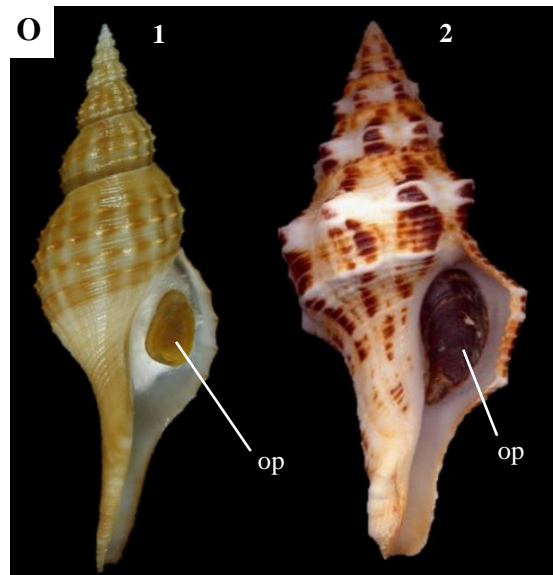
0. Absent

1. Filling entire aperture

2. Not filling entire aperture

The presence of an operculum, which seals the shell aperture, is one of the synapomorphies of Gastropoda; all gastropods possess it in the embryonic stage, but may be reduced or lost

(0) in the adult in several groups such as in *Monetaria annulus* (Ponder & Lindberg, 1997; Simone, 2011). Operculum of *Granulifusus* (clade 4) are highly differentiated; first, it does not fill the entire aperture (2), unlike all other taxa examined (1) and; secondly, has a circular



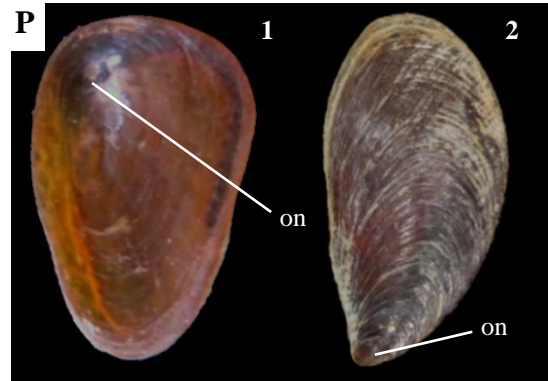
O. Shell in apertural view. **O1**. *Granulifusus kiranus*, shell with operculum that does not fill the entire aperture (2); **O2**. *Latirus polygonus*, operculum fills entire aperture (1); both taken from Femorale (<http://www.femorale.com/shellphotos> accessed vi/09/2016). **op**: operculum.

eccentric nucleus, not terminal like all other fascioliariid (more of this will be discussed in the next section). Because of the outgroup choice, the absence (0) is plesiomorphic, but in the context of Gastropoda, this is an apomorphic state.

### 17. Operculum, nucleus (fig. P)

(L = 1; Ci = 100; Ri = 100)

- 0. Terminal
- 1. Eccentric



**P.** Operculum in dorsal view. **P1.** *Granulifusus poppei* (modified from Preetha *et al.*, 2014) operculum with an eccentric nucleus (1); **P2.** *Fusinus frenguelli*, operculum with a terminal nucleus (0). **on:** operculum nucleus.

In the more basal gastropod taxa, the operculum is generally circular, and larval or very young individuals also have spiral opercula, suggesting that this is the plesiomorphic type (Simone, 2011). The genus *Granulifusus* (clade 4) has a modified operculum in which it does not fill the entire aperture (discussed earlier) and an eccentric nucleus (1), which differs from all other studied opercula with a terminal nucleus (0). Hadorn & Fraussen (2005) described several *Granulifusus* species, and all specimens analyzed have an operculum of this type, being likely that *Pseudolatirus discrepans* (which has belonged to *Granulifusus* [*e.g.*, Poppe, 2008]) also does.



**Q.** Operculum in ventral view. **Q1.** *Buccinum undatum*, round operculum (0); **Q2.** *Fusinus marmoratus*, arrow indicates the slightly curved posterior margin (1); **Q3.** *Peristernia nassatula*, arrow indicates the hook-like posterior margin (2).

### 18. Operculum, lateral margin (fig. Q)

(L = 3; Ci = 66; Ri = 96)

- 0. Round
- 1. Terminally slightly curved
- 2. Terminally hook-like

The posterior margin of the operculum of peristerniines of clade 5 possesses a hook-like extension (2) such that the muscles scar occupies circa 2/3 of the total operculum area. Fascioliariids have



a basal state in which the opercula has the lateral margin slightly curved (1), but does not form such hook-like profile; the muscle scar in this operculum type occupies a much larger area in relation to the rest of the operculum. The genera *Granulifusus* (clade 4a) with its much modified operculum that does not fit the aperture and eccentric nucleus, has a round margin (0), as do other non-fascioliariids such as *Buccinum undatum*.

### 19. Pallial cavity, extension in whorls (fig. R)

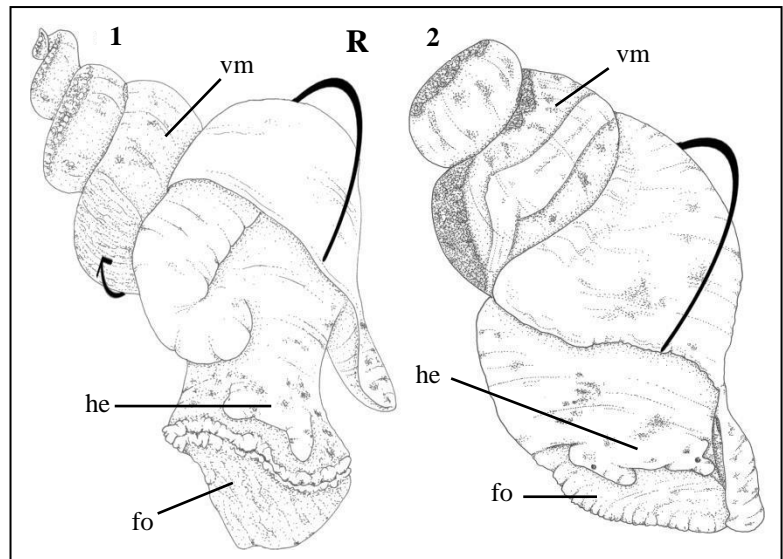
(L = 10; Ci = 10; Ri = 30)

0. Up to 3/4

1. longer than 3/4

Ponder & Lindberg (1997) observed that the range of the length of the pallial cavities were very similar among some of their studied taxa, and did not utilize this character in their study. Nevertheless, this character (the measurement of the length of the pallial cavity, from the mantle edge to the renal membrane and kidney)

showed highly homoplastic. Fascioliariidae have basally a pallial cavity of up to 3/4 whorls (0), with several modifications to a greater extent (1): on clades 1a (*Dolicholatirus* and *Teralatirus roboreus*) 8a (*Pustulatirus*), 15, *Angulofusus neda*, *Peristernia marquesana*, *Aurantilaria aurantiaca* and *Filifusus filamentosus*. An ACCTRAN optimization was used.



**R.** head-foot and visceral mass. **R1.** *Buccinum undatum* (1); **R2.** *Pisania pusio* (0). Arrows indicate the length of the pallial cavity, counted in number of spiral whorls. **fo:** foot; **he:** head; **vm:** visceral mass.

### 20. Mantle border, lobes

(L = 1; Ci = 100; Ri = 100)

0. Two

1. One



The following characters (20, 21 and 22) are synapomorphies of the Cypraeoideans, and no Neogastropoda possess them.

Cypraeoideans have two mantle lobes (left and right) covering most of outer surface of shell. This is a synapomorphy of the superfamily, being a derived character among Caenogastropods (Simone, 2004, 2011). The tendency to internalize the shell reaches its peak in the cypraeoideans, where the mantle extends to the dorsal surface of the shell, being functionally external and the shell is functionally internal, exposed only when the animal is disturbed. In a branch of the cypraeoideans, the Lamellariidae, the shell is permanently internal (Simone, 2004).

## 21. Mantle border, papillae

(L = 1; Ci = 100; Ri = 100)

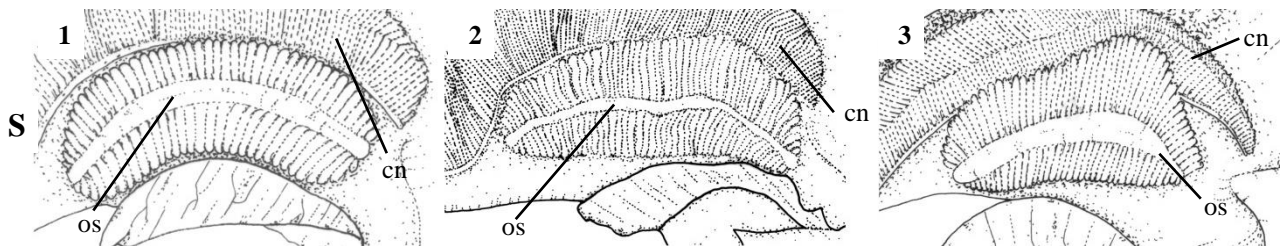
- 0. Present
- 1. Absent

Another synapomorphy of exclusive of the Cypraeoideans is the presence of papillae on the outer surface of the exposed part of mantle and siphon (Simone, 2004).

## 22. Osphradium, branches

(L = 1; Ci = 100; Ri = 100)

- 0. Three
- 1. Two



**S.** Ventral view of the roof of the pallial cavity evidencing the osphradium. **1S.** *Dolicholatirus cayohuesonicus*, symmetrical osphradium (0); **2S.** *Fusinus frenguelli*, slightly asymmetrical osphradium (1); **3S.** *Amiantofusus candoris*, heavily asymmetrical osphradium (2). **cn:** ctenidium; **os:** osphradium.

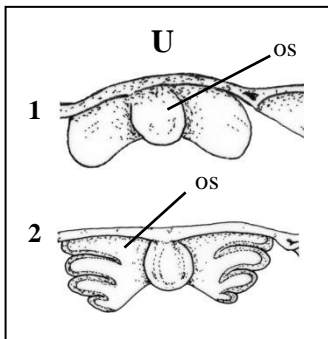
An osphradium bearing two branches is a feature of the “higher” caenogastropods, being an adaptation to increasing the surface of this sensory organ (Simone, 2004, 2011). In the case of the cypraeids, this organ has 3 branches running equidistant from each other; one branch is turned towards the anterior end, another towards the posterior end and another towards the right branch (the right branch is a new acquisition) (Simone, 2004).

### 23. Osphradium, longitudinal shape (fig. S)

(L = 6; Ci = 33; Ri = 77)

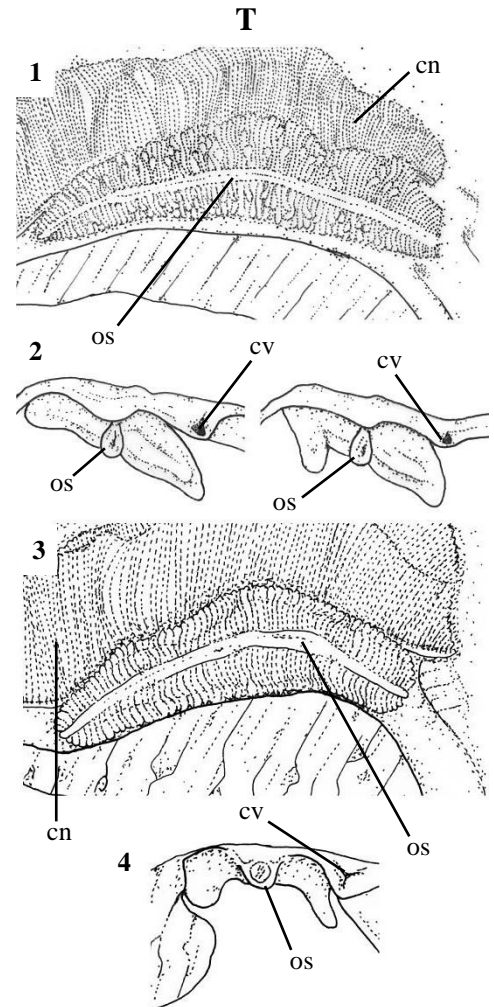
- 0. Symmetrical
- 1. Slightly asymmetrical
- 2. Heavily asymmetrical

Most fascioliariids have some form of asymmetry in the osphradium (the left leaflets smaller than the right ones) with the exception of *Dolicholatirus* and *Teralatirus roboreus*. This character corresponds to the length of the osphradium leaflet, although some variation in form between them occurs.



U. Transversal section of the roof of the pallial cavity in the osphradium region. **U1.** *Dolicholatirus cayohuesonicus*, osphradium profile rounded (0); **U2.** *Fusinus australis*, osphradium profile digitated (1). **os:** osphradium.

The basal state for the family is a symmetrical osphradium (0) and that is maintained for clade 1a. In most fascioliariids beginning in clade 2, there is a slight asymmetry (1). A heavily asymmetrical osphradium (2) occurred independently on clades 2b, 3b<sup>1</sup>, 4a, *Pseudolatirus pallidus* and *Leucozonia ocellata*.



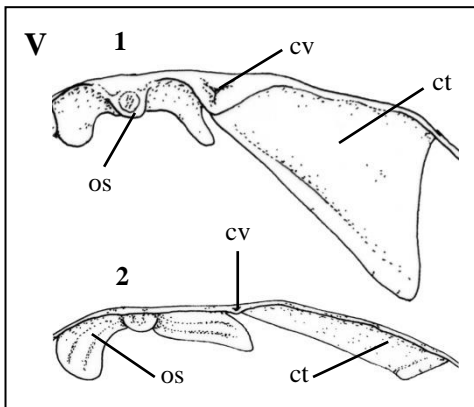
**T.** Ventral view of osphradium and transversal section of the roof of the pallial cavity, evidencing the osphradium. **T1-2.** *Aurantilaria aurantiaca*, osphradium ventral view and profile, evidencing the non-uniform disposition of the leaflets (1); **T3-4.** *Opeatostoma pseudodon*, uniform osphradium leaflets (0). **cn:** ctenidium **cv:** ctenidium vein; **os:** osphradium.

#### 24. Osphradium, leaflets, form (fig. T)

(L = 2; Ci = 50; Ri = 0)

- 0. Uniform
- 1. Non-uniform

The shape of the bi-pectinated osphradium leaflets may be the same shape, *i.e.*, in a uniform fashion (0), or they may have an asymmetry in their shape (1). Only two taxa presented this character as a homoplasy: *Aurantilaria aurantiaca* and *Australaria australasia*.



V. Transversal section of the roof of the pallial cavity in the osphradium and ctenidium region. **V1.** *Opeatostoma pseudodon*, osphradium height: height of ctenidium less than 1/2 (0); **V2.** *Granulifusus* sp. 1/2 or more (1). **cn:** ctenidium **cv,** ctenidium vein; **os:** osphradium

#### 25. Osphradium, leaflets, terminal shape (fig. U)

(L = 1; Ci = 100; Ri = 100)

- 0. Rounded or truncated
- 1. Digitated

In a few taxa, the osphradium leaflets may possess terminally a profile that is digitated, bearing three rounded lobes. This character (1) is a synapomorphy of a *Fusinus frenguelli*, *Fusinus australis* and *Cyrtulus serotinus*, clade 3d, while in all other studied taxa the leaflet is round or truncated (0).

#### 26. Osphradium, leaflets, height: height of ctenidium (fig. V)

(L = 3; Ci = 33; Ri = 66)

- 0. Less than 1/2
- 1. 1/2 or more

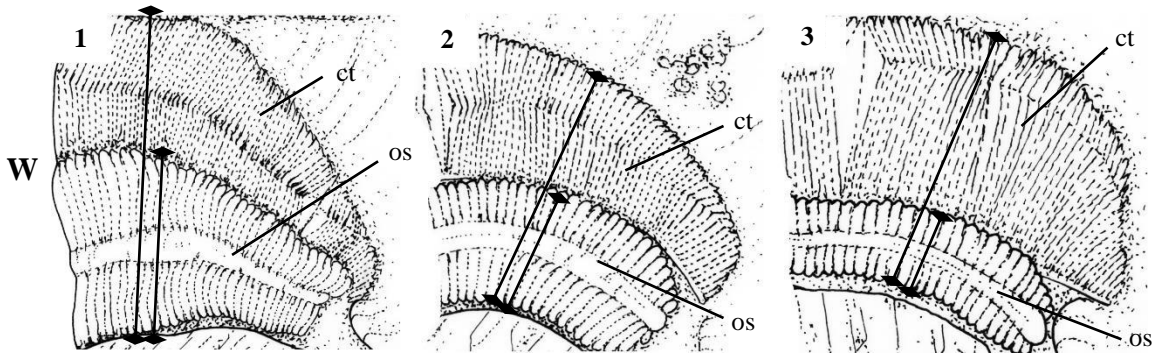
This character corresponds to the proportion between the height of the osphradium by the height of the ctenidium, *i.e.*, osphradia that are taller have the state (1), while those that are low receive a (0). There is an observable tendency that the osphradia become taller in fasciolariiids, including *Pisania pusio*, its sister group, and there is a reversion to the previous state for *Opeatostoma pseudodon*.

## 27. Ctenidium, position

(L = 1; Ci = 100; Ri = 100)

- 0. Not adjacent to osphradium
- 1. Adjacent to osphradium

The position of the ctenidium is always adjacent to the osphradium (1) in all taxa except for *Monetaria annulus*, in which the ctenidium is somewhat distanced laterally from the osphradium (0). This state of character is reported in all cypraeoidean species except lamellariids (Simone, 2004), being linked to the lateralization of the shell. This morphological phenomenon results in an encroachment of the visceral mass at the right region of the pallial cavity, including pericardium and heart, which is dislocated from the posterior part of the gill to its dorsum, and produces some changes in the inner anatomy (*e.g.*, position of the pericardium, genital system, kidney and gill and osphradium position in the pallial cavity) (Simone, 2004).



**W.** Roof of the pallial cavity in the osphradium and ctenidium region. **W1.** *Peristernia nassatula*, ctenidium by osphradium width ratio is less than 1 (0); **W2.** *Dolicholatirus* sp. ctenidium by osphradium width ratio is 1 to less than 1.5 (1); **W3.** *Buccinum undatum*, ctenidium by osphradium width ratio is 1.5 or greater (2). Lines indicate the ratio of the width, evidencing the gradual increase in Ctenidium width by osphradium width ratio. **ct:** ctenidium; **os:** osphradium.

## 28. Ctenidium, width: width of osphradium (fig. W)

(L = 10; Ci = 20; Ri = 72)

- 0. Less than 1.
- 1. 1 to less than 1.5
- 2. 1.5 or greater

This character is an increase in the ratio of the width of the ctenidium by the width of the osphradium. This highly homoplastic character received an ACCTRAN optimization, as it is likely that *Dolicholatirus* sp. will receive the same state as the others of the same group.

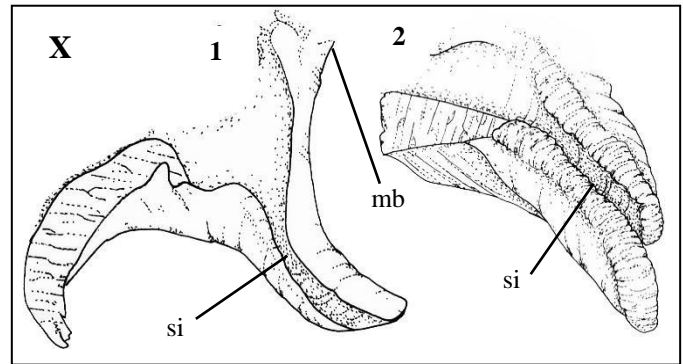
Fasciolariiids have a width of 1 to less than 1.5 of this ratio (1), but this state is only maintained for clade 3b<sup>1</sup> (*Chryseofusus*), *Pseudolatirus pallidus*, *Angulofusus nedae* and clade 2c. A ratio of less than 1 (0) is present in clade 1a, 3c, 4 and on *Pseudolatirus kuroseanus*. A proportion of 1.5 or greater (2) occurs on clade 14 and on *Filifusus filamentosus*.

### 29. Ctenidium, posterior tip position

(L = 1; Ci = 100; Ri = 100)

- 0. Away from pericardium
- 1. Adjacent to pericardium

This is yet another character that is a result of the lateralization of the shell aperture that occurs in cypraeoideans. This results in the transposition of the visceral mass to the right region of the pallial cavity, including pericardium and heart, which leads to a longer ctenidium vein running without gill filaments.



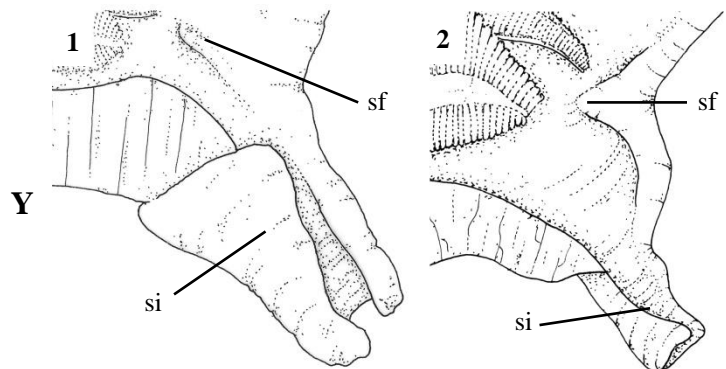
X. Siphon X1. *Granulifusus* sp. margin of the siphon smooth (0); X2. *Leucozonia cerata*, margin bearing longitudinal folds (1). mb: mantle border; si: siphon.

### 30. Siphon, margin (fig. X)

(L = 3; Ci = 33; Ri = 33)

- 0. Smooth
- 1. Bearing longitudinal folds

The presence of longitudinal folds in the margin of the siphon occurs in four taxa: as a synapomorphy of *Pseudolatirus discrepans* and



Y. Siphon. Y1. *Amiantofusus candoris*, siphon flap with a narrow base (0); Y2. *Fusinus marmoratus*, wide base (1). sf: siphon ventral fold; si: siphon.

*Granulifusus kiranus* (clade 4c), *Leucozonia ocellata* and *L. cerata* (clade 14a) and, choosing an ACCTRAN optimization, reversing in *Opeatostoma pseudodon*.

### **31. Siphon, ventral fold, shape** (fig. Y)

(L = 2; Ci = 50; Ri = 60)

- 0. Flap, narrow base
- 1. Flap, wide base

The entrance to the siphon in the pallial cavity occurs near the osphradium and ctenidium, and it bears a muscular flap that project downward. In most fasciolarids this flap has a narrow base (0), but in two groups this flap is strong and muscular with a very broad base (1): in *Chryseofusus*, clade 3b<sup>1</sup> and in *Amiantofusus*, clade 2c as a homoplasy.

### **32. Anal siphon**

(L = 1; Ci = 100; Ri = 100)

- 0. Present
- 1. Absent

Cypraeoideans present an anal siphon in the shell, and in cypraeids and ovulids this appears as a fold differentiated from the mantle border, the anal siphon, which apparently evolved similarly, but in the opposite side, to the incurrent siphon (Simone, 2004). This character occurs only in *Monetaria annulus*.

### **33. Kidney**

(L = 1; Ci = 100; Ri = 100)

- 0. Meronephridial
- 1. Pycnonephridial

Most caenogastropods possess a kidney comprised of excretory tissue with a uniform and characteristic vacuolated appearance. However, a number of taxa possess two distinct lobes of excretory tissue (pycnonephridial *sensu* Perrier [1889] and Ponder [1973]) that are microscopically and macroscopically distinct, including all neogastropods. The traditional bipartite classification of differentiated kidney types (meronephridial vs. pycnonephridial) has been used to distinguished the interdigitating lamellae of the kidney (1) for pycnonephridians to

the simple lamellae (0) for meronephridians (Strong, 2003). This character occurs only in *Monetaria annulus*.

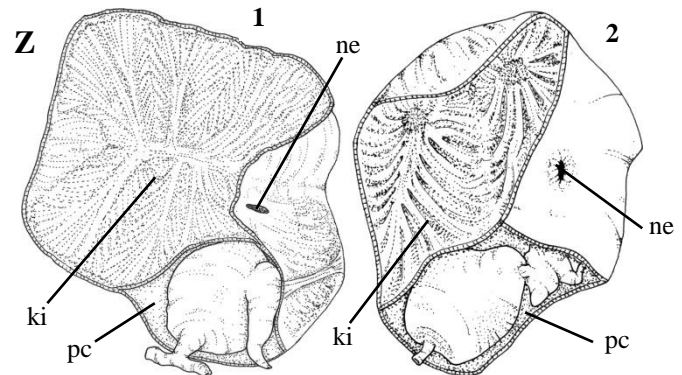
### 34. Renal aperture, lipped margin (fig. Z)

(L = 5; Ci = 20; Ri = 75)

0. Absent

1. Present

The renal aperture, or nephrostome, is situated in the posterior region of the pallial cavity, as an access from the kidney. In Fasciolariidae it occurs as a mere slit (0) or as a slit emarginated by a lipped rim. A DELTRAN optimization was chosen, because there was no data on



**Z.** Kidney and pericardium. **1Z.** *Polygona angulata*, simple renal aperture (0); **2Z.** *Granulifusus* sp. renal aperture bearing a lipped rim (1). **ki:** kidney; **ne:** nephrostome; **pc:** pericardium.

this character for the clade of *Angulofusus nedae*, *Pseudolatirus kuroseanus* and *Amiantofusus*. In Fasciolariidae, the basal state 0 is maintained for clade 1a and 2a, while it attained state 1 beginning on clade 3. Clade 3c<sup>1</sup> and 9 reverted to state 0 (with another reversion in *Latirus pictus* and *Opeatostoma pseudodon*).

### 35. Nephridial gland

(L = 4; Ci = 25; Ri = 57)

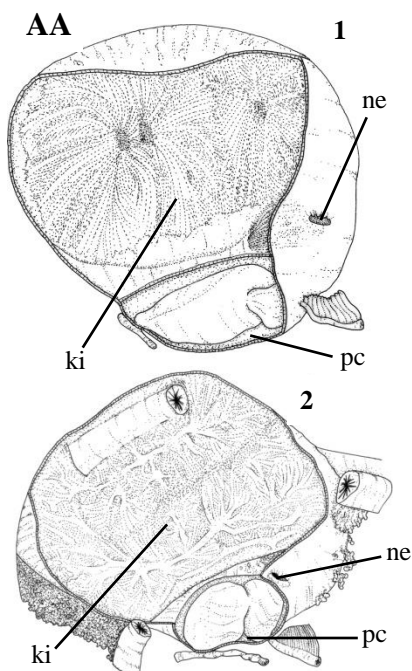
0. Absent

1. Present

The nephridial gland is a mass of glandular tissue immersed between the kidney and pericardium, lined with ciliated cells and penetrated by haemocoelic spaces (Fretter & Graham, 1962). Saccular invaginations of the gland surface bring hemolymph and urine into close contact; hemolymph flows into the haemocoelic spaces of the gland from the renal lamellae, is collected into the efferent nephridial vein, and subsequently flows to the auricle of the heart (Fretter & Graham, 1962; Strong, 2003).



Nephridial gland histology is remarkably uniform across the caenogastropods (Strong, 2003), and is one of the synapomorphies of the predominantly marine taxa except for Cerithioideae and Eulimidae; although it disappeared in some taxa (*e.g.*, xenophorids) (Simone, 2011). In fasciolariiids, the gland is absent in clade 10 of *Latirus polygonus*, *L. pictus* and *Leucozonia* (subsequently reverted in *Leucozonia cerata* and *Opeatostoma pseudodon*), although in order to truly confirm the presence or absence of this structure, a histological study is required. A DELTRAN optimization was chosen



AA. Kidney and pericardium. 1AA. *Pustulatirus ogum*, renal aperture situated centrally in the membrane (0); AA2. *Aurantilaria aurantiaca*, renal aperture situated close to pericardium (1). **ki**: kidney; **ne**: nephrostome; **pc**: pericardium.

### 36. Renal aperture, position in membrane (fig. AA)

(L = 2; Ci = 50; Ri = 75)

- 0. Centrally
- 1. Close to pericardium

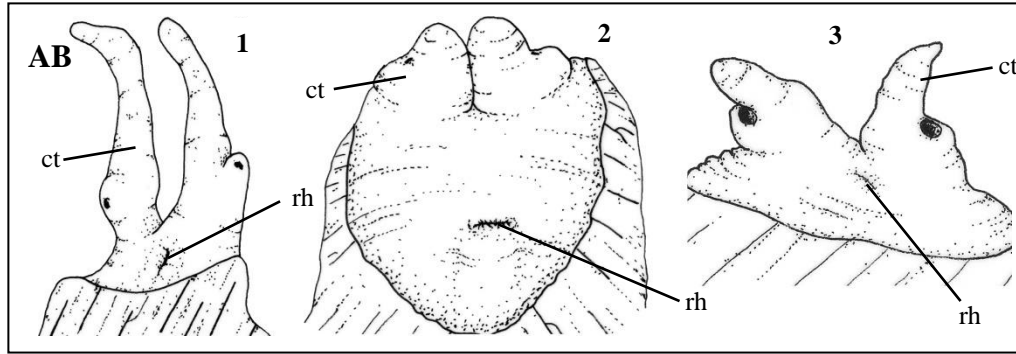
The renal aperture may occur centrally in the membrane separating pericardium and kidney (0) or dislocated closer to pericardium (1). This is a synapomorphy of Fasciolarinae (clade 6c), and a homoplastic autapomorphy for *Opeatostoma pseudodon*. DELTRAN was chosen because of the missing data of *Latirus vischii*.

### 37. Rhynchostome, distance from cephalic tentacles (fig. AB)

(L = 2; Ci = 50; Ri = 0)

- 0. Close to base
- 1. Distanced from base

The rhynchostome is the outer opening of the introverted proboscis, being only visible when the proboscis is in a contracted state. In fasciolariiids this structure is located ventrally close to the cephalic tentacles (0), except for *Leucozonia ocellata* and *L. cerata* (clade 14a), which is located distant from the cephalic tentacle (1). ACCTTRAN was chosen as an optimization, meaning in *Opeatostoma pseudodon* there was a reversion.

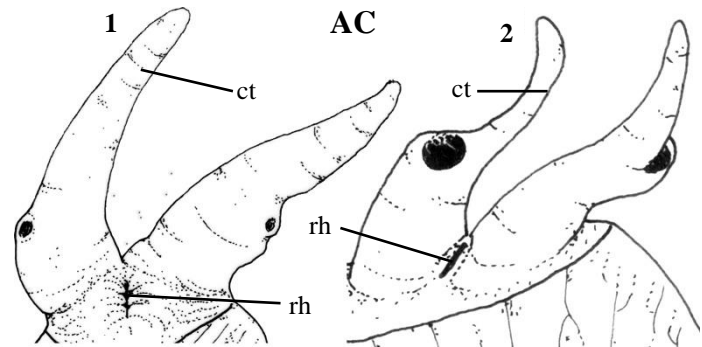


**AB.** Head in ventral view. **AB1.** *Granulifusus kiranus*, rhynchostome located close to the base of cephalic tentacles (char. 38: 0) as a longitudinal slit (char. 39: 1); **AB2.** *Leucozonia cerata*, located distanced from the base of cephalic tentacles (char. 38: 1) as a transverse slit (char. 39: 0); **AB3.** *Hemipolygona beckyae*, located close to the base of cephalic tentacles (char. 38: 0) as an oblique slit (char. 39: 2). **ct:** cephalic tentacle; **rh:** rhynchostome.

### 38. Rhynchostome, position (fig. AB)

(L = 9; Ci = 22; Ri = 66)

- 0. Transverse
- 1. Longitudinal
- 2. Oblique



The position of the rhynchostome is an important character; it may be a slit transverse to the body axis (0), longitudinal (1) or oblique (2). For fascioliariids, the basal state is a

**AC.** Head in ventral view. **1AC.** *Granulifusus* sp. rhynchostome bearing longitudinal folds (char. 40: 1) and a lipped rim (char.41: 1); **2AC.** *Dolicholatirus cayohuesonicus*, rhynchostome without longitudinal folds (char. 40: 0) and a simple margin (char. 41:0). **ct:** cephalic tentacle; **rh:** rhynchostome.

longitudinal slit which occurs in most fusinines, *Dolicholatirus* and *Teralatirus roboreus*, and in *Nodolatirus nodatus*. In most peristerniines (clade 7) and fascioliariines (clade 6b), the slit is transverse, with reversions occurring independently in *Pustulatirus ogum* and *Polygona infundibulum*. In *Hemipolygona beckyae* the slit is oblique (2), it is an autapomorphy. The optimization chosen was DELTRAN.

### 39. Rhynchostome, longitudinal folds in margin (fig. AC)

(L = 6; Ci = 16; Ri = 70)

- 0. Absent
- 1. Present

The rhynchostome in fascioliariids sometimes bear, internally and protruding externally, longitudinal folds or ridges. Basally, fascioliariids lack these folds (0), but it appeared (1) in *Amiantofusus pacificus* and clade 3 and reverted to the absence of the folds (0) in *Chryseofusus archeruisus* and in clade 14 of *Leucozonia* and *Opeatostoma pseudodon*. An ACCTRAN optimization was chosen.

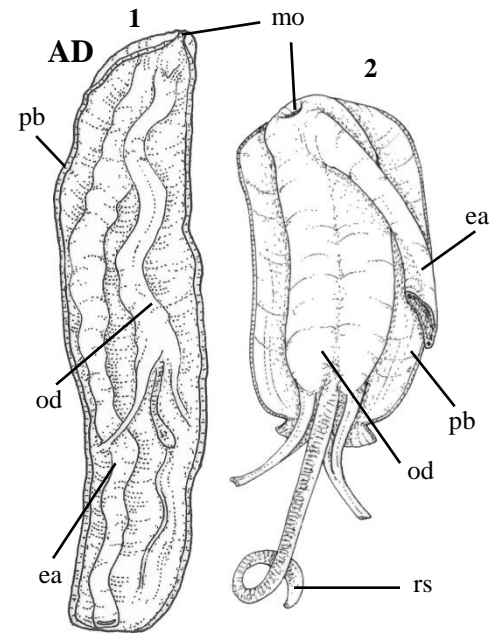
#### 40. Rhynchostome, lipped rim (fig. AC)

(L = 7; Ci = 14; Ri = 72)

0. Absent

1. Present

The presence of a lipped rim is independent of the presence/absence of longitudinal folds (character 39), and is highly homoplastic. The absence of a lip (0) is the plesiomorphic state, while the presence (1) occurred several times independently: In *Fusinus* and *Cyrtulus serotinus* (clade 3c), clade 4 and 14; it reverted back to the plesiomorphic state in *Peristernia nassatula*, *Latirus vischii* and in clade 8.



**AD.** Proboscis opened laterally. **AD1.** *Polygona angulata*. radular sac contained within proboscis (1); **AD2.** *Thais speciosa*, radular sac extending beyond proboscis (0). **ea:** anterior esophagus; **mo:** mouth opening; **od:** odontophore tube; **pb:** proboscis; **rs:** radular sac.

#### 41. Odontophore, radular sac (fig. AD)

(L = 1; Ci = 100; Ri = 100)

0. Extending beyond proboscis

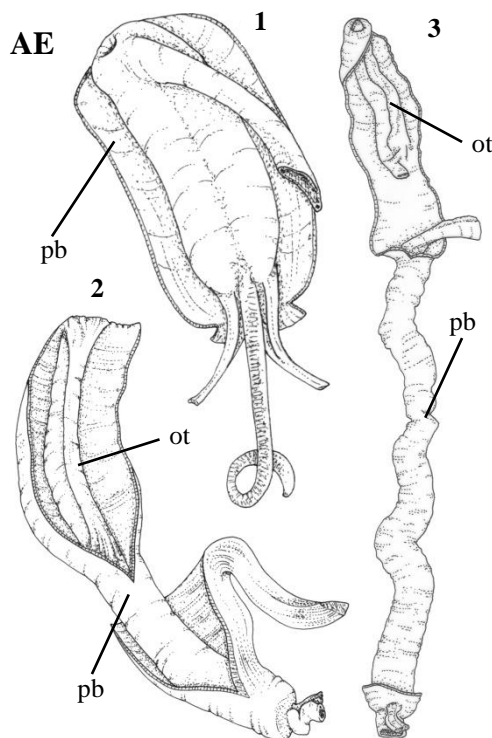
1. Contained within proboscis

The foregut anatomy is rather uniform in all buccinoideans, and is characterized by a long proboscis, large paired or fused salivary glands, usually a well-developed valve and gland of Leiblein, and by the absence of accessory salivary glands (Fraussen *et al.*, 2007). This occurs for all Neogastropoda with the exception of Conoidea (Simone, 2011). The features of the anterior digestive system will be discussed throughout the following characters (characters 41 to 71).

The odontophore is the organ that produces and moves the radula, and is thought to be homologous among gastropods (the possibility of non-homology between the cartilages of the heterobranchs and other gastropods has been raised by several authors, *e.g.*, Golding *et al.*, [2009]) (Simone, 2011). The odontophore characters show great importance of the structure in comparative studies, being utilized up to species-level (Simone, 2004; 2007; Simone *et al.*, 2011; Couto & Pimenta, 2012; Couto *et al.*, 2015; 2016). Although detailed studies on the odontophore are surprisingly scarce in the literature, it shows surprising variation for phylogenetic analysis, and characters related to this structure will be discussed in the next five characters.

The radular sac in which the radular nucleus is located (where the teeth of the radula is formed), is situated posteriorly, storing the teeth that may migrate to the buccal cavity while the teeth have been spent or lost. The radular portion inside the radular sac is coiled and its teeth are

positioned inwards (Simone, 2011). The length of the radular sac may be correlated to feeding patterns although Ponder & Lindberg (1997) could not find any correlations in their studied taxa; these same authors utilized the coiling of the radular sac as a synapomorphy for Sorbeoconcha. In buccinoids including fascioliariids, the radular sac is confined within the proboscis, *i.e.*, it does not extend to the haemocoel (1); however, the outgroup taxa *Monetaria annulus* (Cypraeoidea) and *Thais speciosa* (Muricoidea) the radular sac projects posteriorly into the haemocoel (0).



**AE.** Proboscis opened laterally **AE1.** *Thais speciosa*, odontophore by proboscis lengths is one (0); **AE2.** *Granulifusus* sp., ratio is between one to 1/2 (1); **AE3.** *Fusinus brasiliensis*, ratios is less than 1/2 (2). **ot:** oral tube; **pb,** proboscis.

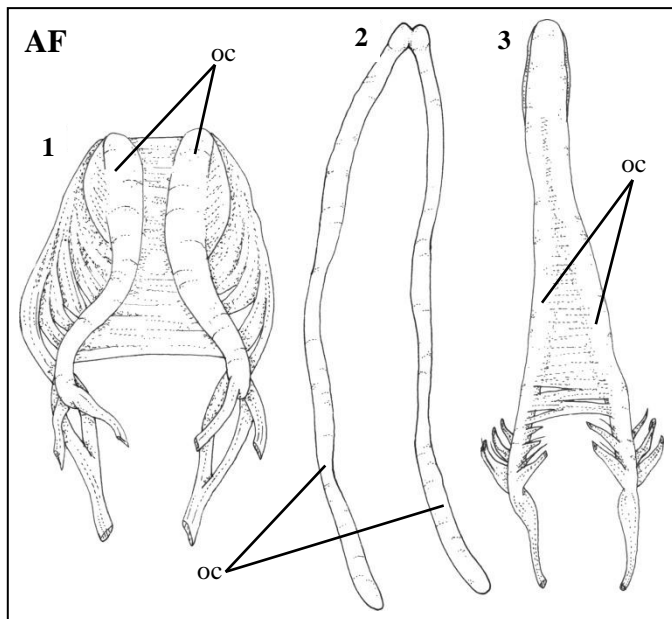
#### 42. Odontophore, length: proboscis length (fig. AE)

(L = 9; Ci = 22; Ri = 72)

- 0. One
- 1. Between 1 and 1/2
- 2. 1/2 or less

This character corresponds to the relation between the lengths of the odontophore by the proboscis. Fasciolariids have this ratio between one and 1/2 of the length (0), and that is the synapomorphic state for the family, although a few modifications in this ratio occurred.

On clades 2c of *Amiantofusus*, 6c of the traditional fasciolariines and 14 of *Leucozonia* (although it returned to the previous state in *Opeatostoma pseudodon*), the odontophore shortened in relation to the proboscis obtaining a ratio of 1 (0), as some species in the outgroup (e.g., *Pisania pusio*, *Bullia laevissima*). The opposite happened on clade 3a, whose related taxa *Fusinus*, *Chryseofusus*, *Cyrtulus serotinus* and *Pseudolatirus pallidus* all possess an extremely long proboscis in relation to the odontophore (2). This relates to character 66, the coiling of the proboscis within its sheath; however, this will be discussed later. Because of the hypothesized quantitative nature of this character, an additive parsimony model was chosen (0–1–2), with a DELTRAN optimization.



**AF.** Ventral view of odontophore cartilages and associated muscles **AF1.** *Thais speciosa*, cylindrical odontophore cartilages (char. 44: 0) not fused (char. 45: 0); **AF2.** *Chryseofusus archeruisius*, concave odontophore cartilages (char. 44: 1), muscles removed, and fused less than 15% (char. 45: 1); **AF3.** *Fusinus brasiliensis*, cylindrical cartilages (char. 44: 0) and fused more than 15% (char. 45: 2). **oc:** odontophore cartilage.

#### **43. Odontophore cartilages shape (fig. AF)**

(L = 1; Ci = 100; Ri = 100)

- 0. Cylindrical
- 1. Concave

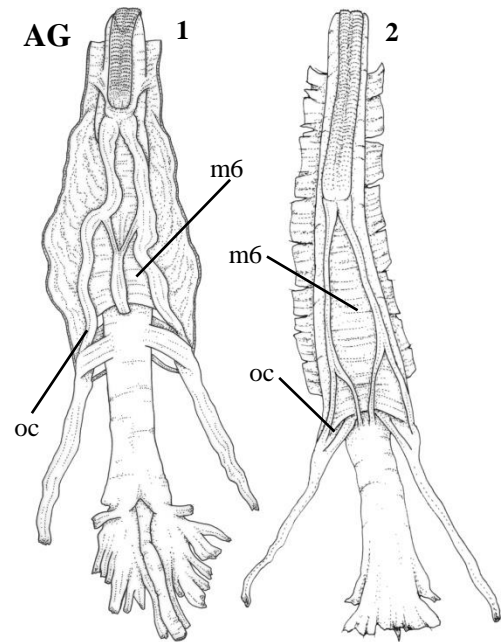
Only the outgroup species *Monetaria annulus* and *Thais speciosa* possess cylindrical odontophore cartilages (0). Concave cartilages (1) correspond to buccinoideans in the analysis, and all species of the superfamily have a similar odontophore (e.g., Simone. 2011; Couto & Pimenta, 2012; Couto *et al.*, 2015; Simone *et al.*, 2013; Abbate & Simone, 2015).

#### 44. Odontophore cartilages, anterior fusion (fig. AF)

(L = 8; Ci = 25; Ri = 71)

- 0. Not fused
- 1. Fused 15% or less
- 2. Fused greater than 15%

Another notable modification in the odontophore is the fusion of the cartilages in the anterior region of some Buccinoidea (e.g., Buccinidae, Nassaridae, Columbellidae) (e.g., Simone Couto *et al.*, 2012; 2015; Simone *et al.*, 2013; Abbate & Simone, 2015). Strong (2003) observed that caenogastropods may possess several degrees of fusion in the odontophore. Members of Fascioliidae exhibit odontophore cartilages that are fused, like most buccinoideans and unlike the cypraeoidean (*Monetaria annulus*) and muricoidean (*Thais speciosa*) which have two separate cartilages, unfused (0). *Teralatirus roboreus*, and likely the genus *Dolicholatirus*, (clade 1a) have odontophore cartilages fused in more than 15% (2), much like most buccinoideans analyzed. Species in clade 2 possess a fusion of less than 15% (1), except for those clades that reverted to the previous state, *i.e.*, clade 3c and 8 (*Latirus polygonus* and *Leucozonia cerata* acquired independently a greater percentage of fusion). Due to the quantitative nature of this character, an additive parsimony model was chosen (0–1–2).



**AG.** Odontophore in ventral view **AG1.** *Pustulatirus ogum*, free portion of m6 more than 1/6 of cartilage length (0); **AG2.** *Fusinus* sp. 1/6 or less (1); **m6:** horizontal muscle; **oc:** odontophore cartilage.

#### 45. Odontophore, m6, posterior free portion: odontophore length (fig. AG)

(L = 8; Ci = 12; Ri = 65)

- 0. More than 1/6
- 1. 1/6 or less

The horizontal muscle (m6) is the easiest to compare among the taxa because of its peculiar situation (Simone, 2011), as it is single muscle bearing transverse fibers connecting the left and right odontophore cartilages. Neogastropods have this muscle very thin, as also observed by Simone (2011), being inserted anteriorly on the opposite cartilage; posteriorly, the cartilages have a portion that is not connected by m6. The length of this portion is more than of the ratio between the odontophore length (0) in fasciolarids, with several independent reversions to the previous state (1/6 or less) (1) in clades 3b, 5a, 14a, *Granulifusus hayashi* and *Fasciolaria tulipa*.

#### 46. Odontophore cartilages, m11

(L = 1; Ci = 100; Ri = 100)

- 0. Origin in haemocoel
- 1. Origin odontophore cartilage

Traditionally, the pair of ventral tensor muscles (m11) insert internally in the subradular membrane; runs posteriorly along the subradular membrane connected to it, and progress out to the haemocoelic cavity, one on each side of the radular sac (Simone, 2011). According to Simone (2011), this muscle is somewhat modified in the Neogastropoda (excluding Conoidea), that apparently reverted to the sliding movement, which is also corroborated by the loss of the thickness of the subradular cartilages in this taxon (Golding *et al.*, 2009).

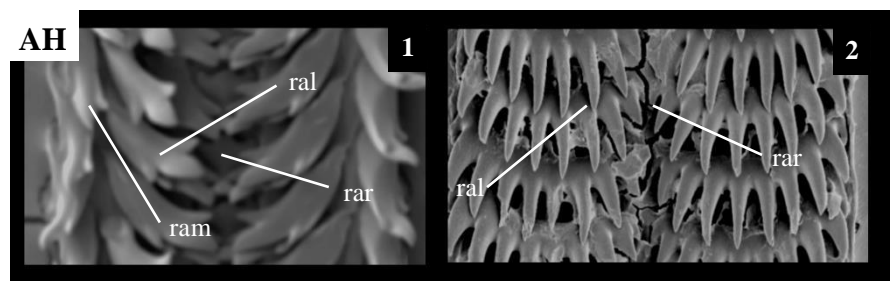
The haemocoelic origin of m11 (0) is only present in the cypraeoidean *Monetaria annulus*, while all other taxa its origin is ventrally and posteriorly in the odontophore cartilages (1).

#### 47. Radula, marginal tooth (fig. AH)

(L = 1; Ci = 100; Ri = 100)

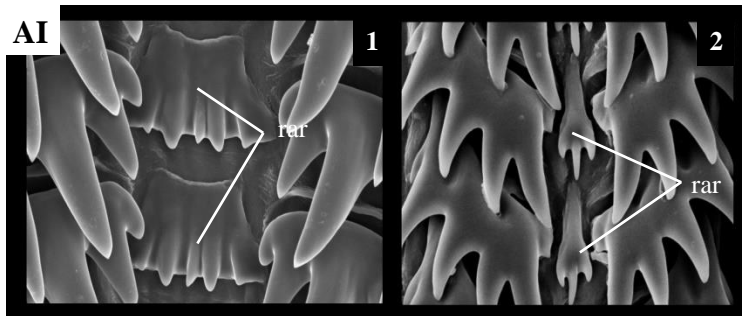
- 0. Present
- 1. Absent

Next to the shell, the radula is the most accessible character complex in gastropods, being used

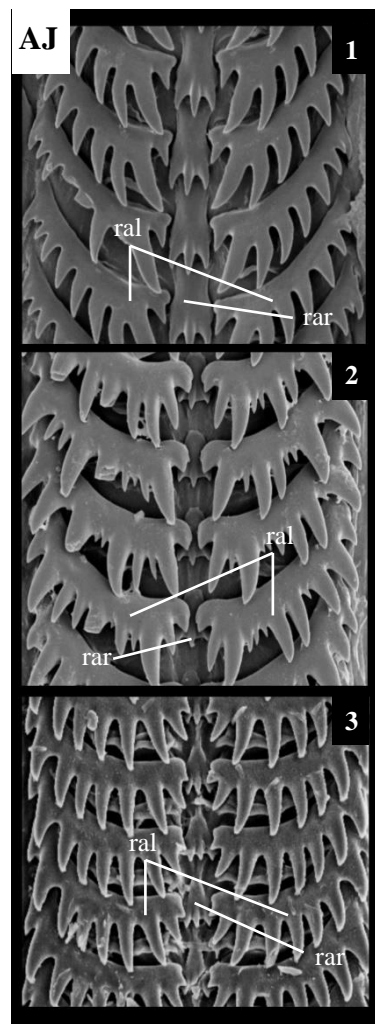


**AH.** Radula. **HA1.** *Monetaria annulus* (modified from Simone, 2004), marginal teeth present (0); **AH2.** *Fusinus australis*, no marginal teeth (1). **ral**: radula lateral; **ram**: radula marginal; **rar**: radula rachidian.





**AI.** Radula, detail of rachidian. **AI1.** *Fusinus frenguelli*, rachidian square to trapezoidal (char 49: 0) with terminal cusps (char: 50: 0); **AI2.** *Pseudolatirus kuroseanus*, rachidian triangular (char. 49: 1) bearing sub-terminal cusps (char. 50: 1). **rar:** radula rachidian.



**AJ.** Radula. **AJ1.** *Latirus pictus*, ratio of the width of the base by the width of the edge of rachidian is one (0); **AJ2.** *Fusolatirus bruijnii*, ratio is less than 1 and more than 1/2 (1); **AJ3.** *Cyrtulus serotinus*, ratio is 1/2 or less (2). **ral:** radula lateral; **rar:** radula rachidian.

diversely for taxonomical and cladistic studies; in fact, classical studies (e.g., Gray, 1854; Thiele, 1929) has produced many classification such as Rachiglossa, Toxoglossa, Taeniglossa, etc. that are based on radulae. This structure has shown to be a reliable source of phylogenetic information, and

the next 17 characters are all radular characters. Although homology problems arise when comparing distantly related species, it is usually not the case for closely related taxa (Ponder & Lindberg, 1997; Strong, 2003), such in the case of fasciolaridiids presented here.

Neogastropods presumably have a radula of the rachiglossate type, which is assumed to have arisen from a taenioglossate ancestral type (Ponder & Lindberg, 1997). The rachiglossate radula has three teeth per row (a central or rachidian, flanked by laterals), and a lack of marginal teeth. *Monetaria annulus* is the only species in which marginal teeth are present (0), while other taxa, all neogastropods, lack them (1).

#### 48. Radula, rachidian, shape (fig. AI)

(L = 2; Ci = 50; Ri = 75)

- 0. Square to trapezoidal
- 1. Triangular

The rachidian in fasciolaridiids is square or trapezoidal shaped (0), being the plesiomorphic state present in all outgroup species. Certain groups modified this basic scheme to a very thin and triangular shaped rachidian (1): in clade 2a (*Amiantofusus*, *Pseudolatirus kuroseanus*, *Angulofusus nedae*) and *Peristernia marquesana*. This has a direct correlation to character 49, discussed next.

#### 49. Radula, rachidian, lateral edge (fig. AI)

(L = 1; Ci = 100; Ri = 100)

- 0. Terminal
- 1. Subterminal

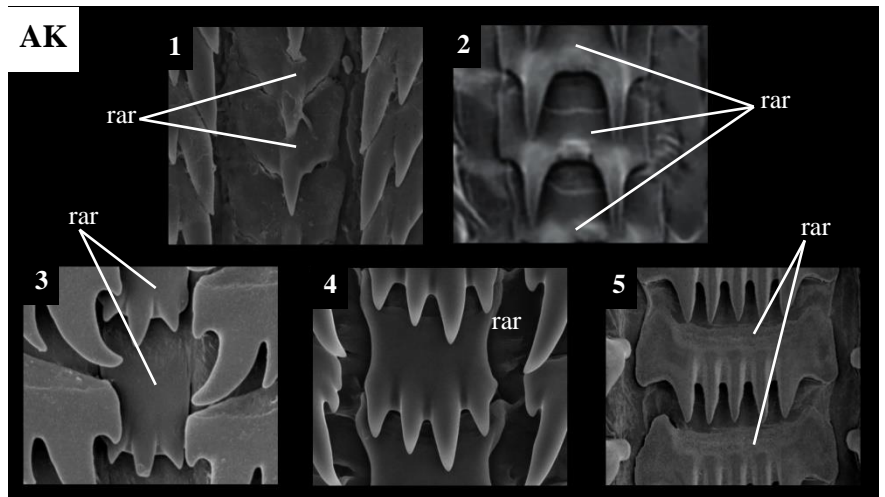
Cusps in the rachidian are present terminally, i.e., they originate in the terminal edge of the tooth and project forward (0), and this is the plesiomorphic state. For clade 2a, the lateral cusps originate somewhat in the lateral edge of the tooth (1), in a way that the lateral base is not visible.

#### 50. Radula, rachidian, base width: edge width (fig. AJ)

(L = 9; Ci = 22; Ri = 75)

- 0. One
- 1. Less than 1 and more than 1/2
- 2. 1/2 or less

This character measures the ratio of the width of the base by the width of the cusped edge, i.e., square or rectangular-like rachidians have a ratio of one (0). This is the case for most outgroups and for clade 1a of *Dolicholatirus* and *Teralatirus roboreus*; in clade 2, however, the rachidian became more or less trapezoidal in shape, with a ratio of less than one and more than 1/2 (1). Clade 5b and 3a saw the occurrence of a ratio of 1/2 or less (i.e., very thin rachidian base), with a posterior reversion in *Fusinus* sp. and *Fusinus frenguelli*.



**AK1.** Radula detail of rachidian. **AK1.** *Latirus* sp. rachidian tooth, one cusp (0); **AK2.** *Pugilina tupiniquim*, (modified from Abbate & Simone, 2015) two cusps (1); **AK3.** *Nodolatirus nodatus*, three cusps (2); **AK4.** *Pustulatirus ogum*, four cusps (3); **AK5.** *Buccinum undatum*, five or more cusps (4). **rar:** radula rachidian.

Beyond the peristerniine clade 6 there was a reversion to state 0, which also occurred in *Granulifusus hayashi*; The fasciolarines *Aurantilaria aurantiaca* and *Fasciolaria tulipa* reverted to a lesser ratio (state 1) independently. *Opeatostoma pseudodon* has a very variable rachidian; hence the states in this taxon were coded 1, 2 and 3.

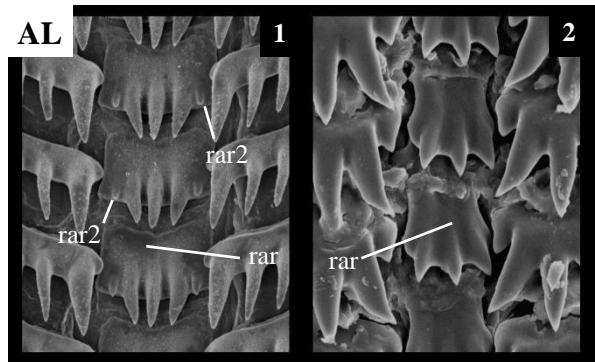
Due to the quantitative nature of this character, an additive parsimony model was used (0–1–2), and a DELTRAN optimization.

### 51. Radula, rachidian, number of principal cusps (fig. AK)

(L = 11; Ci = 36; Ri = 50)

- 0. One
- 1. Two
- 2. Three
- 3. Four
- 4. Five or more

Typically, the rachidian tooth bears three primary cusps, and some taxa may have secondary ones. This pattern of three cusps (2) is the plesiomorphic state, and it remains more or less constant within fasciolariid, with a few modifications. *Dolicholatirus* and *Teralatirus roboreus* (clade 1a) have reduced this number to only one principal cusp (0). Only the outgroup species *Pugilina tupiniquim* has 2 cusps (1), while other outgroup species corresponding to nassariids and buccinids (e.g., *Nassarius reticulatus*, *Buccinum undatum*) have increased the cusp number to five or more (4). In one specimen of *Opeatostoma pseudodon*, there are over ten cusps, while in another it bears five; this may be the case of an anomaly, but in either way, it is coded for state 4. An increase to four cusps (3) occurs in clade 8a (genus *Pustulatirus*) and in *Peristernia nassatula*. An additive parsimony model was used in this case (0–1–2–3–4), with each increase or decrease in cusp number counting as one step.



**AL.** Radula, detail of rachidian. **AL1.** *Aurantilaria aurantiaca*, rachidian tooth, secondary cusps present (1); **AL2.** *Pustulatirus pallidus*, no secondary cusps (1). **rar:** radula rachidian; **rar2,** radula rachidian secondary cusp.

**52. Radula, rachidian, secondary cusps** (fig. AL)

(L = 7; Ci = 14; Ri = 14)

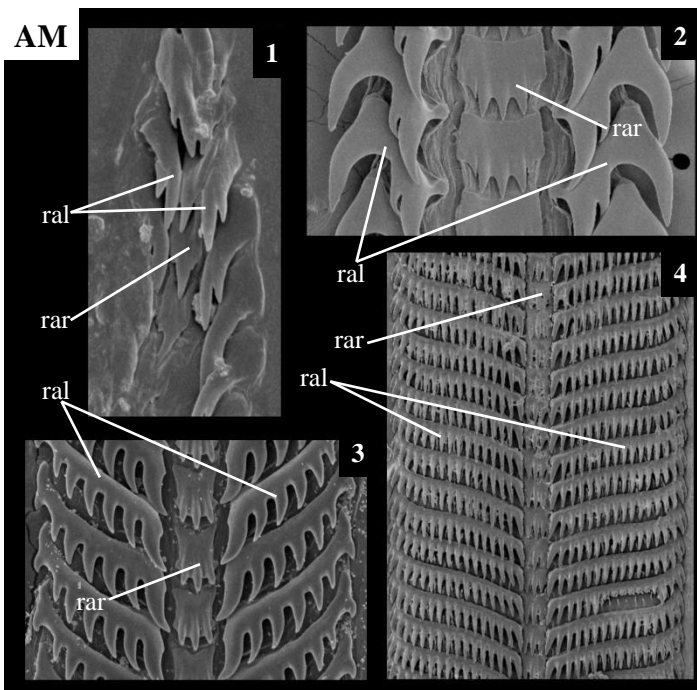
0. Absent

1. Present

This highly homoplastic character explains the minute cusps some fasciolarids and other outgroup species possess. The absence (0) is plesiomorphic in the family, while the occurrence (1) originated independently as autapomorphies in four species: *Fusinus frenguelli*, *Aurantilaria aurantiaca*, *Filifusus filamentosus* and *Polygona infundibulum*. Because of the highly independent origins of the secondary cusps, a DELTRAN optimization was chosen, as independent origins for *Pisania pusio* and clade 1a

**53. Radula, rachidian, width: lateral width** (fig. AM)

(L = 9; Ci = 33; Ri = 78)



**AM.** Radula. **AM1.** *Dolicholatirus cayohuesonicus*, ratio of the width of the rachidian by the lateral tooth is one or more (0); **AM2.** *Pisania pusio*, ratio is 1/2 to less than 1 (1); **AM3.** *Leucozonia nassa*, ratio is 1/4 to less than 1/2 (2); **AM4.** *Latirus vischii*, ratio is less than 1/4 (3). **ral:** radula lateral; **rar:** radula rachidian.

0. One or more

1. 1/2 to less than 1

2. 1/4 to less than 1/2

3. Less than 1/4

The ratio of the width of the rachidian by the lateral is expressed in this character. The plesiomorphic state for, which is retained for *Dolicholatirus* and for *Teralatirus roboreus* (clade 1a), is the rachidian tooth as wide, or wider, than the laterals, with a ratio of rachidian by lateral width equal to one or more (0). This is the overall plesiomorphic radular type for neogastropods; however, beyond clade 2, (*i.e.*, all fasciolarids except clade 1a), there was significant increase in lateral

width, also expressed by the number of lateral cusps, leading to a smaller ratio of 1/4 to less than 1/2 (2).

Bandel (1984) also noted the smaller rachidian by lateral proportion, and argued that *Dolicholatirus* should not belong in Fasciolariidae, but should be placed in Buccinidae instead. Fraussen *et al.* (2007) characterized the radula of fasciolariids in the context of Buccinoidea, as having wider than longer laterals and a very small rachidian, also excluding *Dolicholatirus* from this diagnosis.

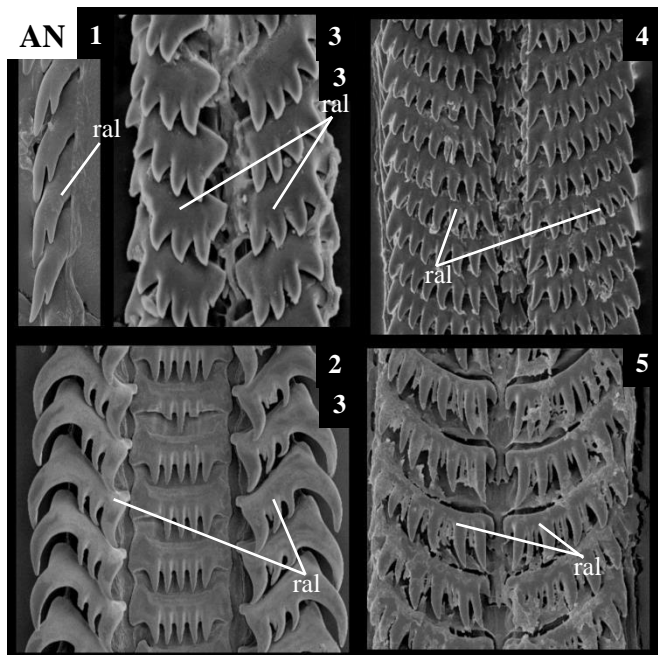
There is a general tendency for the ratio of the rachidian by lateral width to decrease even more. A ratio of less than 1/4 (3) occurs several times in fasciolariids: clade 2a, 6b, *Peristernia marquesana*, *Latirus polygonus* and *L. pictus*. Although this proportion is more or less the same in these clades, the cause for this is likely not; species of clade 2a, and *Peristernia marquesana*, have a very minute rachidian, leading to a much smaller ratio. On the other hand, other taxa which have this proportion have increased the number of cusps in the lateral and consequently its width; that is especially true for fasciolariines.

*Opeatostoma pseudodon* received an ambiguous state due to the variation in rachidian shape, as already mentioned, and it received state 1 (ratio of 1/2 to less than one) and 2 (ratio of 1/4 to less than 1/2; this state was only received for outgroup taxa *Pugilina tupiniquim* and *Pisania pusio*). The optimization was DELTRAN, utilizing an additive parsimony model.

#### 54. Radula, lateral, position (fig. AN)

(L = 2; Ci = 50; Ri = 83)

- 0. Close to rachidian
- 1. Distanced from rachidian



AN. Radula. AN1. *Dolicholatirus cayohuesonicus*, lateral teeth close to rachidian (char. 55: 0), ratio of the lateral length by it width is more than 1 (char. 56: 0); AN2. *Buccinum undatum*, laterals distanced from rachidian (char. 55: 1), ratio is one (char. 56: 1); AN3. *Amiantofusus candoridis*, lateral close to rachidian (char. 55: 0), ratio is less than 1 to more than 1/2 (char. 56: 2); AN4. *Chryseofusus graciliformis*, lateral close to rachidian (char. 55: 0), ratio is 1/2 to 1/3 (char. 56: 3); AN5. *Peristernia marquesana*, lateral close to rachidian (char. 55: 0), ratio is less than 1/3 (char. 56: 4). **ral**: radula lateral.

In the non-fasciolariid buccinoideans, the lateral teeth are somewhat distanced from the rachidian (1), while fasciolariids have them closely set (0).

**55. Radula, lateral, length: width** (fig. AN)

(L = 8; Ci = 50; Ri = 89)

- 0. More than 1
- 1. One
- 2. Less than 1 to more than 1/2
- 3. 1/2 to 1/3
- 4. Less than 1/3

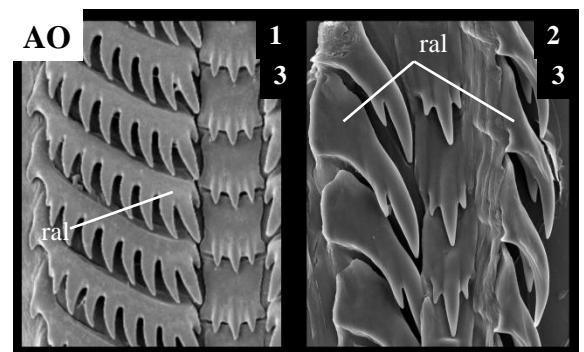
The proportion of the lateral length by its width corresponds to this character, and hypothesized with an additive parsimony model. As with the previous character 54, there is a tendency for this ratio to decrease in fasciolariids, however, the present character does not take into consideration the rachidian width (and this may have contributed to same character states in very distinct groups for character 54).

Fasciolariidae (clade 1) have a ratio of lateral length by width of one (1), but this is only retained for *Dolicholatirus* sp.; clade 1b reversed to a ratio of more than one (0) (*i.e.*, laterals longer than wider). Clade 2's lateral length by width ratio dropped to less than 1 to more than 1/2 (2) and this was preserved for clade 2a; an even greater decrease to 1/2 to 1/3 in the lateral length by width proportion (3) occurred on clade 3. Finally the decrease in the length by width ratio of the lateral tooth to less than 1/3 (4) occurred four times independently: clades 5b (*Peristernia*), 6a, 8a (*Pustulatirus*) and in *Latirus polygonus*.

**56. Radula, lateral, cusps** (fig. AO)

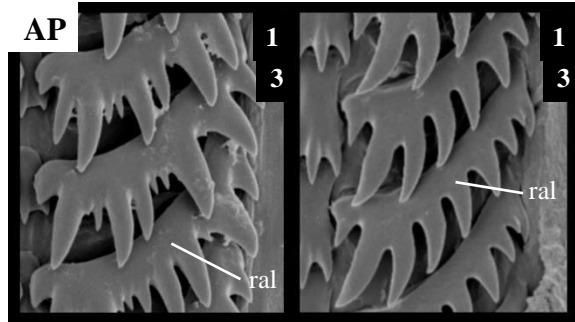
(L = 1; Ci = 100; Ri = 100)

- 0. Curved inward
- 1. Curved outward



AO. Radula. AO1. *Hemipolygona armata*, lateral cusps curved inward (0); AO2. *Dolicholatirus cayohuesonicus*, cusps curved outward (1). ral: radula lateral.

The cusps in the lateral tooth may be curved inward, facing the rachidian tooth (0) or outward (1), facing the lateral extremities. This is a synapomorphy to clade 1a of *Dolicholatirus* and *Teralatirus roboreus*.



AP. Radula, detail of lateral. AP1. *Fusolatirus bruijnii*, non-uniform lateral cusps (1); AP2. *Latirus pictus*, uniform (0). ral: radula lateral.

### 57. Radula, lateral, cusps, variability (fig. AP)

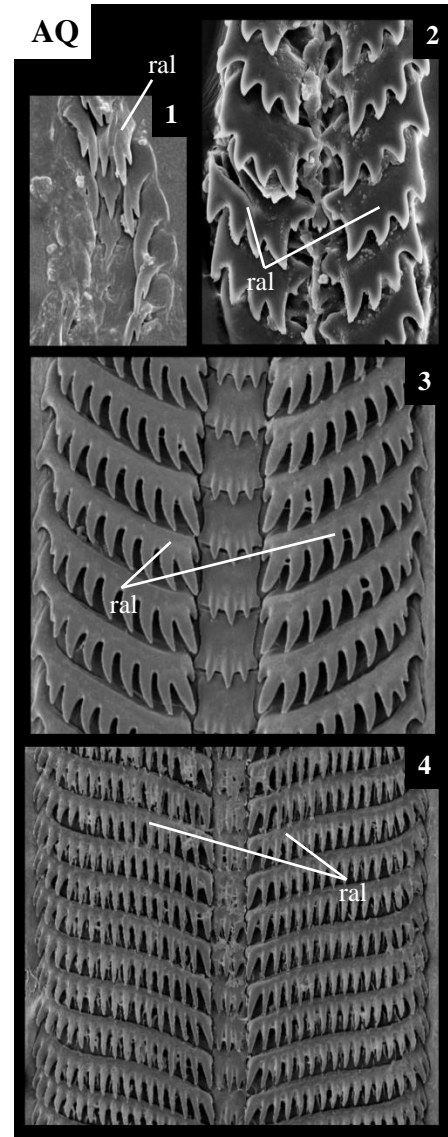
(L = 1; Ci = 100; Ri = 100)

0. Uniform

1. Not uniform

The lateral cusps of the lateral teeth usually occur in a uniform pattern, *i.e.*, the cusps are of approximately equal size or there is a gradual decrease in length centrally or outwardly (0). In clade 5a of *Peristernia* and *Fusolatirus bruijnii*, the lateral cusps are not uniform in this sense, with an irregular pattern (1), bearing secondary cusps that are unevenly distributed across teeth of the same row or not. These secondary cusps will be discussed in character 65.

This has been observed by Bandel (1984) and by Taylor & Lewis (1995), stating that all fasciolaridiids have a radula with comb-like, multicuspidate, lateral teeth; while those of *Peristernia* have both large and small cusps with great variability in cusp pattern between teeth in sequential row. The genus *Fusolatirus* was established on the grounds that the type species “has the shell of *Latirus*-form and the radula of *Peristernia*-formula” (Kuroda & Habe, 1971). Later works on *Fusolatirus* radulae have showed the same pattern (*e.g.*, Snyder & Bouchet, 2006); while this genus and *Peristernia* were shown to be polyphyletic in respect to each other in the phylogenetic study of Couto *et al.* (2016).



AQ. Radula. AQ1. *Dolicholatirus cayohuesonicus*, radula, lateral with up to four cusps (0); AQ2. *Amiantofusus pacificus*, five to six cusps (1); AQ3. *Hemipolygona armata*, seven to 15 cusps (2); AQ4. *Pleuroploca trapezium*, 7 to 15 cusps (3). ral: radula lateral.



**58. Radula, lateral, cusps, number** (fig. AQ)

(L = 5; Ci = 60; Ri = 93)

- 0. Up to 4
- 1. 5 to 6
- 2. 7 to 15.
- 3. 16 or more

Character 59 is another evidence of an increase in the length and cusp number of the laterals, as already discussed previously in character 53 and 55. With the exception of *Dolicholatirus* and *Teralatirus roboreus* (clade 1a), that only have up to four cusps (0), all fasciolariids have increased the number of cusps in the lateral, being a diagnostic characteristic for fasciolariids in the buccinoidean context.

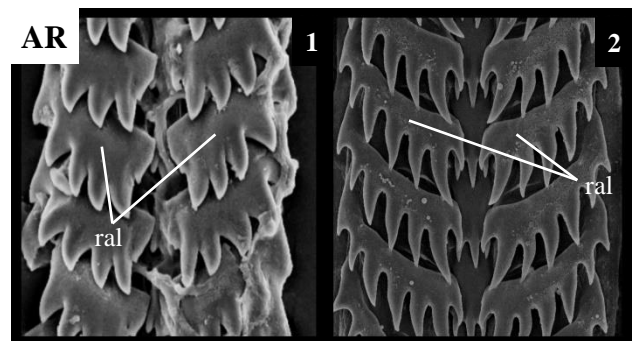
Clade 2 saw an increase in the number of cusps in the laterals to five to six (1), but that was retained only for clade 2a; clade 3 increased to seven to 15 cusps (2), and this was maintained for most fasciolariids. *Leucozonia ocellata* reverted to the previous state of five to six cusps; however, a group that corresponds mostly to fasciolariines but also *Nodolatirus nodatus* and *Latirus vischii* greatly increased the number cusps to more than 16 (3), although *Australaria australasia* reverted back to the previous state of seven to 15 cusps. The evident transitional transformation of increased cusp number denotes an additive parsimony model is desirable (0–1–2–3).

**59. Radula, lateral, base** (fig. AR)

(L = 6; Ci = 16; Ri = 64)

- 0. Straight
- 1. Curved

The lateral tooth's base exists in two ways: a straight (0) or curved (1). The former occurs as the basal state for fasciolariids, while the latter appeared three times independently, in *Angulofusus neda*, clade 3b (*Chryseofusus*, *Fusinus* and *Cyrtulus serotinus*) and 5 (most of the peristerniines).

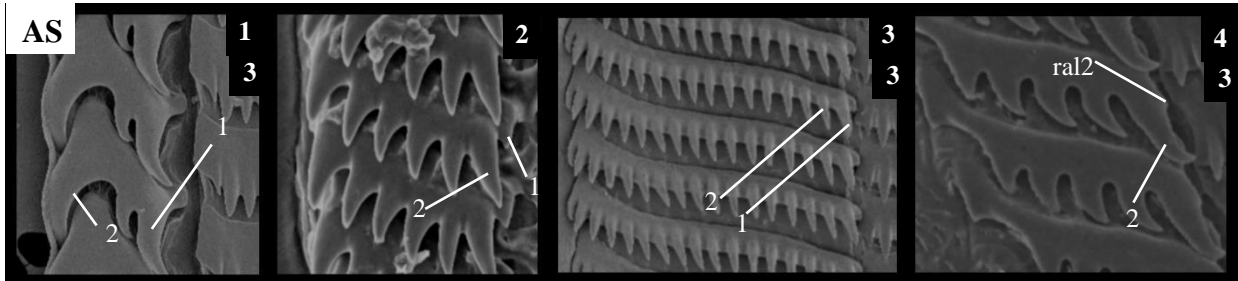


**AR. Radula. AR1.** *Amiantofusus candoris*, radula, lateral base straight (0); **AR2.** *Polygona angulata*, lateral base curved (1). **ral:** radula lateral.

## 60. Radula, lateral, cusp 1 (fig. AS)

(L = 3; Ci = 66; Ri = 95)

0. Present, same or greater size
1. Present, reduced size
2. Absent



**AS.** Radula, detail of lateral. **AS1.** *Pisania pusio*, radula lateral teeth, cusp 1 same or greater size (char. 61: 0), cusp 2 twice as other cusps (char. 62: 1), secondary cusp in cusp 2 absent (char. 63: 0); **AS2.** *Pseudolatirus discrepans*, cusp 1 reduced size (char. 61: 1), cusp 2 same length other cusps (char. 62: 0), secondary cusp in cusp 2 absent (char. 63: 0); **AS3.** *Filifusus filamentosus*, cusp 1 absent (char. 61: 2), cusp 2 same length other cusps (char. 62: 0), secondary cusp in cusp 2 absent (char. 63: 0); **AS4.** *Leucozonia ocellata*, cusp 1 absent (char. 61: 2), cusp 2 twice as other cusps (char. 62: 1), secondary cusp in cusp 2 present (char. 63: 1). Numbers indicate cusp number as indicated by text. **ral**: radula lateral; **ral2**: radula lateral secondary cusp.

The first cusp of the lateral tooth of the radula is hereinafter referred to as the innermost cusp (cusp 1). Bandel (1984) argued that the radula of fasciolarids is much like that of other buccinids, but while in the latter the outermost cusp is the largest, in the former the innermost cusp is largest. This can be confirmed here, as the innermost cusp is bigger or at least the same size as the other cusps in the non-fasciolarid buccinoidean studied; in fasciolarids however (except clade 1a), it is exactly the opposite.

In *Dolicholatirus* and *Teralatirus roboreus* (clade 1a) radular modifications did not take place (as discussed in characters 54, 56, 59: increase in width and cusp number of the lateral tooth), remaining much like other buccinoideans: cusp 1 the same length as other cusps (0). A synapomorphy of the remaining fasciolarids is the reduction of this cusp (1), whereas the complete absence (2) occurred twice independently, on clades 6b (fasciolarines and *Latirus vischii*) and 14 (*Leucozonia* and *Opeatostoma pseudodon*).

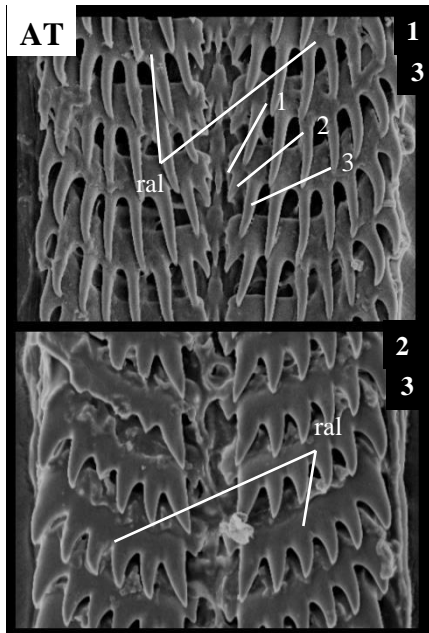
Differences in fasciolarid radulae were observed previously in the literature, more specifically those among peristerniines. Bullock (1974) noted that the feature that distinguishes

*Latirus* and related species (*sic*) from *Leucozonia* is: the absence in *Leucozonia* of a ‘denticle’ in the form of a small projection at the base of the lateral, next to the rachidian tooth, whereas is present in *Latirus*. Couto & Pimenta (2012) and Couto *et al.* (2015) observed that the ‘denticle’ that is present in some *Leucozonia* species, corresponds to the same structure as the cusp 1 of other fascioliariids; this view is rejected here based on observed anatomical differences: the cusp 1 of fascioliariines emerges from the base of the tooth whereas in *Leucozonia* this denticle emerges laterally from the innermost cusp (*i.e.*, cusp 2). More on this ‘denticle’ will be discussed on character 63.

### 61. Radula, lateral, cusp 2, length (fig. AS)

(L = 3; Ci = 33; Ri = 86)

- 0. Same or smaller than other cusps
- 1. Twice as other cusps



AT. Radula. AT1. *Cyrtulus serotinus*, innermost cusps with a gradual increase in length (1); AT2. *Pseudolatirus discrepans*, no gradual lengthening (0). Numbers indicate cusp number as indicated by text. **ral**: radula lateral.

The size of cusp 2 (*i.e.*, the second innermost principal cusp of the lateral tooth) is generally longer than the other cusps in non-fascioliariid buccinoideans (*e.g.*, Abbate & Simone, 2015: Melongenidae; Bandel, 1984: Columbelloidea, Buccinidae, Nassariidae). Clade 1a lacks any cusps other than cusp 1; in clade 2, as well as the reduction of the first cusp (discussed more thoroughly in the character 61), cusp 2 became the same size or smaller than the other cusps (0).

As previously discussed (character 60), clade 14 has completely lost cusp 1; and here it has also observed an increase in the length of cusp 2 to twice the size of the other cusps (1) even though cusp 2 is functionally the innermost cusp. The optimization that best suits the hypothesis that the non-*Dolicholatirus* fascioliariids have reduced the length of cusp 2 is DELTRAN, so it is used here.

**62. Radula, lateral, cusp 2, secondary inner cusp (fig. AS)**

(L = 2; Ci = 50; Ri = 75)

- 0. Absent
- 1. Present

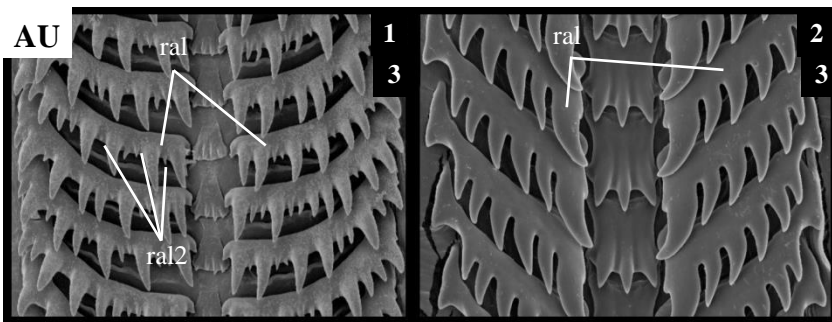
The presence of a secondary cusp occurring in the lateral innermost cusp of the lateral tooth (1) is expressed as this character; because this secondary cusp only occurs in taxa in which cusp 1 is absent, the innermost cusp is cusp 2. As previously discussed in character 60, this secondary cusp is not the ‘denticle’ *sensu* Bullock (1984), Couto & Pimenta (2012) and Couto *et al.* (2015). This character is absent (0) in all fasciolariids except in clade 15 and in *Leucozonia ocellata*.

**63. Radula, lateral, innermost cusps (1 to 3) (fig. AT)**

(L = 1; Ci = 100; Ri = 100)

- 0. Same length
- 1. Progressive increase in length

It is here defined as a progressive increase in the length of the innermost cusps (1) as a gradual lengthening of the cusps outwards from the cusp of the lateral closest to the rachidian; hence cusp 1 is smallest, followed by cusp 2 and sometimes cusp 3. This occurs for clade 3c only (*Fusinus* and *Cyrtulus serotinus*), while in all other fasciolariids this increase does not occur (0).



AU. Radula. AU1. *Peristernia nassatula*, laterals bearing secondary cusps (1); AU2. *Leucozonia ponderosa*, laterals without secondary cusps (0). **ral**: radula lateral; **ral2**: radula lateral secondary cusp.

**64. Radula, lateral, secondary cusps (fig. AU)**

(L = 1; Ci = 100; Ri = 100)

- 0. Absent
- 1. Present

Secondary cusps in the teeth may occur in the rachidian

(character 55, fig. AL) but in the laterals as well. In fasciolariids, secondary cusps in the lateral tooth (1) occur in clade 5a of *Fusolatirus bruijnii* and *Peristernia*, whose non-uniform cusp

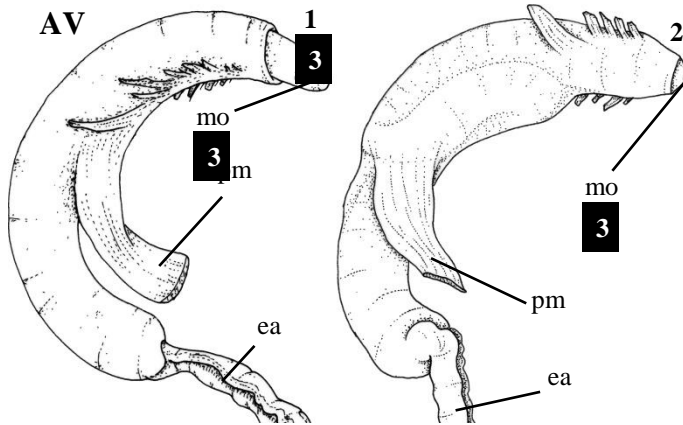
distribution (as mentioned in character 58, fig AP), with its alternating principal and secondary cusps are characteristic for this group. Species in clade 1a (*Dolicholatirus* and *Teralatirus roboreus*) also bear a minute secondary cusp in the lateral tooth; while it may occur in outgroup species of nassariids and some buccinids. All the remaining fascioliids this feature does not occur (0). A DELTRAN optimization was chosen to account for the multiple independent origins of secondary cusps in the groups antecedent Fascioliidae.

### 65. Proboscis, shape (fig. AV)

(L = 1; Ci = 100; Ri = 100)

- 0. Straight
- 1. Coiled

A proboscis is formed from the invagination of the snout and is found in most caenogastropods, and two main types are recognized: an acrembolic type with the retractor muscles at the tip, and



**AV.** Proboscis. **AV1.** *Granulifusus* sp. proboscis retracted straight into the sheath (0); **AV2.** *Fusinus frenguelli*, proboscis coiled within its sheath (1). **ea:** anterior esophagus; **mo:** mouth; **pm:** proboscis retractor muscle.

the pleurembolic type, with retractors inserted in the middle of the proboscis; although several other subtypes have been described (Ponder & Lindberg, 1997). A separation between snout and proboscis is not clear, except the fact that a snout lacks any retractor muscles (Simone, 2011).

In Fascioliidae, there is but a single proboscis type, pleurembolic; for most members, the proboscis is retracted within the rhynchodeum (also called proboscis sheath) in a straight fashion (0), however in a group that consists of *Chryseofusus*, *Fusinus*, *Cyrtulus serotinus* and *Pseudolatirus pallidus* (clade 3a), it is retracted in a coiled manner (1). In this latter group the proboscis is very long, and as discussed in character 43, the small buccal mass occurs at the very tip of the proboscis.

Kosyan *et al.* (2009) examined the anatomy of several fasciolariids, including one *Fusinus* species (*F. tenerifensis*); these authors characterized the proboscis of all species as straight and never coiled within the rhynchodeum like in the buccinid *Troschelia berniciensis* (proboscis extremely long, narrow compactly folded within rhynchodeum). Because these authors reported paired proboscis retractor muscles (instead of one) and did not characterize the radula for *F. tenerifensis*, the suspicion is that this species analyzed by Kosyan *et al.* (2009) does not belong in the genus *Fusinus*; although no image of the shell was provided in order to confirm the taxonomy.

This characteristic coiling of the proboscis occurs in other buccinids (*Troschelia* Mörch, 1876; Kosyan *et al.*, 2009; *Aulacofusus*: Kosyan & Kantor, 2013; *Calagrassor* Kantor *et al.*, 2013; Kantor *et al.*, 2013). Although Buccinidae is evidently a polyphyletic group, as demonstrated by many molecular studies (*e.g.*, Kosyan *et al.*, 2009; Zou *et al.*, 2011; Couto *et al.*, 2016) this characteristic proboscis probably emerged in parallel, as the possession of a particular proboscis type does not necessarily indicate homology (Ponder & Lindberg, 1997). Kantor (1990) has shown, on the basis of differences in musculature, that a pleurembolic proboscis has evolved independently in the Tonnoidea and Neogastropoda, and advocates an independent evolution of the proboscis of all major groups of marine predatory gastropods, a hypothesis refuted by Simone (2011), which demonstrated all higher caenogastropod proboscis are of a same, homologous type, raising the name Rhynchogastropoda (proboscis-bearing) to that branch.

## **66. Proboscis, retractor muscles, origin** (fig. AW)

(L = 1; Ci = 100; Ri = 100)

0. Haemocoel

1. Columellar muscle

Studies of comparative morphological investigation suggest that the muscles in the proboscis and snout anatomy are not yet fully understood. Caenogastropods show that there is undescribed diversity in both snout/proboscis wall composition and introversion/retraction musculature with morphological evidence that suggests that a proboscis evolved separately in at least four separate caenogastropod groups, each characterized by the presence of novel retractor muscles and different modifications of plesiomorphic “aortic muscles” (Golding *et al.*, 2009).

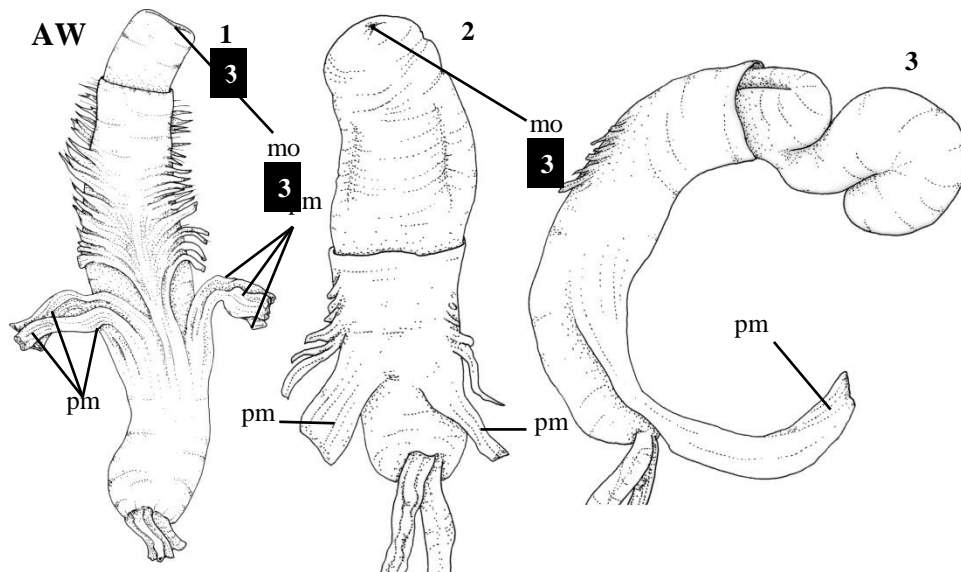
These muscles are important for higher but also for family-level studies; being one of the diagnostic characteristic for the family Fasciolariidae, *sensu* Fraussen *et al.* (2007): in Buccinidae the retractors are usually numerous and are attached in bundles laterally to the proboscis sheath (or rhynchodeum); in Fasciolariidae there is either the single pair of the retractors, or a single powerful retractor. In either of these cases (a pair or single), the retractors originate in the columellar muscle (1), posteriorly, close to the diaphragmatic septum and run anteriorly, inserting posterior or anterior to the rhynchodeum. Non-fasciolariids, which have bundles of fibers instead of a pair or a single muscle, on the other hand, have these originating through several insertion points at the base of the haemocoel (0).

### 67. Proboscis, retractor muscles, bundles of muscles (fig. AW)

(L = 3; Ci = 33; Ri = 80)

0. Two bundles

1. One bundle

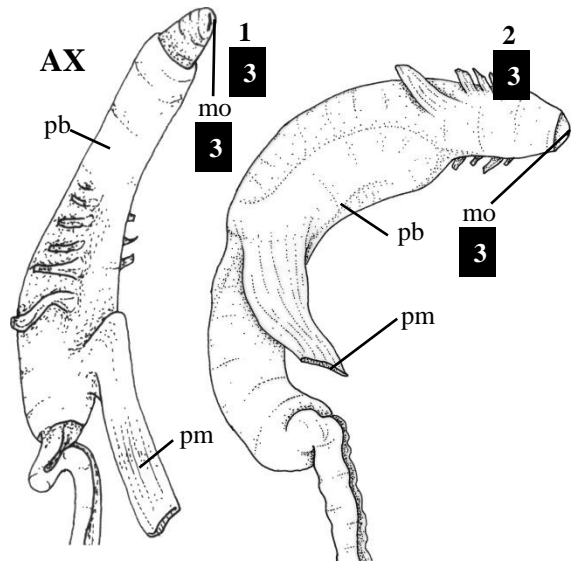


**AW.** Proboscis. **AW1.** *Pisania pusio*, proboscis retractor muscles as multiple fibers, inserted in haemocoel wall (char. 68: 0), arranged in two bundles (char. 68: 0); **AW2.** *Pustulaturus ogum*, retractor muscles originating in columellar muscles (char. 67: 1) and arranged in two bundles (char. 68: 0); **AW3.** *Fusinus marmoratus*, retractor muscles originating in columellar muscles (char. 67: 1) and arranged as a single powerful muscle (1). **mo:** mouth opening; **pm:** proboscis retractor muscle.



Neogastropods have the proboscis muscles arranged in two lateral bundles, one in each side, of the proboscis (e.g., *Enigmaticolus* Fraussen, 2008; Kantor *et al.*, 2013; *Aulacofusus*: Kosyan & Kantor, 2013). Non-fascioliariids have the several muscle fibers with haemocoelic origins; fascioliariids on the other hand have one or two strong muscles with the origin in the columellar muscle (as previously discussed).

The scenario hypothesized here suggests that Fascioliariidae arranged each of these bundles into a single muscle (creating, thus, two bundles one in each side of the proboscis) with columellar muscle origin; posteriorly the left muscle tuft was lost and, for most of the fascioliariids remained so. This is congruent with a DELTRAN optimization, in which there were two independent losses of the right muscle tuft (1): one for *Dolicholatirus cayohuesonicus* and another for clade 2 (containing most members of the family). Species of *Pustulatirus* (clade 8a) reverted to the previous state, and have two bundles of muscles.



**AX.** Proboscis. **AX1.** *Dolicholatirus cayohuesonicus*, proboscis retractor muscle inserted posteriorly in rhynchodeum (0); **AX2.** *Fusinus frenguelli*, proboscis retractor inserted medially (1). **mo**: mouth opening; **pb**: proboscis; **pm**: proboscis retractor muscle.

## 68. Proboscis, retractor muscles, position in proboscis (fig. AX)

(L = 13; Ci = 7; Ri = 45)

- 0. Posterior
- 1. Median

This highly homoplastic character denotes the insertion of the proboscis retractor muscles in the rhynchodeum wall. In most fascioliariids species, being the plesiomorphic state, the muscles are inserted in the posterior region of the proboscis (0), while an insertion medially (1) in the rhynchodeum occurs in several clades or species independently: in *Dolicholatirus cayohuesonicus*, clade 2c (*Amiantofusus*), *Pseudolatirus pallidus*, *Fusinus australis*, clade 4b, 6c, *Hemipolygona armata*, clade 8a (*Pustulatirus*) and 12. The optimization chosen was DELTRAN.

## 69. Salivary glands, position (fig. AY)

(L = 3; Ci = 33; Ri = 91)

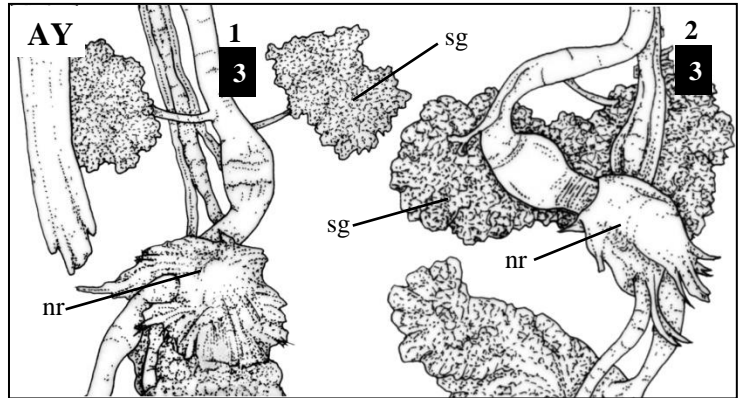
- 0. Close to nerve ring
- 1. Free

Kosyan *et al.* (2009) found that some fasciolariids have ‘separate’ salivary glands while others have ‘free’ salivary glands, this former probably refers to the state 0 (close to nerve ring). There same authors listed

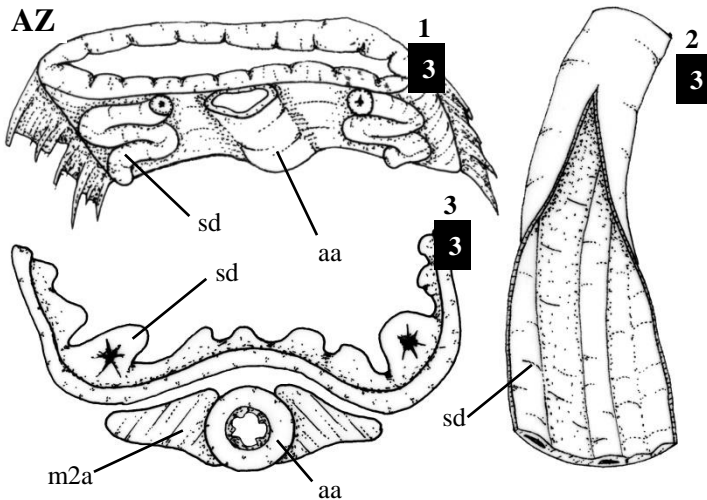
*Fusinus tenerifensis* has having the salivary glands ‘separate’ and *Opeatostoma pseudodon* and *Pustulatirus mediamericus* as ‘fused’; this is the opposite state found in the present study for *Fusinus* and for the two latter species. The meaning for this is doubtful, but perhaps preservation quality plays a crucial role for this character in particular

Fraussen *et al.* (2007) reported that the genus *Amiantofusus* has salivary glands that are

situated on both sides of the anterior part of the rhynchodeum and the nerve ring, suggesting that they have correspond to state ‘close to nerve ring’ (0), much like most fasciolariids. Contrarily, clade 6 has salivary glands that are separate from each other (1), and this occurs on the outgroup species *Buccinum undatum* and *Pisania pusio*.



AY. Mid-esophagus. AY1. *Fasciolaria tulipa*, salivary glands as paired and free amorph masses (1); AY2. *Fusinus* sp. salivary glands close to nerve ring (0). nr: nerve ring; sg: salivary glands.



AZ. Section of the anterior esophagus immediately after valve of Leiblein. AZ1. *Buccinum undatum*, salivary ducts immersed in anterior esophagus wall (0); AZ2. *Polygonia infundibulum*, salivary ducts immersed in esophagus wall (1); AZ3. *Fusinus australis*, salivary ducts immersed in esophagus wall (1). aa: anterior aorta; m2a: accessory odontophore retractor muscles; sd: salivary gland duct.

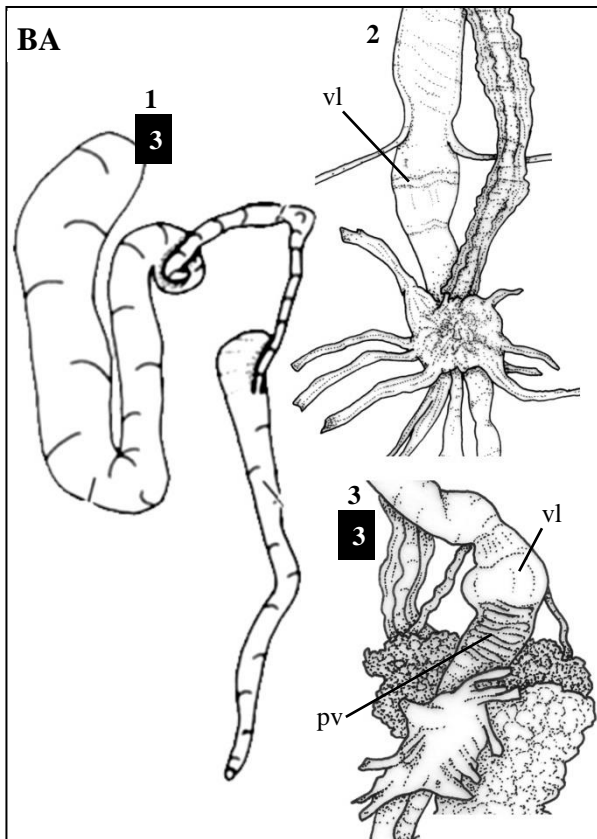
## 70. Salivary ducts (fig. AZ)

(L = 1; Ci = 100; Ri = 100)

- 0. Free
- 1. Immersed in esophagus wall

The salivary gland ducts which bypass the nerve ring is an important character for distinguishing the Neogastropoda from other mesogastropods (Ponder & Lindberg, 1997; Strong, 2003; Simone, 2011). In the scope of the superfamily Buccinoidea, however, there are some differences that are worth noting. In the family Buccinidae, the ducts, after leaving the salivary glands, follow freely along the anterior esophagus towards the anterior part of the proboscis, where they enter the walls of the esophagus close to their entrance into the buccal cavity (Fraussen *et al.*, 2007); in Fasciolariidae (e.g., *Leucozonia nassa*: Couto & Pimenta, 2012; *Pustulaturus ogum* and *Hemipolygona beckyae*: Couto *et al.*, 2015; *Latirus polygonus*: Kosyan *et al.*, 2009), the ducts, shortly after leaving the glands, enter the anterior esophagus walls in front of the valve of

Leiblein.



**BA.** Anterior and middle esophagus. **BA1.** *Pugilina tupiniquim* (modified from Abbate & Simone, 2015), valve of Leiblein absent (char. 72: 0) and ventral glandular region absent (char. 73: 0); **BA2.** *Aurantilaria aurantiaca*, valve of Leiblein present (char. 72: 1) and ventral glandular region absent (char. 73: 0); **BA3.** *Fusinus frenguelli*, valve of Leiblein present (char. 72: 1) and ventral glandular region present (char. 73: 1). **pv:** ventral glandular region of mid esophagus; **vl,** valve of leiblein.

Kosyan *et al.* (2009) observed mixed results for this feature in fasciolariids: while in *Latirus polygonus* the salivary ducts are embedded in the esophagus wall, in *Pustulaturus mediamericus*, *Turrilatirus turritus*, *Peristernia nassatula*, *P. ustulata* and *Opeatostoma pseudodon* the ducts are reported as free. This contradicts the diagnosis for the family of Fraussen *et al.* (2007); Couto *et al.* (2015) has pointed that this fact deserves further investigation. I have dissected four out of the six species that Kosyan *et al.* (2009) reported as having the salivary ducts free from the anterior esophagus and found this not to be true. Likely, these authors mistakenly identified the accessory odontophore retractor muscles (m2a) that follow the aorta anteriorly from the nerve ring, ventral to the anterior esophagus as the ducts, while these run immersed in the gut wall.

Fasciolariids have, with the outgroup species *Pisania pusio* the ducts immersed in the

anterior esophagus wall immediately posterior to the valve of Leiblein (1). The ducts follow their openings into the buccal cavity under the lateral folds of the esophagus. This condition is also true for other neogastropods (Simone, 2011), although they become immersed only near the buccal mass, much more anterior (0).

#### **71. Valve of Leiblein** (fig. BA)

(L = 3; Ci = 33; Ri = 0)

0. Absent

1. Present

The valve of Leiblein, a pyriform bulbous or pear-shaped organ lying at the transition of the anterior and mid-esophagus, is restricted to the non-conoideans neogastropods (Ponder, 1973; Ponder & Lindberg, 1997; Strong, 2003; Simone, 2011). It is composed of a cone-shaped bulge that is enclosed in a chamber formed by the expanded walls of the anterior portion of the mid-esophagus (Kantor & Fedosov, 2009) and is fringed with extremely long cilia (Fretter & Graham, 1962). The main function of the valve is to prevent the reflow of food from the posterior esophagus during proboscis elongation, acting partially mechanically, partially chemically (exposure to secretions of the digestive gland or stomach contents causes the valve to close (Kantor & Fedosov, 2009). The supposition was done earlier in the studies of the valve, since there is a correlation between presence or absence of the valve and size or placement of the gland of Leiblein; taxa lacking a gland or have duct of the gland of Leiblein that bypasses the esophagus, lack a valve of Leiblein (Ponder, 1994; Strong, 2003).

Fedosov & Kantor (2009) have demonstrated significant differences in the morphology and embryogenesis of the valve of Leiblein in different neogastropods, (Muricidae and Buccinidae at least). This suggests that the homology of the valve of Leiblein within Neogastropoda is questionable despite the superficial similarity.

According to these authors, Neogastropoda have three key autapomorphies: the accessory salivary glands, the rectal (or anal) gland and the valve of Leiblein. Because buccinoideans lack the two former neogastropod autapomorphies, if these authors' assumption is correct, then buccinoideans do not share any of the previously hypothesized autapomorphies with the rest of neogastropods. This raises the prospect of a paraphyletic Neogastropoda with two stems, one

including of Buccinoidea, and another with the remaining neogastropod families. This scenario is in conformation with some molecular studies that challenge the neogastropod concept (*e.g.*, Winnepeninckx *et al.*, 1998; Colgan *et al.*, 2007; Cunha *et al.*, 2009). Another likely scenario is the secondary loss of these structures independently by some buccinoids.

This global discussion on valve of Leiblein morphology and homology is beyond the present study, since undoubtedly fascioliid valves have the same origin (1), and only a few outgroup species such as *Pugilina tupiniquim* lack this structure (0).

## **72. Mid-esophagus, posterior ventral glandular region (fig. BA)**

(L = 3; Ci = 100; Ri = 100)

0. Absent

1. Present

In some fascioliids, namely *Fusinus* and *Cyrtulus serotinus* (clade 3c), there is a series of transverse rings, generally orange to brown color, posterior to the valve of Leiblein (1). This structure is not visible (0) in other fascioliids.

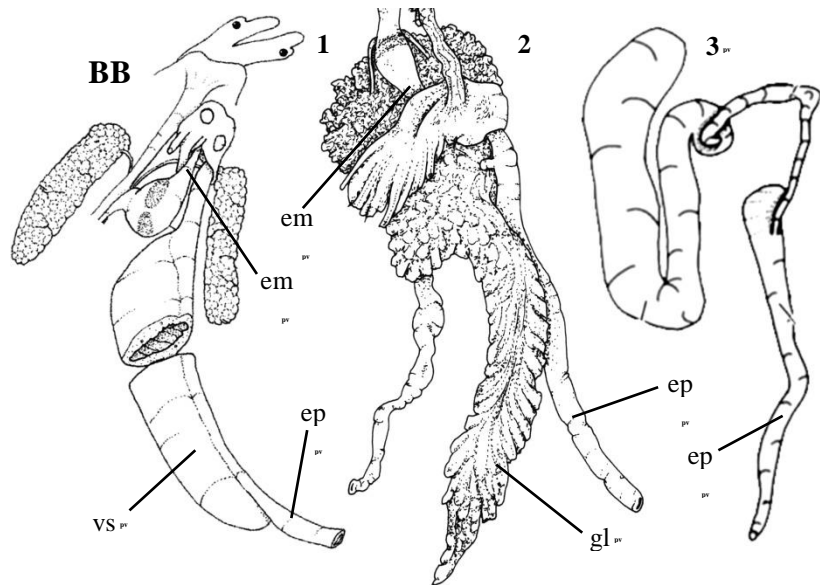
These circular structures are likely the remnants of the ‘glande framboisée’ (framboise gland) *sensu* Amaudrut (1898). Andrews & Thorogood (2005) and Simone (2011) described this part of the mid-esophagus, anterior to the nerve ring, as a section rich in mucous glands on the hypertrophied dorsal folds (the pre-torsional left larger than the right); being an autapomorphy of some Muricidae (Simone 2011: including, *e.g.*, *Phyllonotus* Swainson, 1833, *Siratus* Jousseume, 1880, *Chicoreus* Montfort, 1810; but not including genus *Thais*). The assumption of homology is based on the position and arrangement of the mid-esophagus; however, no further investigation has been undertaken, neither histological nor embryological. What is clear is that the (re?)appearance of this feature is unique in the clade of *Fusinus* and *Cyrtulus serotinus*, with all other fascioliids lacking.

### 73. Esophageal gland, form (fig. BB)

(L = 3; Ci = 66; Ri = 0)

- 0. Ventral septated sac
- 1. Gland of Leiblein
- 2. Absent

The esophagus in gastropods is not merely a passage between mouth and stomach, and food content generally undergoes several digestive processes as a result of intense glandular activity found in it (Fretter & Graham, 1962; Salvini-Plawén, 1988; Ponder & Lindberg, 1997; Strong, 2003; Simone,



**BB.** Anterior digestive system. **BB1.** *Teralatirus roboreus* (modified from Simone *et al.*, 2013), esophageal gland as a ventral septated sac (0); **BB2.** *Granulifusus* sp. esophageal gland as the gland of Leiblein (1); **BB3.** *Pugilina tupiniquim* (modified from Abbate & Simone, 2015), esophageal gland absent (2). **em:** mid-esophagus; **ep:** posterior esophagus; **gl:** gland of Leiblein; **vs:** ventral septated sac.

2011). In some archeogastropods the esophagus bears a pair of esophageal pouches laterally, but this does not have the same origin as the dorsal esophageal gland and the gland of Leiblein (Strong, 2003; Simone, 2011) of interest in this study.

The esophageal gland is located in the mid-posterior esophagus, and is present in most caenogastropods; while it is derived from a dorsal glandular strip, torsion shifted its position to ventral (Simone, 2011). In some taxa such as Naticoidea and Cypraeoidea the middle region of the esophagus possesses a large ventral diverticulum being nodose or transversely (Simone, 2011).

In neogastropods, the esophageal gland lacks septa, and has a uniform tissue; it is connected to the ventral surface of the esophagus by means of a duct. In some Cancellarioidea, Muricoidea (*sensu* Simone, 2011: muricoideans, buccinoideans, olivoideans and pseudolivoideans) and Conoidea, a gland of Leiblein occurs; conoideans have a modified variation, the venom gland (Strong, 2033; Simone, 2011). The gland of Leiblein is absorptive as well as secretory, acting as a reservoir for solute-rich liquid entering it from the esophagus in both directions (Andrews & Thorogood, 2005). Preliminary ultrastructural examination indicates

that the gland absorbs cadmium not only from the blood but also directly from its lumen and that it may have the capacity to sequester a wide range of toxins, that contributed to a modified secretory function of some gastropods (*e.g.*, Conidae: venom gland) (Andrews & Thorogood, 2005).

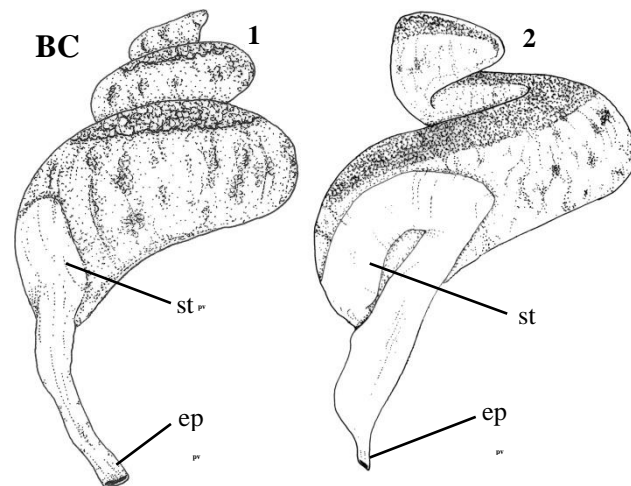
Some buccinoideans have secondarily lost the gland of Leiblein, according to most morphological analysis (Ponder & Lindberg, 1997; Strong, 2003; Simone, 2011). The possibility that Neogastropoda is not monophyletic, as was discussed earlier on character 73, raises the hypothesis that these taxa did not secondarily lose this structure, instead never acquired it. This is not, however, the scope of this study. Melongenids (*Pugilina tupiniquim*) lack a valve or a gland of Leiblein (2), nor any gland in the mid-esophagus.

All Fascioliariids have a gland of Leiblein (1), except *Teralatirus roboreus*, which has an esophagus that resembles those of non-neogastropods, bearing a ventral expansion (0); it greatly resembles the esophagus corresponding to non-neogastropod taxa, such as cypraeoideans, illustrated by Simone (2011: fig. 16C). Some cancellariids have a glandular strip within the mid-esophagus that is homologous to the gland of Leiblein (Strong, 2003) and that seems to be the case in *Teralatirus roboreus* as well; it is certain however, that the reversal to a state without a gland of Leiblein occurred on several occasions within caenogastropods.

#### 74. Posterior esophagus, diameter (fig. BC)

(L = 6; Ci = 33; Ri = 50)

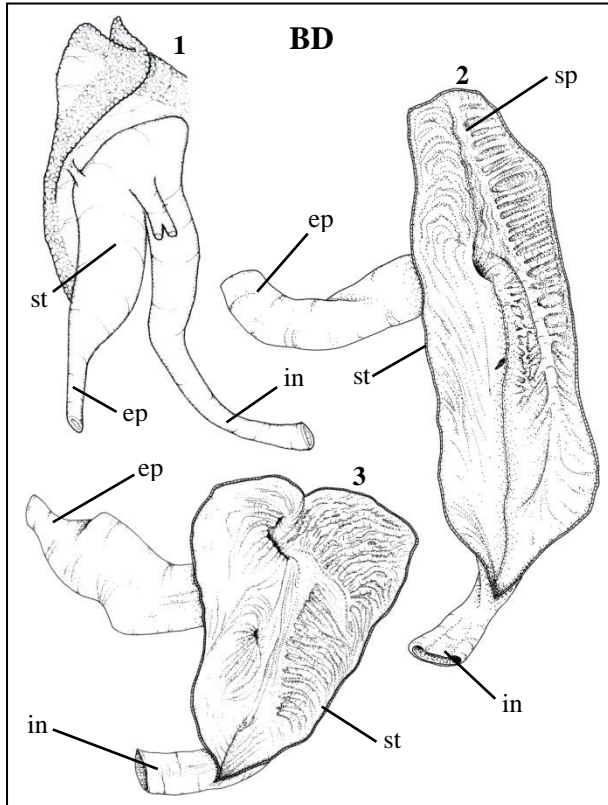
- 0. Constant
- 1. Broadening in visceral region
- 2. Broadening in haemocoel



**BC.** Visceral mass. **BC1.** *Polygona angulata*, posterior esophagus constant in diameter (0); **BC2.** *Aurantilaria aurantiaca*; posterior esophagus with a broadening anterior to the stomach (1). **ep:** posterior esophagus; **st:** stomach.



The posterior esophagus penetrates the diaphragmatic septum posteriorly and follows into the stomach, in the visceral region. In most fascioliariids, the transition between the septum is smooth, the diameter of the esophagus in this region is constant (0). In the clade of fascioliariines



**BD.** Stomach in dorsal view and lumen. **BD1.** *Monetaria annulus* (modified from Simone, 2011), stomach as a simple passage from esophagus to intestine (0); **BD2.** *Pisania pusio*, stomach bearing a dorsal posterior bulge with sorting area (1); **BD3.** *Fasciolaria tulipa*, stomach with dorsal posterior bulge, no sorting area (2). **ep:** posterior esophagus; **in:** intestine; **sp:** stomach posterior sorting area; **st:** stomach.

(clade 6c) and in *Opeatostoma pseudodon*, there is a sudden broadening in the diameter (1), right before entering the stomach. A broadening in the haemocoel (2) occurs in the nassariids *Engoniophos unicinctus* and *Bullia laevissima*.

### 75. Stomach, posterior bulge (fig. BD)

(L = 3; Ci = 65; Ri = 75)

- 0. Absent
- 1. Present, with sorting area
- 2. Present, without sorting area

The stomach is one of the most complex organ of the digestive (Kantor, 2003) and remains as a poorly studied structure, that is intensified by the fact that it is usually too poorly fixed for examination. Observations on the circulatory patterns of the ciliary currents in the stomachs in live specimens suggest that food absorption occurs through

the stomach walls, rather than in the tubules of the digestive gland (Kantor, 2003).

The stomach in caenogastropods is divided into two chambers: the proximal (or gastric) chamber and a distal chamber (or style sac) (Strong, 2003). Strong (2003) revised several stomach (*sic* midgut) characters and revealed that the evolution of midgut structure is highly mosaic, reflected on patterns of feeding, diet and foregut complexity. One such simplification occurred in predatory carnivores, with an emphasis on extracellular digestion, and the gastric shield, crystalline sac and/or gastric caecum may, but not always will be, lost independently

(Strong, 2003). Despite this correlation of alimentary habits/stomach types, there is evidence that similarities in stomach anatomy more likely reflect phylogenetic relationships, rather than similarities in diet (Kantor, 2003; Strong, 2003).

Basal clades of Caenogastropoda are herbivorous or microphages, while the terminal branches are predatory carnivores; a contrast to this is the cypraeoideans that have a very simplified stomach but are herbivores, supposedly grazing feeders (Simone, 2011). Stomach of this type is a mere passage from the posterior esophagus to the intestine (0), and only the outgroup taxa *Monetaria annulus* possess this type.

In Neogastropods, the gastric (or proximal) chamber may have a more or less long, blind, posterior extension called caecum or posterior sorting area (not to be mistaken with the caecum of vetigastropod stomach) (Kantor, 2003). All buccinoideans in the present analysis have a stomach with a posterior mixing area (1), except all studied fascioliids. Kantor (2003) distinguished species of Fascioliidae from other buccinoideans by the low relief of the folds on the inner stomach wall; presence of transverse striations on the low longitudinal fold; absence of clear differentiation of the gastric chamber into dorsal and ventral parts; a shallow lateral sulcus; and absence of a posterior mixing area. The absence of a posterior mixing area was also appointed by Fraussen *et al.* (2007) as diagnostic for the family; and this was the same result for the fascioliids in this study (2).

## **76. Rectum**

(L = 1; Ci = 100; Ri = 100)

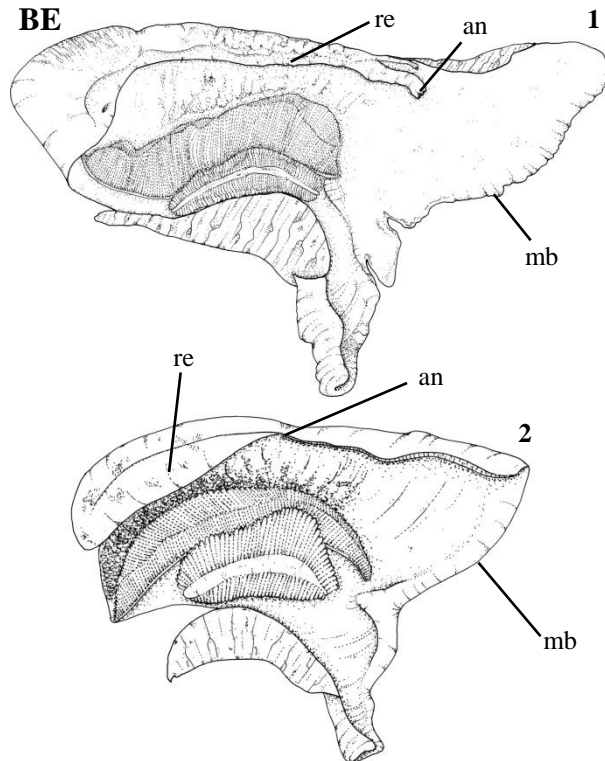
- 0. Free from pallial gonoduct
- 1. Enveloped by the pallial gonoduct

The rectum runs laterally in the left side of the pallial cavity, being completely free from the pallial gonoduct (0) in the Cypraeoideans (*Monetaria annulus*); in the neogastropods examined, including all fascioliids, the rectum is enveloped with the pallial gonoduct (prostate or oviduct) by a thin longitudinal membrane (1).

**77. Anus, position in pallial cavity: total pallial cavity length (fig. BE)**

(L = 9; Ci = 11; Ri = 61)

- 0. Less than 1/3
- 1. 1/3 or more



**BE.** Roof of the pallial cavity in ventral view. **BE1.** *Opeatostoma pseudodon*, anus position from mantle edge is less than 1/3 the total length of the pallial cavity (0); **BE2.** *Amiantofusus candoris*, anus position from the mantle edge is 1/3 or more of the total length of the pallial cavity (1). **an:** anus; **mb:** mantle border; **re:** rectum.

The rectum terminates in the anus on the left side of the animal; the depth of which the anus occurs in the pallial cavity is measured by the distance from the pallial border by the total pallial cavity length. Fasciolariids have a basal state of more than 1/3 of this ratio (1), while in five groups this ratio reverted to less than 1/3 (0): clades 3d, 5a, 13, *Granulifusus* sp., *Pustulaturus ogum* and *Polygona angulata*. This character was optimized under an ACCTRAN optimization.

**78. Oviduct, seminal receptacle (fig. BF)**

(L = 6; Ci = 16; Ri = 50)

- 0. Present
- 1. Absent

The following 12 characters correspond to female and male reproductive systems. It is worth noting that due to the maturation of

certain specimens and the availability of either male or female, these characters (characters 78 to 90) contain the largest amount of missing data, nonetheless they remain very informative.

The presence of a seminal receptacle (0) as observed in a few fasciolariids, while the basal state for the family is the absence (1). It is present in clades 4b, 15 and in *Leucozonia ocellata*. The optimization used was DELTRAN.

### 79. Bursa copulatrix, position

(L = 1; Ci = 100; Ri = 100)

0. Posterior

1. Anterior

Characters 79 and 80 (seminal receptacle and bursa copulatrix respectively) are structures derived from the pallial oviduct responsible for storing sperm; the former storing oriented (head attached to epithelium and tail aligned) and the latter storing unoriented sperm (Ponder & Lindberg, 1997; Strong, 2003). In non-caenogastropods, the seminal receptacles are not homologous with those of caenogastropods, given their different position and structure (Ponder & Lindberg, 1997). Normally in

animals that possess both of these organs the bursa copulatrix is the structure that receives the sperm, spermatophore, or equivalent, during copulation; afterwards the spermatozoa are transferred to the seminal receptacle via a ciliated furrow. The sperm responsible for fertilization is supplied from the seminal receptacle (Simone, 2011).

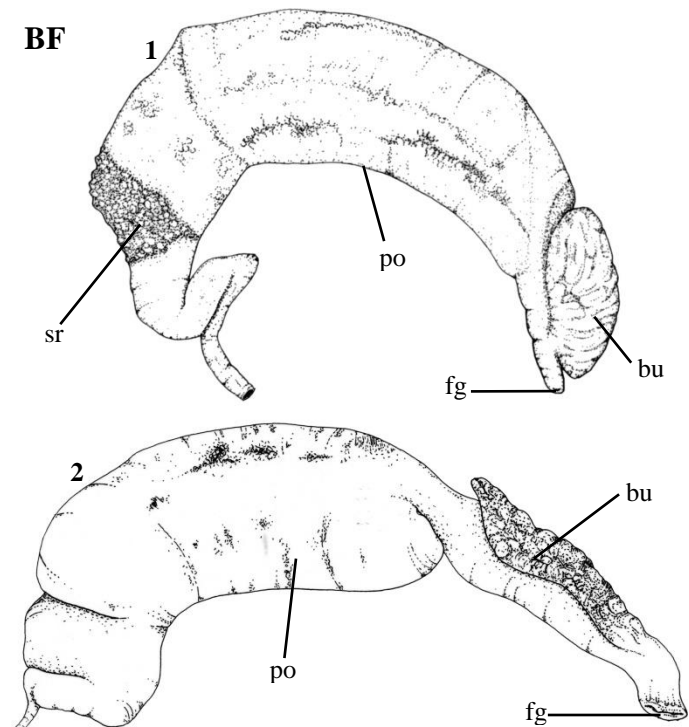
The bursa copulatrix in the outgroup taxa *Monetaria annulus* is posterior to the gonopore, laterally to the seminal receptacle (0). In all other taxa, including Fasciolariidae, the bursa occurs anteriorly, i.e., terminally in the pallial oviduct (1).

### 80. Bursa copulatrix, length: length of oviduct (fig. BF)

(L = 3; Ci = 33; Ri = 71)

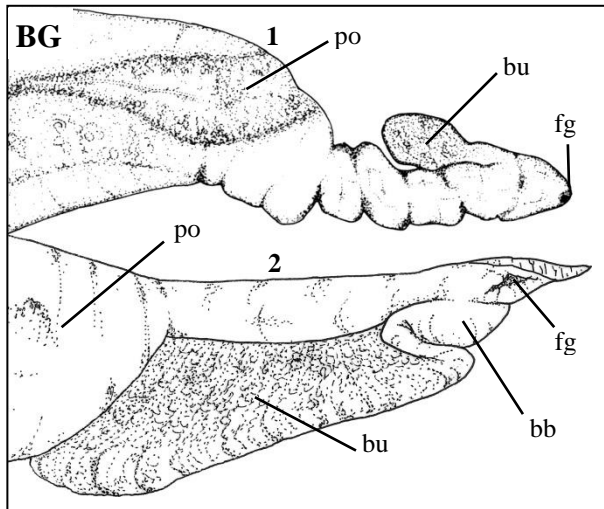
0. Less than 1/4

1. 1/4 or more



**BF.** Pallial oviduct. **BF1.** *Leucozonia ocellata*, seminal receptacle present (char.79: 0), ratio of the length of the bursa copulatrix by the length of oviduct is less than 1/4 (char. 81: 0); **BF2.** *Opeatostoma pseudodon*, seminal receptacle absent (char. 79: 1), ratio of the length of the bursa copulatrix by the length of oviduct is 1/4 or more (char. 81: 1). **bu:** bursa copulatrix; **fg:** female gonopore; **po:** pallial oviduct; **sr:** seminal receptacle.

The ratio between length of the bursa copulatrix by the total length of the oviduct is represented in this character. While this may vary according to sexual maturation, a synapomorphy of the family, fasciolariids have this proportion of less than 1/4 (1), with two independent reversions to a ratio of less than 1/4 (0), in a group of *Leucozonia* (clade 15) and in *Chryseofusus archeruisius*. An ACCTRAN optimization was used.



**BG.** Terminal portion of pallial oviduct. **BG1.** *Granulifusus hayashi*, bursa copulatrix with bulb absent (0); **BG2.** *Polygona angulata*, bursa copulatrix with an anterior bulb (1). **bb:** bursa copulatrix bulb; **br:** bursa copulatrix; **fg:** female gonopore; **po:** pallial oviduct.

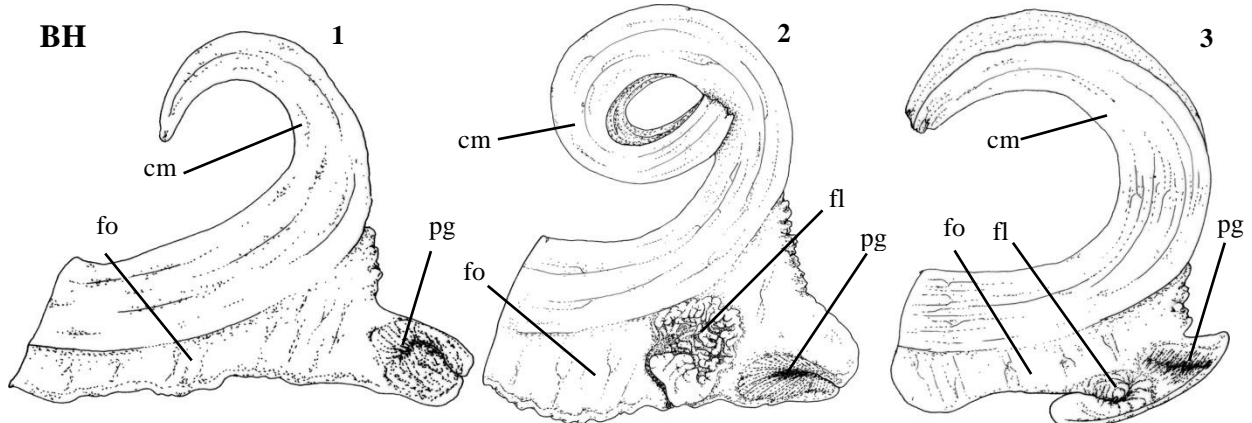
### 81. Bursa copulatrix, anterior bulb (fig. BG)

(L = 3; Ci = 33; Ri = 0)

0. Absent

1. Present

In most fasciolariids, the bursa copulatrix connects to the terminal portion of the pallial oviduct with a simple duct (0); in *Granulifusus* sp. and in *Polygona angulata*, however, the presence of an anterior bulb was observed. This bulb (1) occurs anteriorly to the bursa, close to the gonopore, being muscular than the bursa itself, suggesting a pumping function.



**BH.** Longitudinal section of foot and columellar muscle, haemocoel removed. **BH1.** *Pseudolatirus discrepans*, cement gland absent (char. 83: 0); **BH2.** *Filifusus filamentosus*, cement gland present (char. 83: 1), multi-branched (char. 84: 1) its opening centrally in the foot (char. 85: 0); **BH3.** *Dolicholatirus cayohuesonicus*, cement gland present (char. 83: 1) single branched (char. 84: 0) its opening anteriorly in the foot (char. 85: 1). **cm:** columellar muscle; **fl:** female cement gland; **fo:** foot; **pg:** pedal gland.

**82. Cement gland** (fig. BH)

(L = 3; Ci = 33; Ri = 60)

0. Absent

1. Present

The cement gland (ventral pedal gland *sensu* Strong, 2003) is an unpaired glandular structure that is situated in median line of the foot sole (Simone, 2011). This organ is different from the pedal gland of some caenogastropods that also play a role in reproduction (Strong, 2003). Both Strong (2003) and Simone (2011) agree that this structure has received little attention on homology assessment and requires additional studies. Additionally, it is possible that the gland has not been observed in some taxa because females were not sexually mature, as well as much less obviously developed in some *e.g.*, those with lens-shaped capsules (Simone, 2011).

In Fasciolariidae, clade 4a (*Granulifusus* and *Pseudolatirus discrepans*) lacks this structure (0). All the remaining members of the family have a cement gland (1), which is the basal state for the family. An ACCTRAN optimization was chosen.

**83. Cement gland, form** (fig. BH)

(L = 1; Ci = 100; Ri = 100)

0. One or two branches

1. Multi-branched

In a clade of fasciolariine species (6d), the cement gland occurs as several saccular vesicles ramifying from a main branch (1). This type of gland differs from the more common one or two branching patterns (0) of most fasciolariids.

**84. Cement gland, opening position in foot** (fig. BH)

(L = 9; Ci = 11; Ri = 11)

0. Centrally

1. Anteriorly

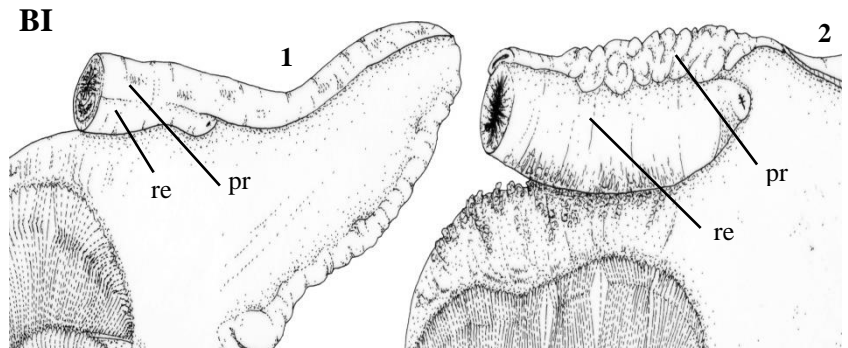
Simone (2011) described the position of the cement gland opening in the anterior third of the foot sole; this is true for most fasciolariids herein, with the opening anteriorly (1). The opening has migrated posteriorly on several occasions in Fasciolariidae, assuming a more or less central position in the foot sole (0). Based on an ACCTTRAN optimization, clades 3b<sup>1</sup> (*Chryseofusus*), 6a, 8a (*Pustulaturus*), 14a and *Fusinus frenguelli* assumed a central opening in the foot sole (and posteriorly *Leucozonia ocellata* reverted to an anterior opening).

**85. Prostate, shape** (fig. BI)

(L = 2; Ci = 40==50; Ri = 0)

0. Simple

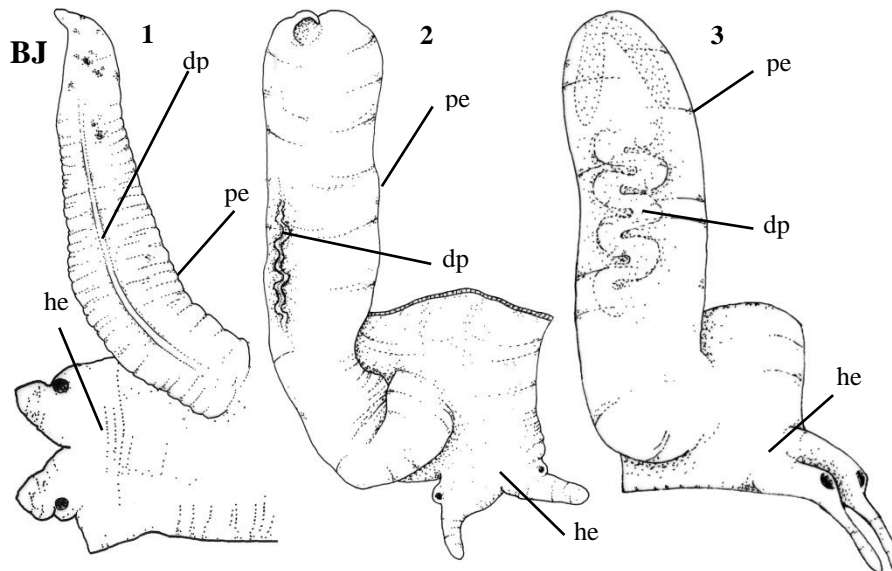
1. Coiled



**BI.** Right side of roof of pallial cavity, male. **BI1.** *Latirus vischii*, prostate as a simple, linear tube (0); **BI2.** *Buccinum undatum*, proboscis coiled (1). **pr:** prostate; **re:** rectum.

Characters 86 to 90 are features of the male reproductive system.

The prostate is, like the seminal vesicle, a modification of the vas deferens that runs on the right side of the roof of the pallial cavity, adjacent to the rectum; it is normally a glandular thickening of the epithelium (Simone, 2011).



**BJ.** Penis and adjacent head-foot in dorsal view. **BJ1.** *Pustulaturus ogum*, duct of penis linear (0); **BJ2.** *Pseudolatirus pallidus*, duct of penis sinuous (1); **BJ3.** *Dolicholatirus cayohuesonicus*, duct of penis convolute (2). **dp:** duct of penis; **he:** head; **pe:** penis.

The prostate in fasciolariids is always a simple tube (0), and a prostate gland is almost inconspicuous in certain species, regardless of sexual maturation. In some outgroup species however, the prostate is visible as a convolution of the vas deferens, somewhat muscular (1). The optimization utilized was ACCTTRAN.



## 86. Penis, duct

(L = 1; Ci = 100; Ri = 100)

- 0. Open
- 1. Closed

Strong (2003) appointed as a synapomorphy of Neogastropoda the prostate that communicates with the mantle cavity via a small duct, *i.e.*, the vas deferens is completely closed without communication with the pallial cavity. In the analysis of Simone (2011) the condition of a closed vas deferens, much like that of the penis, occurred several times independently.

A fully closed system is the plesiomorphic condition here for fasciolarids, and the penis duct is no exception, being closed (1). Only the outgroup species *Monetaria annulus* has this open (0).

## 87. Penis, duct, shape (fig. BJ)

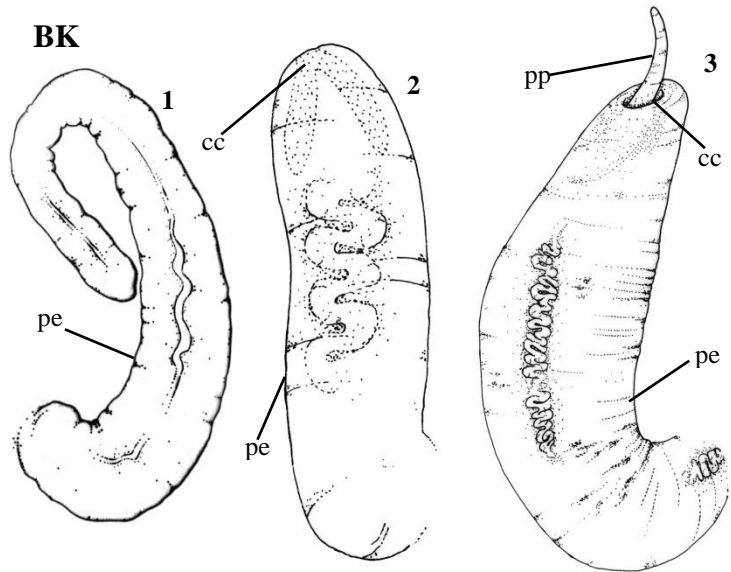
(L = 10; Ci = 20; Ri = 27)

- 0. Linear
- 1. Sinuous
- 2. Convolute

The penis is an exophalic copulatory structure used in the transference of the sperm and/or spermatophore, characteristically positioned at the head-foot, close and posterior to the male right cephalic tentacle and innervated by the pedal ganglia (Ponder & Lindberg, 1997; Simone, 2011). The history of a copulatory organ in the evolution of caenogastropods is a convergent one, with several novelties and losses independently in distinct groups (Strong, 2003; Simone, 2011). The caenogastropod penis differs from those found in heterobranchs because in the former it is permanently exteriorized (exophalic) while in the latter it is retractile (Simone, 2001).

Because of a fully closed male reproductive system, the duct of the penis extends from base to tip, and may occur in several fashions: linear (0), sinuous (1) or convolute *i.e.*, when the curves are tangent to one another (2). This character has been idealized as additive because of the hypothesized increase in the curvature of the duct.

The penis duct is sinuous for most fasciolariids, being this the basal state for the family. In clade 1b the duct is convolute (although because of missing data for *Dolicholaturus* sp. it is impossible to know if this is a synapomorphy for clade 1a). On the other hand, the duct reverted to linear in *Fusinus frenguelli*, *Aurantilaria aurantiaca*, *Pustulaturus ogum* and in clade 14a. The optimization used was DELTRAN.

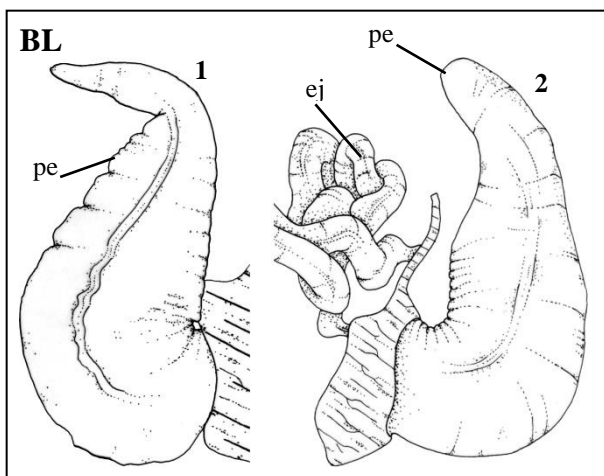


**BK.** Penis. **BK1.** *Leucozonia ocellata*, penis without a pre-copulatory chamber (0); **BK2.** *Dolicholaturus cayohuesonicus*, penis with copulatory chamber bearing short papilla (1); **BK3.** *Pisania pusio*, penis with copulatory chamber bearing long papilla (2). **cc:** pre-copulatory chamber; **pe:** penis; **pp:** penis papilla.

### 88. Penis, pre-copulatory chamber (fig. BK)

(L = 3; Ci = 66; Ri = 50)

- 0. Absent
- 1. Present bearing short papilla
- 2. Present bearing long papilla



**BL.** Penis and section of tegument. **BL1.** *Fusinus frenguelli*, haemocoelic ejaculatory duct absent (0); **BL2.** *Opeatostoma pseudodon*, haemocoelic ejaculatory duct present (1). **ej:** ejaculatory haemocoelic duct; **pe:** penis.

The pre-copulatory chamber is a cavity present at the tip of the penis of certain species and is the preputial-like protection *sensu* Simone (2011). The cavity may house a short papilla (1) or along one (2), in a way that it extends out of the chamber; in most fasciolariids, though, it is absent (0).

Conoideans have a preputial-like protection and a short papilla (Simone, 2011); in the present study the only group in which this occurs is clade 1b with a short papilla (and possibly 1a, if not for the uncertainty in

*Dolicholatirus* sp.); and the outgroup species *Pisania pusio* with a long papilla. As with the previous character, the optimization utilized was DELTRAN.

### 89. Ejaculatory haemocoel duct (fig. BL)

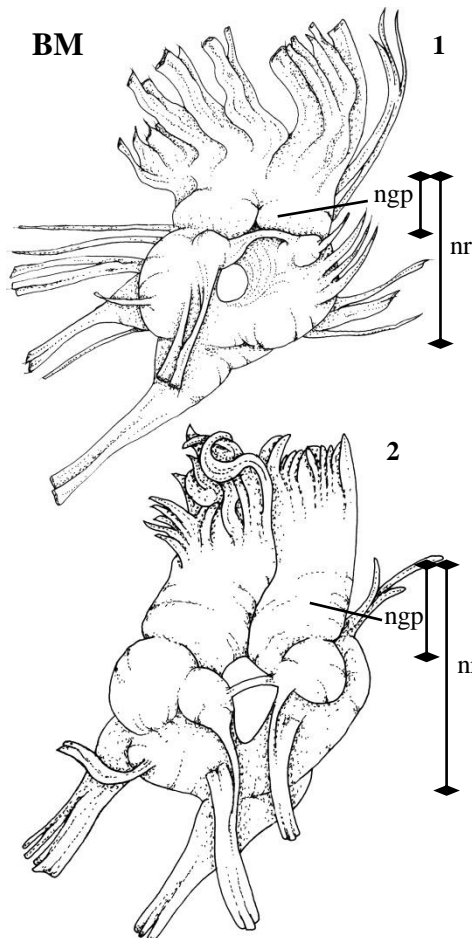
(L = 3; Ci = 33; Ri = 0)

0. Absent

1. Present

The Ejaculatory tube is a long, convoluted muscular portion of the pallial vas deferens immersed in the haemocoelic spaces, on the right side, and protruding into pallial floor. This has been

observed as a synapomorphy of the Conoidea by Simone (2011). This highly homoplastic character (1) occurs in two fascioliids independently, in *Pseudolatirus pallidus* and *Opeatostoma pseudodon*; all other fascioliids lack this structure (0).



**BM.** Nerve ring in dorsal view. **BM1.** *Fusinus* sp. pedal ganglia length is less than 1/2 of total nerve ring length (0); **BM2.** *Filifusus filamentosus*, pedal ganglia length is 1/2 or greater than total nerve ring length (1). **ngp:** pedal ganglion; **nr:** nerve ring.

### 90. Pedal ganglia, length: length of nerve ring (fig. BM)

(L = 2; Ci = 20; Ri = 50)

0. Less than 1/2

1. 1/2 or greater

Much emphasis has been given in the configuration of the nervous system of higher gastropod classification, as reflected in names *e.g.*, Streptoneura, Euthyneura, (Taylor & Sohl, 1962), Triganglionata and Pentaganglionata (Salvini-Plawén & Haszprunar, 1987); much like the gill and radulae (Ponder & Lindberg, 1997).

The central nervous system is located posteriorly of the buccal mass in caenogastropods, and it

corresponds to the nerve ring in the examined taxa. This circumesophageal (*i.e.*, surrounds the esophagus) nerve ring in caenogastropods is in an epiathroid condition in which the pair of pleural ganglia is located closer to the cerebral and far from the pedals, a condition that is convergent with heterobranchs, although much more concentrated in the former group (Strong, 2003; Simone, 2011). It appears that nervous system characters, while useful, should be used with caution in defining major taxonomic divisions (Ponder & Lindberg, 1997; Strong, 2003; Simone, 2011).

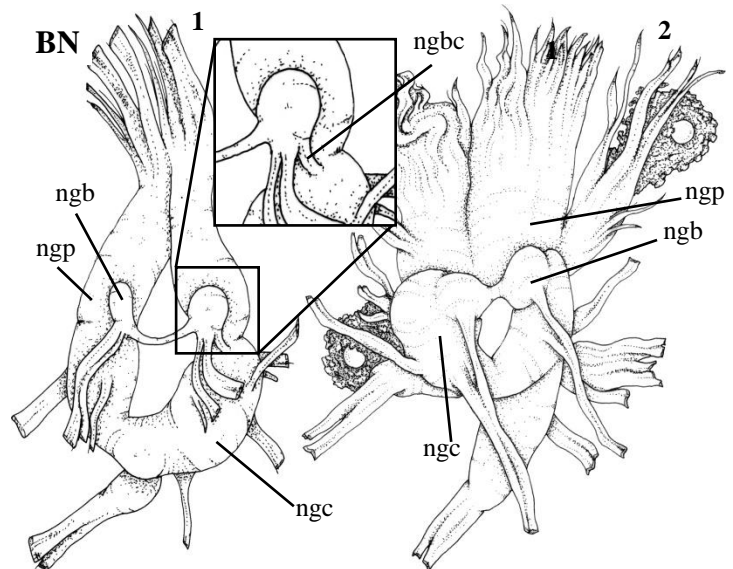
Caenogastropods have a nervous system that is concentrated with well-defined cerebral and pedal ganglia (Ponder *et al.*, 2008). Despite the trend, in Gastropoda in general, for the concentration of ganglia in the nerve ring, the pedal ganglia are one of the few that are undoubtedly distinguishable. Fascioliariids have as a synapomorphy the ratio between the length of the pedal ganglia by the total length of the nerve ring equal to 1/2 or greater (1). For some taxa however, there was a reversion to the previous state of a proportion of less than 1/2 (0): In clades 3c<sup>1</sup> and in *Leucozonia ponderosa*. An ACCTTRAN optimization was used here.

### 91. Buccal ganglia, position (fig. BN)

(L = 2; Ci = 100; Ri = 100)

0. Close to buccal mass
1. On nerve ring
2. Immersed in nerve ring

The presence of short buccal connectives is the plesiomorphic condition for Caenogastropoda (Simone, 2011), but most groups have long connectives (probably due to the tendency for the buccal ganglia to be situated far from the nerve ring). The



**BN.** Nerve ring in dorsal view. **BN1.** *Buccinum undatum*, buccal connective observed (char. 92: 1), buccal ganglia dorsal to pedal ganglia (char. 93: 0); **BN2.** *Hemipolygona beckyae*, buccal connective not observed (char. 92: 2), buccal ganglia dorsal to cerebral ganglia (char. 93: 1). **ngb:** buccal ganglion; **ngbc:** buccal ganglion commissure; **ngc:** cerebral ganglion; **ngp:** pedal ganglion.

muricoideans (*i.e.*, also included here the buccinoideans *sensu* Simone, 2011) have reverted to the plesiomorphic condition, possessing buccal ganglia closer to, or even incorporated into the nerve

ring (Simone, 2011). This is the scenario observed here, with very short connectives that are strongly associated with the adjacent ganglia

This is the scenario observed for all studied taxa, including the buccinoideans (but not the cypraeoidean species *Monetaria annulus*, in which the buccal ganglia is not incorporated in the nerve ring [0]). The buccal ganglia are visible as a bulge in the nerve ring, and several degrees of fusion with the adjacent pedal/cerebro ganglia are observed: The buccal ganglia may rest dorsally in the nerve ring but its connectives are still observable (1); or the buccal ganglia are firmly attached, dorsally to the nerve ring and its connectives are not visible (2). The latter state was observed solely and for all fasciolarids, and it is a synapomorphy.

**92. Buccal ganglia, position in nerve ring (fig. BN)**

(L = 1; Ci = 100; Ri = 100)

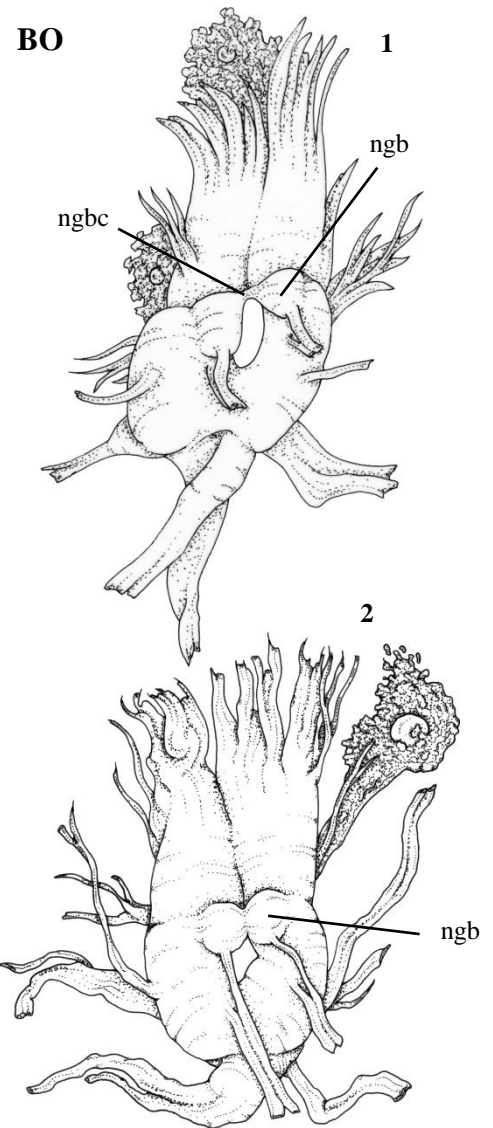
- 0. Dorsal to pedal ganglia
- 1. Dorsal to cerebral ganglia

The topological optimization of this character is strictly associated with the previous character (character 91), due to the fact that when the buccal ganglia is immersed in the nerve ring (in the sense that the connectives aren't visible), its position is always dorsal to the cerebral (1) ganglia; as opposed to dorsal to the pedal ganglia (0). The former state is a synapomorphy to the fasciolarids.

**93. Buccal ganglia, commissure (fig. BO)**

(L = 7; Ci = 14; Ri = 33)

- 0. Conspicuous
- 1. Inconspicuous



**BO.** Nerve ring in dorsal view. **BO1.** *Leucozonia ponderosa* buccal ganglia commissure conspicuous (0); **BO2.** *Pustulaturus ogum*, buccal commissure inconspicuous (1). **ngb:** buccal ganglion; **ngbc:** buccal ganglia commissure.

The buccal ganglia commissure is the only visible commissure in the highly concentrated nerve ring of fasciolariids (and the buccinoideans studied). The fact that the degree of concentration of ganglia in the nerve ring is associated with the degree of dilatation of the esophagus (which passes through it) (Simone, 2011) suggests that this character is associated with the alimentary habits of the animal. This means that predatory carnivorous that ingest the prey whole have a longer commissure, or that the animal had just ingested on the moment it was killed. It is not certain if this holds true for this level of phylogenetic analysis, but in greater groups this has been observed (*e.g.*, Calyptraeidea: Simone, 2011).

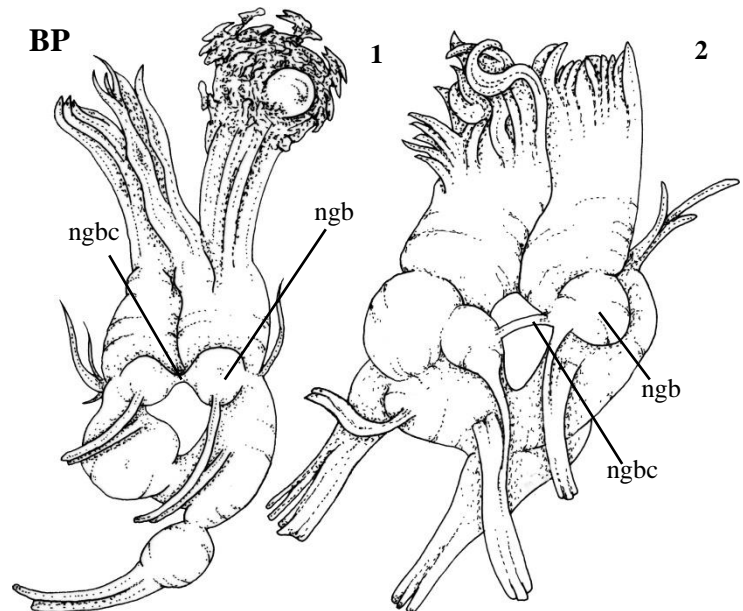
In Fasciolariidae, the buccal commissure is conspicuous (0), with several groups having reduced the distance between the buccal ganglia and the commissure was internalized (1). The latter scenario occurred for clades 1a, 2c (*Amiantofusus*), 8a (*Pustulaturus*), *Peristernia marquesana*, *Hemipolygona armata*, *Polygona angulata*, *P. infundibulum* and *Leucozonia ocellata*. This highly homoplastic character was optimized under an ACCTRAN optimization.

**94. Buccal ganglia, commissure, length: buccal ganglia length (fig. BP)**

(L = 8; Ci = 12; Ri = 46)

- 0. Less than 1/2
- 1. 1/2 or greater

On the fasciolariid taxa in which a buccal commissure occurs, this character measures their length by the total length of the buccal ganglia. This is the ratio of the commissure by the length of the buccal ganglion. As discussed in the previous character (character 93), this may be related to the alimentary habits of the animal Fasciolariids have this proportion of less than 1/2 (0), and several increases in the



**BP.** Nerve ring in dorsal view. **BP1.** *Granulifusus* sp. short buccal commissure, less than 1/2 the total length of the buccal ganglia (0); **BP2.** *Filifusus filamentosus*, long buccal commissure, 1/2 or greater than the total length of the buccal ganglia (1). **ngb:** buccal ganglion; **ngbc:** buccal ganglia commissure.

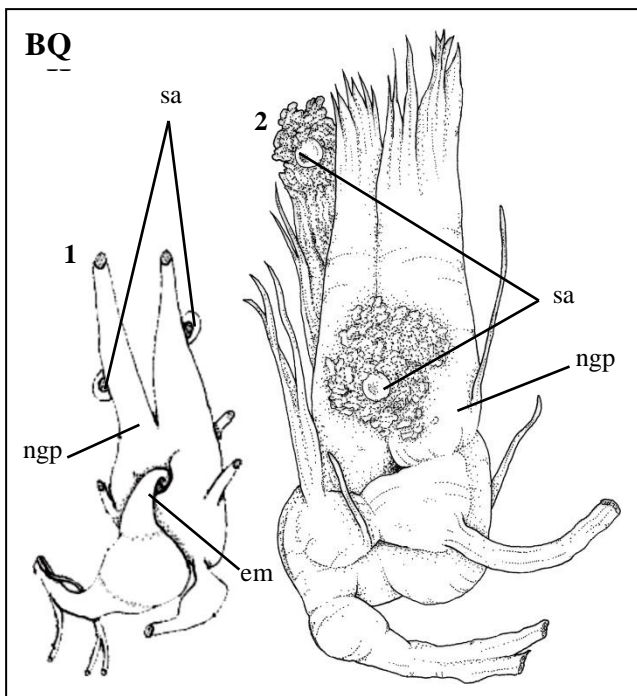
length to 1/2 or greater (1) occurred: on clades 3c of *Fusinus* (*Cyrtulus serotinus* reverting to the

previous state), 6a, of the fascioliariines and *Nodolatirus nodatus* and in *Leucozonia cerata*. An ACCTRAN was used for optimization.

### 95. Statocysts (fig. BQ)

(L = 2; Ci = 50; Ri = 80)

- 0. Both anterior
- 1. Anterior and posterior



**BQ.** Nerve ring. **BQ1.** *Teralatirus roboreus* (modified from Simone *et al.*, 2013), dorsal view showing both statocysts located anteriorly (0); **BQ2.** *Polygona angulata*, ventral view showing statocysts positioned asymmetrically (1). **em:** mid-esophagus; **ngp:** pedal ganglion; **sa:** statocyst.

Statocysts are structures responsible for the balance and positioning of gastropods. It consists of hollow vesicles covered internally by sensitive cells, which have one statolith or several staconia within; due to gravity, these objects tend to stay at the bottom of the vesicle, which is then detected for equilibrium purposes (Simone, 2011). Haszprunar (1988) assumed it to be a synapomorphy of conchiferan mollusks based on their positioning and formation.

The statocyst is innervated by the cerebral ganglia but associated with the pedal ganglia (Ponder & Lindberg, 1997; Simone, 2011); it is immersed in the musculature of the foot and connected with the nerve ring by narrow nerves (Simone, 2011). Statocysts in

the Hypsgastropoda (*sensu* Ponder & Lindberg, 1997: “higher caenogastropods”) bear a single statolith, as opposed to many staconia as opposed to many staconia in archeogastropods and heterobranchs (Simone, 2011)

The Neogastropod statocysts are ventral in position (Strong, 2003) associated with the pedal gland, however, in some cases there may be some slight asymmetry between the right and left sides (Strong, 2003). Most fascioliariids have an asymmetry in the positioning of the



statocysts in the nerve ring: the left is positioned more posteriorly in the nerve ring, more closely related to the cerebral ganglia (1). However, for all outgroup taxa except *Pisania pusio*, and for the fasciolariid *Teralatirus roboreus*, the statocysts are symmetrical, and anteriorly positioned (0).

7.1 Character matrix

TAXON	CHARACTER																		
	0	0	0	0	0	0	0	0	0	1	1	1	1	1	1	1	1	1	1
<i>Monetaria annulus</i>	0	0	0	0	0	0	0	0	0	0	0	0	0	0	0	0	-	-	0
<i>Thais speciosa</i>	1	1	1	0	0	1	0	0	0	1	?	0	0	0	0	1	0	1	0
<i>Pugilina tupiniquim</i>	1	1	1	0	0	1	1	0	1	1	0	0	0	0	0	1	0	1	1
<i>Nassarius reticulatus</i>	1	1	0	0	0	0	0	0	0	0	?	0	2	0	1	1	0	0	1
<i>Bullia laevis</i>	1	1	0	0	0	0	0	0	0	0	0	0	1	1	1	1	0	0	0
<i>Pisania pusio</i>	1	0	1	1	0	0	1	0	1	0	0	0	1	1	0	1	0	1	0
<i>Engoniophos uncinatus</i>	1	1	1	0	0	0	0	0	0	0	0	0	0	0	0	1	0	1	0
<i>Buccinum undatum</i>	1	1	1	0	0	1	0	0	0	0	0	0	2	1	0	1	0	0	1
<i>Teralatirus roboreus</i>	1	1	0	0	0	1	1	1	1	1	?	1	1	1	0	1	0	1	1
<i>Dolicholatirus aff. cayohuesonicus</i>	1	1	0	0	0	1	1	1	1	1	?	1	1	1	0	1	0	1	1
<i>Dolicholatirus sp.</i>	1	1	0	0	0	1	1	0	0	1	?	?	?	?	?	?	?	?	?
<i>Angulofusus netae</i>	1	1	1	2	0	1	1	1	1	0	1	1	0	0	0	1	0	1	1
<i>Amiantofusus pacificus</i>	1	1	1	0	0	1	0	0	1	0	?	1	0	0	0	1	0	1	0
<i>Amiantofusus candoris</i>	1	1	1	0	0	1	0	0	1	0	?	1	0	0	0	1	0	1	0
<i>Pseudolatirus kuroseanus</i>	1	1	1	0	0	1	0	0	1	0	?	1	2	2	0	?	?	?	0
<i>Pseudolatirus discrepans</i>	1	1	1	0	0	1	0	1	2	0	?	1	0	0	0	?	?	?	0
<i>Granulifusus aff. kiranus</i>	1	1	1	0	0	1	0	0	2	0	?	1	2	2	0	2	1	0	0
<i>Granulifusus hayashi</i>	1	1	1	0	0	1	0	0	2	0	?	1	2	2	0	2	1	0	0
<i>Granulifusus sp.</i>	1	1	1	0	0	1	0	0	2	0	?	1	2	2	0	2	1	0	0
<i>Pseudolatirus pallidus</i>	1	1	1	0	0	1	1	0	2	0	?	1	0	0	0	?	?	?	0
<i>Chryseofusus acherusius</i>	1	1	0	0	0	1	0	0	2	0	?	1	0	0	0	1	0	1	0
<i>Chryseofusus graciliformis</i>	1	1	0	0	0	1	0	0	2	0	?	1	2	2	0	1	0	1	0
<i>Fusinus australis</i>	1	1	1	0	0	1	1	0	2	0	1	1	1	1	0	1	0	1	0
<i>Cyrtulus serotinus</i>	1	1	1	0	0	0	1	0	2	0	?	1	1	1	0	?	?	?	0
<i>Fusinus frenguelli</i>	1	1	1	0	0	1	0	0	2	0	?	1	0	0	0	1	0	1	0
<i>Fusinus brasiliensis</i>	1	1	1	0	0	1	0	0	2	0	1	1	0	0	0	1	0	1	0
<i>Fusinus marmoratus</i>	1	1	1	0	0	1	0	0	2	0	1	1	1	1	0	1	0	1	0
<i>Fusinus sp.</i>	1	1	1	0	0	1	0	0	2	0	?	1	1	1	0	1	0	1	0
<i>Fusolatirus bruijnii</i>	1	1	0	0	0	1	1	1	2	1	3	1	0	0	0	1	0	2	0
<i>Peristernia marquesana</i>	1	1	1	0	0	1	1	1	1	1	?	1	0	0	0	1	0	2	1
<i>Peristernia nassatula</i>	1	1	1	0	0	1	1	1	1	1	3	1	0	0	0	1	0	2	0
<i>Pustulatirus mediamericus</i>	1	1	1	0	0	1	2	1	1	1	?	1	1	1	0	1	0	2	?
<i>Pustulatirus ogum</i>	1	1	1	0	0	1	2	1	1	1	?	1	1	1	0	1	0	2	1
<i>Latirus polygonus</i>	1	1	1	0	0	1	2	1	1	1	3	1	1	1	0	1	0	2	0
<i>Nodolatirus nodatus</i>	1	1	1	0	0	1	1	1	2	1	3	1	1	1	0	1	0	2	0
<i>Hemipolygona beckya</i>	1	1	1	0	0	1	2	1	1	1	?	1	0	0	0	1	0	2	0
<i>Hemipolygona armata</i>	1	1	1	0	0	1	2	1	1	1	?	1	1	1	0	1	0	2	0
<i>Latirus vischii</i>	1	1	1	0	0	1	1	1	2	1	?	1	1	1	0	?	?	?	?
<i>Australaria australasia</i>	1	0	1	0	0	1	1	1	1	0	3	1	0	0	0	1	0	2	0
<i>Pleuroploca trapezium</i>	1	0	1	0	0	1	1	1	1	0	3	1	0	0	0	1	0	2	0
<i>Filifusus filamentosus</i>	1	0	0	0	0	1	1	1	1	0	3	1	0	0	0	1	0	2	1
<i>Aurantilaria aurantiaca</i>	1	0	1	0	0	1	1	1	1	0	2	1	1	1	0	1	0	2	1
<i>Fasciolaria tulipa</i>	1	0	0	0	0	1	1	1	1	0	3	1	1	1	0	1	0	2	0
<i>Polygona infundibulum</i>	1	1	1	0	0	1	2	1	1	1	?	1	0	0	0	?	?	?	?
<i>Polygona angulata</i>	1	1	1	0	0	1	2	1	1	1	?	1	1	1	0	1	0	2	0
<i>Latirus pictus</i>	1	1	1	0	0	1	2	1	1	1	3	1	0	0	0	?	?	?	0
<i>Leucozonia ocellata</i>	1	1	1	0	0	1	2	1	1	1	3	1	0	0	0	1	0	2	0
<i>Leucozonia cerata</i>	1	1	1	0	0	1	2	1	1	1	3	1	0	0	0	1	0	2	0
<i>Leucozonia nassa nassa</i>	1	1	1	0	2	1	2	1	1	1	3	1	1	1	0	1	0	2	1
<i>Leucozonia nassa cingulifera</i>	1	1	1	0	2	1	2	1	1	1	3	1	1	1	0	1	0	2	1
<i>Leucozonia nassa brasiliensis</i>	1	1	1	0	2	1	2	1	1	1	3	1	1	1	0	1	0	2	1
<i>Leucozonia ponderosa</i>	1	1	1	0	2	1	2	1	1	1	3	1	1	1	0	1	0	2	1
<i>Opeatostoma pseudodon</i>	1	1	0	0	1	1	2	1	1	1	3	1	0	0	0	1	0	2	0

TAXON	CHARACTER	2	2	2	2	2	2	2	2	2	2	3	3	3	3	3	3	3	3	3		
		0	1	2	3	4	5	6	7	8	9	0	1	2	3	4	5	6	7	8	9	
<i>Monetaria annulus</i>		0	0	0	0	0	0	0	0	0	0	0	0	0	0	0	0	0	0	0	0	
<i>Thais speciosa</i>		1	1	1	0	0	0	0	1	1	1	0	0	1	1	0	0	0	0	0	0	0
<i>Pugilina tupiniquim</i>		1	1	1	0	0	0	1	1	1	1	0	0	1	1	0	0	0	0	1	0	0
<i>Nassarius reticulatus</i>		1	1	1	0	0	0	0	1	2	1	0	0	1	1	0	0	0	0	1	1	1
<i>Bullia laevissima</i>		1	1	1	0	0	0	0	1	2	1	0	0	1	1	0	0	0	0	1	1	1
<i>Pisania pusio</i>		1	1	1	0	0	0	1	1	1	1	0	0	1	1	0	0	0	0	0	0	0
<i>Engoniophos uncinatus</i>		1	1	1	0	0	0	0	1	1	1	0	0	1	1	0	0	0	0	0	0	0
<i>Buccinum undatum</i>		1	1	1	0	0	0	0	1	2	1	0	0	1	1	0	1	0	0	1	0	0
<i>Teralatirus roboreus</i>		1	1	1	0	0	?	?	1	0	1	0	0	1	1	?	?	?	0	1	0	0
<i>Dolicholatirus aff. cayohuesonicus</i>		1	1	1	0	0	0	1	1	0	1	0	0	1	1	0	0	0	0	1	0	0
<i>Dolicholatirus sp.</i>		?	?	?	?	?	?	?	?	?	?	?	?	?	?	?	?	?	?	?	?	?
<i>Angulofusus nedae</i>		1	1	1	1	0	?	1	1	1	1	0	?	1	?	?	?	?	0	?	?	?
<i>Amiantofusus pacificus</i>		1	1	1	?	?	?	?	?	?	?	0	1	1	1	?	?	?	0	1	1	1
<i>Amiantofusus candoris</i>		1	1	1	2	0	0	1	1	1	1	0	1	1	1	?	?	?	0	1	0	0
<i>Pseudolatirus kuroseanus</i>		1	1	1	2	0	0	1	1	0	?	0	0	1	1	?	?	?	0	1	0	0
<i>Pseudolatirus discrepans</i>		1	1	1	2	0	0	1	1	0	1	1	0	1	1	1	0	0	0	1	1	1
<i>Granulifusus aff. kiranus</i>		1	1	1	2	0	0	1	1	0	1	1	0	1	1	1	0	0	0	1	1	1
<i>Granulifusus hayashi</i>		1	1	1	2	0	0	1	1	0	1	0	0	1	1	1	0	0	0	1	1	1
<i>Granulifusus sp.</i>		1	1	1	2	0	0	1	1	0	1	0	0	1	1	1	?	0	0	1	1	1
<i>Pseudolatirus pallidus</i>		1	1	1	2	0	0	1	1	1	1	0	0	1	1	?	?	?	0	1	1	1
<i>Chryseofusus acherusius</i>		1	1	1	2	0	0	1	1	1	1	0	1	1	1	?	?	?	0	1	0	0
<i>Chryseofusus graciliformis</i>		1	1	1	2	0	0	1	1	1	1	0	1	1	1	1	?	?	0	1	1	1
<i>Fusinus australis</i>		1	1	1	1	0	1	1	1	0	1	0	0	1	1	1	0	0	0	1	1	1
<i>Cyrtulus serotinus</i>		1	1	1	1	0	1	1	1	0	1	0	0	1	1	1	0	0	0	1	1	1
<i>Fusinus frenguelli</i>		1	1	1	1	0	1	1	1	0	1	0	0	1	1	1	0	0	0	1	1	1
<i>Fusinus brasiliensis</i>		1	1	1	1	0	0	1	1	0	1	0	0	1	1	0	?	0	0	1	1	1
<i>Fusinus marmoratus</i>		1	1	1	1	0	0	1	1	0	1	0	0	1	1	0	?	0	0	1	1	1
<i>Fusinus sp.</i>		1	1	1	?	?	?	?	?	?	?	0	0	1	?	?	?	?	0	1	1	1
<i>Fusolatirus bruijnii</i>		1	1	1	1	0	0	1	1	0	1	0	0	1	?	?	?	?	0	1	1	1
<i>Peristernia marquesana</i>		1	1	1	1	0	0	1	1	0	1	0	0	1	?	?	?	?	0	1	1	1
<i>Peristernia nassatula</i>		1	1	1	1	0	0	1	1	0	1	0	0	1	?	?	?	?	0	1	1	1
<i>Pustulatirus mediamericus</i>		1	1	1	1	0	0	1	1	0	1	0	0	1	?	?	?	?	0	0	1	1
<i>Pustulatirus ogum</i>		1	1	1	1	0	0	1	1	0	1	0	0	1	1	1	0	0	0	1	1	1
<i>Latirus polygonus</i>		1	1	1	1	0	0	1	1	0	1	0	0	1	1	0	1	0	0	0	1	1
<i>Nodolatirus nodatus</i>		1	1	1	1	0	0	1	1	0	1	0	0	1	1	1	0	0	0	1	1	1
<i>Hemipolygona beckyae</i>		1	1	?	?	?	?	?	?	?	?	0	0	1	1	?	?	?	0	2	1	1
<i>Hemipolygona armata</i>		1	1	1	1	0	0	1	1	0	1	0	0	1	1	1	0	0	0	0	1	1
<i>Latirus vischii</i>		1	1	1	1	0	0	1	1	0	1	0	0	1	?	?	?	?	0	0	1	1
<i>Australaria australasia</i>		1	1	1	1	1	0	1	1	0	1	0	0	1	1	1	0	1	0	0	1	1
<i>Pleuroploca trapezium</i>		1	1	1	1	0	0	1	1	0	1	0	0	1	1	1	0	1	0	0	1	1
<i>Filifusus filamentosus</i>		1	1	1	1	0	0	1	1	2	1	0	0	1	?	?	?	?	0	0	1	1
<i>Aurantilaria aurantiaca</i>		1	1	1	1	1	0	1	1	0	1	0	0	1	1	1	0	1	0	0	1	1
<i>Fasciolaria tulipa</i>		1	1	1	1	0	0	1	1	0	1	0	0	1	1	1	0	1	0	0	1	1
<i>Polygona infundibulum</i>		1	1	1	1	0	?	?	1	0	1	0	0	1	?	?	?	?	0	1	1	1
<i>Polygona angulata</i>		1	1	1	1	0	0	1	1	0	1	0	0	1	1	0	0	0	0	0	1	1
<i>Latirus pictus</i>		1	1	1	1	0	0	1	1	0	1	0	0	1	1	1	1	0	0	0	1	1
<i>Leucozonia ocellata</i>		1	1	1	2	0	0	1	1	2	1	1	0	1	1	0	1	0	1	0	0	0
<i>Leucozonia cerata</i>		1	1	1	1	0	0	1	1	2	1	1	0	1	?	?	0	?	1	0	0	0
<i>Leucozonia nassa nassa</i>		1	1	1	1	0	0	1	1	2	1	0	0	1	1	0	1	0	0	0	0	0
<i>Leucozonia nassa cingulifera</i>		1	1	1	1	0	0	1	1	2	1	0	0	1	1	0	1	0	0	0	0	0
<i>Leucozonia nassa brasiliana</i>		1	1	1	1	0	0	1	1	2	1	0	0	1	1	0	1	0	0	0	0	0
<i>Leucozonia ponderosa</i>		1	1	1	1	0	0	1	1	2	1	0	0	1	1	0	1	0	0	0	0	0
<i>Opeatostoma pseudodon</i>		1	1	1	1	0	0	0	1	2	1	0	0	1	1	1	0	1	0	0	0	0

TAXON	CHARACTER	5	5	5	5	5	5	5	5	5	5	6	6	6	6	6	6	6	6	6	
		0	1	2	3	4	5	6	7	8	9	0	1	2	3	4	5	6	7	8	9
<i>Monetaria annulus</i>		0	2	0	0	0	0	0	0	0	0	0	0	0	0	0	0	0	0	0	
<i>Thais speciosa</i>		0	2	1	0	1	0	0	0	0	0	0	-	-	-	0	0	0	0	1	0
<i>Pugilina tupiniquim</i>		0	1	0	1	1	1	0	0	0	1	0	1	0	0	0	0	0	0	0	0
<i>Nassarius reticulatus</i>		0	4	0	0	1	1	0	0	0	1	0	1	0	0	1	0	0	0	0	0
<i>Bullia laevissima</i>		0	4	0	0	1	1	0	0	0	1	0	1	0	0	1	0	0	0	1	0
<i>Pisania pusio</i>		0	2	1	1	1	1	0	0	0	0	0	1	0	0	1	0	0	0	1	1
<i>Engoniophos uncinatus</i>		0	4	0	0	1	1	0	0	0	1	0	1	0	0	0	0	0	0	0	0
<i>Buccinum undatum</i>		0	4	0	0	1	1	0	0	0	0	0	1	0	0	1	0	0	0	1	1
<i>Teralatirus roboreus</i>		?	?	?	?	0	0	1	0	0	0	0	-	-	0	1	0	1	0	1	0
<i>Dolicholatirus aff. cayohuesonicus</i>		0	0	1	0	0	0	1	0	0	0	0	-	-	0	1	0	1	1	0	0
<i>Dolicholatirus sp.</i>		0	0	1	0	0	1	1	0	0	0	0	-	-	0	1	?	?	?	?	?
<i>Angulofusus nedae</i>		1	2	0	3	0	2	0	0	1	1	1	0	0	0	0	0	1	1	1	0
<i>Amiantofusus pacificus</i>		1	2	0	3	0	2	0	0	1	0	1	0	0	0	0	0	1	1	0	0
<i>Amiantofusus candoris</i>		1	2	0	3	0	2	0	0	1	0	1	0	0	0	0	0	1	1	0	0
<i>Pseudolatirus kuroseanus</i>		1	2	0	3	0	2	0	0	1	0	1	0	0	0	0	0	1	1	1	0
<i>Pseudolatirus discrepans</i>		1	2	0	2	0	3	0	0	2	0	1	0	0	0	0	0	1	1	0	0
<i>Granulifusus aff. kiranus</i>		1	2	0	2	0	3	0	0	2	0	1	0	0	0	0	0	1	1	0	0
<i>Granulifusus hayashi</i>		0	2	0	2	0	3	0	0	2	0	1	0	0	0	0	0	1	1	0	0
<i>Granulifusus sp.</i>		1	2	0	2	0	3	0	0	2	0	1	0	0	0	0	0	1	1	1	0
<i>Pseudolatirus pallidus</i>		2	2	0	2	0	3	0	0	2	0	1	0	0	0	0	1	1	1	0	0
<i>Chryseofusus acherusius</i>		2	2	0	2	0	3	0	0	2	1	1	0	0	0	0	1	1	1	1	0
<i>Chryseofusus graciliformis</i>		2	2	0	2	0	3	0	0	2	1	1	0	0	0	0	1	1	1	1	0
<i>Fusinus australis</i>		2	2	0	2	0	3	0	0	2	1	1	0	0	1	0	1	1	1	0	0
<i>Cyrtulus serotinus</i>		2	2	0	2	0	3	0	0	2	1	1	0	0	1	0	1	1	1	1	0
<i>Fusinus frenguelli</i>		1	2	1	2	0	3	0	0	2	1	1	0	0	1	0	1	1	1	1	0
<i>Fusinus brasiliensis</i>		2	2	0	2	0	3	0	0	2	1	1	0	0	1	0	1	1	1	1	0
<i>Fusinus marmoratus</i>		2	2	0	2	0	3	0	0	2	1	1	0	0	1	0	1	1	1	1	0
<i>Fusinus sp.</i>		1	2	0	2	0	3	0	0	2	1	1	0	0	1	0	1	1	1	1	0
<i>Fusolatirus bruijnii</i>		1	2	0	2	0	3	0	1	2	1	1	0	0	1	0	1	1	1	1	0
<i>Peristernia marquesana</i>		2	2	0	3	0	4	0	1	2	1	1	0	0	1	0	1	1	1	1	0
<i>Peristernia nassatula</i>		2	3	0	2	0	4	0	1	2	1	1	0	0	1	0	1	1	1	1	0
<i>Pustulatirus mediamericus</i>		0	3	0	2	0	4	0	0	2	1	1	0	0	0	0	0	1	0	0	1
<i>Pustulatirus ogum</i>		0	3	0	2	0	4	0	0	2	1	1	0	0	0	0	0	1	0	0	1
<i>Latirus polygonus</i>		0	2	0	3	0	4	0	0	2	1	1	0	0	0	0	0	1	1	1	1
<i>Nodolatirus nodatus</i>		0	2	0	2	0	4	0	0	3	1	1	0	0	0	0	0	1	1	1	1
<i>Hemipolygona beckyae</i>		0	2	0	2	0	3	0	0	2	1	1	0	0	0	0	0	1	1	0	1
<i>Hemipolygona armata</i>		0	2	0	2	0	3	0	0	2	1	1	0	0	0	0	0	1	1	0	1
<i>Latirus vischii</i>		0	2	0	3	0	4	0	0	3	1	2	0	0	0	0	0	1	1	1	1
<i>Australaria australasia</i>		0	2	0	3	0	4	0	0	2	1	2	0	0	0	0	0	1	1	0	1
<i>Pleuroploca trapezium</i>		0	2	0	3	0	4	0	0	3	1	2	0	0	0	0	0	1	1	0	1
<i>Filifusus filamentosus</i>		0	2	1	3	0	4	0	0	3	1	2	0	0	0	0	0	1	1	0	1
<i>Aurantilaria aurantiaca</i>		1	2	1	3	0	4	0	0	3	1	2	0	0	0	0	0	1	1	0	1
<i>Fasciolaria tulipa</i>		1	2	0	3	0	4	0	0	3	1	2	0	0	0	0	0	1	1	0	1
<i>Polygona infundibulum</i>		0	2	1	2	0	3	0	0	2	1	1	0	0	0	0	0	1	1	1	1
<i>Polygona angulata</i>		0	2	0	2	0	3	0	0	2	1	1	0	0	0	0	0	1	1	1	1
<i>Latirus pictus</i>		0	2	0	3	0	3	0	0	2	1	1	0	0	0	0	0	1	1	0	1
<i>Leucozonia ocellata</i>		0	2	0	2	0	3	0	0	1	1	2	1	1	0	0	0	1	1	0	1
<i>Leucozonia cerata</i>		0	2	0	2	0	3	0	0	2	1	2	1	0	0	0	0	1	1	0	1
<i>Leucozonia nassa nassa</i>		0	2	0	2	0	3	0	0	2	1	2	1	1	0	0	0	1	1	0	1
<i>Leucozonia nassa cingulifera</i>		0	2	0	2	0	3	0	0	2	1	2	1	1	0	0	0	1	1	0	1
<i>Leucozonia nassa brasiliana</i>		0	2	0	2	0	3	0	0	2	1	2	1	1	0	0	0	1	1	0	1
<i>Leucozonia ponderosa</i>		0	2	0	2	0	3	0	0	2	1	2	1	1	0	0	0	1	1	0	1
<i>Opeatostoma pseudodon</i>		0-1-2	4	0	1-2	0	3	0	0	2	?	2	1	0	0	0	0	1	1	0	1

TAXON	CHARACTER	7	7	7	7	7	7	7	7	7	8	8	8	8	8	8	8	8	8	9	9	9	9	9	9					
		0	1	2	3	4	5	6	7	8	9	0	1	2	3	4	5	6	7	8	9	0	1	2	3	4	5			
<i>Monetaria annulus</i>		0	0	-	0	0	0	0	0	0	0	0	0	-	-	0	0	0	0	0	0	0	0	0	0					
<i>Thais speciosa</i>		0	1	0	1	0	2	1	0	? ?	? ? ? ? ?	0	1	1	0	1	0	1	0	1	0	1	0	0	1	0				
<i>Pugilina tupiniquim</i>		0	0	-	2	0	1	1	0	0	-	-	-	1	0	0	0	1	1	0	0	0	0	1	0	- ?				
<i>Nassarius reticulatus</i>		0	1	0	1	0	?	1	1	1	-	-	-	0	-	-	?	?	?	?	?	?	1	1	0	0	0	0		
<i>Bullia laevis</i>		0	0	-	1	2	1	1	0	0	-	-	-	1	0	1	?	1	0	0	0	0	0	1	0	?	?	0		
<i>Pisania pusio</i>		1	1	0	1	0	1	1	1	1	1	0	0	1	0	1	1	1	2	2	0	0	0	1	0	0	1	1		
<i>Engoniophos uncinatus</i>		0	1	0	1	2	?	1	0	0	-	-	-	1	0	1	0	1	0	0	0	0	0	1	0	0	1	0		
<i>Buccinum undatum</i>		0	1	0	1	0	1	1	1	1	1	0	1	1	0	0	1	1	2	0	0	0	1	1	0	0	1	?		
<i>Teralatirus roboreus</i>		?	1	?	0	0	2	1	1	?	1	?	?	?	?	1	0	1	2	1	0	0	1	2	1	1	-	0		
<i>Dolicholatirus aff. cayohuesonicus</i>		?	1	0	1	0	2	1	1	?	?	?	?	1	0	1	0	1	2	1	0	0	1	2	1	1	0	1		
<i>Dolicholatirus sp.</i>		?	?	?	?	?	?	?	?	?	?	?	?	?	?	?	?	?	?	?	?	?	?	?	?	?	?	?	?	
<i>Angulofusus neda</i>		1	1	0	1	?	2	1	1	?	?	?	?	?	?	?	?	?	?	?	?	?	?	?	?	?	?	?	?	
<i>Amiantofusus pacificus</i>		1	1	0	1	?	2	1	1	?	1	?	?	?	?	?	0	1	1	0	?	?	?	?	?	?	?	?	?	
<i>Amiantofusus candoris</i>		1	1	0	1	?	?	1	1	?	1	?	?	?	?	?	?	?	?	?	?	?	?	?	?	?	?	?	?	
<i>Pseudolatirus kuroseanus</i>		1	1	0	1	0	?	1	1	?	1	?	?	?	?	?	0	1	1	0	?	?	?	?	?	?	?	?	?	
<i>Pseudolatirus discrepans</i>		1	1	0	1	0	?	1	1	0	1	1	0	0	-	-	?	?	?	?	?	?	?	?	?	?	?	?	?	
<i>Granulifusus aff. kiranus</i>		1	1	0	1	0	?	1	1	?	1	?	?	?	0	-	-	0	1	1	0	0	0	1	1	0	0	1	1	
<i>Granulifusus hayashi</i>		1	1	0	1	0	?	1	1	0	1	1	0	0	-	-	?	?	?	?	?	?	?	?	?	?	?	?	?	
<i>Granulifusus sp.</i>		1	1	0	1	0	?	1	0	1	1	1	1	0	-	-	?	?	?	?	?	?	?	?	?	?	?	?	?	
<i>Pseudolatirus pallidus</i>		1	1	0	1	0	2	1	1	?	1	?	?	?	?	?	0	1	1	0	1	0	1	1	0	0	1	1	1	
<i>Chryseofusus acherusius</i>		1	1	0	1	0	2	1	1	1	1	0	0	1	0	0	0	1	1	0	0	0	1	1	0	0	1	1	1	
<i>Chryseofusus graciliformis</i>		1	1	0	1	0	2	1	1	?	1	?	?	1	0	?	0	1	1	0	0	0	1	1	0	0	1	1	1	
<i>Fusinus australis</i>		1	1	1	1	0	?	1	0	1	1	1	0	1	0	1	0	1	1	0	0	0	1	1	0	0	1	1	1	
<i>Cyrtulus serotinus</i>		1	1	1	1	0	?	1	0	?	1	?	?	?	?	?	?	?	?	?	?	?	?	?	?	?	?	?	?	
<i>Fusinus frenguelli</i>		1	1	1	1	0	2	1	0	?	1	?	?	1	0	0	0	1	0	0	0	0	1	0	0	0	?	?	?	?
<i>Fusinus brasiliensis</i>		1	1	1	1	0	2	1	1	?	1	?	?	1	0	1	0	1	1	0	0	0	0	1	1	0	0	1	1	
<i>Fusinus marmoratus</i>		1	1	1	1	0	2	1	1	?	1	?	?	1	0	1	0	1	1	0	0	0	?	?	?	?	?	?	?	?
<i>Fusinus sp.</i>		1	1	1	1	0	2	1	1	?	1	?	?	1	0	1	?	?	?	?	?	?	?	?	?	?	?	?	?	
<i>Fusolatirus bruijnii</i>		1	1	0	1	0	?	1	0	1	1	1	0	1	0	1	?	?	?	?	?	?	?	?	?	?	?	?	?	
<i>Peristernia marquesana</i>		1	1	0	1	0	?	1	0	?	?	?	?	?	?	?	?	?	?	?	?	?	?	?	?	?	?	?	?	
<i>Peristernia nassatula</i>		1	1	0	1	0	2	1	0	1	1	1	0	1	?	?	?	0	1	1	0	?	?	?	?	?	?	?	?	
<i>Pustulatirus mediamericus</i>		1	1	0	1	0	2	1	1	?	1	?	?	1	0	0	?	?	?	?	?	?	?	?	?	?	?	?	?	
<i>Pustulatirus ogum</i>		1	1	0	1	0	2	1	0	?	1	?	?	?	?	?	0	1	0	0	0	0	1	2	1	1	-	1	1	
<i>Latirus polygonus</i>		1	1	0	1	0	2	1	1	1	1	1	0	1	0	1	?	?	?	?	?	?	?	?	?	?	?	?	?	
<i>Nodolatirus nodatus</i>		1	1	0	1	0	?	1	1	?	?	?	?	?	?	?	0	1	1	0	0	0	1	2	1	0	1	1	1	
<i>Hemipolygona beckyae</i>		1	1	0	1	0	2	1	1	?	1	?	?	1	0	1	0	1	1	0	0	0	1	2	1	0	0	1	1	
<i>Hemipolygona armata</i>		1	1	0	1	0	2	1	1	?	?	?	?	1	0	1	0	1	1	0	0	0	1	2	1	1	-	1	1	
<i>Latirus vischii</i>		1	1	0	1	0	?	1	?	?	?	?	?	?	?	?	?	?	?	?	?	?	?	?	?	?	?	?	?	
<i>Australaria australasia</i>		1	1	0	1	1	?	1	1	1	1	1	0	1	1	0	?	?	?	?	?	?	?	?	?	?	?	?	?	
<i>Pleuroploca trapezium</i>		1	1	0	1	1	?	1	1	?	?	?	?	?	?	?	?	?	?	?	?	?	?	?	?	?	?	?	?	
<i>Filifusus filamentosus</i>		1	1	0	1	1	?	1	1	?	1	?	?	?	?	?	?	?	?	?	?	?	?	?	?	?	?	?	?	
<i>Aurantilaria aurantiaca</i>		1	1	0	1	1	2	1	1	1	1	1	0	1	0	1	0	1	0	0	0	0	?	?	?	?	?	?	?	
<i>Fasciolaria tulipa</i>		1	1	0	1	1	2	1	1	1	1	1	0	1	0	0	0	1	1	0	0	0	?	?	?	?	?	?	?	
<i>Polygona infundibulum</i>		1	1	0	1	0	?	1	?	?	?	?	?	?	?	?	?	?	?	?	?	?	?	?	?	?	?	?	?	
<i>Polygona angulata</i>		1	1	0	1	0	2	1	0	1	1	1	1	0	1	0	1	1	0	0	0	0	1	2	1	1	-	1	1	
<i>Latirus pictus</i>		1	1	0	1	0	2	1	0	?	?	?	?	?	?	?	0	1	1	0	0	0	1	2	1	0	0	1	1	
<i>Leucozonia ocellata</i>		1	1	0	1	0	2	1	0	0	1	1	0	1	0	1	0	1	0	0	0	0	1	2	1	1	-	1	1	
<i>Leucozonia cerata</i>		1	1	0	1	0	2	1	0	?	?	?	?	1	0	0	0	1	0	0	0	0	1	2	1	0	1	1	1	
<i>Leucozonia nassa nassa</i>		1	1	0	1	0	2	1	0	0	1	0	0	1	0	1	0	1	1	0	0	0	1	2	1	0	0	1	1	
<i>Leucozonia nassa cingulifera</i>		1	1	0	1	0	2	1	0	0	1	0	0	1	0	1	0	1	1	0	0	0	1	2	1	0	0	1	1	
<i>Leucozonia nassa brasiliensis</i>		1	1	0	1	0	2	1	0	0	1	0	0	1	0	1	0	1	1	0	0	0	1	2	1	0	0	1	1	
<i>Leucozonia ponderosa</i>		1	1	0	1	0	2	1	0	0	1	0	0	1	0	1	0	1	1	0	0	0	0	2	1	0	0	?	?	
<i>Opeatostoma pseudodon</i>		1	1	0	1	1	2	1	0	1	1	1	0	1	0	0	0	1	0	0	1	0	1	2	1	0	0	1	1	

## 8. References

Abbate D. 2016. **Estudo Filogenético da subfamília Nassariinae (Neogastropoda, Buccinoidea, Nassariidae)**. Tese (Doutorado em Ciências, área de Zoologia) - Instituto de Biociências, Universidade de São Paulo, São Paulo. 234p.

Abbate D. & Simone L.R.L. 2015. Review of *Pugilina* from the Atlantic, with description of a new species from Brazil (Neogastropoda, Melongenidae). **African Invertebrates**, 56(3): 559-577.

Abbate D. & Simone L.R.L. 2016. Anatomy of *Bullia laevis* from Cape Town, South Africa (Mollusca, Caenogastropoda, Nassariidae). **Spixiana**, 39(1): 1-10.

Abbott R.T. 1958. The marine mollusks of Grand Cayman Island, British West Indies. **Monographs of the Academy of Natural Sciences of Philadelphia**, 11: 1-138.

Absalão R.S., Caetano C.H.S. & Fortes R.R. 2006. Filo Mollusca. In: Lavrado H.P. & Ignacio B.L. (Eds). **Biodiversidade bentônica da região central da Zona Econômica Exclusiva Brasileira**. Rio de Janeiro, Museu Nacional. p. 211-260. (Série Livros 18)

Amaudrut A. 1898. La partie antérieure du tube digestif et la torsion chez les mollusques gastéropodes. **Annales des Sciences Naturelles, Serie 8**, 7:1-291, pls. 1-10.

Andrews E.B. & Thorogood K.E. 2005. An ultrastructural study of the gland of Leiblein of muricid and nassariid neogastropods in relation to function, with a discussion on its homologies in other caenogastropods. **Journal of Molluscan Studies**, 71(3): 269-300. <http://doi.org/10.1093/mollus/eyi036>.

Bandel K. 1984. The radulae of Caribbean and other Mesogastropoda and Neogastropoda. **Zoologische Verhandelingen**. 214: 1-188.

Bandel K. 1993. Caenogastropoda during Mesozoic times. **Scripta Geologica**, (Special issue 2): 7-56.

Bellardi L. 1884. **I molluschi dei terreni terziarii del Piemonte e della Liguria. Parte IV. Fasciolariidae e Turbinellidae**, Torino, Ermano Loescher. 62p.

Benton M.J. 1993. **The Fossil Record**. Chapman & Hall, London, v. 2, 845p.

Beu A.G. 2011. Marine Mollusca of isotope stages of the last 2 million years in New Zealand. Part 4. Gastropoda (Ptenoglossa, Neogastropoda, Heterobranchia). **Journal of the Royal Society of New Zealand**, 41(1): 1-153.

Bieler R. & Simone L.R.L. 2005. Anatomy and morphology of *Stephopoma nucleogranosum* Verco, 1904 (Caenogastropoda: Siliquariidae) from Esperance Bay, Western Australia. *In*: Wells F., Walker D.I. & Kendrick G.A. (Eds.). **The Marine Flora and Fauna of Esperance, Western Australia**. Western Australian Museum, Perth. p. 159-175.

Bouchet P. & Rocroi J.P. 2005. Classification and nomenclator of gastropod families. **Malacologia**, 47: 1-397.

Bouchet P. & Snyder M.A. 2013. New and old species of *Benimakia* (Neogastropoda: Fasciolariidae) and a description of *Nodolatirus*, new genus. **Journal of Conchology**, 41(3): 331-341.

Bouchet P. & Waren A. 1985. Revision of the Northeast Atlantic bathyal and abyssal Neogastropoda excluding Turridae (Mollusca, Gastropoda). **Bollettino Malacologico**, (Suppl 1): 1- 296.

Bronwen J., Scott J. & Kenny R. 1998. Morphology and Physiology of the Mollusca. *In*: Beesley P.L., Ross G.J.B. & Wells A. **Mollusca: The Southern Synthesis. Fauna of Australia**. CSIRO Publishing, Melbourne. p. 11-23.

Bullock R.C. 1974. A contribution to the systematics of some West Indian *Latirus* (Gastropoda: Fasciolariidae). **The Nautilus**, 88: 69-79.

Buzzurro G. & Russo P. 2007. **Fusinus del Mediterraneo**. published by the authors. 280p.



Callomon P. & Snyder M.A. 2004. On some *Fusinus* (Gastropoda: Fascioliariidae) from Japan, with type selections. **Venus: Japanese Journal of Malacology**, 63(1): 13-27.

Callomon P. & Snyder M.A. 2007. On the Genus *Fusinus* in Japan III: Nine Further Species, with Type Selections. **Venus: Japanese Journal of Malacology**, 66(1): 19-47.

Callomon P. & Snyder M.A. 2009. On the genus *Fusinus* in Japan V: further species, an unnamed form and discussion. **Venus: Japanese Journal of Malacology**, 67 (3-4): 1-14.

Callomon P. & Snyder M.A. 2006. On the Genus *Fusinus* in Japan II: *F. undatus*, *F. similis* and Related Pacific Taxa, with the Description of *F. mauiensis* n. sp. (Gastropoda: Fascioliariidae). **Venus: Japanese Journal of Malacology**, 65(3): 177-191.

Colgan D.J., Ponder W.F., Beacham E. & Macaranas J. M. 2003. Gastropod phylogeny based on six segments from four genes representing coding or non-coding and mitochondrial or nuclear DNA. **Molluscan Research**, 23: 123-148. <http://doi.org/10.1071/MR03002>

Colgan D.J., Ponder W.F., Beacham E. & Macaranas, J. 2007. Molecular phylogenetics of Caenogastropoda (Gastropoda: Mollusca). **Molecular Phylogenetics and Evolution**, 42(3): 717-737. <http://doi.org/10.1016/j.ympev.2006.10.009>.

Cossmann M. 1901. **Essais de paléonchologie comparée**, 4. The author and Société d'Éditions Scientifiques. Paris. 293p.

Couto D.R. & Pimenta A.D. 2012. Comparative morphology of *Leucozonia* from Brazil (Neogastropoda: Buccinoidea: Fascioliariidae). **American Malacological Bulletin**, 30: 103-116.

Couto D.R., Bouchet P., Kantor Y.I., Simone L.R.L. & Giribet G. 2016. A multilocus molecular phylogeny of Fascioliariidae (Neogastropoda: Buccinoidea). **Molecular phylogenetics and evolution**, 99: 309-322.

Couto D.R., Simone L.R.L. & Pimenta A.D. 2015a. Comparative anatomy of the fascioliariids *Pustulatirus ogum* and *Hemipolygona beckyae* from Brazil (Gastropoda: Buccinoidea: Peristerniinae). **Scientia Marina**, 79(1): 1–17.

Couto D.R., Simone L.R.L. & Pimenta A.D. 2015b. Morphology of *Fasciolaria tulipa* from Venezuela (Gastropoda: Buccinoidea: Fasciolariidae). *Journal of Conchology*, 42(2), 163–173.

Cunha R.L., Grande C. & Zardoya R. 2009. Neogastropod phylogenetic relationships based on entire mitochondrial genomes. *BMC Evolutionary Biology*, 9(210): 1-16. <http://doi.org/10.1186/1471-2148-9-210>.

Dall W.H. 1894. The mechanical cause of folds in the aperture of the shell of Gastropoda. *American Naturalist*, 28: 909-914.

Faber M.J. 2010. Marine gastropods from the ABC islands and other localities 34. The genus *Teralatirus* Coosmans, 1965 (Gastropoda: Fasciolariidae). *Miscellanea Malacologica*, 4(1): 9-12.

Farris J.S. 1969. A Successive Approximations Approach to Character Weighting. *Systematic Zoology* 18 (4): 374-385. <http://doi:10.2307/2412182>.

Fedosov A. & Kantor Y.I. 2012. A new species and genus of enigmatic turritiform Fasciolariidae from the Central Indo-Pacific (Gastropoda: Neogastropoda). *Archiv Für Molluskenkunde*, 141(2): 137–144. <http://doi.org/10.1127/arch.moll/1869-0963/141/137-144>.

Fedosov A., Puillandre N., Kantor Y.I. & Bouchet P. 2015. Phylogeny and systematics of mitriform gastropods (Mollusca: Gastropoda: Neogastropoda). *Zoological Journal of the Linnaean Society*: 1-24. <http://doi.org/10.1111/zoj.12278>.

Fitch W. 1971. Toward defining the course of evolution: minimal change for a specific tree topology. *Systematic Zoology*, 20: 406-416.

Fraussen K., Kantor Y.I. & Hadorn R. 2007. *Amiantofusus* gen. nov. for *Fusinus amiantus* Dall, 1889 (Mollusca: Gastropoda: Fasciolariidae) with description of a new and extensive Indo-West Pacific radiation. *Novapex*, 8(3-4): 79-101.

Fretter V. & Graham A. 1962. **British Prosobranch Molluscs. Their functional anatomy and ecology.** Ray Society Publications, London. 755p.

Galindo L.A., Puillandre N., Strong E.E. & Bouchet P. 2014. Using microwaves to prepare gastropods for DNA barcoding. **Molecular Ecology Resources**, 14:700-705. <http://doi.org/10.1111/1755-0998.12231>.

Galindo L.A., Puillandre N., Utge J., Lozouet P. & Bouchet P. 2016. The phylogeny and systematics of the Nassariidae revisited (Gastropoda, Buccinoidea). **Molecular Phylogenetics and Evolution**, 99: 337-353. <http://doi.org/10.1016/j.ympev.2016.03.019>.

Giribet G. 2015. Morphology should not be forgotten in the era of genomics - a phylogenetic perspective. **Zoologischer Anzeiger**, 256: 96–103. <http://doi.org/10.1016/j.jcz.2015.01.003>.

Giribet G., Edgecombe G.D. & Wheeler W.C. 2001. Arthropod Phylogeny Based on Eight Molecular Loci and Morphology. **Nature**, 413: 157-161.

Giribet G., Edgecombe G.D., Wheeler W.C. & Babbitt C. 2002. Phylogeny and Systematic Position of Opiliones: A Combined Analysis of Chelicerate Relationships Using Morphological and Molecular data. **Cladistics**, 18: 5-70.

Golding R.E., Ponder W.F. & Byrne M. 2009. Three-dimensional reconstruction of the odontophoral cartilages of caenogastropoda (mollusca: gastropoda) using micro-ct: Morphology and phylogenetic significance. **Journal of Morphology**, 270: 558-587. <http://doi.org/10.1002/jmor.10699>.

Goloboff P.A. 1993. Estimating character weights during tree search. **Cladistics**, 9: 83-91.

Goloboff P.A., Carpenter J.M., Arias J.S. & Miranda-Esquivel D.R. 2008. Weighting against homoplasy improves phylogenetic analysis of morphological data sets. **Cladistics**, 24: 758-773. <http://doi.org/10.1111/j.1096-0031.2008.00209.x>.

Grabau A.W. 1907. Studies of Gastropoda, III. On Orthogenetic variation in Gastropoda. **The American Naturalist**, 41(490): 607-651.

Gray J.E. 1854. On the division of ctenobranchous gasteropodous Mollusca into larger groups and families. **Proceedings of the Zoological Society of London**, 21: 32-44.

Habe T. 1958. On the radulae of Japanese marine gastropods. **Venus – Japanese Journal of Malacology**, 20: 43-60.

Hadorn R. 1999. Two new *Fusinus* (Gastropoda: Fascioliariidae) from South Mozambique and Natal: *Fusinus rogersi* sp. nov. and *Fusinus kilburni* sp. nov. **Vita Marina**, 46(3-4): 101-110.

Hadorn R. & Fraussen K. 2003. The deep-water Indo-Pacific radiation of *Fusinus* (*Chryseofusus* subgen. nov.)(Gastropoda: Fascioliariidae). **Iberus**, 21: 207-240.

Hadorn R. & Fraussen K. 2002. Four new *Fusinus* from East Africa (Gastropoda: Fascioliariidae). **Iberus**, 20(1), 63-72.

Hadorn R. & Fraussen K. 2005. Revision of the genus *Granulifusus* Kuroda & Habe 1954 with description of some new species (Gastropoda: Prosobranchia: Fascioliariidae). **Archiv Für Molluskenkunde**, 134(2): 129-171.

Hadorn R. & Fraussen K. 2006. Five new species of *Fusinus* (Gastropoda: Fascioliariidae) from western Pacific and Arafura Sea. **Novapex**, 7(4): 91–102.

Hadorn R. & Rogers B. 2000. Revision of recent *Fusinus* (Gastropoda: Fascioliariidae) from tropical western Atlantic, with description of six new species. **Argonauta**, 14(1): 5-57.

Hadorn R., Snyder M.A. & Fraussen K. 2008. A new *Chryseofusus* (Gastropoda: Fascioliariidae: *Fusinus*) from South and Western Australia. **Novapex**, 9(2-3): 95-99.

Hanken J. & Wake D.B. 1993. Miniaturization of body size: organismal consequences and evolutionary significance. **Annual Review of Ecology and Systematics**, 24: 501-519.

Harasewych M.G. 1990. Studies on bathyal and abyssal Buccinidae (Gastropoda: Neogastropoda): 1. *Metula fusiformis* Clench and Aguayo, 1941. **The Nautilus**, 104: 120-130.

Harasewych M.G. 1998. Family Fascioliariidae. *In*: Beesley P.L., Ross G.J.B. & Wells A. (Eds) **Mollusca: The Southern Synthesis. Fauna of Australia**. CSIRO Publishing, Melbourne, Australia. p. 832-833.

Harasewych M.G., Adamkewicz S.L., Blake J.A., Saudek D., Spriggs T. & Bult C.J. 1997. Neogastropod phylogeny: a molecular perspective. **Journal of Molluscan Studies**, 63, 327-351. <http://doi.org/10.1093/mollus/63.3.327>.

Harasewych M.G. & Kantor Y.I. 2004. The deep-sea Buccinoidea (Gastropoda: Neogastropoda) of the Scotia Sea and adjacent abyssal plains and trenches. **The Nautilus**, 118(1): 1-42.

Haszprunar G. 1988. On the origin and evolution of major gastropods group, with special reference to the Streptoneura. **Journal of Molluscan Studies**, 54: 367-441. <http://doi.org/10.1093/mollus/54.4.367>.

Hayashi S. 2005. Molecular phylogeny of the Buccinidae (Caenogastropoda: Neogastropoda) as inferred from the complete mitochondrial 16S rRNA gene sequences of selected. **Molluscan Research**, 25(2): 85–98.

Kantor Y.I. 1990. Anatomical basis for the origin and evolution of the toxoglossan mode of feeding. **Malacologia**, 32 (1): 3-18.

Kantor Y.I. 1996. Phylogeny and relationships of Neogastropoda *In*: Taylor, J.D. (Ed.). **Origin and evolutionary radiation of the Mollusca**. Oxford University Press, Oxford. p. 221-230

Kantor Y.I. 2003. Comparative Anatomy of the Stomach of Buccinoidea (Neogastropoda). **Journal of Molluscan Studies**, 69: 203–220. <http://doi.org/10.1093/mollus/69.3.203>.

.Kantor Y.I. & Fedosov A. 2009. Morphology and development of the valve of *Leiblein* in Neogastropoda: possible evidence for paraphyly of the Neogastropoda. **The Nautilus**, 123(3): 73-82.

Kantor Y.I., Puillandre N., Fraussen K., Fedosov A. & Bouchet P. 2013. Deep-water Buccinidae (Gastropoda: Neogastropoda) from sunken wood, vents and seeps: molecular phylogeny and taxonomy. **Journal of the Marine Biological Association of the United Kingdom**, 93(8): 2177-2195. <http://doi.org/10.1017/S0025315413000672>.

Kier W.M. & Smith K.K. 1985. Tongues, tentacles and trunks: the biomechanics of movement in muscular-hydrostats. **Zoological Journal of the Linnean Society**, 83: 307-324.

Kishino H. & Hasegawa M. 1989. Evaluation of the maximum likelihood estimate of the evolutionary tree topologies from DNA sequence data, and the branching order in Hominoidea. **Journal of Molecular evolution**, 29: 170–179.

Kosyan A.R. 2006. Two new species of the genus *Pararetifusus* Kosuge, 1967 (Buccinidae: Colinae), with notes on the morphology of *Pararetifusus tenuis* (Okutani, 1966). **Ruthenica**, 16(1-2): 5-15.

Kosyan A.R. & Kantor Y.I. 2009. Phylogenetic analysis of the subfamily Colinae (Neogastropoda: Buccinidae) based on morphological characters. **The Nautilus**, 123: 83-94.

Kosyan A.R. & Kantor Y.I. 2013. Revision of the genus *Aulacofusus* Dall, 1918 (Gastropoda : Buccinidae). **Ruthenica**, 23(1): 1-33.

Kosyan A.R., Modica M.V. & Oliverio M. 2009. The anatomy and relationships of *Troschelia* (Neogastropoda: Buccinidae): New evidence for a closer fascioliid-buccinid relationship? **The Nautilus**, 123(3): 95-105.

Kuroda T. & Habe T. 1952. **Checklist and bibliography of the recent marine Mollusca of Japan**. Tokyo, L.W. Stalch. p.59.

Kuroda T. & Habe T. 1971. Descriptions of genera and species. *In*: Kuroda T., Habe T. & Oyama K. **The Sea Shells of Sagami Bay collected by his majesty the emperor of Japan**. Maruzen, Tokio.741p.

Kuroda T., Habe T. & Oyama K. 1971. **The Sea Shells of Sagami Bay collected by his majesty the emperor of Japan**. Maruzen, Tokio.741p.

Küster H.C. & Kobelt W. 1844-1876. Die geschwänzten unbewehrten Purpurschnecken. Erste hälfte: *Turbinella* und *Fasciolaria*. *In*: Martini F.H.W. & Chemnitz J.H. (Eds). **Systematisches Conchylien-Cabinet**. 2. ed. p.1-164, pls. 1-32, 9a, 9b, 13b.

Landau B. & Vermeij G.J. 2012. The Peristerniinae (Mollusca: Gastropoda, Buccinoidea, Fasciolariidae) from the Neogene of Venezuela. **Cainozoic Research**, 9(1): 87-99.

Leal J.H. 1991. **Marine Prosobranch Gastropods from Oceanic Islands off Brazil: Species Composition and Biogeography**. Universal Book Services/W, Backhuys. 418p.

Lyons W.G. 1972. A New *Fasciolaria* from the Northeastern Gulf Of Mexico. **The Nautilus**, 85(3): 96–99.

Lyons W.G. 1991. Post-Miocene species of *Latirus* Montfort, 1810 (Mollusca: Fasciolariidae) of Southern Florida, with a review of regional marine biostratigraphy. **Biological Sciences**, 35(3): 131-208.

Lyons W.G. & Snyder M.A. 2013. The genus *Pustulatirus* Vermeij and Snyder, 2006 (Gastropoda: Fasciolariidae: Peristerniinae) in the western Atlantic, with descriptions of three new species. **Zootaxa**, 3636: 35-58.

Maddison W.P. & Maddison D.R. 2016. **Mesquite: a modular system for evolutionary analysis**. Version 3.10 <http://mesquiteproject.org>. Last access vi/2016.

Marcus E. & Marcus E. 1962. On *Leucozonia* nassa. **Boletim da Faculdade de Filosofia, Ciências e Letras da Universidade de São Paulo, Zoologia** 24: 11-30.

Matthews-Cascon H., Matthews H.R. & Kotzian C.B. 1989. Os gêneros *Fasciolaria* Lamarck, 1799 e *Leucozonia* Gray, 1847 no nordeste brasileiro (Mollusca: Gastropoda: Fasciolariidae). **Memórias do Instituto Oswaldo Cruz**, 84(Supplement IV): 357-364.

McCormack J.E., Hird S.M., Zellmer A.J., Carstens B.C. & Brumfield R.T. 2013. Applications of next-generation sequencing to phylogeography and phylogenetics. **Molecular Phylogenetics and Evolution**, 66(2): 526-538.

Nixon K.C. & Carpenter J.M. 1993. On Outgroups. **Cladistics**, 9: 413-426. <http://doi:10.1111/j.1096-0031.1993.tb00234.x>.

Nixon K.C. 1999-2002. **WinClada ver. 1.0000** Published by the author, Ithaca, NY.

Okutani T. 2000. **Marine Mollusks in Japan**. Tokai University Press, Tokyo. 1173p.

Oliverio M. & Modica M.V. 2010. Relationships of the hematophagous marine snail *Colubraria* (Rachiglossa: Colubrariidae), within the neogastropod phylogenetic framework. **Zoological Journal of the Linnaean Society**, 158(4): 779-800. <http://doi.org/10.1111/j.1096-3642.2009.00568.x>.

Osca D., Templado J. & Zardoya R. 2015. Caenogastropod mitogenomics. **Molecular Phylogenetics and Evolution**, 93: 118-128. <http://doi.org/10.1016/j.ympev.2015.07.011>.

Perrier R. 1889. Recherches sur l'anatomie et l'histologie du rein des gastéropodes, Prosobranchiata. **Annales des Sciences Naturelles. Zoologie et Biologie Animale**, 8: 61-192.

Petuch E.J. 1979. New gastropods from the Abrolhos Archipelago and reef complex, Brazil. **Proceedings of the Biological Society of Washington**, 92(3): 510-526.

Philippe H., Brinkmann H., Lavrov D.V., Littlewood D.T.J., Manuel M., Wörheide G. & Baurain D. 2011. Resolving difficult phylogenetic questions: Why more sequences are not enough. **PLoS Biology**, 9(3): 1-10. <http://doi.org/10.1371/journal.pbio.1000602>.



Platnick N.I., Griswold C.E. & Coddington J.A. 1991. On missing entries in cladistic analysis. **Cladistics**, 7: 337-343.

Ponder W.F. & Lindberg D.R. 1997. Towards a phylogeny of gastropod molluscs: an analysis using morphological characters. **Zoological Journal of the Linnaean Society**, 119: 83-265. <http://doi.org/10.1006/zjls.1996.0066>.

Ponder W.F. 1973. The origin and evolution of the Neogastropoda. **Malacologia**, 12: 295-338.

Ponder W.F., Colgan D.J., Healy J.M., Nützel A., Simone L.R.L. & Strong E.E. 2008. Caenogastropoda. *In*: Ponder W.F. & Lindberg D.R. (Eds.). **Phylogeny and Evolution of the Mollusca**. University of California Press. p. 331-383.

Ponder W.F. 1972. Notes on some Australian Species and Genera of the Family Buccinidae (Neogastropoda). **Journal of the Malacological Society of Australia**, 2(3): 249-265. <http://doi.org/10.1080/00852988.1972.10673857>.

Poppe G.T. 2008. **Philippine Marine Mollusks: Gastropoda**. Hackenheim, ConchBooks. v.2, pt. 2, 848p.

Preetha K., Ravinesh R., Bijukumar A., Dhaneesh K.V. & George S. 2014. First record of *Granulifusus poppei* (Mollusca: Fascioliidae) from Indian coast. **Marine Biodiversity Records**, 7(e95): 1-3. <http://doi.org/10.1017/S1755267214000992>.

Price R.M. 2003. Columellar muscle of neogastropods: muscle attachment and the function of columellar folds. **Biological Bulletin**, 205: 351-366. <http://doi.org/10.1086/277797>.

Riedel F. 2000. Ursprung und evolution der “höheren” Caenogastropoda. **Berliner Geowissenschaftliche Abhandlungen Reihe e Paläobiologie**, 32: 1-240.

Rios E.C. 2009. **Compendium of Brazilian Sea Shells**. Rio Grande, RS, Evangraf. 676p.

Rosenberg G. 1992. **The encyclopedia of Seashells**. Robert Hale Ltda, London. 224p.

Rosenberg G. 2009. Malacolog 4.1.1: **A Database of Western Atlantic Marine Mollusca**. [WWW database (version 4.1.1)] URL <http://www.malacolog.org/>.

Salvini-Plawen L.V. 1988. The structure and function of molluscan digestive systems. *In*: Trueman E.R. & Clarke M.R. (Eds) **The Mollusca: Form and function**. Academic Press, London. p. 301-379.

Salvini-Plawen L.V. & Haszprunar G. 1987. The Vetigastropoda and systematics of streptoneurous Gastropoda (Mollusca). **Journal of Zoology**, London, 211: 747-770.

Shendure J. & Ji H. 2008. Next-generation DNA sequencing. **Nature Biotechnology**, 26(10): 1135-1145. <http://doi.org/10.1038/nbt1486>.

Shimodaira H. 2002. An approximately unbiased test of phylogenetic tree selection. **Systematic Biology**, 51: 492-508.

Shimodaira H. & Hasegawa M. 1999. Multiple comparisons of log-likelihoods with applications to phylogenetic inference. **Molecular Biology and Evolution**, 16: 1114-1116.

Shuto T. 1958. *Granulifusus* from the Miyazaki group (Paleontological study of the Miyazaki group - V). **Transactions and Proceedings of the Paleontological Society of Japan**, 31: 253-264.

Simone L.R.L. 1996. Anatomy and systematics of *Buccinanops gradatus* (Deshayes, 1844) and *Buccinanops moniliferus* (Kiener, 1834) (Neogastropoda, Muricoidea) from the Southeastern coast of Brazil. **Malacologia**, 38(1-2): 87-102.

Simone L.R.L. 2001. Phylogenetic analyses of Cerithioidea (Mollusca, Caenogastropoda) based on comparative morphology. **Arquivos de Zoologia**, São Paulo, 36(2): 147-263.

Simone L.R.L. 2004. **Morphology and phylogeny of the Cypraeoidea (Mollusca, Caenogastropoda)**. Papel Virtual. 185p.

Simone L.R.L. 2005. Comparative morphological study of representatives of the three families of Stromboidea and the Xenophoroidea (Mollusca, Caenogastropoda), with an assessment of their phylogeny. **Arquivos de Zoologia**, São Paulo, 37(2): 141-267.

Simone L.R.L. 2011. Phylogeny of the Caenogastropoda (mollusca), based on comparative morphology. **Arquivos de Zoologia**, São Paulo, 42(4): 161-323.

Simone L.R.L., Cavallari D.C. & Abbate D. 2013. Revision of the genus *Teralatirus* Coomans 1965 in the Western Atlantic, with an anatomical description of *T. roboreus* (Reeve 1845). **Archiv Für Molluskenkunde**, 142(2): 215-226. <http://doi.org/10.1127/arch.moll/1869-0963/142/215-226>.

Simone L.R.L., Herbert G.S. & Merle D. 2009. Unusual anatomy of the ectoparasitic muricid *Vitularia salebrosa* (King & Broderip, 1832) (neogastropoda: muricidae) from the pacific coast of Panama. **The Nautilus**, 123(3): 137-147.

Simone L.R.L. & Pastorino G. 2014. Comparative morphology of *Dorsanum miran* and *Bullia granulosa* from Morocco (Mollusca: Caenogastropoda: Nassariidae). **African Invertebrates**, 55(1): 125-142. <http://doi.org/10.5733/afin.055.0107>

Simone L.R.L. & Ramos L.V. 1986. Variação constatada em *Leucozonia nassa* no litoral do Brasil (Buccinacea, Fascioliidae, Peristeniinae). Informativo da Sociedade Brasileira de **Malacologia**, São Paulo, v. 58: 15-16.

Snyder M.A. 2003. Four new species of *Latirus* (Gastropoda: Fascioliidae) from the Philippine Islands and the southern Caribbean. **Iberus**, 21(1), 1-9.

Snyder M.A. & Bouchet P. 2006. New species and new records of deep-water *Fusolatirus* (neogastropoda: fascioliidae) from the West Pacific. **Journal of Conchology**, 39(1): 1-12.

Snyder M.A. & Callomon P. 2005. On some *Fusolatirus* from Japan and the Philippines, with description of a new species (Gastropoda: Fascioliidae). **Venus: Japanese Journal of Malacology**, 63(3-4): 109-119.

Snyder M.A., Vermeij G.J. & Lyons W.G. 2012. The genera and biogeography of Fasciolarinae (Gastropoda, Neogastropoda, Fasciolaridae). **Basteria**, 76(1-3): 31-70.

Taylor D.W. & Sohl N.F. 1962. An outline of gastropod classification. **Malacologia**, 1: 7-32.

Taylor J.D. & Lewis A. 1995. Diet and radular morphology of *Peristernia* and *Latirolagena* (Gastropoda: Fasciolaridae) from Indo-Pacific coral reefs. **Journal of Natural History**, 29: 1143-1154. <http://doi.org/10.1080/00222939500770481>.

Thiele J. 1929-1935. **Handbuch der Systematischen Weichtierkunde**. Gustav Fischer, Jena. 1134p.

Troschel F.H. & Thiele J. 1865-1893. **Das Gebiss der Schnecken, zur Begründung einer natürlichen Classification**. Berlin, Nicolaische Verlags-Buchhandlungen. 2 v.

Tryon G.W. 1880-1881. **Manual of conchology, structural and systematic, with illustrations of the species. Volume 3. Tritonidae, Fusidae, Buccinidae**. Philadelphia. p.1-64, pls 1-24 [1880]; p. 65-310, pls 25-87 [1881].

Turner H. & Zandee R. 1995. The behaviour of Goloboff's tree fitness measure F. **Cladistics**, 11: 57-72.

Vermeij G.J. 1997. The genus *Leucozonia* (Gastropoda: Fasciolaridae) in the Neogene of tropical America. **Tulane Studies in Geology and Paleontology**, 29: 129-134.

Vermeij G.J. 2001. Innovation and evolution at the edge: origins and fates of gastropods with a labral tooth. **Biological Journal of the Linnean Society** 72: 461-508.

Vermeij G.J. 2002. Characters in context: molluscan shells and the forces that mold them. **Paleobiology**, 28(1): 41-54. [http://doi.org/10.1666/0094-8373\(2002\)028<0041:CICMSA>2.0.CO;2](http://doi.org/10.1666/0094-8373(2002)028<0041:CICMSA>2.0.CO;2).

Vermeij G.J. & Rosenberg G. 2003. *Dentifusus*, a new genus of fasciolariid gastropod from the Philippine with labral tooth. **Proceedings of the Academy of Natural Sciences of Philadelphia**, 153: 23-26. [http://doi.org/10.1635/0097-3157\(2003\)153\[0023:DANGOF\]2.0.CO](http://doi.org/10.1635/0097-3157(2003)153[0023:DANGOF]2.0.CO).

Vermeij G.J. & Snyder M.A. 1998. *Leucozonia ponderosa*, a new fasciolariid gastropod from Brazil. **The Nautilus**, 112: 117-119.

Vermeij G.J. & Snyder M.A. 2002. *Leucozonia* and related genera of fasciolariid gastropods: shell-based taxonomy and relationships. **Proceedings of the Academy of Natural Sciences of Philadelphia** 152: 23-44.

Vermeij G.J. & Snyder M.A. 2003. The fasciolariid gastropod genus *Benimakia*: New species and a discussion of Indo-Pacific genera in Brazil. **Proceedings of the Academy of Natural Sciences of Philadelphia**, 153:15-22. [http://doi.org/10.1635/0097-3157\(2003\)153\[0015:TFGGBN\] 2.0.CO;2](http://doi.org/10.1635/0097-3157(2003)153[0015:TFGGBN] 2.0.CO;2).

Vermeij G.J. & Snyder M.A. 2006. Shell characters and taxonomy of *Latirus* and related fasciolariid groups. **Journal of Molluscan Studies**, 72: 413-424. <http://doi.org/10.1093/mollus/eyl020>.

Wahlberg N., Braby M.F., Brower A.V.Z., de Jong R., Lee M., Nylin S., Pierce N.E., Sperling F.A.H., Vila R., Warren A.D. & Zakharov E. 2005. Synergistic effects of combining morphological and molecular data in resolving the phylogeny of butterflies and skippers. **Proceedings of the Royal Society B, Biological Science**, 272: 1577-1586.

Watson R.B. 1886. Report on the Scaphopoda and Gasteropoda collected by HMS Challenger during the years 1873-1876. *In: Reports of the scientific results of the voyage of H.M.S. "Challenger", Zoology*. London, H.M. Stationary Off. v.15 (part 42): 1-756, pl. 1-50.

Wenz W. 1938-1944. Teil 1: Allgemeiner Teil und Prosobranchia. *In: Schindewolf, O.H. (Ed.). Handbuch der Paläozoologie, Band 6, Gastropoda*. Berlin, Borntraeger. 1639p.

Winnepenninckx B., Steiner G., Backeljau T. & Wachter R. 1998. Details of gastropod phylogeny inferred from 18S rRNA sequences. **Molecular Phylogenetics and Evolution**, 9(1): 55-63. <http://doi.org/10.1006/mpev.1997.0439>.

WoRMS 2016. **World Register of Marine Species**. <http://www.marinespecies.org/> (accessed November 22, 2016).

Zenetos A., Çinar M.E., Pancucci-Papadopoulou M.A., Harmelin J.G. & Furnari G. 2005. Annotated list of marine alien species in the Mediterranean with records of the worst invasive species. **Mediterranean Marine Science**, 6(2): 63-118.

Zou S., Li Q. & Kong L. 2011. Additional gene data and increased sampling give new insights into the phylogenetic relationships of Neogastropoda, within the caenogastropod phylogenetic framework. **Molecular Phylogenetics and Evolution**. 61: 425-435.

**Molecular phylogeny of Fascioliidae with a total evidence analysis  
in POY (Gastropoda: Buccinoidea)**

## 1. Introduction

In the age of phylogenomics, it is crucial that molecular data be integrated into phylogenetic frameworks. Common practice in phylogenetics today involves the use of molecular datasets, and is partly due to the unprecedented amount of information that DNA sequences provide researchers with, in the form of nucleotide bases or amino-acids numbers, as opposed to morphological characters. Likewise, a thorough use of morphology requires greater amounts of time to extract a character, since dissection and study of specimens is more time consuming than current procedures of DNA isolation, amplification and sequencing.

The use of a mixed dataset, comprising of both molecular and morphological data is known as a total evidence analysis, and it may be pursued through a statistical model, such as MrBayes (utilizing a Bayesian inference analysis) or a parsimonious model, such as in POY. The inclusion of morphological data in molecular studies helps to resolve many internal clades, (*e.g.*, as encountered in other groups such as butterflies by Wahlberg *et al.*, 2005; arthropods by Giribet *et al.* 2001; Opiliones by Giribet *et al.*, 2002).

Couto *et al.* (2016) have endeavored in an extensive phylogenetic molecular study, and their results were discussed extensively in Chapter I of this dissertation, by comparing the clades obtained through morphology/molecular data. This work proves especially useful, as most terminals were scored for both the molecular and morphological datasets, providing a useful tool for comparison.

## 2. Objectives

1. To complement the molecular analysis of Couto *et al.* (2016) through the use of a parsimony criterion in the program POY;
2. To analyze the molecular data from Couto *et al.* (2016) with the morphological matrix from Chapter I in a total evidence analysis;
3. Upon the combined analysis, to provide a more realistic scenario of evolution in which the taxonomy may be more firmly rooted.



### 3. Material and Methods

The ultimate goal of this study is to include morphological data in a combined analysis with the use of direct optimization, implemented in the program POY 5.1.1 (Varón *et al.*, 2010). This method allows for DNA transformations to be assessed without the need for a previous multiple sequence alignment, in which indels appear as transformations linking ancestral and descendent sequences without the need of a fifth character state. The character and the character state are accessed at the same time (Wheeler, 1996) and the included morphological character transformations are weighted according to each parameter set. This averts the use of an ad hoc hypothesis of alignment.

Six analyses using only molecular data was used in order to determine the best parameter of weighting scheme (1110, 2110, 3221, 1210, 2210 and 3211). These will be explained subsequently. For full description of taxon sampling, DNA extraction, amplification, molecular markers and sequencing see Couto *et al.* (2016) (Appendix).

#### 3.1 Parsimony analyses – molecular data

POY analyses were done in Inspiron 5537, Intel(R) Core(TM) i7 4500U CPU with 8.00GB personal computer. Processor number was set to four in POY 5.1.1; four independent timed searches of 6h were performed in order to obtain a global optimum.

In order to better ascertain the homology of the nucleotides, each individual sequence of the non-protein encoding genes (18S rRNA, 28S rRNA and 16S rRNA) was partitioned (using the pound sign '#'). In this way isolating homologous fragments, corresponding more-or-less to the stem regions of the DNA, which are more conserved. The loop regions that, contrarily, are more variable, were analyzed with greater certainty of base correspondence. For the protein encoding genes Cytochrome *c* Oxidase subunit I (COI) e Histone H3 a single fragment was used because these lack any indels (Table 1)

Parameters used for this study follows other works that include parsimonious analysis using POY (*e.g.*, Edgecombe & Giribet, 2006; 2009; Aktipis *et al.*, 2011; Giribet & Edgecombe. 2013; Giribet *et al.*, 2014). Each parameter corresponds to different weighting schemes for indel opening, transversions, transitions and indel extensions. Six parameters routinely used were chosen for this study:

1. 1110 (indel opening cost = 1; transversions = transitions = 1; indel extension cost = 0);
2. 2110 (indel opening cost = 2; transversions = transitions = 1; indel extension cost = 0);
3. 3221 (indel opening cost = 3; transversions = transitions = 2; indel extension cost = 1);
4. 1210 (indel opening cost = 1; transversions = 2; transitions = 1; indel extension cost = 0);
5. 2210 (indel opening cost = 2; transversions = 2; transitions = 1; indel extension cost = 0);
6. 3211 (indel opening cost = 3; transversions = 2; transitions = 1; indel extension cost = 1).

Nodal support for the optimal parameter set was estimated via jackknifing (50 replicates) with a 50% of characters removed per pseudo-replicate. Jackknife was estimated via the Cyber infrastructure for Phylogenetic Research (CIPRES) gateway (Miller *et al.*, 2010) (<https://www.phylo.org/>) for the optimal parameter chosen.

POY Scripts for all analysis are found in the appendix section.

Table 1: Number of taxa and fragments analyzed for each coding or non-coding loci.

<b>16S rRNA:</b>	104 taxa	8 fragments	non-coding
<b>18S rRNA:</b>	133 taxa	9 fragments	
<b>28S rRNA:</b>	132 taxa	17 fragments	
<b>Cytochrome c Oxidase COI:</b>	129 taxa	1 fragment	coding
<b>Histone H3:</b>	127 taxa	1 fragment	

### 3.2 Parsimony analyses – Total evidence data

Total evidence analysis, combining the molecular data aforementioned with the morphological data from Chapter I of this dissertation was done in the Cyber infrastructure for Phylogenetic Research (CIPRES) portal (Miller *et al.*, 2010). For the morphological methodology, character descriptions, and morphological matrix, refer to chapter I. The weighting scheme parameter was the same as specified for the molecular analysis.

Out of the 140 taxa analyzed for both the molecular and the morphological part, eight species were excluded, because they lacked any molecular data: *Pugilina tupiniquim*, *Engoniophos uncinatus*, *Bullia laevissima*, *Pisania pusio*, *Fusinus marmoratus*, *Fusinus* sp., *Hemipolygona beckyae* and *Pustulatirus mediamericanus*. This was opted because the results obtained with the inclusion of these species did not provide any information on their position, and sometimes with misleading topologies. Table 2 lists all taxa for the total evidence analysis.

Table 2: Taxa used for morphological (chapter I) and molecular analyses. All taxa from the Molecular column were employed in the total evidence analysis. Shadings: light grey, same-genus species; dark grey, outgroup species.

MORPHOLOGY	MOLECULAR	MORPHOLOGY	MOLECULAR
<i>Amiantofusus candoris</i>	<i>Amiantofusus candoris</i>		<i>Peristernia</i> sp.4
<i>Amiantofusus pacificus</i>	<i>Amiantofusus pacificus</i>		<i>Peristernia</i> sp.5
	<i>Amiantofusus sebalis</i>	<i>Hemipolygona armata</i>	<i>Hemipolygona armata</i>
<i>Angulofusus nedae</i>	<i>Angulofusus nedae</i>		<i>Hemipolygona mcgintyi</i>
<i>Chryseofusus archeriusis</i>	<i>Chryseofusus acherusius</i>		<i>Lamellilaturus lamyi</i>
	<i>Chryseofusus bradneri</i>		<i>Latirolagena smaragdulus</i>
<i>Chryseofusus graciliformis</i>	<i>Chryseofusus graciliformis</i>		<i>Latirus amplustre</i>
<i>Cyrtulus serotinus</i>	<i>Cyrtulus serotinus</i>		<i>Latirus belcheri</i>
	<i>Fusinus agatha</i>		<i>Latirus gibbulus</i>
<i>Fusinus australis</i>	<i>Fusinus australis</i>	<i>Latirus pictus</i>	<i>Latirus pictus</i>
<i>Fusinus brasiliensis</i>	<i>Fusinus brasiliensis</i>	<i>Latirus polygonus</i>	<i>Latirus polygonus</i>
	<i>Fusinus colus</i>	<i>Latirus vischii</i>	<i>Latirus vischii</i>
	<i>Fusinus crassiplicatus</i>	<i>Leucozonia cerata</i>	<i>Leucozonia cerata</i>
	<i>Fusinus excavatus</i>	<i>Leucozonia nassa brasiliiana</i>	<i>Leucozonia nassa brasiliiana</i>
	<i>Fusinus filosus</i>	<i>Leucozonia nassa cingulifera</i>	<i>Leucozonia nassa cingulifera</i>
	<i>Fusinus forceps</i>	<i>Leucozonia nassa nassa</i>	<i>Leucozonia nassa nassa</i>
	<i>Fusinus gracillimus</i>	<i>Leucozonia ocellata</i>	<i>Leucozonia ocellata</i>
	<i>Fusinus longissimus</i>	<i>Leucozonia ponderosa</i>	<i>Leucozonia ponderosa</i>
	<i>Fusinus maiiensis</i>	<i>Nodolaturus nodatus</i>	<i>Nodolaturus nodatus</i>
	<i>Fusinus pulchellus</i>	<i>Opeatostoma pseudodon</i>	<i>Opeatostoma pseudodon</i>
	<i>Fusinus salisburyi</i>	<i>Polygona angulata</i>	<i>Polygona angulata</i>
	<i>Fusinus sandvichensis</i>		<i>Polygona bernadensis</i>
	<i>Fusinus similis</i>	<i>Polygona infundibulum</i>	<i>Polygona infundibulum</i>
	<i>Fusinus syracusanus</i>	<i>Pustulaturus ogum</i>	<i>Pustulaturus ogum</i>
	<i>Fusinus virginiae</i>		<i>Pustulaturus praestantior</i>
<i>Granulifusus aff kiranus</i>	<i>Granulifusus aff kiranus</i>		<i>Pseudolaturus aff. pallidus</i>
	<i>Granulifusus aff niponicus</i>	<i>Pseudolaturus discrepans</i>	<i>Pseudolaturus discrepans</i>
	<i>Granulifusus bacciballus</i>		<i>Pseudolaturus kurodai</i>
	<i>Granulifusus benjamini</i>	<i>Pseudolaturus kuroseanus</i>	<i>Pseudolaturus kuroseanus</i>
<i>Granulifusus hayashi</i>	<i>Granulifusus hayashi</i>	<i>Pseudolaturus pallidus</i>	<i>Pseudolaturus pallidus</i>
	<i>Granulifusus niponicus</i>		<i>Pseudolaturus</i> sp.
<i>Granulifusus</i> sp.1	<i>Granulifusus</i> sp.1		<i>Dolicholaturus aff. cayohuesonicus</i>
	<i>Granulifusus</i> sp.2		<i>Dolicholaturus aff. spiceri</i>
	<i>Granulifusus staminatus</i>		<i>Dolicholaturus lancea</i>
<i>Aurantilaria aurantiaca</i>	<i>Aurantilaria aurantiaca</i>		<i>Dolicholaturus</i> sp.
<i>Australaria australasia</i>	<i>Australaria australasia</i>		<i>Dolicholaturus spiceri</i>
	<i>Cinctura hunteria</i>		<i>Teralaturus noumeensis</i>
	<i>Fasciolaria bullisi</i>	<i>Teralaturus roboreus</i>	<i>Teralaturus roboreus</i>
	<i>Fasciolaria</i> sp.		<i>Turrilaturus turritus</i>
<i>Fasciolaria tulipa</i>	<i>Fasciolaria tulipa</i>		<i>Turrilaturus craticulatus</i>
<i>Filifusus filamentosus</i>	<i>Filifusus filamentosus</i>		<i>Triplofusus giganteus</i>
<i>Pleuroploca trapezium</i>	<i>Pleuroploca trapezium</i>		<i>Thais speciosa</i>
	<i>Benimakia fastigium</i>		<i>Thais nodosa</i>
	<i>Benimakia lanceolata</i>	<i>Buccinum undatum</i>	<i>Buccinum undatum</i>
<i>Fusolaturus bruijnii</i>	<i>Fusolaturus bruijnii</i>		<i>Neptunea antiqua</i>
	<i>Fusolaturus pachyus</i>		<i>Mitrella scripta</i>
	<i>Fusolaturus pearsoni</i>		<i>Columbella aureomexicana</i>
	<i>Fusolaturus rikae</i>		<i>Euthria cumulata</i>
	<i>Fusolaturus</i> sp.1		<i>Euthria</i> sp.
	<i>Fusolaturus</i> sp.2		<i>Manaria</i> sp.
<i>Peristernia nassatula</i>	<i>Peristernia forskalii</i>		<i>Prodotia</i> sp.
	<i>Peristernia gemmata</i>		<i>Nassarius glans</i>
	<i>Peristernia marquesana</i>		<i>Nassarius reticulatus</i>
	<i>Peristernia nassatula</i>		<i>Busycon africanus</i>
	<i>Peristernia reincarnata</i>		<i>Conus angasi</i>
	<i>Peristernia</i> sp.1		<i>Phymorhynchus</i> sp.
	<i>Peristernia</i> sp.2		<i>Erosaria erosa</i>
	<i>Peristernia</i> sp.3	<i>Monetaria annulus</i>	<i>Monetaria annulus</i>

## 4. Results

The tree obtained through the molecular data of five loci is shown in Figure 1, using a parsimony criterion of direct optimization as implemented in POY 5.1.1. Jackknife support is indicated above each node; this tree was obtained through the optimal parameter set as discussed hereinafter.

One parameter set, 3221, follows the proposal of DeLaet (2005) in which gap openings are assigned a cost of 3, nucleotide transformations (transversions = transitions) are assigned a cost of 2 and gap extensions cost is 1. This was the parameter chosen (and the resulting tree hypothesis), and was also the one used for fissurellid gastropods in Aktipis *et al.* (2011).

Usually in the case of multiple parameters, a sensitivity analysis (Wheeler, 1995) is done in order to determine the best tree. However this was not the case here as one can explore an infinite number of parameters given an infinite number of hypotheses and still the choice is an arbitrary one: sensitivity analysis is therefore independent of hypothesis selection (Giribet, 2003). The optimality criterion aims at choosing the optimal set of parameters (among the explored ones) for a given data set, *i.e.*, the parameters that maximize precision among partitions (the agreement among data, using an ILD-derived index: Wheeler, 1995; DeLaet, 2005; 2014).

As mentioned above, sensitivity analyses do not conflict with the notion of choosing the best (most corroborated) phylogenetic hypothesis (*i.e.*, the tree obtained under the most congruent parameter set or under the most likely model). Sometimes several trees are presented simultaneously, usually side by side with the strict consensus of all the analyzed parameters (Wheeler, 1995; Wheeler & Hayashi, 1998; Edgecombe *et al.*, 1999, 2002; Giribet & Boyer, 2002; Giribet & Wheeler, 2002). Figures 2-6 illustrate the chosen hypothesis tree plotted with Navajo rugs: a graphic representation in which the parameter space (including the ML and the BI analyses of Couto *et al.*, 2016) is represented as a grid with each square corresponding to a different parameter (as evidenced in the bottom right). Filled squares indicate that the node is corroborated for the specified hypothesis.

The molecular results evidence three major well-supported deep clades of Fasciolariidae, but none of these correspond to the traditional contents of the recognized subfamilies, apart from the clade of *Dolicholatirus* and *Teralatirus* species. A first split (corroborated in all but parameter 3211) divides fasciolariids into a clade mostly corresponding to Fusininae, but also including the

clearly non-monophyletic genus *Pseudolatirus* traditionally classified in the Peristerniinae. Because this clade includes *Fusinus colus*, the type species of *Fusinus* (type genus of Fusiniinae), it is henceforth referred to as the *Fusinus colus* clade. Fasciolariinae, which appears monophyletic and fully supported in all parameter sets, is nested within a subclade of Fasciolariinae and Peristerniinae; as it includes *Fasciolaria tulipa*, the type species of *Fasciolaria* (type genus of Fasciolariinae), we will refer to it as the *Fasciolaria tulipa* clade. Finally, its sister group is a fully supported clade containing various taxa of Peristerniinae; as it includes *Peristernia nassatula* the type species of *Peristernia* (type genus of Peristerniinae), we will refer to it as the *Peristernia nassatula* clade.

The clade containing *Dolicholatirus* and *Teralatirus* was highly supported, its monophyly confirmed in all parameters, despite not included in Fasciolariidae. Its position varied among parameter sets, however.

Total evidence analysis based on the parameter 3221 is shown in the Figure 7. This is the most complete analysis of the family Fasciolariidae: five molecular loci (totaling circa 5.3 kbp) and 95 morphological characters. The topology evidences the same major clades as the previous molecular analysis and those of Couto *et al.* (2016): A *Fusinus colus* clade, a *Peristernia nassatula* clade, a *Fasciolaria tulipa* clade and a *Dolicholatirus* and *Teralatirus* clade. The latter one was shown to be monophyletic, but not belonging to the family Fasciolariidae.

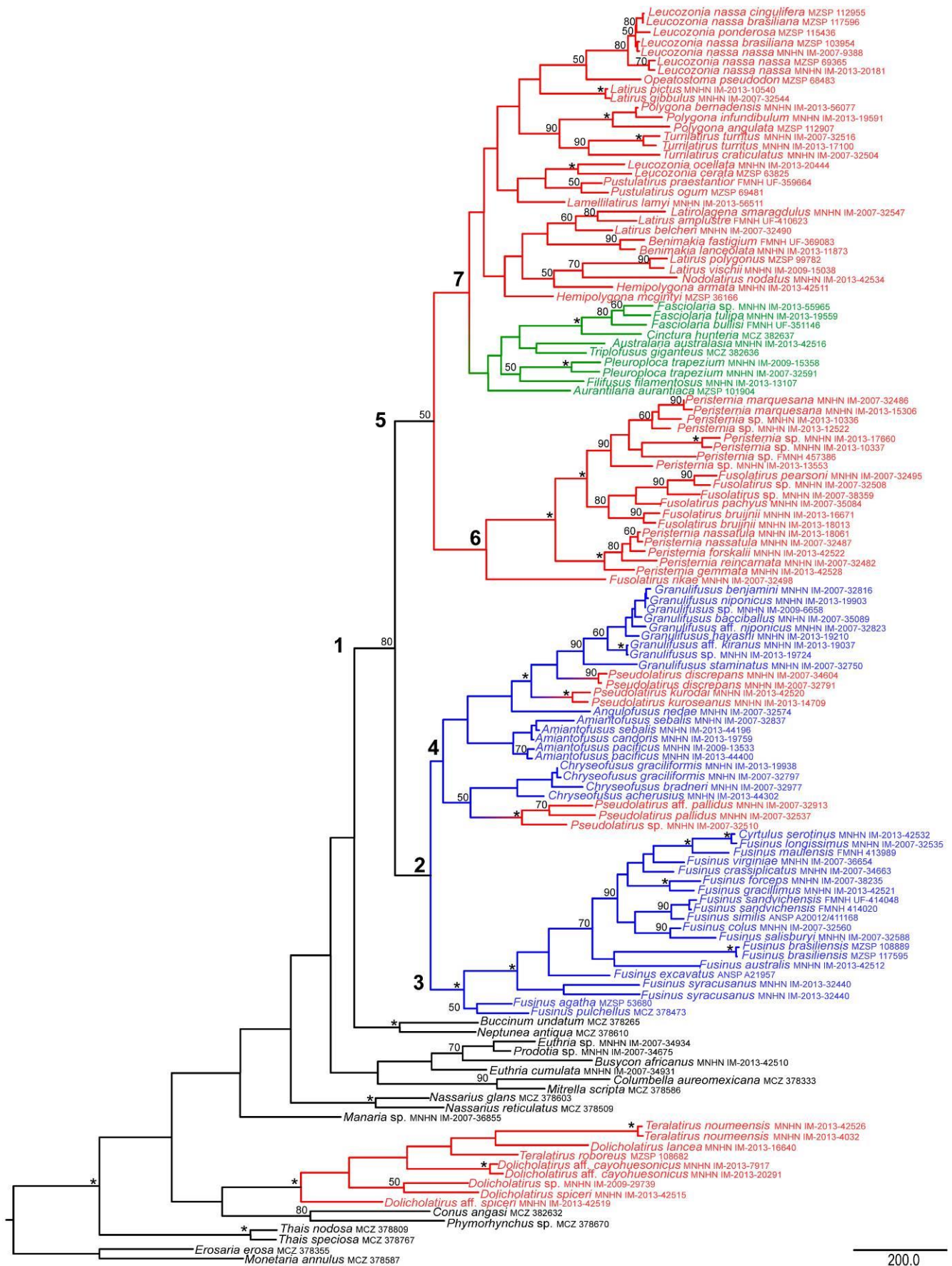


Figure 1. Phylogenetic relationships based on a parsimonious analysis done in POY under parameter 3221. Small numbers on nodes indicate jackknife support, only supports over 50 are shown, \* indicate full support. Color scheme: Black: non-fasciolariids. Blue: fusinines. Red: peristerniines. Green: fasciolariines.

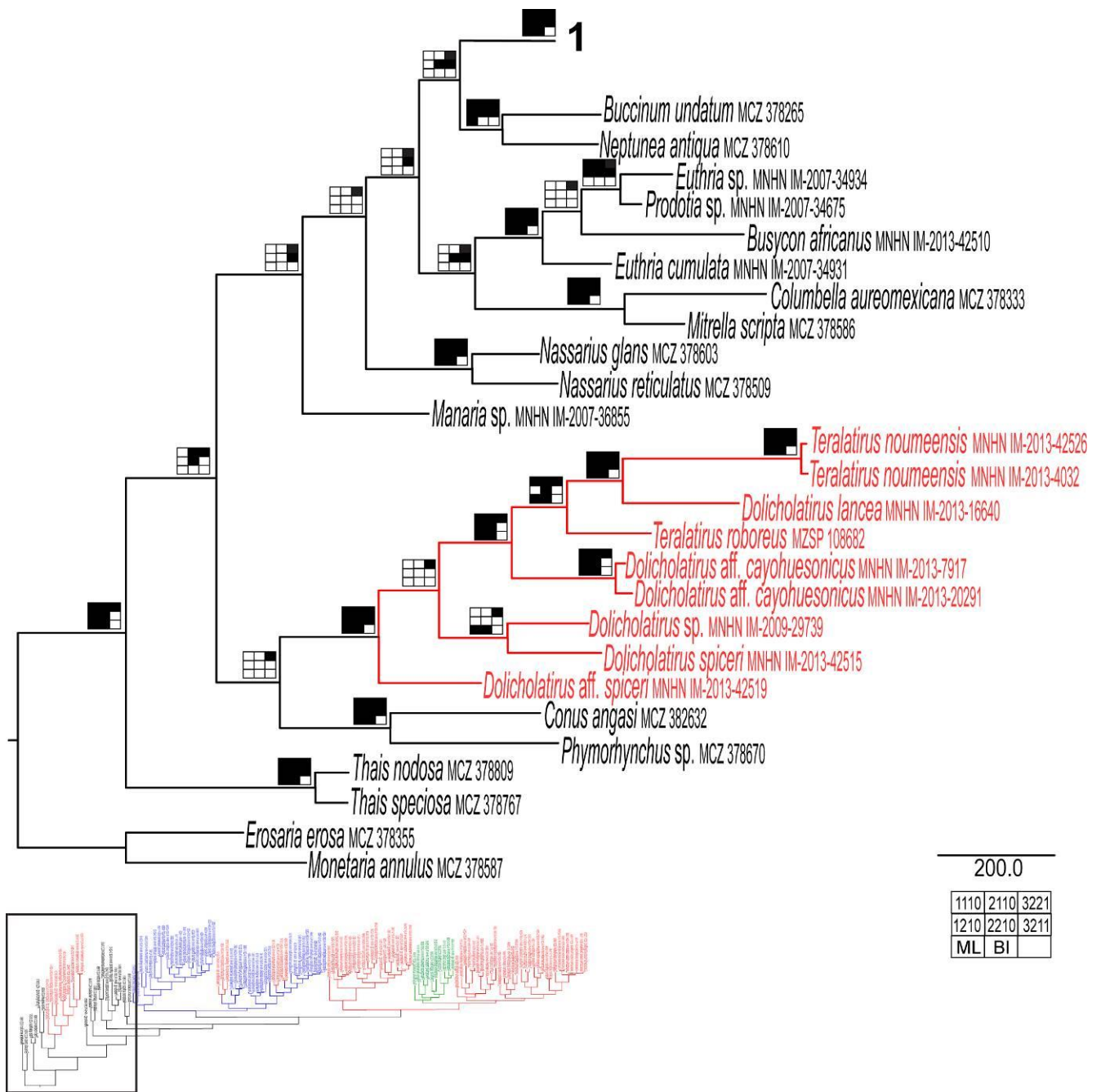


Figure 2. Phylogenetic relationships (part one) based on a parsimonious analysis done in POY under parameter 3221. Navajo rugs indicate support for the given parameter (bottom right). Node numbers are the same across all figures. Color scheme: Black: non-fasciolaridiids. Blue: fusinines. Red: peristerniines. Green: fasciolarines.



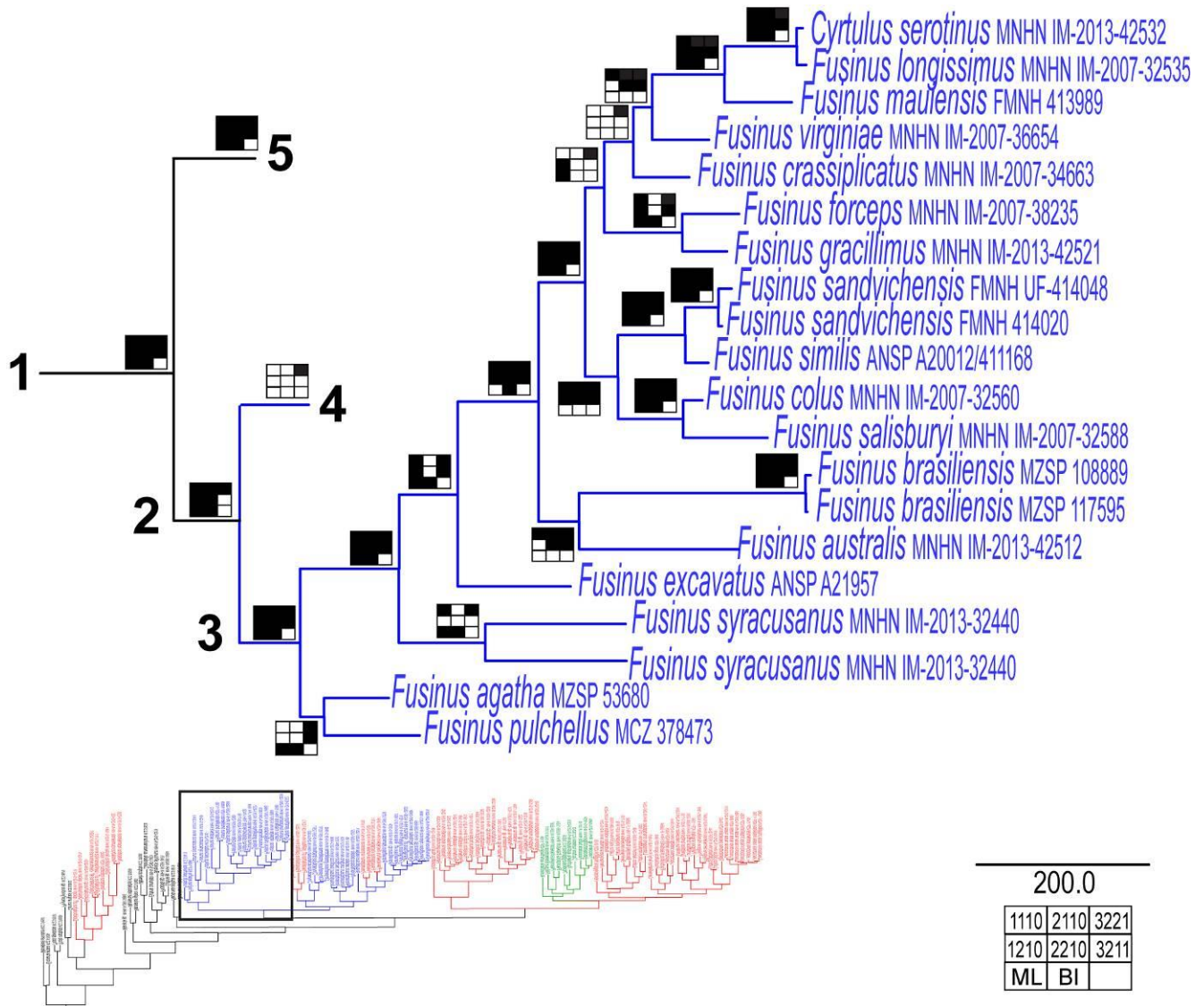


Figure 3. Phylogenetic relationships (part two) based on a parsimonious analysis done in POY under parameter 3221. Navajo rugs indicate support for the given parameter (bottom right). Node numbers are the same across all figures. Color scheme: Black: non-fasciolariids. Blue: fusinines. Red: peristerniines. Green: fasciolariines.



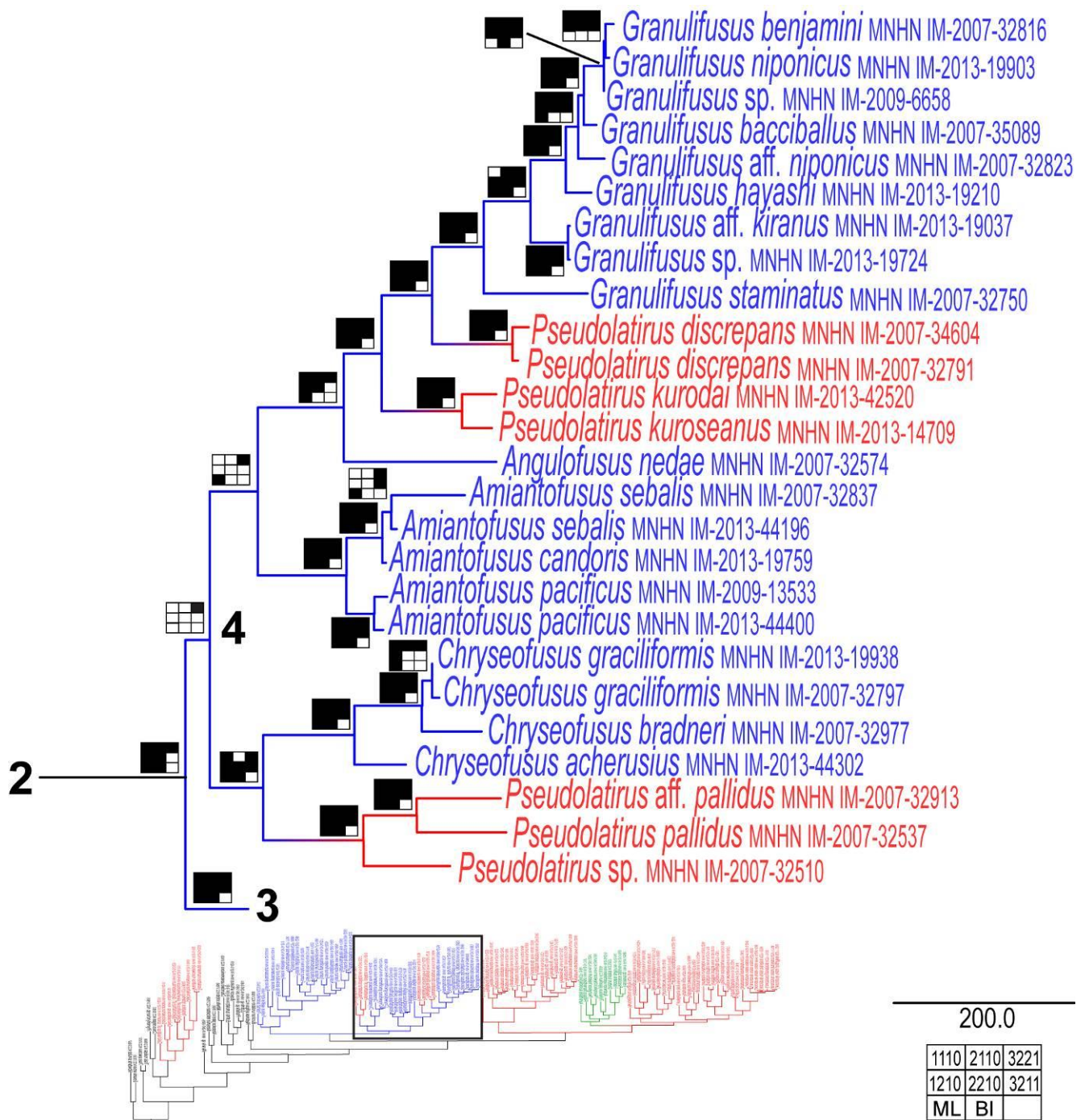


Figure 4. Phylogenetic relationships (part three) based on a parsimonious analysis done in POY under parameter 3221. Navajo rugs indicate support for the given parameter (bottom right). Node numbers are the same across all figures. Color scheme: Black: non-fascioliariids. Blue: fusinines. Red: peristerniines. Green: fascioliariines.

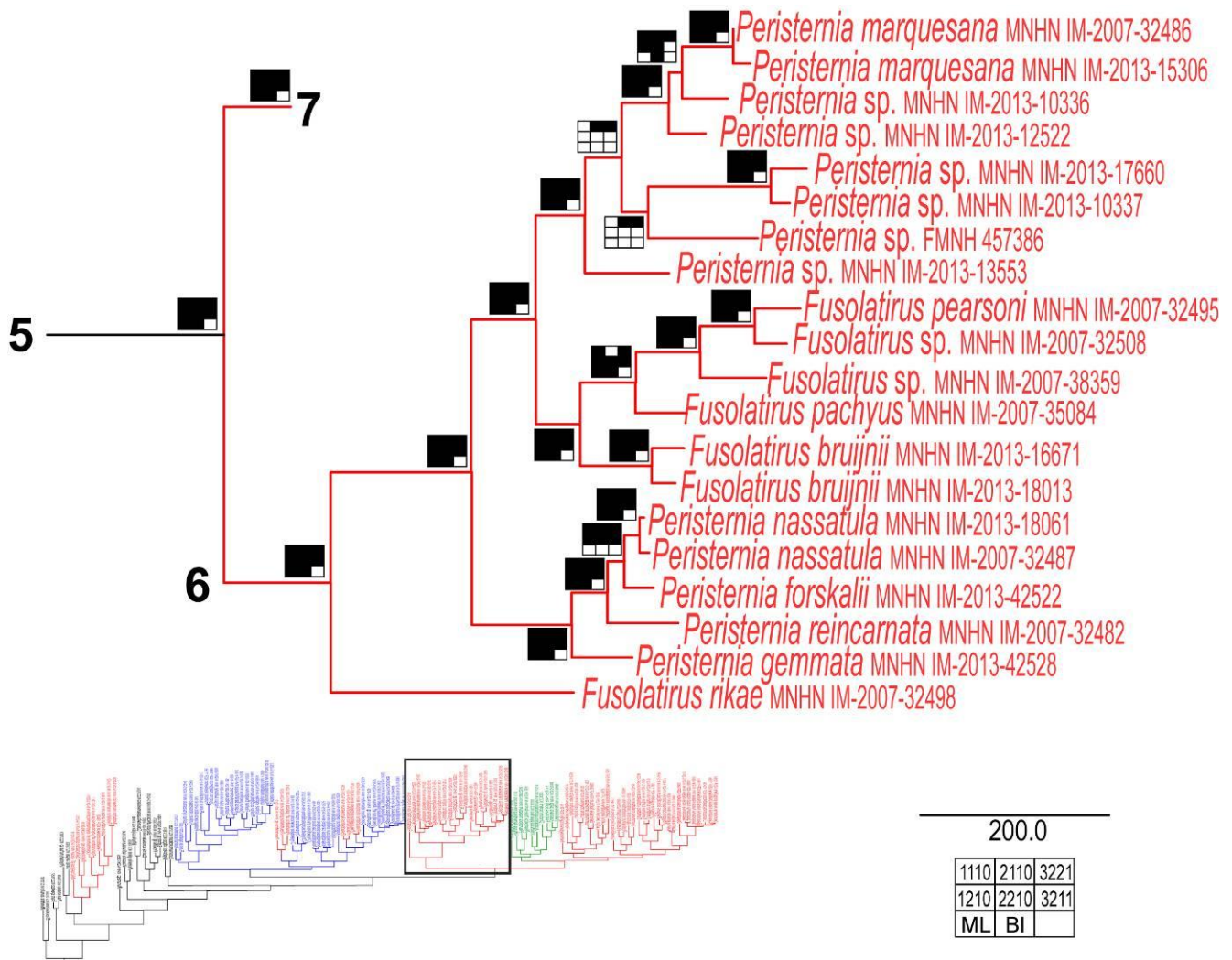
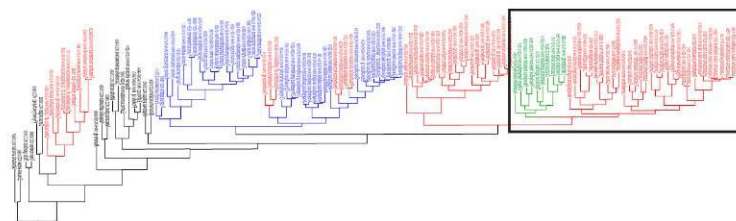
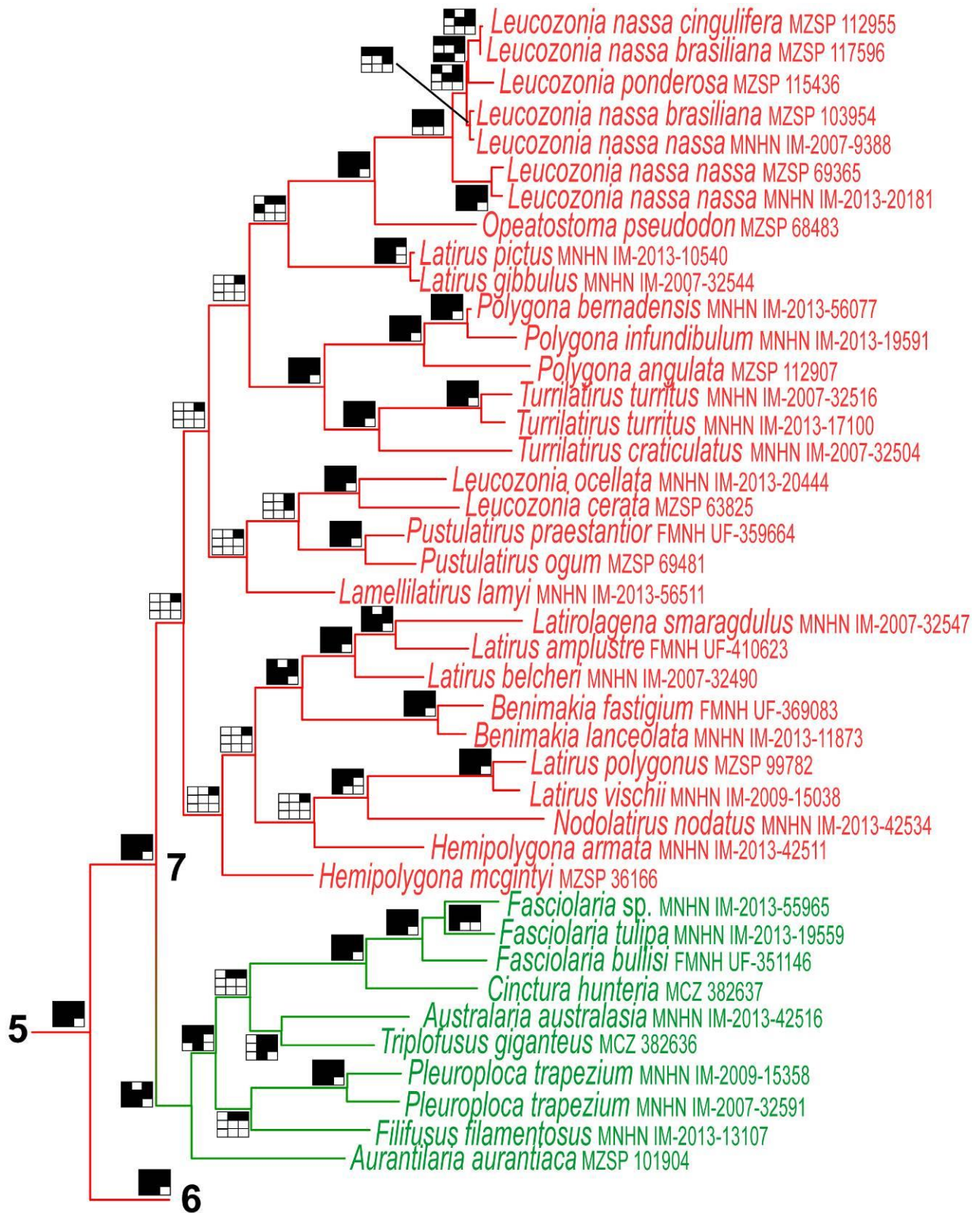


Figure 5. Phylogenetic relationships (part four) based on a parsimonious analysis done in POY under parameter 3221. Navajo rugs indicate support for the given parameter (bottom right). Node numbers are the same across all figures. Color scheme: Black: non-fascioliariids. Blue: fusinines. Red: peristerniines. Green: fascioliariines.

Figure 6 (following page). Phylogenetic relationships (part five) based on a parsimonious analysis done in POY under parameter 3221. Navajo rugs indicate support for the given parameter (bottom right) Node numbers are the same across all figures. Color scheme: Black: non-fascioliariids. Blue: fusinines. Red: peristerniines. Green: fascioliariines.





200.0

1110	2110	3221
1210	2210	3211
ML	BI	

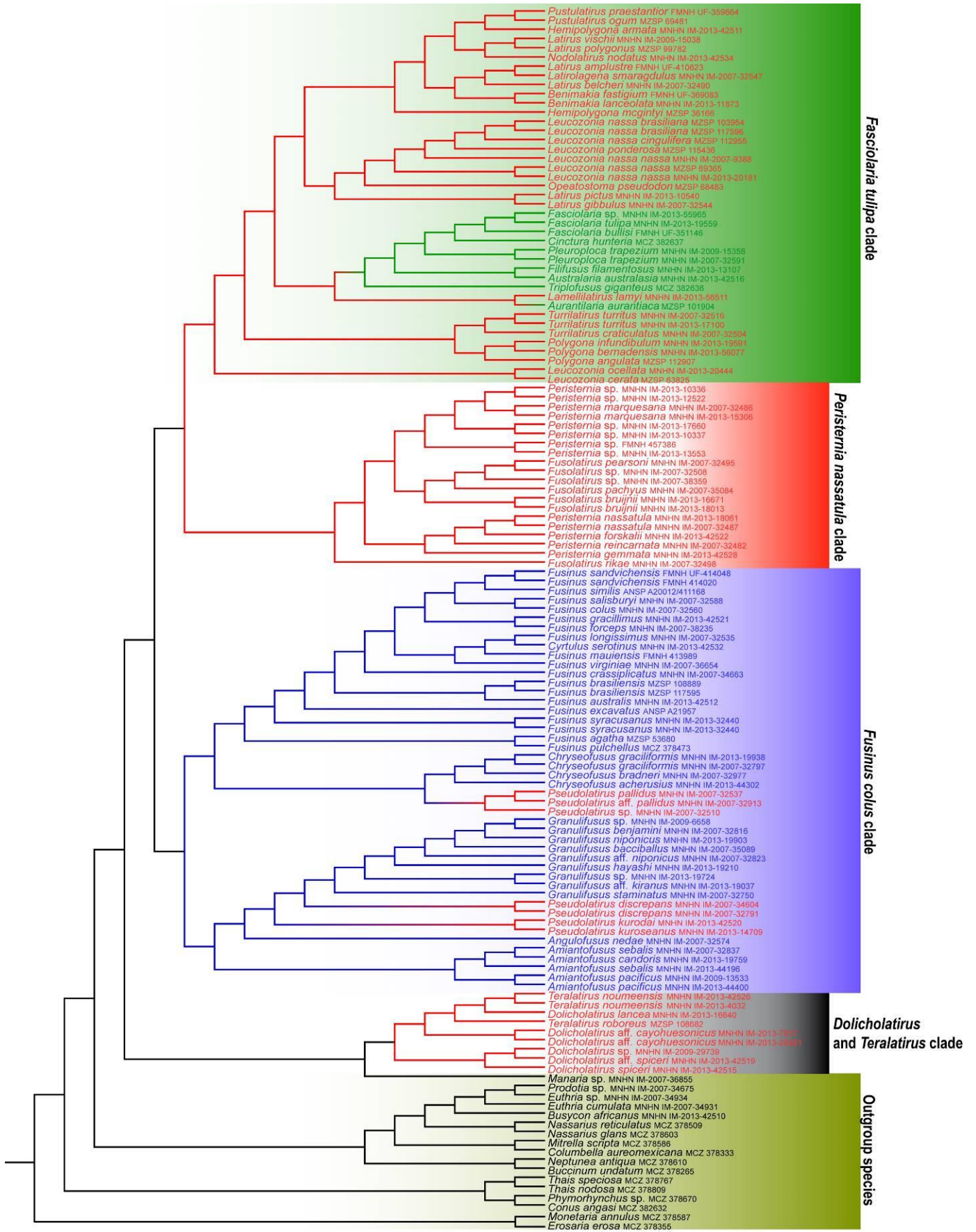


Figure 7. Phylogenetic relationships of Fasciolariidae for the total evidence analysis as implemented in POY under parameter 3221. Color scheme for text: Black: non-fasciolariids. Blue: fusinines. Red: peristerniines. Green: fasciolariines. Color shadings for each clade represent the supported clades.

## 5. Discussion

This is the most extensive phylogenetic analysis of the family Fascioliariidae endeavored to date being the first to include morphological and molecular data in a combined analysis. Within this brief section will be discussed the main differences and similarities between the total evidence analysis done in POY (Fig. 7) with the morphological analysis from Chapter I of this dissertation; a more extensive taxonomical and morphological discussion is also undertaken at the Chapter I. It is for the sake of readability that the section will be divided into the four main clades plus the outgroup species.

### 5.1 *Outgroup species*

Muricoids (species of *Thais*, Muricidae) and Conoids (*Conus angasi* and *Phymorhynchus* sp.) form a monophyletic group, that is the sister group of the remaining buccinoids, including Buccinidae, Nassariidae, Columbellidae and Fascioliariidae families. This agrees with Strong (2003), in which Buccinoidea is the sister taxon of Conoidea and Muricoidea in a polytomy. However, this scenario does not concur with Ponder & Lindberg (1997: Buccinoidea + Muricoidea sister to Cancellarioidea) or Simone (2011: Muricoidea + Cancellarioidea sister to Conoidea), but because very few taxa were sampled, it is not possible to make a concrete inference.

As with most analyses discussed so far, Buccinidae is not monophyletic, and in this case, assumes a polyphyletic state, with species of Nassariidae and Columbellidae intercalating buccinid species.

The inclusion of morphological data from outgroup species reveals the incongruence between the molecular data and morphology, as the achieved topology was not recovered in any of the analyzed weighting parameters or from Couto *et al.* (2016).

### 5.2 *Dolicholatirus and Teralatirus clade*

The clade containing species of the Fascioliariidae sensu lato *Dolicholatirus* and *Teralatirus* forms the sister group of a buccinid, *Manaria* sp. This genus possess species which superficially resemble fascioliariids, more specifically the genus *Amiantofusus*, but distinguish from it by the more reticulated shell pattern across the whole of the shell surface (Bouchet & Warén, 1985).

*Manaria* are related to deep-sea buccinids, e.g., *Eosipho*, *Termosipho*, etc. (Kantor *et al.*, 2013) and are very conchologically similar to *Amiantofusus*.

In all analyses (morphological, molecular, total evidence) the clade of *Dolicholatirus* and *Teralatirus* appear as highly supported, with virtually the same topology; neither genera is monophyletic. No further insights into the group may be given that have not already been done in Chapter I of this dissertation.

### 5.3 *Fusinus colus* clade

The combined molecular and morphological dataset evidences two main groups: a first split separates the more fusiform shells of the genera *Fusinus*, *Cyrtulus* and *Chryseofusus* (corresponding to clade 3a from Chapter I), from the remaining genera *Amiantofusus*, *Angulofusus* and *Granulifusus*. The polyphyletic genus *Pseudolatirus* corresponds to two lineages, being related to *Chryseofusus* and the other to *Granulifusus*, much like discussed in Chapter I and in Couto *et al.* (2016).

### 5.4 *Peristernia nassatula* clade

This clade groups *Peristernia* and *Fusolatirus* species. Clade 5a from Chapter I, is highly supported in both analyses of Couto *et al.* (2016) and in the parsimony analysis done in POY. The topology within this node is virtually identical among all analyses, which shows the congruence between the analyzed genes and morphology.

### 5.5 *Fasciolaria tulipa* clade

This clade has suffered the most modifications from the inclusion of morphological data in the analysis. As with the previous cases, the deep nodes evidenced much incongruence among the topologies, with each parameter analyzed generating a different relationship scheme, and different hypotheses of relation between the ML and the BI analysis of Couto *et al.* (2016).

Because the bulk of the peristerniines (clade 7 of Chapter I) appeared as a grade in the morphological analysis, only a few clades matched those of the combined dataset analysis. Clade 14 containing the genera *Leucozonia* and *Opeatostoma* was well recovered in both topologies, while clade 6d containing the precious fasciolariines, but here is included *Lamellilatirus lamyi*. Lyons & Snyder (2007) described the genus *Lamellilatirus* (type *Fusus ceramidus* Dall, 1889)



distinguishing it from *Fusinus* because of its peristerniine-like radula (ten cusps in the wide laterals, three cusps in the rachidian). The radula of *Lamellilaturus ceramidus* (Lyons & Snyder, 2007: fig. 3a) indeed resembles a typical peristerniine, lacking the gradual increase in the lateral inner cusps like *Fusinus* and the reduced cusp one of the lateral (resembling somewhat *Hemipolygona armata* and *Pustulaturus ogum* (Figs. 80, 83, Chapter I). The species *L. lamyi* was not analyzed morphologically, but if the radula resembles *L. ceramidus*, as illustrated by Lyons & Snyder (2007), than likely this species would be placed near clade 7 (Fig. 6, Chapter I). Another prospect is that this is the plesiomorphic radula type for this clade. The type species of *Lamellilaturus lamyi* (<https://science.mnhn.fr/institution/mnhn/collection/im/item/2000-25714>) resembles *Hemipolygona armata*.

Based on the total evidence analysis, the clade of *Dolicholaturus* and *Teralaturus* does not belong to Fasciolariidae, despite morphological evidence. The results obtained through the molecular dataset show a strong dissimilarity between *Dolicholaturus/Teralaturus* species from the remaining taxa, while exhibiting a strong affinity among themselves. This can be easily observed in the individual gene analyses of Couto *et al.* (2016: suppl. mat. 1-5): in all trees, *Dolicholaturus* and *Teralaturus* is well supported (in detriment to most of the other major groups).

The inclusion of morphological data has done little in altering the topology of the three major clades of Fasciolariidae. All three main clades suffered minor modifications internally but remained with the same inclusion of taxa as in the molecular analysis. However, with the inclusion of molecular data, the morphological tree suffered more drastically.

The main difference in Fasciolariidae that occurs for the analyzed molecular dataset (including the total evidence analysis) from the morphological dataset occurs within the clade of fusinines: in the first it is a crown-group, sister to the remaining fasciolariids, while in the latter it is a stem-group, comprising of three major clades (the clade of mainly *Amiantofusus*, *Chryseofusus* and *Fusinus*, and a clade of *Granulifusus*). The other major groups, *Peristernia* and *Fusolaturus* and Fasciolariinae remained more-or-less stable for morphological and most molecular analyses.

## 6. Conclusions

1. The molecular data was more determinant for the final topology than the morphological data;

2. *Dolicholattirus* and *Teralattirus* form a monophyletic group, external to Fasciolariidae;

3. The remaining fasciolariids were recovered as a monophyletic clade that fall into three main clades that correspond to the three currently recognized subfamilies, but with their taxonomic extension considerably revised;

4. The *Fusinus colus* clade, containing all the Fusinae, consisting of five major lineages corresponding to the genera *Amiantofusus*, *Angulofusus*, *Chryseofusus*, *Fusinus* and *Granulifusus*, and also including the non-monophyletic *Pseudolattirus*;

5. *Pseudolattirus*, a polyphyletic fusinine genus, is present in two lineages: related to *Chryseofusus* and another to *Granulifusus*;

6. The *Peristernia nassatula* clade, consisting of the non-monophyletic genera *Peristernia* and *Fusolattirus*; the name Peristerniinae can be retained for this clade;

7. The *Fasciolaria tulipa* clade, consisting of a monophyletic *Fasciolaria-Pleuroploca* clade and many other genera currently classified as peristerniines; the taxonomic extension of the subfamily Fasciolariinae can be revised to encompass this third clade;

8. The *Fasciolaria – Pleuroploca* clade also groups *Lamellilattirus lamyi*;

9. The genus *Leucozonia* is non-monophyletic; *L. cerata – L. ocellata* forms a monophyletic group; the *L. nassa* complex forms a monophyletic clade that is sister of *Opeatostoma pseudodon*;

10. The genera *Lattirus* and *Hemipolygona* are polyphyletic;



## 7. References

- Aktipis S.W., Boehm E. & Giribet G. 2011. Another step towards understanding the slit-limpets (Fissurellidae, Fissurelloidea, Vetigastropoda, Gastropoda): A combined five-gene molecular phylogeny. **Zoologica Scripta**, 40(3): 238-259. <http://doi.org/10.1111/j.1463-6409.2010.00468.x>.
- Bouchet P. & Warén A. 1985. Revision of the Northeast Atlantic bathyal and abyssal Neogastropoda excluding Turridae (Mollusca, Gastropoda). **Bollettino Malacologico** (Suppl 1): 1-296.
- Couto D.R., Bouchet P., Kantor Y.I., Simone L.R.L. & Giribet G. 2016. A multilocus molecular phylogeny of Fasciolaridae (Neogastropoda: Buccinoidea). **Molecular phylogenetics and evolution**, 99: 309-322.
- De Laet J. 2005. Parsimony and the problem of inapplicables in sequence data. *In*: Albert V.A. (Ed), **Parsimony, phylogeny, and genomics**. Oxford, Oxford University Press. p. 81-116.
- De Laet J. 2014. Parsimony analysis of unaligned sequence data: Maximization of homology and minimization of homoplasy, not minimization of operationally defined total cost or minimization of equally weighted transformations. **Cladistics**, 31(5): 550-567, 2015. <http://doi.org/10.1111/cla.12098>.
- Edgecombe G.D. & Giribet G. 2006. A century later - A total evidence re-evaluation of the phylogeny of scutigermorph centipedes (Myriapoda: Chilopoda). **Invertebrate Systematics**, 20(5): 503-525. <http://doi.org/10.1071/IS05044>.
- Edgecombe G.D. & Giribet G. 2009. Phylogenetics of scutigermorph centipedes (Myriapoda: Chilopoda) with implications for species delimitation and historical biogeography of the Australian and New Caledonian faunas. **Cladistics**, 25(4): 406-427. <http://doi.org/10.1111/j.1096-0031.2009.00253.x>.
- Edgecombe G.D., Giribet G. & Wheeler W.C. 1999. Phylogeny of Chilopoda: Combining 18S and 28S rRNA sequences and morphology. *In*: Melic A., De Haro J.J., Mendes, M. &

- Ribera I. (Eds). Evolución y Filogenia de Arthropoda, **Boletín de la Sociedad Entomológica Aragonesa** 26: 293-331.
- Edgecombe G.D., Giribet G. & Wheeler W.C. 2002. Phylogeny of Henicopidae (Chilopoda: Lithobiomorpha): A combined analysis of morphology and five molecular loci. **Systematic Entomology** 27: 31-64.
- Giribet G. 2003. Stability in phylogenetic formulations and its relationship to nodal support. **Systematic Biology**, 52(4): 554-564.
- Giribet G. & Boyer S.L. 2002. A cladistic analysis of the cyphophthalmid genera (Opiliones, Cyphophthalmi). **Journal of Arachnology**, 30(1): 110-128.
- Giribet G. & Edgecombe G.D. 2013. Stable phylogenetic patterns in scutigermorph centipedes (Myriapoda: Chilopoda: Scutigermorpha): dating the diversification of an ancient lineage of terrestrial arthropods. **Invertebrate Systematics**, 27: 485-501.
- Giribet G., Edgecombe G.D. & Wheeler W.C. 2001. Arthropod Phylogeny Based on Eight Molecular Loci and Morphology. **Nature**, 413: 157-161.
- Giribet G., Edgecombe G.D., Wheeler W.C. & Babbitt C. 2002. Phylogeny and Systematic Position of Opiliones: A Combined Analysis of Chelicerate Relationships Using Morphological and Molecular data. **Cladistics**, 18: 5-70.
- Giribet G., McIntyre E., Christian E., Espinasa L., Ferreira R.L., Francke O.F., Harvey M.S., Isaia M., Kováč L., McCutchen L., Souza M.F.V.R. & Zagamajster M. 2014. The first phylogenetic analysis of Palpigradi (Arachnida) - The most enigmatic arthropod order. **Invertebrate Systematics**, 28: 350-360. <http://doi.org/10.1071/IS13057>.
- Giribet G. & Wheeler W.C. 2002. On bivalve phylogeny: a high-level analysis of the Bivalvia (Mollusca) based on combined morphology and DNA sequence data. **Invertebrate Biology**, 121(4): 271-324. <http://doi.org/10.1111/j.1744-7410.2002.tb00132.x>.

- Kantor Y.I., Puillandre N., Fraussen K., Fedosov A. & Bouchet P. 2013. Deep-water Buccinidae (Gastropoda: Neogastropoda) from sunken wood, vents and seeps: molecular phylogeny and taxonomy. **Journal of the Marine Biological Association of the United Kingdom**, 93(8): 2177-2195. <http://doi.org/10.1017/S0025315413000672>.
- Lyons W.G. & Snyder M.A. 2007. New genera and species of Peristerniinae (Gastropoda: Fascioliariidae) from the Caribbean region, with comments on the fascioliariid fauna of Bermuda. **The Veliger**, 50(3): 225-240.
- Miller M.A., Pfeiffer W. & Schwartz T. 2010. Creating the CIPRES Science Gateway for inference of large phylogenetic trees. **Gateway Computing Environments Workshop (GCE)**, 1-8.
- Ponder W.F. & Lindberg D.R. 1997. Towards a phylogeny of gastropod molluscs: an analysis using morphological characters. **Zoological Journal of the Linnean Society**, 119: 83-265. <http://doi.org/10.1006/zjls.1996.0066>.
- Simone L.R.L. 2011. Phylogeny of the Caenogastropoda (mollusca), based on comparative morphology. **Arquivos de Zoologia**, São Paulo, 42(4): 161-323.
- Varón A., Vinh L.S. & Wheeler W.C. 2010. POY version 4: Phylogenetic analysis using dynamic homologies. **Cladistics**, 26:72-85. <http://doi.org/10.1111/j.1096-0031.2009.00282.x>.
- Wahlberg N., Braby M.F., Brower A.V.Z., de Jong R., Lee M., Nylin S., Pierce N.E., Sperling F.A.H., Vila R., Warren A.D. & Zakharov E. 2005. Synergistic Effects of Combining Morphological and Molecular Data in Resolving the Phylogeny of Butterflies and Skippers. **Proceedings of the Royal Society of London, B**, 272: 1577-1586.
- Wheeler W.C. 1995. Sequence alignment, parameter sensitivity, and the phylogenetic analysis of molecular data. **Systematic Biology**, 44(3): 321-331. <http://doi.org/10.1080/10635150290155881>.

Wheeler W.C. 1996. Optimization Alignment: the End of Multiple Sequence Alignment in Phylogenetics? **Cladistics**, 12: 1-9. <http://doi.org/10.1006/clad.1996.0001>.

Wheeler W.C. & Hayashi C.Y. 1998. The phylogeny of the extant chelicerate orders. **Cladistics**, 14(2): 173-192.

**A complement to the phylogenetic analysis of the work of Simone (2011): “Phylogeny of the Caenogastropoda (Mollusca), based on comparative morphology”**

## 1. Introduction

The classification and phylogeny of Caenogastropoda were analyzed by Simone (2011) in his work entitled "Phylogeny of the Caenogastropoda (Mollusca), based on comparative Morphology". This taxon is considered the most diverse among Mollusca, representing more than half of the number of species of the phylum (Ponder *et al.*, 2008, Simone, 2011). Its phylogenetical implications to the morphology and taxonomy in the fasciolariid framework have been extensively discussed in Chapter I of this dissertation.

In Simone's (2011) work a total 305 species were examined, including representatives of most families of Caenogastropoda, totaling 270 ingroup and 35 outgroups species. The morphological data was compiled through using several anatomical characters, from shell to all soft-parts, including detailed structures of the odontophore and nerve-ring, as well as behavioral and ecological data. In total 676 morphological characters were coded. The polarization was based on non-caenogastropod representatives, comprising of 27 heterobranchs, neritimorphs, cocculiniforms, patellogastropods and vetigastropods; eight representatives of other classes were also included; Rooting was in done in a Polyplacophora. Phylogenetic analysis resulted in 48 most parsimonious trees and the Strict consensus ( $L = 3.036$ ;  $CI = 51$ ;  $RI = 94$ ) was used to discuss groups and character evolution (See Chapter I, Fig. 107).

The Caenogastropoda monophyly is supported by 60 synapomorphies, and this clade is the sister group of Heterobranchia. The paraphyly of architaenoglossates was also corroborated. Among the most relevant results of this analysis is the monophyly of Neogastropoda, which include three superfamilies: Cancellarioidea, Conoidea and Muricoidea. The analysis did not recognize, nor had sufficient taxon sampling at this level, the Buccinoidea as a separate entity, although some representatives were recovered as a monophyletic clade within the superfamily Muricoidea.

The inclusion of more taxa in the analysis will increase the robustness of the analysis. It is likely that an increased pool of representatives, especially of buccinoideans, will corroborate more recent classifications which include Buccinoidea as a separate superfamily (*e.g.*, Bouchet & Rocroi, 2005; WoRMS, 2016).

## 2. Objectives

1. To insert the analyzed taxa present in Chapter I of this dissertation in the data matrix of Simone (2011) in order to test the phylogenetic position of Fasciolariidae and consequently, Buccinoidea.

## 3. Material and Methods

The examined material is the same as analyzed in chapter I of this dissertation. These taxa were inserted in the morphological data matrix of Simone (2011).

For full reference of taxa, characters and character states present see Simone (2011); additionally, the following character states were added in order to implement the analysis:

1. Character 98 (Retractor muscles of snout): state 8 (one, inserted laterally).
2. Character 285 (Nephridial gland): state 2 (present, inconspicuous).
3. Character 450 (Salivary ducts): state 5 (free from nerve ring and immersed in esophagus wall).

For search strategies, algorithms and full phylogenetic methodology the reader is referred to the chapter I of this dissertation.

## 4. Results

The traditional search through a TBR algorithm, using prior weighting only (best hit scored 742 times out of 1000, best TBR = 3207 [overflow was achieved and trees were than subjected to another round of TBR with the trees stored in memory]), generated 1296 equally parsimonious trees of 5518 steps (L), a consistency index of 28 (Ci) and a retention index of 92 (Ri). The resulting strict consensus generated a tree with L = 5533, Ci = 28 and Ri = 92 (Figs. 1, 2).

The topology of the tree (Fig. 1) revealed a monophyletic Buccinoidea and, more inclusively, Fasciolariidae. *Thais speciosa* (Muricoidea) and *Monetaria annulus* (Cypraeoidea) are not shown in this clade since they were recovered within cypraeids and muricids, respectively.

Within Fasciolariidae, many polytomies are present, but few groups are recognizable: 1) The Fusinae clade with three major groups: 1.1) A clade grouping *Fusinus*, *Chryseofusus*, *Cyrtulus serotinus* and *Pseudolatirus pallidus*; 1.2) *Amiantofusus* and *Pseudolatirus kuroseanus* and; 1.3) *Granulifusus* and *Pseudolatirus discrepans*. 2) The genus *Pustulatirus*. 3) A group of mainly *Leucozonia* species and *Opeatostoma pseudodon*. 4) *Dolicholatirus* and *Teralatirus* and *Leucozonia nassa brasiliiana* and *L. ponderosa*. 5) The traditional Fasciolariinae, *Latirus vischii* and *Nodolatirus nodatus*.

Color scheme used for all terminals and branches in the trees correspond to each of the assigned subfamilies: black: outgroup species, non-fasciolariids; blue: fusinines; red: peristerniines; green: fasciolariines. This does not correspond to the natural subfamilies but the one previously assigned (pre-analysis).



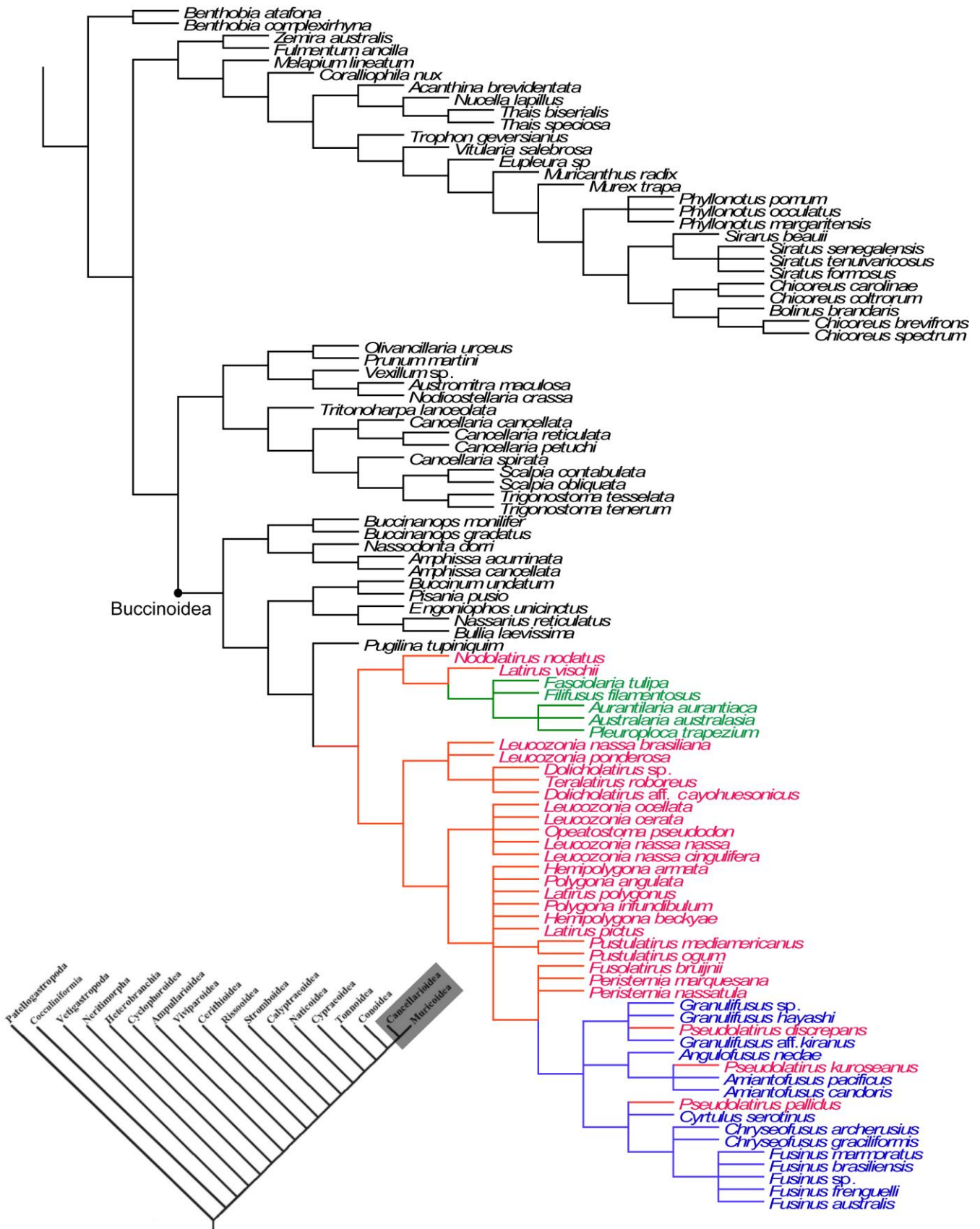


Figure 1: Phylogenetic tree obtained through parsimonious analysis in TnT using prior, unweighted characters; the Fascioliidae taxa were included in the morphological dataset from Simone (2011). Figure shows clade of Muricoidea and Cancellarioidea (bottom left) in detail. Color reference, see text.

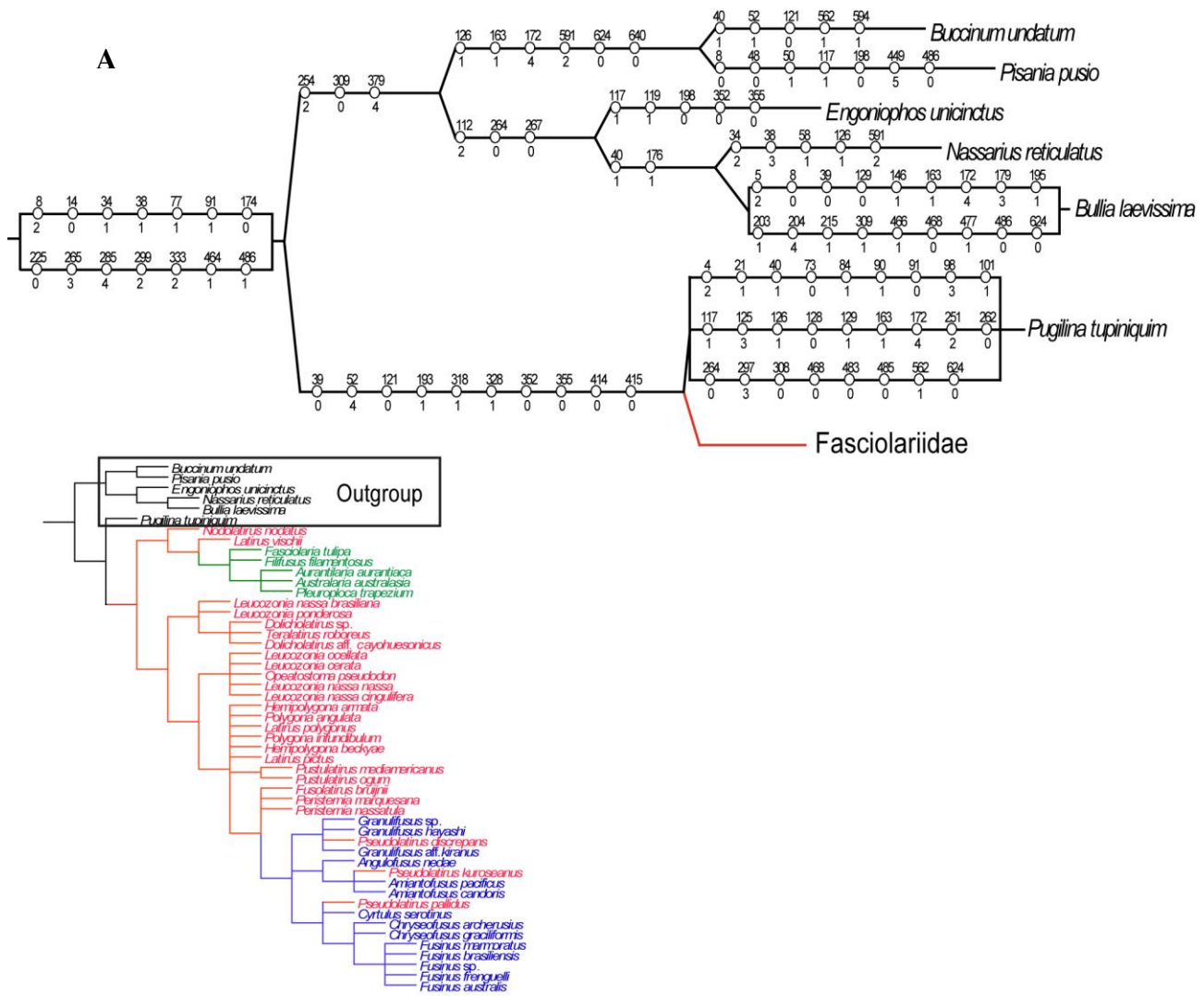


Figure 2A: Phylogenetic tree of the included taxa, with synapomorphies (dark circles) and homoplasies (empty circles). Number above each symbol represents the character, while the number below indicates the character state of according to Simone (2011). Color reference, see text.

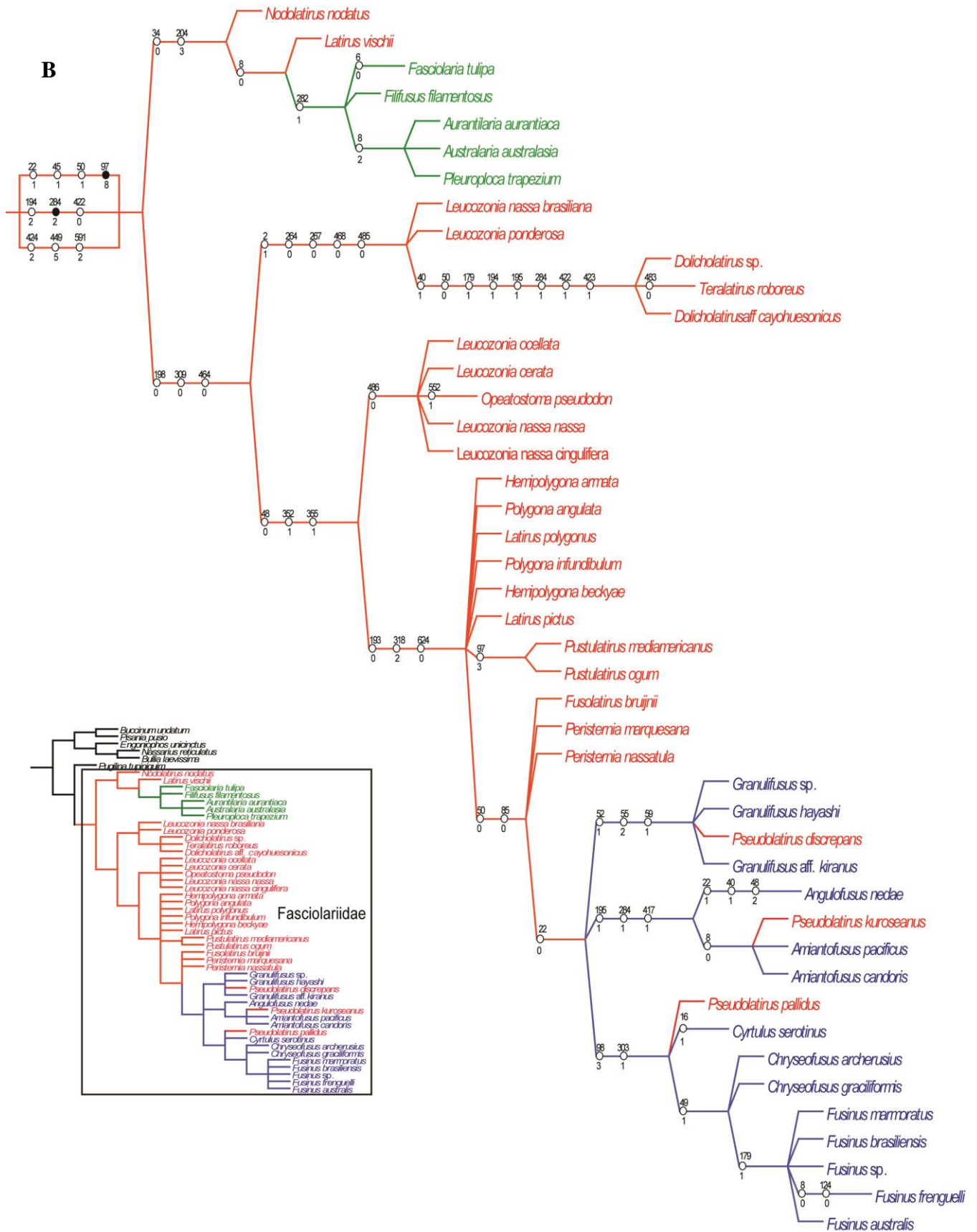


Figure 2B: Phylogenetic tree of the included taxa, with synapomorphies (dark circles) and homoplasies (empty circles). Number above each symbol represents the character, while the number below indicates the character state of according to Simone (2011). Color reference, see text.

## 5. Discussion

The analysis of Simone (2011) recovered three main clades in Neogastropoda: The first split separates Conoidea from the remaining Cancellarioidea and Muricoidea, although with the taxonomy of ingroup species thoroughly revised (as that would require some taxa to be included in Cancellarioidea, *e.g.*, *Cancellaria*).

Contrarily, in the present analysis Buccinoidea was recovered monophyletic, with all buccinoid species from Simone (2011) present in this clade: *Buccinanops gradatus*, *B. monolifer*, *Amphissa acuminata*, *A. cancellata* and *Nassodonta dorri*. In this context, Cancellarioidea *sensu* Simone (2011) is the sister group of Buccinoidea, and this is the sister group of Muricoidea (Fig. 1). This in turn would be the sister clade of Conoidea. This scenario of evolution is congruent with the idea that the superfamily Buccinoidea is considered highly derived in the Neogastropoda scheme (due to several losses of typical neogastropod synapomorphies: mainly the accessory salivary glands and the rectal gland [Kantor & Fedosov, 2009]).

The superfamily was supported by many homoplasies, shown in Fig. 2. Worth noting is the head-foot groove (char 77: 1), the inconspicuous nephridial gland (char 285: 2) and Gland of Leiblein with a long duct (char 486: 1). The gland of Leiblein is highly variable in Neogastropoda; Kantor & Fedosov (2009) argue in favor of independent origins of the Gland and valve of Leiblein. These authors hypothesized that the Neogastropoda is paraphyletic, mainly because the main synapomorphies that support Neogastropoda are lacking in Buccinoidea (anal gland, accessory salivary glands), since the Gland and Valve of Leiblein are not homologous among the different lineages.

The family Fasciolariidae contained many polytomies in the internal nodes; this is because the characters provided in the dataset from Simone (2011) lack the resolution to clarify the internal relationship among the many lineages. Despite this, there are some striking differences the present analysis has from the one presented in Chapter I. Notable, the clade of *Dolicholatirus* and *Teralatirus* is immersed within fasciolariid, not basally, as the analysis in Chapter I. The Fusinines also appeared as a crown group, as opposed to a paraphyletic, stem group. Finally, the *Fasciolaria* and *Pleuroploca* clade, despite appearing with the same topology as the previous analysis, represents the first split in the group of Fasciolariids.

The purpose of this analysis, in verifying the position of the studied Fasciolaridae taxa in a broader context, within Neogastropoda and Buccinoidea, including the dataset from Simone (2011), proved successful. On the other hand, the characters used in this analysis are considered more conservative and, therefore, of limited utility for more inclusive groups, such as the case for fasciolarids.

It is good to remark that this analysis has made possible the resolution of the superfamily Buccinoidea, which was not recovered in the original analysis of Simone (2011). This proves that the inclusion of a variable pool of taxa is needed in order to clarify the relationship of more inclusive groups. The inclusion of more buccinoid taxa will most certainly clarify the relationship between the families contained in the superfamily, proving that an ample taxonomical sampling is vital.

### 5.1 Character matrix

TAXON	CHARACTER	0	0	0	0	0	0	0	0	0	1	1	1	1	1	1	1	1	1	1	2	2	2	2	2	2	2	2	2	2	3	3	3	3	3	3	3	3	3	3		
		1	2	3	4	5	6	7	8	9	0	1	2	3	4	5	6	7	8	9	0	1	2	3	4	5	6	7	8	9	0	1	2	3	4	5	6	7	8	9		
<i>Monetaria annulus</i>		4	4	0	2	3	2	7	0	0	0	-	-	-	1	0	1	1	1	0	1	0	0	0	0	0	0	1	1	0	0	1	1	0	0	0	0	0				
<i>Thais speciosa</i>		4	2	0	0	0	1	1&2	0	5	0	0	-	-	-	1	0	0	0	-	0	-	0	0	1	0	0	0	1	1	0	0	1	0	1	0	0	0				
<i>Pugilina tupiniquim</i>		4	1	0	0	2	1	1&2	0	2	0	0	-	-	-	0	0	0	0	-	0	-	1	0	0	0	0	0	1	1	0	0	1	1	1	0	0	0	1			
<i>engoniophos uncinatus</i>		4	1	0	0	0	1	1&2	0	2	0	0	-	-	-	0	0	0	0	-	0	-	0	0	0	0	0	0	1	1	0	0	1	1	1	1	0	1	0	1		
<i>Nassarius reticulatus</i>		4	1	0	0	0	1	1&2	0	2	0	0	-	-	-	0	0	0	0	-	0	-	0	0	0	0	0	1	1	0	0	1	1	0	1	1	2	0	1	0	3	
<i>Bullia laevissima</i>		4	1	0	0	0	2	1&2	0	0	0	0	-	-	-	0	0	0	0	-	0	-	0	0	0	0	0	1	1	0	0	1	1	0	1	1	0	0	0	1		
<i>Buccinum undatum</i>		4	1	0	0	0	1	1&2	0	2	0	0	-	-	-	0	0	0	0	-	0	-	0	0	0	0	0	1	1	0	0	1	1	0	1	1	0	1	0	1		
<i>Pisania pusio</i>		4	1	0	0	0	1	1&2	0	0	0	0	-	-	-	0	0	0	0	-	0	-	0	0	0	0	0	1	1	0	0	1	1	0	0	0	0	1	0	0		
<i>Dolicholatus sp.</i>		4	1	1	0	0	1	1&2	0	2	0	0	-	-	-	0	0	0	0	-	0	-	0	1	0	0	0	0	1	1	0	0	1	1	0	0	0	0	1	0	0	
<i>Teralatirus roboreus</i>		4	1	1	0	0	1	1&2	0	2	0	0	-	-	-	0	0	0	0	-	0	-	0	1	0	0	0	0	1	1	0	0	1	1	0	0	0	0	1	0	0	
<i>Dolicholatus aff. cayohuesonicus</i>		4	1	1	0	0	1	1&2	0	2	0	0	-	-	-	0	0	0	0	-	0	-	0	1	0	0	0	0	1	1	0	0	1	1	0	0	0	0	1	0	0	
<i>Angulofusus neda</i>		4	1	0	0	0	1	1&2	0	2	0	0	-	-	-	0	0	0	0	-	0	-	0	1	0	0	0	0	1	1	0	0	1	1	0	0	0	0	1	0	0	
<i>Pseudolatus kuroseanus</i>		4	1	0	0	0	1	1&2	0	0	0	0	-	-	-	0	0	0	0	-	0	-	0	0	0	0	0	1	1	0	0	1	1	0	0	0	0	1	0	0	0	
<i>Amiantofusus pacificus</i>		4	1	0	0	0	1	1&2	0	0	0	0	-	-	-	0	0	0	0	-	0	-	0	0	0	0	0	1	1	0	0	1	1	0	0	0	0	1	0	0	0	
<i>Amiantofusus candoris</i>		4	1	0	0	0	1	1&2	0	0	0	0	-	-	-	0	0	0	0	-	0	-	0	0	0	0	0	1	1	0	0	1	1	0	0	0	0	1	0	0	0	
<i>Pseudolatus pallidus</i>		4	1	0	0	0	1	1&2	0	2	0	0	-	-	-	0	0	0	0	-	0	-	0	0	0	0	0	1	1	0	0	1	1	0	0	0	0	1	0	0	0	
<i>Chryseofusus archerius</i>		4	1	0	0	0	1	2	0	0	0	0	-	-	-	0	0	0	0	-	0	-	0	0	0	0	0	1	1	0	0	1	1	0	0	1	1	0	0	0	0	
<i>Chryseofusus graciliformis</i>		4	1	0	0	0	1	2	0	0	0	0	-	-	-	0	0	0	0	-	0	-	0	0	0	0	0	1	1	0	0	1	1	0	0	0	0	1	0	0	0	
<i>Fusinus marmoratus</i>		4	1	0	0	0	1	1&2	0	2	0	0	-	-	-	0	0	0	0	-	0	-	0	0	0	0	0	1	1	0	0	1	1	0	0	0	0	1	0	0	0	
<i>Fusinus brasiliensis</i>		4	1	0	0	0	1	1&2	0	2	0	0	-	-	-	0	0	0	0	-	0	-	0	0	0	0	0	1	1	0	0	1	1	0	0	0	0	1	0	0	0	
<i>Fusinus sp.</i>		4	1	0	0	0	1	1&2	0	2	0	0	-	-	-	0	0	0	0	-	0	-	0	0	0	0	0	1	1	0	0	1	1	0	0	0	0	1	0	0	0	
<i>Fusinus frenguelli</i>		4	1	0	0	0	1	1&2	0	0	0	0	-	-	-	0	0	0	0	-	0	-	0	0	0	0	0	1	1	0	0	1	1	0	0	0	0	1	0	0	0	
<i>Fusinus australis</i>		4	1	0	0	0	1	1&2	0	2	0	0	-	-	-	0	0	0	0	-	0	-	0	0	0	0	0	1	1	0	0	1	1	0	0	0	0	1	0	0	0	
<i>Cyrtulus serotinus</i>		4	1	0	0	0	1	1&2	0	2	0	0	-	-	-	0	0	1	0	-	0	-	0	0	0	0	0	1	1	0	0	1	1	0	0	0	0	1	0	0	0	
<i>Granulifusus sp.</i>		4	1	0	0	0	1	1&2	0	2	0	0	-	-	-	0	0	0	0	-	0	-	0	0	0	0	0	1	1	0	0	1	1	0	0	0	0	1	0	0	0	
<i>Granulifusus hayashi</i>		4	1	0	0	0	1	1&2	0	2	0	0	-	-	-	0	0	0	0	-	0	-	0	0	0	0	0	1	1	0	0	1	1	0	0	0	0	1	0	0	0	
<i>Pseudolatus discrepans</i>		4	1	0	0	0	1	1&2	0	2	0	0	-	-	-	0	0	0	0	-	0	-	0	0	0	0	0	1	1	0	0	1	1	0	0	0	0	1	0	0	0	
<i>Granulifusus aff. kiranus</i>		4	1	0	0	0	1	1&2	0	2	0	0	-	-	-	0	0	0	0	-	0	-	0	0	0	0	0	1	1	0	0	1	1	0	0	0	0	1	0	0	0	
<i>Fusolatus bruijnii</i>		4	1	0	0	0	1	1&2	0	2	0	0	-	-	-	0	0	0	0	-	0	-	0	1	0	0	0	1	1	0	0	1	1	0	0	0	0	1	0	0	0	
<i>Peristernia marquesana</i>		4	1	0	0	0	1	1&2	0	2	0	0	-	-	-	0	0	0	0	-	0	-	0	1	0	0	0	1	1	0	0	1	1	0	0	0	0	1	0	0	0	
<i>Peristernia nassatula</i>		4	1	0	0	0	1	1&2	0	2	0	0	-	-	-	0	0	0	0	-	0	-	0	1	0	0	0	1	1	0	0	1	1	0	0	0	0	1	0	0	0	
<i>Nodolatus nodatus</i>		4	1	0	0	0	1	1&2	0	2	0	0	-	-	-	0	0	0	0	-	0	-	0	1	0	0	0	1	1	0	0	1	1	0	0	0	0	0	1	0	0	0
<i>Latirus vischii</i>		4	1	0	0	0	1	1&2	0	0	0	0	-	-	-	0	0	0	0	-	0	-	0	1	0	0	0	1	1	0	0	1	1	0	0	0	0	0	1	0	0	0
<i>Aurantilaria aurantiaca</i>		4	1	0	0	0	1	1&2	0	2	0	0	-	-	-	0	0	0	0	-	0	-	0	1	0	0	0	1	1	0	0	1	1	0	0	0	0	0	1	0	0	0
<i>Fasciolaria tulipa</i>		4	1	0	0	0	1	0	0	0	0	0	-	-	-	0	0	0	0	-	0	-	0	1	0	0	0	1	1	0	0	0	0	0	0	0	0	0	0	0	0	
<i>Australaria australasia</i>		4	1	0	0	0	1	1&2	0	2	0	0	-	-	-	0	0	0	0	-	0	-	0	1	0	0	0	1	1	0	0	0	0	0	0	0	0	0	0	0	0	
<i>Pleuroploca trapezium</i>		4	1	0	0	0	1	1&2	0	2	0	0	-	-	-	0	0	0	0	-	0	-	0	1	0	0	0	1	1	0	0	0	0	0	0	0	0	0	0	0	0	
<i>Filifusus filamentosus</i>		4	1	0	0	0	1	1	0	0	0	0	-	-	-	0	0	0	0	-	0	-	0	1	0	0	0	1	1	0	0	0	0	0	0	0	0	0	0	0	0	
<i>Hemipolygona armata</i>		4	1	0	0	0	1	1&2	0	2	0	0	-	-	-	0	0	0	0	-	0	-	0	1	0	0	0	1	1	0	0	0	0	0	0	0	0	0	0	0	0	
<i>Pustulatus mediamericus</i>		4	1	0	0	0	1	1&2	0	2	0	0	-	-	-	0	0	0	0	-	0	-	0	1	0	0	0	1	1	0	0	0	0	0	0	0	0	0	0	0	0	
<i>Pustulatus ogun</i>		4	1	0	0	0	1	1&2	0	2	0	0	-	-	-	0	0	0	0	-	0	-	0	1	0	0	0	1	1	0	0	0	0	0	0	0	0	0	0	0	0	
<i>Polygona angulata</i>		4	1	0	0	0	1	1&2	0	2	0	0	-	-	-	0	0	0	0	-	0	-	0	1	0	0	0	1	1	0	0	0	0	0	0	0	0	0	0	0	0	
<i>Latirus polygonus</i>		4	1	0	0	0	1	1&2	0	2	0	0	-	-	-	0	0	0	0	-	0	-	0	1	0	0	0	1	1	0	0	0	0	0	0	0	0	0	0	0	0	
<i>Polygona infundibulum</i>		4	1	0	0	0	1	1&2	0	2	0	0	-	-	-	0	0	0	0	-	0	-	0	1	0	0	0	1	1	0	0	0	0	0	0	0	0	0	0	0	0	
<i>Hemipolygona beckyae</i>		4	1	0	0	0	1	1&2	0	2	0	0	-	-	-	0	0	0	0	-	0	-	0	1	0	0	0	1	1	0	0	0	0	0	0	0	0	0	0	0	0	
<i>Latirus pictus</i>		4	1	0	0	0	1																																			









TAXON	CHARACTER	16	16	16	16	16	16	16	16	16	17	17	17	17	17	17	17	17	17	17	18	18	18	18	18	18	18	18	18	18	19	19	19	19	19	19	19	19	19	19	
		0	1	2	3	4	5	6	7	8	9	0	1	2	3	4	5	6	7	8	9	0	1	2	3	4	5	6	7	8	9	0	1	2	3	4	5	6	7	8	9
<i>Monetaria annulus</i>		5	2	3	0	0	1	2	2	1	3	1	0	1	0	0	2	1	1	0	3	1	0	8	5	0	0	1	0	-	-	0	2	1	1	0	1	0	1	1	1
<i>Thais speciosa</i>		0	0	0	0	0	0	1	0	0	-	-	-	-	4	1	1	2	1	0	3	1	0	1	0	0	0	1	0	-	-	0	1	0	0	0	1	0	1	1	1
<i>Pugilina tupiniquim</i>		0	0	0	0	1	0	1	0	0	-	-	-	-	4	0	0	2	2	0	3	2	0	1	0	0	0	1	0	-	-	0	1	0	0	1	1	0	1	1	1
<i>engoniophos uncinatus</i>		0	0	0	0	0	0	1	0	0	-	-	-	-	0	0	0	2	2	0	3	2	0	1	0	0	0	1	0	-	-	0	1	0	0	0	1	0	1	1	0
<i>Nassarius reticulatus</i>		0	0	0	0	0	0	1	0	0	-	-	-	-	0	0	0	2	1	0	3	2	0	1	0	0	0	1	0	-	-	0	1	0	0	0	1	0	1	1	1
<i>Bullia laevisima</i>		0	0	0	0	1	0	1	0	0	-	-	-	-	4	0	0	2	1	0	3	3	0	1	0	0	0	1	0	-	-	0	1	0	0	0	1	1	1	1	1
<i>Buccinum undatum</i>		0	0	0	0	1	0	1	0	0	-	-	-	-	4	0	0	2	2	0	3	2	0	1	0	0	0	1	0	-	-	0	1	0	0	0	1	0	1	1	1
<i>Pisania pusio</i>		0	0	0	0	1	0	1	0	0	-	-	-	-	4	0	0	2	2	0	3	2	0	1	0	0	0	1	0	-	-	0	1	0	0	0	1	0	1	1	0
<i>Dolicholatus sp.</i>		0	0	0	0	0	0	1	0	0	-	-	-	-	0	0	0	2	2	0	3	1	0	1	0	0	0	1	0	-	-	0	1	0	0	1	1	1	1	1	0
<i>Teralatirus roboreus</i>		0	0	0	0	0	0	1	0	0	-	-	-	-	0	0	0	2	2	0	3	1	0	1	0	0	0	1	0	-	-	0	1	0	0	1	1	1	1	1	0
<i>Dolicholatus aff. cayohuesonicus</i>		0	0	0	0	0	0	1	0	0	-	-	-	-	0	0	0	2	2	0	3	1	0	1	0	0	0	1	0	-	-	0	1	0	0	1	1	1	1	1	0
<i>Angulofusus netae</i>		0	0	0	0	0	0	1	0	0	-	-	-	-	0	0	0	2	2	0	3	2	0	1	0	0	0	1	0	-	-	0	1	0	0	2	1	1	1	0	
<i>Pseudolatus kuroseanus</i>		0	0	0	0	0	0	1	0	0	-	-	-	-	0	0	0	2	2	0	3	2	0	1	0	0	0	1	0	-	-	0	1	0	0	2	1	1	1	0	
<i>Amiantofusus pacificus</i>		0	0	0	0	0	0	1	0	0	-	-	-	-	0	0	0	2	2	0	3	2	0	1	0	0	0	1	0	-	-	0	1	0	0	2	1	1	1	0	
<i>Amiantofusus candoris</i>		0	0	0	0	0	0	1	0	0	-	-	-	-	0	0	0	2	2	0	3	2	0	1	0	0	0	1	0	-	-	0	1	0	0	2	1	1	1	0	
<i>Pseudolatus pallidus</i>		0	0	0	0	0	0	1	0	0	-	-	-	-	0	0	0	2	2	0	3	2	0	1	0	0	0	1	0	-	-	0	1	0	0	2	0	1	1	0	
<i>Chryseofusus archeruisus</i>		0	0	0	0	0	0	1	0	0	-	-	-	-	0	0	0	2	2	0	3	2	0	1	0	0	0	1	0	-	-	0	1	0	0	2	0	1	1	0	
<i>Chryseofusus graciliformis</i>		0	0	0	0	0	0	1	0	0	-	-	-	-	0	0	0	2	2	0	3	2	0	1	0	0	0	1	0	-	-	0	1	0	0	2	0	1	1	0	
<i>Fusinus marmoratus</i>		0	0	0	0	0	0	1	0	0	-	-	-	-	0	0	0	2	2	0	3	1	0	1	0	0	0	1	0	-	-	0	1	0	0	2	0	1	1	0	
<i>Fusinus brasiliensis</i>		0	0	0	0	0	0	1	0	0	-	-	-	-	0	0	0	2	2	0	3	1	0	1	0	0	0	1	0	-	-	0	1	0	0	2	0	1	1	0	
<i>Fusinus sp.</i>		0	0	0	0	0	0	1	0	0	-	-	-	-	0	0	0	2	2	0	3	1	0	1	0	0	0	1	0	-	-	0	1	0	0	2	0	1	1	0	
<i>Fusinus frenguelli</i>		0	0	0	0	0	0	1	0	0	-	-	-	-	0	0	0	2	2	0	3	1	0	1	0	0	0	1	0	-	-	0	1	0	0	2	0	1	1	0	
<i>Fusinus australis</i>		0	0	0	0	0	0	1	0	0	-	-	-	-	0	0	0	2	2	0	3	1	0	1	0	0	0	1	0	-	-	0	1	0	0	2	0	1	1	0	
<i>Cyrtulus serotinus</i>		0	0	0	0	0	0	1	0	0	-	-	-	-	0	0	0	2	2	0	3	2	0	1	0	0	0	1	0	-	-	0	1	0	0	2	0	1	1	0	
<i>Granulifusus sp.</i>		0	0	0	0	0	0	1	0	0	-	-	-	-	0	0	0	2	2	0	3	2	0	1	0	0	0	1	0	-	-	0	1	0	0	2	0	1	1	0	
<i>Granulifusus hayashi</i>		0	0	0	0	0	0	1	0	0	-	-	-	-	0	0	0	2	2	0	3	2	0	1	0	0	0	1	0	-	-	0	1	0	0	2	0	1	1	0	
<i>Pseudolatus discrepans</i>		0	0	0	0	0	0	1	0	0	-	-	-	-	0	0	0	2	2	0	3	2	0	1	0	0	0	1	0	-	-	0	1	0	0	2	0	1	1	0	
<i>Granulifusus aff. kiranus</i>		0	0	0	0	0	0	1	0	0	-	-	-	-	0	0	0	2	2	0	3	2	0	1	0	0	0	1	0	-	-	0	1	0	0	2	0	1	1	0	
<i>Fusolatus bruijnii</i>		0	0	0	0	0	0	1	0	0	-	-	-	-	0	0	0	2	2	0	3	2	0	1	0	0	0	1	0	-	-	0	1	0	0	2	0	1	1	0	
<i>Peristernia marquesana</i>		0	0	0	0	0	0	1	0	0	-	-	-	-	0	0	0	2	2	0	3	2	0	1	0	0	0	1	0	-	-	0	1	0	0	2	0	1	1	0	
<i>Peristernia nassatula</i>		0	0	0	0	0	0	1	0	0	-	-	-	-	0	0	0	2	2	0	3	2	0	1	0	0	0	1	0	-	-	0	1	0	0	2	0	1	1	0	
<i>Nodolatus nodatus</i>		0	0	0	0	0	0	1	0	0	-	-	-	-	0	0	0	2	2	0	3	2	0	1	0	0	0	1	0	-	-	0	1	0	0	1	2	0	1	1	1
<i>Latirus vischii</i>		0	0	0	0	0	0	1	0	0	-	-	-	-	0	0	0	2	2	0	3	2	0	1	0	0	0	1	0	-	-	0	1	0	0	1	2	0	1	1	1
<i>Aurantilaria aurantiaca</i>		0	0	0	0	0	0	1	0	0	-	-	-	-	0	0	0	2	2	0	3	2	0	1	0	0	0	1	0	-	-	0	1	0	0	1	2	0	1	1	1
<i>Fasciolaria tulipa</i>		0	0	0	0	0	0	1	0	0	-	-	-	-	0	0	0	2	2	0	3	2	0	1	0	0	0	1	0	-	-	0	1	0	0	1	2	0	1	1	1
<i>Australaria australasia</i>		0	0	0	0	0	0	1	0	0	-	-	-	-	0	0	0	2	2	0	3	2	0	1	0	0	0	1	0	-	-	0	1	0	0	1	2	0	1	1	1
<i>Pleuroploca trapezium</i>		0	0	0	0	0	0	1	0	0	-	-	-	-	0	0	0	2	2	0	3	2	0	1	0	0	0	1	0	-	-	0	1	0	0	1	2	0	1	1	1
<i>Filifusus filamentosus</i>		0	0	0	0	0	0	1	0	0	-	-	-	-	0	0	0	2	2	0	3	2	0	1	0	0	0	1	0	-	-	0	1	0	0	1	2	0	1	1	1
<i>Hemipolygona armata</i>		0	0	0	0	0	0	1	0	0	-	-	-	-	0	0	0	2	2	0	3	2	0	1	0	0	0	1	0	-	-	0	1	0	0	2	0	1	1	0	
<i>Pustulatus mediamericus</i>		0	0	0	0	0	0	1	0	0	-	-	-	-	0	0	0	2	2	0	3	2	0	1	0	0	0	1	0	-	-	0	1	0	0	2	0	1	1	0	
<i>Pustulatus ogum</i>		0	0	0	0	0	0	1	0	0	-	-	-	-	0	0	0	2	2	0	3	2	0	1	0	0	0	1	0	-	-	0	1	0	0	2	0	1	1	0	
<i>Polygona angulata</i>		0	0	0	0	0	0	1	0	0	-	-	-	-	0	0	0	2	2	0	3	2	0	1	0	0	0	1	0	-	-	0	1	0	0	2	0	1	1	0	
<i>Latirus polygonus</i>		0	0	0	0	0	0	1	0	0	-	-	-	-	0	0	0	2	2	0	3	2	0	1	0	0	0	1	0	-	-	0	1	0	0	2	0	1	1	0	
<i>Polygona infundibulum</i>		0	0	0	0	0	0	1	0	0	-	-	-	-	0	0	0	2	2	0	3	2	0	1	0	0	0	1	0	-	-	0	1	0	0	2	0	1	1	0	
<i>Hemipolygona beckyae</i>		0	0	0	0	0	0	1	0	0	-	-	-	-	0	0	0	2	2	0	3	2	0	1	0	0	0	1	0	-	-	0	1	0	0	2	0	1	1	0	
<i>Latirus pictus</i>		0	0	0	0	0	0	1	0	0	-	-	-	-	0	0	0	2	2	0	3	2	0	1	0	0	0	1	0	-	-	0	1	0	0	2	0	1	1	0	
<i>Leucozonia ocellata</i>		0	0	0	0	0	0	1	0	0</																															

TAXON	CHARACTER	20	20	20	20	20	20	20	20	20	21	21	21	21	21	21	21	21	21	21	22	22	22	22	22	22	22	22	22	22	23	23	23	23	23	23	23	23						
		0	1	2	3	4	5	6	7	8	9	0	1	2	3	4	5	6	7	8	9	0	1	2	3	4	5	6	7	8	9	0	1	2	3	4	5	6	7	8	9			
<i>Monetaria annulus</i>		1	1	4	0	0	0	0	0	0	0	0	0	0	-	0	0	1	1	2	1	1	0	1	1	2	0	1	1	1	1	1	1	1	1	1	1	1						
<i>Thais speciosa</i>		1	1	0	0	0	0	0	0	0	0	1	1	2																														
<i>Pugilina tupiniquim</i>		1	1	0	0	0	1	0	0	0	?	0	0	0	?	?	0	0	1	1	2	1	1	0	1	0	?	0	1	1	1	1	1	?	?	0	0	0	1	0	0	1	?	
<i>engoniophos uncinatus</i>		1	1	0	0	0	1	0	0	0	?	0	0	0	?	?	0	0	1	1	2	1	1	0	1	0	?	0	1	1	1	1	1	?	?	0	0	0	1	0	0	1	?	
<i>Nassarius reticulatus</i>		1	1	0	0	0	0	0	0	0	?	0	0	0	?	?	0	0	1	1	2	1	1	0	1	0	?	0	1	1	1	1	1	?	?	0	0	0	1	0	0	1	?	
<i>Bullia laevisima</i>		1	1	0	0	1	4	0	0	0	?	0	0	0	?	?	?	0	1	1	2	1	1	0	1	0	?	0	1	1	1	1	1	?	?	0	0	0	1	0	0	1	?	
<i>Buccinum undatum</i>		1	1	0	0	0	0	0	0	0	?	0	0	0	?	?	0	0	1	1	2	1	1	0	1	0	?	0	1	1	1	1	1	1	?	?	0	0	0	1	0	0	1	?
<i>Pisania pusio</i>		1	1	0	0	0	0	0	0	0	?	0	0	0	?	?	0	0	1	1	2	1	1	0	1	0	?	0	1	1	1	1	1	?	?	0	0	0	1	0	0	1	?	
<i>Dolicholatus</i> sp.		1	1	0	0	0	0	0	0	0	?	0	0	0	?	?	0	0	1	1	2	1	1	0	1	0	?	0	1	1	1	1	1	?	?	0	0	0	1	0	0	1	?	
<i>Teralatirus roboreus</i>		1	1	0	0	0	0	0	0	0	?	0	0	0	?	?	0	0	1	1	2	1	1	0	1	0	?	0	1	1	1	1	1	?	?	0	0	0	1	0	0	1	?	
<i>Dolicholatus</i> aff. <i>cayohuesonicus</i>		1	1	0	0	0	0	0	0	0	?	0	0	0	?	?	0	0	1	1	2	1	1	0	1	0	?	0	1	1	1	1	1	?	?	0	0	0	1	0	0	1	?	
<i>Angulofusus neda</i>		1	1	0	0	0	0	0	0	0	?	0	0	0	?	?	0	0	1	1	2	1	1	0	1	0	?	0	1	1	1	1	1	?	?	0	0	0	1	0	0	1	?	
<i>Pseudolatus kuroseanus</i>		1	1	0	0	0	0	0	0	0	?	0	0	0	?	?	0	0	1	1	2	1	1	0	1	0	?	0	1	1	1	1	1	?	?	0	0	0	1	0	0	1	?	
<i>Amiantofusus pacificus</i>		1	1	0	0	0	0	0	0	0	?	0	0	0	?	?	0	0	1	1	2	1	1	0	1	0	?	0	1	1	1	1	1	?	?	0	0	0	1	0	0	1	?	
<i>Amiantofusus candoris</i>		1	1	0	0	0	0	0	0	0	?	0	0	0	?	?	0	0	1	1	2	1	1	0	1	0	?	0	1	1	1	1	1	?	?	0	0	0	1	0	0	1	?	
<i>Pseudolatus pallidus</i>		1	1	0	0	0	0	0	0	0	?	0	0	0	?	?	0	0	1	1	2	1	1	0	1	0	?	0	1	1	1	1	1	?	?	0	0	0	1	0	0	1	?	
<i>Chryseofusus archeruisus</i>		1	1	0	0	0	0	0	0	0	?	0	0	0	?	?	0	0	1	1	2	1	1	0	1	0	?	0	1	1	1	1	1	?	?	0	0	0	1	0	0	1	?	
<i>Chryseofusus graciliformis</i>		1	1	0	0	0	0	0	0	0	?	0	0	0	?	?	0	0	1	1	2	1	1	0	1	0	?	0	1	1	1	1	1	?	?	0	0	0	1	0	0	1	?	
<i>Fusinus marmoratus</i>		1	1	0	0	0	0	0	0	0	?	0	0	0	?	?	0	0	1	1	2	1	1	0	1	0	?	0	1	1	1	1	1	?	?	0	0	0	1	0	0	1	?	
<i>Fusinus brasiliensis</i>		1	1	0	0	0	0	0	0	0	?	0	0	0	?	?	0	0	1	1	2	1	1	0	1	0	?	0	1	1	1	1	1	?	?	0	0	0	1	0	0	1	?	
<i>Fusinus</i> sp.		1	1	0	0	0	0	0	0	0	?	0	0	0	?	?	0	0	1	1	2	1	1	0	1	0	?	0	1	1	1	1	1	?	?	0	0	0	1	0	0	1	?	
<i>Fusinus frenguelli</i>		1	1	0	0	0	0	0	0	0	?	0	0	0	?	?	0	0	1	1	2	1	1	0	1	0	?	0	1	1	1	1	1	?	?	0	0	0	1	0	0	1	?	
<i>Fusinus australis</i>		1	1	0	0	0	0	0	0	0	?	0	0	0	?	?	0	0	1	1	2	1	1	0	1	0	?	0	1	1	1	1	1	?	?	0	0	0	1	0	0	1	?	
<i>Cyrtulus serotinus</i>		1	1	0	0	0	0	0	0	0	?	0	0	0	?	?	0	0	1	1	2	1	1	0	1	0	?	0	1	1	1	1	1	?	?	0	0	0	1	0	0	1	?	
<i>Granulifusus</i> sp.		1	1	0	0	0	0	0	0	0	?	0	0	0	?	?	0	0	1	1	2	1	1	0	1	0	?	0	1	1	1	1	1	?	?	0	0	0	1	0	0	1	?	
<i>Granulifusus hayashi</i>		1	1	0	0	0	0	0	0	0	?	0	0	0	?	?	0	0	1	1	2	1	1	0	1	0	?	0	1	1	1	1	1	?	?	0	0	0	1	0	0	1	?	
<i>Pseudolatus discrepans</i>		1	1	0	0	0	0	0	0	0	?	0	0	0	?	?	0	0	1	1	2	1	1	0	1	0	?	0	1	1	1	1	1	?	?	0	0	0	1	0	0	1	?	
<i>Granulifusus</i> aff. <i>kiranus</i>		1	1	0	0	0	0	0	0	0	?	0	0	0	?	?	0	0	1	1	2	1	1	0	1	0	?	0	1	1	1	1	1	?	?	0	0	0	1	0	0	1	?	
<i>Fusolatus bruijnii</i>		1	1	0	0	0	0	0	0	0	?	0	0	0	?	?	0	0	1	1	2	1	1	0	1	0	?	0	1	1	1	1	1	?	?	0	0	0	1	0	0	1	?	
<i>Peristernia marquesana</i>		1	1	0	0	0	0	0	0	0	?	0	0	0	?	?	0	0	1	1	2	1	1	0	1	0	?	0	1	1	1	1	1	?	?	0	0	0	1	0	0	1	?	
<i>Peristernia nassatula</i>		1	1	0	0	0	0	0	0	0	?	0	0	0	?	?	0	0	1	1	2	1	1	0	1	0	?	0	1	1	1	1	1	?	?	0	0	0	1	0	0	1	?	
<i>Nodolatus nodatus</i>		1	1	0	0	0	3	0	0	0	?	0	0	0	?	?	0	0	1	1	2	1	1	0	1	0	?	0	1	1	1	1	1	?	?	0	0	0	1	0	0	1	?	
<i>Latirus vischii</i>		1	1	0	0	0	3	0	0	0	?	0	0	0	?	?	0	0	1	1	2	1	1	0	1	0	?	0	1	1	1	1	1	?	?	0	0	0	1	0	0	1	?	
<i>Aurantilaria aurantiaca</i>		1	1	0	0	0	3	0	0	0	?	0	0	0	?	?	0	0	1	1	2	1	1	0	1	0	?	0	1	1	1	1	1	?	?	0	0	0	1	0	0	1	?	
<i>Fasciolaria tulipa</i>		1	1	0	0	0	3	0	0	0	?	0	0	0	?	?	0	0	1	1	2	1	1	0	1	0	?	0	1	1	1	1	1	?	?	0	0	0	1	0	0	1	?	
<i>Australaria australasia</i>		1	1	0	0	0	3	0	0	0	?	0	0	0	?	?	0	0	1	1	2	1	1	0	1	0	?	0	1	1	1	1	1	?	?	0	0	0	1	0	0	1	?	
<i>Pleuroploca trapezium</i>		1	1	0	0	0	3	0	0	0	?	0	0	0	?	?	0	0	1	1	2	1	1	0	1	0	?	0	1	1	1	1	1	?	?	0	0	0	1	0	0	1	?	
<i>Filifusus filamentosus</i>		1	1	0	0	0	3	0	0	0	?	0	0	0	?	?	0	0	1	1	2	1	1	0	1	0	?	0	1	1	1	1	1	?	?	0	0	0	1	0	0	1	?	
<i>Hemipolygona armata</i>		1	1	0	0	0	0	0	0	0	?	0	0	0	?	?	0	0	1	1	2	1	1	0	1	0	?	0	1	1	1	1	1	?	?	0	0	0	1	0	0	1	?	
<i>Pustulatus mediamericus</i>		1	1	0	0	0	0	0	0	0	?	0	0	0	?	?	0	0	1	1	2	1	1	0	1	0	?	0	1	1	1	1	1	?	?	0	0	0	1	0	0	1	?	
<i>Pustulatus ogum</i>		1	1	0	0	0	0	0	0	0	?	0	0	0	?	?	0	0	1	1	2	1	1	0	1	0	?	0	1	1	1	1	1	?	?	0	0	0	1	0	0	1	?	
<i>Polygona angulata</i>		1	1	0	0	0	0	0	0	0	?	0	0	0	?	?	0	0	1	1	2	1	1	0	1	0	?	0	1	1	1	1	1	?	?	0	0	0	1	0	0	1	?	
<i>Latirus polygonus</i>		1	1	0	0	0	0	0	0	0	?	0	0	0	?	?	0	0	1	1	2	1	1	0	1	0	?	0	1	1	1	1	1	?	?	0	0	0	1	0	0	1	?	
<i>Polygona infundibulum</i>		1	1	0	0	0	0	0	0	0	?	0	0	0	?	?	0	0	1	1	2	1	1	0	1	0	?	0	1	1	1	1	1	?	?	0	0	0	1	0	0	1	?	
<i>Hemipolygona beckyae</i>		1																																										



TAXON	CHARACTER																																							
	28	28	28	28	28	28	28	28	28	28	29	29	29	29	29	29	29	29	29	29	30	30	30	30	30	30	30	30	30	30	31	31	31	31	31	31	31	31		
<i>Monetaria annulus</i>	0	0	0	8	1	1	0	0	2	2	0	0	0	0	0	0	0	1	0	1	0	2	0	0	2	-	0	0	0	1	1	2	0	5	1	2	0	0	0	1
<i>Thais speciosa</i>	0	0	0	0	1	1	0	0	0	2	0	0	0	0	0	0	0	1	0	1	0	2	0	0	0	0	0	0	1	1	2	0	0	?	0	0	4	0	2	
<i>Pugilina tupiniquim</i>	?	?	?	0	1	1	4	?	?	2	0	0	0	0	0	0	3	0	2	0	2	0	0	0	0	0	0	0	1	1	?	?	0	-	-	0	0	0	1	
<i>engoniophos uncinatus</i>	?	?	?	0	1	1	4	?	?	2	0	0	0	0	0	0	3	0	2	0	2	0	0	0	0	0	0	1	0	?	?	?	0	-	-	0	0	0	2	
<i>Nassarius reticulatus</i>	?	?	?	0	1	1	4	?	?	2	0	0	0	0	0	0	2	0	2	0	2	0	0	0	0	0	0	1	0	?	?	?	0	-	-	0	0	0	2	
<i>Bullia laevis</i>	?	?	?	0	1	1	4	?	?	2	0	0	0	0	0	0	3	0	2	0	2	0	0	0	0	0	0	1	1	?	?	?	0	-	-	0	0	0	2	
<i>Buccinum undatum</i>	?	?	?	0	1	1	4	?	?	2	0	0	0	0	0	0	1	0	2	0	2	0	0	0	0	0	0	1	0	?	?	?	0	-	-	0	0	0	2	
<i>Pisania pusio</i>	?	?	?	0	1	1	4	?	?	2	0	0	0	0	0	0	1	0	2	0	2	0	0	0	0	0	0	1	0	?	?	?	0	-	-	0	0	0	2	
<i>Dolicholatirus sp.</i>	?	?	?	0	1	1	4	?	?	2	0	0	0	0	0	0	2	0	2	0	2	0	0	0	0	0	0	1	0	?	?	?	0	-	-	0	0	0	1	
<i>Teralatirus roboreus</i>	?	?	?	0	1	1	4	?	?	2	0	0	0	0	0	0	2	0	2	0	2	0	0	0	0	0	0	1	0	?	?	?	0	-	-	0	0	0	1	
<i>Dolicholatirus aff. cayohuesonicus</i>	?	?	?	0	1	1	4	?	?	2	0	0	0	0	0	0	2	0	2	0	2	0	0	0	0	0	0	1	0	?	?	?	0	-	-	0	0	0	1	
<i>Angulofusus neda</i>	?	?	?	0	1	1	4	?	?	2	0	0	0	0	0	0	2	0	2	0	2	0	0	0	0	0	0	1	0	?	?	?	0	-	-	0	0	0	2	
<i>Pseudolatirus kuroseanus</i>	?	?	?	0	1	1	4	?	?	2	0	0	0	0	0	0	2	0	2	0	2	0	0	0	0	0	0	1	0	?	?	?	0	-	-	0	0	0	2	
<i>Amiantofusus pacificus</i>	?	?	?	0	1	1	4	?	?	2	0	0	0	0	0	0	2	0	2	0	2	0	0	0	0	0	0	1	0	?	?	?	0	-	-	0	0	0	2	
<i>Amiantofusus candoris</i>	?	?	?	0	1	1	4	?	?	2	0	0	0	0	0	0	2	0	2	0	2	0	0	0	0	0	0	1	0	?	?	?	0	-	-	0	0	0	2	
<i>Pseudolatirus pallidus</i>	?	?	?	0	1	2	4	?	?	2	0	0	0	0	0	0	2	0	2	0	2	0	1	0	0	0	0	1	0	?	?	?	0	-	-	0	0	0	2	
<i>Chryseofusus archerius</i>	?	?	?	0	1	2	4	?	?	2	0	0	0	0	0	0	2	0	2	0	2	0	1	0	0	0	0	1	0	?	?	?	0	-	-	0	0	0	2	
<i>Chryseofusus graciliformis</i>	?	?	?	0	1	2	4	?	?	2	0	0	0	0	0	0	2	0	2	0	2	0	1	0	0	0	0	1	0	?	?	?	0	-	-	0	0	0	2	
<i>Fusinus marmoratus</i>	?	?	?	0	1	2	4	?	?	2	0	0	0	0	0	0	2	0	2	0	2	0	1	0	0	0	0	1	0	?	?	?	0	-	-	0	0	0	2	
<i>Fusinus brasiliensis</i>	?	?	?	0	1	2	4	?	?	2	0	0	0	0	0	0	2	0	2	0	2	0	1	0	0	0	0	1	0	?	?	?	0	-	-	0	0	0	2	
<i>Fusinus sp.</i>	?	?	?	0	1	2	4	?	?	2	0	0	0	0	0	0	2	0	2	0	2	0	1	0	0	0	0	1	0	?	?	?	0	-	-	0	0	0	2	
<i>Fusinus frenguelli</i>	?	?	?	0	1	2	4	?	?	2	0	0	0	0	0	0	2	0	2	0	2	0	1	0	0	0	0	1	0	?	?	?	0	-	-	0	0	0	2	
<i>Fusinus australis</i>	?	?	?	0	1	2	4	?	?	2	0	0	0	0	0	0	2	0	2	0	2	0	1	0	0	0	0	1	0	?	?	?	0	-	-	0	0	0	2	
<i>Cyrtulus serotinus</i>	?	?	?	0	1	2	4	?	?	2	0	0	0	0	0	0	2	0	2	0	2	0	1	0	0	0	0	1	0	?	?	?	0	-	-	0	0	0	2	
<i>Granulifusus sp.</i>	?	?	?	0	1	2	4	?	?	2	0	0	0	0	0	0	2	0	2	0	2	0	0	0	0	0	0	1	0	?	?	?	0	-	-	0	0	0	2	
<i>Granulifusus hayashi</i>	?	?	?	0	1	2	4	?	?	2	0	0	0	0	0	0	2	0	2	0	2	0	0	0	0	0	0	1	0	?	?	?	0	-	-	0	0	0	2	
<i>Pseudolatirus discrepans</i>	?	?	?	0	1	2	4	?	?	2	0	0	0	0	0	0	2	0	2	0	2	0	0	0	0	0	0	1	0	?	?	?	0	-	-	0	0	0	2	
<i>Granulifusus aff. kiranus</i>	?	?	?	0	1	2	4	?	?	2	0	0	0	0	0	0	2	0	2	0	2	0	0	0	0	0	0	1	0	?	?	?	0	-	-	0	0	0	2	
<i>Fusolatirus bruijnii</i>	?	?	?	0	1	2	4	?	?	2	0	0	0	0	0	0	2	0	2	0	2	0	0	0	0	0	0	1	0	?	?	?	0	-	-	0	0	0	2	
<i>Peristernia marquesana</i>	?	?	?	0	1	2	4	?	?	2	0	0	0	0	0	0	2	0	2	0	2	0	0	0	0	0	0	1	0	?	?	?	0	-	-	0	0	0	2	
<i>Peristernia nassatula</i>	?	?	?	0	1	2	4	?	?	2	0	0	0	0	0	0	2	0	2	0	2	0	0	0	0	0	0	1	0	?	?	?	0	-	-	0	0	0	2	
<i>Nodolatirus nodatus</i>	?	?	?	0	1	2	4	?	?	2	0	0	0	0	0	0	1	0	2	0	2	0	0	0	0	0	0	1	1	?	?	?	0	-	-	0	0	0	1	
<i>Latirus vischii</i>	?	?	?	0	1	2	4	?	?	2	0	0	0	0	0	0	1	0	2	0	2	0	0	0	0	0	0	1	1	?	?	?	0	-	-	0	0	0	1	
<i>Aurantilaria aurantiaca</i>	?	?	?	1	1	2	4	?	?	2	0	0	0	0	0	0	1	0	2	0	2	0	0	0	0	0	0	1	1	?	?	?	0	-	-	0	0	0	1	
<i>Fasciolaria tulipa</i>	?	?	?	1	1	2	4	?	?	2	0	0	0	0	0	0	1	0	2	0	2	0	0	0	0	0	0	1	1	?	?	?	0	-	-	0	0	0	1	
<i>Australaria australasia</i>	?	?	?	1	1	2	4	?	?	2	0	0	0	0	0	0	1	0	2	0	2	0	0	0	0	0	0	1	1	?	?	?	0	-	-	0	0	0	1	
<i>Pleuroploca trapezium</i>	?	?	?	1	1	2	4	?	?	2	0	0	0	0	0	0	1	0	2	0	2	0	0	0	0	0	0	1	1	?	?	?	0	-	-	0	0	0	1	
<i>Filifusus filamentosus</i>	?	?	?	1	1	2	4	?	?	2	0	0	0	0	0	0	1	0	2	0	2	0	0	0	0	0	0	1	1	?	?	?	0	-	-	0	0	0	1	
<i>Hemipolygona armata</i>	?	?	?	0	1	2	4	?	?	2	0	0	0	0	0	0	2	0	2	0	2	0	0	0	0	0	0	1	0	?	?	?	0	-	-	0	0	0	2	
<i>Pustulatirus mediamericus</i>	?	?	?	0	1	2	4	?	?	2	0	0	0	0	0	0	2	0	2	0	2	0	0	0	0	0	0	1	0	?	?	?	0	-	-	0	0	0	2	
<i>Pustulatirus ogum</i>	?	?	?	0	1	2	4	?	?	2	0	0	0	0	0	0	2	0	2	0	2	0	0	0	0	0	0	1	0	?	?	?	0	-	-	0	0	0	2	
<i>Polygona angulata</i>	?	?	?	0	1	2	4	?	?	2	0	0	0	0	0	0	2	0	2	0	2	0	0	0	0	0	0	1	0	?	?	?	0	-	-	0	0	0	2	
<i>Latirus polygonus</i>	?	?	?	0	1	2	4	?	?	2	0	0	0	0	0	0	2	0	2	0	2	0	0	0	0	0	0	1	0	?	?	?	0	-	-	0	0	0	2	
<i>Polygona infundibulum</i>	?	?	?	0	1	2	4	?	?	2	0	0	0	0	0	0	2	0	2	0	2	0	0	0	0	0	0	1	0	?	?	?	0	-	-	0	0	0	2	
<i>Hemipolygona beckyae</i>	?	?	?	0	1	2	4	?	?	2	0	0	0	0	0	0	2	0	2	0	2	0	0	0	0	0	0	1	0	?	?	?	0	-	-	0	0	0	2	
<i>Latirus pictus</i>	?	?	?	0	1	2	4	?	?	2	0	0	0	0	0	0	2	0	2	0	2	0	0	0	0	0	0	1	0	?	?	?	0	-	-	0	0	0	2	
<i>Leucozonia ocellata</i>	?	?	?	0	1	2	4	?	?	2	0	0	0	0	0	0	2	0	2	0	2	0	0	0	0	0	0	1	0	?	?	?	0	-	-	0	0	0	1	
<i>Leucozonia cerata</i>	?	?	?	0	1	2	4	?	?	2	0	0	0	0	0	0	2	0	2	0	2	0	0	0	0	0	0	1	0	?	?	?	0	-	-	0	0	0	1	
<i>Opeatostoma pseudodon</i>	?	?	?	0	1	2	4	?	?	2	0	0	0	0	0	0	2	0	2	0	2	0	0																	

TAXON	CHARACTER	32	32	32	32	32	32	32	32	32	33	33	33	33	33	33	33	33	33	34	34	34	34	34	34	34	34	34	35	35	35	35	35	35	35	35	35	35			
		0	1	2	3	4	5	6	7	8	9	0	1	2	3	4	5	6	7	8	9	0	1	2	3	4	5	6	7	8	9	0	1	2	3	4	5	6	7	8	9
<i>Monetaria annulus</i>		0	0	0	0	0	0	0	0	2	0	2	0	3	0	1	3	1	0	0	0	0	0	0	0	0	0	0	1	1	1	0	0	0	2	1	2	1	2		
<i>Thais speciosa</i>		0	0	0	0	1	0	0	0	4	2	1	0	0	0	1	3	1	2	1	0	0	0	-	0	?	2	2	1	0	2	0	1	0	1	0	2	1	1	0	0
<i>Pugilina tupiniquim</i>		0	0	?	0	0	-	0	0	3	1	1	0	0	0	2	3	1	?	1	-	0	0	-	0	?	2	2	1	?	2	0	2	0	0	1	2	0	1	0	0
<i>engoniophos uncinatus</i>		0	0	?	0	0	-	0	0	3	2	1	0	0	0	2	3	1	?	1	-	0	0	-	0	?	2	2	1	?	2	0	2	0	0	1	2	0	1	0	0
<i>Nassarius reticulatus</i>		0	0	?	0	0	-	0	0	3	2	1	0	0	0	2	3	1	?	1	-	0	0	-	0	?	2	2	1	?	2	0	2	0	1	1	2	1	1	0	0
<i>Bullia laevisima</i>		0	0	?	0	0	-	0	0	3	2	1	0	0	0	2	3	1	?	1	-	0	0	-	0	?	2	2	1	?	2	0	2	0	1	1	2	1	1	0	0
<i>Buccinum undatum</i>		0	0	?	0	0	-	0	0	3	2	1	0	0	0	2	3	1	?	1	-	0	0	-	0	?	2	2	1	?	2	0	2	0	1	1	2	1	1	0	0
<i>Pisania pusio</i>		0	0	?	0	0	-	0	0	3	2	1	0	0	0	2	3	1	?	1	-	0	0	-	0	?	2	2	1	?	2	0	2	0	1	1	2	1	1	0	0
<i>Dolicholatirus sp.</i>		0	0	?	0	0	-	0	0	3	1	1	0	0	0	2	3	1	?	1	-	?	0	-	0	?	2	2	1	?	2	0	2	0	0	1	2	0	1	0	0
<i>Teralatirus roboreus</i>		0	0	?	0	0	-	0	0	3	1	1	0	0	0	2	3	1	?	1	-	?	0	-	0	?	2	2	1	?	2	0	2	0	0	1	2	0	1	0	0
<i>Dolicholatirus aff. cayohuesonicus</i>		0	0	?	0	0	-	0	0	3	1	1	0	0	0	2	3	1	?	1	-	?	0	-	0	?	2	2	1	?	2	0	2	0	0	1	2	0	1	0	0
<i>Angulofusus netae</i>		0	0	?	0	0	-	0	0	3	1	1	0	0	0	2	3	1	?	1	-	0	0	-	0	?	2	2	1	?	2	0	2	0	1	1	2	1	1	0	0
<i>Pseudolatirus kuroseanus</i>		0	0	?	0	0	-	0	0	3	1	1	0	0	0	2	3	1	?	1	-	0	0	-	0	?	2	2	1	?	2	0	2	0	1	1	2	1	1	0	0
<i>Amiantofusus pacificus</i>		0	0	?	0	0	-	0	0	3	1	1	0	0	0	2	3	1	?	1	-	0	0	-	0	?	2	2	1	?	2	0	2	0	1	1	2	1	1	0	0
<i>Amiantofusus candoris</i>		0	0	?	0	0	-	0	0	3	1	1	0	0	0	2	3	1	?	1	-	0	0	-	0	?	2	2	1	?	2	0	2	0	1	1	2	1	1	0	0
<i>Pseudolatirus pallidus</i>		0	0	?	0	0	-	0	0	3	1	1	0	0	0	2	3	1	?	1	-	0	0	-	0	?	2	2	1	?	2	0	2	0	1	1	2	1	1	0	0
<i>Chryseofusus archerius</i>		0	0	?	0	0	-	0	0	3	1	1	0	0	0	2	3	1	?	1	-	0	0	-	0	?	2	2	1	?	2	0	2	0	1	1	2	1	1	0	0
<i>Chryseofusus graciliformis</i>		0	0	?	0	0	-	0	0	3	1	1	0	0	0	2	3	1	?	1	-	0	0	-	0	?	2	2	1	?	2	0	2	0	1	1	2	1	1	0	0
<i>Fusinus marmoratus</i>		0	0	?	0	0	-	0	0	3	1	1	0	0	0	2	3	1	?	1	-	0	0	-	0	?	2	2	1	?	2	0	2	0	1	1	2	1	1	0	0
<i>Fusinus brasiliensis</i>		0	0	?	0	0	-	0	0	3	1	1	0	0	0	2	3	1	?	1	-	0	0	-	0	?	2	2	1	?	2	0	2	0	1	1	2	1	1	0	0
<i>Fusinus sp.</i>		0	0	?	0	0	-	0	0	3	1	1	0	0	0	2	3	1	?	1	-	0	0	-	0	?	2	2	1	?	2	0	2	0	1	1	2	1	1	0	0
<i>Fusinus frenguelli</i>		0	0	?	0	0	-	0	0	3	1	1	0	0	0	2	3	1	?	1	-	0	0	-	0	?	2	2	1	?	2	0	2	0	1	1	2	1	1	0	0
<i>Fusinus australis</i>		0	0	?	0	0	-	0	0	3	1	1	0	0	0	2	3	1	?	1	-	0	0	-	0	?	2	2	1	?	2	0	2	0	1	1	2	1	1	0	0
<i>Cyrtulus serotinus</i>		0	0	?	0	0	-	0	0	3	1	1	0	0	0	2	3	1	?	1	-	0	0	-	0	?	2	2	1	?	2	0	2	0	1	1	2	1	1	0	0
<i>Granulifusus sp.</i>		0	0	?	0	0	-	0	0	3	1	1	0	0	0	2	3	1	?	1	-	0	0	-	0	?	2	2	1	?	2	0	2	0	1	1	2	1	1	0	0
<i>Granulifusus hayashi</i>		0	0	?	0	0	-	0	0	3	1	1	0	0	0	2	3	1	?	1	-	0	0	-	0	?	2	2	1	?	2	0	2	0	1	1	2	1	1	0	0
<i>Pseudolatirus discrepans</i>		0	0	?	0	0	-	0	0	3	1	1	0	0	0	2	3	1	?	1	-	0	0	-	0	?	2	2	1	?	2	0	2	0	1	1	2	1	1	0	0
<i>Granulifusus aff. kiranus</i>		0	0	?	0	0	-	0	0	3	1	1	0	0	0	2	3	1	?	1	-	0	0	-	0	?	2	2	1	?	2	0	2	0	1	1	2	1	1	0	0
<i>Fusolatirus bruijnii</i>		0	0	?	0	0	-	0	0	3	1	1	0	0	0	2	3	1	?	1	-	0	0	-	0	?	2	2	1	?	2	0	2	0	1	1	2	1	1	0	0
<i>Peristernia marquesana</i>		0	0	?	0	0	-	0	0	3	1	1	0	0	0	2	3	1	?	1	-	0	0	-	0	?	2	2	1	?	2	0	2	0	1	1	2	1	1	0	0
<i>Peristernia nassatula</i>		0	0	?	0	0	-	0	0	3	1	1	0	0	0	2	3	1	?	1	-	0	0	-	0	?	2	2	1	?	2	0	2	0	1	1	2	1	1	0	0
<i>Nodolatirus nodatus</i>		0	0	?	0	0	-	0	0	3	1	1	0	0	0	2	3	1	?	1	-	0	0	-	0	?	2	2	1	?	2	0	2	0	0	1	2	0	1	0	0
<i>Latirus vischii</i>		0	0	?	0	0	-	0	0	3	1	1	0	0	0	2	3	1	?	1	-	0	0	-	0	?	2	2	1	?	2	0	2	0	0	1	2	0	1	0	0
<i>Aurantilaria aurantiaca</i>		0	0	?	0	0	-	0	0	3	1	1	0	0	0	2	3	1	?	1	-	0	0	-	0	?	2	2	1	?	2	0	2	0	0	1	2	0	1	0	0
<i>Fasciolaria tulipa</i>		0	0	?	0	0	-	0	0	3	1	1	0	0	0	2	3	1	?	1	-	0	0	-	0	?	2	2	1	?	2	0	2	0	0	1	2	0	1	0	0
<i>Australaria australasia</i>		0	0	?	0	0	-	0	0	3	1	1	0	0	0	2	3	1	?	1	-	0	0	-	0	?	2	2	1	?	2	0	2	0	0	1	2	0	1	0	0
<i>Pleuroploca trapezium</i>		0	0	?	0	0	-	0	0	3	1	1	0	0	0	2	3	1	?	1	-	0	0	-	0	?	2	2	1	?	2	0	2	0	0	1	2	0	1	0	0
<i>Filifusus filamentosus</i>		0	0	?	0	0	-	0	0	3	1	1	0	0	0	2	3	1	?	1	-	0	0	-	0	?	2	2	1	?	2	0	2	0	0	1	2	0	1	0	0
<i>Hemipolygona armata</i>		0	0	?	0	0	-	0	0	3	1	1	0	0	0	2	3	1	?	1	-	0	0	-	0	?	2	2	1	?	2	0	2	0	1	1	2	1	1	0	0
<i>Pustulatirus mediamericus</i>		0	0	?	0	0	-	0	0	3	1	1	0	0	0	2	3	1	?	1	-	0	0	-	0	?	2	2	1	?	2	0	2	0	1	1	2	1	1	0	0
<i>Pustulatirus ogum</i>		0	0	?	0	0	-	0	0	3	1	1	0	0	0	2	3	1	?	1	-	0	0	-	0	?	2	2	1	?	2	0	2	0	1	1	2	1	1	0	0
<i>Polygona angulata</i>		0	0	?	0	0	-	0	0	3	1	1	0	0	0	2	3	1	?	1	-	0	0	-	0	?	2	2	1	?	2	0	2	0	1	1	2	1	1	0	0
<i>Latirus polygonus</i>		0	0	?	0	0	-	0	0	3	1	1	0	0	0	2	3	1	?	1	-	0	0	-	0	?	2	2	1	?	2	0	2	0	1	1	2	1	1	0	0
<i>Polygona infundibulum</i>		0	0	?	0	0	-	0	0	3	1	1	0	0	0	2	3	1	?	1	-	0	0	-	0	?	2	2	1	?	2	0	2	0	1	1	2	1	1	0	0
<i>Hemipolygona beckyae</i>		0	0	?	0	0	-	0	0	3	1	1	0	0	0	2	3	1	?	1	-	0	0	-	0	?	2	2	1	?	2	0	2	0	1	1	2	1	1	0	0
<i>Latirus pictus</i>		0	0	?	0	0	-	0	0	3	1	1	0	0	0	2	3	1	?	1	-	0	0	-	0	?	2	2	1	?	2	0	2	0	1	1	2				



TAXON	CHARACTER																																							
	40	40	40	40	40	40	40	40	40	40	41	41	41	41	41	41	41	41	41	41	42	42	42	42	42	42	42	42	42	42	43	43	43	43	43	43	43	43	43	43
<i>Monetaria annulus</i>	0	0	0	1	0	0	0	1	3	0	2	1	1	1	2	0	4	0	1	0	0	0	1	3	1	0	0	0	0	0	2	0	2	3	0	2	2	0	2	0
<i>Thais speciosa</i>	1	0	0	1	0	0	0	2	3	0	3	1	1	1	2	5	7	0	0	0	0	0	1	5	0	5	0	2	1	0	0	-	-	-	-	-	-	-	-	-
<i>Pugilina tupiniquim</i>	1	0	0	2	0	0	0	2	0	0	3	1	1	1	2	0	0	0	0	0	0	0	1	5	0	5	0	2	1	0	0	-	-	-	-	-	-	-	-	-
<i>engoniophos uncinatus</i>	1	0	0	2	0	0	0	2	0	0	3	1	1	1	2	5	1	0	0	0	0	0	1	5	0	5	0	2	1	0	0	-	-	-	-	-	-	-	-	-
<i>Nassarius reticulatus</i>	1	0	0	2	0	0	0	2	0	0	3	1	1	1	2	5	1	0	0	0	0	0	1	5	0	5	0	2	1	0	0	-	-	-	-	-	-	-	-	-
<i>Bullia laevis</i>	1	0	0	2	0	0	0	2	0	0	3	1	1	1	2	5	1	0	0	0	0	0	1	5	0	5	0	2	1	0	0	-	-	-	-	-	-	-	-	-
<i>Buccinum undatum</i>	1	0	0	2	0	0	0	2	0	0	3	1	1	1	2	5	1	0	0	0	0	0	1	5	0	5	0	2	1	0	0	-	-	-	-	-	-	-	-	-
<i>Pisania pusio</i>	1	0	0	2	0	0	0	2	0	0	3	1	1	1	2	?	?	0	0	0	0	0	1	5	0	5	0	2	1	0	0	-	-	-	-	-	-	-	-	-
<i>Dolicholatus</i> sp.	1	0	0	2	0	0	0	2	0	0	3	1	1	1	2	0	0	0	0	0	0	0	1	1	1	2	0	2	1	0	0	-	-	-	-	-	-	-	-	-
<i>Teralatus roboreus</i>	1	0	0	2	0	0	0	2	0	0	3	1	1	1	2	0	0	0	0	0	0	0	1	1	1	2	0	2	1	0	0	-	-	-	-	-	-	-	-	-
<i>Dolicholatus</i> aff. <i>cayohuesonicus</i>	1	0	0	2	0	0	0	2	0	0	3	1	1	1	2	0	0	0	0	0	0	0	1	1	1	2	0	2	1	0	0	-	-	-	-	-	-	-	-	-
<i>Angulofusus neda</i>	1	0	0	2	0	0	0	2	0	0	3	1	1	1	2	0	4	0	1	0	0	0	1	0	0	2	0	2	1	0	0	-	-	-	-	-	-	-	-	-
<i>Pseudolatus kuroseanus</i>	1	0	0	2	0	0	0	2	0	0	3	1	1	1	2	0	4	0	1	0	0	0	1	0	0	2	0	2	1	0	0	-	-	-	-	-	-	-	-	-
<i>Amiantofusus pacificus</i>	1	0	0	2	0	0	0	2	0	0	3	1	1	1	2	0	4	0	1	0	0	0	1	0	0	2	0	2	1	0	0	-	-	-	-	-	-	-	-	-
<i>Amiantofusus candoris</i>	1	0	0	2	0	0	0	2	0	0	3	1	1	1	2	0	4	0	1	0	0	0	1	0	0	2	0	2	1	0	0	-	-	-	-	-	-	-	-	-
<i>Pseudolatus pallidus</i>	1	0	0	2	0	0	0	2	0	0	3	1	1	1	2	0	4	0	0	0	0	0	1	0	0	2	0	2	1	0	0	-	-	-	-	-	-	-	-	-
<i>Chryseofusus archerius</i>	1	0	0	2	0	0	0	2	0	0	3	1	1	1	2	0	4	0	0	0	0	0	1	0	0	2	0	2	1	0	0	-	-	-	-	-	-	-	-	-
<i>Chryseofusus graciliformis</i>	1	0	0	2	0	0	0	2	0	0	3	1	1	1	2	0	4	0	0	0	0	0	1	0	0	2	0	2	1	0	0	-	-	-	-	-	-	-	-	-
<i>Fusinus marmoratus</i>	1	0	0	2	0	0	0	2	0	0	3	1	1	1	2	0	4	0	0	0	0	0	1	0	0	2	0	2	1	0	0	-	-	-	-	-	-	-	-	-
<i>Fusinus brasiliensis</i>	1	0	0	2	0	0	0	2	0	0	3	1	1	1	2	0	4	0	0	0	0	0	1	0	0	2	0	2	1	0	0	-	-	-	-	-	-	-	-	-
<i>Fusinus</i> sp.	1	0	0	2	0	0	0	2	0	0	3	1	1	1	2	0	4	0	0	0	0	0	1	0	0	2	0	2	1	0	0	-	-	-	-	-	-	-	-	-
<i>Fusinus frenguelli</i>	1	0	0	2	0	0	0	2	0	0	3	1	1	1	2	0	4	0	0	0	0	0	1	0	0	2	0	2	1	0	0	-	-	-	-	-	-	-	-	-
<i>Fusinus australis</i>	1	0	0	2	0	0	0	2	0	0	3	1	1	1	2	0	4	0	0	0	0	0	1	0	0	2	0	2	1	0	0	-	-	-	-	-	-	-	-	-
<i>Cyrtulus serotinus</i>	1	0	0	2	0	0	0	2	0	0	3	1	1	1	2	0	4	0	0	0	0	0	1	0	0	2	0	2	1	0	0	-	-	-	-	-	-	-	-	-
<i>Granulifusus</i> sp.	1	0	0	2	0	0	0	2	0	0	3	1	1	1	2	0	4	0	0	0	0	0	1	0	0	2	0	2	1	0	0	-	-	-	-	-	-	-	-	-
<i>Granulifusus hayashi</i>	1	0	0	2	0	0	0	2	0	0	3	1	1	1	2	0	4	0	0	0	0	0	1	0	0	2	0	2	1	0	0	-	-	-	-	-	-	-	-	-
<i>Pseudolatus discrepans</i>	1	0	0	2	0	0	0	2	0	0	3	1	1	1	2	0	4	0	0	0	0	0	1	0	0	2	0	2	1	0	0	-	-	-	-	-	-	-	-	-
<i>Granulifusus</i> aff. <i>kiranus</i>	1	0	0	2	0	0	0	2	0	0	3	1	1	1	2	0	4	0	0	0	0	0	1	0	0	2	0	2	1	0	0	-	-	-	-	-	-	-	-	-
<i>Fusolatus bruijnii</i>	1	0	0	2	0	0	0	2	0	0	3	1	1	1	2	0	4	0	0	0	0	0	1	0	0	2	0	2	1	0	0	-	-	-	-	-	-	-	-	-
<i>Peristernia marquesana</i>	1	0	0	2	0	0	0	2	0	0	3	1	1	1	2	0	4	0	0	0	0	0	1	0	0	2	0	2	1	0	0	-	-	-	-	-	-	-	-	-
<i>Peristernia nassatula</i>	1	0	0	2	0	0	0	2	0	0	3	1	1	1	2	0	4	0	0	0	0	0	1	0	0	2	0	2	1	0	0	-	-	-	-	-	-	-	-	-
<i>Nodolatus nodatus</i>	1	0	0	2	0	0	0	2	0	0	3	1	1	1	2	0	0	0	0	0	0	0	1	0	0	2	0	2	1	0	0	-	-	-	-	-	-	-	-	-
<i>Latirus vischii</i>	1	0	0	2	0	0	0	2	0	0	3	1	1	1	2	0	0	0	0	0	0	0	1	0	0	2	0	2	1	0	0	-	-	-	-	-	-	-	-	-
<i>Aurantularia aurantiaca</i>	1	0	0	2	0	0	0	2	0	0	3	1	1	1	2	0	0	0	0	0	0	0	1	0	0	2	0	2	1	0	0	-	-	-	-	-	-	-	-	-
<i>Fasciolaria tulipa</i>	1	0	0	2	0	0	0	2	0	0	3	1	1	1	2	0	0	0	0	0	0	0	1	0	0	2	0	2	1	0	0	-	-	-	-	-	-	-	-	-
<i>Australaria australasia</i>	1	0	0	2	0	0	0	2	0	0	3	1	1	1	2	0	0	0	0	0	0	0	1	0	0	2	0	2	1	0	0	-	-	-	-	-	-	-	-	-
<i>Pleuroploca trapezium</i>	1	0	0	2	0	0	0	2	0	0	3	1	1	1	2	0	0	0	0	0	0	0	1	0	0	2	0	2	1	0	0	-	-	-	-	-	-	-	-	-
<i>Filifusus filamentosus</i>	1	0	0	2	0	0	0	2	0	0	3	1	1	1	2	0	0	0	0	0	0	0	1	0	0	2	0	2	1	0	0	-	-	-	-	-	-	-	-	-
<i>Hemipolygona armata</i>	1	0	0	2	0	0	0	2	0	0	3	1	1	1	2	?	?	0	0	0	0	0	1	0	0	2	0	2	1	0	0	-	-	-	-	-	-	-	-	-
<i>Pustulatus mediamericus</i>	1	0	0	2	0	0	0	2	0	0	3	1	1	1	2	?	?	0	0	0	0	0	1	0	0	2	0	2	1	0	0	-	-	-	-	-	-	-	-	-
<i>Pustulatus ogum</i>	1	0	0	2	0	0	0	2	0	0	3	1	1	1	2	?	?	0	0	0	0	0	1	0	0	2	0	2	1	0	0	-	-	-	-	-	-	-	-	-
<i>Polygona angulata</i>	1	0	0	2	0	0	0	2	0	0	3	1	1	1	2	?	?	0	0	0	0	0	1	0	0	2	0	2	1	0	0	-	-	-	-	-	-	-	-	-
<i>Latirus polygonus</i>	1	0	0	2	0	0	0	2	0	0	3	1	1	1	2	?	?	0	0	0	0	0	1	0	0	2	0	2	1	0	0	-	-	-	-	-	-	-	-	-
<i>Polygona infundibulum</i>	1	0	0	2	0	0	0	2	0	0	3	1	1	1	2	?	?	0	0	0	0	0	1	0	0	2	0	2	1	0	0	-	-	-	-	-	-	-	-	-
<i>Hemipolygona beckyae</i>	1	0	0	2	0	0	0	2	0	0	3	1	1	1	2	?	?	0	0	0	0	0	1	0	0	2	0	2	1	0	0	-	-	-	-	-	-	-	-	-
<i>Latirus pictus</i>	1	0	0	2	0	0	0	2	0	0	3	1	1	1	2	?	?	0	0	0	0	0	1	0	0	2	0	2	1	0	0	-	-	-	-	-	-	-	-	-
<i>Leucozonia ocellata</i>	1	0	0	2	0	0	0	2	0	0	3	1	1	1	2	0	0	0																						





TAXON	CHARACTER																																								
	48	48	48	48	48	48	48	48	48	48	49	49	49	49	49	49	49	49	49	49	50	50	50	50	50	50	50	50	50	50	51	51	51	51	51	51	51	51	51	51	
<i>Monetaria annulus</i>	-	-	0	-	0	-	0	-	-	1	0	0	0	1	0	0	1	0	0	0	-	0	0	0	-	-	-	0	0	2	0	1	0	0	0	1	1	0	1	1	
<i>Thais speciosa</i>	-	-	0	-	1	1	1	0	?	1	0	0	4	1	0	0	0	0	0	0	-	0	0	0	-	-	-	0	0	0	0	4	0	2	0	1	1	0	1	1	
<i>Pugilina tupiniquim</i>	-	-	0	-	0	0	0	-	-	?	?	?	?	?	?	?	?	?	?	?	?	?	?	?	-	-	-	?	?	?	?	?	?	2	?	?	?	?	0	?	?
<i>engoniophos uncinatus</i>	-	-	0	-	1	0	1	1	2	?	?	?	?	?	?	?	?	?	?	?	?	?	?	?	0	-	-	-	?	?	?	?	?	2	?	?	?	?	0	?	?
<i>Nassarius reticulatus</i>	-	-	0	-	1	0	1	1	2	?	?	?	?	?	?	?	?	?	?	?	?	?	?	?	0	-	-	-	?	?	?	?	?	2	?	?	?	?	0	?	?
<i>Bullia laevisima</i>	-	-	0	-	1	0	1	0	2	?	?	?	?	?	?	?	?	?	?	?	?	?	?	?	0	-	-	-	?	?	?	?	?	2	?	?	?	?	0	?	?
<i>Buccinum undatum</i>	-	-	0	-	1	0	1	1	2	?	?	?	?	?	?	?	?	?	?	?	?	?	?	?	0	-	-	-	?	?	?	?	?	2	?	?	?	?	0	?	?
<i>Pisania pusio</i>	-	-	0	-	1	0	1	0	2	?	?	?	?	?	?	?	?	?	?	?	?	?	?	?	0	-	-	-	?	?	?	?	?	2	?	?	?	?	0	?	?
<i>Dolicholatus sp.</i>	-	-	0	-	1	0	0	1	2	?	?	?	?	?	?	?	?	?	?	?	?	?	?	?	0	-	-	-	?	?	?	?	?	2	?	?	?	?	0	?	?
<i>Teralatirus roboreus</i>	-	-	0	-	0	0	0	1	2	?	?	?	?	?	?	?	?	?	?	?	?	?	?	?	0	-	-	-	?	?	?	?	?	2	?	?	?	?	0	?	?
<i>Dolicholatus aff. cayohuesonicus</i>	-	-	0	-	1	0	0	1	2	?	?	?	?	?	?	?	?	?	?	?	?	?	?	?	0	-	-	-	?	?	?	?	?	2	?	?	?	?	0	?	?
<i>Angulofusus neda</i>	-	-	0	-	1	0	1	1	2	?	?	?	?	?	?	?	?	?	?	?	?	?	?	?	0	-	-	-	?	?	?	?	?	2	?	?	?	?	0	?	?
<i>Pseudolatus kuroseanus</i>	-	-	0	-	1	0	1	1	2	?	?	?	?	?	?	?	?	?	?	?	?	?	?	?	0	-	-	-	?	?	?	?	?	2	?	?	?	?	0	?	?
<i>Amiantofusus pacificus</i>	-	-	0	-	1	0	1	1	2	?	?	?	?	?	?	?	?	?	?	?	?	?	?	?	0	-	-	-	?	?	?	?	?	2	?	?	?	?	0	?	?
<i>Amiantofusus candoris</i>	-	-	0	-	1	0	1	1	2	?	?	?	?	?	?	?	?	?	?	?	?	?	?	?	0	-	-	-	?	?	?	?	?	2	?	?	?	?	0	?	?
<i>Pseudolatus pallidus</i>	-	-	0	-	1	0	1	1	2	?	?	?	?	?	?	?	?	?	?	?	?	?	?	?	0	-	-	-	?	?	?	?	?	2	?	?	?	?	0	?	?
<i>Chryseofusus archeruisus</i>	-	-	0	-	1	0	1	1	2	?	?	?	?	?	?	?	?	?	?	?	?	?	?	?	0	-	-	-	?	?	?	?	?	2	?	?	?	?	0	?	?
<i>Chryseofusus graciliformis</i>	-	-	0	-	1	0	1	1	2	?	?	?	?	?	?	?	?	?	?	?	?	?	?	?	0	-	-	-	?	?	?	?	?	2	?	?	?	?	0	?	?
<i>Fusinus marmoratus</i>	-	-	0	-	1	0	1	1	2	?	?	?	?	?	?	?	?	?	?	?	?	?	?	?	0	-	-	-	?	?	?	?	?	2	?	?	?	?	0	?	?
<i>Fusinus brasiliensis</i>	-	-	0	-	1	0	1	1	2	?	?	?	?	?	?	?	?	?	?	?	?	?	?	?	0	-	-	-	?	?	?	?	?	2	?	?	?	?	0	?	?
<i>Fusinus sp.</i>	-	-	0	-	1	0	1	1	2	?	?	?	?	?	?	?	?	?	?	?	?	?	?	?	0	-	-	-	?	?	?	?	?	2	?	?	?	?	0	?	?
<i>Fusinus frenguelli</i>	-	-	0	-	1	0	1	1	2	?	?	?	?	?	?	?	?	?	?	?	?	?	?	?	0	-	-	-	?	?	?	?	?	2	?	?	?	?	0	?	?
<i>Fusinus australis</i>	-	-	0	-	1	0	1	1	2	?	?	?	?	?	?	?	?	?	?	?	?	?	?	?	0	-	-	-	?	?	?	?	?	2	?	?	?	?	0	?	?
<i>Cyrtulus serotinus</i>	-	-	0	-	1	0	1	1	2	?	?	?	?	?	?	?	?	?	?	?	?	?	?	?	0	-	-	-	?	?	?	?	?	2	?	?	?	?	0	?	?
<i>Granulifusus sp.</i>	-	-	0	-	1	0	1	1	2	?	?	?	?	?	?	?	?	?	?	?	?	?	?	?	0	-	-	-	?	?	?	?	?	2	?	?	?	?	0	?	?
<i>Granulifusus hayashi</i>	-	-	0	-	1	0	1	1	2	?	?	?	?	?	?	?	?	?	?	?	?	?	?	?	0	-	-	-	?	?	?	?	?	2	?	?	?	?	0	?	?
<i>Pseudolatus discrepans</i>	-	-	0	-	1	0	1	1	2	?	?	?	?	?	?	?	?	?	?	?	?	?	?	?	0	-	-	-	?	?	?	?	?	2	?	?	?	?	0	?	?
<i>Granulifusus aff. kiranus</i>	-	-	0	-	1	0	1	1	2	?	?	?	?	?	?	?	?	?	?	?	?	?	?	?	0	-	-	-	?	?	?	?	?	2	?	?	?	?	0	?	?
<i>Fusolatus bruijnii</i>	-	-	0	-	1	0	1	1	2	?	?	?	?	?	?	?	?	?	?	?	?	?	?	?	0	-	-	-	?	?	?	?	?	2	?	?	?	?	0	?	?
<i>Peristernia marquesana</i>	-	-	0	-	1	0	1	1	2	?	?	?	?	?	?	?	?	?	?	?	?	?	?	?	0	-	-	-	?	?	?	?	?	2	?	?	?	?	0	?	?
<i>Peristernia nassatula</i>	-	-	0	-	1	0	1	1	2	?	?	?	?	?	?	?	?	?	?	?	?	?	?	?	0	-	-	-	?	?	?	?	?	2	?	?	?	?	0	?	?
<i>Nodolatus nodatus</i>	-	-	0	-	1	0	1	1	2	?	?	?	?	?	?	?	?	?	?	?	?	?	?	?	0	-	-	-	?	?	?	?	?	2	?	?	?	?	0	?	?
<i>Latirus vischii</i>	-	-	0	-	1	0	1	1	2	?	?	?	?	?	?	?	?	?	?	?	?	?	?	?	0	-	-	-	?	?	?	?	?	2	?	?	?	?	0	?	?
<i>Aurantularia aurantiaca</i>	-	-	0	-	1	0	1	1	2	?	?	?	?	?	?	?	?	?	?	?	?	?	?	?	0	-	-	-	?	?	?	?	?	2	?	?	?	?	0	?	?
<i>Fasciolaria tulipa</i>	-	-	0	-	1	0	1	1	2	?	?	?	?	?	?	?	?	?	?	?	?	?	?	?	0	-	-	-	?	?	?	?	?	2	?	?	?	?	0	?	?
<i>Australaria australasia</i>	-	-	0	-	1	0	1	1	2	?	?	?	?	?	?	?	?	?	?	?	?	?	?	?	0	-	-	-	?	?	?	?	?	2	?	?	?	?	0	?	?
<i>Pleuroploca trapezium</i>	-	-	0	-	1	0	1	1	2	?	?	?	?	?	?	?	?	?	?	?	?	?	?	?	0	-	-	-	?	?	?	?	?	2	?	?	?	?	0	?	?
<i>Filifusus filamentosus</i>	-	-	0	-	1	0	1	1	2	?	?	?	?	?	?	?	?	?	?	?	?	?	?	?	0	-	-	-	?	?	?	?	?	2	?	?	?	?	0	?	?
<i>Hemipolygona armata</i>	-	-	0	-	1	0	1	1	2	?	?	?	?	?	?	?	?	?	?	?	?	?	?	?	0	-	-	-	?	?	?	?	?	2	?	?	?	?	0	?	?
<i>Pustulatus mediamericus</i>	-	-	0	-	1	0	1	1	2	?	?	?	?	?	?	?	?	?	?	?	?	?	?	?	0	-	-	-	?	?	?	?	?	2	?	?	?	?	0	?	?
<i>Pustulatus ogum</i>	-	-	0	-	1	0	1	1	2	?	?	?	?	?	?	?	?	?	?	?	?	?	?	?	0	-	-	-	?	?	?	?	?	2	?	?	?	?	0	?	?
<i>Polygona angulata</i>	-	-	0	-	1	0	1	1	2	?	?	?	?	?	?	?	?	?	?	?	?	?	?	?	0	-	-	-	?	?	?	?	?	2	?	?	?	?	0	?	?
<i>Latirus polygonus</i>	-	-	0	-	1	0	1	1	2	?	?	?	?	?	?	?	?	?	?	?	?	?	?	?	0	-	-	-	?	?	?	?	?	2	?	?	?	?	0	?	?
<i>Polygona infundibulum</i>	-	-	0	-	1	0	1	1	2	?	?	?	?	?	?	?	?	?	?	?	?	?	?	?	0	-	-	-	?	?	?	?	?	2	?	?	?	?	0	?	?
<i>Hemipolygona beckyae</i>	-	-	0	-	1	0	1	1	2	?	?	?	?	?	?	?	?	?	?	?	?	?	?	?	0	-	-	-	?	?	?	?	?	2	?	?	?	?	0	?	?
<i>Latirus pictus</i>	-	-	0	-	1	0	1	1	2	?	?	?	?	?	?	?	?	?	?	?	?	?	?	?	0	-	-	-	?	?	?	?	?	2	?	?	?	?	0	?	?
<i>Leucozonia ocellata</i>	-	-	0	-	1	0	1	0	2	?	?	?	?	?	?	?	?	?	?	?	?	?	?	?	0	-	-	-	?	?	?	?	?	2	?	?	?	?	0	?	?
<i>Leucozonia cerata</i>	-	-	0	-	1	0	1	0	2	?	?	?	?	?	?	?	?	?	?	?	?	?	?	?	0	-	-	-	?	?	?	?	?	2	?	?	?	?	0	?	?
<i>Opeatostoma pseudodon</i>	-	-	0	-	1	0	1	0	2	?	?	?	?	?	?	?	?	?	?	?	?	?	?	?	0	-	-	-	?	?	?	?	?	2	?	?	?	?	0	?	?
<i>Leucozonia nassa nassa</i>	-	-	0	-	1	0	1	0	2	?	?	?	?	?	?	?	?	?	?	?	?	?	?	?	0																







TAXON	CHARACTER																																				
	64	64	64	64	64	64	64	64	65	65	65	65	65	65	65	65	66	66	66	66	66	66	66	66	67	67	67	67	67	67							
<i>Monetaria annulus</i>	0	0	1	0	6	0	0	1	2	1	2	1	2	2	3	3	1	2	2	0	1	0	1	0	0	0	0	2	0	0	0	0	0	-	0	0	
<i>Thais speciosa</i>	0	1	1	0	6	0	0	0	1	2	1	2	1	3	2	3	3	1	1	4	0	1	0	1	0	1	0	1	2	0	1	1	1	0	-	0	1
<i>Pugilina tupiniquim</i>	0	1	1	0	6	0	0	0	1	2	1	2	1	3	2	?	?	1	1	5	0	1	0	1	0	1	?	1	2	?	0	1	1	0	-	0	1
<i>engoniophos uncinatus</i>	0	1	1	0	6	0	0	0	1	2	1	2	1	3	2	?	?	1	1	5	0	1	0	1	0	1	?	1	2	?	0	1	1	0	-	0	1
<i>Nassarius reticulatus</i>	0	1	1	0	6	0	0	0	1	2	1	2	1	3	2	?	?	1	1	5	0	1	0	1	0	1	?	1	2	?	0	1	1	0	-	0	1
<i>Bullia laevissima</i>	0	1	1	0	6	0	0	0	1	2	1	2	1	3	2	?	?	1	1	5	0	1	0	1	0	1	?	1	2	?	0	1	1	0	-	0	1
<i>Buccinum undatum</i>	0	0	1	0	6	0	0	0	1	2	1	2	?	3	2	?	?	1	1	5	0	1	0	1	0	1	?	1	2	?	0	1	1	0	-	0	1
<i>Pisania pusio</i>	0	0	1	0	6	0	0	0	1	2	1	2	1	3	2	?	?	1	1	5	0	1	0	1	0	1	?	1	2	?	0	1	1	0	-	0	1
<i>Dolicholatirus sp.</i>	0	1	1	0	6	0	0	0	1	2	1	2	1	3	2	?	?	1	1	5	0	1	0	1	0	1	?	1	2	?	0	1	1	0	-	0	1
<i>Teralatirus roboreus</i>	0	1	1	0	6	0	0	0	1	2	1	2	1	3	2	?	?	1	1	5	0	1	0	1	0	1	?	1	2	?	0	1	1	0	-	0	1
<i>Dolicholatirus aff. cayohuesonicus</i>	0	1	1	0	6	0	0	0	1	2	1	2	1	3	2	?	?	1	1	5	0	1	0	1	0	1	?	1	2	?	0	1	1	0	-	0	1
<i>Angulofusus neda</i>	0	1	1	0	6	0	0	0	1	2	1	2	1	3	2	?	?	1	1	5	0	1	0	1	0	1	?	1	2	?	0	1	1	0	-	0	1
<i>Pseudolatirus kuroseanus</i>	0	1	1	0	6	0	0	0	1	2	1	2	1	3	2	?	?	1	1	5	0	1	0	1	0	1	?	1	2	?	0	1	1	0	-	0	1
<i>Amiantofusus pacificus</i>	0	1	1	0	6	0	0	0	1	2	1	2	1	3	2	?	?	1	1	5	0	1	0	1	0	1	?	1	2	?	0	1	1	0	-	0	1
<i>Amiantofusus candoris</i>	0	1	1	0	6	0	0	0	1	2	1	2	1	3	2	?	?	1	1	5	0	1	0	1	0	1	?	1	2	?	0	1	1	0	-	0	1
<i>Pseudolatirus pallidus</i>	0	1	1	0	6	0	0	0	1	2	1	2	1	3	2	?	?	1	1	5	0	1	0	1	0	1	?	1	2	?	0	1	1	0	-	0	1
<i>Chryseofusus archerius</i>	0	1	1	0	6	0	0	0	1	2	1	2	1	3	2	?	?	1	1	5	0	1	0	1	0	1	?	1	2	?	0	1	1	0	-	0	1
<i>Chryseofusus graciliformis</i>	0	1	1	0	6	0	0	0	1	2	1	2	1	3	2	?	?	1	1	5	0	1	0	1	0	1	?	1	2	?	0	1	1	0	-	0	1
<i>Fusinus marmoratus</i>	0	1	1	0	6	0	0	0	1	2	1	2	1	3	2	?	?	1	1	5	0	1	0	1	0	1	?	1	2	?	0	1	1	0	-	0	1
<i>Fusinus brasiliensis</i>	0	1	1	0	6	0	0	0	1	2	1	2	1	3	2	?	?	1	1	5	0	1	0	1	0	1	?	1	2	?	0	1	1	0	-	0	1
<i>Fusinus sp.</i>	0	1	1	0	6	0	0	0	1	2	1	2	1	3	2	?	?	1	1	5	0	1	0	1	0	1	?	1	2	?	0	1	1	0	-	0	1
<i>Fusinus frenguelli</i>	0	1	1	0	6	0	0	0	1	2	1	2	1	3	2	?	?	1	1	5	0	1	0	1	0	1	?	1	2	?	0	1	1	0	-	0	1
<i>Fusinus australis</i>	0	1	1	0	6	0	0	0	1	2	1	2	1	3	2	?	?	1	1	5	0	1	0	1	0	1	?	1	2	?	0	1	1	0	-	0	1
<i>Cyrtulus serotinus</i>	0	1	1	0	6	0	0	0	1	2	1	2	1	3	2	?	?	1	1	5	0	1	0	1	0	1	?	1	2	?	0	1	1	0	-	0	1
<i>Granulifusus sp.</i>	0	1	1	0	6	0	0	0	1	2	1	2	1	3	2	?	?	1	1	5	0	1	0	1	0	1	?	1	2	?	0	1	1	0	-	0	1
<i>Granulifusus hayashi</i>	0	1	1	0	6	0	0	0	1	2	1	2	1	3	2	?	?	1	1	5	0	1	0	1	0	1	?	1	2	?	0	1	1	0	-	0	1
<i>Pseudolatirus discrepans</i>	0	1	1	0	6	0	0	0	1	2	1	2	1	3	2	?	?	1	1	5	0	1	0	1	0	1	?	1	2	?	0	1	1	0	-	0	1
<i>Granulifusus aff. kiranus</i>	0	1	1	0	6	0	0	0	1	2	1	2	1	3	2	?	?	1	1	5	0	1	0	1	0	1	?	1	2	?	0	1	1	0	-	0	1
<i>Fusolatirus bruijnii</i>	0	1	1	0	6	0	0	0	1	2	1	2	1	3	2	?	?	1	1	5	0	1	0	1	0	1	?	1	2	?	0	1	1	0	-	0	1
<i>Peristernia marquesana</i>	0	1	1	0	6	0	0	0	1	2	1	2	1	3	2	?	?	1	1	5	0	1	0	1	0	1	?	1	2	?	0	1	1	0	-	0	1
<i>Peristernia nassatula</i>	0	1	1	0	6	0	0	0	1	2	1	2	1	3	2	?	?	1	1	5	0	1	0	1	0	1	?	1	2	?	0	1	1	0	-	0	1
<i>Nodolatirus nodatus</i>	0	1	1	0	6	0	0	0	1	2	1	2	1	3	2	?	?	1	1	5	0	1	0	1	0	1	?	1	2	?	0	1	1	0	-	0	1
<i>Latirus vischii</i>	0	1	1	0	6	0	0	0	1	2	1	2	1	3	2	?	?	1	1	5	0	1	0	1	0	1	?	1	2	?	0	1	1	0	-	0	1
<i>Aurantilaria aurantiaca</i>	0	1	1	0	6	0	0	0	1	2	1	2	1	3	2	?	?	1	1	5	0	1	0	1	0	1	?	1	2	?	0	1	1	0	-	0	1
<i>Fasciolaria tulipa</i>	0	1	1	0	6	0	0	0	1	2	1	2	1	3	2	?	?	1	1	5	0	1	0	1	0	1	?	1	2	?	0	1	1	0	-	0	1
<i>Australaria australasia</i>	0	1	1	0	6	0	0	0	1	2	1	2	1	3	2	?	?	1	1	5	0	1	0	1	0	1	?	1	2	?	0	1	1	0	-	0	1
<i>Pleuroploca trapezium</i>	0	1	1	0	6	0	0	0	1	2	1	2	1	3	2	?	?	1	1	5	0	1	0	1	0	1	?	1	2	?	0	1	1	0	-	0	1
<i>Filifusus filamentosus</i>	0	1	1	0	6	0	0	0	1	2	1	2	1	3	2	?	?	1	1	5	0	1	0	1	0	1	?	1	2	?	0	1	1	0	-	0	1
<i>Hemipolygona armata</i>	0	1	1	0	6	0	0	0	1	2	1	2	1	3	2	?	?	1	1	5	0	1	0	1	0	1	?	1	2	?	0	1	1	0	-	0	1
<i>Pustulatirus mediamericus</i>	0	1	1	0	6	0	0	0	1	2	1	2	1	3	2	?	?	1	1	5	0	1	0	1	0	1	?	1	2	?	0	1	1	0	-	0	1
<i>Pustulatirus ogum</i>	0	1	1	0	6	0	0	0	1	2	1	2	1	3	2	?	?	1	1	5	0	1	0	1	0	1	?	1	2	?	0	1	1	0	-	0	1
<i>Polygona angulata</i>	0	1	1	0	6	0	0	0	1	2	1	2	1	3	2	?	?	1	1	5	0	1	0	1	0	1	?	1	2	?	0	1	1	0	-	0	1
<i>Latirus polygonus</i>	0	1	1	0	6	0	0	0	1	2	1	2	1	3	2	?	?	1	1	5	0	1	0	1	0	1	?	1	2	?	0	1	1	0	-	0	1
<i>Polygona infundibulum</i>	0	1	1	0	6	0	0	0	1	2	1	2	1	3	2	?	?	1	1	5	0	1	0	1	0	1	?	1	2	?	0	1	1	0	-	0	1
<i>Hemipolygona beckyae</i>	0	1	1	0	6	0	0	0	1	2	1	2	1	3	2	?	?	1	1	5	0	1	0	1	0	1	?	1	2	?	0	1	1	0	-	0	1
<i>Latirus pictus</i>	0	1	1	0	6	0	0	0	1	2	1	2	1	3	2	?	?	1	1	5	0	1	0	1	0	1	?	1	2	?	0	1	1	0	-	0	1
<i>Leucozonia ocellata</i>	0	1	1	0	6	0	0	0	1	2	1	2	1	3	2	?	?	1	1	5	0	1	0	1	0	1	?	1	2	?	0	1	1	0	-	0	1
<i>Leucozonia cerata</i>	0	1	1	0	6	0	0	0	1	2	1	2	1	3	2	?	?	1	1	5	0	1	0	1	0	1	?	1	2	?	0	1	1	0	-	0	1
<i>Opeatostoma pseudodon</i>	0	1	1	0	6	0	0	0	1	2	1	2	1	3	2	?	?	1	1	5	0	1	0	1	0	1	?	1	2	?	0	1	1	0	-	0	1
<i>Leucozonia nassa nassa</i>	0	1	1	0	6	0	0	0	1	2	1	2	1	3																							

## 6. References

- Bouchet P. & Rocroi J.P. 2005. Classification and nomenclator of gastropod families. **Malacologia**, 47: 1-397.
- Kantor Y.I. & Fedosov A. 2009. Morphology and development of the valve of Leiblein in Neogastropoda: possible evidence for paraphyly of the Neogastropoda. **The Nautilus**, 123(3): 73-82.
- Ponder W.F., Colgan D.J., Healy J.M., Nützel A., Simone L.R.L. & Strong E.E. 2008. Caenogastropoda. In: Ponder W.F. & Lindberg D.R. (Eds.). *Phylogeny and Evolution of the Mollusca*. University of California Press. p. 331-383.
- Simone L.R.L. 2011. Phylogeny of the Caenogastropoda (mollusca), based on comparative morphology. **Arquivos de Zoologia**, São Paulo, 42(4): 161-323.
- WoRMS 2016. **World Register of Marine Species**. <http://www.marinespecies.org/> (accessed November 22, 2016).

## APPENDIX



```
(*script for POY parameter set 1110*)
```

```
set (seed:1234,log:"Faciollaridae_POY.log")  
read ("16S-align-POY.fasta")  
read ("18S-align-POY.fasta")  
read ("28S-align-POY.fasta")  
read ("COI-align.fasta")  
read ("H3-align.fasta")
```

```
transform (tcm:(1, 1), gap_opening:0)
```

```
search(max_time:0:6:0)  
search(max_time:0:6:0)  
search(max_time:0:6:0)  
search(max_time:0:6:0)
```

```
report ("all.tre", trees:(newick))  
report ("all.txt", treestats)  
select()
```

```
report ("best.tre", trees:(newick))  
report ("best.txt", treestats)  
report ("align_file.fas", fasta:all)  
report ("test.tre", trees:(total, branches:true))  
report ("fasciolaridae", diagnosis, consensus, "consensus",  
graphconsensus)
```

```
exit()
```

```
(*script for POY parameter set 2110*)
```

```
set (seed:1234,log:"Faciollaridae_POY.log")  
read ("16S-align-POY.fasta")  
read ("18S-align-POY.fasta")  
read ("28S-align-POY.fasta")  
read ("COI-align.fasta")  
read ("H3-align.fasta")
```

```
transform (tcm:(1, 2), gap_opening:0)
```

```
search(max_time:0:6:0)  
search(max_time:0:6:0)  
search(max_time:0:6:0)  
search(max_time:0:6:0)
```

```
report ("all.tre", trees:(newick))  
report ("all.txt", treestats)  
select()
```

```
report ("best.tre", trees:(newick))  
report ("best.txt", treestats)  
report ("align_file.fas", fasta:all)  
report ("test.tre", trees:(total, branches:true))  
report ("fasciolaridae", diagnosis, consensus, "consensus",  
graphconsensus)
```

```
exit()
```

```
(*script for POY parameter set 3221*)
```

```
set (seed:1234,log:"Faciollaridae_POY.log")  
read ("16S-align-POY.fasta")  
read ("18S-align-POY.fasta")  
read ("28S-align-POY.fasta")  
read ("COI-align.fasta")  
read ("H3-align.fasta")
```

```
transform (tcm:(2, 2), gap_opening:1)
```

```
search(max_time:0:6:0)  
search(max_time:0:6:0)  
search(max_time:0:6:0)  
search(max_time:0:6:0)
```

```
report ("all.tre", trees:(newick))  
report ("all.txt", treestats)  
select()
```

```
report ("best.tre", trees:(newick))  
report ("best.txt", treestats)  
report ("align_file.fas", fasta:all)  
report ("test.tre", trees:(total, branches:true))  
report ("fasciolaridae", diagnosis, consensus, "consensus",  
graphconsensus)
```

```
exit()
```

```
(*script for POY parameter set 1210*)
```

```
set (seed:1234,log:"Faciollaridae_POY.log")  
read ("16S-align-POY.fasta")  
read ("18S-align-POY.fasta")  
read ("28S-align-POY.fasta")  
read ("COI-align.fasta")  
read ("H3-align.fasta")
```

```
transform (tcm:(*READ_MATRIX*))
```

```
search(max_time:0:6:0)  
search(max_time:0:6:0)  
search(max_time:0:6:0)  
search(max_time:0:6:0)
```

```
report ("all.tre", trees:(newick))  
report ("all.txt", treestats)  
select()
```

```
report ("best.tre", trees:(newick))  
report ("best.txt", treestats)  
report ("align_file.fas", fasta:all)  
report ("test.tre", trees:(total, branches:true))  
report ("fasciolaridae", diagnosis, consensus, "consensus",  
graphconsensus)
```

```
exit()
```

```
(*READ_MATRIX:  
0 2 1 2 1  
2 0 2 1 1  
1 2 0 2 1  
2 1 2 0 1  
1 1 1 1 0*)
```

```
(*script for POY parameter set 2210*)
```

```
set (seed:1234,log:"Faciollaridae_POY.log")
read ("16S-align-POY.fasta")
read ("18S-align-POY.fasta")
read ("28S-align-POY.fasta")
read ("COI-align.fasta")
read ("H3-align.fasta")
```

```
transform (tcm:(*READ_MATRIX*))
```

```
search(max_time:0:6:0)
search(max_time:0:6:0)
search(max_time:0:6:0)
search(max_time:0:6:0)
```

```
report ("all.tre", trees:(newick))
report ("all.txt", treestats)
select()
```

```
report ("best.tre", trees:(newick))
report ("best.txt", treestats)
report ("align_file.fas", fasta:all)
report ("test.tre", trees:(total, branches:true))
report ("fasciolaridae", diagnosis, consensus, "consensus",
graphconsensus)
```

```
exit()
```

```
(*READ_MATRIX:
0 2 1 2 2
2 0 2 1 2
1 2 0 2 2
2 1 2 0 2
2 2 2 2 0*)
```

```
(*script for POY parameter set 3211*)
```

```
set (seed:1234,log:"Faciollaridae_POY.log")  
read ("16S-align-POY.fasta")  
read ("18S-align-POY.fasta")  
read ("28S-align-POY.fasta")  
read ("COI-align.fasta")  
read ("H3-align.fasta")
```

```
transform (tcm:(*READ_MATRIX*))
```

```
search(max_time:0:6:0)  
search(max_time:0:6:0)  
search(max_time:0:6:0)  
search(max_time:0:6:0)
```

```
report ("all.tre", trees:(newick))  
report ("all.txt", treestats)  
select()
```

```
report ("best.tre", trees:(newick))  
report ("best.txt", treestats)  
report ("align_file.fas", fasta:all)  
report ("test.tre", trees:(total, branches:true))  
report ("fasciolaridae", diagnosis, consensus, "consensus",  
graphconsensus)
```

```
exit()
```

```
(*READ_MATRIX:  
0 2 1 2 2  
2 0 2 1 2  
1 2 0 2 2  
2 1 2 0 2  
2 2 2 2 0*)
```

## Comparative anatomy of the fasciolariiids *Pustulaturus ogum* and *Hemipolygona beckyae* from Brazil (Gastropoda: Buccinoidea: Peristerniinae)

Diogo R. Couto<sup>1</sup>, Luiz R. L. R. Simone<sup>1</sup>, Alexandre D. Pimenta<sup>2</sup>

<sup>1</sup>Laboratório de Malacologia, Museu de Zoologia da Universidade de São Paulo. Avenida Nazaré, 481, Ipiranga. CEP 04263-000 São Paulo, SP, Brazil. E-mail: [diogoaut@gmail.com](mailto:diogoaut@gmail.com)

<sup>2</sup>Setor de Malacologia, Departamento de Invertebrados, Museu Nacional, Universidade Federal do Rio de Janeiro. Quinta da Boa Vista s/n, São Cristóvão. CEP 20940-040 Rio de Janeiro, RJ, Brazil.

**Summary:** The Brazilian species *Pustulaturus ogum* and *Hemipolygona beckyae* were examined, and certain morphological characters were described. Both species were originally assigned to the genus *Latirus*, considered as a heterogeneous complex. The radulae of both species are like that which characterizes *Latirus*, in which the innermost cusp of the rachidian tooth is well developed but always smaller than the other cusps. This feature differs from *Leucozonia*, in which this cusp is reduced or absent. The penis tapers terminally, and the tapered part may be long (more than half the total penis length), as in *H. beckyae*, or very short (less than half the total penis length), as in *P. ogum*. The anatomical data observed in both species are discussed under the framework of fasciolariid systematics and they appear to be widespread among other fasciolariid species. For this reason, to date, the soft-part features here provided and those known from previously studied species of *Latirus* are not useful for delineating precise generic diagnoses.

**Keywords:** morphology; Caenogastropoda; Fasciolariiidae; *Latirus*; western Atlantic.

**Anatomía comparada de los fascioláridos *Pustulaturus ogum* y *Hemipolygona beckyae* de Brasil (Gastropoda: Buccinoidea: Peristerniinae)**

**Resumen:** Se describe la morfología y anatomía de las especies brasileñas *Pustulaturus ogum* y *Hemipolygona beckyae*. Ambas especies han sido tradicionalmente asignadas al género *Latirus*, que en la actualidad se considera que agrupa a un conjunto heterogéneo de especies. Las rádulas de ambas especies son como la que caracteriza a *Latirus*, con la cúspide más interna del diente raquídeo bien desarrollada y siempre menor que las otras cúspides. Esta característica difiere de la que presentan las especies del género *Leucozonia*, en las que esta cúspide está reducida o ausente. El pene se estrecha en su parte terminal, y la parte cónica puede ser larga (más de la mitad de la longitud total del pene), como en *H. beckyae*, o muy corta (menos de la mitad de la longitud total del pene), como en *P. ogum*. Los caracteres morfológicos observados en ambas especies se discuten en el marco de la sistemática de los Fasciolariiidae y parecen estar ampliamente distribuidos en otras especies de fascioláridos. Por ello, hasta la fecha, las características de las partes blandas del animal aquí descritas y las conocidas previamente de otras especies de *Latirus* no se consideran de utilidad para la diagnosis de los géneros en esta familia.

**Palabras clave:** morfología; Caenogastropoda; Fasciolariiidae; *Latirus*; Atlántico occidental.

**Citation/Como citar este artículo:** Couto D.R., Simone L.R.L.R., Pimenta A.D. 2015. Comparative anatomy of the fasciolariiids *Pustulaturus ogum* and *Hemipolygona beckyae* from Brazil (Gastropoda: Buccinoidea: Peristerniinae). *Sci. Mar.* 79(1): 000-000. doi: <http://dx.doi.org/10.3989/scimar.04144.08A>

**Editor:** J. Templado.

**Received:** September 1, 2014. **Accepted:** December 16, 2014. **Published:** February 12, 2015.

**Copyright:** © 2015 CSIC. This is an open-access article distributed under the Creative Commons Attribution-Non Commercial License (by-nc) Spain 3.0.

### INTRODUCTION

The neogastropod family Fasciolariiidae comprises more than 1300 living species, distributed in the tropics and subtropics (Gofas 2014), and divided into three subfamilies, Fasciolarinae, Fussiniinae and Peristerni-

inae. Members of the subfamily Peristerniinae inhabit hard bottoms, although other fasciolariiids dwell mostly in soft and muddy substrates (Harasewych 1998, Vermeij and Snyder 2006).

Members of the Peristerniinae are represented in Brazil by at least 16 species, in the genera *Polygona*

Schumacher, 1817 (7 spp.), *Hemipolygona* Rovereto, 1899 (2 spp.), *Pustulatirus* Vermeij and Snyder, 2006 (3 spp.) and *Leucozonia* Gray, 1847 (4 spp.) (Rosenberg 2009). Most species included in *Hemipolygona* and *Pustulatirus* were previously grouped in *Latirus*. However, this genus is now restricted to the Indo-West Pacific (Vermeij and Snyder, 2006); it was previously regarded as a heterogeneous assemblage, and was recently the target of some taxonomic revisions (Vermeij and Snyder 2002, 2006).

*Pustulatirus ogum* and *Hemipolygona beckyae*, which occur in Brazilian waters, were treated in the most recent bibliographic records as subgenera of *Latirus* (Rios 1994, 2009). The former species occurs from Espírito Santo to Bahia state, and the latter only in Espírito Santo; *P. ogum* inhabits tide pools, while *H. beckyae* occurs at depths of about 30 m.

Kosyan et al. (2009) studied the anatomy of some species of Fasciolariidae, including *Turrilatirus turritus* (Gmelin, 1791), *Pustulatirus mediamericus* (Hertlein and Strong, 1951) and *Latirus polygonus* (Gmelin, 1791), all of which were previously regarded as members of *Latirus*. In Brazil, only the anatomy of species belonging to *Leucozonia* has been studied: *L. nassa* (Gmelin, 1791) by Marcus and Marcus (1962); *L. nassa* (Gmelin, 1791), *L. ocellata* (Gmelin, 1791) and *L. ponderosa* (Vermeij and Snyder 1998) by Couto and Pimenta (2012); and *Teralatirus roboreus* by Simone et al. (2013).

Fraussen et al. (2007) reported that a combination of traits is diagnostic for Fasciolariidae: multicuspitate lateral teeth and straight rachidian teeth, proboscis retractor muscle as a single or paired tuft of fibres, ducts of the salivary glands embedded in the esophagus wall, and a stomach without a posterior mixing area. Kosyan et al. (2009) studied the anatomy of eight fasciolarid species belonging to seven genera. These authors distinguished fasciolarids from buccinids studied by them and by Kosyan and Kantor (2009), based on the stomach morphology: low folds with transverse striations, absence of differentiation of the gastric chamber, absence of a posterior mixing area (Kantor 2003), and proboscis retractor muscles as a single muscle or paired (Fraussen et al. 2007). The orange-red colour of the foot and head-foot mass is typical for fasciolarids.

Morphological characters may prove useful in validating phylogenetic relationships and may help to resolve internal clades (Strong 2003, Simone 2011). However, no formal anatomical characterization within *Latirus* and related species exists. They are presently distinguished solely on shell features (Vermeij and Snyder 2006, Lyons and Snyder 2013), and hence prone to hypotheses of polymorphism and convergence. The present contribution provides morphological descriptions and comparisons of *Pustulatirus ogum* and *Hemipolygona beckyae*.

## MATERIALS AND METHODS

The material used for this study is deposited in the Museu Nacional / Universidade Federal do Rio de Ja-

neiro (MNRJ) and Museu de Zoologia / Universidade de São Paulo (MZSP).

The specimens collected were fixed in 70% ethanol. Shells were measured with a caliper, and photographs of individuals were taken with a digital camera. The anatomical dissections were done under a stereomicroscope. All drawings were made using a camera lucida. Radulae were manually extracted and prepared by immersion in KOH, followed by ultrasonic cleaning and subsequent immersion in distilled water for scanning electron microscope photography.

## RESULTS

### Genus *Pustulatirus* Schumacher, 1817

*Pustulatirus* Vermeij and Snyder, 2006. Type species: *Latirus mediamericus* Hertlein and Strong, 1951 by original designation.

*Diagnosis.* See Vermeij and Snyder (2006).

### *Pustulatirus ogum* (Petuch, 1979) (Figs 1-5)

*Latirus ogum*: Petuch 1979: 519 (Figs 3A-B); Rios 1985: 107 (pl. 36, Fig. 470); Mallard and Robin 2005: 18 (pl. 47).

*Latirus (Polygona) ogum*: Petuch 1987: 140 (pl. 27, Figs 1-2); Rios 1994: 133, (pl. 42, Fig. 574); Snyder 2003: 152, 306; Rios 2009: 253.

*Benimakia ogum*: Vermeij and Snyder 2003: 17 (Figs 6A-B).

*Polygona ogum*: Rosenberg 2009.

*Pustulatirus ogum*: Landau and Vermeij 2012: 88; Lyons and Snyder 2013: 49 (Figs 52-62).

*Type locality.* West of Coroa Vermelha, in tide pool, Abrolhos reef, Bahia state, Brazil, 17°57'S, 39°13'W.

*Types.* Holotype: USNM 780654.

*Examined material.* Brazil: Bahia, Alcobaça (20-25 m), MZSP 68475, 16 specimens (vi/2006), MZSP 68835, 1 specimen (viii/2005); Espírito Santo, Guarapari (A. Bodart col., 20-25 m, i/2006), MZSP 69477, 6 specimens, MZSP 69481, 10 specimens; Rio de Janeiro, Arraial do Cabo, 30-35 m, MZSP 69301, 2 specimens (P. Conçalves col., i/2005).

*Distribution.* Abrolhos reef, Bahia state; Espírito Santo to Rio de Janeiro states, southeast coast of Brazil.

*Shell* (Fig. 1A-F). Shell elliptical, fusiform, height up to 39.2 mm, width 2/5-1/2 of height. Colour chestnut to dark brown. Spire high, angle 45°-50°, ~1/2 of total shell height. Protoconch small with 2 whorls, smooth, terminal varix low. Teleoconch with 7-8 rounded whorls; subsutural ramp slightly concave, suture deep, base of shell concave. Spiral sculpture of 6-7 continuous spiral cords along entire teleoconch, 3 in abapical half of each whorl, more evidenced in first whorls, 3-4 strong spiral cords marking siphonal canal; several secondary spiral cords along entire teleoconch. Axial sculpture of 7-8 strong rounded ribs. Aperture elliptical to pyriform, height ~3× width. Columella bearing 3 folds medially. Outer lip crenulated, marked internally by 10 discontinuous lirae. Siphonal canal moderately long, length ~1/2 of length of aperture. Siphonal fasciole indistinct. Pseudoumbilicus as shallow slit.



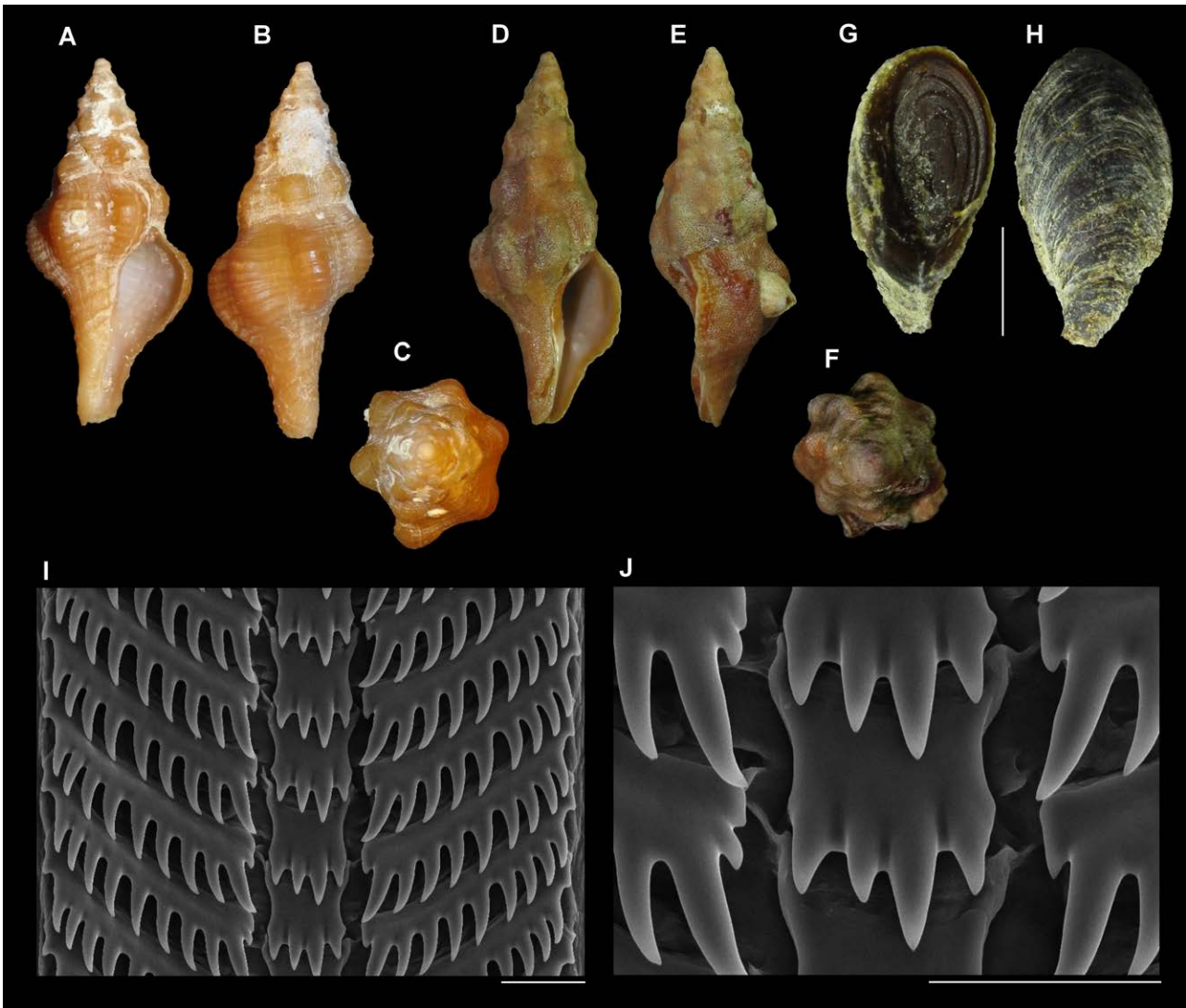


Fig. 1. – *Pustulaturus ogum*. A-C, 22.2 mm (MZSP 68475); D-F, 39.2 mm (MZSP 69301); G, operculum internal view; H, operculum external view; I, radula; J, detail of rachidian tooth. Scale bars: G-H, 3 mm; I-J, 30 mm.

**Head-foot** (Fig. 2A-B). colour cream in fixed species. Head prominent, of medium size (width  $\sim 1/3$  of adjacent width of head-foot), cephalic tentacles blunt and short (length  $\sim 1/2$  of anterior width of head), situated very close to each other; bases lying side by side. Eyes dark, small, rounded, situated in middle region of outer edge of tentacles. Foot short, rounded, anterior region bifid. Pedal gland as shallow median anterior slit, with anterior furrow extending along entire anterior edge. Columellar muscle thick, with  $\sim 1.25$  whorls in length.

**Operculum** (Fig. 1G-H). Operculum corneous, unguiculate (width  $\sim 2/3$  of length), filling entire aperture; outer surface opaque, with anterior nucleus inner surface with attachment scar elongated, elliptical, situated posteriorly, occupying  $\sim 2/3$  of inner area.

**Pallial complex** (Fig. 2C-D). Pallial cavity wide, of one whorl. Mantle border simple, thickened. Siphon short (length about  $1/4$  of free portion of mantle edge), its margin smooth; right fold of siphon base extend-

ing into pallial cavity, ending close to anterior end of ctenidium. Osphradium elongated, tapering anteriorly; length  $\sim 1/2$  of ctenidium; almost symmetrical longitudinally; osphradium leaflets rounded, short (height  $\sim 1/2$  of ctenidial filament height at middle region of pallial cavity),  $\sim$ equal in size. Ctenidium curved,  $\sim 1/4$  of total pallial cavity area, width slightly larger than osphradium; anterior and posterior region pointed, posterior end situated close to pericardium; filaments triangular; ctenidial vein (efferent branchial vessel) uniformly narrow along its length. Hypobranchial gland thin and loosely fixed, situated between gill and rectum, except for posterior  $1/2$  of pallial cavity. Rectum elongated. Anus elliptical, situated at  $1/4$  of mantle edge.

**Circulatory and excretory systems** (Fig. 4G). Pericardium spanning  $\sim 1/5$  of total renal cavity area. Auricle pyriform, wall thin, translucent; ventricle large and rounded ( $\sim$ larger than auricle), triangular in shape, with thick walls. Aorta bifurcate immediately after leaving ventricle; posterior aorta following visceral mass close to stomach; anterior aorta crossing diaphragmatic sep-

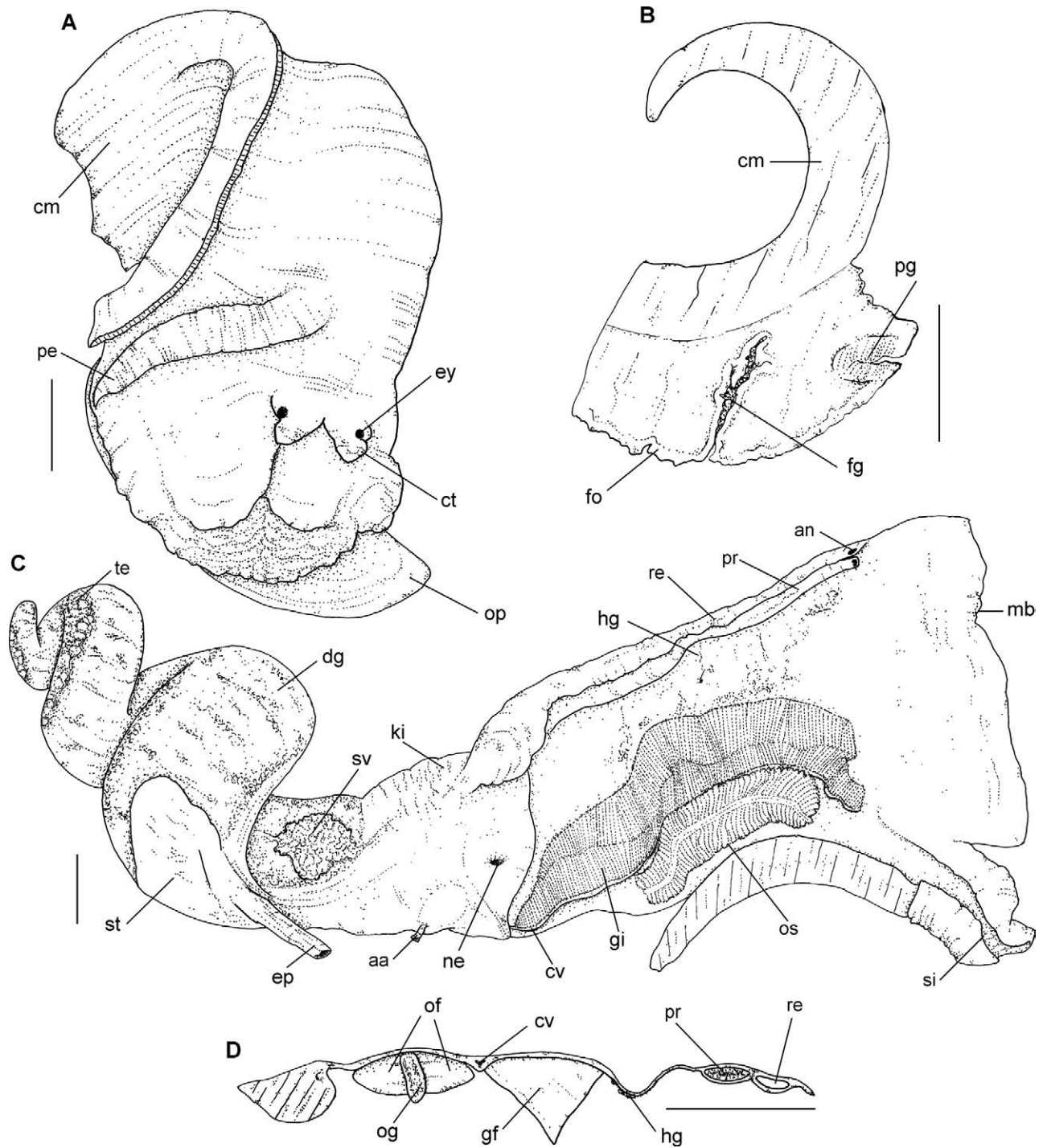


Fig. 2. – *Pustulaturus ogum*. A, head-foot mass in dorsal view; B, longitudinal section of head-foot mass, female; C, roof of pallial cavity in ventral view, male; D, transverse section of roof of pallial cavity. Abbreviations: aa, anterior aorta; an, anus; cm, columellar muscle; ct, cephalic tentacle; cv, ctenidial vein; dg, digestive gland; ep, posterior esophagus; ey, eye; fg, female cement gland; fo, foot; gf, gill filament gi, gill; hg, hypobranchial gland; ki, kidney; mb, mantle border; ne, nephrostome; of, osphradium filament; og, osphradium ganglia; op, operculum; os, osphradium; pe, penis; pg, pedal gland; pr, prostate; re, rectum; si, siphon; st, stomach; sv, seminal vesicle; te, testis. Scale bars: 2 mm.

tum anteriorly. Anterior aorta running anteriorly along whole length of posterior esophagus, crossing gland of Leiblein in mid-esophagus, with branches forming sinus surrounding nerve ring. Anterior aorta bifurcating anteriorly to nerve ring; one branch following anteriorly to pedal ganglia as pedal aorta, another branch accompanying anterior esophagus, following anteriorly to buccal mass and odontophore. Kidney bearing ventral

and dorsal lamellar lobes similar in shape; nephridial gland situated on dorsal side of membrane between renal cavity and pericardium; renal aperture as slit in membrane between pallial and renal cavities, flanked on its right side by transversal folds, longitudinal to roof of pallial cavity. Part of intestine running longitudinally on inner side of kidney, ventrally adhered to its membrane



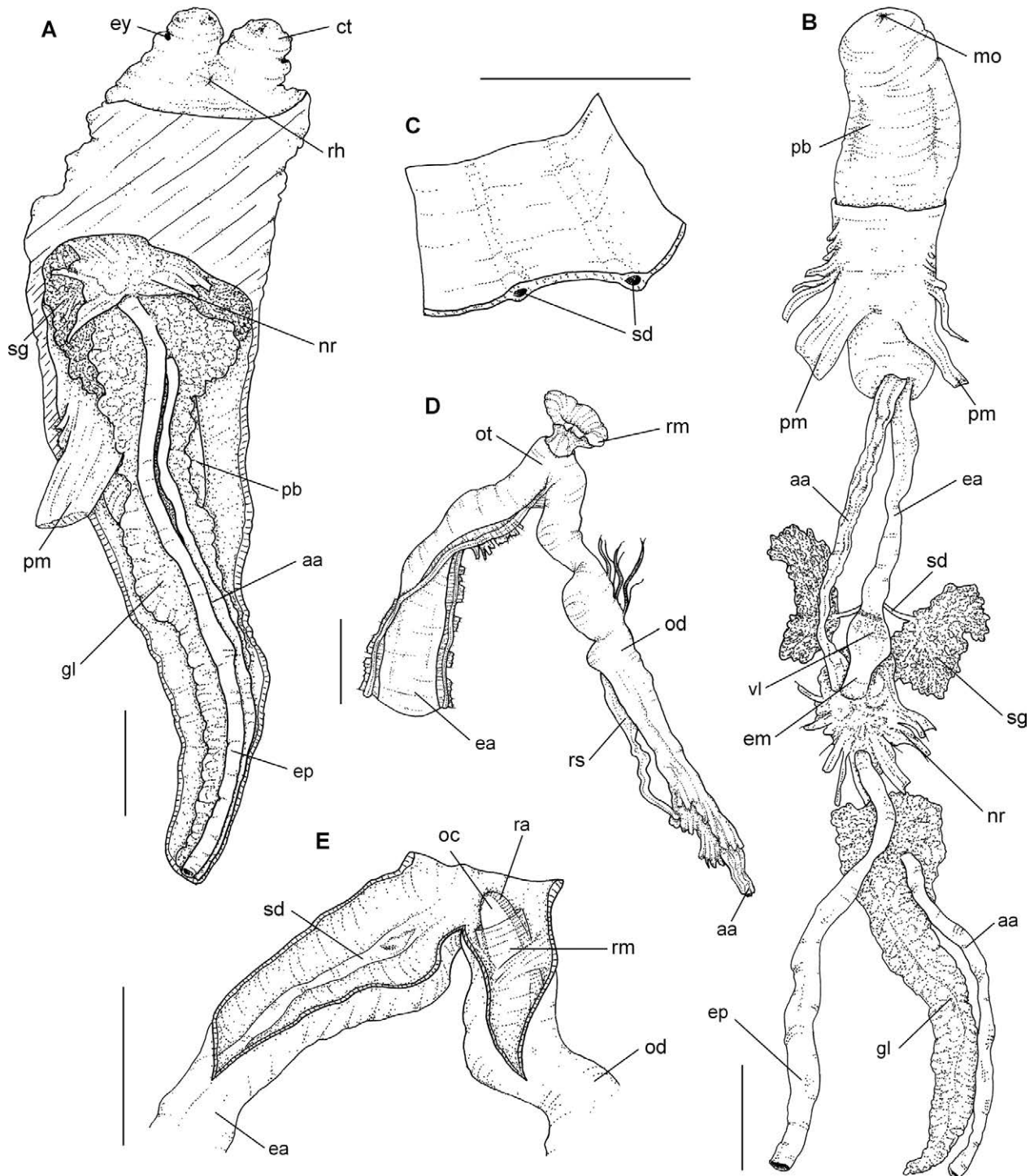


Fig. 3.- *Pustulatirus ogum*. A, haemocoel in ventral view; B, anterior digestive system; C, lumen of anterior esophagus; D, buccal mass in lateral view; E, buccal mass in lateral view, opened longitudinally. Abbreviations: aa, anterior aorta; ct, cephalic tentacle; ea, anterior esophagus; ep, posterior esophagus; ey, eye; gl, gland of Leiblein; mo, mouth opening; nr, nerve ring; oc, odontophore cartilage; od, odontophore tube; ot, oral tube; pb, proboscis; pm, proboscis retractor muscles; ra, radula; rh, rhynchostoma; rm, subradular membrane; rs, radular sac; sd, salivary gland duct; sg, salivary gland; vl, valve of Leiblein. Scale bars: A-B, 2 mm; C-E, 1 mm.

**Digestive system** (Figs 3A-E, 4A-E). Rhynchostome as small longitudinal slit, located between and below cephalic tentacles. Proboscis straight, of moderate length (~2/3 of haemocoel length), with thick muscular walls bearing 2 lateral grooves. Pair of proboscis retractor muscles originating in ventral posterior wall of proboscis; series of short lateral muscle fibres connected to inner walls of haemocoel. Mouth small,

circular. Odontophore long, slender (~same length as proboscis), pair of odontophore cartilages dorsally concave, fused anteriorly at ~1/4 of total cartilage length. Series of transversal muscle fibres connecting odontophore tube with anterior esophagus; superficial circular muscles (m3) enveloping entirely odontophore, except for most posterior end; horizontal muscle (m6), originating on ventral surface of odontophore

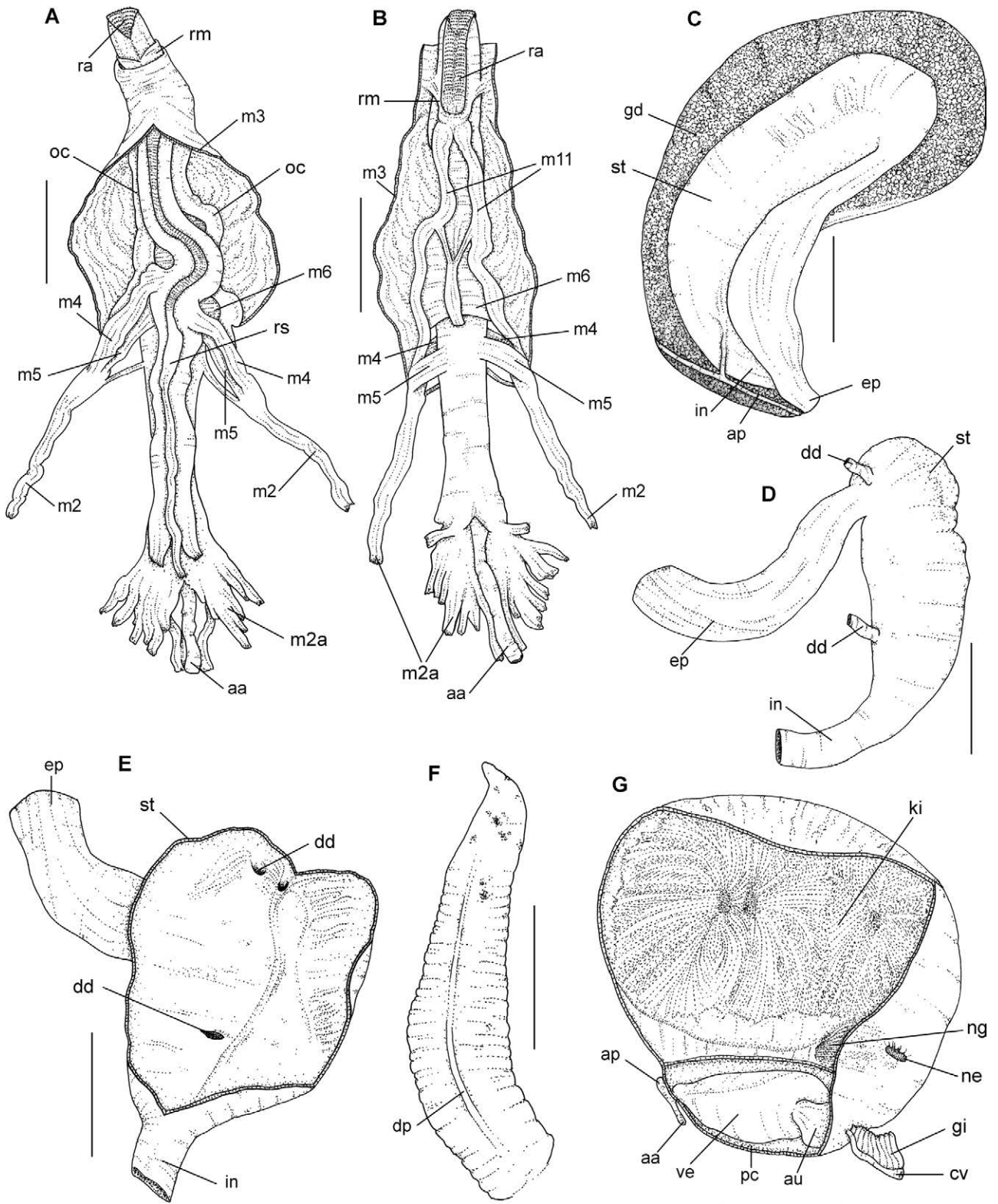


Fig. 4. – *Pustulaturus ogum*. A, odontophore in dorsal view; B, odontophore in ventral view; C, stomach in dorsal view; D, stomach in ventral view; E, stomach shown internally; F, penis in dorsal; G, renal cavity and pericardium in ventral view. Abbreviations: aa, anterior aorta; ap, posterior aorta; au, auricle; bu, bursa; cv, ctenidial vein; dd, duct of digestive gland; dg, digestive gland; dp, duct of penis; ep, posterior esophagus; in, intestine; ki, kidney; m11, ventral tensor muscles of radula; m2, odontophore retractor muscles; m2a, accessory odontophore retractor muscles; m3, superficial circular muscles; m4, dorsal tensor muscles of radula; m5, auxiliary dorsal tensor muscles of radula; m6, horizontal muscle; ne, nephrostome; ng, nephridial gland; oc, odontophore cartilage; pc, pericardium; ra, radula; re, rectum; rm, subradular membrane; rs, radular sac; ve, ventricle. Scale bars: A-B, 1 mm; C-G, 2 mm.



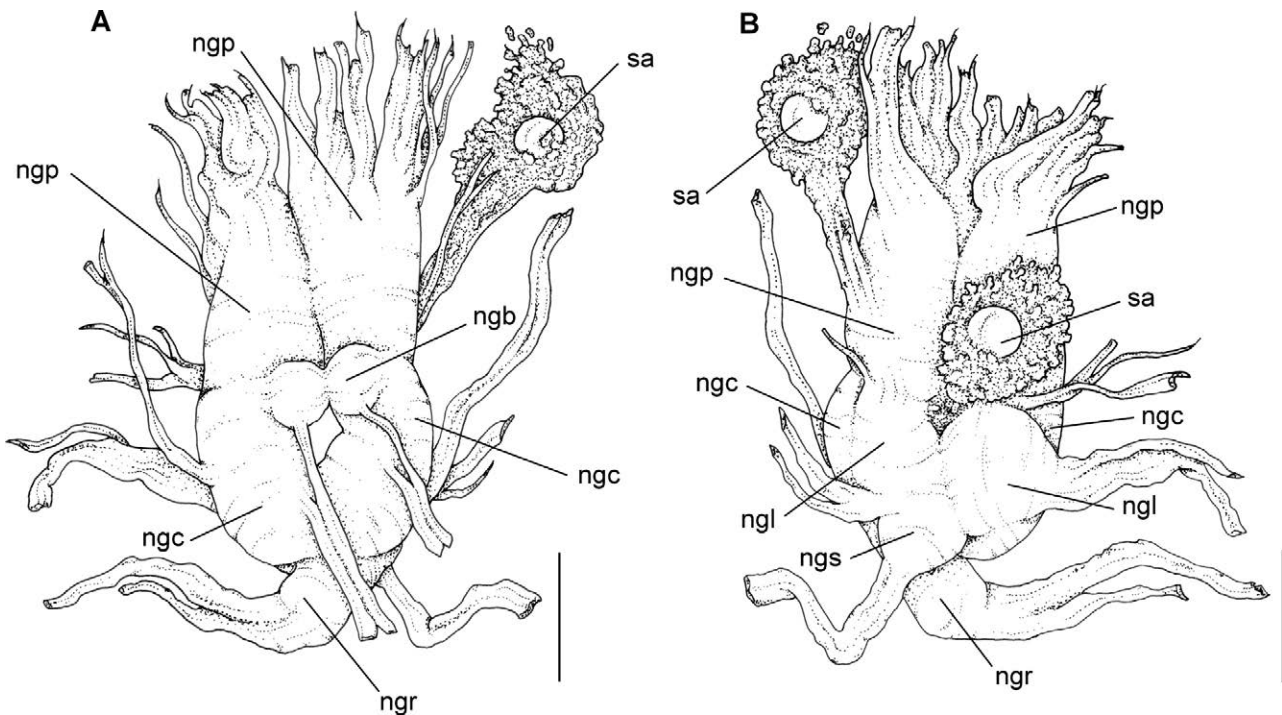


Fig. 5. – *Pustulaturus ogum*. A, nerve ring in dorsal view; B, nerve ring in ventral view. Abbreviations: ngb, buccal ganglion; ngc, cerebral ganglion; nbl, pleural ganglion; ngp, pedal ganglion; ngr, supra-esophageal ganglion; ngs, subesophageal ganglion; sa, statocyst. Scale bars: 0.5 mm.

cartilages, except for most posterior region (~1/5 of total odontophore length). Pair of odontophore retractor muscles (m2) originating from posterior end of odontophore cartilages, near to radular sac, inserted in inner wall of proboscis; pair of accessory odontophore retractor muscles (m2a), originating from inner surface of proboscis, near origin of m2, running adjacent to esophagus, insertion enveloping radular sac; pair of secondary, long branch of m2a accompanying anterior aorta reaching up to posterior level of nerve ring. Pair of dorsal tensor muscles of radula (m4) originating from posterior dorsal end of odontophore, covering its dorsal surface, inserting m2a; pair of auxiliary dorsal tensor muscles of radula (m5) originating from posterior end of odontophore, covering its ventral surface, inserting in m2a; pair of ventral tensor muscles of radula (m11), inserting anteriorly in subradular membrane, running, ventrally adhered (~3/4 of total odontophore length), origin bifid: main branch originating in ventral posterior cartilage of odontophore near origin of m2, secondary branch originating ventrally in m2a, crossing dorsally m6, connecting in main branch (at ~1/2 of total m11 length). Radula long and thin; radular sac extending beyond posterior end of odontophore; Radular teeth (Fig. 11-I-J): rachidian tooth straight, slightly rectangular, their base with concave outline, cusped margin convex, bearing 4 sharp cusps of ~equal size, except for right central, slightly larger than others; lateral tooth wider than long, bearing 11 prominent, centrally recurved cusps of approximately same size, except for innermost ~1/5 smaller, and outermost ~1/4 smaller and separated from rest. Anterior esophagus moderately long and broad (~2× proboscis length), dorsally-ventrally compressed, originating in oral tube. Valve of Leiblein pyriform, forming orange

ring around esophagus, ~1.5 of esophagus width. Salivary glands just anterior to valve of Leiblein, forming pair of branching and amorphous masses; free portion of salivary ducts short, extending along esophagus, anteriorly to valve of Leiblein, becoming embedded with esophageal wall, running immersed anteriorly, opening in oral lumen, immediately before oral tube. Accessory salivary glands absent. Middle esophagus short. Duct of gland of Leiblein short and narrow, inserted posterior to nerve ring. Gland of Leiblein brownish, long, of ~same length as posterior esophagus, posterior end acute. Posterior and anterior esophagus of ~same width. Inner wall of anterior esophagus smooth, salivary ducts immersed in marked lateral folds. Stomach wide, walls thin, bearing many internal folds. Digestive gland dark brown, occupying all whorls of visceral mass, from apex to kidney/pericardium area, surrounding stomach, emitting two narrow, branching ducts discharging near esophagus and intestine apertures. Intestine bearing expansion near posterior region of pallial cavity in region preceding rectum, internally bearing many longitudinal folds.

*Male genital system* (Fig. 4F). Testis brownish, occupying all whorls of visceral mass, except for last one; surrounding apically entire length of digestive gland. Visceral vas deferens running from testis. Seminal vesicle coiled, located on mid-ventral region of last whorl of visceral mass; vas deferens narrow, simple, running along ventral wall of kidney. Prostate thin and long, tubular, located along right side of roof of pallial cavity, next to rectum and ~equal in width. Penis long, close to head-foot, ~circular in transverse section; penis becoming narrower at middle of its length, terminating in extension of ~1/2 of total penis length; duct of penis linear, simple.

**Female genital system** (Fig. 2B). Ovaries brownish, with same texture and length as testis. Female cement gland opening at ~1/2 from anterior edge of foot, forming somewhat elongated and deep sac of ~same depth as foot thickness, recurved anteriorly. Pallial oviduct not observed.

**Nervous system** (Fig. 5A-B). Nerve ring highly concentrated, occupying ~1/6 of total haemocoel area, surrounding mid-esophagus posteriorly. All commissures internal. Cerebral ganglia bean-shaped, occupying ~1/2 of total nerve ring volume, right ganglion slightly larger and more dorsal than left ganglion, its posterior halves broadly connected with each other; pair of lateral tentacular nerves following anteriorly to pedal aorta. Pleural ganglia as pair of bulges ventral to cerebral ganglia, strongly attached to these; left pleural ganglia emitting thick nerve accompanying proboscis anteriorly. Pedal ganglia anterior, elongated, ~1/2 of total nerve ring volume; bearing anterior nerves; right pedal ganglion slightly larger and dorsal than left pedal ganglion. Buccal ganglia circular, small, ~1/5 of cerebral ganglia and dorsal to these, emitting pair of cerebro-buccal nerves, following anteriorly to anterior aorta. Supra-esophageal ganglion posterior to cerebro-pleural ganglia complex, slightly larger than buccal ganglia, emitting thick osphradial nerve. Subesophageal ganglion as ventral bulge in left cerebro-pleural ganglia complex emitting thick pallial-siphon nerve. Pair of vitreous statocysts with one anterior and associated with right pedal ganglion; and one posterior, associated with left pedal ganglion.

#### Genus *Hemipolygona* Rovereto, 1899

*Hemipolygona* Rovereto, 1899: 104. New name for *Chascax* Watson, 1873, non Ritgen 1828 (Reptilia). Type species: *Chascax maderensis* Watson, 1873 by monotypy.

**Diagnosis.** Shell extremely nodulose with blunt to sharp nodes where axial ribs cross spiral cords, especially on shoulder angulation and central cord, but also on base of shell and subsutural ramp; columella bearing up to 3 weak to strong folds medially; outer lip crenulated, marked internally by several beaded lirae; siphonal fasciole and pseudoumbilicus usually present.

#### *Hemipolygona beckyae* (Snyder, 2000) (Figs 6-9)

*Latirus beckyae*: Snyder 2000: 161 (Figs 1-2); Snyder 2003: 48, 300; Mallard and Robin 2005: 17 (pl. 40).

*Hemipolygona beckyae*: Vermeij and Snyder 2006: 417 (Fig. 2D); Rosenberg 2009.

**Type locality.** Off Vitória, 30-50 m depth, Espírito Santo state, Brazil.

**Types.** Holotype: USNM 880231; Paratypes: USNM 880232; IBU-FRJ 9121; MORG 39008; MNRJ 7696.

**Examined material.** Brazil: Espírito Santo, Vitória (30-50 m, v/1994), MNRJ 7696, paratype, 1 shell; (viii/2005) MZSP 68835, 1 specimen; Vitória (viii/2003, 30-35 m), MZSP 69482, 3 specimens; Guarapari, MZSP 57053, 1 specimen, (30-35 m, viii/2000), MZSP 69764, 1 specimen.

**Distribution.** Espírito Santo to São Paulo states, southeast coast of Brazil.

**Shell** (Fig. 6A-G). Shell elliptical, fusiform, height up to 55.4 mm, width ~1/3 of height. Colour light orange with spiral cords whitish. Spire high, angle 50°-55°, ~1/2 of total shell height. Protoconch small with 1.5 whorls, smooth, terminal varix low. Teleoconch with 6-9 rounded whorls; suture raised, subsutural lamellar spiral cord, base of shell concave. Spiral sculpture of 8-9 continuous whitish spiral cords per whorl, more prominent in shoulder angulation; 14-18 whitish spiral in base; several secondary spiral cords along teleoconch. Axial sculpture of 7-8 strong, wide, rounded ribs; lamellar striae occurring between spiral cords, eroded in early whorls. Aperture elliptical, height ~3× width. Columella bearing 3 folds medially. Outer lip crenulated, marked internally by 10-11 discontinuous lirae, not present where they cross outer lip growth scars. Siphonal canal moderately long, length ~1/2 of length of aperture. Siphonal fasciole present. Pseudoumbilicus as shallow slit.

**Head-foot** (Fig. 7A-B). Colour cream in fixed species, Head prominent, small (width ~1/4 of adjacent width of head-foot), cephalic tentacles blunt and of medium size (length ~same as anterior width of head), situated very close to each other, bases lying side by side. Eyes dark, small, rounded, situated in middle region of outer edge of tentacles. Foot short, rounded, its anterior region bifid. Pedal gland as shallow median anterior slit, with anterior furrows extending along entire anterior edge.

**Operculum** (Fig. 6H-I). Corneous, unguiculate (width ~2/3 of length), filling entire aperture; outer surface opaque, with anterior nucleus; inner surface with attachment scar elongated, elliptical, situated posteriorly, occupying ~2/3 of inner area. Columellar muscle thick, with ~1 whorl in length.

**Pallial complex.** Pallial cavity of 3/4 whorl; mantle border simple, thickened. Siphon short (length about 1/4 of free portion of mantle edge), margin smooth. Gill, hypobranchial gland osphradium and pallial portion of digestive system not observed.

**Circulatory and excretory systems.** Not analysed.

**Digestive system** (Figs 7C-D, 8, 9A-C). Rhynchostome as transversal slit, located slightly below right cephalic tentacle. Proboscis straight, of moderate length (~2/3 of haemocoel length), with thick muscular walls; strong proboscis retractor muscles originating in right ventral posterior wall of proboscis; laterally to proboscis, series of short muscle fibres connect to inner walls of haemocoel. Mouth small, circular. Odontophore long, very slender (~1/2 total length of proboscis). Pair of odontophore cartilages dorsally concave, fused anteriorly at ~1/5 of total cartilage length; series of transversal muscle fibres connect odontophore tube with anterior esophagus, and series of





Fig. 6. – *Hemipolygona beckyae*. A-B, 55.4 mm (MZSP 69764); C-E, 52.4 mm (MZSP 57053); F-G, 38.2 mm (MZSP 69482); H, operculum internal view; I, operculum external view; J, radula; K, detail of rachidian tooth. Scale bars: H-I, 3 mm; J-K, 30  $\mu$ m.

thin muscle fibres, superficial circular muscles (m3) entirely envelope odontophore, except for most posterior end. Horizontal muscle (m6), on ventral surface of odontophore cartilages, except for most posterior region (~1/6 of total odontophore length). Pair of odontophore retractor muscles (m2) originating from posterior end of odontophore cartilages, near to radular sac, inserted in inner wall of proboscis. Pair of accessory odontophore retractor muscles (m2a), originating from

inner surface of proboscis, near origin of m2, running adjacent to esophagus, insertion enveloping radular sac; pair of secondary, long branches of m2a accompanying anterior aorta reaching up to posterior level of nerve ring. Pair of dorsal tensor muscles of radula (m4) originating from posterior dorsal end of odontophore, covering its dorsal surface, inserting m2a. Pair of auxiliary dorsal tensor muscles of radula (m5) originating from posterior end of odontophore, covering its ventral

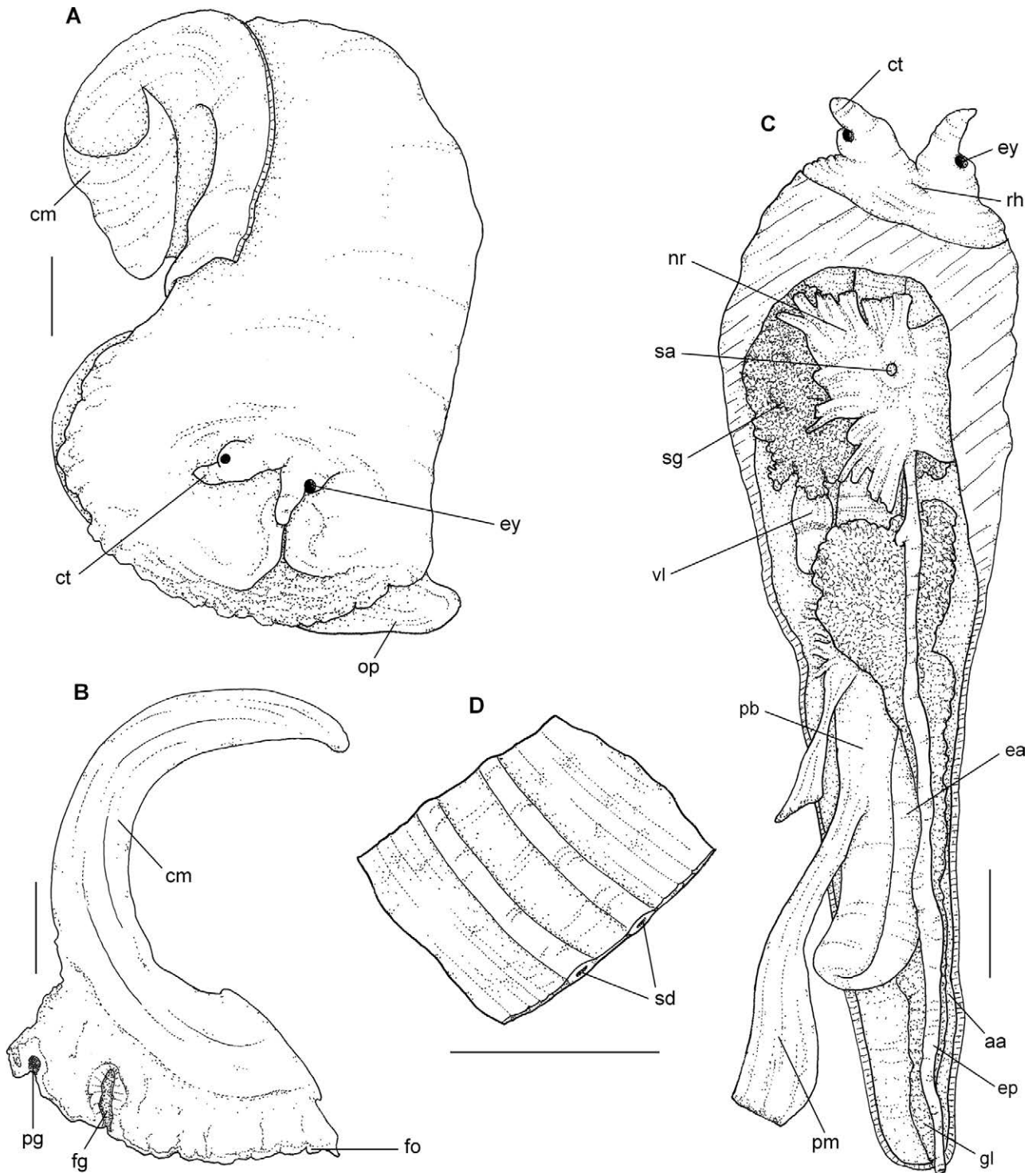


Fig. 7. – *Hemipolygona beckyae*. A, head-foot mass in dorsal view; B, longitudinal section of head-foot mass, female; C, haemocoel in ventral view; D, lumen of anterior esophagus. Abbreviations: aa, anterior aorta; cm, columellar muscle; ct, cephalic tentacle; ea, anterior esophagus; ep, posterior esophagus; ey, eye; fg, female cement gland; fo, foot; gl, gland of Leiblein; nr, nerve ring; op, operculum; pb, proboscis; pg, pedal gland; rh, rhynchostoma; sa, statocyst; sd, salivary gland duct; sg, salivary gland. Scale bars: A-C, 2 mm; D, 0.5 mm.

surface, inserting in m2a. Pair of ventral tensor muscles of radula (m11), inserting anteriorly in subradular membrane, running ventrally adhered (~2/3 of total odontophore length), their origin bifid: main branch originating in ventral posterior cartilage of odontophore near origin of m2; secondary branch originating ventrally in m2a, crossing m6 dorsally, connecting in

main branch, (at ~2/3 of total m11 length). Radula long and thin; radular sac extending beyond posterior end of odontophore. Radular teeth (Fig. 6J-K): rachidian tooth straight, rectangular, its base with concave outline and its cusped margin slight convex outline, with 3 sharp cusps of equal size; lateral tooth wider than long, bearing 8-9 prominent and centrally recurved cusps of



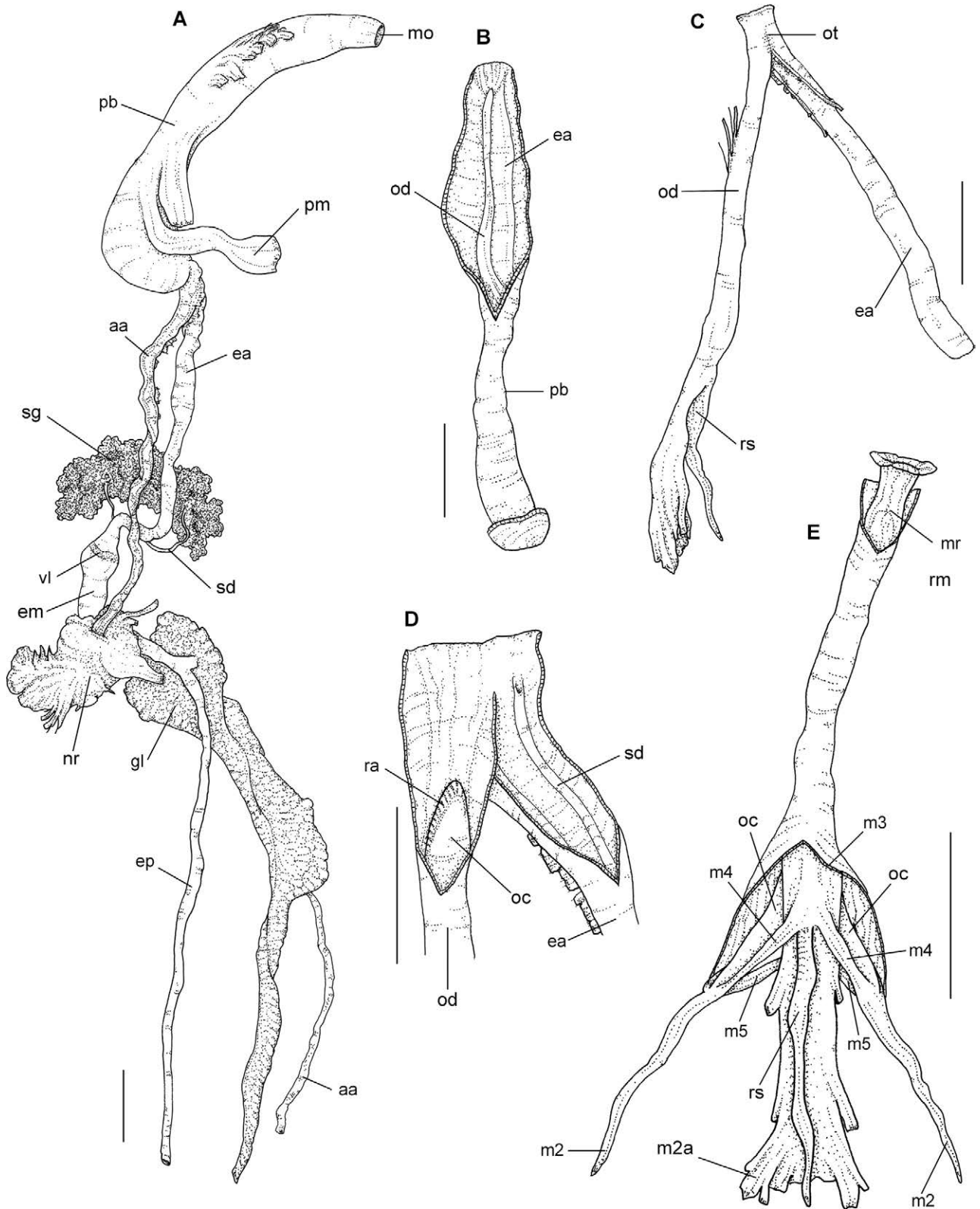


Fig. 8. – *Hemipolygona beckyae*. A, anterior digestive system; B, proboscis opened anteriorly in lateral view; C, buccal mass in lateral view; D, buccal mass in lateral view, opened longitudinally; E, odontophore in dorsal view. Abbreviations: aa, anterior aorta; ea, anterior esophagus; ep, posterior esophagus; gl, gland of Leiblein; m2, odontophore retractor muscles; m2a, accessory odontophore retractor muscles; m3, superficial circular muscles; m4, dorsal tensor muscles of radula; m5, auxiliary dorsal tensor muscles of radula; m6, horizontal muscle; mo, mouth opening; nr, nerve ring; oc, odontophore cartilage; od, odontophore tube; ot, oral tube; ra, radula; rm, subradular membrane; rs, radular sac; sd, salivary gland duct; sg, salivary gland; vl, valve of Leiblein. Scale bars: A-B, 2 mm; C-E, 1 mm.

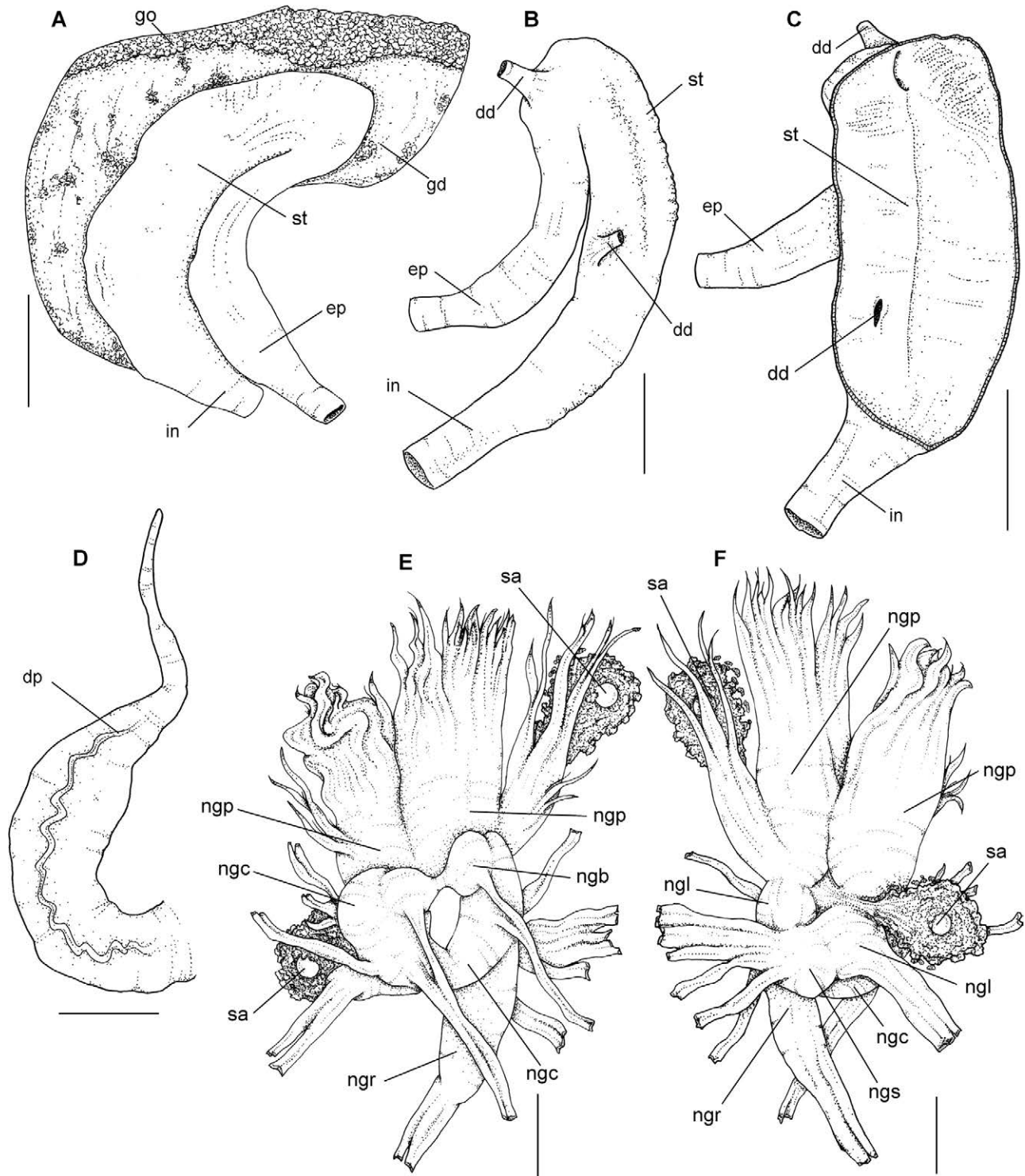


Fig. 9. – *Hemipolygona beckyae*. A, stomach in dorsal view; B, stomach in ventral view; C, stomach shown internally; D, penis in dorsal; E, nerve ring in dorsal view; F, nerve ring in ventral view. Abbreviations: dd, duct of digestive gland; dp, duct of penis; ep, posterior esophagus; in, intestine; nbl, pleural ganglion; ngb, buccal ganglion; ngc, cerebral ganglion; ngp, pedal ganglion; ngr, supra-esophageal ganglion; ngs, subesophageal ganglion; sa, statocyst. Scale bars: A-D, 2 mm; E-F, 0.5 mm.

approximately same size, except for innermost ~1/2 smaller than rest, lateral margin acute, terminating in external cusp. Anterior esophagus moderately long and broad (~2× proboscis length), dorsally-ventrally compressed, originating in oral tube. Valve of Leiblein pyriform, as an orange ring around esophagus,

~2× esophagus width. Salivary glands just anterior to valve of Leiblein, as pair of amorphous masses; free portion of salivary ducts short, extending to esophagus anteriorly to valve of Leiblein, where ducts become embedded with esophagus wall, following anteriorly and opening in esophagus lumen, immediately before

oral tube. Accessory salivary glands absent. Middle esophagus short; duct of gland of Leiblein short, situated after nerve ring. Gland of Leiblein brownish, long, of ~same length as posterior esophagus, posterior end acute. Posterior and anterior esophagus of ~same width. Inner wall of anterior esophagus with thin dorsal longitudinal folds, salivary ducts immersed in marked lateral folds. Stomach as wide sac with thin walls bearing many internal folds. Digestive gland dark brown, occupying all whorls of visceral mass, from apex to kidney/pericardium area, surrounding stomach and emitting two narrow ducts that discharge into stomach near esophagus and intestine apertures. Pallial portion of digestive system not analysed.

*Male genital system* (Fig. 9D). Testis brownish. Visceral and pallial portion of male genital system not observed. Penis long and thin, close to head-foot mass, ~circular in transverse section; at ~2/3 of its length penis becomes narrower (~1/4 diameter), terminating in short, blunt extension; duct of penis linear.

*Female genital system* (Fig. 7B). Ovaries same colour and texture as testis. Female cement gland opening at ~1/3 from anterior edge of foot, forming shallow sac (~1/2 foot thickness).

*Nervous system* (Fig. 9E-F). Nerve ring highly concentrated, occupying ~1/4 of total hemocoel area, surrounding mid-esophagus posteriorly. All commissures and internal. Cerebral ganglia bean-shaped, occupying ~1/3 of total nerve ring volume, of about same size, posterior halves broadly connected; pair of lateral tentacular nerves follow pedal aorta anteriorly. Pleural ganglia as pair of bulges ventral to cerebral ganglia, strongly attached to these; left pleural ganglia emits thick nerve that accompanies proboscis anteriorly. Pedal ganglia anterior, elongated, ~1/2 of total nerve ring volume, emitting anterior zigzag nerves; right pedal ganglion slightly larger and dorsal than left. Buccal ganglia subcircular, ~1/3 of cerebral ganglia and dorsal to these, emitting pair of nerves that form cerebro-buccal nerves, that follow anterior aorta anteriorly. Supra-esophageal ganglion posterior to cerebro-pleural ganglia complex, elongated, ~same volume as cerebral ganglion, emitting thick osphradial nerve. Subesophageal ganglion as ventral bulge in left cerebro-pleural ganglia complex that emits thick branching pallial-siphon. Pair of vitreous statocysts with one anterior and associated with right pedal ganglion, and one posterior, associated with left pedal ganglion.

## DISCUSSION

Ponder (1973) pointed out the anatomical similarity among members of the Buccinoidea, concluding that there are no consistent differences among the families; hence they could be treated as subfamilies (e.g. Buccininae, Fasciolarinae). However, later taxonomic studies (e.g. Bouchet and Rocroi 2005) recognized family entities within the superfamily Buccinoidea. The morphological results obtained in this study are

in agreement with the diagnostic characteristics established by Fraussen et al. (2007) for Fasciolaridae. These are the multicuspidate lateral teeth, the straight shape of the rachidian teeth of the radula, the proboscis retractor muscle as a single or paired tuft of fibres, ducts of the salivary glands embedded in the esophagus wall, and the stomach without a posterior mixing area.

The taxonomy of fasciolarids is based on the shell and radula (e.g. Tryon 1880, Thiele 1929-1935, Vermeij and Snyder 2002, 2006), and taxonomic approaches based on soft-part anatomy are few. Anatomical data for the buccinoideans, particularly the stomach (e.g. Kosyan and Kantor 2013, Kantor 1996, Strong 2003), the anterior digestive system including the radula (e.g. Kosyan et al. 2009, Simone 1996) and the reproductive system (Fraussen et al. 2007), suggest that they are highly advanced Neogastropoda that lack accessory salivary glands and anal glands.

The accessory salivary glands and anal glands are synapomorphic to neogastropods (Ponder and Lindberg 1997, Harasewych 1998, Strong 2003, Simone 2011), although these organs are lacking in buccinoideans. Kantor and Fedosov (2009) asserted the dual appearance of the valve of Leiblein in Buccinoidea; therefore, this clade shares none of the previously hypothesized autapomorphies with other neogastropods; and in this case, Neogastropoda is a paraphyletic group.

Historically, the taxonomy of the subfamily Peristerniinae, especially that of *Latirus*, has been confused, because the genus was used indiscriminately to include several species, some of them doubtfully related. *Latirus* was initially considered to have a worldwide distribution. However, Vermeij and Snyder (2006) considered the known geographic range of the genus to be restricted to the western Indo-Pacific, and consequently raised several taxa previously considered as subgenera to genus rank (e.g. *Hemipolygona*) and proposed new genera (e.g. *Pustulatirus*, *Turrilatirus*).

Vermeij and Snyder (2003) transferred several species to the genus *Benimakia* Habe, 1958, including *Benimakia ogum*, originally described in *Latirus*. These authors characterized *Benimakia* as high-spined fasciolarids with prominent axial ribs and a labral tooth at the end of the central cord of the outer lip. *Benimakia ogum* differs from other species of the genus in having a discontinuous beaded lira on the inner side of the outer lip (Fig. 1A, D), in this respect resembling *Latirus* (Vermeij and Snyder 2003) and *Pustulatirus* (Vermeij and Snyder 2006). Species included in *Benimakia* by Habe (1958) and Vermeij and Snyder (2003) occur in the western Pacific, with the exception of *B. ogum*, which putatively differs from other members of Peristerniinae related to *Latirus* in having a small labral tooth at the end of the basal cord. However, the presence of this tooth is questionable. A labral tooth is not mentioned in the original description by Petuch (1979), nor was it found in the present study (Fig. 1A-F). A pseudoumbilicus is also present, differentiating it from *Benimakia*, although it occurs in *Pustulatirus*. Therefore *B. ogum* clearly belongs to the genus *Pustulatirus*, in agreement with Landau and Vermeij (2012) and Lyons and Snyder (2013).



Table 1. – Main comparative radular features of the Peristerniinae based on our data and those of <sup>1</sup>Couto and Pimenta (2012), <sup>2</sup>Kosyan et al. (2009), <sup>3</sup>Bandel (1984) and <sup>4</sup>Snyder and Bouchet (2006).

	format	Raquidian	cusps	first cusp	Lateral	cusps
<i>Pustulatirus ogum</i>	square, base broad		4	developed		11 curved
<i>Hemipolygona beckyae</i>	rectangular, thin, base broad		3	developed		8-9 somewhat curved
<i>Leucozonia nassa</i> <sup>1</sup>	square, broad, base broad		3	vestigial		7-8 curved
<i>Leucozonia ocellata</i> <sup>1</sup>	square, broad, base broad		3	reduced		5-6 curved
<i>Pustulatirus mediamericanus</i> <sup>2</sup>	square, broad, base broad		4	developed		11-12
<i>Peristernia nassatula</i> <sup>2</sup>	Trapezoidal, thin, base thin		3 laterally recurved	well developed	11-12	alternating smaller/larger
<i>Peristernia ustulata</i> <sup>2</sup>	Trapezoidal, thin, base thin		3 laterally recurved	well developed	11-12	alternating smaller/larger
<i>Opeatostoma pseudodon</i> <sup>2</sup>	square, broad, base broad		5	absent		8, central larger
<i>Tarantinae lignaria</i> <sup>2</sup>	square, broad, base broad		3	developed		9 curved
<i>Latirus polygonus</i> <sup>2,3</sup>	square, broad, base broad		3, central longer	developed		11-12 curved
<i>Turritatirus turritus</i> <sup>2,3</sup>	rectangular, base broad		3	well developed		7 curved
<i>Latirus infundibulum</i> <sup>3</sup>	rectangular, thin, base broad		3 centrally recurved	well developed		7-8 curved
<i>Latirolagena smaragdula</i> <sup>3</sup>	square, base broad		3, central longer	reduced		15-16
<i>Polygona angulata</i> <sup>3</sup>	Trapezoidal, thin, base thin		3	well developed		8-9 curved
<i>Fusolatirus elsiae</i> <sup>4</sup>	Trapezoidal, thin, base thin		3	well developed	12-13	alternating smaller/larger

*Hemipolygona beckyae* was originally included in *Latirus* by Petuch (1979), and was later allocated to *Hemipolygona* by Snyder (2003), as agreed to by Vermeij and Snyder (2006), due to the highly nodulose shell with a deep slit-like pseudoumbilicus and whitish spiral cords (Fig. 6A-G).

The morphology of the two species is similar and in accordance with other descriptions of fascioliariids (Fraussen et al. 2007, Kosyan et al. 2009, Couto and Pimenta 2012), with the main differences occurring in the anterior digestive and male reproductive systems. Details of the anatomy, histology and ultrastructure of the anterior digestive system (including the radula) have been noted as useful traits for phylogenetic analyses (Ponder and Lindberg 1997), and the anterior structures of the foregut are generally used to distinguish neogastropod families (Fraussen et al. 2007). A recent phylogenetic analysis based on comparative morphology (Simone 2011) consistently recovered all the major caenogastropod clades.

The rhynchostome occurs as a lip-like slit bearing longitudinal lamellar folds, which may be longitudinal to the adjacent head-foot mass as in *P. ogum* (Fig. 3A) or transverse, although located slightly to the right side of the animal, not between its cephalic tentacles as in *H. beckyae* (Fig. 7C).

Golding et al. (2009a) studied the snout and proboscis morphology in species belonging to 33 caenogastropod families, among them a buccinoidean (Columbellidae), but included no fascioliariid. In their study they reported the ventro-lateral insertion of the proboscis retractor muscles as occurring in all Neogastropoda, and the presence of aortic muscles that flank the aorta in the anterior esophagus; both characters are confirmed for members of Fascioliariidae so far studied. On the other hand, Goulding et al. (2009b) studied the anatomy of odontophoral cartilages in Caenogastropoda through the use of micro-CT scanning, although none of the species studied were buccinoideans. This method allows observation of the cartilages in their natural orientation, without anatomical dissections that would otherwise cut or displace structures. Despite the methodological differences, *Pustulatirus ogum* and *H. beckyae* showed a close resemblance to the muricoid-ean studied by Golding et al. (2009b) in having greatly

elongated anterior cartilages and lacking subradular cartilages. As noted by these authors, the Neogastropoda possess the most dramatic modifications of the plesiomorphic odontophoral cartilage morphology. Also, the morphology of the odontophoral cartilages may be conserved within families and superfamilies: hence the resemblance of these structures among the Fascioliariidae (Couto and Pimenta 2012) and to other buccinoideans (Simone 1996, 2011)

The lateral teeth of the radula of the Peristerniinae observed in this study and in *Leucozonia* (Couto and Pimenta 2012) have the innermost cusp (defined as a 'denticle' by Bullock, 1974) as a small projection at its base, next to the rachidian tooth. This projection may vary considerably in size and shape. In *Leucozonia*, it is reduced or even absent (Couto and Pimenta 2012: 1Q, 5G and 9O), while in *P. ogum* (Fig. 1A-J) and *Hemipolygona beckyae* (Fig. 6J-K) it is developed, although smaller than the outer cusps, and recurved outward. All species of Peristerniinae studied by Bullock (1974) and Bandel (1984) have this same conformation, and Bullock (1974) also noted that this feature distinguishes *Latirus* and related species from *Leucozonia*.

Within the Fascioliariidae, members of Peristerniinae possess fewer cusps of the lateral teeth than members of other subfamilies (Bandel 1984, Taylor and Lewis 1995, Snyder and Bouchet 2006). However, recent findings from moderate/deep-sea regions of the Indo-West Pacific led to the description of several species and genera that deviate from this pattern (e.g. *Amiantofusus*, Fraussen et al. 2007; *Chryseofusus*, Hadorn et al. 2008; and *Angulofusus*, Fedosov and Kantor 2012). All aforementioned genera have the radula closer to Peristerniinae than to Fusiniinae. Table 1 lists relevant radular features of *P. ogum* and *H. beckyae*, as well as those of other members of Peristerniinae compiled from the literature.

According to Fraussen et al. (2007), the ducts of the salivary glands embedded in the esophagus wall is diagnostic for the family; this feature was reported for *Latirus polygonus*, but not for *Pustulatirus mediamericanus*, *Turritatirus turritus*, *Peristernia nassatula*, *P. ustulata*, *Opeatostoma pseudodon* and *Tarantinae lignaria* studied by Kosyan et al. (2009), and therefore a reinvestigation is needed in these species. In the species

Table 2. – Comparison between major anatomical features among Peristeriinae species based on this study and literature. Data was extracted, when available, from <sup>1</sup>Couto and Pimenta (2012) and <sup>2</sup>Kosyan et al. (2009); shell characters were taken from various sources.

	<i>Leucozonia nassa</i> <sup>1</sup>	<i>Leucozonia ocellata</i> <sup>1</sup>	<i>Pustulaturus ogum</i>	<i>Hemipolygona beckyae</i>	<i>Latirus polygonus</i> <sup>2</sup>	<i>Turriturris turritus</i> <sup>2</sup>	<i>Peristeria nassatula</i> <sup>2</sup>	<i>Opeatostoma pseudodon</i> <sup>2</sup>	<i>Tarantinia lignaria</i> <sup>2</sup>
Protoconch	2 whorls	1,5 whorls	2 whorls	2 whorls	-	-	-	-	-
Labral tooth	present or absent	absent	absent	absent	absent	absent	absent	present	absent
Outer lip - margin	smooth	smooth	crenulated	crenulated	crenulated	crenulated	-	-	-
Outer lip - inner side	discontinuous lirae	discontinuous lirae	continuous or discontinuous lirae	continuous or discontinuous lirae	discontinuous lirae	continuous lirae	-	-	-
Siphonal fasciole	present or absent	present or absent	absent	absent	absent	absent	-	-	-
Pseudombilicus	usually present	usually absent	present	present	present	absent	-	-	-
Head	prominent, 1/2 width of foot	prominent, 1/2 width of foot	medium-sized, 1/3 width of foot	small, 1/4 width of foot	-	-	-	-	-
Cephalic tentacles	large, length 1/2 the width of head	small, length 1/5 the width of head	large, length 1/2 the width of head	very large, same length of width of head	-	-	-	-	-
Columellar muscle	1.5 whorls	1.5 whorls	1.25 whorls	1 whorl	-	-	-	-	-
Pallial cavity	1 whorl	3/4 whorl	1 whorl	1 whorl	-	-	-	-	-
Osphradium	symmetrical	non-symmetrical	symmetrical	3/4 whorl	-	-	-	-	-
Osphradium leaflets	sharp, 2/3 height of ctenidium filaments	rounded, same height of ctenidium filaments	sharp, 1/2 the height of ctenidium filaments	triangular, twice the width of same width of	non-symmetrical	-	non-symmetrical	non-symmetrical	non-symmetrical
Ctenidium filaments	triangular, 1.5 times width of osphradium	triangular, twice the width of osphradium	triangular, twice the width of osphradium	triangular, twice the width of osphradium	-	-	-	-	-
Rhynchostome	osphradium transversal, central, smooth	osphradium transversal, central, smooth	osphradium longitudinal, central, rimmed by longitudinal folds	osphradium longitudinal, central, rimmed by longitudinal folds	-	-	-	-	-
Odontophore	40% fused	30% fused	25% fused	25% fused	-	-	-	-	-
Buccal mass	same length as proboscis	same length as proboscis	2/3 length of proboscis	2/3 length of proboscis	same length as proboscis	1/2 length of proboscis	1/2 length of proboscis	same length as proboscis	same length as proboscis
Proboscis muscles	single embedded	single embedded	1 pair embedded	1 pair embedded	1 pair embedded	single free	single free	1 pair free	single free
Salivary ducts	1.5 width of esophagus	same width of esophagus	1.5 width of esophagus	1.5 width of esophagus	-	-	-	-	-
Valve of Leiblein	1/2 total penis length	1/3 total penis length	diminute	diminute	-	-	-	-	-
Penis tapering	indistinct	indistinct	distinct	distinct	-	-	-	-	-
Nephridial gland	1/3 renal cavity area	1/3 renal cavity area	1/5 renal cavity area	1/5 renal cavity area	-	-	-	-	-
Pericardium	1/2 the length of buccal ganglia	internal commissure ventral to pedal ganglia	internal commissure ventral to pedal ganglia	internal commissure ventral to pedal ganglia	-	-	-	-	-
Buccal ganglia	1/2 the length of buccal ganglia	internal commissure ventral to pedal ganglia	ventral to pedal ganglia	1/3 the length of buccal ganglia left of pedal ganglia	-	-	-	-	-
Posterior statocyst	ventral to pedal ganglia	ventral to pedal ganglia	ventral to pedal ganglia	ventral to pedal ganglia	-	-	-	-	-

studied here and those reported by other authors (e.g. Marcus and Marcus 1962, Couto and Pimenta 2012, Fedosov and Kantor 2012), this feature also occurs.

*Hemipolygona beckyae* has a single powerful proboscis retractor muscle, which emerges posteriorly and ventrally from the proboscis (Fig. 8A). *Pustulaturus ogum* has a pair of muscles (Fig. 3B). In the species studied by Kosyan et al. (2009), all fascioliids but *Latirus polygonus* and *Fusinus tenerifensis* have a single muscle, while in the buccinids multiple fibres occur posteriorly to the proboscis. Golding et al. (2009a) distinguished different proboscis types among caenogastropods, although they studied only one species of Buccinoidea, the columbellid *Euplica scripta*, which possesses two ventro-lateral proboscis retractors, resembling those of *H. beckyae*. Both fascioliids have the proboscis retractor passing outside the nerve ring and originating in the posterior hemocoel floor, near the diaphragm septum.

Kantor (2003) distinguished species of Fascioliariidae from other buccinoideans by the low relief of the folds on the inner stomach wall; presence of transverse striations on the low longitudinal fold; absence of clear differentiation of the gastric chamber into dorsal and ventral parts; absence of a posterior mixing area; and a shallow lateral sulcus. Despite this thorough examination of representatives of the three subfamilies (Fascioliariinae: *Fasciolaria lilium*, *F. filamentosa*; Fusiniinae: *Fusinus nicobaricus* and Peristerniinae: *Leucozonia nassa*), Kantor (2003) noted the difficulties of examination and the necessity of specially preserved specimens for stomach analysis, although the differences observed are likely due to phylogenetic relationships. While both *P. ogum* and *H. beckyae* have stomach morphology similar to the fascioliids cited by Kantor (2003), species-level differentiation is unlikely.

Both species, as well as *Leucozonia* (Marcus and Marcus 1962, Couto and Pimenta 2012), have penises with terminal tapering. In *Leucozonia* (Couto and Pimenta 2012: Figs 4E and 8F) and *H. beckyae* (Fig. 9D) the terminal extension extends for more than half of the total penis length, while in *P. ogum* it extends less than half of its length (Fig. 4F).

Several morphological characters occur in both species and also occur diffused among other fascioliids (Fraussen et al. 2007, Kosyan et al. 2009, Couto and Pimenta 2012). These include the outline of the gill lamellae, the length and anterior fusion of the odontophore cartilages, and the extension of the anus to the edge of the pallial cavity. For this reason, the soft-part traits of *Latirus* and related species studied so far do not allow a precise anatomical diagnosis. Table 2 lists the main differentiating characteristics.

#### ACKNOWLEDGEMENTS

The authors are grateful to two anonymous reviewers who made insightful comments and suggestions on this manuscript. Dr. J. Reid, from Virginia Museum of Natural History for revising the English text. This work was funded in part by the Conselho de Desenvolvimento Científico e Tecnológico (CNPq) for a M.S. scholar-

ship and Fundação de Amparo à Pesquisa do Estado de São Paulo (FAPESP) for a PhD scholarship.

#### REFERENCES

- Bandel K. 1984. The Radulae of Caribbean and other Mesogastropoda and Neogastropoda. Rijksmuseum van Natuurlijke Historie, 346 pp. 22 pls.
- Bouchet P., Rocroi J.P. 2005. Classification and nomenclator of gastropod families. *Malacologia* 47(1-2): 397 pp.
- Bullock R.C. 1974. A contribution to the systematics of some West Indian *Latirus* (Gastropoda: Fascioliariidae). *Nautilus* 88(3): 69-79.
- Couto D.R., Pimenta A.D. 2012. Comparative morphology of *Leucozonia* from Brazil (Neogastropoda: Buccinoidea: Fascioliariidae). *Am. Malacol. Bull.* 30(1): 103-116. <http://dx.doi.org/10.4003/006.030.0108>
- Fedosov A.E., Kantor Y.I. 2012. A new species and genus of enigmatic turritiform Fascioliariidae from the Central Indo-Pacific (Gastropoda: Neogastropoda). *Arch. Molluskenkunde* 141(2): 137-144.
- Fraussen K., Kantor Y.I., Hadorn R. 2007. *Amiantofusus* gen. nov. for *Fusus amiantus* Dall, 1889 (Mollusca: Gastropoda: Fascioliariidae) with description of a new and extensive Indo-West Pacific radiation. *Novapex* 8(3-4): 79-101.
- Gofas S. 2014. Fascioliariidae Gray, 1853. Accessed through: World Register of Marine Species on 2014-07-15, at <http://www.marinespecies.org/aphia.php?p=taxdetails&id=23038>
- Golding R.E., Ponder W.F., Byrne M. 2009a. The evolutionary and biomechanical implications of snout and proboscis morphology in Caenogastropoda (Mollusca: Gastropoda). *J. Nat. Hist.* 43(43-44): 2723-2763. <http://dx.doi.org/10.1080/00222930903219954>
- Golding R.E., Ponder W.F., Byrne M. 2009b. Three-Dimensional Reconstruction of the Odontophoral Cartilages of Caenogastropoda (Mollusca: Gastropoda) Using Micro-CT: Morphology and Phylogenetic Significance. *J. Morphol.* 270: 558-587.
- Habe T. 1958. On the radulae of Japanese marine gastropods. *Venus* 20: 43-60.
- Hadorn R., Snyder M.A., Fraussen K. 2008. A new *Chryseofusus* (Gastropoda: Fascioliariidae: Fusinus) from South and Western Australia. *Novapex* 9(2-3): 95-99.
- Harasewych M.G. 1998. Family Fascioliariidae. In: Beesley P.L., Ross G.J.B., Wells A. (eds), *Mollusca: The Southern Synthesis. Fauna of Australia*. CSIRO publishing, Melbourne, pp 832-833.
- Kantor Y.I. 1996. Phylogeny and relationships of Neogastropoda. In: Taylor J.D. *Origin and evolutionary radiation of the Mollusca*. Oxford Univ. Press, pp 221-230.
- Kantor Y.I. 2003. Comparative anatomy of the stomach of Buccinoidea (Neogastropoda). *J. Moll. Stud.* 69(3): 203-220. <http://dx.doi.org/10.1093/mollus/69.3.203>
- Kantor Y.I., Fedosov A. 2009. Morphology and development of the valve of Leiblein: possible evidence for paraphyly of the Neogastropoda. *Nautilus* 123(3): 1-73.
- Kosyan A.R., Kantor Y.I. 2009. Phylogenetic analysis of the subfamily Colinae (Neogastropoda, Buccinidae) based on morphological characters. *Nautilus* 123: 83-94.
- Kosyan A.R., Kantor Y.I. 2013. Revision of the genus *Aulacofusus* Dall, 1918 (Gastropoda: Buccinidae). *Ruthenica* 23(1): 1-33.
- Kosyan A.R., Modica M.V., Oliverio M. 2009. The anatomy and relationships of *Troschelia* (Neogastropoda, Buccinidae): New evidence for a closer fascioliariid-buccinid relationship? *Nautilus* 123: 95-105.
- Landau B., Vermeij G.J. 2012. The Peristerniinae (Mollusca: Gastropoda, Buccinoidea, Fascioliariidae) from the Neogene of Venezuela. *Cainozoic Res.* 9(1): 87-99.
- Lyons W.G., Snyder M.A. 2013. The genus *Pustulaturus* Vermeij and Snyder, 2006 (Gastropoda: Fascioliariidae: Peristerniinae) in the western Atlantic, with descriptions of three new species. *Zootaxa* 3636(1): 35-58. <http://dx.doi.org/10.11646/zootaxa.3636.1.2>
- Mallard D., Robin A. 2005. Fascioliariidae. La Mothe Achard, Les Sables-d'Olonne, France, 27 pp. 70 pls.
- Marcus E., Marcus E. 1962. On *Leucozonia nassa*. *Bol. Fac. Fil. Cienc. Letr. Univ. São Paulo, Zool.* 24: 11-30.
- Petuch E.J. 1979. New Gastropods from the Abrolhos reef archipelago and reef complex, Brazil. *Proc. Biol. Soc. Wash.* 92(3): 520-526.

- Petuch E.J. 1987. New Caribbean Molluscan Faunas. The Coastal education and Research foundation [CERF], Charlottesville, Virginia. 154 pp. A1-A4.
- Ponder W.F. 1973. The Origin and Evolution of the Neogastropoda. *Malacologia* 12(2): 295-338.
- Ponder W.F., Lindberg D.R. 1997. Towards a phylogeny of gastropod molluscs: an analysis using morphological characters. *Zool. J. Linn. Soc.* 119: 83-265.  
<http://dx.doi.org/10.1111/j.1096-3642.1997.tb00137.x>
- Rios E.C. 1985. Seashells of Brazil. Museu Oceanográfico, Fundação Univesidade do Rio Grande, Rio Grande, 328 pp.
- Rios E.C. 1994. Seashells of Brazil. Museu Oceanográfico Prof. E. C. Rios, Fundação Universidade do Rio Grande, Rio Grande, 368 pp. 113 pls.
- Rios E.C. 2009. Compendium of Brazilian Sea Shells. Museu Oceanográfico Prof. E. C. Rios, Fundação Universidade do Rio Grande, Rio Grande, 668 pp.
- Rosenberg G. 2009. Malacolog 4.1.0: A Database of Western Atlantic Marine Mollusca <http://www.malacolog.org/>
- Simone L.R.L. 1996. Anatomy and systematics of *Buccinanops gradatus* (Deshayes, 1844) and *Buccinanops moniliferus* (Kiener, 1834) (Neogastropoda, Muricoidea) from the Southeastern coast of Brazil. *Malacologia* 38(1-2): 87-102.
- Simone L.R.L. 2011. Phylogeny of the Caenogastropoda (Mollusca), based on comparative morphology. *Arq. Zool. Mus. Zoo. Univ. São Paulo* 42(2-4): 83-323.
- Simone L.R.L., Cavallari D.C., Abbate D. 2013. Revision of the genus *Teralatirus* Coomans 1965 in the Western Atlantic, with an anatomical description of *T. roboreus* (Reeve 1845) (Gastropoda: Neogastropoda: Fascioliariidae). *Arch. Molluskenkunde* 142(2): 215-226.
- Snyder M.A. 2000. *Latirus beckyae*, a new species of Fascioliariidae (Gastropoda: Neogastropoda) from Brazil. *Nautilus* 114(4): 161-163.
- Snyder M.A. 2003. Catalogue of the marine gastropod family Fascioliariidae. *Acad. Nat. Sci. Phila. Spec. Publ.* 21. Philadelphia, iv + 431 pp.
- Snyder M.A., Bouchet P. 2006. New species and new records of deep-water *Fusolatirus* (Neogastropoda: Fascioliariidae) from the West Pacific. *J. Conchology* 39: 1-12.
- Strong E.E. 2003. Refining molluscan characters: morphology, character coding and a phylogeny of the Caenogastropod. *Zool. J. Linn. Soc.* 137: 447-554.  
<http://dx.doi.org/10.1046/j.1096-3642.2003.00058.x>
- Taylor J.D., Lewis A. 1995. Diet and radular morphology of *Peristernia* and *Latrolagena* (Gastropoda: Fascioliariidae) from Indo-Pacific coral reefs. *J. Nat. Hist.* 29(5): 1143-1154.  
<http://dx.doi.org/10.1080/00222939500770481>
- Thiele J. 1929-1935. *Handbuch der Systematischen Weichtierkunde*. Gustav Fischer, Jena vol 1: vi + 778 pp. vol. 2: v + 779-1134 pp.
- Tryon G.W. 1880. *Manual of Conchology, Structural and Systematic, with Illustrations of the Species*. Philadelphia. 310 pp. 87 pls.
- Vermeij G.J., Snyder M.A. 1998. *Leucozonia ponderosa*, a new fascioliariid gastropod from Brazil. *Nautilus* 112: 117-119.
- Vermeij G.J., Snyder M.A. 2002. *Leucozonia* and related genera of Fascioliariid Gastropods: shell-based taxonomy and relationships. *Proc. Acad. Nat. Sci. Phila.* 152: 23-44.  
[http://dx.doi.org/10.1635/0097-3157\(2002\)152\[0023:LARGOF\]2.0.CO;2](http://dx.doi.org/10.1635/0097-3157(2002)152[0023:LARGOF]2.0.CO;2)
- Vermeij G.J., Snyder M.A. 2003. The fascioliariid gastropod genus *Benimakia*: new species and a discussion of Indo-Pacific genera in Brazil. *Proc. Acad. Nat. Sci. Phila.* 153: 15-22.  
[http://dx.doi.org/10.1635/0097-3157\(2003\)153\[0015:TFGGBN\]2.0.CO;2](http://dx.doi.org/10.1635/0097-3157(2003)153[0015:TFGGBN]2.0.CO;2)
- Vermeij G.J., Snyder M.A. 2006. Shell characters and taxonomy of *Latirus* and related fascioliariid groups. *J. Moll. Stud.* 72(4): 413-424.  
<http://dx.doi.org/10.1093/mollus/eyl020>



# MORPHOLOGY OF *FASCIOLARIA TULIPA* FROM VENEZUELA (GASTROPODA: BUCCINOIDEA: FASCIOLARIIDAE)

DIOGO R. COUTO<sup>1</sup>, LUIZ RICARDO L. SIMONE<sup>1</sup>, ALEXANDRE D. PIMENTA<sup>2</sup>

<sup>1</sup>Laboratório de Malacologia, Museu de Zoologia da Universidade de São Paulo. Avenida Nazaré, 481, Ipiranga. CEP 04263-000 São Paulo, SP, Brazil

<sup>2</sup>Setor de Malacologia, Departamento de Invertebrados, Museu Nacional, Universidade Federal do Rio de Janeiro. Quinta da Boa Vista s/n, São Cristóvão. CEP 20940-040 Rio de Janeiro, RJ, Brazil

*Abstract* The morphology of *Fasciolaria tulipa*, type species for the genus, is described and illustrated. Features of the shell, head-foot, pallial organs, circulatory, excretory, digestive and reproductive systems are presented, along with comparisons of published descriptions of other members of Fasciolariidae. The anatomical features concord with previous characterizations of the family: proboscis retractor as a single and powerful muscle, lateral teeth of the radula wide and multicuspidate, ducts of the salivary glands immersed in the esophagus wall, and stomach without a posterior sorting area. *Fasciolaria tulipa* is notable for a large, thin walled auricle, a conspicuous nephridial gland, and a renal aperture sited close to the pericardium; also the odontophore cartilages are fused anteriorly in only 10% of their length, and the radula has the central side of the base of the lateral tooth rounded, a trait that is shared with other species of the subfamily Fasciolariinae. As the type of the genus, the soft-parts anatomy of *F. tulipa* is of great importance, especially because recent taxonomic revisions of the Fasciolariinae have not considered anatomical data.

*Key words* Fasciolariidae, *Fasciolaria tulipa*, anatomy, morphology

## INTRODUCTION

The Neogastropod family Fasciolariidae comprises more than 1300 living species distributed in the tropics and subtropics (Gofas, 2014). Members of the subfamily Fasciolariinae are usually easily recognized by their ample shell, sinuous columella, and oblique columellar folds. The genus *Fasciolaria* is restricted to the western Atlantic and its fossil record dates from the early Pliocene, which is relatively late in comparison with other fasciolariids (Snyder *et al.* 2012).

Two species of Fasciolariinae are recognized from Brazil: *Pleuroploca aurantiaca* (Lamarck, 1816) and *Fasciolaria tulipa* (Linnaeus, 1758) (Rosenberg, 2009). Although the former species was allocated to the new genus *Aurantilaria* by Snyder *et al.* (2012), no recent taxonomic rearrangement has been undertaken for the latter species, as it is the type for the genus *Fasciolaria*. Although *F. tulipa* occurs on virtually every Caribbean island, despite its non-planktotrophic mode of development, in Brazil this species is restricted to the northern border of Amapá state (Rosenberg, 2009; Snyder *et al.* 2012), implying the possible presence of a geographic barrier formed by the Amazon River mouth.

Present knowledge on the anatomy of the Fasciolariidae is as described by Fraussen *et al.* (2007), with a combination of traits diagnostic for the family: multicuspidate lateral teeth and straight rachidian teeth, proboscis retractor muscle as a single or paired tuft of fibres, ducts of the salivary glands immersed in the esophagus wall, and the stomach without a posterior caecum. However, anatomical diagnoses of species within Fasciolariidae have not been developed.

In Brazil, few species of Fasciolariidae have undergone a thorough anatomical study. The anatomy of some species belonging to *Leucozonia* has been studied in detail: *L. nassa* (Gmelin, 1791) by Marcus & Marcus (1962), and *L. nassa* (Gmelin, 1791), *L. ocellata* (Gmelin, 1791) and *L. ponderosa* (Vermeij & Snyder, 1998) by Couto & Pimenta (2012). Recently, Simone *et al.* (2013) thoroughly described the anatomy of *Teralatirus roboreus* (Reeve, 1845). Matthews-Cascon *et al.* (1989) contributed a superficial characterization of *Aurantilaria aurantiaca*; however, no other member of Fasciolariinae from Brazil has had its anatomy studied. Kosyan *et al.* (2009) studied the anatomy of eight species of Fasciolariidae, including *Fasciolaria lignaria* (Linnaeus, 1758), although none of these occurs in Brazil.

The taxonomy of gastropod groups is based mainly on shell and radula features (*e.g.*, Tryon,



1880; Thiele, 1929–1935; Snyder *et al.*, 2012). Therefore, approaches using soft-part anatomy will prove useful in delimiting groups that have similar conchological features and/or those prone to polymorphisms and convergences. Also, morphological data will prove useful in validating phylogenetic relationships and resolve internal clades (Ponder & Lindberg, 2008; Simone, 2011). This study provides a thorough morphological description of the type species for the genus *Fasciolaria*, *F. tulipa*, from Venezuela, in order to provide supporting information for future comparative analyses.

### MATERIAL AND METHODS

Material for this study is deposited in the Museu de Zoologia da Universidade de São Paulo (MZSP).

The specimens collected were fixed in 70% ethanol. Shells were measured with a caliper, and photographs of individuals were taken with a digital camera. The anatomical dissections were made with the aid of a stereomicroscope. All drawings were done using a camera lucida. Radulae were extracted manually and prepared by immersion in KOH, followed by ultrasonic cleaning and rinsing in distilled water for SEM photography.

### RESULTS

#### *Fasciolaria tulipa* (Linnaeus, 1758) (figs 1–30)

*Murex tulipa* Linnaeus, 1758: 754.  
*Colus achatinus* Röding, 1798: 117.  
*Colus marmoratus* Röding, 1798: 117.  
*Neptunea laevigata* Link, 1807: 117–118.  
*Fasciolaria canaliculata* Valenciennes, 1832: 286.  
*Fasciolaria tulipa* var. *concolor* Kobelt, 1875: 362.  
*Fasciolaria tulipa* var. *rugosa* Kobelt, 1875: 362.  
*Fasciolaria scheepmakeri* Kobelt, 1875: 362.  
*Fasciolaria rugosa*: Dall (1885:115).  
*Fasciolaria* var. *obsoleta* Dall, 1890: 102.  
*Fasciolaria tulipa*: Warmke & Abbott, 1961: 119 (pl. 2d); Rios, 1970: 96; 1975: 102 (pl. 29, fig. 431); 1985: 106 (pl. 36, fig. 465); 1994: 131(pl. 42, fig. 564); 2009: 248; Abbott, 1974: 227–228 (fig. 2500); (Vokes & Vokes, 1983: 26, (pl. 16, fig. 6); Bandel, 1984: 144, (pl. 17, figs 9, 10); Abbott & Morris, 1995: 233 (pl. 56, fig. 1); Redfern, 2001: 101, (pl. 46, fig. 428A–B); Snyder, 2003: 211, 235; Mallard

& Robin, 2005: 8 (pl. 2); Jensen & Pearce, 2009: 143; Rosenberg, 2009; Tunnel *et al.*, 2010: 221; Snyder *et al.*, 2012: 40 (fig. 1).

*Type locality* Not given.

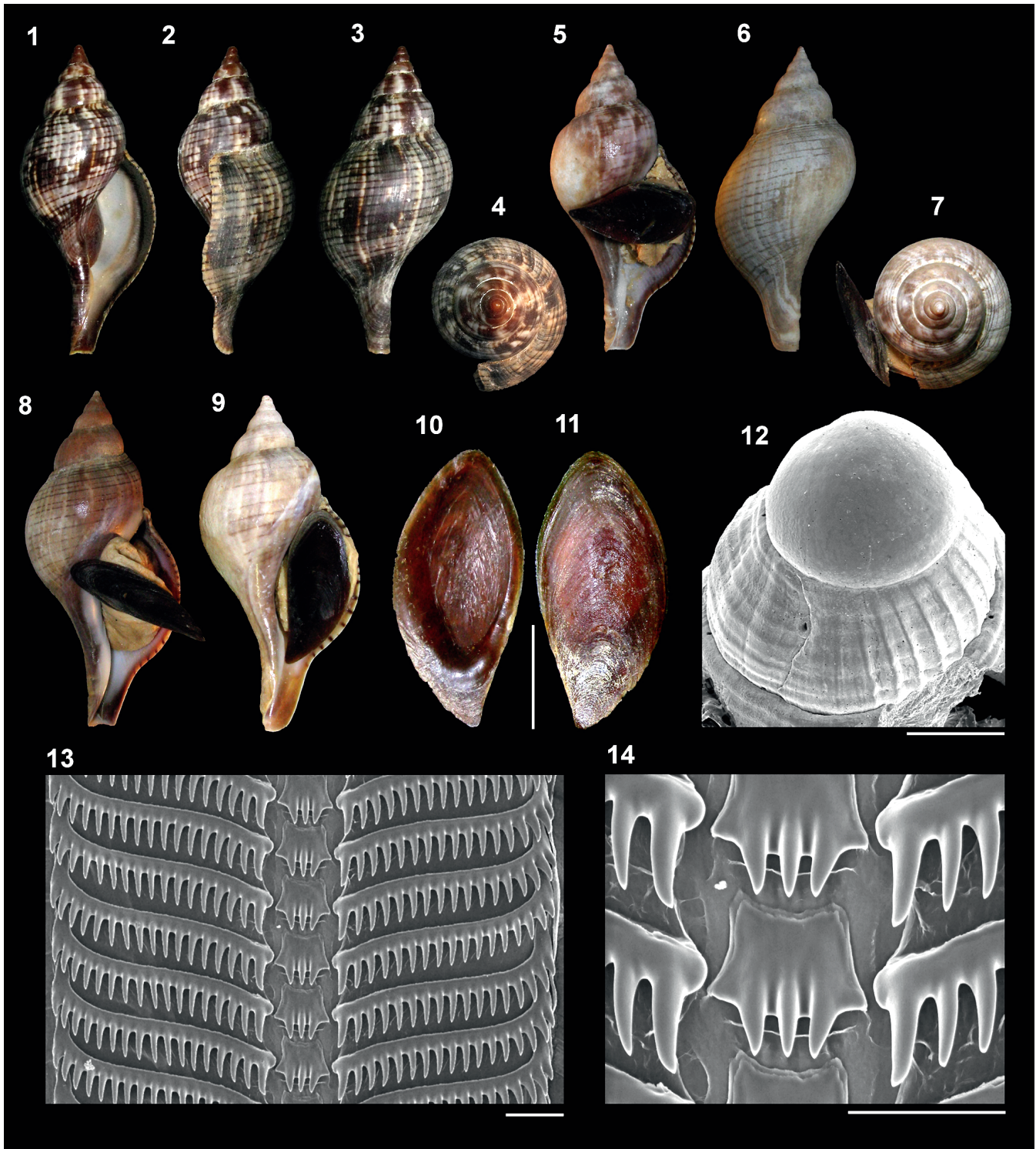
*Type material* *Murex Tulipa* P–Z 0010859. Linnean Society of London Collection, 3 specimens. Available online: <http://linnean-online.org/17116/>

*Examined material* HONDURAS; Roatan Island, 16°22'49.2"N, 86°24'39.6"W (80–100m depth, Femorale col. iii/2006), MZSP 69277, 1 specimen. VENEZUELA; Marguerite Island, 10°56'38.9"N, 64°01'31.1"W, (L. R. Simone col.), MZSP 35530, 2 specimens; 10°53'51.3"N, 63°58'11.9"W, (El Yaque, 2m depth, Simone col. 28/i/1998), MZSP 56870, 2 specimens.

*Geographic distribution* North Carolina, USA; Caribbean islands; west coast of central America to Amapá state, Brazil.

*Description* *Shell* (figs 1–9) Elliptical and moderately fusiform, height up to 106mm, width usually less than 1/2 of height. Colour chestnut to brown, with darker blotches. Spire moderately high, angle 55°–65°, ~2/5 of total shell height. Protoconch small with 1 1/2 whorls, sculptured with axial ribs in last 1/2 whorl, terminal varix low. Teleoconch with 5–7 rounded whorls; suture slightly raised. Spiral sculpture of 17–27 main spiral cords, color dark brown, usually grouped in pairs, along entire teleoconch but usually obsolete in siphonal canal. Axial sculpture indistinct. Aperture elliptical, ample, height ~3x width. Columella bearing 3 folds medially, close to siphonal canal. Outer lip thin, marked internally by 45–50 discontinuous lirae, crenulated by spiral sculpture and forming brownish sharp protuberances. Siphonal canal short, length ~1/3 of length of aperture. Siphonal fasciole indistinct. Pseudoumbilicus indistinct.

*Head-foot* (figs 15, 16) Colour cream in fixed species. Head prominent, of medium size, width ~1/3 of adjacent width of head-foot; cephalic tentacles blunt and medium-sized, length ~2/3 of anterior width of head, situated very close to each other; bases lying side by side. Eyes dark, small, rounded, situated in middle region of outer edge of tentacles. Foot short, rounded, anterior region



**Figures 1–14** *Fasciolaria tulipa*. 1–4: 69,5mm (MZSP 69277); 5–7: 92,3mm (MZSP 56870); 8: 77,5mm (MZSP 35530); 9: 107,9mm (MZSP 35530); 10: operculum, internal view; 11: operculum, external view; 12: detail of protoconch, lateral view; 13: radula; 14: detail of rachidian tooth of radula. Scale bars: 10–11: 10mm; 12: 1mm; 13–14: 100µm.

bifid. Pedal gland as a shallow median anterior slit, with anterior furrow extending along entire anterior edge. Columellar muscle thick, ~1 1/2 whorls in length.

*Operculum* (figs 10, 11) Corneous, unguiculated (width ~2/3 of length), filling entire aperture; outer surface opaque, with anterior nucleus; inner surface with attachment scar elongated,



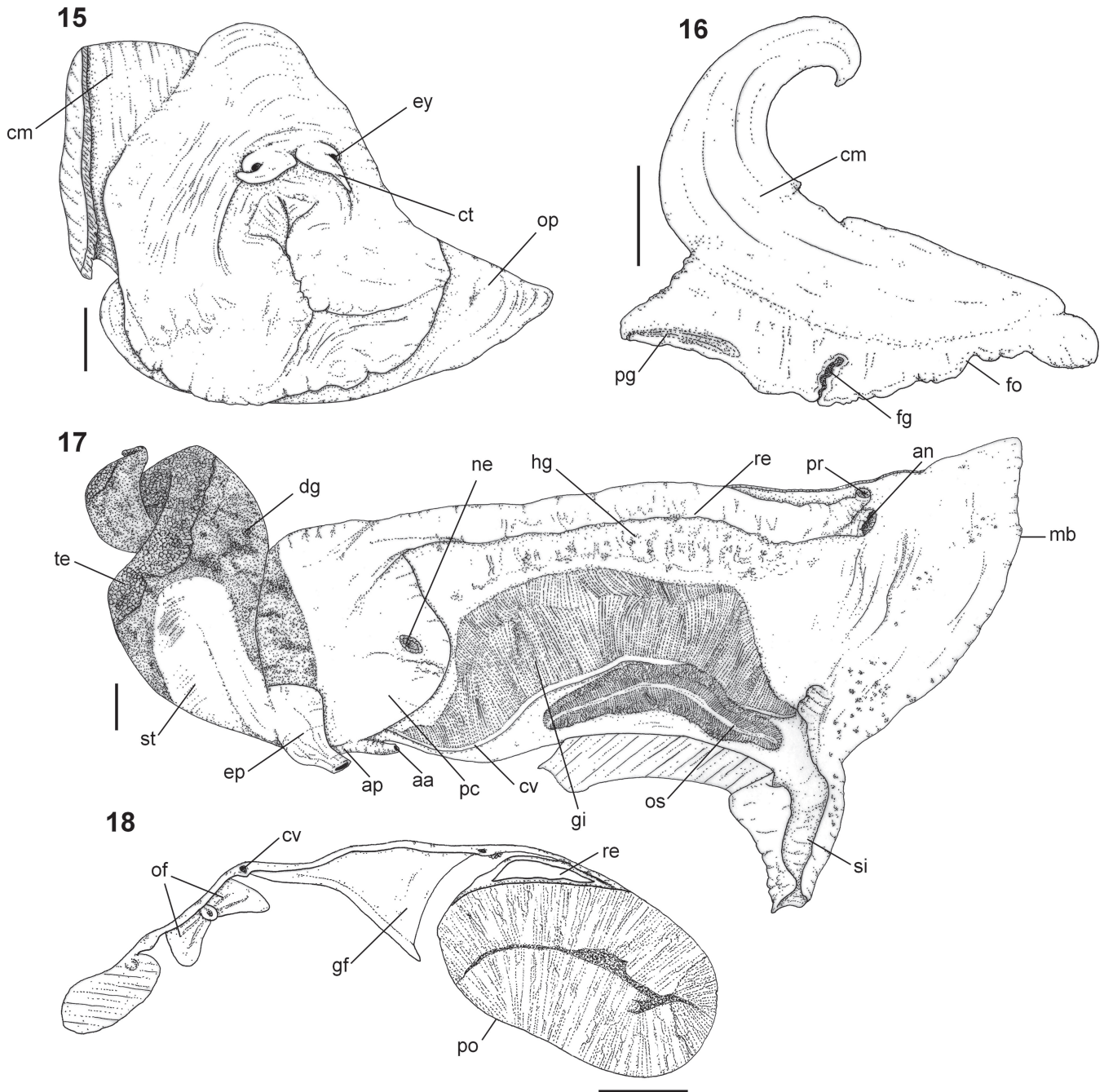
elliptical, situated posteriorly, occupying  $\sim 2/3$  of inner area.

*Pallial complex* (figs 17, 18) Pallial cavity wide than longer, of  $1/2$  whorl. Mantle border simple, thickened. Siphon short (length  $\sim 1/4$  of free portion of mantle edge), its margin smooth; right fold of siphon base extending into pallial cavity, ending as a thickened transversal flap, close to anterior end of ctenidium and osphradium. Osphradium elongated, tapering posteriorly; length  $\sim 2/3$  of ctenidium; almost symmetrical longitudinally; osphradium leaflets rounded, short (height  $\sim 1/2$  of ctenidial filament height at middle region of pallial cavity),  $\sim$ equal in size. Ctenidium curved,  $\sim 1/3$  of total pallial cavity area, width  $\sim$ twice than osphradium; anterior and posterior region pointed, posterior end situated close to pericardium; filaments triangular; ctenidial vein (efferent branchial vessel) uniformly narrow along its length. Hypobranchial gland thin, loosely fixed, situated in all the area between gill and rectum. Rectum elongated. Anus elliptical, situated at  $\sim 1/3$  of mantle edge.

*Circulatory and excretory systems* (fig. 30) Pericardium ample, spanning  $\sim 1/3$  of total renal cavity area. Auricle large, translucent, walls thin, posterior wall elongated ending close to renal aperture; ventricle large and rounded ( $\sim$ larger than auricle), rounded, with thick walls. Aorta bifurcating immediately after ventricle; posterior aorta following visceral mass close to stomach; anterior aorta crossing diaphragmatic septum anteriorly. Kidney small,  $\sim 1/4$  whorl, bearing ventral and dorsal lamellar lobes similar in shape; nephridial gland prominent, situated on dorsal side of membrane between renal cavity and pericardium; renal aperture sub-circular, situated in membrane closer to pericardium, flanked by thick folds, longitudinal to roof of pallial cavity. Part of intestine running longitudinally on inner side of kidney, ventrally adhered to its membrane.

*Digestive system* (figs 19–28) Rhynchostome as ample transversal slit, located between and below cephalic tentacles, flanked by lip-like folds bearing longitudinal lamellae. Proboscis straight, of moderate length ( $\sim 2/3$  of haemocoel length), with thick muscular walls bearing 2 lateral grooves; a single proboscis retractor muscles originating in ventral posterior wall of the

proboscis; series of short lateral muscles fibers connected to inner walls of haemocoel. Mouth small, circular. Odontophore long, slender,  $\sim$ same length as proboscis; pair of odontophore cartilages dorsally concave, fused anteriorly at  $\sim 1/10$  of total cartilage length; series of transversal muscle fibers connecting odontophore tube with anterior esophagus; superficial circular muscles ( $m^3$ ) enveloping entirely odontophore, except for most posterior end; horizontal muscle ( $m^6$ ), originating on ventral surface of odontophore cartilages, except for most posterior region,  $\sim 1/6$  of total odontophore length; pair of odontophore retractor muscles ( $m^2$ ) originating from posterior end of odontophore cartilages, near to radular sac, inserted in inner wall of proboscis; pair of accessory odontophore retractor muscles ( $m^2a$ ), originating from inner surface of proboscis, near origin of  $m^2$ , enveloping radular sac, a long branch of  $m^2a$  accompanies anterior aorta posteriorly to nerve ring; pair of dorsal tensor muscles of radula ( $m^4$ ) originating from posterior dorsal end of odontophore, covering its dorsal surface, inserting  $m^2a$ ; pair of auxiliary dorsal tensor muscles of radula ( $m^5$ ) originating from posterior end of odontophore, covering its ventral surface, inserting in  $m^2a$ ; pair of ventral tensor muscles of radula ( $m^{11}$ ), inserting anteriorly in sub-radular membrane, running, ventrally adhered ( $\sim 2/3$  of total odontophore length), its origin bifid: main branch originating in ventral posterior cartilage of odontophore near origin of  $m^2$ , secondary branch originating ventrally in  $m^2a$ , crossing  $m^6$  dorsally, connecting in main branch, at  $\sim 2/3$  of total  $m^{11}$  length. Radula long and thin; radular sac extending to posterior end of odontophore; Radular teeth (figs 13, 14): rachidian tooth straight, trapezoidal, its base with concave outline, cusped margin convex, bearing 3 sharp cusps of  $\sim$ equal size; lateral tooth wider than long, bearing 17–18 prominent, slightly centrally recurved cusps of approximately same size, central side of base rounded. Anterior esophagus moderately long and broad ( $\sim 2x$  proboscis length), dorsally-ventrally compressed, originating in oral tube. Valve of Leiblein pyriform, forming orange ring around esophagus,  $\sim$ of same width. Salivary glands just anterior to valve of Leiblein, forming pair of branching and amorphous masses; free portion of salivary ducts short, extending along esophagus, anteriorly to valve of Leiblein, becoming merged with esophageal wall, running

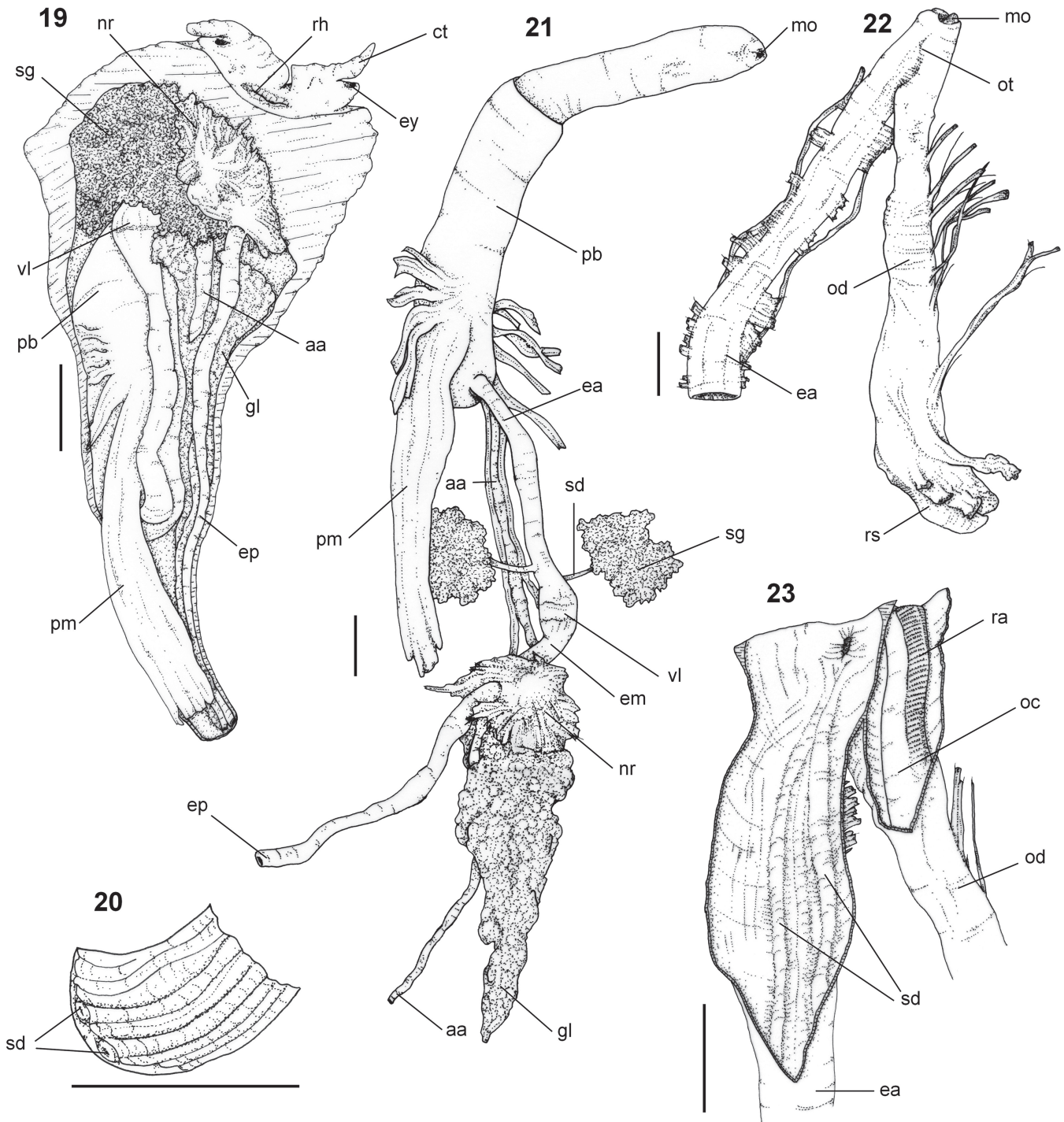


**Figures 15–18** *Fasciolaria tulipa*. 15: head-foot mass in dorsal view; 16: longitudinal section of foot, female; 17: roof of pallial cavity in ventral view, male 18: transversal section of roof of pallial cavity, female. Abbreviations: **aa**, anterior aorta; **an**, anus; **cm**, columellar muscle; **ct**, cephalic tentacle; **cv**, ctenidial vein; **dg**, digestive gland; **ep**, posterior esophagus; **ey**, eye; **fg**, female cement gland; **fo**, foot; **gf**, gill filament; **gi**, gill; **hg**, hypobranchial gland; **ki**, kidney; **mb**, mantle border; **ne**, nephrostome; **of**, osphradium filament; **op**, operculum; **os**, osphradium; **pc**, pericardium; **pe**, penis; **pg**, pedal gland; **po**, pallial oviduct; **pr**, prostate; **re**, rectum; **si**, siphon; **st**, stomach; **sv**, seminal vesicle; **te**; testis. Scale bars: 4mm.

immersed anteriorly, opening in oral lumen, immediately before oral tube. Accessory salivary glands absent. Middle esophagus short. Duct of gland of Leiblein short and narrow, inserted posterior to nerve ring. Gland of Leiblein brownish,

long, of ~same length as posterior esophagus, posterior end acute. Posterior and anterior esophagus of ~same width. Inner wall of anterior esophagus bearing many longitudinal folds, salivary ducts immersed in marked lateral folds.





**Figures 19–23** *Fasciolaria tulipa*. 19: hemocoel in ventral view; 20: longitudinal section of anterior esophagus; 21: anterior digestive system; 22: buccal mass in lateral view; 23: buccal mass in lateral view opened longitudinally. Abbreviations: **aa**, anterior aorta; **ct**, cephalic tentacle; **ea**, anterior esophagus; **ep**, posterior esophagus; **ey**, eye; **gl**, gland of leiblein; **mo**, mouth opening; **nr**, nerve ring; **oc**, odontophore cartilage; **od**, odontophore tube; **ot**, oral tube; **ra**, radula; **rh**, rhynchostoma; **rs**, radular sac; **sd**, salivary gland duct; **sg**, salivary gland; **vl**, valve of leiblein. Scale bars: 19–20: 4mm; 21–23: 2mm.

Sudden broadening of posterior esophagus anteriorly to stomach. Stomach wide, walls thin, bearing many internal folds. Digestive gland dark-brown, occupying all whorls of visceral

mass, from apex to kidney/pericardium area, surrounding stomach, emitting two narrow, branching ducts discharging near esophagus and intestine apertures. Intestine ~same width

of posterior esophagus and rectum, with smooth lumen.

*Male genital system* (fig. 29) Testis cream colored, occupying all whorls of visceral mass; surrounding apically entire length of digestive gland. Visceral vas deferens running along testis. Seminal vesicle indistinct; vas deferens narrow, simple, running along ventral wall of kidney. Prostate thin and long, tubular, located along right side of roof of pallial cavity, next to rectum and of its ~equal width. Penis medium-sized, close to head-foot, ~circular in transverse section; penis becoming narrower at mid of its length, terminating in tip-like extension; duct of penis sinuous.

*Female genital system* (fig. 18) Ovaries brownish, with same texture and length as testis. Cement gland opening centrally on foot, forming somewhat elongated and deep sac of depth of ~2/3 of foot thickness. Pallial oviduct ample, occupying ~1/2 of total pallial cavity area, covering part of ctenidium and renal aperture. Pallial oviduct glands not analyzed due to poor preservation.

## DISCUSSION

The anatomy of the fascioliid *Fasciolaria tulipa* is consistent with the framework within the Neogastropoda, as well as Buccinoidea, in lacking accessory salivary glands and an anal gland. The proboscis retractor as a single and powerful muscle, the multicuspidate lateral teeth of the radula, the stomach without a posterior sorting area (caecum), and the ducts of the salivary glands immersed in the esophagus wall confirm the species as a member of the Fascioliidae in the context of Buccinoidea as diagnosed by Fraussen *et al.* (2007).

Snyder *et al.* (2012) noted that the distributions of both species of Fascioliinae (*F. tulipa* and *Aurantilaria aurantiaca*) overlap in northern Brazil. Fascioliinae have a free-swimming larval stage of up to six days, allowing some species to occur over a wide range, supposedly because the veligers gain access to floating objects and disperse to areas inaccessible to crawlers (Snyder *et al.*, 2012). Juveniles of *A. aurantiaca* hatch from egg capsules attached to the bottom and crawl directly onto the surrounding substrate (Meirelles & Matthews-Cascon, 2005); the protoconch morphology also indicates a direct mode

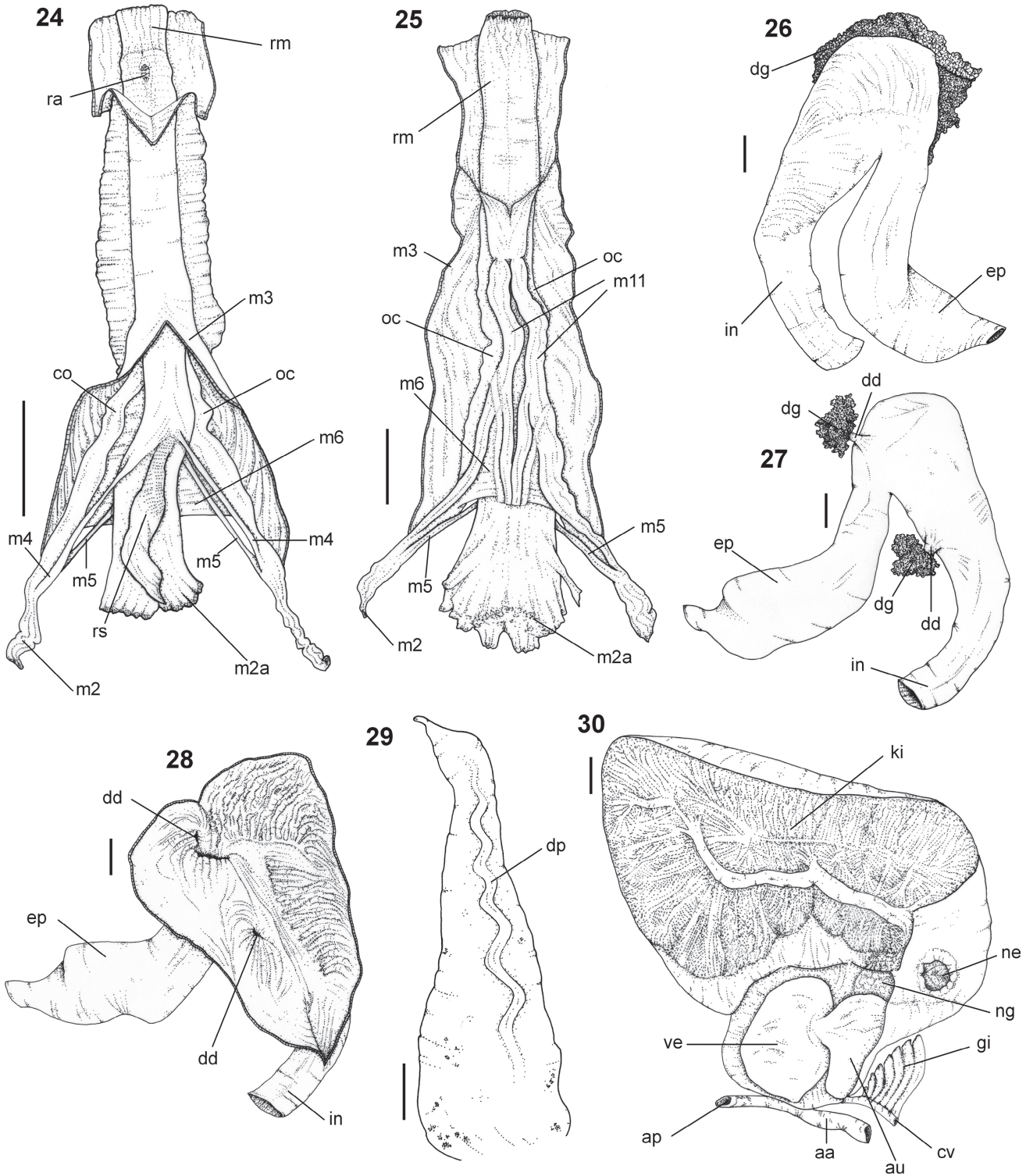
of development. However, *F. tulipa* has a wide distribution and probably has a free-swimming larva during its development, albeit briefly (Leal, 1991), and its protoconch indicates this. The distinction of the *Fasciolaria* species from the West Atlantic is problematic (Lyons, 1972); Rosenberg (2009) argued for the occurrence of at least seven distinct species occurring in sympatry in the Caribbean Sea: *Fasciolaria tulipa* (Linnaeus, 1758); *F. bullisi* Lyons, 1972; *F. hollisteri* Weisbord, 1962; *F. tephрина* de Souza, 2002; *F. branhamae* Rehder & Abbott, 1951; *F. hunteria* (G. Perry, 1811) and *F. liliium* G. Fischer, 1807. However, Snyder *et al.* (2012) recognized only the first four of these as belonging to this genus.

Shells of members of Fascioliinae are morphologically similar to those of Peristerniinae: both groups are characterized by the presence of folds in the columella, with one fold marking the entrance to the siphonal canal, and an outer lip with lirae internally. The folds in Fascioliinae, however, are orientated obliquely, whereas in Peristerniinae they are transverse (Snyder *et al.* 2012).

The central side of the base of the lateral tooth with a rounded outline is unique for Fascioliinae. Bandel (1984) illustrated many fascioliid radulae, with three species of *Fasciolaria*, including *F. tulipa*; all the radulae that he described agree with this pattern. All the cusps of the laterals are more or less equal in size, and the number of these is generally larger than in other fascioliids (see Bandel, 1984, figs 257–268, for examples of radulae of Peristerniinae and Fusiniinae). The radula of *Fasciolaria lignaria* (Küster & Kobelt, 1876; Kosyan *et al.*, 2009) resembles that of many *Latirus*-like species in having a minute cusp on the inner side of the base of the lateral tooth, as well as fewer, shorter and more strongly curved cusps. Snyder *et al.* (2012) tentatively placed the species in the genus *Tarantinae* Monterosato (1917) (see also Gofas & Bouchet, 2014), previously a subgenus of *Fasciolaria*, due to the presence of an adapical sinus on the outer lip. Moreover, this species was considered a member of Peristerniinae “pending molecular confirmation” by these same authors.

Two other features of the anterior digestive system are noteworthy for *F. tulipa*. The odontophore cartilages are fused anteriorly along only 10% of their length, less than in other fascioliids: 30–40% in *Leucozonia* (Couto & Pimenta, 2012) and 25% in *Polygona*. The posterior esophagus





**Figures 24–30** *Fasciolaria tulipa*. 24: odontophore in dorsal view; 25: odontophore in ventral view; 26: stomach in dorsal view; 27: stomach in ventral view; 28: stomach opened longitudinally; 29: penis in dorsal view; 30: renal cavity and pericardium opened ventrally. Abbreviations: **aa**, anterior aorta; **ap**, posterior aorta; **au**, auricle; **cv**, ctenidial vein; **dd**, duct of digestive gland; **dg**, digestive gland; **dp**, duct of penis; **ep**, posterior esophagus; **in**, intestine; **ki**, kidney; **m<sup>11</sup>**, ventral tensor muscles of radula; **m<sup>2</sup>**, odontophore retractor muscles; **m<sup>2a</sup>**, accessory odontophore retractor muscles; **m<sup>3</sup>**, superficial circular muscles; **m<sup>4</sup>**, dorsal tensor muscles of radula; **m<sup>5</sup>**, auxiliary dorsal tensor muscles of radula; **m<sup>6</sup>**, horizontal muscle; **ne**, nephrostome; **ng**, nephridial gland; **oc**, odontophore cartilage; **pc**, pericardium; **ra**, radula; **re**, rectum; **rm**, sub-radular membrane; **rs**, radular sac; **ve**, ventricle. Scale bars: 2mm.

broadens anteriorly to the entrance of the stomach; this suggests a premature digestion in this part of the esophagus, although histological procedures are required to verify this statement.

As in many groups, the morphology of the anterior digestive and male reproductive systems is more informative for species-level taxonomy, and this is also true for Fascioliidae (Fraussen *et al.* 2007; Kosyan *et al.* 2009; Couto & Pimenta, 2012; Couto *et al.* 2015). The radula is especially important, as an easily preserved structure that distinguishes fairly well the families of Neogastropoda (Fraussen *et al.* 2007).

A renal aperture of *F. tulipa* is situated very close to the pericardium, instead of being located centrally in the membrane; this is not seen in any other fascioliid (*e.g.*, Marcus & Marcus, 1962; Couto & Pimenta 2012, Couto *et al.* submitted). This occurs together with two other unique features: a large auricle with thin, translucent walls, its posterior end elongated and terminating close to the renal aperture; and a very conspicuous nephridial gland. The posterior end of the auricle seems to be attached to the roof of the pericardium wall, hence the elongation of its wall; the nephridial gland is conspicuous, visible through the transparent wall between the pericardium and renal cavity. No other member of Fascioliidae is so far known to present these features (Marcus & Marcus, 1962; Couto & Pimenta, 2012), whereas both occur in *A aurantiaca* (Couto, pers. obs.).

Fraussen *et al.* (2007) defined a diagnostic character for *F. tulipa*: the ducts of the salivary gland do not run free alongside the anterior esophagus, as they do in other fascioliids (Marcus & Marcus, 1962; Couto & Pimenta, 2012; Fedosov & Kantor, 2012), but are merged in its wall anteriorly to the valve of Leiblein. This feature was reported only for *Latirus polygonus*, among the fascioliids examined by Kosyan *et al.* (2009).

An important diagnostic feature for the family *sensu* Fraussen *et al.* (2007) is the proboscis retractor as a single ventral-lateral muscle. All fascioliids except *Latirus polygonus* and *Fusinus tenerifensis* have a single muscle, while in the buccinids, multiple fibers occur posteriorly to the proboscis, distinguishing the Fascioliidae from the Buccinidae (Kosyan *et al.*, 2009). Other studies that mention the proboscis retractor for Fascioliidae agree on this (Marcus & Marcus,

1962; Couto & Pimenta, 2012; Fedosov & Kantor, 2012; Couto *et al.*, submitted).

*Fasciolaria tulipa* is the type species of the genus, so the study of its anatomy is fundamental in resolving species-level taxonomy, particularly because the subfamily Fascioliinae has undergone a thorough taxonomic revision in recent years, albeit only conchologically (Snyder *et al.* 2012). A more detailed understanding of the morphology of soft-parts will be able to provide further data, and possibly help to define groups that are currently doubtful, as is the case for many *Latirus*- and *Fusinus*-like species. Moreover, knowledge of anatomical characters is imperative for phylogenetic analysis, as the relationships of most groups within the Buccinoidea, including family and genus level are still unknown. This analysis is in effect a permanent work in progress, of which the present study is a part.

#### ACKNOWLEDGMENTS

The authors are grateful to Lara Guimarães for helping with the SEM. This work was funded in part by the Conselho de Desenvolvimento Científico e Tecnológico (CNPq) for a M.S. scholarship and Fundação de Amparo à Pesquisa do Estado de São Paulo (FAPESP) for a Ph.D. scholarship.

#### REFERENCES

- ABBOTT RT & MORRIS PA 1995 *A field guide to shells: Atlantic and Gulf Coasts and the West Indies*. Houghton Mifflin Co. Boston, MA. 350p.
- ABBOTT RT 1974 *American Seashells*. second edition. Van Nostrand Reinhold Co, New York. 663p. 24pls.
- BANDEL K 1984 *The Radulae of Caribbean and other Mesogastropoda and Neogastropoda*. Rijksmuseum van Natuurlijke Historie, 346p. 22pls.
- COUTO DR & PIMENTA AD 2012 Comparative morphology of *Leucozonia* from Brazil (Neogastropoda: Buccinoidea: Fascioliidae). *American Malacological Bulletin* 30(1): 103–116.
- COUTO DR, SIMONE LRL & PIMENTA, AD 2015 Comparative anatomy of the fascioliids *Pustulatirus ogum* and *Hemipolygona beckyae* from Brazil (Gastropoda: Buccinoidea: Peristerniinae). *Scientia Marina*, 79(1): 89–105.
- DALL WH 1885 List of marine Mollusca comprising the Quaternary fossils and Recent forms from American localities between Cape Hatteras and Cape Roque including the Bermudas. *Bulletin of the United States Geological Survey* 24: 1–336.
- DALL WH 1890 Contributions to the Tertiary fauna of Florida, with especial reference to the Miocene



- silex-beds of Tampa and the Pliocene beds of the Caloosahatchie River. Part I. Pulmonate, opisthobranchiate and orthodont gastropods. *Transactions of the Wagner Free Institute of Science of Philadelphia* **3**: 1–200, 1–12pls.
- FEDOSOV AE & KANTOR YI 2012 A new species and genus of enigmatic turriiform Fascioliidae from the Central Indo-Pacific (Gastropoda: Neogastropoda). *Archiv für Molluskenkunde* **141**(2): 137–144.
- FRAUSSEN K, KANTOR Y & HADORN R 2007 *Amiantofusus* gen. nov. for *Fusus amiantus* Dall, 1889 (Mollusca: Gastropoda: Fascioliidae) with description of a new and extensive Indo-West Pacific radiation. *Novapex* **8**(3–4): 79–101.
- GOFAS S & BOUCHET P 2014 *Tarantinaea lignaria* (Linnaeus, 1758). Accessed through: World Register of Marine Species (WoRMS) on 2014-07-15 at <http://www.marinespecies.org/aphia.php?p=taxdetails&id=607879>.
- GOFAS S 2014 Family Fascioliidae Gray, 1853. Accessed through: World Register of Marine Species (WoRMS) on 2014-07-15 at <http://www.marinespecies.org/aphia.php?p=taxdetails&id=23038>.
- JENSEN RH & PEARCE TA 2009 *Marine Mollusks of Bermuda: Checklist and Bibliography*. Delaware Museum of Natural History: Wilmington, Delaware. 473p.
- KOBELT W 1875 Catalog der Gattung *Fasciolaria* Lam. *Jahrbücher der Deutschen Malakozoologischen Gesellschaft* **2**: 362–364.
- KOSYAN AR, MODICA MV & OLIVERIO M 2009 The anatomy and relationships of *Troschelia* (Neogastropoda, Buccinidae): new evidence for a closer fascioliid-buccinid relationship? *The Nautilus* **123**(3): 95–105.
- KÜSTER HC & KOBELT W 1844–1876 Die geschwänzten unbewehrten Purpurschnecken. Erste Hälfte: *Turbinella* und *Fasciolaria*. - In: FHW Martini & JH Chemnitz. *Systematisches Conchylien-Cabinet*, second edition (Küster HC) (3a): 1–164, 1–32pls, 9a, 9b, 13b.
- LEAL JH 1991 *Marine Prosobranch Gastropods from Oceanic Islands off Brazil*. Backhuys/U.B.S. Oegstgeest, The Netherlands. 419p.
- LINK DHF 1807 *Beschreibung der naturalien-Sammlung der Universität zu Rostock*. Abtheilung **3**: 101–165.
- LINNAEUS C 1758 *Systema Naturae per regna tria naturae, secundum classes, ordines, genera, species, cum characteribus, differentiis, synonymis, locis*. Editio decima, reformata. Laurentius Salvius: Holmiae. ii, 824 p.
- LYONS WG 1972 A New *Fasciolaria* from the Northeastern gulf of Mexico. *The Nautilus* **85**(3): 96–99.
- MALLARD D & ROBIN A 2005 *Fascioliidae*. La Mother Achard, Les Sables-d'Olonne. 27p. 70pls.
- MARCUS E & MARCUS E 1962 On *Leucozonia nassa*. *Boletim da faculdade de Filosofia Ciências e Letras da Universidade de São Paulo, Zoologia* **24**: 1–30.
- MATTHEWS-CASCON H, MATTHEWS HR & KOTZIAN CB 1989 Os Gêneros *Fasciolaria* Lamarck, 1799 e *Leucozonia* Gray, 1847 no Nordeste Brasileiro (Mollusca: Gastropoda: Fascioliidae). *Memórias do Instituto Oswaldo Cruz* **84**, Supl. IV: 357–364.
- MEIRELLES CAO & MATTHEWS-CASCON H 2005 Family Fascioliidae Gray, 1853 *Pleuroploca aurantiaca* (Lamarck, 1816). 51–53, pl. 12 In: Matthews-Cascon H, Rocha-Barreira CA & Meirelles CAO. Egg Masses of Some Brazilian Mollusks. Expressão Gráfica e Editora, Fortaleza. 119p.
- PONDER WF & LINDBERG DR 2008 *Phylogeny and Evolution of the Mollusca*. University of California Press, Berkeley. xi, 469p.
- REDFERN C 2001 *Bahamian Seashells: A Thousand Species from Abaco, Bahamas*. Bahamian-seashells.com, Inc, Boca Raton, Florida. x, 280p, 124pls.
- RIOS EC 1970 *Coastal Brazilian Seashells*. Museu Oceanográfico de Rio Grande, Rio Grande. 255p. 60pls. 4 maps.
- RIOS EC 1975 *Brazilian Marine Mollusks Iconography*. Museu Oceanográfico da FURG, Rio Grande, 331p. 91pls.
- RIOS EC 1985 *Seashells of Brazil*. Museu Oceanográfico, Fundação Univesidade do Rio Grande, Rio Grande, 328p.
- RIOS EC 1994 *Seashells of Brazil*. Museu Oceanográfico Prof. E. C. Rios, Fundação Universidade do Rio Grande, Rio Grande, 368p. 113pls.
- RIOS EC 2009 *Compendium of Brazilian Sea Shells*. Museu Oceanográfico Prof. E. C. Rios, Fundação Universidade do Rio Grande, Rio Grande, 668p.
- RÖDING PF 1798 *Museum Boltenianus sive Catalogus cimeliorum e tribus regnis naturae quae olim collegerat. Pars secunda continens Conchylia sive Testacea univalvia, bivalvia & multivalvia*. Hamburg, Johan Christi Trappii. viii, 199p.
- ROSENBERG G 2009 Malacolog 4.1.0: A Database of Western Atlantic Marine Mollusca [WWW database (version 4.1.0)] URL <http://www.malacolog.org/>.
- SIMONE LRL 2011 Phylogeny of the Caenogastropoda (Mollusca), Based on Comparative Morphology. *Arquivos de Zoologia do Museu de Zoologia da Universidade de São Paulo*, **42**(2–4): 83–323.
- SIMONE LRL, CAVALLARI DC & ABBATE D 2013. Revision of the genus *Teralatirus* Coomans 1965 in the Western Atlantic, with an anatomical description of *T. roboreus* (Reeve 1845) (Gastropoda: Neogastropoda: Fascioliidae). *Archiv für Molluskenkunde* **142**(2): 215–226.
- SNYDER MA, VERMEIJ GJ & LYONS WG 2012 The genera and biogeography of Fascioliinae (Gastropoda, Neogastropoda, Fascioliidae). *Basteria* **76**(1–3): 31–70.
- SNYDER MA 2003 Catalogue of the marine gastropod family Fascioliidae. *Academy of Natural Sciences of Philadelphia Special Publications* **21**. Philadelphia. iv, 431p.
- THIELE J 1929–1935 *Handbuch der Systematischen Weichtierkunde*. Gustav Fischer, Jena vol 1: vi, 778p. vol. 2: v, 779–1134p.
- TRYON GW 1880 *Manual of Conchology, Structural and Systematic, with Illustrations of the Species*. Philadelphina. 310p. 87pls.

- TUNNEL JW, ANDREWS J, BARRERA NC & MORETZSOHN F 2010 *Encyclopedia of Texas Seashells – Identification, Ecology, Distribution & History*. Texas A&M University Press. Corpus Christi. xi, 512p.
- VALENCIENNES A 1832 Coquilles univalves marines de l'Amérique équinoxiale, recueillies pendant le voyage de MM de Humboldt et Bonpland: 262–339. In Humboldt VA & Bonpland A (eds) *Recueil d'observations de zoologie et d'anatomie compar : faites dans l'ocn atlantique, dans l'intieur du nouveau continent et dans la mer du sud pendant les anns 1799, 1800, 1801, 1802 et 1803* , Deuxieme Volume, 352p pls 41–57.
- VOKES HE & VOKES EH 1983 Distribution of Shallow-Water Marine Mollusca, Yucatan Peninsula, Mexico. *Middle American Research Institute, New Orleans* 54: 183p. 50pls.
- WARMKE GL & ABBOTT RT 1961 *Caribbean Seashells: A Guide to Marine Mollusks of Puerto Rico and Other West Indian Islands. Bermuda and the Lower Florida Keys*: Livingston Publishing Co., Narberth, Pennsylvania. xx, 348p. 44pls.





# A multilocus molecular phylogeny of Fascioliariidae (Neogastropoda: Buccinoidea)



Diogo R. Couto<sup>a,b,\*</sup>, Philippe Bouchet<sup>c</sup>, Yuri I. Kantor<sup>d</sup>, Luiz R.L. Simone<sup>b</sup>, Gonzalo Giribet<sup>a</sup>

<sup>a</sup> Museum of Comparative Zoology, Department of Organismic and Evolutionary Biology, Harvard University, 26 Oxford Street, Cambridge, MA 02138, USA

<sup>b</sup> Laboratório de Malacologia, Museu de Zoologia da Universidade de São Paulo, Avenida Nazaré 481, 04263-000 São Paulo, Brazil

<sup>c</sup> Institut de Systématique, Évolution, Biodiversité, ISYEB, UMR 7205, CNRS, MNHN, UPMC, EPHE, Muséum National d'Histoire Naturelle, Sorbonne Universités, 55 rue Buffon, CP26, F-75005 Paris, France

<sup>d</sup> A.N. Severtzov Institute of Ecology and Evolution, Russian Academy of Sciences, Leninski Prospect 33, Moscow 119071, Russia

## ARTICLE INFO

### Article history:

Received 5 November 2015

Revised 17 March 2016

Accepted 18 March 2016

Available online 23 March 2016

### Keywords:

Fascioliariinae

Peristerniinae

Fusiniinae

Evolution

*Dolicholaturus*

*Radula*

## ABSTRACT

The neogastropod family Fascioliariidae Gray, 1853 – tulips, horse-conchs, spindles, etc., comprises important representatives of tropical and subtropical molluscan assemblages, with over 500 species in the subfamilies Fascioliariinae Gray, 1853, Fusiniinae Wrigley, 1927 and Peristerniinae Tryon, 1880. Fascioliariids have had a rather complicated taxonomical history, with several genus names for a long time used as waste baskets to group many unrelated species; based on shell characters, recent taxonomic revisions have, however, began to set some order in its taxonomy. The present work is the first molecular approach to the phylogeny of Fascioliariidae based on a multigene dataset, which provides support for fascioliariids, an old group with a fossil record dating back to the Cretaceous. Molecular markers used were the mitochondrial genes 16S rRNA and cytochrome *c* oxidase subunit I, and the nuclear genes 18S rRNA, 28S rRNA and histone H3, sequenced for up to 116 ingroup taxa and 17 outgroups. Phylogenetic analyses revealed monophyly of *Dolicholaturus* Bellardi, 1884 and *Teralaturus* Coomans, 1965, however it was not possible to discern if the group is the sister clade to the remaining fascioliariids; the latter, on the other hand, proved monophyletic and contained highly supported groups. A first split grouped fusinines and *Pseudolaturus* Bellardi, 1884; a second split grouped the peristerniine genera *Peristernia* Mörch, 1852 and *Fusolaturus* Kuroda and Habe, 1971, while the last group comprised fascioliariines and the remaining peristerniines. None of these clades correspond to the present-day accepted circumscription of the three recognized subfamilies.

© 2016 Elsevier Inc. All rights reserved.

## 1. Introduction

Neogastropoda, the most diverse caenogastropod mollusk clade, is supported by morphology-based phylogenetic analyses (Ponder and Lindberg, 1997; Strong, 2003) and by a Bayesian inference analysis of a combined morphological and molecular data (Ponder et al., 2008), but it has been challenged in several molecular studies (Harasewych et al., 1997; Colgan et al., 2000, 2003, 2007). In their complete mitochondrial genome and three nuclear-gene phylogeny, Osca et al. (2015) failed to recover Neogastropoda, and proposed the inclusion of Tonnoidea, or the exclusion of Cancellarioidea and possibly Volutidae from Neogastropoda. In the first case tonnoideans would have secondarily lost the traditional neogastropod synapomorphies, while in the latter

these synapomorphies would be considered homoplastic, in this sense agreeing with Kantor and Fedosov (2009). The superfamily Buccinoidea includes the families Buccinidae, Belomitridae, Busyconidae, Colubrariidae, Columbelloidea, Nassariidae, Melongenidae and Fascioliariidae (Bouchet and Rocroi, 2005; WoRMS, 2016). They are considered highly derived in the Neogastropoda scheme due to the probable loss of the accessory salivary glands and the rectal glands.

Knowledge of the phylogenetic position of Fascioliariidae and of the families included in Buccinoidea is scant, and studies that deal specifically with the taxonomic position of these taxa are few. Hayashi (2005), utilizing sequences from the complete mitochondrial 16S rRNA gene, obtained a phylogeny based on 22 buccinoid species; Kosyan et al. (2009) used 20 species of buccinoids from partial 16S rRNA sequence data; finally, Oliverio and Modica (2010), analyzed 16S rRNA data from 30 buccinoids. All these analyses failed to recover Buccinidae as monophyletic due to the

\* Corresponding author at: Laboratório de Malacologia, Museu de Zoologia da Universidade de São Paulo, Avenida Nazaré 481, 04263-000 São Paulo, Brazil.

E-mail address: [diogout@gmail.com](mailto:diogout@gmail.com) (D.R. Couto).

intercalation of Nassariidae and/or Fascioliariidae. There are no phylogenetic hypotheses that deal specifically with the family Fascioliariidae, based either on morphological or molecular characters, and the studies that do include some fascioliariid species (e.g., Hayashi, 2005; Kosyan et al., 2009; Zou et al., 2011) lack the resolution and coverage to clarify their relationships or to test their monophyly, as the family may potentially comprise multiple paraphyletic groups (Fedosov and Kantor, 2012).

Fascioliariidae, Melongenidae, Cancellariidae and Buccinidae date back to the early Cretaceous (Valanginian, ~140 Mya) (Tracey et al., 1993), whereas other neogastropod families appeared between the late Cretaceous to early Paleogene, suggesting that the former families represent the first offshoots of Neogastropoda (Hayashi, 2005). While Fascioliariidae appeared during the Albian (Bandel, 1993), the fossil record indicates that the family – especially Fascioliariidae and Peristerniinae (Vermeij and Snyder, 2006) – diversified extensively during the early Neogene (Aquitanian, 24 Mya).

With 541 extant species in 51 genera worldwide (WoRMS, 2016), Fascioliariidae are a diverse element of the molluscan predatory fauna in shallow to deep coastal waters, especially on soft bottoms. Fascioliariids are gonochoristic with internal fertilization and, usually, direct development (Leal, 1991). They inhabit depths down to 1900 m (Callomon and Snyder, 2009) where they prey on sedentary polychaetes, bivalves, cirripedes and other gastropods (Taylor et al., 1980). The family is currently comprised of three subfamilies: Peristerniinae, which includes, among other genera, *Peristernia* and *Latirus*; Fusiniinae, the spindles; and Fascioliariinae with the conspicuous and well-known tulips and horse-conchs. For a long time, the name '*Fusus*' has been used indiscriminately for numerous Cretaceous, Cenozoic and Recent spindle-shaped shells (Snyder, 2003), and likewise *Latirus*, *Fasciolaria* and *Pleuroploca* were also used for evidently heterogeneous assemblages. More recently, however, the group has undergone extensive taxonomical revision (e.g., Vermeij and Snyder, 2002, 2006; Snyder et al., 2012; Lyons and Snyder, 2013), elevating several subgenera to genus rank and establishing new genera.

Sampling of multiple independently evolving genes is recommended to produce a resolved and strongly supported phylogeny avoiding issues of incongruence among single gene analyses. The use of such a multi-gene molecular approach has helped resolve problems in different molluscan clades (e.g., Puillandre et al., 2011; Aktipis and Giribet, 2010; Tëmkin, 2010; Sharma et al., 2013). The present study aims to improve the phylogenetic understanding of the Fascioliariidae and investigate the diversification patterns of its members by conducting multi-gene phylogenetic analyses.

## 2. Material and methods

### 2.1. Taxon sampling

The present study is largely based on material vouchered in MNHN, collected during multiple expeditions conducted by MNHN and IRD, and other ad hoc fieldwork (see Acknowledgements). Before 2012, specimens were treated with an isotonic solution of magnesium chloride until relaxed (showing no response to touch), and then a tissue clip was cut. Starting from early 2012, specimens were processed using a microwave oven (Galindo et al., 2014), i.e., in most cases the entire body, or at least the last 1–1.5 whorls, were available for study. Tissue samples were preserved in 96% EtOH. Additional specimens were used from the following institutions: Academy of Natural Sciences of Philadelphia (ANSP); Florida Museum of Natural History (FMNH); Museum of Comparative Zoology, Harvard University, Cambridge, MA (MCZ); Museum of Zoology, University of São Paulo (MZSP); and Santa Barbara

Museum of Natural History (SBMNH). Some museum specimens were preserved in 70% EtOH. In total 116 specimens of Fascioliariidae were sequenced. The 116 ingroup taxa sampled consist of 10 Fascioliariinae, 67 Peristerniinae and 39 Fusiniinae. Outgroup taxa for the study consisted of 11 Buccinoidea, 2 Conoidea, 2 Muri-coidea and 2 Cypraeoidea. The list of specimens, including collection voucher numbers, GenBank accession codes and collection details is found in Table 1.

### 2.2. Molecular methods

Total DNA was extracted from foot tissue using Qiagen's DNeasy tissue kit (Qiagen, Valencia, CA, USA). Molecular markers consisted of 2 nuclear ribosomal genes (18S rRNA and 28S rRNA), a mitochondrial ribosomal gene (16S rRNA), a mitochondrial protein-encoding gene (cytochrome *c* oxidase subunit I [COI]) and one nuclear protein-encoding gene (histone H3) Primer sequences are listed in Table 2. Purified genomic DNA was used as a template for polymerase chain reaction (PCR) amplification.

Polymerase chain reactions (PCR) were performed on a Mastercycler Pro<sup>®</sup> Eppendorf (Hamburg, Germany) in a 25  $\mu$ L volume reaction, and consisted of 1  $\mu$ L of template DNA, 1  $\mu$ M of each primer, 200  $\mu$ M of deoxynucleotide triphosphates (dNTP's; Invitrogen, Carlsbad, CA, USA), 1X PCR buffer containing 1.5 mM MgCl<sub>2</sub> (Promega, Madison, WI, USA) and 1.25 units of GoTaq DNA polymerase (Promega). The fragments were amplified under the following conditions: initial denaturing at 95 °C for 15 min, 40 cycles of 94 °C for 30 s, 43–64 °C (annealing temperatures, Table 2) for 70 s and 72 °C for 90 s, and final extension step at 72 °C for 10 min. Numerous PCR additives were utilized in order to optimize DNA amplification, including BSA (Bovine serum albumin) and DMSO (Dimethyl sulfoxide). BSA was utilized with different optimal concentrations per template (0.8–5.6  $\mu$ g/mL). It exerts its effect through interacting with interfering substances and also stabilizing Taq DNA polymerase (Nagai et al., 1998). DMSO was used with a final concentration of 5% to reduce secondary structures that could inhibit the progress of the polymerase, being especially useful for GC-rich templates (Meyer et al., 2010).

Double-stranded PCR products were visualized by agarose gel electrophoresis (1% agarose) and purified using 2  $\mu$ L of diluted (1:2) ExoSAP-IT (Affymetrix, Santa Clara, CA, USA) in a volume of 25  $\mu$ L PCR product and incubated at 37 °C for 20 min followed by enzyme inactivation at 80 °C for 15 min. Sequencing reactions were performed in a 10  $\mu$ L reaction volume with Big-Dye Terminator v.3.1 (Applied Biosystems, Foster City, CA, USA) following the manufacturer's instructions. using the thermal cycler described above, with an initial denaturation step for 3 min at 94 °C and 25 cycles of 94 °C for 10 s, 50 °C for 5 s and 60 °C for 4 min.

Sequenced products were purified using Sephadex (Amersham Biosciences) and sequenced on an ABI Prism 3730 Genetic Analyzer (Applied Biosystems). Chromatograms obtained were visualized and edited in Geneious v.8.1.2 (<http://www.geneious.com>, Kearsse et al., 2012). All new sequences have been deposited in GenBank under accession numbers KT753546–KT754145. The 5 genes were analyzed as follows:

18S rRNA: The complete gene was amplified with three overlapping markers (*a*, *b*, *c*). In the present study we include 116 ingroup specimens plus 17 outgroups, for a total of 1777–1787 bp per complete sequence. From the 116 ingroup sequences, all but 3 were complete.

28S rRNA: A 2.2 Kb fragment of the gene was amplified with three overlapping markers (*a*, *b*, *c*), as described in Giribet and Shear (2010). The dataset includes 115 ingroup specimens plus 17 outgroups, for a total of 2085–2139 bp, showing considerable length variation in 28S rRNA. Fragment *a* was sequenced for 115

**Table 1**

List of species sampled and gene fragments included in phylogenetic analyses with GenBank accession numbers. Outgroup species appear in bold.

Taxon		Voucher #	Locality	18S rRNA	28S rRNA	16S rRNA	COI	H3	
<i>Amiantofusus candoris</i>	Bu	f	MNHN IM-2013-19759	Bismarck Sea	KT753546	KT753679	KT753807	KT753912	KT754043
<i>Amiantofusus pacificus</i>	Bu	f	MNHN IM-2009-13533	New Caledonia	KT753552	KT753685	KT753812	KT753918	KT754049
<i>Amiantofusus pacificus</i>	Bu	f	MNHN IM-2013-44400	Taiwan	KT753581	KT753714	KT753837	KT753947	KT754078
<i>Amiantofusus sebalis</i>	Bu	f	MNHN IM-2007-32837	Solomon Islands	KT753545	KT753678	–	KT753911	KT754042
<i>Amiantofusus sebalis</i>	Bu	f	MNHN IM-2013-44196	Taiwan	KT753592	KT753725	KT753846	KT753958	KT754089
<i>Angulofusus nedae</i>	Bu	f	MNHN IM-2007-32574	Vanuatu	KT753618	KT753751	–	KT753984	KT754114
<i>Aurantilaria aurantiaca</i>	Bu	f	MZSP 101904	northeast Brazil	KT753649	KT753782	KT753888	KT754013	KT754143
<i>Australaria australasia</i>	Bu	f	MNHN IM-2013-42516	Western Australia	KT753624	KT753757	KT753875	KT753990	KT754120
<i>Benimakia fastigium</i>	Bu	f	FMNH UF-369083	Vanuatu	KT753645	KT753778	–	KT754010	KT754139
<i>Benimakia lanceolata</i>	Bu	f	MNHN IM-2013-11873	Papua New Guinea	KT753593	KT753726	KT753847	KT753959	KT754090
<i>Chryseofusus acherusius</i>	Bu	f	MNHN IM-2013-44302	Taiwan	KT753590	KT753723	KT753844	KT753956	KT754087
<i>Chryseofusus bradneri</i>	Bu	f	MNHN IM-2007-32977	New Caledonia	KT753577	KT753710	KT753833	KT753943	KT754074
<i>Chryseofusus graciliformis</i>	Bu	f	MNHN IM-2007-32797	Solomon Islands	KT753582	KT753715	KT753838	KT753948	KT754079
<i>Chryseofusus graciliformis</i>	Bu	f	MNHN IM-2013-19938	Solomon Sea	KT753597	KT753730	KT753851	KT753963	KT754094
<i>Cinctura hunteria</i>	Bu	f	MCZ 382637	Florida	KT753646	KT753779	KT753887	KT754011	KT754140
<i>Cyrtulus serotinus</i>	Bu	f	MNHN IM-2013-42532	Marchesas Islands	KT753603	KT753736	KT753857	KT753969	KT754099
<i>Dolicholaturus aff. cayohuesonicus</i>	Bu	f	MNHN IM-2013-7917	Guadeloupe	KT753540	KT753673	KT753802	KT753907	KT754037
<i>Dolicholaturus aff. cayohuesonicus</i>	Bu	f	MNHN IM-2013-20291	Guadeloupe	KT753550	KT753683	KT753810	KT753916	KT754047
<i>Dolicholaturus aff. spiceri</i>	Bu	f	MNHN IM-2013-42519	Western Australia	KT753564	KT753697	–	KT753930	KT754061
<i>Dolicholaturus lancea</i>	Bu	f	MNHN IM-2013-16640	Papua New Guinea	KT753572	KT753705	KT753828	KT753938	KT754069
<i>Dolicholaturus sp.</i>	Bu	f	MNHN IM-2009-29739	Western Australia	KT753541	KT753674	KT753803	–	KT754038
<i>Dolicholaturus spiceri</i>	Bu	f	MNHN IM-2013-42515	Western Australia	KT753570	KT753703	KT753826	KT753936	KT754067
<i>Fasciolaria bullisi</i>	Bu	f	FMNH UF-351146	Florida	KT753622	KT753755	KT753874	KT753988	KT754118
<i>Fasciolaria sp.</i>	Bu	f	MNHN IM-2013-55965	French Guyane	KT753626	KT753759	KT753876	KT753992	KT754122
<i>Fasciolaria tulipa</i>	Bu	f	MNHN IM-2013-19559	Guadeloupe	KT753588	KT753721	KT753842	KT753954	KT754085
<i>Filifusus filamentosus</i>	Bu	f	MNHN IM-2013-13107	Papua New Guinea	KT753543	KT753676	KT753805	KT753909	KT754040
<i>Fusinus agatha</i>	Bu	f	MZSP 53680	northeast Brazil	KT753627	KT753760	–	KT753993	–
<i>Fusinus australis</i>	Bu	f	MNHN IM-2013-42512	Western Australia	KT753557	KT753690	KT753816	KT753923	KT754054
<i>Fusinus brasiliensis</i>	Bu	f	MZSP 117595	southeast Brazil	KT753620	KT753753	KT753872	KT753986	KT754116
<i>Fusinus brasiliensis</i>	Bu	f	MZSP 108889	southeast Brazil	KT753640	KT753773	KT753882	KT754005	KT754134
<i>Fusinus colus</i>	Bu	f	MNHN IM-2007-32560	New Caledonia	KT753533	KT753666	KT753796	KT753901	KT754030
<i>Fusinus crassiplicatus</i>	Bu	f	MNHN IM-2007-34663	New Caledonia	KT753551	KT753684	KT753811	KT753917	KT754048
<i>Fusinus excavatus</i>	Bu	f	ANSP A21957	Barbados	KT753634	KT753767	KT753879	KT754000	KT754129
<i>Fusinus filiosus</i>	Bu	f	MNHN IM-2013-42523	Congo	KT753553	KT753686	–	KT753919	KT754050
<i>Fusinus forceps</i>	Bu	f	MNHN IM-2007-38235	Madagascar	KT753574	KT753707	KT753830	KT753940	KT754071
<i>Fusinus gracillimus</i>	Bu	f	MNHN IM-2013-42521	Mozambique	KT753558	KT753691	KT753817	KT753924	KT754055
<i>Fusinus longissimus</i>	Bu	f	MNHN IM-2007-32535	Philippines	KT753534	KT753667	–	–	KT754031
<i>Fusinus mauiensis</i>	Bu	f	FMNH 413989	Hawaii	KT753621	KT753754	KT753873	KT753987	KT754117
<i>Fusinus pulchellus</i>	Bu	f	MCZ 378473	France	KT753630	KT753763	–	KT753996	KT754125
<i>Fusinus salisburyi</i>	Bu	f	MNHN IM-2007-32588	New Caledonia	KT753609	KT753742	KT753863	KT753975	KT754105
<i>Fusinus sandvichensis</i>	Bu	f	FMNH UF-414048	Hawaii	KT753637	KT753770	–	KT754002	KT754131
<i>Fusinus sandvichensis</i>	Bu	f	FMNH 414020	Hawaii	KT753644	KT753777	KT753886	KT754009	KT754138
<i>Fusinus similis</i>	Bu	f	ANSP A20012/411168	Japan	KT753652	KT753785	KT753890	KT754016	KT754146
<i>Fusinus syracusanus</i>	Bu	f	MNHN IM-2013-32440	Tunisia	KT753602	KT753735	KT753856	KT753968	KT754098
<i>Fusinus virginiae</i>	Bu	f	MNHN IM-2007-36654	Madagascar	KT753578	KT753711	KT753834	KT753944	KT754075
<i>Fusolaturus bruijnii</i>	Bu	f	MNHN IM-2013-16671	Papua New Guinea	KT753538	KT753671	KT753800	KT753905	KT754035
<i>Fusolaturus bruijnii</i>	Bu	f	MNHN IM-2013-18013	Papua New Guinea	KT753613	KT753746	KT753867	KT753979	KT754109
<i>Fusolaturus pachyus</i>	Bu	f	MNHN IM-2007-35084	New Caledonia	KT753595	KT753728	KT753849	KT753961	KT754092
<i>Fusolaturus pearsoni</i>	Bu	f	MNHN IM-2007-32495	Vanuatu	KT753555	KT753688	KT753814	KT753921	KT754052
<i>Fusolaturus rikae</i>	Bu	f	MNHN IM-2007-32498	Vanuatu	KT753610	KT753743	KT753864	KT753976	KT754106
<i>Fusolaturus sp.</i>	Bu	f	MNHN IM-2007-38359	Madagascar	KT753573	KT753706	KT753829	KT753939	KT754070
<i>Fusolaturus sp.</i>	Bu	f	MNHN IM-2007-32508	Vanuatu	KT753616	KT753749	KT753870	KT753982	KT754112
<i>Granulifusus aff. kiranus</i>	Bu	f	MNHN IM-2013-19037	Bismarck Sea	KT753600	KT753733	KT753854	KT753966	KT754096
<i>Granulifusus aff. niponicus</i>	Bu	f	MNHN IM-2007-32823	New Caledonia	KT753584	KT753717	–	KT753950	KT754081
<i>Granulifusus bacciballus</i>	Bu	f	MNHN IM-2007-35089	New Caledonia	KT753563	KT753696	KT753822	KT753929	KT754060
<i>Granulifusus benjamini</i>	Bu	f	MNHN IM-2007-32816	New Caledonia	KT753566	KT753699	–	KT753932	KT754063
<i>Granulifusus hayashi</i>	Bu	f	MNHN IM-2013-19210	Bismarck Sea	KT753589	KT753722	KT753843	KT753955	KT754086
<i>Granulifusus niponicus</i>	Bu	f	MNHN IM-2013-19903	Solomon Sea	KT753569	KT753702	–	KT753935	KT754066
<i>Granulifusus sp.</i>	Bu	f	MNHN IM-2013-19724	Bismarck Sea	KT753556	KT753689	KT753815	KT753922	KT754053
<i>Granulifusus sp.</i>	Bu	f	MNHN IM-2009-6658	Solomon Islands	KT753561	KT753694	KT753820	KT753927	KT754058
<i>Granulifusus staminatus</i>	Bu	f	MNHN IM-2007-32750	Philippines	KT753607	KT753740	KT753861	KT753973	KT754103
<i>Hemipolygona armata</i>	Bu	f	MNHN IM-2013-42511	Senegal	KT753608	KT753741	KT753862	KT753974	KT754104
<i>Hemipolygona mcgintyi</i>	Bu	f	MZSP 36166	Florida USA	KT753659	KT753792	–	KT754023	KT754152
<i>Lamellilaturus lamyi</i>	Bu	f	MNHN IM-2013-56511	French Guyane	KT753642	KT753775	KT753884	KT754007	KT754136
<i>Latirolagena smaragdulus</i>	Bu	f	MNHN IM-2007-32547	Vanuatu	KT753598	KT753731	KT753852	KT753964	–
<i>Latirus amplustris</i>	Bu	f	FMNH UF-410623	Kiribati	KT753657	KT753790	KT753894	KT754021	KT754150
<i>Latirus belcheri</i>	Bu	f	MNHN IM-2007-32490	Vanuatu	KT753587	KT753720	–	KT753953	KT754084
<i>Latirus gibbulus</i>	Bu	f	MNHN IM-2007-32544	Philippines	KT753542	KT753675	KT753804	KT753908	KT754039
<i>Latirus pictus</i>	Bu	f	MNHN IM-2013-10540	Papua New Guinea	KT753601	KT753734	KT753855	KT753967	KT754097
<i>Latirus polygonus</i>	Bu	f	MZSP 99782	Djibouti	KT753629	KT753762	KT753878	KT753995	KT754124
<i>Latirus vischii</i>	Bu	f	MNHN IM-2009-15038	south Madagascar	KT753547	KT753680	KT753808	KT753913	KT754044
<i>Leucozonia cerata</i>	Bu	f	MZSP 63825	Ecuador	KT753643	KT753776	KT753885	KT754008	KT754137
<i>Leucozonia nassa brasiliana</i>	Bu	f	MZSP 117596	southeast Brazil	KT753628	KT753761	KT753877	KT753994	KT754123
<i>Leucozonia nassa brasiliana</i>	Bu	f	MZSP 103954	southeast Brazil	KT753648	KT753781	–	KT754012	KT754142

(continued on next page)



Table 1 (continued)

Taxon		Voucher #	Locality	18S rRNA	28S rRNA	16S rRNA	COI	H3	
<i>Leucozonia nassa cingulifera</i>	Bu	f	MZSP 112955	offshore northeast Brazil	KT753655	KT753788	KT753892	KT754019	KT754148
<i>Leucozonia nassa nassa</i>	Bu	f	MNHN IM-2013-20181	Guadeloupe	KT753535	KT753668	KT753797	KT753902	KT754032
<i>Leucozonia nassa nassa</i>	Bu	f	MNHN IM-2007-9388	Guadeloupe	KT753568	KT753701	KT753825	KT753934	KT754065
<i>Leucozonia nassa nassa</i>	Bu	f	MZSP 69365	Dominican Republic	KT753636	KT753769	–	–	–
<i>Leucozonia ocellata</i>	Bu	f	MNHN IM-2013-20444	Guadeloupe	KT753612	KT753745	KT753866	KT753978	KT754108
<i>Leucozonia ponderosa</i>	Bu	f	MZSP 115436	southeast Brazil	KT753654	KT753787	KT753891	KT754018	–
<i>Nodolattirus nodatus</i>	Bu	f	MNHN IM-2013-42534	Austral Islands	KT753539	KT753672	KT753801	KT753906	KT754036
<i>Opeatostoma pseudodon</i>	Bu	f	MZSP 68483	Ecuador	KT753661	–	KT753897	KT754025	–
<i>Peristernia forskalii</i>	Bu	f	MNHN IM-2013-42522	Mozambique	KT753537	KT753670	KT753799	KT753904	KT754034
<i>Peristernia gemmata</i>	Bu	f	MNHN IM-2013-42528	Marchesas Islands	KT753614	KT753747	KT753868	KT753980	KT754110
<i>Peristernia marquesana</i>	Bu	f	MNHN IM-2013-15306	Papua New Guinea	KT753548	KT753681	–	KT753914	KT754045
<i>Peristernia marquesana</i>	Bu	f	MNHN IM-2007-32486	Vanuatu	KT753567	KT753700	KT753824	KT753933	KT754064
<i>Peristernia nassatula</i>	Bu	f	MNHN IM-2007-32487	Vanuatu	KT753579	KT753712	KT753835	KT753945	KT754076
<i>Peristernia nassatula</i>	Bu	f	MNHN IM-2013-18061	Papua New Guinea	KT753591	KT753724	KT753845	KT753957	KT754088
<i>Peristernia reincarnata</i>	Bu	f	MNHN IM-2007-32482	Vanuatu	KT753575	KT753708	KT753831	KT753941	KT754072
<i>Peristernia</i> sp.	Bu	f	MNHN IM-2013-17660	Papua New Guinea	KT753560	KT753693	KT753819	KT753926	KT754057
<i>Peristernia</i> sp.	Bu	f	MNHN IM-2013-10337	Papua New Guinea	KT753580	KT753713	KT753836	KT753946	KT754077
<i>Peristernia</i> sp.	Bu	f	MNHN IM-2013-10336	Papua New Guinea	KT753599	KT753732	KT753853	KT753965	KT754095
<i>Peristernia</i> sp.	Bu	f	MNHN IM-2013-12522	Papua New Guinea	KT753604	KT753737	KT753858	KT753970	KT754100
<i>Peristernia</i> sp.	Bu	f	MNHN IM-2013-13553	Papua New Guinea	KT753611	KT753744	KT753865	KT753977	KT754107
<i>Peristernia</i> sp.	Bu	f	FMNH 457386	Guam	KT753656	KT753789	KT753893	KT754020	KT754149
<i>Pleuroploca trapezium</i>	Bu	f	MNHN IM-2009-15358	south Madagascar	KT753576	KT753709	KT753832	KT753942	KT754073
<i>Pleuroploca trapezium</i>	Bu	f	MNHN IM-2007-32591	Vanuatu	KT753596	KT753729	KT753850	KT753962	KT754093
<i>Polygona angulata</i>	Bu	f	MZSP 112907	northeast Brazil	KT753619	KT753752	KT753871	KT753985	KT754115
<i>Polygona bernadensis</i>	Bu	f	MNHN IM-2013-56077	French Guyane	KT753635	KT753768	–	KT754001	KT754130
<i>Polygona infundibulum</i>	Bu	f	MNHN IM-2013-19591	Guadeloupe	KT753585	KT753718	KT753840	KT753951	KT754082
<i>Pseudolattirus aff. pallidus</i>	Bu	f	MNHN IM-2007-32913	Philippines	KT753586	KT753719	KT753841	KT753952	KT754083
<i>Pseudolattirus discrepans</i>	Bu	f	MNHN IM-2007-34604	Philippines	KT753562	KT753695	KT753821	KT753928	KT754059
<i>Pseudolattirus discrepans</i>	Bu	f	MNHN IM-2007-32791	Solomon Islands	KT753594	KT753727	KT753848	KT753960	KT754091
<i>Pseudolattirus kurodai</i>	Bu	f	MNHN IM-2013-42520	New Caledonia	KT753531	KT753664	–	KT753899	KT754028
<i>Pseudolattirus kuroseanus</i>	Bu	f	MNHN IM-2013-14709	Papua New Guinea	KT753571	KT753704	KT753827	KT753937	KT754068
<i>Pseudolattirus pallidus</i>	Bu	f	MNHN IM-2007-32537	Solomon Islands	KT753544	KT753677	KT753806	KT753910	KT754041
<i>Pseudolattirus</i> sp.	Bu	f	MNHN IM-2007-32510	New Caledonia	KT753565	KT753698	KT753823	KT753931	KT754062
<i>Pustulattirus ogum</i>	Bu	f	MZSP 69481	southeast Brazil	KT753653	KT753786	–	KT754017	KT754147
<i>Pustulattirus praestantior</i>	Bu	f	FMNH UF-359664	west Panama	KT753650	KT753783	–	KT754014	KT754144
<i>Teralattirus noumeensis</i>	Bu	f	MNHN IM-2013-42526	Austral Islands	KT753549	KT753682	KT753809	KT753915	KT754046
<i>Teralattirus noumeensis</i>	Bu	f	MNHN IM-2013-4032	Papua New Guinea	KT753632	KT753765	–	KT753998	KT754127
<i>Teralattirus roboreus</i>	Bu	f	MZSP 108682	Grenada	KT753660	KT753793	KT753896	KT754024	–
<i>Triplofusus giganteus</i>	Bu	f	MCZ 382636	Florida	KT753638	KT753771	KT753880	KT754003	KT754132
<i>Turrillattirus craticulatus</i>	Bu	f	MNHN IM-2007-32504	Vanuatu	KT753554	KT753687	KT753813	KT753920	KT754051
<i>Turrillattirus turritus</i>	Bu	f	MNHN IM-2007-32516	Vanuatu	KT753532	KT753665	–	KT753900	KT754029
<i>Turrillattirus turritus</i>	Bu	f	MNHN IM-2013-17100	Papua New Guinea	KT753615	KT753748	KT753869	KT753981	KT754111
<b><i>Buccinum undatum</i></b>	<b>Bu</b>	<b>b</b>	<b>MCZ 378265</b>	<b>Sweden</b>	<b>KT753631</b>	<b>KT753764</b>	–	<b>KT753997</b>	<b>KT754126</b>
<b><i>Busycyon africanus</i></b>	<b>Bu</b>	<b>b</b>	<b>MNHN IM-2013-42510</b>	<b>Senegal</b>	<b>KT753536</b>	<b>KT753669</b>	<b>KT753798</b>	<b>KT753903</b>	<b>KT754033</b>
<b><i>Euthria cumulata</i></b>	<b>Bu</b>	<b>b</b>	<b>MNHN IM-2007-34931</b>	<b>New Caledonia</b>	<b>KT753583</b>	<b>KT753716</b>	<b>KT753839</b>	<b>KT753949</b>	<b>KT754080</b>
<b><i>Euthria</i> sp.</b>	<b>Bu</b>	<b>b</b>	<b>MNHN IM-2007-34934</b>	<b>New Caledonia</b>	<b>KT753559</b>	<b>KT753692</b>	<b>KT753818</b>	<b>KT753925</b>	<b>KT754056</b>
<b><i>Manaria</i> sp.</b>	<b>Bu</b>	<b>b</b>	<b>MNHN IM-2007-36855</b>	<b>Madagascar</b>	<b>KT753605</b>	<b>KT753738</b>	<b>KT753859</b>	<b>KT753971</b>	<b>KT754101</b>
<b><i>Neptunea antiqua</i></b>	<b>Bu</b>	<b>b</b>	<b>MCZ 378610</b>	<b>Sweden</b>	<b>KT753623</b>	<b>KT753756</b>	–	<b>KT753989</b>	<b>KT754119</b>
<b><i>Prodotia</i> sp.</b>	<b>Bu</b>	<b>b</b>	<b>MNHN IM-2007-34675</b>	<b>New Caledonia</b>	<b>KT753606</b>	<b>KT753739</b>	<b>KT753860</b>	<b>KT753972</b>	<b>KT754102</b>
<b><i>Columbella aureomexicana</i></b>	<b>Bu</b>	<b>c</b>	<b>MCZ 378333</b>	<b>Baja California, Mexico</b>	<b>KT753633</b>	<b>KT753766</b>	–	<b>KT753999</b>	<b>KT754128</b>
<b><i>Mitrella scripta</i></b>	<b>Bu</b>	<b>c</b>	<b>MCZ 378586</b>	<b>southeast France</b>	<b>KT753658</b>	<b>KT753791</b>	<b>KT753895</b>	<b>KT754022</b>	<b>KT754151</b>
<b><i>Nassarius glans</i></b>	<b>Bu</b>	<b>n</b>	<b>MCZ 378603</b>	<b>east Australia</b>	<b>KT753641</b>	<b>KT753774</b>	<b>KT753883</b>	<b>KT754006</b>	<b>KT754135</b>
<b><i>Nassarius reticulatus</i></b>	<b>Bu</b>	<b>n</b>	<b>MCZ 378509</b>	<b>Sweden</b>	<b>KT753617</b>	<b>KT753750</b>	–	<b>KT753983</b>	<b>KT754113</b>
<b><i>Conus angasi</i></b>	<b>Co</b>	<b>c</b>	<b>MCZ 382632</b>	<b>East Australia</b>	<b>KT753663</b>	<b>KT753795</b>	<b>KT753898</b>	<b>KT754027</b>	<b>KT754154</b>
<b><i>Phymorhynchus</i> sp.</b>	<b>Co</b>	<b>r</b>	<b>MCZ 378670</b>	<b>Unknown</b>	<b>KT753662</b>	<b>KT753794</b>	–	<b>KT754026</b>	<b>KT754153</b>
<b><i>Thais nodosa</i></b>	<b>Mu</b>	<b>m</b>	<b>MCZ 378809</b>	<b>Cameroon</b>	<b>KT753639</b>	<b>KT753772</b>	<b>KT753881</b>	<b>KT754004</b>	<b>KT754133</b>
<b><i>Thais speciosa</i></b>	<b>Mu</b>	<b>m</b>	<b>MCZ 378767</b>	<b>Baja California, Mexico</b>	<b>KT753647</b>	<b>KT753780</b>	–	–	<b>KT754141</b>
<b><i>Erosaria erosa</i></b>	<b>Cy</b>	<b>c</b>	<b>MCZ 378355</b>	<b>east Australia</b>	<b>KT753625</b>	<b>KT753758</b>	–	<b>KT753991</b>	<b>KT754121</b>
<b><i>Monetaria annulus</i></b>	<b>Cy</b>	<b>c</b>	<b>MCZ 378587</b>	<b>east Australia</b>	<b>KT753651</b>	<b>KT753784</b>	<b>KT753889</b>	<b>KT754015</b>	<b>KT754145</b>

Bu – Buccinoidea, f – Fascioliariidae, b – Buccinidae, c – Columbellidae, n – Nassariidae, Co – Conoidea, c – Conidae, r – Raphitomidae, Mu – Muricoidea, m – Muricidae, Cy – Cypraeoidea, c – Cypraeidae.

ingroup taxa and 16 outgroups, fragment *b* for 116 and 17, and fragment *c* for 113 and 17.

16S rRNA: This gene was amplified for 94 ingroup and 10 outgroup terminals in a single amplicon between 505–520 bp.

COI: Amplified for 113 ingroup and 16 outgroup terminals in a single amplicon using a combination of different primer pairs. It showed no length variation among all sampled specimens (658 bp analyzed), being analyzed as a single fragment.

Histone H3: A single amplicon was amplified for 110 ingroup and 17 outgroup specimens. It was analyzed in a single fragment without variation in length among individuals sequenced (328 bp).

### 2.3. Phylogenetic analyses

Maximum likelihood (ML) and Bayesian inference (BI) analyses were conducted on static alignments using MUSCLE v.3.6 (Edgar, 2004) as implemented in the Geneious v.8.1.2 platform. In order to confirm codon position of protein encoding genes COI and histone H3, their sequences were translated into amino acids using the Geneious v.8.1.2 platform.

ML analysis was conducted using RAxML v.8.2.X (Stamatakis, 2014) on the complete dataset. For the ML searches, the General Time Reversible model with a discrete gamma distribution of



**Table 2**

List of primer sequences utilized for amplification and sequencing with original references, indicating primer pairs and optimal annealing temperatures used.

Primer	Sequence	Reference	Primer pairs	Annealing temp	
18S	1F	5'-TACCTGGTTGATCTGCCAGTAG-3'	Forward	1F/4R	43–45 °C
	4R	5'-GAATTACCGCGGCTGCTGG-3'	Reverse		
	3F	5'-GTTTCGATTCGGAGAGGGA-3'	Forward	3F/bi	
	bi	5'-GAGTCTCGTTTCGTTATCGGA-3'	Reverse		
	a2.0	5'-ATGGTTGCAAAGCTGAAAC-3'	Forward	a2.0/9R	
	9R	5'-GATCCTCCGAGTTCACCTAC-3'	Reverse		
28S	Rd1a	5'-CCSCGTAAYTTAGGCATAT-3'	Forward	Rd1a/Rd4b	47 °C
	Rd4b	5'-CCTTGGTCCGTTTCAAGAC-3'	Reverse	ZX1 f/Rd4b	47–64 °C
	ZX1 f	5'-ACCGCTGAATTTAAGCATAT-3'	Forward		62–64 °C
	A	5'-GACCCGCTTGAAGCACGGA-3'	Forward	A/Rd5b	44–45 °C
	Rd5b	5'-CCACAGCGCCAGTTCTGCTTAC-3'	Reverse		
	Rd 4.8a	5'-ACCTATTCTCAAACCTTAAATGG-3'	Forward	Rd 4.8a/Rd7b1	44–45 °C
	Rd7b1	5'-GACTTCCCTTACCTACAT-3'	Reverse		
16S	a	5'-CGCCTGTTTATCAAAAACAT-3'	Forward	a/b	44–48 °C
	b	5'-CTCCGGTTTGAACCTCAGATCA-3'	Reverse		
COI	LCO1490	5'-GGTCAACAATCATAAAGATATTGG-3'	Forward	LCO1490/HCO2198	45 °C
	HCO2198	5'-TAAACTTCAGGGTGACCAAAAAATCA-3'	Reverse		
	HCOout	5'-CCAGGTAAAATTAATAAATAAATTC-3'	Reverse	LCO1490/HCOout	44–45 °C
	jgLCO1490	5'-TITCIACIAAYCAYARGAYATTGG-3'	Forward		
	jgHCO2198	5'-TAIACYTCIGGRTGICCRARAAYCA-3'	Reverse		
H3	H3af	5'-ATGGCTCGTACCAAGCAGACVGC-3'	Forward	H3af/H3ar	47 °C
	H3ar	5'-ATATCTTRGGCATRATRTGTGAC-3'	Reverse		

site-rate heterogeneity ( $GTR + \Gamma$ ) was specified for each individual gene. Nodal support was estimated via 1000 replicates of a rapid bootstrapping algorithm (Stamatakis et al., 2008) using the GTR-GAMMA model, via the Cyber infrastructure for Phylogenetic Research (CIPRES) portal (Miller et al., 2010). Bootstrap resampling frequencies were thereafter mapped onto the optimal tree from the independent searches.

In order to assess the monophyly of Fasciolariidae, a constrained phylogeny was generated by RAXML, and site-wise log-likelihoods were calculated for the best tree topology and for the constrained tree with fasciolariid monophyly. These values were used in CONSEL v.0.1.j (Shimodaira and Hasegawa, 2001) to calculate the probabilities according to the approximately unbiased test (AU; Shimodaira, 2002), the Kishino–Hasegawa test (KH; Kishino and Hasegawa, 1989), and the Shimodaira–Hasegawa test (SH; Shimodaira and Hasegawa, 1999).

A Bayesian inference analysis was conducted using MrBayes v.3.2.5 (Ronquist et al., 2012) with a unique model of sequence evolution with corrections for a discrete gamma distribution and/or a proportion of invariant sites ( $GTR + \Gamma + I$ ) on each partition, as selected in jModelTest 2 v.2.1.7 (Guindon and Gascuel, 2003; Durrin et al., 2012) as implemented in the CIPRES gateway (Miller et al., 2010). Default priors were used starting with random trees and three runs, each with three hot and one cold Markov chains, were conducted until the average deviation of split frequencies reached <0.01 (7,000,000 generations). Stationarity was checked using Tracer v.1.6 (Rambaut et al., 2014). After the burn-in of 25% samples was discarded, a majority-rule consensus topology was generated from the sampled trees.

### 3. Results

The ML analysis of the concatenated genes (133 specimens in total) resulted in a tree topology with a  $-\ln L = 50219.14$  (Fig. 1). The BI analysis ( $-\ln L = 102047.8$  for run1;  $-\ln L = 102507.2$  for run2) recovered a topology highly congruent with that of the ML analysis (Fig. 2).

Leaving aside *Dolicholaturus/teralaturus*, both analyses recovered three major well-supported deep clades of Fasciolariidae, but none of these correspond to the traditional contents of the recognized subfamilies. A first split divides fasciolariids into a clade mostly

corresponding to Fusiniinae, but also including the clearly non-monophyletic genus *Pseudolaturus* (BS = 87%; PP = 1.00) – traditionally classified in the Peristerniinae (BS = 99%; PP = 1.00). As it includes *Fusinus colus* (Linnaeus, 1758), the type species of *Fusinus* (type genus of Fusiniinae), we will refer to this clade as the *Fusinus colus* clade. Fasciolariinae, which appears monophyletic, is nested within a subclade of Fasciolariinae + Peristerniinae (BS = 99%; PP = 1.00); as it includes *Fasciolaria tulipa* (Linnaeus, 1758), the type species of *Fasciolaria* (type genus of Fasciolariinae), we will refer to it as the *Fasciolaria tulipa* clade. Finally, its sister group is a clade containing various taxa of Peristerniinae (BS = 95%; PP = 1.00); as it includes *Peristernia nassatula* (Lamarck, 1822), the type species of *Peristernia* (type genus of Peristerniinae), we will refer to it as the *Peristernia nassatula* clade.

A clade containing *Dolicholaturus* and *teralaturus* was highly supported (BS = 100%; PP = 1.00). Its position varied in the ML and BI analyses, but in neither of them did it appear as a sister group to, or nested within, the remaining fasciolariids. The ML analysis for the constrained tree (fasciolariid monophyly) resulted in a tree topology with a  $-\ln L = 50257.70$ , and the probability values (AU, KH and SH) calculated in CONSEL showed no significant statistical difference between the relaxed ML tree and the constrained tree.

Single ML gene trees obtained from 16S rRNA (104 sequences) displayed the same overall topology but with less resolution in the internal nodes. Gene trees from 18S rRNA (133 sequences), 28S rRNA (132 sequences) and COI (129 sequences) displayed rival topologies with many outgroup taxa nested within Fasciolariidae, and low nodal support as initially expected. Histone H3 is a conserved gene that generated a tree with short branch lengths for closely related species and low support for nodes. Individual ML trees are available in Supplementary Material Figs. S1–S5.

### 4. Discussion

This study presents the first comprehensive molecular phylogenetic analysis using combined sequences from nuclear and mitochondrial genes to infer the relationships of Fasciolariidae. None of the three traditionally recognized subfamilies (Fasciolariinae, Fusiniinae and Peristerniinae) was recovered with their currently accepted contents. The taxa currently included in Peristerniinae appeared among all three major lineages: the *Peristernia nassatula*

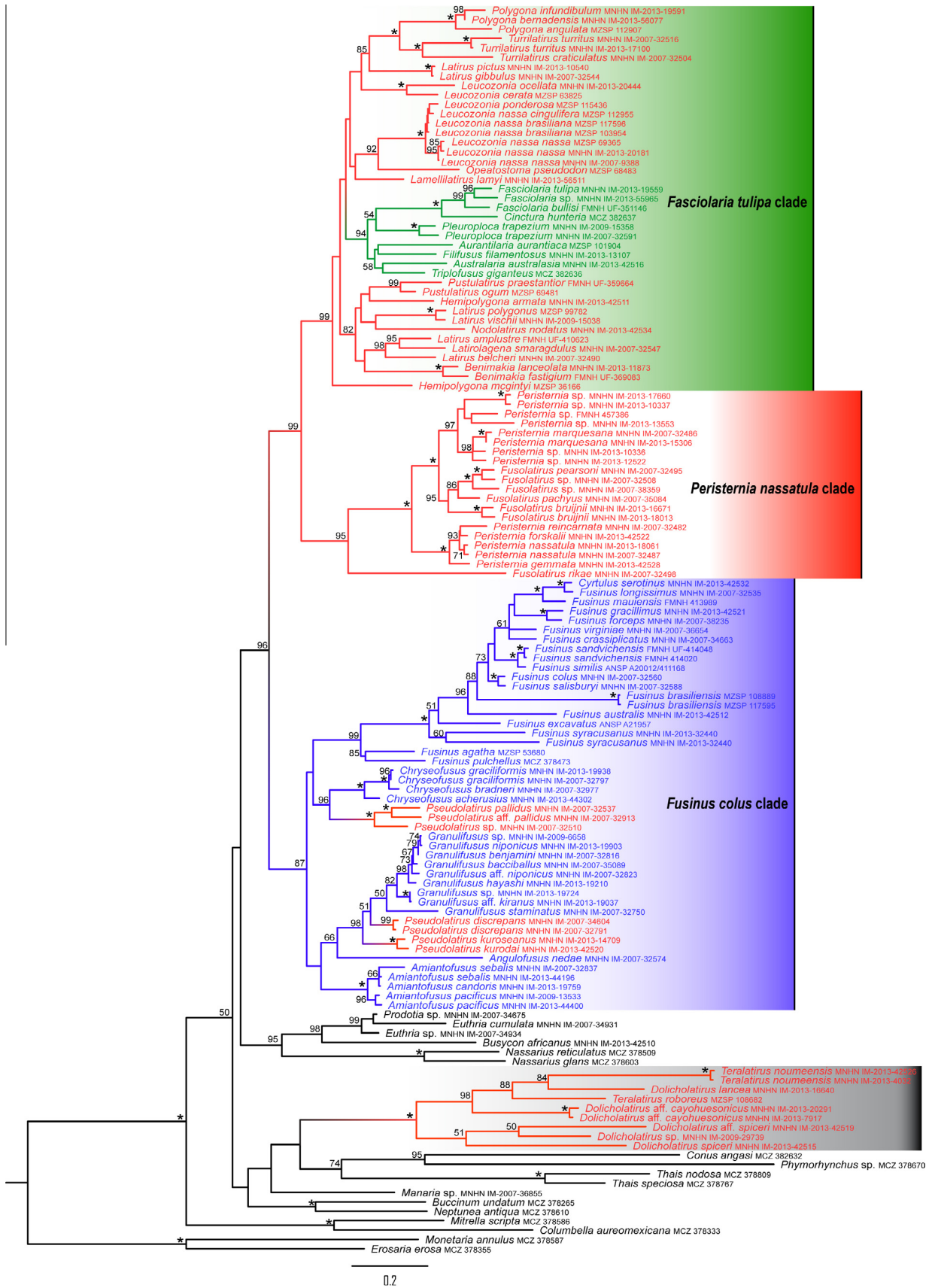


**Fig. 1.** Phylogenetic relationships of Fasciolariidae based on maximum likelihood analysis of five genes (–lnL = 50219.139606). Numbers on nodes indicate bootstrap resampling, only bootstraps over 50 are shown, \* indicate BS = 100%. Color of taxon names indicates traditional subfamily placement (green: Fasciolariinae; blue: Fusiniinae; red: Peristeriinae). (For interpretation of the references to color in this figure legend, the reader is referred to the web version of this article.)

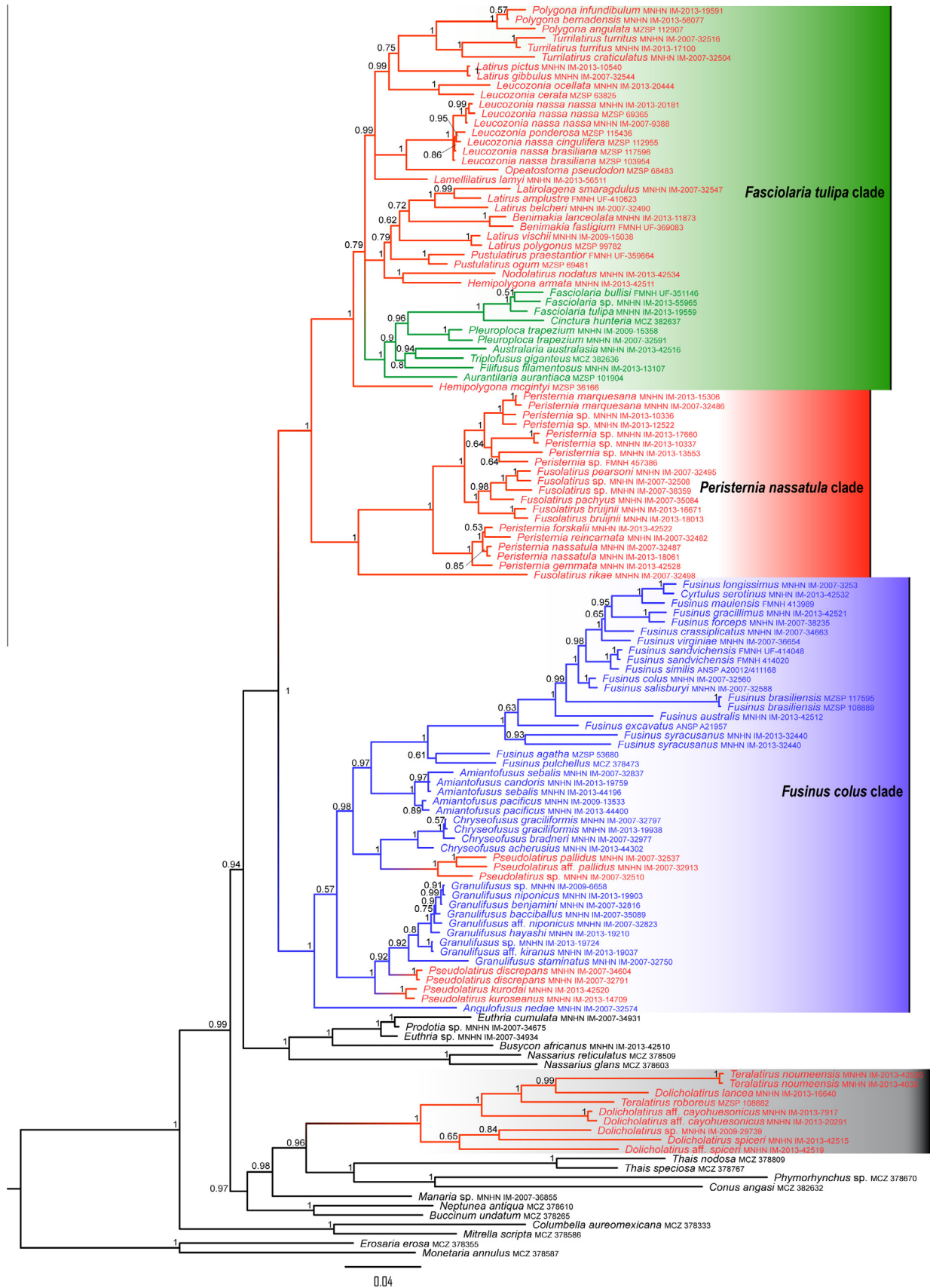


**Fig. 2.** Phylogenetic relationships of Fascioliariidae based on Bayesian inference analysis of five genes. Numbers on nodes indicate posterior probabilities, only posterior probabilities over 0.5 are shown. Color of taxon names indicates traditional subfamily placement (green: Fascioliariinae; blue: Fusiniinae; red: Peristeriinae). (For interpretation of the references to color in this figure legend, the reader is referred to the web version of this article.)



clade (containing *Peristernia* and *Fusolatirus*); the *Fusinus colus* clade (containing *Pseudolatirus*); and a more derived *Fasciolaria tulipa* clade (containing *Polygona*, *Turrilatirus*, *Leucozonina*, *Opeatosoma*, *Lamellilatirus*, *Pustulatirus*, *Hempolygona*, *Nodolatirus*, *Benimakia*, and the clearly polyphyletic *Latirus*).

Our study demonstrates the monophyly of a clade containing *Dolicholatirus* and *Teralatirus* (BS = 100%; PP = 1.00) (Fig. 3). Its position as the sister group to the remaining fascioliids remains uncertain, as the tests could not statistically discriminate between the constrained and unconstrained topologies. *Dolicholatirus* and *Teralatirus* are small buccinoids with distinctive shell characters, whose taxonomic position in Fascioliidae is ambiguous, although currently generally accepted (e.g., Snyder, 2003). Originally established (Bellardi, 1884) as a section of *Latirus* for two fossil species, the genus *Dolicholatirus* was attributed to Fascioliidae without any arguments or analysis, obviously on the basis of its fusiform shell superficially resembling many fascioliids, although the presence of paired weak columellar plaits (uncommon in Fascioliidae) was mentioned. Cossmann (1901) raised *Dolicholatirus* to full genus, designated the type species (*Turbinella bronni* Micheliotti, 1847) and classified it in the family Fusidae [which Cossmann used in place of Fascioliidae], subfamily Fusinae, also without providing supporting arguments. Subsequently, almost half of the genera included in Cossmann's Fusinae have since been transferred to other families of Neogastropoda (*Columbarium*, now Columbarinae, Turbinellidae; *Exilia*, now Ptychactractidae; *Thersitea*, now Thersiteidae; *Euthriofusus*, now Buccinidae). Thiele (1929) reverted to *Dolicholatirus* as a section of *Latirus*, still included in the family Fascioliidae, a position followed by Wenz (1943) and finally by Snyder (2003; but see Vermeij and Snyder, 2006). Thus the current inclusion of *Dolicholatirus* in the Fascioliidae goes back to Bellardi (1884) and is uncritically based on shell characters. Abbott (1958) was the first to examine the radula of *D. cayohuesonicus* (Sowerby II, 1878) and found it to be “the most highly modified of the Fascioliidae radulae, and somewhat resembl[ing] those of Vasidae.” Based on the shape of the egg capsules and differences in radula and shell morphology, Vermeij and Snyder (2006) argued that *Dolicholatirus* likely belongs to Turbinellidae, a view followed by Beu (2011). Simone et al. (2013) pointed out the similarities between *Dolicholatirus* and *Teralatirus*, and suggested that most likely these should be better placed together, a hypothesis confirmed here as *Teralatirus* nests within *Dolicholatirus*. Nevertheless Simone et al. (2013) followed a conservative approach with regard to the classification of *Dolicholatirus/Teralatirus* and no changes were made.

In our current phylogeny, the two Indo-Pacific *T. noumeensis* and *D. lancea* are the sister group to the Australian *T. roboreus*, and these are the sister group to *D. cayohuesonicus*, which in turn are the sister clade to the Caribbean *D. spiceri*. The genus *Dolicholatirus* is therefore paraphyletic with respect to *Teralatirus*, which is also non-monophyletic. The similarity of the radula of *Crassicantharus norfolkensis* illustrated by Ponder (1972: Fig. 14) suggests that *Crassicantharus* may belong in the same clade.

A *Dolicholatirus* sp. (Fig. 3C) from western Australia is nested in the same clade (BS = 51%; PP = 0.65). The radular morphology of another *Dolicholatirus* sp. (Fig. 3D) is virtually identical to that of *D. cayohuesonicus* (Fig. 3E) and *T. roboreus* figured by Simone et al. (2013: Figs. 31–34). This characteristic radula type likely occurs within all species in this clade (A radula of *Dolicholatirus* was supposedly figured by Bandel (1984), however we suspect a misidentification as this radula does not match our own observations [bicuspidate laterals, internal cusp hook-like], and we believe Bandel's specimen to have been a buccinid instead).

At least one species of *Teralatirus*, *T. roboreus* has conflicting characters in favor and against its inclusion in Fascioliidae (Simone et al., 2013). It has salivary ducts attached to the anterior esophagus, the retractor muscle of the proboscis in a single beam,

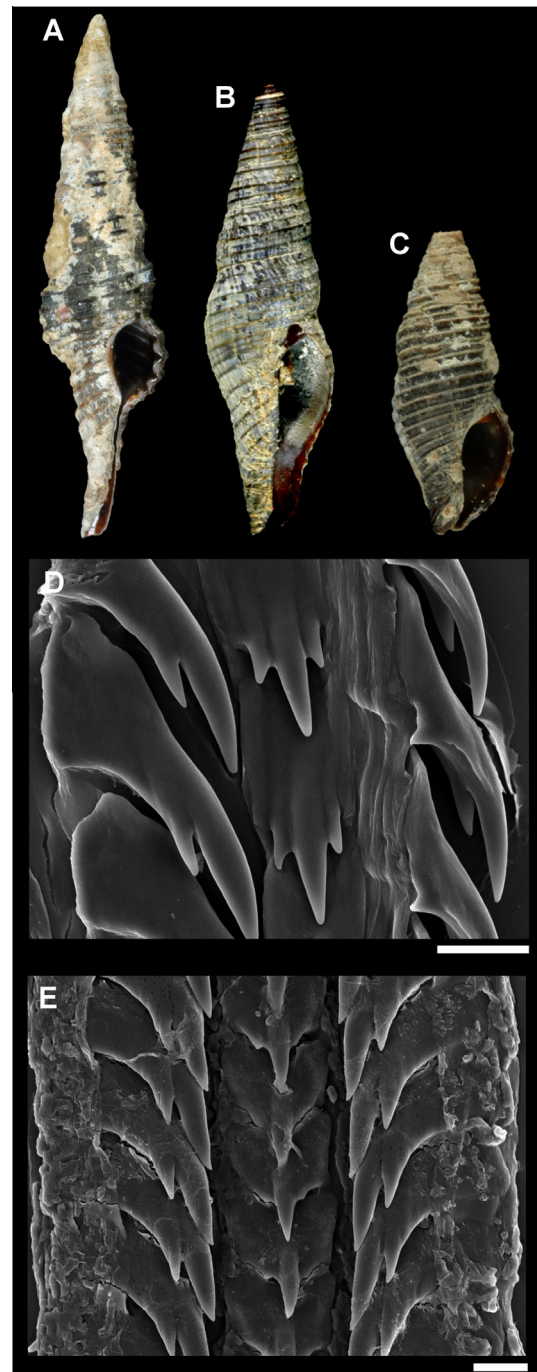


**Fig. 3.** Vouchers of sequenced non-Fascioliidae specimens and radulae: A: *Dolicholatirus lancea*, MNHN IM-2013-16640, Papua New Guinea; B: *Dolicholatirus spiceri*, MNHN IM-2013-42515, Mozambique; C: *Dolicholatirus* sp., MNHN IM-2009-29739, Western Australia; D: radula of *Dolicholatirus cayohuesonicus*, MNHN IM-2013-20291, Guadeloupe; E: radula of *Dolicholatirus* sp., MNHN IM-2009-29739, Western Australia. Scale bars = 10  $\mu$ L.

and a simple stomach, which are fascioliid-like characters; however, its radula, the lack of gland of Leiblein, and the huge esophageal gland are not. In conclusion, although the molecular results do not reliably establish their position outside the remaining fascioliids, *Dolicholatirus* and *Teralatirus* form a monophyletic group and there is strong morphological evidence suggesting a non-fascioliid position.

For the ML analysis, deep nodes were unresolved and/or weakly supported in all major outgroups sampled, resulting in conflicting

topologies with the BI analysis. Perhaps phylogenomic analyses will be able to recover this part of the Neogastropoda tree with high support, as is usually the case with deep nodes in mollusks (Kocot et al., 2011; Smith et al., 2011; Zapata et al., 2014; Goodheart et al., 2015).

#### 4.1. The *Fasciolaria tulipa* clade

Vermeij and Snyder (2006) considered Fascioliariinae as derived from early peristerniines and that the two groups are part of a single clade Fascioliariinae; Snyder et al. (2012) noted that the subfamilies are morphologically similar. Our analysis confirmed that fascioliariines (Fig. 4) are a clade derived from a group of Peristerniinae (BS = 94%; PP = 1.00). Historically, most members of this clade have been assigned to the genera *Fasciolaria* or *Pleuroploca*. However, Snyder et al. (2012), after a thorough re-examination of their taxonomy, proposed several additional genera. Species with broad axial ribs and nodose spiral sculpture appear first as several lineages among members of this clade (*Aurantilaria aurantiaca*, *Filifusus filamentosus*, *Australaria australasia*, *Triplofusus giganteus* and *Pleuroploca trapezium* – all traditionally in the genus *Pleuroploca*); while *Fasciolaria* and *Cinctura* (BS = 100%; PP = 1.00) represent a Caribbean lineage with obsolete axial sculpture and weakly convex spiral whorls (Fig. 4B). Vermeij and Snyder (2002, 2006) revised the taxonomy of many *Latirus* and related genera, elevated previous subgenera to genus rank (e.g., *Polygona*, *Hemipolygona*) and described new ones (e.g., *Turrilatirus*, *Pustulatirus*). Genus-level taxonomy and phylogenetic relationships of this group have been problematic, with names such as *Latirus* and *Leucozonia* applied

indiscriminately. Fascioliariinae and Peristerniinae have a long history of divergence from the Cretaceous (~140 Mya) but diversifying extensively during the Neogene (24 Mya to the present) (Vermeij and Snyder, 2006). In our study, many deep relationships within this clade received little or no support and are incongruent between the ML and BI analyses. However, all genera, with the exception of *Hemipolygona* (represented by *H. mcgintyi* and *H. armata*), are monophyletic and have high support (*Pustulatirus* [BS = 99%; PP = 1.00], *Benimakia* [BS = 100%; PP = 1.00], *Polygona* [BS = 100%; PP = 1.00], *Turrilatirus* [BS = 100%; PP = 1.00]).

A supported clade (BS = 82%; PP = 1.00) grouped species that were historically associated to *Latirus* (*Latirus*, *Benimakia*, *Pustulatirus*, *Hemipolygona*, *Nodolatirus*) (Fig. 4C–F), including notably a clade with *Latirus amplustre* and *Latirolagena smaragdula* (BS = 95%; PP = 0.99). *Latirolagena smaragdula* and *Latirus amplustre* grouped with *Latirus belcheri* with high support (BS = 99%; PP = 1.00).

The clade consisting of *Leucozonia nassa* and *L. ponderosa* was strongly supported (BS = 100%; PP = 1.00), but the genus was not monophyletic. *Leucozonia nassa* is a widely distributed species occurring from southeastern Brazil to North Carolina, including records from several locations in the Caribbean. Three distinct forms can be identified, which correspond to three subspecies *sensu* Abbott (1958) and Vermeij and Snyder (2002), or three species *sensu* Vermeij (1997): the typical *L. nassa nassa* which occurs in Caribbean islands and from North Carolina to Florida and the Gulf of Mexico; *L. nassa cingulifera*, found offshore in NE Brazilian waters, off Bahia and the islands of Fernando de Noronha and Atol das Rocas; and *L. nassa brasiliana*, from the SE to NE Brazilian coast.

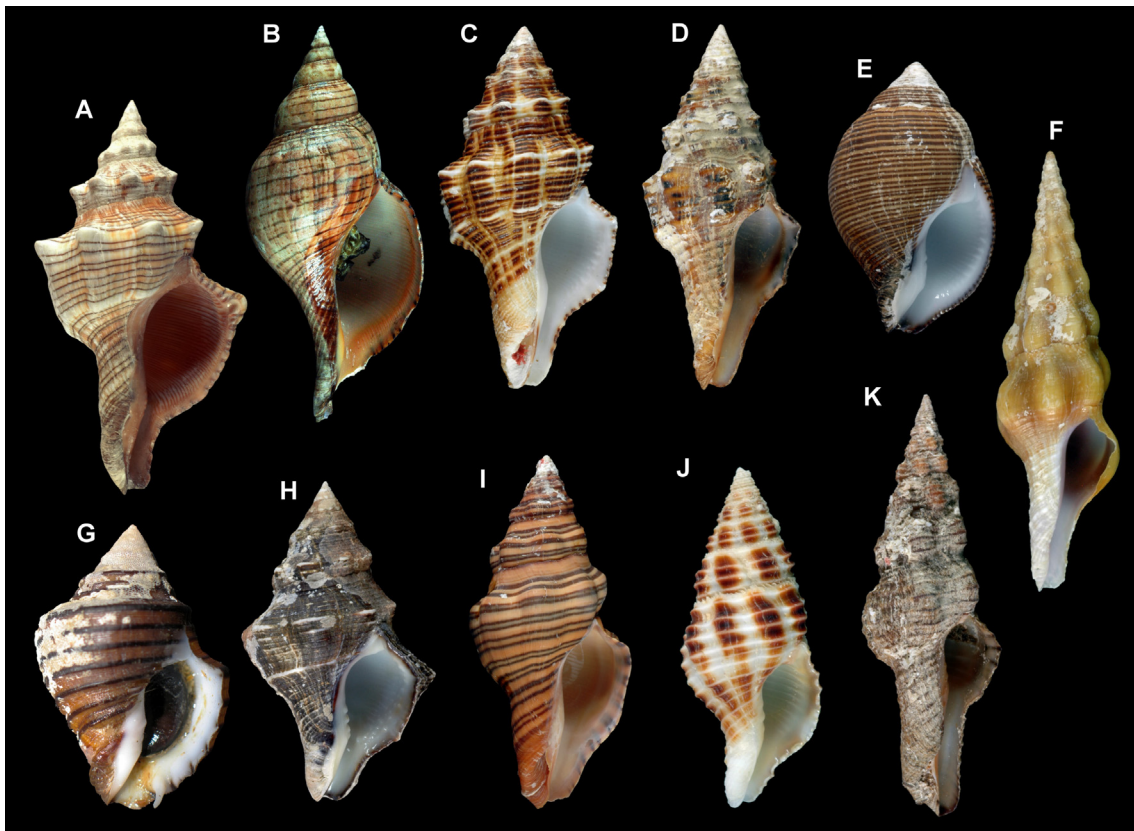


**Fig. 4.** Vouchers of sequenced specimens of Fascioliariidae: A: *Pleuroploca trapezium*, MNHN IM-2007-32591, Vanuatu; B: *Fasciolaria tulipa*, MNHN IM-2013-19559, Guadeloupe; C: *Latirus vischii*, MNHN IM-2009-15038, south Madagascar; D: *Latirus belcheri*, MNHN IM-2007-32490, Vanuatu; E: *Latirolagena smaragdulus*, MNHN IM-2007-32547, Vanuatu; F: *Benimakia lanceolata*, MNHN IM-2013-11873, Papua New Guinea; G: *Opeatostoma pseudodon*, MZSP 68483, Ecuador; H: *Leucozonia nassa nassa*, MNHN IM-2013-20181, Guadeloupe; I: *Latirus gibbulus*, MNHN IM-2007-32544, Philippines; J: *Turrilatirus craticulatus*, MNHN IM-2007-32504, Vanuatu; K: *Polygona infundibulum*, MNHN IM-2013-19591, Guadeloupe.



Shell characters alone may be insufficient to allow unambiguous separation among the various forms (Vermeij and Snyder, 2002). Due to overlapping geographic ranges and the presence of intermediate forms, *L. nassa* is recognized as a single species (WoRMS, 2016). *Leucozonia ponderosa* was described by Vermeij and Snyder (1998) as endemic to Trindade Island, SE Brazil, while Vermeij and Snyder (2002) argued that it may be a local variant of the widespread *L. nassa* “with the hope that molecular investigations resolve this issue”. Couto and Pimenta (2012) examined several specimens from both *L. ponderosa* and *L. nassa* and found no anatomical variation among them; however, they distinguished the species by their unique shell morphology.

In our study, we had representatives of all three geographical subspecies of *Leucozonia nassa*, and they grouped as a single well supported clade (BS = 100%; PP = 1.00). *Leucozonia ponderosa* appeared as sister to *L. nassa cingulifera* from the Fernando de Noronha Archipelago, NE Brazil. These insular species grouped with the coastal SE Brazilian *L. nassa brasiliensis*, a clade that is sister group to the three Caribbean specimens corresponding to *L. nassa*. The Caribbean clade was highly supported in both ML and BI analysis (BS = 95%; PP = 1.00), albeit the other nodes within this group received weak support and conflicting topologies among analyses.

*Opeatostoma pseudodon* is the sister group to the western Atlantic *Leucozonia nassa* complex clade with high support (BS = 92%; PP = 1.00) (Fig. 4G and H). The radula of *Opeatostoma pseudodon* has similar lateral tooth morphology to other *Leucozonia* species. Bullock (1974) called attention to the fact that the shell of the Indo-Pacific *Latirus gibbulus*, the type of the genus, has features – notably its radula – that suggest affinity with species now classified in *Leucozonia*, rather than with the other species of *Latirus*. The radula of the species of *Latirus* and related genera (e.g., *Polygona*, *Turrilatirus*) has a small denticle on the inner side of the laterals, but this is reduced or absent in species of *Leucozonia* and *Opeatostoma*.

*Latirus gibbulus* (Fig. 4I) is grouped with *L. pictus* (BS = 100%; PP = 1.00), and *Leucozonia ocellata* with *L. cerata* (BS = 100%; PP = 1.00). However, deeper nodes are incongruent and have little support for their position among the other major lineages. Like the clade of *Leucozonia* + *Opeatostoma*, their radulae are similar because *L. nassa* and *O. pseudodon* lack the small denticle on the inner side of the lateral teeth.

Lyons (1991) suggested that, if *L. gibbulus* proves to be allied with *Leucozonia*, *Leucozonia* will become a junior synonym of *Latirus* and many species classified in *Latirus* will have to be re-classified. While *L. gibbulus* is in fact allied to *Polygona* and *Turrilatirus* (BS = 85%; PP = 0.75), *Leucozonia* is not monophyletic so *L. ocellata* and *L. cerata* must be placed in a different genus. On the same note, *Latirus* proved to be polyphyletic, comprising three distinct lineages: (1): *Latirus gibbulus* + *L. pictus*, (2): *L. amplustre* + *L. belcheri* + *Latirolagena smaragdulus* (BS = 98%; PP = 1.00) and (3): *Latirus polygonus* + *L. vischii* (BS = 100%; PP = 1.00).

*Latirus gibbulus* + *L. pictus* received support with (*Polygona* + *Turrilatirus*) in the ML tree (BS = 85%) (Fig. 4J and K). Several authors have recognized informal groups within *Polygona* (Lyons, 1991; Vermeij and Snyder, 2006; Vermeij and Snyder (2006) also grouped species of *Polygona* into two groups but opted against giving them formal status in view of the “absence of more definitive molecular evidence”. The first group with *Polygona infundibulum* and the second with *P. angulata*. In our analyses, *Polygona infundibulum* grouped with *P. bernadensis* (BS = 100%; PP = 1.00), while this clade is sister group to *P. angulata*; although a more thorough sampling of *Polygona* species is desirable, these groups concur with those recognized by Vermeij and Snyder (2006) and may indeed justify formal separation, possibly as subgenera.

#### 4.2. The *Peristernia nassatula* clade

The genera *Peristernia* and *Fusolatirus* have strong support, both in the ML and BI analysis (BP = 95%; PP = 1.00) (Fig. 5) and in radular features, confirming the distinctiveness of the subfamily Peristerniinae.

*Peristernia nassatula* (type species of the genus) forms a well-supported clade with *P. forskalii*, *P. reincarnata* and *P. gemmata* (BS = 100%; PP = 1.00) (Fig. 5A–C); *Peristernia marquesana* clustered with several related and possibly new species with high support (BS = 97%; PP = 1.00), and this clade is sister to some species of *Fusolatirus* (BS = 100%; PP = 1.00). Because *Peristernia* is paraphyletic, the species in the clade of *P. marquesana* will have to be classified in a new genus. Vermeij (2001) assigned *P. marquesana* to the genus *Benimakia*; however *B. fastigium* and *B. lanceolata* cluster in the *Fasciolaria tulipa* clade.

The clade including *Peristernia marquesana* and its closest relatives is supported in both analysis (Fig. 5D–F), and it likely includes species related to *P. ustulata* (<https://science.mnhn.fr/institution/mnhn/collection/im/item/2000-6506>) and *P. lyrata* (see Poppe (2008: 108–109) for the illustration of several forms). All four sequenced specimens in this clade have a dark spot in the siphonal canal and a pseudo-umbilicus, as well as varying degree of coloration of the spire. The genus *Peristernia* and its allies have not been the subject of taxonomical revisions, and several species (e.g., Fig. 5E and F) are most likely new to science.

The genus *Fusolatirus* (Fig. 5G and H) appeared diphyletic. *Fusolatirus rikae* is the sister taxon to *Peristernia* and all other *Fusolatirus* species (BS = 100%; PP = 1.00), and a clade nested within *Peristernia* comprises *Fusolatirus pearsoni*, *F. pachyus* and *F. bruijnii* (BP = 95%; PP = 1.00). Snyder and Bouchet (2006) considered *Fusolatirus* a valid genus of peristerniine fascioliids with long siphonal canal, imbricated subsutural spiral ridge and *Peristernia*-like radula. In fact all radulae of *Peristernia* and *Fusolatirus* figured in the literature (e.g., Bandel, 1984; Taylor and Lewis, 1995; Kosyan et al., 2009 [*Peristernia*]; Snyder and Bouchet, 2006 [*Fusolatirus*]) have *Peristernia*-like radula, with the lateral teeth with alternating smaller and larger cusps, while in other Fascioliariidae the lateral teeth have regular cusp sizes.

#### 4.3. The *Fusinus colus* clade

The clade containing all members of Fusiniinae is monophyletic and highly supported (BS = 87%; PP = 1.00) (Fig. 6), with five major groups corresponding roughly to the five genera *Fusinus* (BS = 99%; PP = 1.00), *Amiantofusus* (BS = 100%; PP = 1.00), *Granulifusus* (BS = 50%; PP = 1.00), *Chryseofusus* (BS = 100%; PP = 1.00) and *Angulofusus* (monotypic). The genus *Pseudolatirus*, previously assigned to Peristerniinae, is polyphyletic and nested in two of these groups. However, due to the low support and incongruence of deeper nodes, the relationships among them are not well resolved. Vermeij and Snyder (2002) suggested that fusinines are a stem-group distinguished from the other subfamilies by the absence of columellar folds. Shells of fusinine generalized morphology extend back to the early Cretaceous and probably represent the plesiomorphic shell type of Neogastropoda (Harasewych, 1990; Riedel, 2000).

The central Pacific species *Cyrtulus serotinus* is endemic to the Marquesas Archipelago in French Polynesia, being the only species of the genus. The shape of its shell is unique within fusinines, with a last whorl embracing the earlier whorls, accompanied by a loss of ornamentation. Grabau (1907), in his article about ontogenetic variation, noted that “no one can distinguish the young of *Cyrtulus serotinus* from that of any member of the *Fusus* series (. . .). Nevertheless, it remains true that *Cyrtulus serotinus* is a derivation of

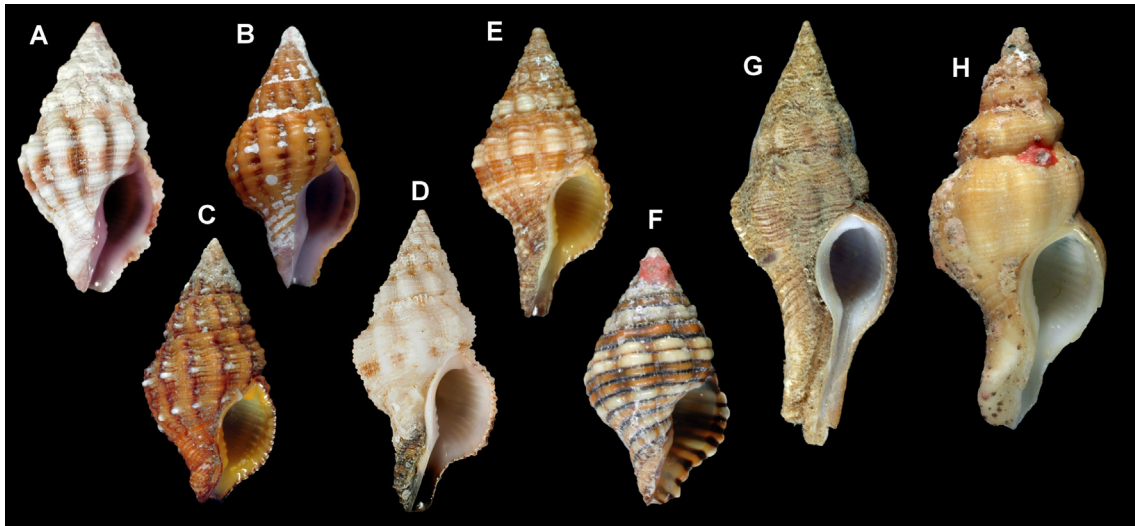


**Fig. 5.** Vouchers of sequenced specimens of Fascioliariidae: Peristerniinae clade. A: *Peristernia nassatula*, MNHN IM-2007-32487, Vanuatu; B: *Peristernia reincarnata*, MNHN IM-2007-32482, Vanuatu; C: *Peristernia gemmata*, MNHN IM-2013-42528, Marquesas Islands; D: *Peristernia marquesana*, MNHN IM-2007-32486, Vanuatu; E: *Peristernia* sp., MNHN IM-2013-12522, Papua New Guinea; F: *Peristernia* sp., MNHN IM-2013-10337, Papua New Guinea; G: *Fusolaturus bruijnii*, MNHN IM-2013-18013, Papua New Guinea; H: *Fusolaturus pachyus*, MNHN IM-2007-35084, New Caledonia.

modern *Fusus*." It is clear that this species is a *Fusinus* (*Fusus*, sensu Grabau (1907)) if one takes a look at a growth series (Fig. 6A and B). This species, nested within *Fusinus*, is sister to the Philippine *Fusinus longissimus* (BS = 100%; PP = 1.00). We thus agree with Grabau (1907) and consider *Cyrtulus serotinus* as part of the genus *Fusinus*, albeit highly derived.

*Amiantofusus* (Fig. 6E) was described to accommodate deep-water species that possess shells that are strikingly similar to Buccinidae, but with unique protoconch morphology and fascioliariid-like radula and soft-part morphology (Fraussen et al., 2007). In our analyses, the genus was strongly supported in both analyses (BS = 100%; PP = 1.00), but the relationship with other Fusininae proved controversial. In the BI analysis, *Amiantofusus* is sister group to *Fusinus* (PP = 0.97) and this clade is in turn sister group to *Chryseofusus* + *Pseudolaturus* (PP = 0.98); (*Amiantofusus* + *Fusinus* + *Chryseofusus* + *Pseudolaturus*) is sister group to *Granulifusus* + *Pseudolaturus* (PP = 0.57); and *Angulofusus* is a basal group to all the remaining fusinines (PP = 0.57). In the ML analysis, *Amiantofusus* is the sister genus to (*Granulifusus* + *Pseudolaturus* + *Angulofusus*), albeit unsupported (BS = 33%), while this group is sister group to the remaining fusinines (BS = 44%).

In our phylogeny, *Chryseofusus* (Fig. 6F), is monophyletic and highly supported (BS = 100%; PP = 1.00), forming a clade with the *Pseudolaturus pallidus* complex in both analyses (BS = 96%; PP = 1.00).

The genus *Pseudolaturus* is currently classified in Peristerniinae (Snyder, 2003), however, Stahlschmidt and Fraussen (2012) noted that the type species is conchologically more similar to those of the subfamily Fusininae rather than to Peristerniinae, which is confirmed in the present study. *Pseudolaturus* proved non-monophyletic in our analysis, as it forms two main clades nested within the Fusininae. The lineage of *Pseudolaturus* that is sister group to *Chryseofusus* comprises a species complex of *Pseudolaturus pallidus* (Fig. 6G–I); Callomon and Snyder (2009) pointed that many shells of this species differ somewhat among them (e.g., having finer and more broadly spaced axial sculpture, more slender profile), suggesting that this species, as well as others in the genus, require additional attention. Both *P. pallidus* and *P. aff. pallidus* have a different placement of the axial sculpture as noted by Callomon and Snyder (2009), and both appear together with an undescribed species (Fig. 6I). Since grouping with *Chryseofusus* seems an unlikely choice based on conchological characters alone, one must

assume that the *Pseudolaturus* shell morphology is plesiomorphic, which is corroborated by the fact that this form is present in two independent clades (see below). *Pseudolaturus* also appears as a grade of two lineages that are basal to *Granulifusus* (BS = 98%; PP = 1.00) (Fig. 6J and K). *Pseudolaturus discrepans* is closest to *Granulifusus*, although this clade is poorly supported in the ML analysis (BS = 51%; PP = 0.92). This species has been considered a *Granulifusus* by several authors (e.g., Poppe, 2008), and based on our tree topology and on the sculpture of the initial whorls (which closely resembles that of many *Granulifusus*), we agree with the placement of *Pseudolaturus discrepans* in *Granulifusus*.

In the clade of *Granulifusus* + *Pseudolaturus*, a first split separates *Pseudolaturus kuroseanus* + *P. kurodai* from the rest, and while they share some similarities, there are very few resemblances between them and a *Granulifusus*-like shell. A more conservative approach is taken here, as taking any taxonomic actions herein requires additional research, including the investigation of type specimens and synonymies; however we consider *Pseudolaturus* to be a heterogeneous assemblage in the subfamily Fusininae.

*Granulifusus* is an Indo-Pacific genus, being one of the Indo-Pacific elements occurring in Japanese warm waters (Shuto, 1958). The genus was revised by Hadorn and Fraussen (2005), who described several new species (e.g., *G. bacciballus*, *G. benjamini*) and transferred several others to it. In our phylogeny, *Granulifusus* is monophyletic (BS = 51%; PP = 0.92), a first split separates *G. discrepans* from of the remaining *Granulifusus* (BS = 50%; PP = 0.92). A second split separates *Granulifusus staminatus* from the rest (BS = 82%; PP = 1.00), including an undescribed species (Fig. 6L) with a canaliculated suture and reduced granulated surface; this new species is sister to *G. kiranus* (BS = 100%; PP = 1.00).

In the original description of *Angulofusus nedae*, the only representative of the genus *Angulofusus*, a superficial conchological resemblance to some Conoidea was noted by its authors (Fedosov and Kantor, 2012), notably the distinctive anal sinus. However its anatomy and radula structure placed it unambiguously in the family Fascioliariidae and Fedosov and Kantor (2012) noted that the radula, soft-part coloration and internal anatomy of *Angulofusus nedae* are very similar to those of species in the genus *Amiantofusus*; however, upon examination of its COI sequence through BLAST scores in the NCBI database, a closer relationship to *Granulifusus* was proposed. Indeed, in our multi-gene





**Fig. 6.** Vouchers of sequenced specimens of Fascioliariidae: *Fusinus colus* clade. A–C: *Cyrtulus serotinus* growth series, Marquesas Islands: A: MNHN IM-2013-42530; B: MNHN IM-2013-4251; C: MNHN IM-2013-42532; D: *Fusinus colus*, MNHN IM-2007-32560, New Caledonia; E: *Amiantofusus sebalis*, MNHN IM-2007-32837, Solomon Islands. F: *Chryseofusus graciliformis*, MNHN IM-2007-32797, Solomon Islands; G: *Pseudolaturus pallidus*, MNHN IM-2007-32537, Solomon Islands; H: *Pseudolaturus* aff. *pallidus*, MNHN IM-2007-32913, Philippines; I: *Pseudolaturus* sp., MNHN IM-2007-32510, New Caledonia; J: *Pseudolaturus kurodai*, MNHN IM-2013-42520, New Caledonia; K: *Pseudolaturus discrepans*, MNHN IM-2007-34604, Philippines; L: *Granulifusus* sp., MNHN IM-2013-19724, Bismarck Sea.

ML analysis, *Angulofusus neda* is grouped with the (*Granulifusus* + *Pseudolaturus*) clade, albeit weakly supported (BS = 66%).

By using a dense taxon sampling and a multigene analysis of the putative members of the Fascioliariidae we were able to test the monophyly of the family and its main subclades. While the current molecular data are not able to conclude unambiguously whether the family includes or not the *Dolicholaturus/Teralaturus* clade, it showed reliable structure and three clades, each including the type species of the type genus of the three currently recognized subfamilies. These clades do not strictly correspond to the currently accepted taxonomy, as only Fascioliariinae is monophyletic but deeply nested within a clade of taxa hitherto classified as peristerniines. The type species of the type genus of Peristerniinae is present in another, Peristerniinae-only, clade. And, finally, Fusiniinae includes also members of the hitherto peristerniine genus *Pseudolaturus*. Our phylogenetic hypothesis thus provides a compelling new classification of the Fascioliariidae where the three

current subfamilies are maintained, albeit with completely revised taxonomic extensions.

## 5. Conclusions

The clade consisting of *Dolicholaturus/Teralaturus* is monophyletic; however, topology tests do not reject its inclusion in Fascioliariidae or its relationship to the remaining fascioliariids. The remaining fascioliariids are monophyletic and strongly supported, and fall into three main clades that correspond to the three currently recognized subfamilies, but with their taxonomic extension considerably revised:

- (1) *Fusinus colus* clade, containing all the Fusiniinae, consisting of five major lineages corresponding to the genera *Amiantofusus*, *Angulofusus*, *Chryseofusus*, *Fusinus* and *Granulifusus*, and also including the non-monophyletic *Pseudolaturus*.

- (2) *Peristernia nassatula* clade, consisting of the non-monophyletic *Peristernia* and *Fusolatirus*; the name *Peristerniinae* can be retained for this clade.
- (3) *Fasciolaria tulipa* clade, consisting of a monophyletic *Fasciolaria-Pleuroploca* clade and many other genera currently classified as *peristerniinae*, among which the genera *Latirus*, *Leucozonia*, and *Hemipolygona* appeared non-monophyletic; deep nodes within this clade were unresolved or poorly supported. The taxonomic extension of the subfamily *Fasciolariinae* can be revised to encompass this third clade.

## Acknowledgements

Most molecular material in this paper originates from numerous shore-based expeditions and deep-sea cruises, conducted respectively by MNHN and Pro-Natura International as part of the Our Planet Reviewed programme, and by MNHN and IRD as part of the Tropical Deep-Sea Benthos programme. Funders and sponsors include the French Ministry of Foreign Affairs, the Philippines Bureau of Fisheries and Aquatic Resources, the Total Foundation, Prince Albert II of Monaco Foundation, Stavros Niarchos Foundation, and Richard Lounsbery Foundation. We thank Gary Rosenberg (ANSP), Gustav Paulay (FMNH), Daniel Geiger (SBMNH), Gregory Herbert (USF) and Daniel Cavallari (MZSP) for loan of additional specimens and sending samples for this work; Virginie Héros, Philippe Maestrati, Pierre Lozouet, Barbara Buge, Laurent Charles (MNHN) and Ellen Strong (NMNH) for their role in specimen processing during the expeditions and curation; Lee Ann Galindo (MNHN) and Patricia Álvarez (UAM) provided helpful insights during the early stages of the lab work; Alexander Fedosov and Nicolas Puillandre (MNHN) for sending useful sequence information; Paul Callomon (ANSP) and William Lyons greatly helped in the identification of the sequenced specimens; Carlo Magenta (ANSP) for the valuable help during a visit to the Academy. Martin Snyder assisted with identifications and provided constructive insights to the manuscript. Rosa Fernández, Sarah Lemer, David Combosch, Erin McIntyre, Tauana Cunha, Ana Tourinho, Beka Buckham and Rafaela Jorge Trad (MCZ) helped with many aspects of bench work and analysis. Adam Baldinger (MCZ) for help in collection and management. John Slapcinsky (FMNH) sent photographic material. Two anonymous reviewers are acknowledged for their comments, which helped to improve this article. This work was funded in part by grant #2012/14821-3, #2013/27005-2 and #2014/10951-5, Fundação de Amparo à Pesquisa do Estado de São Paulo (FAPESP), Brazil and by internal funds from the MCZ and the Faculty of Arts and Sciences, Harvard University.

## Appendix A. Supplementary material

Supplementary data associated with this article can be found, in the online version, at <http://dx.doi.org/10.1016/j.ympev.2016.03.025>.

## References

Abbott, R.T., 1958. The marine mollusks of Grand Cayman Island, British West Indies. *Monogr. Acad. Nat. Sci. Philadelphia* 11, 1–138.

Aktipis, S.W., Giribet, G., 2010. A phylogeny of Vetigastropoda and other “archaeogastropods”: re-organizing old gastropod clades. *Invertebr. Biol.* 129, 220–240.

Auwera, G.V., Chapelle, S., De Wächter, R., 1994. Structure of the large ribosomal subunit RNA of *Phytophthora megasperma*, and phylogeny of the Oomycetes. *FEBS Lett.* 338, 133–136.

Bandel, K., 1984. The radulae of Caribbean and other Mesogastropoda and Neogastropoda. *Zool. Verh.* 214, 1–188.

Bandel, K., 1993. Caenogastropoda during Mesozoic times. *Scr. Geol. Special* 2, 7–56.

Bellardi, L., 1884. I molluschi dei terreni terziarii del Piemonte e della Liguria. Parte IV. Fasciariidae e Turbinellidae. Torino, pp. 62.

Beu, A., 2011. Marine Mollusca of isotope stages of the last 2 million years in New Zealand. Part 4. Gastropoda (Ptenoglossa, Neogastropoda, Heterobranchia). *J. R. Soc. N.Z.* 41, 11–53.

Bouchet, P., Rocroi, J.P., 2005. Classification and nomenclator of gastropod families. *Malacologia* 47, 1–397.

Bullock, R.C., 1974. A contribution to the systematics of some West Indian *Latirus* (Gastropoda: Fasciariidae). *Nautilus* 88, 69–79.

Callomon, P., Snyder, M.A., 2009. On the genus *Fusinus* in Japan V: further species, an unnamed form and discussion. *Venus* 67 (3–4), 1–14.

Carpenter, J.M., Wheeler, W.C., 1999. Towards simultaneous analysis of morphological and molecular data in Hymenoptera. *Zool. Scr.* 28, 251–260.

Colgan, D., Ponder, W.F., Egger, P.E., 2000. Gastropod evolutionary rates and phylogenetic relationships assessed using partial 28S rDNA and histone H3 sequences. *Zool. Scr.* 29, 29–63.

Colgan, D.J., McLauchlan, A., Wislon, G.D.F., Livingston, S., Edgcombe, G.D., Macaranas, J., Cassis, G., Gray, M.R., 1998. Molecular phylogenetics of the Arthropoda: relationships based on histone H3 and U2 snRNA DNA sequences. *Aust. J. Zool.* 46, 419–437.

Colgan, D.J., Ponder, W.F., Beacham, E., Macaranas, J.M., 2003. Molecular phylogenetic studies of Gastropoda based on six gene segments representing coding or non-coding and mitochondrial or nuclear DNA. *Moll. Res.* 23, 123–148.

Colgan, D.J., Ponder, W.F., Beacham, E., Macaranas, J., 2007. Molecular phylogenetics of Caenogastropoda (Gastropoda: Mollusca). *Mol. Phylogenet. Evol.* 42, 717–737.

Cossmann, M., 1901. Essais de paléontologie comparée, 4. The author and Société d'Éditions Scientifiques, Paris, pp. 293.

Couto, D.R., Pimenta, A.D., 2012. Comparative morphology of *Leucozonia* from Brazil (Neogastropoda: Buccinoidea: Fasciariidae). *Am. Malacol. Bul.* 30, 103–116.

Darriba, D., Taboada, G.L., Doallo, R., Posada, D., 2012. JModelTest 2: more models, new heuristics and parallel computing. *Nat. Meth.* 9, 772.

Edgar, R.C., 2004. MUSCLE: multiple sequence alignment with high accuracy and high throughput. *Nucl. Acids Res.* 32, 1792–1797.

Edgcombe, G.D., Giribet, G., 2006. A century later – a total evidence re-evaluation of the phylogeny of scutigermorph centipedes (Myriapoda: Chilopoda). *Invertebr. Syst.* 20, 503–525.

Fedosov, A.E., Kantor, Y.I., 2012. A new species and genus of enigmatic turritiform Fasciariidae from the Central Indo-Pacific (Gastropoda: Neogastropoda). *Arch. Molluskenkunde* 141, 137–144.

Folmer, O., Black, M., Hoeh, W., Lutz, R., Vrijenhoek, R., 1994. DNA primers for amplification of mitochondrial cytochrome c oxidase subunit I from diverse metazoan invertebrates. *Mol. Mar. Biol. Biotechnol.* 3, 294–299.

Fraussen, K., Kantor, Y., Hadorn, R., 2007. *Amiantofusus* gen. nov. for *Fusus amiantus* Dall, 1889 (Mollusca: Gastropoda: Fasciariidae) with description of a new and extensive Indo-West Pacific radiation. *Novapex* 8, 79–101.

Galindo, L.A., Puillandre, N., Strong, E.E., Bouchet, P., 2014. Using microwaves to prepare gastropod for DNA barcoding. *Mol. Ecol. Res.* 14, 700–705.

Geller, J., Meyer, C., Parker, M., Hawk, H., 2013. Redesign of PCR primers for mitochondrial cytochrome c oxidase subunit I for marine invertebrates and application in all-taxa biotic surveys. *Mol. Ecol. Resour.* 13, 851–861.

Giribet, G., Carranza, S., Bagnà, J., Riutort, M., Ribera, C., 1996. First molecular evidence for the existence of a Tardigrada + Arthropoda clade. *Mol. Biol. Evol.* 13, 76–84.

Giribet, G., Shear, W.A., 2010. The genus *Siro* Latreille, 1796 (Opiliones, Cyphophthalmi, Sironidae), in North America with a phylogenetic analysis based on molecular data and the description of four new species. *Bull. Mus. Comp. Zool.* 160, 1–33.

Goodheart, J., Camacho-García, Y., Padula, V., Schrödl, M., Cervera, J.L., Gosliner, T. M., Valdés, Á., 2015. Systematics and biogeography of *Pleurobranchus* Cuvier, 1804, sea slugs (Heterobranchia: Nudipleura: Pleurobranchidae). *Zool. J. Linn. Soc.* 174, 322–362.

Grabau, A.W., 1907. Studies of Gastropoda III. On orthogenetic variation in Gastropoda. *Am. Nat.*, 607–651.

Guindon, S., Gascuel, O., 2003. A simple, fast, and accurate algorithm to estimate large phylogenies by maximum likelihood. *Syst. Biol.* 52, 696–704.

Hadorn, R., Fraussen, K., 2005. Revision of the genus *Granulifusus* Kuroda & Habe 1954, with description of some new species (Gastropoda: Prosobranchia: Fasciariidae). *Archiv für Molluskenkunde* 134, 129–171.

Harasewych, M.G., 1990. Studies on bathyal and abyssal Buccinidae (Gastropoda: Neogastropoda): 1. *Metula fusiformis* Clench and Aguayo, 1941. *Nautilus* 104, 120–130.

Harasewych, M.G., Adamkewicz, S.L., Blake, J.A., Saudek, D., Spriggs, T., Bult, C.J., 1997. Neogastropod phylogeny: a molecular perspective. *J. Moll. Stud.* 63, 327–351.

Hayashi, S., 2005. The molecular phylogeny of the Buccinidae (Caenogastropoda: Neogastropoda) as inferred from the complete mitochondrial 16S rRNA gene sequences of selected representatives. *Moll. Res.* 25, 85–98.

Kantor, Y.I., Fedosov, A., 2009. Morphology and development of the valve of *Leiblein*: possible evidence for parphyly of the Neogastropoda. *Nautilus* 123, 1–73.

Kearse, M., Moir, R., Wilson, A., Stones-Havas, S., Cheung, M., Sturrock, S., Buxton, S., Cooper, A., Stones-Havas, S., Duran, C., Thierer, S., Ashton, B., Meintjes, P., Drummond, A., 2012. Geneious Basic: an integrated and extendable desktop software platform for the organization and analysis of sequence data. *Bioinformatics* 28, 1647–1649.

- Kishino, H., Hasegawa, M., 1989. Evaluation of the maximum likelihood estimate of the evolutionary tree topologies from DNA sequence data, and the branching order in Hominoidae. *J. Mol. Evol.* 29, 170–179.
- Kocot, K.M., Cannon, J.T., Todt, C., Citarella, M.R., Kohn, A.B., Meyer, A., Santos, S.R., Schander, C., Moroz, L.L., Lieb, A., Halanych, K.M., 2011. Phylogenomics reveals deep molluscan relationships. *Nature* 477, 452–456.
- Kosyan, A.R., Modica, M.V., Oliverio, M., 2009. The anatomy and relationships of *Troschelia* (Neogastropoda, Buccinidae): new evidence for a closer fascioliid-buccinid relationship? *Nautilus* 123, 95–105.
- Leal, J.H., 1991. Marine Prosobranch Gastropods from Oceanic Islands Off Brazil: Species Composition and Biogeography. Universal Book Services/W. Backhuys, pp. 418.
- Lyons, W.G., 1991. Post-Miocene species of *Latirus* Montfort, 1810 (Mollusca: Fascioliariidae) of southern Florida, with a review of regional marine biostratigraphy. *Bull. Fla. Mus. Nat. Hist. (Biol. Sci.)* 34, 131–208.
- Lyons, W.G., Snyder, M.A., 2013. The genus *Pustulaturus* Vermeij and Snyder, 2006 (Gastropoda: Fascioliariidae: Peristerniinae) in the western Atlantic, with descriptions of three new species. *Zootaxa* 3636, 35–58.
- Meyer, A., Todt, C., Mikkelsen, N., Lieb, B., 2010. Fast evolving 18S rRNA sequences from Solenogastres (Mollusca) resist standard PCR amplification and give new insights into mollusk substitution rate heterogeneity. *BMC Evol. Biol.* 10, 70.
- Miller, M.A., Pfeiffer, W., Schwartz, T., 2010. Creating the CIPRES Science Gateway for inference of large phylogenetic trees. *Gateway Computing Environments Workshop (GCE)*, pp. 1–8.
- Nagai, M., Yoshida, A., Sato, N., 1998. Additive effects of bovine serum albumin, dithiothreitol and glycerol on PCR. *Int. Union Biochem. Mol. Biol. Life* 44, 157–163.
- Oliverio, M., Modica, M.V., 2010. Relationships of the haematophagous marine snail *Colubraria* (Rachiglossa: Colubrariidae), within the neogastropod phylogenetic framework. *Zool. J. Linn. Soc.* 158, 779–800.
- Osca, D., Templado, J., Zardoya, R., 2015. Caenogastropod mitogenomics. *Mol. Phylogenet. Evol.* 98, 118–128.
- Palumbi, S.R., 1996. Nucleic acids II: the polymerase chain reaction. *Mol. Syst.* 2, 205–247.
- Ponder, W.F., Colgan, D.J., Healy, J.M., Nützel, A., Simone, L.R.L., Strong, E.E., 2008. Caenogastropoda. In: Ponder, W.F., Lindberg, D.R. (Eds.), *Phylogeny and Evolution of the Mollusca*. Univ. Calif. Press, pp. 331–383.
- Ponder, W.F., 1972. Notes on some Australian species and genera of the family Buccinidae (Neogastropoda). *J. Malacol. Soc. Aust.* 2, 249–265.
- Ponder, W.F., Lindberg, D.R., 1997. Towards a phylogeny of gastropod molluscs: an analysis using morphological characters. *Zool. J. Linn. Soc.* 119, 83–265.
- Poppe, G.T., 2008. *Philippine Marine Mollusks: Gastropoda*, Pt. 2. ConchBooks, pp. 848.
- Puillandre, N., Kantor, Y.I., Sysoev, A., Couloux, A., Meyer, C., Rawlings, T., Todd, J.A., Bouchet, P., 2011. The dragon tamed? A molecular phylogeny of the Conoidea (Gastropoda). *J. Moll. Stud.* 77, 259–272.
- Rambaut, A., Suchard, M.A., Xie, D., Drummond, A.J., 2014. Tracer v1. 6. Computer Program and Documentation Distributed by the Author, website <<http://beast.bio.ed.ac.uk/Tracer>> (accessed 27 July 2014).
- Riedel, F., 2000. Ursprung und evolution der "höheren" Caenogastropoda. *Berl. Geowiss. Abhandl. Reihe E Paläobiol.* 32, 1–240.
- Ronquist, F., Teslenko, M., van der Mark, P., Ayres, D., Darling, A., Höhna, S., Larget, B., Liu, L., Suchard, M.A., Huelsenbeck, J.P., 2012. MrBayes 3.2: efficient Bayesian phylogenetic inference and model choice across a large model space. *Syst. Biol.* 61, 539–542.
- Schwendinger, P.J., Giribet, G., 2005. The systematics of the south-east Asian genus *Fangensis* Rambla (Opiliones: Cyphophthalmi: Stylocellidae). *Inv. Syst.* 19, 297–323.
- Sharma, P.P., Zardus, J.D., Boyle, E.E., González, V.L., Jennings, R.M., McIntyre, E., Wheeler, W.C., Etter, R.J., Giribet, G., 2013. Into the deep: a phylogenetic approach to the bivalve subclass Protobranchia. *Mol. Phylogenet. Evol.* 69, 188–204.
- Shimodaira, H., 2002. An approximately unbiased test of phylogenetic tree selection. *Syst. Biol.* 51, 492–508.
- Shimodaira, H., Hasegawa, M., 1999. Multiple comparisons of log-likelihoods with applications to phylogenetic inference. *Mol. Biol. Evol.* 16, 1114–1116.
- Shimodaira, H., Hasegawa, M., 2001. CONSEL: for assessing the confidence of phylogenetic tree selection. *Bioinformatics* 17, 1246–1247.
- Shuto, T., 1958. *Granulifusus* from the Miyazaki Group. *Trans. Proc. Palaeont. Soc. Japan NS* 31, 253–264.
- Simone, L.R.L., Cavallari, D.C., Abbate, D., 2013. Revision of the genus *Teralaturus* Coomans 1965 in the Western Atlantic, with an anatomical description of *T. roboreus* (Reeve 1845) (Gastropoda: Neogastropoda: Fascioliariidae). *Arch. Molluskenkunde* 142, 215–226.
- Smith, S.A., Wilson, N.G., Goetz, F.E., Feehery, C., Andrade, S.C., Rouse, G.W., Giribet, G., Dunn, C.W., 2011. Resolving the evolutionary relationships of molluscs with phylogenomic tools. *Nature* 480, 364–367.
- Snyder, M.A., 2003. Catalogue of the marine gastropod family Fascioliariidae. *Acad. Nat. Sci. Philadelphia*, 431.
- Snyder, M.A., Bouchet, P., 2006. New species and new records of deep-water *Fusolaturus* (Neogastropoda: Fascioliariidae) from the West Pacific. *J. Conchol.* 39, 1–12.
- Snyder, M.A., Vermeij, G.J., Lyons, W.G., 2012. The genera and biogeography of Fascioliariinae (Gastropoda, Neogastropoda, Fascioliariidae). *Basteria* 76, 31–70.
- Stahlschmidt, P., Fraussen, K., 2012. *Crassibougia*, a new genus for *Fusus clausicaudatus* Hinds, 1844, from South Africa, with description of a new species (Gastropoda: Fascioliariidae). *Misc. Malacol.* 5, 85–93.
- Stamatakis, A., 2014. RAxML version 8: a tool for phylogenetic analysis and post-analysis of large phylogenies. *Bioinformatics* 31, 1–2.
- Stamatakis, A., Hoover, P., Rougemont, J., 2008. A rapid bootstrap algorithm for the RAxML web servers. *Syst. Biol.* 57, 758–771.
- Strong, E.E., 2003. Refining molluscan characters: morphology, character coding and a phylogeny of the Caenogastropoda. *Zool. J. Linn. Soc.* 137, 447–554.
- Taylor, J.D., Morris, N.J., Taylor, C.N., 1980. Food specialization and the evolution of predatory prosobranch gastropods. *Palaeontology* 23, 375–409.
- Taylor, J.D., Lewis, A., 1995. Diet and radular morphology of *Peristernia* and *Latirologena* (Gastropoda: Fascioliariidae) from Indo-Pacific coral reefs. *J. Nat. Hist.* 29, 1143–1154.
- Tëmkin, I., 2010. Molecular phylogeny of pearl oysters and their relatives (Mollusca, Bivalvia, Pterioidea). *BMC Evol. Biol.* 10, 342.
- Thiele, J., 1929–1935. *Handbuch der Systematischen Weichtierkunde*. Gustav Fischer, Jena, pp. 1134.
- Tracey, S., Todd, J.A., Erwin, D.H., 1993. Mollusca: gastropoda. In: Benton, M.J. (Ed.), *The Fossil Record*, vol. 2. Chapman & Hall, London, pp. 845.
- Vermeij, G.J., 1997. The genus *Leucozonia* (Gastropoda: Fascioliariidae) in the Neogene of tropical America. *Tulane Stud. Geol. Paleont.* 29, 129–134.
- Vermeij, G.J., 2001. Innovation and evolution at the edge: origins and fates of gastropods with a labral tooth. *Biol. J. Linn. Soc.* 72, 461–508.
- Vermeij, G.J., Snyder, M.A., 1998. *Leucozonia ponderosa*, a new fascioliariid gastropod from Brazil. *Nautilus* 112, 117–119.
- Vermeij, G.J., Snyder, M.A., 2002. *Leucozonia* and related genera of fascioliariid gastropods: shell-based taxonomy and relationships. *Proc. Acad. Nat. Sci. Philadelphia* 152, 23–44.
- Vermeij, G.J., Snyder, M.A., 2006. Shell characters and taxonomy of *Latirus* and related fascioliariid groups. *J. Moll. Stud.* 72, 413–424.
- Wenz, W., 1938–1944. Teil 1: Allgemeiner Teil und Prosobranchia. In: Schindewolf, O.H. (Ed.), *Handbuch der Paläozoologie*, Band 6, Gastropoda. Borntraeger, Berlin, pp. 1639.
- Whiting, M.F., Carpenter, J.C., Wheeler, Q.D., Wheeler, W.C., 1997. The Strepsiptera problem: phylogeny of the holometabolous insect orders inferred from 18S and 28S ribosomal DNA sequences and morphology. *Syst. Biol.* 46, 1–68.
- WoRMS, 2016. *World Register of Marine Species*. <<http://www.marinespecies.org/>> (accessed 17 February 2016).
- Zapata, F., Wilson, N.G., Howison, M., Andrade, S.C., Jörgen, K.M., Schrödl, M., Goetz, F.E., Giribet, G., Dunn, C.W., 2014. Phylogenomic analyses of deep gastropod relationships reject Orthogastropoda. *Proc. R. Soc. Lond. B Biol. Sci.* 281, 1–9.
- Zou, S., Li, Q., Kong, L., 2011. Additional gene data and increased sampling give new insights into the phylogenetic relationships of Neogastropoda, within the caenogastropod phylogenetic framework. *Mol. Phylogenet. Evol.* 61, 425–435.